30
12-28-87
RB
DR 0356-5
CONF-870659--Vol.2

DOE/METC-87/6079, Vol. 2
(DE87006496)

Proceedings of the Seventh Annual Gasification and Gas Stream Cleanup Systems Contractors Review Meeting

Volume II

DO NOT MICROFILM
COVER

Editors
M.R. Ghate
K.E. Markel, Jr.
L.A. Jarr
S.J. Bossart

June 1987

Sponsored by
U.S. Department of Energy
Office of Fossil Energy
Morgantown Energy Technology Center
Morgantown, West Virginia

FOSSIL ENERGY

DISTRIBUTION OF THIS DOCUMENT IS UNLIMITED

DISCLAIMER

This report was prepared as an account of work sponsored by an agency of the United States Government. Neither the United States Government nor any agency Thereof, nor any of their employees, makes any warranty, express or implied, or assumes any legal liability or responsibility for the accuracy, completeness, or usefulness of any information, apparatus, product, or process disclosed, or represents that its use would not infringe privately owned rights. Reference herein to any specific commercial product, process, or service by trade name, trademark, manufacturer, or otherwise does not necessarily constitute or imply its endorsement, recommendation, or favoring by the United States Government or any agency thereof. The views and opinions of authors expressed herein do not necessarily state or reflect those of the United States Government or any agency thereof.

DISCLAIMER

Portions of this document may be illegible in electronic image products. Images are produced from the best available original document.

DO NOT MICROFILM
THIS PAGE

DISCLAIMER

This report was prepared as an account of work sponsored by an agency of the United States Government. Neither the United States Government nor any agency thereof, nor any of their employees makes any warranty, express or implied, or assumes any legal liability or responsibility for the accuracy, completeness or usefulness of any information, apparatus, product, or process disclosed, or represents that its use would not infringe privately owned rights. Reference herein to any specific commercial product, process, or service by trade name, trademark, manufacturer, or otherwise, does not necessarily constitute or imply its endorsement, recommendation, or favoring by the United States Government or any agency thereof. The views and opinions of authors expressed herein do not necessarily state or reflect those of the United States Government or any agency thereof.

This report has been reproduced directly from the best available copy.

Available from the National Technical Information Service, U. S. Department of Commerce, Springfield, VA 22161.

Price: Printed copy A19
Microfiche A01

Codes are used for pricing all publications. The code is determined by the number of pages in the publication. Information pertaining to the pricing codes can be found in the current issues of the following publications, which are generally available in most libraries: *Energy Research Abstracts (ERA), Government Reports Announcements* and Index (*GRA* and *I*); *Scientific and Technical Abstract Reports (STAR);* and publication NTIS-PR- 360 available from NTIS at the above address.

DOE/METC-87/6079, Vol. 2
(CONF-870659)
(DE87006496)

DOE/METC--87/6079-Vol.2

DE87 006496

Proceedings of the Seventh Annual Gasification and Gas Stream Cleanup Systems Contractors Review Meeting

Volume II

Editors
M.R. Ghate
K.E. Markel, Jr.
L.A. Jarr
S.J. Bossart

U.S. Department of Energy
Office of Fossil Energy
Morgantown Energy Technology Center
P.O. Box 880
Morgantown, West Virginia 26507-0880

Held at
Sheraton Lakeview Conference Center
Morgantown, West Virginia
June 16-19, 1987

August 1987

NAC.ER

EB

DISTRIBUTION OF THIS DOCUMENT IS UNLIMITED

THIS PAGE

WAS INTENTIONALLY

LEFT BLANK

TABLE OF CONTENTS

Page

VOLUME I

KEYNOTE SPEECH

The Status of Coal Gasification Technology and Its Implications for Electric Power Production -- Seymour B. Alpert for Dr. Dwain F. Spencer, Vice President of Advanced Power Systems, Electric Power Research Institute 1

SESSION 1 -- SYSTEM FOR THE PRODUCTION OF CO-PRODUCTS

Development of a Mild Gasification Process -- UCC Research Corporation 14

Steam Conditioning of Coal for Synfuels Production -- City College of New York 24

Investigation of Reaction of Heteroatoms During Coal Gasification -- Institute of Gas Technology 34

Measurement and Modeling of Advanced Coal Conversion Processes -- Advanced Fuel Research, Inc., and Brigham Young University 43

Applications of Organo-Calcium Chemistry to Control of Contaminant Aromatic Hydrocarbons in Advanced Coal Gasification Processes -- Massachusetts Institute of Technology 53

Novel Concept Development of an Internal Recirculation Catalyst for Mild Gasification -- Institute of Gas Technology 66

Chemical and Physical Development of Char Particles During Devolatilization -- Advanced Fuel Research, Inc. 76

Study of the Effects of Soot, Particulate and Other Contaminants on Molten Carbonate Fuel Cells Fueled by Coal Gas -- Energy Research Corporation 86

Mild Gasification of Coal -- Brookhaven National Laboratory 100

Fundamental Mechanisms of Coal Gasification -- Massachusetts Institute of Technology 110

Upgrading of Condensibles From Coal Devolatilization -- Oak Ridge National Laboratory 117

Assessment of Instrumentation Needs for Advanced Coal Conversion Power Plants -- Gilbert/Commonwealth, Inc. 123

TABLE OF CONTENTS
(Continued)

Page

POSTER SESSION A

Reduced Entrainment Precipitator (REP) for High-Temperature and High-Pressure (Phase I) -- ETS, Inc. 137

Vaporization of Trace Inorganic Species From Coal Under Combustion and Gasification Conditions -- SRI International 145

Hot Gas Cleanup Systems Analysis -- METC 150

Experimental Development of a Multi-Solid Fluidized-Bed Reactor Concept -- Battelle Columbus Division 165

Mechanisms of Mild Gasification and Low Severity Coal Devolatilization -- METC 170

Mild Gasification of Coal -- University of North Dakota Energy Research Center 183

Gasification Systems Analysis -- METC 187

Fundamental Research on Mild Gasification Char Fuel Development -- UCC Research Corporation 200

Effects of Halides on the Performance of Coal Gas-Fueled Molten Carbonate Fuel Cell -- International Fuel Cells 204

Component Systems Enhancement Reduced Girth Seam Weldments for Heavy-Walled Vessels -- CBI Na-Con, Inc. 210

Coal Slurry Letdown Device -- Jet Propulsion Laboratory 215

Development of Iron Aluminides for Coal Gasification Systems -- Martin Marietta Energy Systems, Inc., and Oak Ridge National Laboratory 220

Protective Coatings and Claddings: Application/Evaluation -- Argonne National Laboratory 225

SESSION 2 -- SYSTEM FOR THE PRODUCTION OF INDUSTRIAL FUEL GAS

Ash and Slag Characterization -- University of North Dakota Energy Research Center 230

Experimental and Theoretical Investigation of the Formation and Growth of Ash Agglomerates -- Institute of Gas Technology 241

TABLE OF CONTENTS
(Continued)

Page

Performance Evaluation of a Screenless (Counter-Current) Granular Bed Filter on a Subpilot-Scale PFBC -- Combustion Power Company 251

Testing of Electrostatic Precipitator at New York University -- Cottrell Environmental Sciences 262

Status Report on KILnGAS Commercial Module -- Allis-Chalmers Coal Gas Corporation 270

SESSION 3 -- ENVIRONMENTAL PROJECTS

Evaluation of a Ceramic Cross-Flow Filter In a Bench-Scale Gasifier -- Westinghouse Electric Corporation 279

Environmental Engineering and Analysis -- Radian Corporation 289

Advanced Wastewater Treatment -- University of North Dakota Energy Research Center 299

A Mechanical Analysis of a Ceramic Cross Flow Filter -- Westinghouse Electric Corporation 308

SESSION 4 -- COMPONENTS AND MATERIALS

Zirconia Cell Oxygen Source -- Jet Propulsion Laboratory 321

Materials Development for JPL Oxygen Plant -- Argonne National Laboratory 331

Reduction of Erosion in Elbows Due to Flow Field Modifications -- West Virginia University 341

Ceramic-Fiber Ceramic-Matrix Hot-Gas Filters -- Oak Ridge National Laboratory 351

TABLE OF CONTENTS
(Continued)

Page

VOLUME II

SESSION 5 -- SYSTEM FOR THE PRODUCTION OF SYNTHESIS GAS

Catalytic Gasification Fundamentals -- Lawrence Berkeley Laboratory 363

Production of Hydrogen From Low-Rank Coals -- University of North Dakota Energy Research Center 372

Biological Degradation of Low-Rank Coal -- Georgia Institute of Technology 382

Study of Ammonia Removal in Coal Gasification Processes Using Integrated Systems Approach -- Acurex Corporation 393

Study of Ammonia Removal in Coal Gasification Processes -- SRI International 403

Injection of Densely Loaded Flows Into Entrained-Flow Gasifiers -- Science Applications International Corporation 413

Attrition and Entrainment Studies Related to Fluidized-Bed Coal Gasifiers -- Institute of Gas Technology 422

Mechanisms for Hot Gas Cleanup -- METC 431

Low Temperature, Sulfur Tolerant, Homogenous Catalysts for the Water-Gas Shift Reaction -- SRI International 442

Removal of H_2S From Gasified Coal -- Lawrence Berkeley Laboratory 451

Gas Separation by Pressure Swing Adsorption for Producing Hydrogen From Coal -- State University of New York at Buffalo 461

Gas Separation Using Ion Exchange Membranes for Producing Hydrogen From Synthesis Gas -- National Bureau of Standards 469

Separation of Gas Mixtures by Supported Complexes -- Pacific Northwest Laboratory 477

Measurement of Alkali Vapors in PFBC Process Stream and Their Removal With a Fixed Granular-Bed Sorber -- Argonne National Laboratory 482

A Study of High Temperature Removal of Alkali in a Pressurized Gasification System -- Westinghouse Electric Corporation 495

TABLE OF CONTENTS
(Continued)

Page

LUNCHEON SPEECH

The Present and Future of Gas Supplies -- William F. Morse, Vice President of Research, Columbia Gas 505

POSTER SESSION B

A Novel Approach to Hydrogen Recovery, Storage, and Transport -- United Technologies Research Center 509

Hydrogen Recovery by Novel Solvent Systems -- City College of New York 514

Low Cost Hydrogen/Novel Membrane Technology for Hydrogen Separation From Synthesis Gas -- Membrane Technology and Research, Inc. 519

Advanced Studies of the Biological Conversion of Synthesis Gas to Methane -- University of Arkansas 526

Biological Gasification -- Atlantic Research Corporation 530

Process Development Unit for Coal Gasification Tied to Regenerative Hot Gas Cleanup -- Calderon Energy Company 537

Expansion of High-Temperature, High-Pressure Data Set for Coal Gasification -- The Pennsylvania State University 542

Expansion of High-Temperature, High-Pressure Data Set for Coal Gasification -- Advanced Fuel Research, Inc. 548

Advanced Gasification Entrained Reactor -- METC 553

Sidestream Zinc Ferrite Regeneration Testing -- METC 567

METC Fixed-Bed Gasifier -- METC 579

A Mechanistic Study of the Energetic Heterogeneity of Coal Chars -- Brown University 591

Fundamental Fluidization Research Program at Morgantown Energy Technology Center -- METC 596

Development of a Novel Nested-Fiber Filter Concept for High-Temperature and High-Pressure Physical Cleanup -- Battelle Columbus Division 610

Throwaway Processes for Treatment of Regeneration Tail Gases -- Arthur D. Little, Inc. 614

TABLE OF CONTENTS
(Continued)

Page

Sorbent-Based Recovery of Sulfur From Regeneration Tail Gases -- Research Triangle Institute 619

SESSION 6 -- SYSTEM FOR THE PRODUCTION OF POWER

Modeling Hydrodynamic Mixing in Process Design and Development of Fluidized Bed Gasifiers -- University of Massachusetts 624

Novel Concepts of System Assessment in Coal Gasification -- City College of New York 629

Development of a Hot Gas Cleanup System -- Institute of Gas Technology 642

Sulfur Recovery From Hot Coal Gas Desulfurization Processes -- The Ralph M. Parsons Company 656

KRW Process Development Coal Gasification/Hot Gas Cleanup -- KRW Energy System, Inc. 668

Design Studies for Hot Gas Cleanup System in a Load Following Mode -- General Electric Corporate Research and Development 678

Enhanced Durability and Reactivity for Zinc Ferrite Desulfurization Sorbent -- AMAX Research and Development Center 693

High-Temperature Solid Oxide Electrolyte Fuel Cell Power Generation System -- Westinghouse Electric Corporation 704

Dynamic Simulation Models for High-Temperature Desulfurization Processes -- Louisiana State University 716

Detailed Studies of Novel Regenerable Sorbents for High-Temperature Coal-Gas Desulfurization -- Massachusetts Institute of Technology 726

Integration and Testing of Hot Desulfurization and Entrained Flow Gasification for Power Generation System -- Texaco, Inc. 741

Bench-Scale Testing of Novel Desulfurization Sorbents -- Research Triangle Institute 749

APPENDICES

Appendix A -- Technical Program Agenda 758

Appendix B -- List of Participants 767

CATALYTIC GASIFICATION FUNDAMENTALS

1. CONTRACT NUMBER: DE-AC03-76SF00098

   CONTRACTOR: Lawrence Berkeley Laboratory
   One Cyclotron Road
   Berkeley, CA 94720

   CONTRACTOR PROJECT MANAGER: Dr. Heinz Heinemann

   PRINCIPAL INVESTIGATORS: Dr. Heinz Heinemann
   Professor G.A. Somorjai

   METC PROJECT MANAGER: Dr. H.-Y.L. Lai

   PERIOD OF PERFORMANCE: October 1, 1986 to September 30, 1987

2. SCHEDULE/MILESTONES:

   During fiscal 1987, surface characterization of intermediates in the catalytic steam gasification of chars will have been completed. Mechanisms of gasification with a potassium/nickel oxide catalyst have been illustrated by electronmicroscopy and kinetics derived from movies taken during the gasification in a CAEM chamber of the electron microscope compared with flow reactor kinetics. Comparisons of chars with graphite will have been completed and allow deductions to be made from graphite to char. Ratios of carbon monoxide and carbon dioxide produced along with hydrogen will have been determined as a function of operating conditions as well as catalyst and ash composition of the chars.

3. OBJECTIVES:

   The major purpose of this project is to find catalysts which will permit steam gasification of carbonaceous material at reasonable rates and at lower temperatures than currently practiced. An understanding of the catalytic mechanism is necessary to provide leads towards this aim.

4. BACKGROUND STATEMENT:

   Earlier work in this laboratory has shown that the gasification by steam in the presence of alkali compounds and at temperatures in the range of 600-900K proceeds through formation of a phenoxide and hydrogen production ceases when one-half mol of hydrogen has been produced per mol of alkali hydroxide. The phenoxide can be decomposed at much higher temperature (e.g., 1300K) under release of

CO and reconstitution of the alkali compound. The same result can be accomplished by the presence of a transition metal oxide at much lower temperatures (700-900K). The phenoxide is catalytically decomposed and the overall gasification reaction proceeds catalytically at these low temperatures with continuous production of hydrogen and CO_2 in ratios of between 1.5 and 2:1. The best catalyst composition found is an equimolecular mixture of KOH and NiO, although all alkali hydroxides and most transition metal oxides work. It has been established that this mixture forms a ternary oxide, presence of which is established by XPS measurements. The ternary oxide has been shown to be stable at higher temperatures than its components and in particular preserves the plus two state of nickel in the presence of reducing agents such as carbon and/or hydrogen.

6. RESULTS/ACCOMPLISHMENTS:

Activation energies for K/Ni catalyzed steam gasification of graphite and chars are identical indicating the same mechanism prevails though rates are much higher for chars. This permits extrapolation of findings in high vacuum equipment from graphite to chars. It has been found that the carbon monoxide to carbon dioxide ratio of gases produced with hydrogen varies with different chars. The ratio is .8 for Illinois #6 char and 0.08 for North Dakota char. Methane production is several orders of magnitude smaller and ceases after about two hours of operation. Comparison of K/Ni catalyst for steam gasification of Illinois #6 char with potassium or nickel alone indicates that potassium alone produces much higher CO/CO_2 ratios than potassium/nickel (3.5 versus 0.8) and therefore produces less hydrogen. Nickel alone is almost inactive for the steam gasification of Illinois #6 char except for the short first period of operation. The hydrogen production rate for nickel alone, as in the case of potassium alone, is lower than that for K/Ni. It has further been found that the Ni/K catalyst is very active for the Boudouart reaction. Experiments were carried out with carbon dioxide in the absence of water. A hypothesis has been arrived at that the ratios of $CO/CO_2/CH_4$ obtained during char gasification with steam over Ni/K can be controlled by adjusting the water partial pressure. This assumption based on a few experiments is now being tested. The NiO/K catalyst promotes the hydrogenation of CO to methane in the absence of water at 673K and above. Since CO_2 can be reduced to CO by char, CO_2 also can go to methane.

Table 1 gives the activation energies and n values obtained for Ni/K and K alone catalysts for a number of chars for the production of hydrogen, CO_2, CO and n. Graphite has an activation energy for hydrogen of 29.0±.5 Kcal.

Table 1. Activation Energies and n Values Obtained for the Ni/K and K Alone Catalysts.

CHAR	CATALYST	H_2	CO_2	CO	n
Illinois #6	K/Ni	28.6 ± 0.6	36.0 ± 0.6	35.0 ± 0.4	0.37
Illinois #6	K	60.8 ± 1.8	48.1 ± 2.3	55.3 ± 1.7	0.28
Montana	K/Ni	28.7 ± 1.2	28.4 ± 0.6	43.0 ± 0.7	0.23
North Dakota	K/Ni	29.2 ± 0.6	36.8 ± 0.3	49.8 ± 0.8	0.48

The gas products obtained in the steam gasification of the three chars studied are H_2, CO_2, CO and a slight amount of CH_4. After the first hour, and in all the cases, the product distribution though not the rate remains constant with time and a mass balance is established. The rates of formation of these four gases as a function of time are shown in Figs. 1, 2 and 3 for the steam gasification of Illinois #6, North Dakota and Montana chars

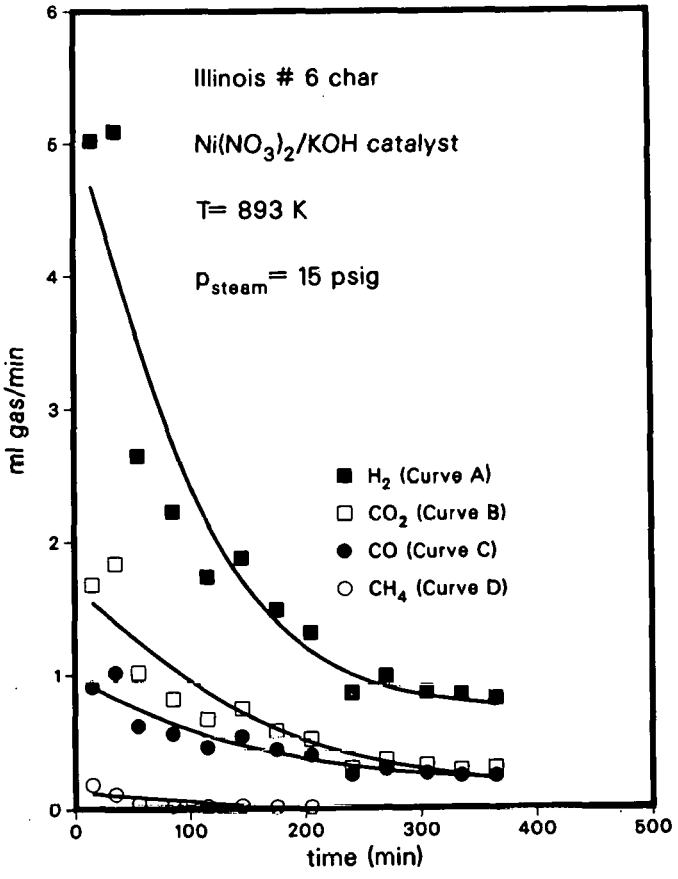

Figure 1.

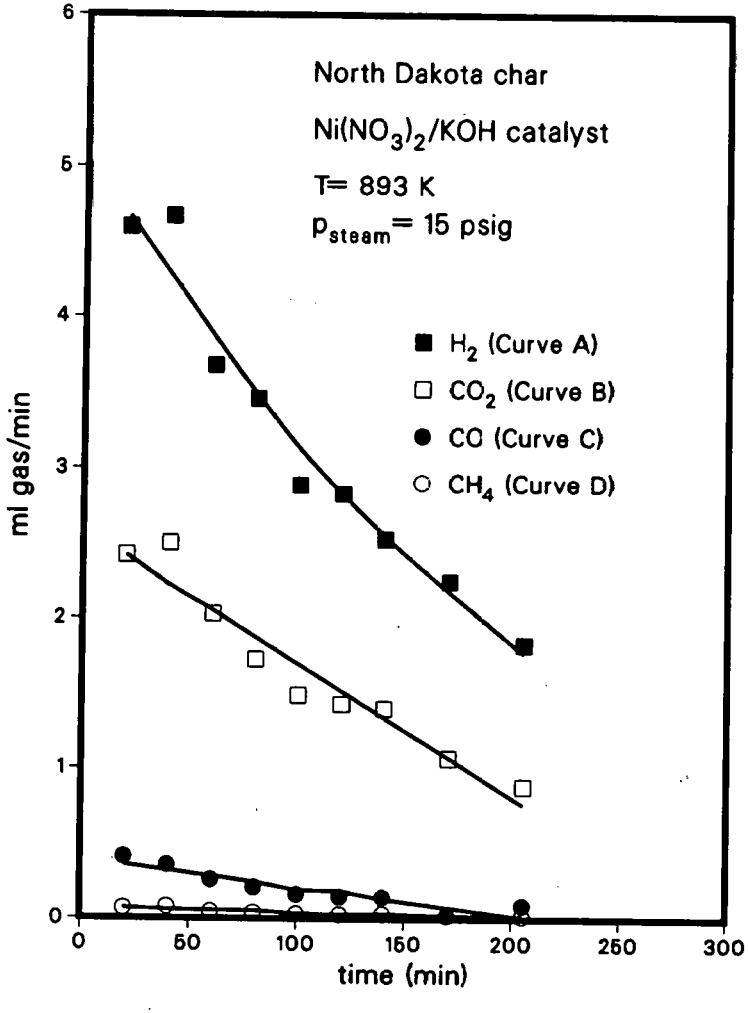

Figure 2.

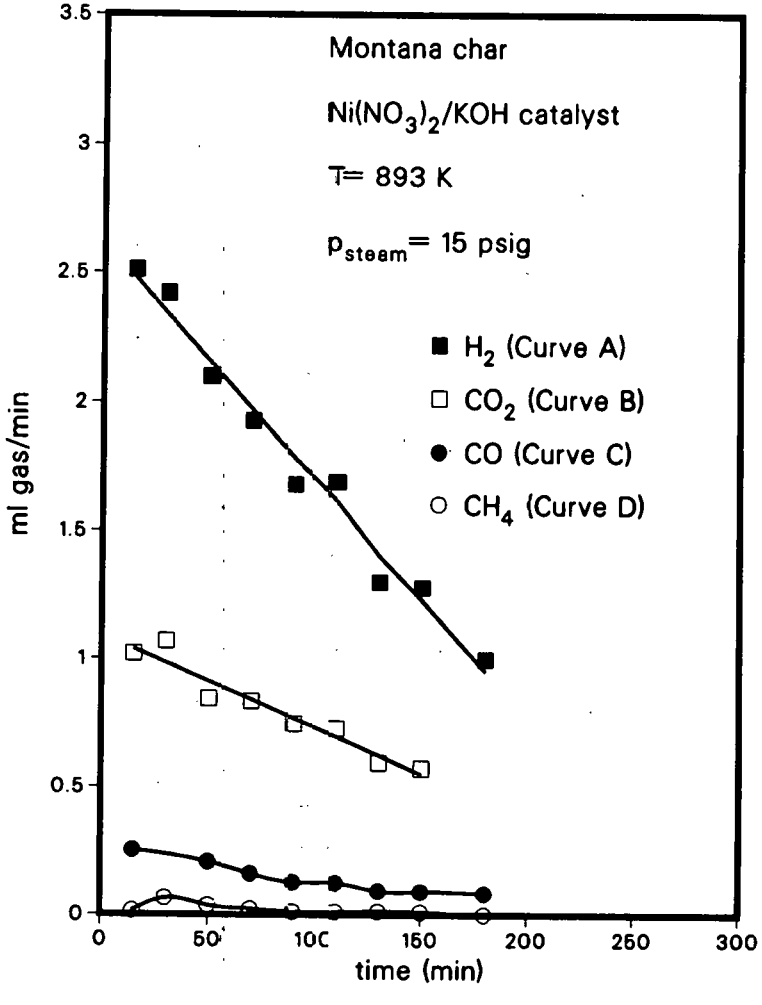

Figure 3.

respectively. By comparing the rates shown in these figures it is clear that the ratio of CO_2 to CO produced depends on the char (see Table II), and due to the stoichiometry of Equations 1 and 2:

$$C + 2H_2O = 2H_2 + CO_2 \quad (1)$$
$$C + H_2O = H_2 + CO \quad (2)$$

this ratio affects the total number of moles of H_2 that are produced per mol of carbon that is gasified. The steam gasification of North Dakota and Montana chars produces almost 2.0 moles of H_2 per mol of carbon consumed, since CO_2 is the main oxygen containing product, while the steam gasification of Illinois #6 char produces 1.6 moles of H_2 per mol of carbon consumed, because CO_2 and CO are produced in a ratio equal to 1.47.

The rate of H_2 production is also dependent on the carbon source. This is reflected in the total H_2 production obtained after 4 hours at 893 K (See Table 2). For North Dakota char gasification this volume (663 ml) is two times higher than that of Montana char (337 ml) and six times higher than the volume previously obtained for graphite (95 ml) [3], even though the product distribution for these three carbon sources is similar.

Table 2. Product Distribution Obtained with the Three Chars and Three Catalysts Studied.

CARBON SOURCE	CATALYST	P_{CO_2}/P_{CO}	H_2prod.[a]
Illinois #6		1.47	458
North Dakota		10.0	663
Montana	$KOH/Ni(NO_3)_2$	5.26	337
Graphite[b]		33.3	95
Montana[c]		.77	173
Illinois #6		0.29	322
North Dakota	KOH	9.09	170
Montana		5.26	449
Illinois #6		-	0
Montana		4.35	314
Montana[c]	$Ni(NO_3)_2$	1.11	55
North Dakota		8.33	511
North Dakota[c]		7.14	342

[a]ml of H_2 produced in 4.0 hours at 893 K.
[b]Taken from reference 3.
[c]Treated in aqua regia.

Fig. 1, 2 and 3 also show that the rate of formation of all the gases decreases with time. This can be prevented by treating the carbon substrate in aqua regia overnight previous to the catalyst loading. This is shown in Fig. 4 for the case of Montana char. The $Ni(NO_3)_2$/KOH mixture maintains 75% of its initial activity after 600 min when the substrate is pretreated in aqua regia while its activity decreases by a factor of three after 200 min when the sample has not been treated. Also, beyond 200 min the rate of gasification of the treated sample becomes higher than that of the untreated one. These results suggest that the decrease in rate of char gasification is due to the deactiviation of the $Ni(NO_3)_2$/KOH catalyst by interaction with some char component that can be removed by the aqua regia treatment.

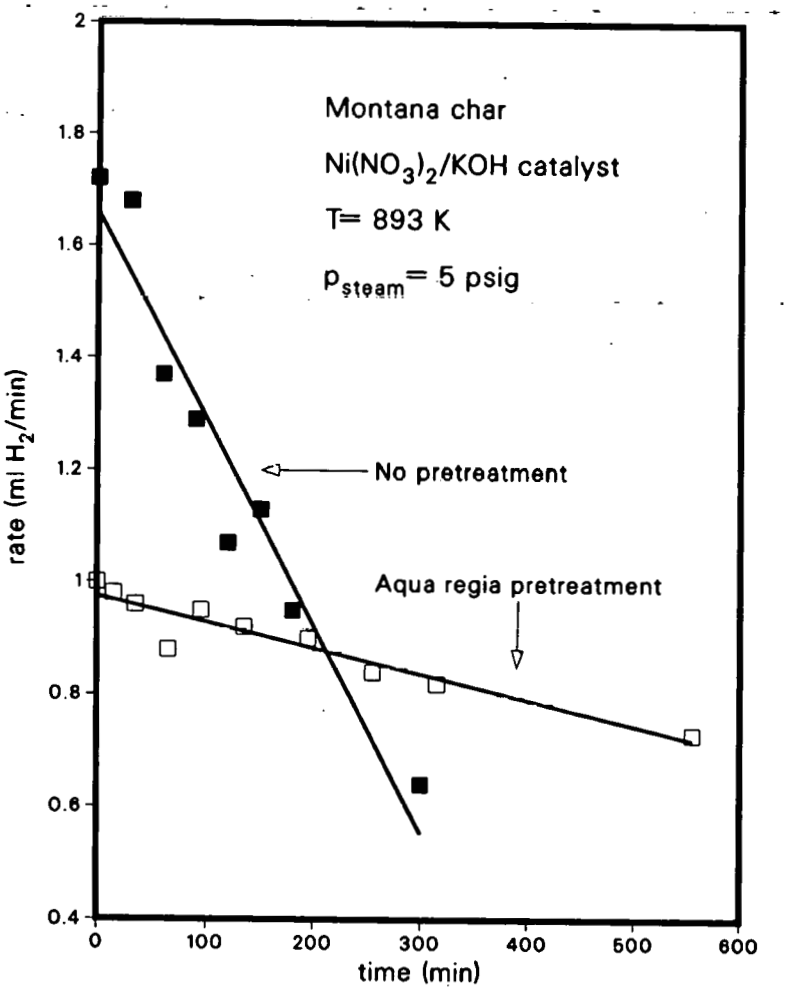

Figure 4.

The dependence of the rates of steam gasification upon temperature has been determined for the three chars. Since the initial rate of gas production decreases rapidly with time, the reaction was carried out isothermally at 893 K for four hours before the temperature was increased. After this period the variations in rate with time at 893 K are small enough to allow the determination of the activation energies. The measurements were carried out in a temperature range where the product distribution does not vary significantly (873 to 993 K) and in a total time period of one and a half hours to diminish the effect of deactivation.

The rates of gas production as a function of temperature for Illinois #6 char are shown in Fig. 5 in the form of a Arrhenius plot. The

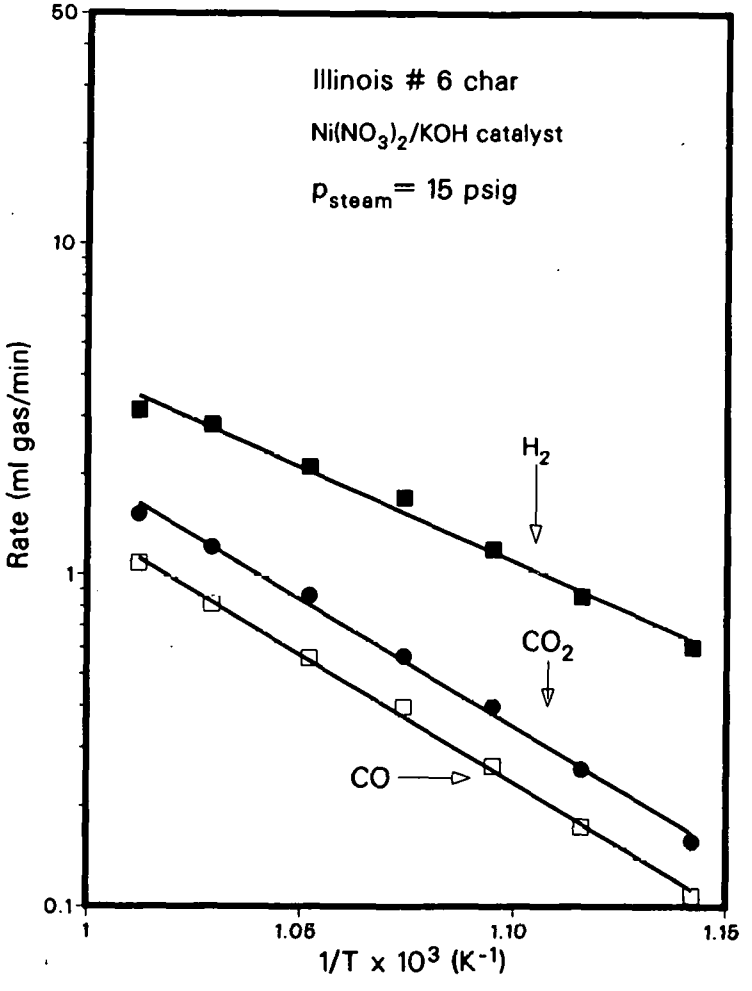

Figure 5.

activation energy for H_2 production is the same in all the cases (29 Kcal/mol), and the activation energies for formation of CO and CO_2 varies with the char. The gasification of the chars that produce much more CO_2 than CO, that is Montana and North Dakota, also show lower activation energies for CO_2 than for CO production. (28.4 vs. 43.0 Kcal/mol in the case of Montana, and 36.8 vs. 49.9 Kcal/mol in the case of North Dakota). Illinois #6 char, which produces a ratio of CO_2 to CO close to one, shows similar activation energies for CO_2 and CO production (36.0 and 35.4 Kcal/mol respectively). These results indicate that the product distribution is controlled by the activation energy for formation of the gases.

The steam gasification of Illinois #6, North Dakota and Montana chars catalyzed by KOH alone was studied isothermally at 893 K and as a function of temperature in order to compare the results with those obtained for the $Ni(NO_3)_2$/KOH mixture.

The ratio of CO_2 to CO in the case of Illinois #6 char is lower than the one obtained with the $Ni(NO_3)_2$/KOH catalyst, (p_{CO_2}/p_{CO} is equal to 0.29 in the case of KOH alone and 1.47 in the case of $Ni(NO_3)_2$/KOH) and therefore the moles of H_2 produced per mol of carbon consumed are lower in this case (1.30 mol H_2/mol carbon) than in the $Ni(NO_3)_2$/KOH case (1.56 mol H_2/mol carbon) (See Table II).

Results obtained for KOH gasification of North Dakota and of Montana char at 893° are identical. For these two chars the product distribution obtained when the reaction is catalyzed by KOH is very similar to the one obtained with the $Ni(NO_3)_2$/KOH catalyst (See Table II). The ratio of CO_2 to CO produced in the gasification of both chars is the same as for the $Ni(NO_3)_2$/KOH catalyzed reaction, but the catalytic activity of KOH alone for the steam gasification of these two chars is lower by two orders of magnitude than that of the $Ni(NO_3)_2$/KOH catalyst.

While $Ni(NO_3)_2$ alone is completely inactive for the steam gasification of Illinois #6 char, its catalytic properties for the steam gasification of North Dakota and Montana chars are similar to those of the $Ni(NO_3)_2$/KOH mixture. As in the case of $Ni(NO_3)_2$/KOH, the rate of H_2 production decreases as a function of time. A treatment of the char in aqua regia previous to the $Ni(NO_3)_2$ loading also eliminates the decrease in rate with time. In contrast with $Ni(NO_3)_2$/KOH, however, if the char is treated in aqua regia previous to the $Ni(NO_3)_2$ loading, the catalyst loses most of its activity, suggesting that the $Ni(NO_3)_2$ activity on the untreated sample was due to its interaction with some inorganic constituent in the char.

The activation energy for gasification of North Dakota char loaded with $Ni(NO_3)_2$ was determined for samples that either had or had not been pretreated in aqua regia. The values do not change after the aqua regia pre-treatment and they are similar to those obtained with the $Ni(NO_3)_2$/KOH catalyst. (33.6 Kcal/mol for H_2 production, 38.2 Kcal/mol for CO_2 production and 48.5 Kcal/mol for CO production). As in the case of $Ni(NO_3)_2$/KOH and KOH alone, the product distribution is controlled by the activation energy for formation of the products.

7. FUTURE WORK:

Future work will establish by XPS measurement the composition of various alkali-transition metal catalysts other than Ni/K and determine the cause of catalyst deactivation. A major future objective should be to explore the reasons for the very low CH_4 formation which is always below equilibrium and to find modes of producing CH_4 as a primary product at low temperatures.

8. REFERENCES:

J. Carrazza, W.T. Tysoe, H. Heinemann and G.A. Somorjai. 1985. J. Catal. 96:234-241

J. Carrazza, R. Pande, D.J. Sullivan, H. Heinemann and G.A. Somorjai. Kinetic Study for Catalytic Steam Gasification of Char. Submitted to Energy and Fuels.

J. Carrazza, J.J. Chludzinsky, H. Heinemann, G.A. Somorjai and R.T.K. Baker. CAEM Study of the Gasification of Graphite Catalysed by a Ni/K Mixture. Submitted to J. Catal.

PRODUCTION OF HYDROGEN FROM LOW-RANK COALS

1. CONTRACT NUMBER DE-FC21-86MC10637-T3

CONTRACTOR: University of North Dakota
Energy Research Center
Box 8213, University Station
Grand Forks, ND 58202
(701) 777-5163

CONTRACTOR PROJECT MANAGER: Rodney E. Sears

PRINCIPAL INVESTIGATORS: Rodney E. Sears
Ronald C. Timpe

METC PROJECT MANAGER: Leland E. Paulson

CONTRACT PERIOD OF PERFORMANCE: April 1, 1986 to April 1, 1987

2. SCHEDULE/MILESTONES:

1986-1987 Program Schedule

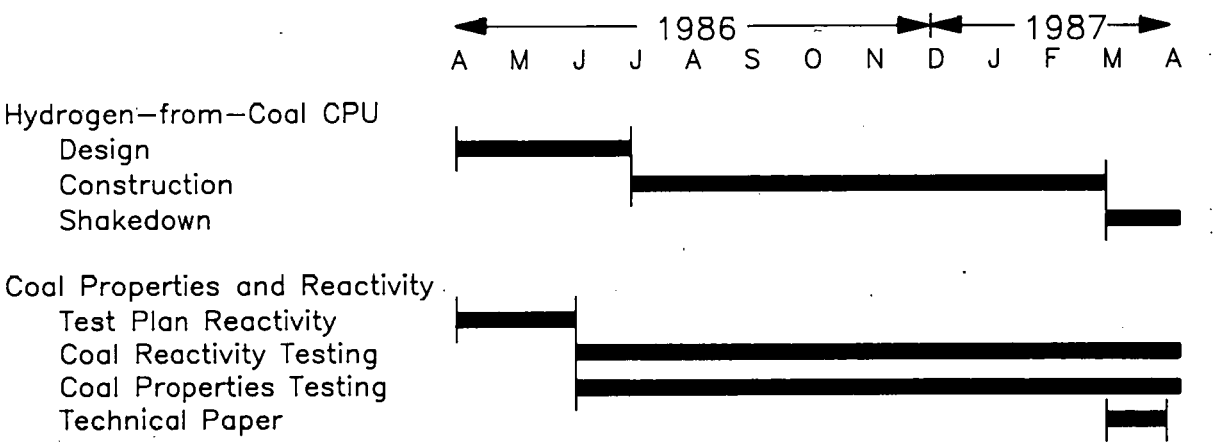

3. OBJECTIVES:

The objective of this research is to evaluate the technical feasibility of producing low-cost hydrogen by catalytic steam gasification of low-rank coals. This approach takes advantage of the high reactivity, volatile matter, moisture concentration, and inherent alkali content of low-rank coals. This effort will provide a proof-of-concept and the early stages of engineering development. In parallel with this process development and systems analysis work, an evaluation of the relationship between the fundamental properties of low-rank coals and their reactivity under hydrogen-producing conditions will be conducted.

4. BACKGROUND STATEMENT:

Over the next 45 years, the demand for hydrogen has been projected to increase by a factor of 19 to 27 (Pohani 1984). Advanced coal gasification technologies appear to be the most probable alternative for meeting the future demand for large quantities of hydrogen. Low-rank coals (lignites and subbituminous coals) are the preferred feedstock for such applications because of their low mining cost and higher reactivity relative to higher-rank coals.

The two most important considerations in the design of a process for producing hydrogen from coal are to maintain operating conditions that thermodynamically favor the production of hydrogen and carbon dioxide over carbon monoxide and methane, and to obtain reaction rates that result in sufficient gasifier throughput. Optimization of the conditions for maximum hydrogen content of the product gas requires steam gasification at relatively mild temperature and pressure. Temperatures in the range of 700° to 800°C at atmospheric pressure maximize hydrogen production. These mild conditions do not, however, promote high reaction rates. As a result, increasing coal reactivity is perhaps the most critical factor in the selection of a gasification process for producing hydrogen from coal.

The primary advantage of lignites and subbituminous coals is their greater reactivity relative to coals of higher rank. This increase in reactivity is caused by higher concentrations of active sites, higher porosity, and a more uniform dispersion of alkali impurities that act as inherent catalysts. In steam gasification tests conducted using bench-scale fixed-bed thermogravimetric analysis (TGA), a dry synthesis gas containing 63% hydrogen was produced from low-rank coal (Galegher 1986), and low-rank coal char reactivities were found to be nearly ten times higher than that of a bituminous coal char gasified at the same conditions (Wiltsee 1986).

A more complete evaluation of the use of low-rank coals in catalytic steam gasification to produce hydrogen is required. To date, much of this work has been performed at the laboratory scale, and has focused only on fundamental reactivity studies. These data must be verified on a larger continuous scale, and a more complete evaluation of the concept must be performed before the technical realities, and also the economic feasibility, of the process can be clearly stated. A fluid-bed system operated with catalyzed low-rank coal offers both excellent heat and mass transfer and processing flexibility; it is, therefore, attractive for process development.

5. PROJECT DESCRIPTION:

The research program will include the design, construction, and testing of a 6-inch diameter fluid-bed system and determination of the optimum operating conditions for producing low-cost hydrogen. Data collected from this process development work will be used to generate an economic assessment of the process. In addition, gas and wastewater treatment, end-use applications, and the integration of thermochemical cycles for

enhancement of hydrogen yield will be evaluated as part of a systems approach study to be performed in conjunction with the process economics study.

A companion TGA study will determine reactivities of a suite of selected low-rank coals computed on both a weight basis and an active site basis. Instrumental analyses to be performed on each coal char and ash that are derived from reactivity studies will include solid ^{13}C Nuclear Magnetic Resonance (NMR) spectroscopy, x-ray diffraction, x-ray fluorescence, and Electron Spectroscopy for Chemical Analysis (ESCA) and Scanning Electron Microscopy (SEM) surface analysis. Coal reactivity will be correlated with identified coal properties to help elucidate the mechanism for catalytic steam gasification to produce hydrogen.

6. RESULTS/ACCOMPLISHMENTS:

HYDROGEN-FROM-COAL CONTINUOUS PROCESS UNIT (CPU)

A simplified schematic diagram of the final design for the CPU is shown in Figure 1. Steam and a small amount of oxygen are heated to nominally 760°C with an electric superheater and fed into the bottom of the fluid-bed gasifier (FBG). Coal sized to 1/4" x 0 is stored after preparation in a coal hopper with a holding capacity of 450 lbs. The coal is fed to the FBG with a star feeder and screw conveyor mechanism, with the star feeder controlling the rate. The outer shell of the FBG is constructed of 304 stainless steel with a 20-inch outside diameter and a 3/8-inch wall thickness. The FBG is refractory lined with 4.5 inches of insulating refractory and 2 inches of high temperature refractory, making the inside diameter of the reactor nominally 6 inches. The FBG was designed and constructed in three sections, one 5-foot section and two 6-foot sections. The inside working height is 16 feet (4-foot expanded bed height and 12-foot freeboard). Fines are removed from the product gas exiting the FBG by a refractory lined cyclone. The product gas is quenched to remove condensables via a two-stage gas/liquid separator and a cryogenic trap. The gas is split into two streams before entering the coaxial first-stage, water-cooled condensers and the coaxial, second-stage, glycol-cooled condensers. The coaxial heat exchangers are easy to maintain and provide sufficient gas velocities to prevent hang-up of any condensables. After the cryogenic trap the product gas is metered and sampled prior to being vented. Feed ranges for the CPU, based on the hydrogen production equilibrium computer code developed at UNDERC (Wiltsee 1986) for a temperature range of 700° to 800°C, steam-to-carbon molar ratio range of 2 - 4, and an average bed superficial velocity of 3 ft/sec, are nominally 13 - 25 lb/hr coal, 24 - 40 lb/hr steam, and 5 - 10 lb/hr oxygen. Design work on the hydrogen-from-coal continuous process unit was completed in early July, and the design for the CPU was reviewed with the Department of Energy (DOE) Contracting Officer's Technical Representative (COTR) for approval to commence construction.

The CPU is housed in the gasification tower for UNDERC's 1-ton/hour slagging fixed-bed gasifier. Prior to assembly of the CPU, the shell for the FBG was assembled and hydrostatically pressure checked by an independent

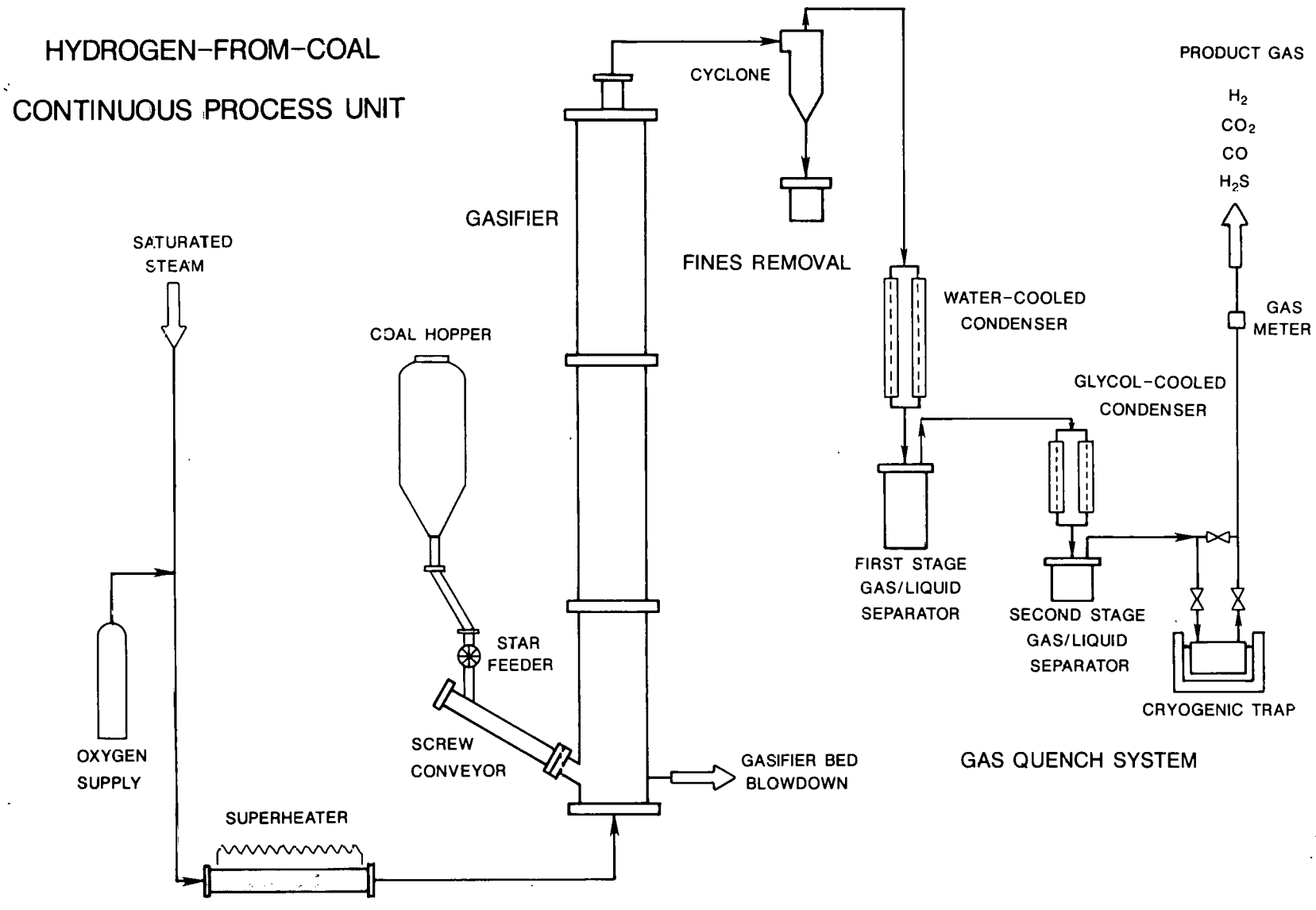

Figure 1. Schematic Diagram of the Hydrogen-from-Coal Continuous Process Unit

laboratory. The gasifier shell was ASME certified by Twin Cities Testing for a working pressure of 200 psi. Construction of the CPU was delayed due to conflicts in operations manpower scheduling and delays in equipment procurement. Access was limited during construction due to other contractual obligations by UNDERC. This moved the beginning of the shakedown period for the CPU to March 1st.

The initial start-up test with the CPU will be with a carbonaceous source that is low in, or free of, volatile matter, such as a commercial lignite char, to avoid problems with tars until operating procedures are more clearly defined. Shakedown of the CPU is expected to continue through April with the unit anticipated to be fully operational in May.

COAL PROPERTIES AND REACTIVITY ANALYSIS

The bench-scale study of the fundamental properties and reactivities of low-rank coal was initiated with the development of a test plan outlining test procedures and methods of analysis. The plan includes methods for studying active sites by gravimetric and spectroscopic means and a discussion of the instrumental tools to be used for analyzing the coal char and ash. Velva (North Dakota) and Martin Lake (Texas) lignites were selected for the study because of an extensive existing data base and because of their differences in geographic origin. In addition, Velva lignite exhibited excellent reactivity in the previous work and can serve as a "model" coal for hydrogen production from the char-steam reaction. The two catalysts chosen for the catalytic portion of the testing include potassium carbonate and trona. Potassium carbonate was selected based on its well documented catalytic effects, and trona, an inexpensive naturally occurring mineral, was selected for its good catalytic performance in previous testing and its potential as a disposable catalyst.

A statistically designed set of bench-scale experiments on the reaction between uncatalyzed and catalyzed Velva and Martin Lake lignite-chars and steam were completed for the temperature range of 650° to 750°C and was studied with two different TGA systems. The kinetic study of weight change of char with time for the char-steam reaction was carried out on a DuPont 951 Thermogravimetric Analyzer interfaced with a DuPont 1090 Thermal Analyzer. Samples of approximately 20 mg of -100 x +140 mesh coal, uncatalyzed or catalyzed, were devolatilized under argon flowing at 160 cc/min and the resulting char reacted with steam ($p(H_2O) = 0.1$). Reactivity parameters (k) for 50% carbon conversion (shown in Table 1) were calculated at each of three temperatures (T), and Arrhenius plots of ln k vs 1/T were constructed for calculating energy of activation (Ea) and frequency factor (A) as in previous work (Timpe 1985). The inherent mineral matter of the Velva lignite had the effect of increasing the reaction rate over that of the Martin Lake lignite. Addition of either potassium or sodium compounds also increased the rate of the char-steam reaction for both the Martin Lake and the Velva chars. Potassium carbonate and trona mixed with the lignite both gave positive catalysis of the char-steam reaction, as shown by the reactivity parameters listed in Table 1.

Table 1. Reactivity Parameters for Velva and Martin Lake Chars.

	Reactivity Parameters (k) (g/hr)/g		
	Uncatalyzed	K_2CO_3 Catalyzed	Trona Catalyzed
Velva			
650°C	0.30	1.43	1.28
700°C	1.40	3.50	3.23
750°C	2.10	5.81	7.04
Activation Energy (kcal/mole)	36.6	32.1	26.4
Martin Lake			
650°C	0.36	0.45	1.05
700°C	0.74	1.41	2.37
750°C	1.70	3.55	3.50
Activation Energy (kcal/mole)	29.2	22.7	26.7

Selected reactivity experiments were duplicated on a large TGA (constructed at UNDERC using a Cahn 1000 electrobalance and a 1200°C vertical tube furnace) for reacting samples >1 g. Total gas samples (product gas plus carrier gas) were collected over the duration of the run and were analyzed by gas chromatography (GC). The normalized product gas compositions on the total gas sample collected during the hydrogen production reaction carried out on the large laboratory TGA for uncatalyzed and trona catalyzed Velva char at 700° and 750°C are shown in Table 2. The normalized hydrogen values approximated those predicted by the engineering thermodynamic model with hydrogen concentrations in the product gas generally over 55%. The values obtained from the samples generated on the large TGA are somewhat more realistic compared to the total gas samples collected from the duPont TGA, since the dilution effect of the carrier gas, and thus the uncertainty in the GC analysis, was reduced.

Catalyzed and uncatalyzed chars subjected to spectroscopic techniques were prepared as in the char-steam reactivity experiments, but were cooled to room temperature under argon. In selected experiments the char was removed from the TGA and stored under argon to prevent exposure to air. These samples were analyzed by ESCA and solid ^{13}C Cross Polarization/Magic Angle Spinning (CP/MAS) NMR spectrometry. Chars were also examined by analytical Scanning Electron Microscopy (SEM), both pictorially and for surface elemental composition. The field was scanned and representative particles were photographed and mapped to determine elemental distribution. All char samples were analyzed for active sites by gravimetric measurement of CO_2 adsorption in a manner similar to that described by Ratcliffe and Vaughn (Ratcliffe 1985).

Table 2. Product Gas from Velva Lignite Char-Steam Reaction Carried Out in the Large TGA (mole %).*

Sample**	Temp., °C	H_2	CO_2	CO	CH_4
With 10 wt% Trona	750	56.23	30.13	13.64	ND
With 10 wt% Trona	700	51.73	43.51	4.55	ND
Uncatalyzed	750	57.70	35.30	6.30	0.72
Uncatalyzed	700	56.20	40.00	2.60	0.90

* Data normalized to exclude carrier gas and air.
** Sample sizes were between 1.0 and 1.4 grams of -100 x +140 mesh "as-received" coal-catalyst.
ND = Absent or below detection limit.

In preliminary ESCA analyses of Velva chars, it was demonstrated that C-O, COOH, and C-N are readily detectable, although the results were not quantitative. Since these sites are thought to be key active sites during the char-steam reaction, their quantitation will give an indication of the relative reactivities of prepared chars. Table 3 shows the ESCA surface carbon/oxygen ratio on the Velva chars prepared at various temperatures. Char prepared at 750°C and exposed to air had a significantly lower surface C/O ratio than that prepared at the same temperature and protected from exposure to air. The latter sample was analyzed at the natural surface, and then at surfaces produced by removal of outer layers of char using ion "sputtering" for the time indicated on Table 3. The low C/O ratio of the exposed sample is due to the adsorption of oxygen on exposure to air due to the highly activated carbon that results during char formation. The chars formed at the other temperatures given on Table 3 exhibited little increase in C/O ratio with temperature. These results indicate that erroneous surface data can be minimized by maintaining an inert atmosphere over the char samples and a more accurate analysis can be carried out.

Table 3. Preliminary ESCA Results---Velva Lignite Char (element %).

Char Temp., °C	Sputter Time, minutes	Element, %			
		C	O	N	C/O
750*	0	74.4	21.0	--	4.73
750	0	82.1	14.3	--	7.69
	10	82.9	13.0	--	8.52
	70	84.3	11.6	--	9.62
700	70	81.9	10.9	0.9	10.03
650	70	80.1	12.3	0.8	8.66
600	70	80.3	12.6	1.0	8.47

*Exposed to air

SEM photographs (Figure 2) show the surface effect upon charring of adding catalyst to the Velva and Martin Lake coals. The ragged, irregular surface and lack of apparent pores in the uncatalyzed char was replaced by the rounded, highly porous surface on the alkali catalyzed char. The degree to which the surface changed with the addition of catalyst differed between the Velva and the Martin Lake chars. The Velva surface contained uniform, evenly spaced nodules of approximately 0.05 um x 0.10 um in size, while those of the Martin Lake char are neither uniform in size nor evenly spaced over the surface. The reactivities differed similarly, with the Velva having the higher reactivity. This suggests that the increase in reactivity of the catalyzed char, which may be due to mechanistic change in the chemical reaction brought about by the alkali, must also be due at least in part to the physical effect of producing a large increase in surface area. The result of this increase in surface area is an increase in available active sites, as shown in Figure 3 for Velva char.

Mapping the surface for inorganic element distribution showed that the potassium was distributed uniformly over the surface of the Velva particles but not over that of the Martin Lake particles. The uniform distribution of the potassium catalyst on the surface of the Velva char implies a surface wetting by a fluid consisting of, or containing, the catalyst. The trona, however, does not exhibit this mode of distribution. Instead the map showed the sodium surface deposits as being associated with those of silicon and aluminum. The irregularly placed surface nodules of non-uniform size were located near the sodium deposits.

7. EVALUATION OF POTENTIAL FUTURE PLANS:

Shakedown of the CPU will be completed in May, at which time a parametric test program with the CPU will begin. The CPU test program will focus on defining and optimizing the steam gasification process for low-cost hydrogen production. This will involve investigating operability parameters in addition to coal/catalyst system testing.

The reactivity and coal properties analysis portion of the project will continue through next year. The characterization of physical and chemical properties of the coal will continue to correlate the various analyses to one another. Also the determination of the reactivities and active site quantitation will be correlated with identified coal properties. Correlations between coal properties and steam gasification kinetics will be developed and aid the process of selecting coals that are well suited for use in hydrogen producing gasification systems.

a) Velva char - Mag. 6000X

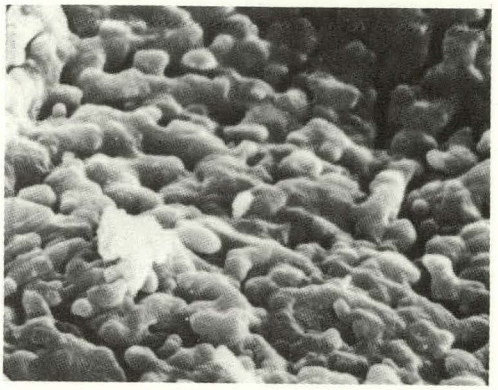

b) Velva/K_2CO_3 Char - Mag. 6000X

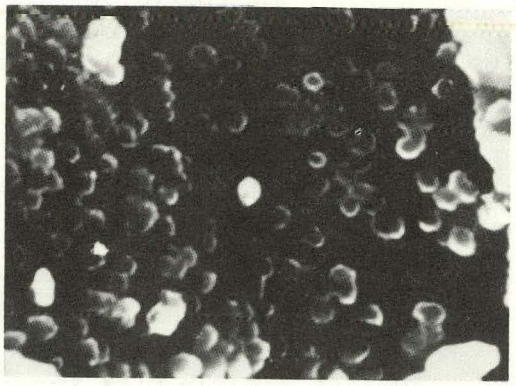

c) Velva/Na_2CO_3 - Mag. 6000X

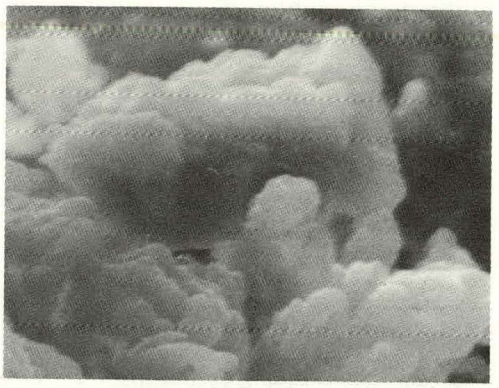

d) Velva/Trona - Mag. 6000X

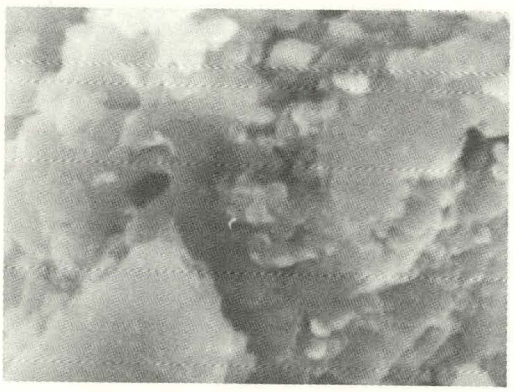

e) Martin Lake Char - Mag. 6000X

f) Martin Lake/K_2CO_3 - Mag. 6000X

Figure 2. SEM Photographs of Coal Chars Prepared at 750°C with and without Alkali Addition.

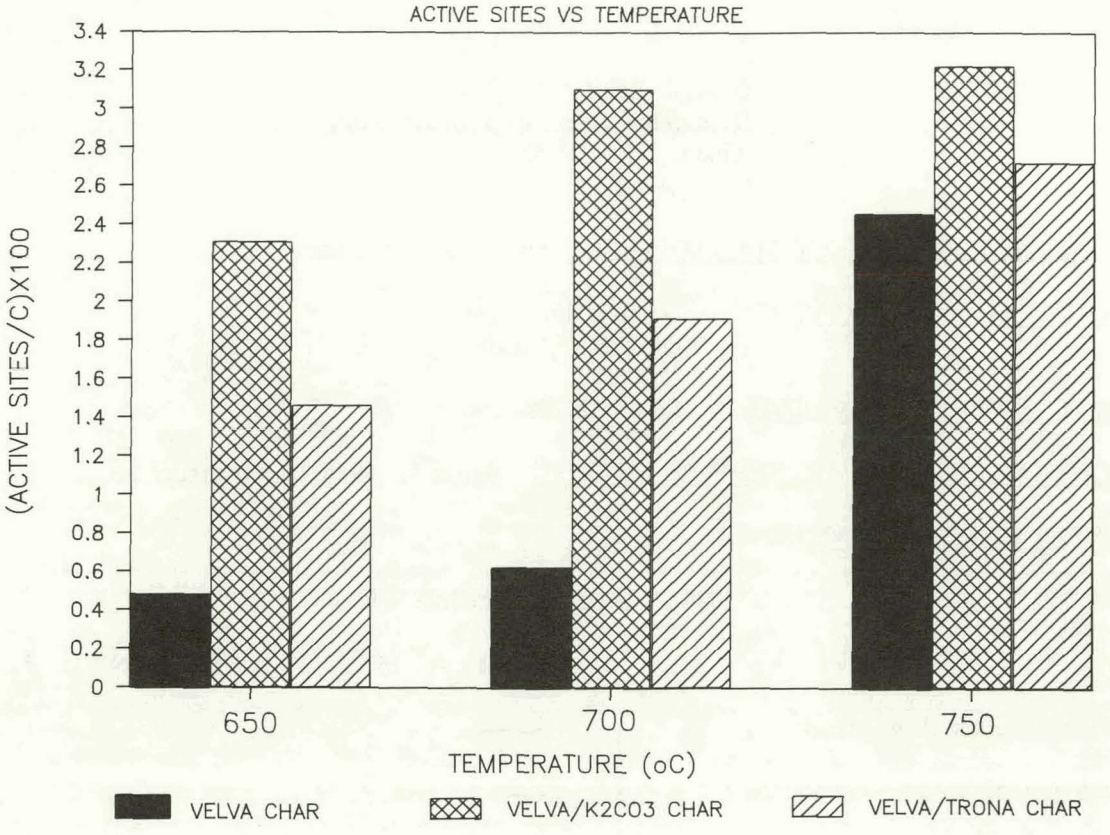

Figure 3. Number of Active Sites per Carbon Atom in Velva Lignite Char with and without Catalyst

8. REFERENCES:

Galegher, S.J., R.C. Timpe, W.G. Willson and S.A. Farnum. Kinetics of Catalyzed Steam Gasification of Low-Rank Coals To Produce Hydrogen. Final Report, June 1986, DOE/FE/60181-2034.

Pohani, B.P., J. Japan. Petrol. Inst., 27, 1, (1984).

Ratcliffe, C.T., Vaughn, S.N., ACS Div. Fuel Preprints, 30, No. 1, 304, (1985).

Timpe, R.C., S.A. Farnum, S.J. Galegher, J.G. Hendrikson, M.M. Fegley, ACS Div. Fuel Preprints, 30, No. 4, 481, (1985).

Wiltsee, George A. Low-rank Coal Research, University of North Dakota Energy Research Center, Quarterly Technical Progress Report, January-March 1986, DOE/UNDERC/QTR-86/1.

BIOLOGICAL DEGRADATION OF LOW-RANK COAL

1. CONTRACT NUMBER: DE-AC18-85FC10625

CONTRACTOR: Georgia Institute of Technology
Research Center for Biotechnology
Atlanta, GA 30332
(404) 894-3700

CONTRACTOR PROJECT MANAGER: Dr. William J. Jones

PRINCIPAL INVESTIGATORS: Dr. William J. Jones
Dr. E.S.K. Chian

METC PROJECT MANAGER: Leland E. Paulson

CONTRACT PERIOD OF PERFORMANCE: August 31, 1985 to November 30, 1987

2. SCHEDULE/MILESTONES:

1986-87 Program Schedule

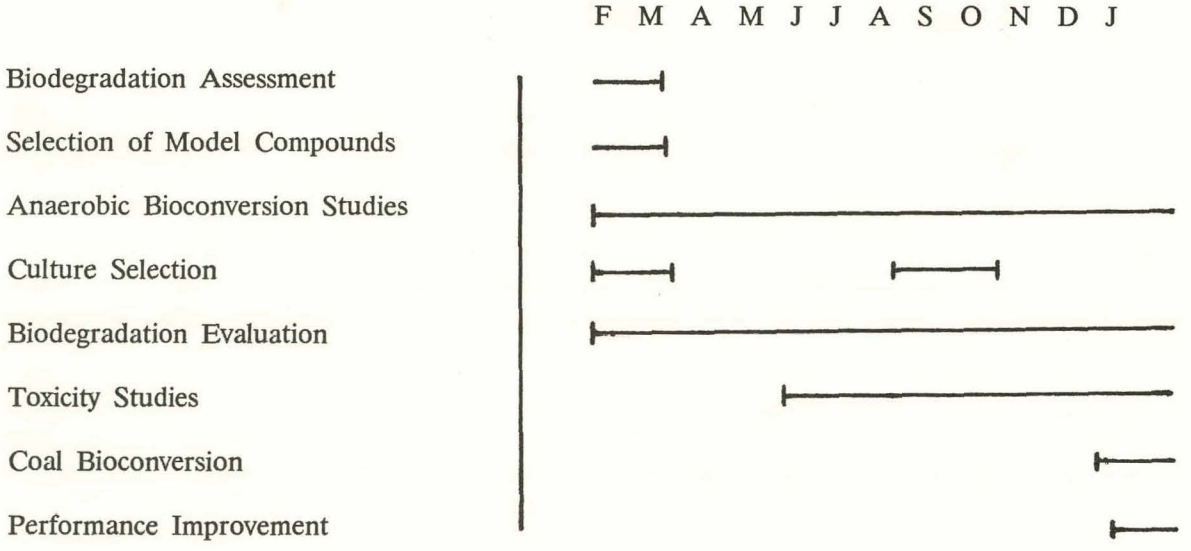

3. OBJECTIVES:

The primary goal of this contract is to assess the anaerobic bioconversion of low-rank coal to fuel products such as methane. Selected "model compounds," representative of constituents of low-rank coal, were tested for anaerobic bioconversion under methanogenic and nitrate-reducing conditions. In addition, studies were performed to evaluate the toxicity (inhibition) of model compounds on growth and activity of diverse microorganisms. The results of these studies will demonstrate the potential for bioconversion of low-rank coals and related aromatic organic compounds using anaerobic bacterial consortia.

4. BACKGROUND STATEMENT:

Microorganisms exhibit extreme diversity and versatility with respect to metabolic and physiological characteristics. The biodegradation/bioconversion/detoxification of a wide array of organic compounds occurs in both natural and man-made habitats colonized by aerobic, facultatively anaerobic, and strictly anaerobic microorganisms (Gibson 1984). The bioconversion of aromatic organic compounds has the most direct relevance to coal technology because of the abundance and variety of aromatic constituents which comprise coals (Larsen 1981, Given 1960). In addition, waste streams from coal conversion processes contain diverse aromatic compounds, the majority of which are phenols (Donaldson 1984). The use of microorganisms as biological catalysts is an alternative solution for the bioconversion of coal and aromatic organic compounds to fuel products.

The microbial conversion of simple and complex aromatic compounds under aerobic conditions has been well documented (Gibson 1984). In addition, investigators have demonstrated bioconversion of less complex aromatic compounds such as phenol under strict anaerobic conditions (Healy 1978). However, no reports are available concerning the anaerobic bioconversion of complex aromatic compounds such as substituted two and three fused-ring compounds of the naphthalene and phenanthrene group (Table 1). Partially oxidized compounds of these groups, such as 2-naphthol or 9-phenanthrol, may be representative constituents of low-rank coals, especially since low-rank coals are differentiated from bituminous coals by increased degree of oxygenation yet similar in aromatic content. Coals are likely derived from lignin-like compounds and it seems likely that coals still retain some structural similarity to lignin derivatives.

Table 1. Various classes of complex aromatic compounds and possible constituents of low-rank coals.

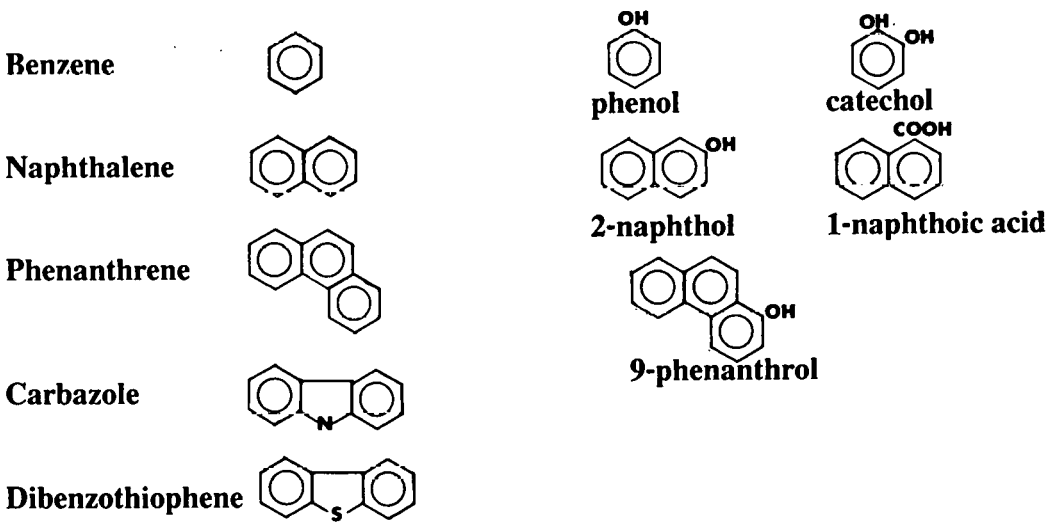

Research concerning the microbial conversion of coal has received little attention until recently. Several strains of fungi, including *Penicillium waksmanii* and *Aspergillus sp.*, and one bacterium, *Streptomyces setonii*, are capable of aerobic liquefaction of certain lignite coals (Scott 1986, Ward 1985, Cohen 1982; Table 2).

Table 2. Examples of microorganisms that are capable of coal liquefaction.

Microorganism	Source
Penicillium waksmanii	Mississippi lignite (B. Ward)
Candida sp. ML13	Mississippi lignite (B. Ward)
Aspergillus sp.	lignite (G. Strandberg)
Poria placenta	ATCC
Polyporous versicolor	ATCC (Cohen and Gabrielle)
Streptomyces setonii	ATCC (G. Strandberg)

These results are exciting since the generally accepted view is that coal and coal-related aromatic compounds are essentially biologically recalcitrant molecules. The potential use of microorganisms for coal beneficiation via production of H_2 and CH_4, as well a means of detoxifying coal processing wastes, is somewhat promising. Other than the above studies, however, no investigations have been reported concerning coal bioconversion under anaerobic conditions. Bioconversion of various organic compounds coupled to methane production is well-documented and may provide an alternative means for coal beneficiation. A primary goal of this research is to assess the potential for anaerobic bioconversion of coal and coal-related organic compounds.

5. PROJECT DESCRIPTION:

As stated previously, the primary goal of this research is to assess the potential for the anaerobic bioconversion of coal to fuel products. Initial experiments were conducted to assess the potential for anaerobic bioconversion of selected model compounds, including phenol, 2-naphthol, and 9-phenanthrol; these compounds were selected as representative constituents of low-rank coals based on available literature of low-rank coal chemistry (Larsen 1981, Benjamin 1978, Given 1960). Experiments were designed to enhance anaerobic bioconversion of the selected 'recalcitrant' substrates via coupling to CH_4 production (use of methanogenic consortia) or via nitrate reduction. Coupling bioconversion to CH_4 production has been demonstrated for a variety of organic substrates and is advantageous because of production of a desirable (energetic) end product (CH_4) and because of thermodynamic considerations. Importantly, the biologically mediated reduction of CO_2 by H_2 to CH_4 provides a mechanism for maintaining low partial pressures of H_2, resulting in favorable thermodynamic reaction kinetics for the H_2-producing species (Table 3).

Table 3. Benzoate fermentation coupled to a H_2-oxidizing methanogen results in more thermodynamically favorable reaction.

	ΔG^o (kJ)
$4\ C_7H_5O_2 + 24\ H_2O \rightarrow 12\ CH_3COO^- + 4\ HCO_3 + 12\ H_2 + 12\ H^+$	(+359)
coupled to H_2 oxidation via CO_2 reduction to CH_4:	
$4\ C_7H_5O_2 + 19\ H_2O \rightarrow 3\ CH_4 + 12\ CH_3COO^- + HCO_3 + 9H^+$	(-48.2)
$(12\ H_2 + 3\ HCO_3 + 3\ H^+ \rightarrow 3\ CH_4 + 9\ H_2O)$	(-406.8)

This concept of "interspecies H_2-transfer" (Iannotti 1973) necessitates that mixed bacterial cultures, or consortia, participate in bioconversion reactions. These syntrophic associations of bacteria have been demonstrated for the anaerobic bioconversion of benzoate (Ferry 1976) and other aromatic compounds to CH_4 and CO_2 and are likely to be important for anaerobic bioconversion of more complex aromatic compounds and possibly coal. Anaerobic bioconversion reactions coupled to nitrate reduction are advantageous simply because of favorable thermodynamic considerations.

All initial biodegradation experiments were conducted under strict anaerobic conditions in 30 ml serum vials (Balch 1979). Headspace gases for media preparation and culture conditions were scrubbed free of traces of O_2 by passing the gas stream through a heated and reduced column of copper turnings. Model compounds to be tested for bioconversion were added individually at final concentrations of 10, 100, and 250 μM. Experimental vials were then inoculated with bacterial consortia from several natural anaerobic habitats which supported methanogenesis. After inoculation, replicate experimental vials were incubated for 30 to 120 days at 25 to 37° C before experimental termination and subsequent analysis for substrate bioconversion.

The composition of the medium used in biodegradation experiments was formulated from current literature (Balch 1979) and was designed to support the growth of diverse anaerobic bacteria (including methanogens) which may be important constituents of the bacterial consortia responsible for bioconversion of complex organic compounds to CH_4. External sources of carbon were not added to media unless otherwise specified. In addition, experimental conditions for denitrifying activity were adjusted primarily via addition of potassium nitrate.

In addition to biodegradation experiments, toxicity studies were performed to assess the inhibitory nature of the model compounds used in biodegradation experiments. Various concentrations of the selected model compounds were added individually to pure cultures of several diverse procaryotic microorganisms, including a methanogen (*Methanospirillum hungatei*), a facultative anaerobic eubacterium (*Escherichia coli*), and a gram positive aerobic bacterium (*Staphylococcus aureus*). Growth of these bacterial cultures, amended with various concentrations of the test model compound, was followed with time by measuring culture optical density. In further experiments, CH_4 production from glucose was followed in the presence of varying concentrations of different model compounds to assess the toxicity on active methanogenic consortia. Results from these studies should be useful in assessing potential toxic effects of model compounds on natural inocula.

6. RESULTS/ACCOMPLISHMENTS:

ANALYTICAL METHODS FOR BIODEGRADATION ASSESSMENT.

Assessment of anaerobic biodegradation of model compounds was achieved by following substrate loss from biodegradation experiments with time. Methods for extraction, separation, and quantitation of amended model compounds from the complex biodegradation test system were optimized. Extraction of two model compounds, 2-naphthol, 9-phenanthrol, and the surrogate compound (fluorene) from a simulated biodegradation experiment are presented in Table 4. Prior to extraction, experimental samples were separated into a sediment and supernatant phase; subsequent analyses indicated the degree of adsorption of model compounds to the sediment fraction. Quantitation of model compounds was achieved by gas chromatography, on a 5% phenylmethyl silicone wide-bore (0.52 mm ID) capillary column, with a temperature program of 130°C (isothermal, 3 min) followed by a temperature increase of 15°C/min to 260°C.

Table 4. % Recovery of surrogate, 2-naphthol, and 9-phenanthrol from a simulated biodegradation experiment.

		%Recovery		
Sample		**Supernatant**	**Sediment**	**Total**
2-naphthol	**(10 μM)**	**80.0 ± 5.9**	**19.6 ± 2.2**	**99.6 ± 3.8**
	(100 μM)	**77.2 ± 2.8**	**25.5 ± 2.8**	**102.7 ± 4.7**
9-phenanthrol	**(10 μM)**	**N.D.**	**59.9 ± 8.3**	**59.9 ± 8.3**
	(100 μM)	**N.D.**	**56.9 ± 4.2**	**56.9 ± 4.2**
Surrogate (fluorene, 2 mg/L)		**78.7 ± 0.8**	**81.4 ± 1.4**	**---**

Results (Table 4) indicated that recovery of 2-naphthol was efficient (99.6 - 102.7%) at both 10 and 100 μM concentrations; the majority (77-80%) of the amended 2-naphthol was recovered from the aqueous phase. Total recovery of 9-phenanthrol was less efficient (56.9-59.9%) and levels of 9-phenanthrol were undetectable in the supernatant liquid phase, indicating that 9-phenanthrol was rapidly adsorbed to 'sediment' inocula. Since adsorption of model compounds may be significant in biodegradation experiments, extraction and analyses were performed on the entire contents of the biodegradation vials; no subsamples were withdrawn.

BIODEGRADATION EXPERIMENTS

Experiments to assess anaerobic biodegradation of the model compounds phenol, 2-naphthol, and 9-phenanthrol are presented in Tables 5-8. Sources of inocula included sludge from anaerobic digestors and anaerobic sediments from a freshwater eutrophic pond.

Results of anaerobic phenol bioconversion, using anaerobic methanogenic sewage sludge as an inocula, are presented in Table 5.

Table 5. Anaerobic bioconversion of phenol to CH_4 by anaerobic consortia.

Time (weeks)	phenol		CH_4
	mg/L	μmol	μmol
0	192	21.2	0
1.5	96	9.6	2.4
4.0	58	5.5	22.9
5.5	0	0	75.8

Experimental yield: 3.6 μmole CH_4/μmole phenol

Phenol degradation was complete after 5.5 weeks of incubation at 30°C and stoichiometric amounts of methane were produced. Additional experiments were performed to determine substrate tolerance for phenol bioconversion. Results presented in Figure 1 indicated that the phenol-degrading consortium was capable of bioconversion of 1400 mg/L phenol after a period of phenol acclimation. Consortia were initially unable to degrade phenol at concentrations greater than 800 mg/L.

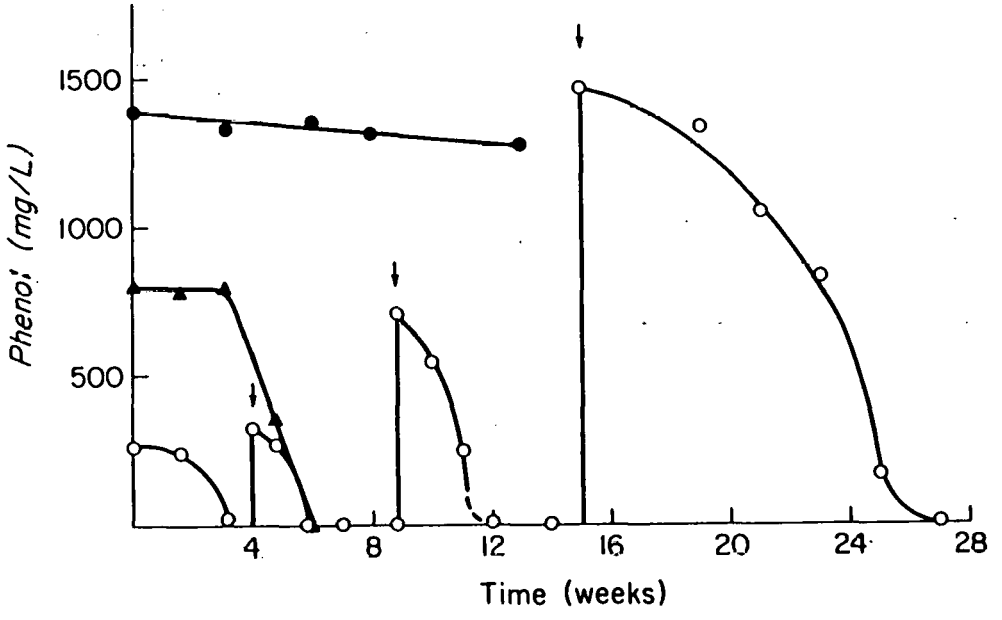

Figure 1. Acclimation of phenol-degrading consortium to high levels of phenol. Arrows indicate addition of phenol.

In contrast to phenol, anaerobic biodegradation of more complex aromatic compounds was less effective. Biodegradation experiments supplemented with 2-naphthol at concentrations of 10 and 100 μM exhibited little or no significant bioconversion after 60 days of incubation (Table 6) for either methanogenic or denitrifying conditions. Similar results were obtained for 1-naphthol bioconversion. In some experiments, glucose was added as a means of stimulating the biodegradation potential of consortia or by promoting co-metabolism; no significant effect on bioconversion was noted.

Table 6. Results of anaerobic bioconversion of 2-naphthol using anaerobic sludge as inoculum. Glucose was added to some experiments to promote co-metabolism.

Sample	Supernatant (μM)	Sediment (μM)	Total 2-naphthol (μM)
T_0	262.0	109.5	372.1
T_{30}	203.5	108.1	311.3
T_{60}	210.0	121.0	331.4
T_0 + glucose	225.0	140.8	365.8
T_{30} + glucose	184.4	156.2	340.6

Results of biodegradation experiments supplemented with 9-phenanthrol at an initial concentration of 100 μM and inoculated with anaerobic sediment and anaerobic sludge are presented in Tables 7 and 8. Samples inoculated with anaerobic sediment appeared to be partially effective in biodegradation of 9-phenanthrol after 60 days of incubation at 30°C (Table 7). The concentration of 9-phenanthrol was reduced by 48% compared to the initial concentration of 9-phenanthrol.

Table 7. Results of anaerobic bioconversion of 9-phenanthrol using inocula from anaerobic sediment.

Sample	% Surrogate Recovery	Corrected 9-phenanthrol (μM)
T_0	84.6	364 ± 18.2
T_{30}	91.0	352 ± 17.6
T_{60}	92.2	189 ± 15.4
T_0 + glucose	92.8	369 ± 18.5
T_{30} + glucose	81.2	278 ± 13.9

Additional experiments with anaerobic sludge as inocula exhibited interesting results (Table 8). In one test system, the concentration of 9-phenanthrol was dramatically lower (92%) after 150 days incubation compared to initial levels of 9-phenanthrol. However, control experiments inoculated with heat-sterilized anaerobic sludge and incubated for 150 days in the presence of 9-phenanthrol also exhibited a significant reduction (16-45%) in 9-phenanthrol concentration compared to initial levels. At this time no definitive conclusions may be made regarding 9-phenanthrol bioconversion.

Table 8. Results of anaerobic bioconversion of 9-phenanthrol using inocula from anaerobic sludge.

Sample		% Surrogate Recovery	Corrected 9-phenanthrol (μM)
T_0	A	60.1	86.2
	B	72.9	103.4
T_{30}	A	73.2	75.1
	B	74.8	92.4
T_{150}	A	88.9	7.7
	B	79.9	84.0
T_0	A sterile	72.6	84.9
	B sterile	76.1	101.2
T_{150}	A sterile	70.8	44.8
	B sterile	59.8	16.3

TOXICITY STUDIES

A series of experiments was performed to assess the potential toxic effects of model comopunds used in biodegradation studies on specific pure and mixed bacterial cultures. The bacterial cultures used for toxicity studies represented diverse groups of the microbial world; examples of important components of bacterial consortia responsible for the bioconversion of organic compounds to CH_4 were included. For example, one test organism, *Methanospirillum hungatei*, is a H_2-oxidizing methanogen routinely found as a predominant organism in the anaerobic digestion of complex organic compounds. Inhibitory effects of model compounds on growth and CH_4 production of *M. hungatei* should provide valuable information regarding toxicity to methanogenic consortia.

Initial toxicity experiments indicated that 9-phenanthrol was inhibitory to all organisms tested at a concentration of 100 μM. Variation in the level of toxicity was observed among the organisms tested. Growth of *M. hungatei* was completed inhibited by 50 μM 9-phenanthrol and 29% inhibited at 25 μM (Table 9), while growth of the gram negative eubacterium *E.*

coli was inhibited by only 21% at 100 μM 9-phenanthrol and growth of *S. aureus* was completely inhibited by 100 μM 9-phenanthrol. In most experiments, little or no inhibition of growth was observed for all organisms tested when exposed to 100 μM or 250 μM levels of 2-naphthol or 1-naphthoic acid.

Table 9. Inhibition of growth of *Methanospirillum hungatei* by various concentrations of 9-phenanthrol.

Methanospirillum hungatei

	Growth (A_{600nm})			
9-phenanthrol	T_0	T_{24}	T_{48}	T_{96} hours
0 (μM)	**0.02**	**0.16**	**0.37**	**0.55**
10	**0.03**	**0.10**	**0.27**	**0.53**
25	**0.03**	**0.08**	**0.19**	**0.39**
50	**0.04**	**0.05**	**0.05**	**0.05**
100	**0.05**	**0.05**	**0.04**	**0.04**

An evaluation of the toxicity of 9-phenanthrol was also made using a mixed bacterial consortia capable of CH_4 production from various soluble carbohydrates. This experiment more closely simulated natural conditions of biodegradation because several metabolic groups of bacteria were represented and because both organic and inorganic "contaminants" from inocula were present. It was previously demonstrated (Table 4) that 9-phenanthrol readily adsorbed to the sediment fraction of an aqueous-sediment slurry and this phenomenon must be considered for an accurate assessment of 9-phenanthrol toxicity to various microbial populations. Results of further experiments (Table 10) indicated that 9-phenanthrol, as well as 2-naphthol and 1-naphthoic acid, exhibited little or no detectable inhibition of methanogenesis from glucose at either 10 or 100 μM concentrations, indicating that the toxic effects of 9-phenanthrol were reduced in complex biodegradation experiments containing "adsorptive" non-biological constituents.

Table 10. CH_4 production from glucose by anaerobic consortia in the presence of 2-naphthol, 1-naphthoic acid, and 9-phenanthrol.

		μmoles CH_4			
Compound		T_0	T_{18}	T_{42}	T_{65} hours
2-naphthol	**(10 μM)**	**0.5**	**8.9**	**28.7**	**53.5**
	(100 μM)	**0.4**	**8.8**	**29.1**	**44.1**
1-naphthoic acid	**(10 μM)**	**0.5**	**8.5**	**29.9**	**56.7**
	(100 μM)	**0.5**	**9.4**	**28.9**	**43.9**
9-phenanthrol	**(10 μM)**	**0.5**	**9.6**	**28.8**	**46.6**
	(100 μM)	**0.5**	**8.0**	**30.1**	**52.7**
control		**0.7**	**8.1**	**28.1**	**57.6**

This evaluation was further tested by supplementing pure cultures of *M. hungatei* with sterilized "sediment" (10% v/v) and assessing the effect of added 9-phenanthrol (100 and 250 μM) on the rate of CH_4 production. As indicated in Table 11, addition of sterile "sediment" completely suppressed the previously observed toxicity of 100 μM 9-phenanthrol; however, complete inhibition of CH_4 production was observed at a higher concentration (250 μM) of 9-phenanthrol.

Table 11. Effect of addition of 9-phenanthrol plus "sterilized sediment" on CH_4 production by *M. hungatei*.

	μ moles CH_4		
9-phenanthrol plus "sediment"	**T_{10}**	**T_{48}**	**T_{120} hours**
0 (μM)	**0.6**	**192**	**471**
100	**0.6**	**32.0**	**475**
250	**0.6**	**1.2**	**1.4**

These results indicate that anaerobic consortia in nature may be more tolerant to the potential toxic effects of aromatic compounds because of adsorptive properties of organic and inorganic constituents of the natural environment.

7. FUTURE WORK:

- Continue assessment of anaerobic bioconversion of model compounds and extracts from low-rank coals to fuel products.
- Assess pretreatment of low-rank coals and coal extracts as a means of increasing biodegradability under anaerobic conditions.
- Determine toxicity of extracts of low-rank coals and pretreated coals on pure cultures of bacteria and anaerobic consortia used as inocula in biodegradation studies.

8. REFERENCES:

Balch, W.E., G.E. Fox, L.J. Magrum, C.R. Woese and R.S. Wolfe. 1979. *Microbiol. Rev.* 43:260.

Benjamin, B.M., V.F. Raaen, P.H. Maupin, L.L. Brown and C.J. Collins. *Fuel* 57:269.

Cohen, M.S. and P.G. Gabriele. 1982. *Appl. Environ. Microbiol.* 44:23.

Donaldson, T.L., G.W. Strandberg, J.D. Hewitt and G.S. Shields. 1984. *Environ. Prog.* 3:248.

Ferry, J.G. and R.S. Wolfe. 1976. *Arch. Microbiol.* 107:33.

Gibson, D.T. 1984. *Microbial Degradation of Organic Compounds.* Marcel Dekker, Inc. New York.

Given, P.H. 1960. *Fuel* 39:147.

Iannotti, E.L., D. Kafkewitz, M.J. Wolin, and M.P. Bryant. 1973. *J. Bacteriol.* 114:1231.

Larsen, J.W. 1981. *Chemistry and Physics of Coal Utilization - 1980.* Amer. Inst. of Physics Proceed., No. 70.

Scott, C.D., G.W. Strandberg, and S.N. Lewis. 1986. *Biotechnol. Progress* 2:131.

Ward, H.B. 1985. *Syst. Appl. Microbiol.* 6:236.

STUDY OF AMMONIA REMOVAL IN COAL GASIFICATION PROCESSES USING INTEGRATED SYSTEMS APPROACH

1. CONTRACT NUMBER: DE-AC21-86MC23275

CONTRACTOR: Acurex Corporation, Environmental Systems Division
485 Clyde Avenue
Mountain View, California 94039

CONTRACTOR PROGRAM MANAGER: Dr. Ramsay Chang

PRINCIPAL INVESTIGATORS: Dr. Ramsay Chang
Mr. Stefan Unnasch

METC PROJECT MANAGER: Mr. V. P. Kothari

PERIOD OF PERFORMANCE: September 26, 1986 to December 24, 1987

2. SCHEDULE/MILESTONES:

Program Schedule.

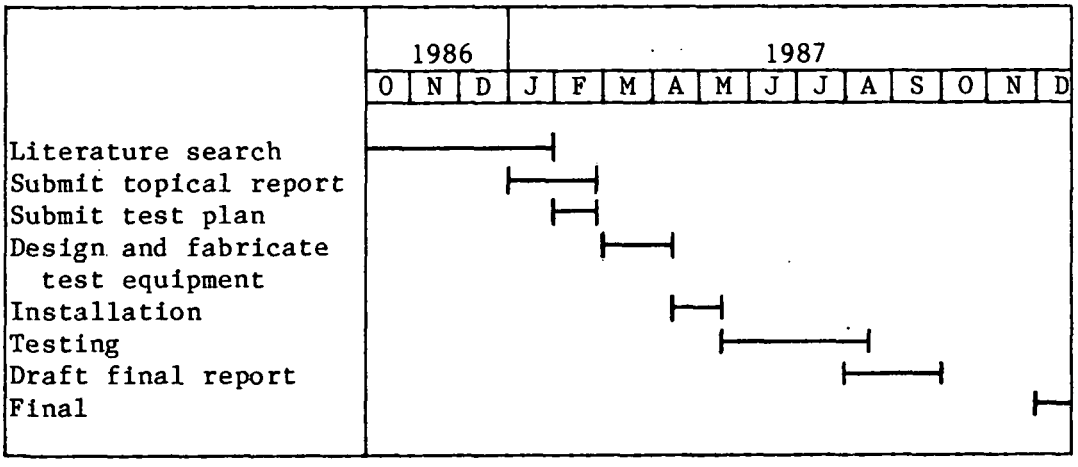

3. OBJECTIVE:

The purpose of this project is to investigate process concepts to eliminate ammonia in the gas stream from a coal gasifier at 1,000° to 1,800°F. It is the objective of this project to review all previous work and to recommend a preferred approach to achieving the goal of reducing the formation of NO_x from ammonia to environmentally acceptable levels. The recommended concept will be proven by laboratory-scale experimentation using simulate coal gases.

4. BACKGROUND:

Gasification offers a promising approach to the utilization of coal, our most abundant fossil energy resource, for a variety of end uses. The ability to utilize the hot gases from coal gasifiers directly in gas

turbines and fuel cells in combined cycle power generation systems can improve the overall efficiency and lower the overall costs of these systems. This will necessitate removal of contaminants such as particulates, sulfur, nitrogen compounds, and alkali vapor in the gas stream.

A major contaminant in the hot fuel gas stream is fuel-bound nitrogen, primarily ammonia, formed from complex nitrogenous compounds in the coal during gasification. Ammonia carried over in the gasifier stream will be partially converted to NO_x during combustion in downstream combustors. Emission standards for NO_x limit emissions to between 0.31 to 0.52 lb NO_x/million Btu for gas turbines and 0.5 lb NO_x/million Btu for steam units fired with coal-derived fuels. Based on an emissions standards of 0.5 lb NO_x/million Btu, the maximum permissible ammonia levels in the fuel gas (based on fuel gas heat value) compared to measured values are shown in Table 1. This table assumes that all the ammonia present is converted into NO_x (NO_x is defined as NO_2) and does not include the contribution from thermal NO_x. Table 1 shows that cleanup of the ammonia will be needed in all cases.

Table 1. Maximum Tolerable NH_3 Levels from Gasifiers.

	Fixed Bed	Fluidized Bed	Entrained Bed
Gross Heat Value (Btu/SCF)	130 (air blown)	94 (air blown)	245 (oxygen blown)
NH_3 Emissions (ppm)	5,000	900	2,000
NH_3 Emissions Limit (ppm)	510	370	960

5. PROJECT DESCRIPTION:

The program is divided into three tasks. In task 1, a literature search was conducted to review concepts for ammonia/nitrogen oxide control. A topical report was submitted to summarize the most promising concepts for ammonia/nitrogen oxide control and to recommend a promising approach for proof-of-concept testing. In task 2, a test plan was constructed to evaluate the most promising approach at the laboratory scale. In task 3, the selected approach will be tested under simulated hot coal gas conditions.

6. RESULTS AND ACCOMPLISHMENTS:

AMMONIA CONTROL APPROACHES

The minimum achievable ammonia level under any conditions is determined by equilibrium and is a function of temperature, pressure, and gas composition. Equilibrium fuel nitrogen values are low and often meet

environmental requirements (Robson 1980) without need for further cleanup. However, actual fuel nitrogen levels in fuel gas are often significantly higher than values predicted by equilibrium and are determined by kinetics and mass transfer. The most promising concepts are shown in Table 2. Theoretically, the fuel nitrogen in fuel gas will approach equilibrium if sufficient time is allowed. As the temperature of the fuel gas is increased, the required time decreases rapidly. The exit temperatures of most gasifier fuel gas are generally not high enough to drive ammonia levels to equilibrium within reasonable time periods. Indirect heating of the fuel gas to higher temperatures is inefficient and expensive.

Table 2. Concepts for Ammonia Removal.

• Residence time/temperature
• Catalytic dissociation of ammonia
• Staged combustion
• Staged catalytic combustion
• Adsorption
• Nitride formation
• NO_x reaction
• Catalytic filter

CATALYTIC DISSOCIATION OF AMMONIA

Catalysts have long been observed to promote the decomposition of ammonia to nitrogen and hydrogen (Winter 1931; Engelhard 1981). The DOE funded an extensive study of ammonia decomposition catalysts by Engelhard (1981). Very high ammonia reductions (80 to 100 percent) were obtained, especially with nickel-based catalysts on alumina supports. However, no catalysts were capable of sustained operation in the presence of 10 ppm H_2S and >5 percent water.

CATALYTIC FILTER

The existence of suitable ammonia reduction catalysts will provide an opportunity for the simultaneous removal of ammonia and particulates from the fuel gas. One of the promising approaches for particulate removal is the use of ceramic filters (Chang 1986; Ciliberti 1983). These ceramic filters are also suitable for use as catalyst supports since they are made of similar alumina-silica based material. The concept of a catalytic particulate filter is worthwhile investigating pending favorable results of catalyst development.

ADSORPTION

Adsorption of ammonia on Zeolites has been proposed by Battelle based on some of their earlier work on the catalytic cracking of tar (1986). The adsorption process generally works effectively at relatively low

temperatures and is actually reversed at higher temperatures. It is uncertain what degree of ammonia removal can be achieved.

NITRIDE FORMATION

The use of a metallic surface to react with ammonia to form nitrides is possible (Kushnir 1968). In the reactive environment of gasifier gas, the metal will be rapidly deactivated by reactions with gases such as hydrogen sulfide. Also, regeneration of the metal surface will be difficult.

NO_X ADDITION

NO_X added directly to the fuel gas may initiate rapid selective reactions with ammonia. However, data to date on the selective reactions of NO_X and ammonia occur in the presence of oxygen. Significant amounts of CO and H_2 in the fuel gas could reduce the NO_X to fuel nitrogen compounds such as HCN instead.

CATALYTIC COMBUSTION

The work performed to date shows that catalytic combustion provides a promising approach for NO_X control in the conversion of coal gas (Kesselring 1980; Matthews 1977). This can be achieved by staging the combustion process and selecting suitable catalysts to support the combustion. The best catalysts appear to be transition metal oxides, including nickel, cobalt, and chromium oxides. Platinum can be added to the base metal catalyst to improve lightoff and combustion characteristics for coal gas.

The major limitation of staged catalytic combustion is the uncertainty with catalyst durability. Thermal shock problems with the support and vaporization of the catalyst limit use temperatures to around 2,200°F. Even at 2,200°F, the long-term durability of the catalyst system is uncertain. In order to combust coal gas within a suitable temperature range for catalyst life, as well as at an optimal window for ammonia reduction, it may be necessary to extract heat from the primary stage or add an inert diluent such as nitrogen to lower the reaction temperature. This would complicate the overall system as well as lower overall system efficiency.

APPROACH RECOMMENDED FOR PROOF-OF-CONCEPT TESTING

The primary approach for ammonia control from gasifier fuel gas to be considered at Acurex is staged combustion which has the potential of controlling both fuel and thermal NO_X during the conversion of fuel containing ammonia (Tyson 1977; Westinghouse 1982). The ammonia is effectively reduced in a first stage burning fuel rich. Sufficient air is then added rapidly in a second stage to completely convert the fuel gas and to adjust the exhaust temperature to turbine inlet conditions. The amount of reduction is dependent on several parameters, including:

- Temperature of the first stage
- Gas composition and combustion stoichiometry
- Pressure
- Residence time
- Ammonia concentrations
- Mixing/transport processes

In general, these conditions can be controlled in the combustor to drive the ammonia to very low levels (near equilibrium), far below environmental requirements. There will also be minimum perturbation to the overall IGCC process because the combustor is part of the overall IGCC train and is needed to produce the hot pressurized gas for the gas turbines.

A significant amount of tests on staged combustion has been performed on different fuels, including gasifier gases. The data to date has shown that fuel nitrogen can be controlled effectively. The major difference in present proposed tests is the high fuel gas inlet temperatures. This high temperature is a result of using high-temperature gas cleanup techniques to increase overall system efficiency. The fuel gas exiting the high temperature zinc ferrite desulfurizer bed will be used directly in the gas turbine combustor. Nominal temperatures of 1,200°F are expected. This high fuel gas preheat will limit the reaction stoichiometries allowable in the first stage. It is uncertain how the changes in fuel gas temperature and reaction stoichiometry will affect first-stage ammonia removal efficiencies as well as second-stage thermal NO_x formation.

The second approach to be considered in the present program will be a combination of staged combustion and catalytic dissociation. The approach may be useful if staged combustion does not provide the ammonia removal desired. Essentially, the first-stage combustion provides just sufficient heat to the fuel gas before it is passed over an ammonia dissociation catalyst. The higher temperature can improve ammonia destruction efficiency of the catalyst. The temperature at the catalyst is not expected to exceed 1,800°F so that only a small fraction of the fuel needs to be converted in the first stage. The rest is converted in the second stage after all the ammonia has been essentially removed. This concept is similar to staged catalytic combustion. Since only a small fuel fraction was utilized in the first stage, there is the possibility that there is sufficient energy content in the fuel gas after the first stage that it can be utilized as a low-Btu, ammonia-free gas directly in a fuel cell or gas turbine.

The two approaches will be evaluated in a bench-scale combustor/reactor system to be constructed at Acurex. Two gasifier fuel gas compositions are selected for testing: the GE air-blown, fixed-bed gasifier and the Texaco oxygen-blown, entrained-flow gasifier. These two gas compositions cover the range of gas compositions of most gasifier types and has high ammonia levels.

TEST PLAN

In order to assess the effect of different operating parameters on the staged combustion control of ammonia, a test matrix was set up to systematically evaluate all the major parameters of interest within the limitations of the test facility available. The range of test parameters expected is given in Table 3.

Table 3. Range of Test Parameters for Staged Combustions

Gasifier Type	GE fixed bed (air blown) and Texaco entrained bed (oxygen blown)
Pressure	15 to 75 psia
Fuel Gas Temperature	800 to 1,600°F (1,200°F nominal)
Air Preheat Temperature	800°F
Ammonia Level	500 to 10,000 ppm (5,000 pm nominal)
First-Stage Stoichiometry	30- to 90-percent theoretical air
First-Stage Residence Time	20 to 200 msec
Burner Firing Rate	50,000 Btu/hr nominal

The existing air compressor is limited to pressures of about 100 psia so that a maximum test pressure of 75 psia will be used. The nominal fuel gas temperature will be 1,200°F, corresponding to the outlet temperature of the zinc ferrite desulfurizer bed. Both a higher and a lower fuel preheat temperature will be examined to determine the sensitivity of ammonia conversion to the preheat. The air preheat will be kept at 800°F corresponding to gas turbine compressor outlet temperatures.

Ammonia levels will be varied between 500 and 10,000 ppm to cover the range of ammonia concentrations expected with different gasifier and coal types. Low hydrogen sulfide levels will be used because the combustor is located after the desulfurizer.

The first-stage stoichiometry will be varied within the limitations of the combustor lining and combustion stability. The amount of second-stage air addition will be determined by the operating temperature required for the gas turbine (around 2,000°F). The first-stage stoichiometry can be varied by adjusting the fuel and air flowrates to maintain the constant residence time in the first-stage. This first-stage temperature will depend on reaction stoichiometry, and fuel and air preheat temperatures.

The residence time of combustion/reaction in the first stage will be controlled by the location of the secondary quench air point. There will be several locations for quench air injection. The requirement of the secondary quench air injection is to prevent the fuel/gas temperature from reaching excessive temperatures that will favor thermal NO_x and at the same time prevent over quenching of the gas reactions.

The use of partial combustion to elevate the temperature of the fuel gas before reaction with an ammonia reduction catalyst represents the backup approach to staged combustion. The range of test parameters to be evaluated is similar to that in Table 3, although first-stage stoichiometry is expected to be fairly low. The fuel gas is expected to be elevated to 1,800°F before reaction on the catalyst. Since this represents only a small change in temperature, the combustion in the first stage may not be stable because very fuel-rich conditions are needed. It may be necessary to stage the fuel gas in the first stage. Part of the fuel gas will be combusted under optimal stoichiometries before the remaining fuel is added. Overall stoichiometry in the first stage is expected to be below 50-percent theoretical air.

Residence time in the first stage is not a significant factor due to the low temperatures expected. The secondary air addition may be more difficult because of the low temperature exiting the first stage. It is uncertain whether proper quench conditions can be maintained during second-stage air injection.

EXPERIMENTAL SYSTEMS

The existing high-pressure, high-temperature reactor test passage at Acurex is modified to accommodate the requirements of the present project. The key components are shown schematically in Figure 1.

Combustion air is heated by in-line electrical heaters. Fuel gas is simulated by blending hydrogen, carbon monoxide, carbon dioxide, methane, and nitrogen, and is heated by a series of external electric heaters. Steam, ammonia, and hydrogen sulfide are added individually to the fuel gas just before entry into the combustor.

A portion of the reacted gas mixture will be extracted and sampled. The gas stream will be passed through an impinger train and the resulting solutions analyzed for ammonia using a specific ion electrode.

From the impinger train, the gas stream will pass through a dryer to remove water and lower the dewpoint. From the dryer, the sample stream will pass through a filter and a secondary dryer to the continuous monitors for measurement of NO_x, CO, CO_2, and O_2 concentrations.

A schematic of the staged combustor/reactor system is shown in Figure 2. A silicon carbide bluff body is used to promote flame stability. Preheated air will enter the burner via an annular space surrounding the fuel tube. Natural gas is used to preheat the combustor before switching to simulated fuel gas.

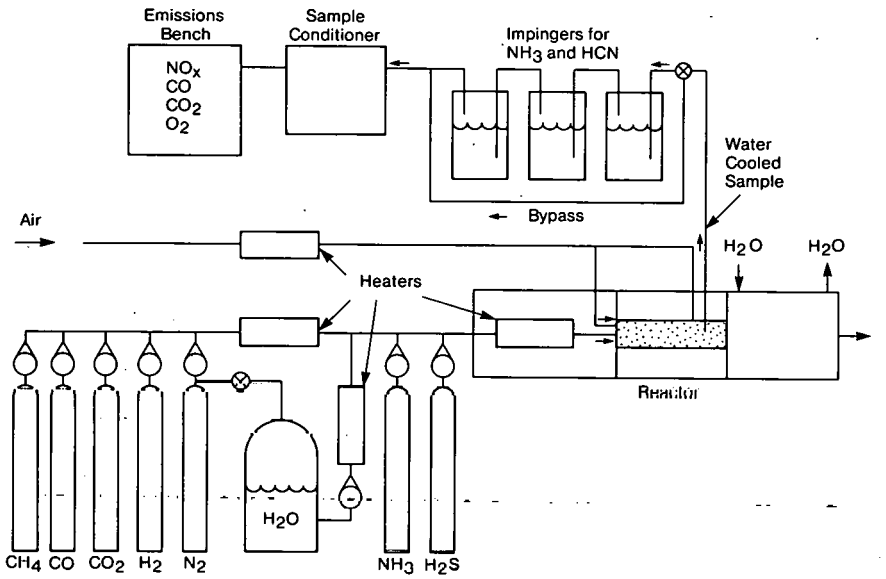

Figure 1. Reactor Piping and Instrumentation

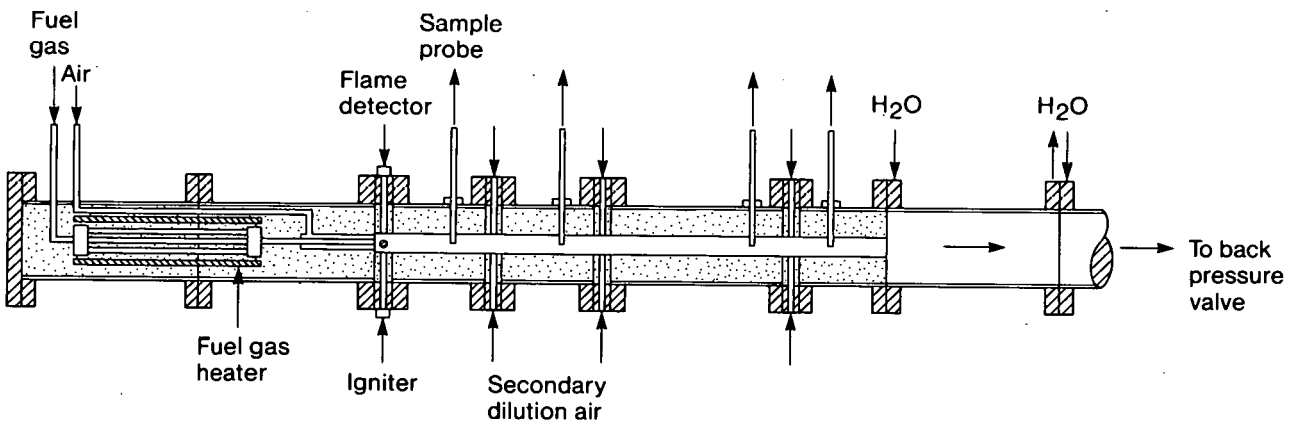

Figure 2. Schematic of Staged Combustor

The reactor/combustor system consists of a series of pressure shells nominally 8 in. in diameter and rated for 300 psi. The shells are also equipped with water-cooled walls.

The shells are lined with approximately 3 in. of ceramic refractory blanket. The combustor chamber is formed from a 2-in.-diameter, rigid ceramic liner machined to allow thermocouple insertion, secondary air injection, and gas sampling probes.

A variety of ports are available for secondary air injection and gas sampling probes. The selection of ports for secondary air injection will depend on the residence time being investigated. The gas sampling probe will be a sufficient distance downstream from the secondary air injection port to allow mixing and reaction.

7. FUTURE WORK:

Construction of the staged combustor is in progress. Testing is expected to start in early June following shakedown of the test unit.

1. REFERENCES

Battelle Northwest Laboratory. 1986. Catalytic tar conversion in coal gasification systems. DOE/METC-86/6042.

Chang, R., et al. 1986. Performance evaluation of a fabric bag filter on a bench-scale gasifier. Acurex Report, Appendix A-3, DOE Contract DE-AC21-84MC21337.

Ciliberti, D.F., et al. 1983. Hot gas cleanup using ceramic cross flow membrane filters. DOE/ET/1591-1565.

Engelhard Corp. 1981. Development and testing of ammonia decomposition catalysts. Unpublished report done under DOE Contract No. DE-AC21-81MC16332.

Kesselring, J.P., et al. 1980. Catalytic combustion component and system prototype development. Acurex Report, EPA Contract No. 68-02-3122.

Kushnir, N.A., Lunez V.M., Romanov, A.A., Sablev, L.P., and Sereda, N.I. 1968. Reaction of ammonia, hydrogen and nitrogen with titanium. Kharkov, USSR: Fiz,-Tekh. Institute.

Matthews, R.D., and Sawyer, R.F. 1977. Fuel nitrogen conversion and catalytic conversion. Paper No. 77-40. Fall Meeting of the Western States Section/Combustion Institute.

Robson, F.L., and Blecher W.A. 1980. Assessment of fuel gas cleanup systems. DOE/MC/12050-149.

Tyson, T.J., et. al. 1977. Low NO_x combustion concepts for advanced power generation systems firing low-Btu gas. EPA-600/2-77-235.

Westinghouse Corp. 1982. Low NO_x heavy fuel combustor concept program phase 1A -- combustion technology generation coal gas fuels. Final Report, DOE/NASA/0146-2.

Winter, E. 1931. The catalytic decomposition of ammonia over iron. Journal of Physics and Chemistry 13.

STUDY OF AMMONIA REMOVAL IN COAL GASIFICATION PROCESSES

1. CONTRACT NUMBER: DE-AC21-86MC 23087

CONTRACTOR:
SRI International
333, Ravenswood avenue
Menlo Park, CA 94025
(415) 859-2627

PROGRAM MANAGER: Gopala N. Krishnan

PRINCIPAL INVESTIGATORS:
Gopala N. Krishnan
Bernard J. Wood
Jon G. McCarty

METC PROJECT MANAGER: Vijendra P. Kothari

PERIOD OF PERFORMANCE: September 29, 1986 to December 28,1987

2. SCHEDULE:

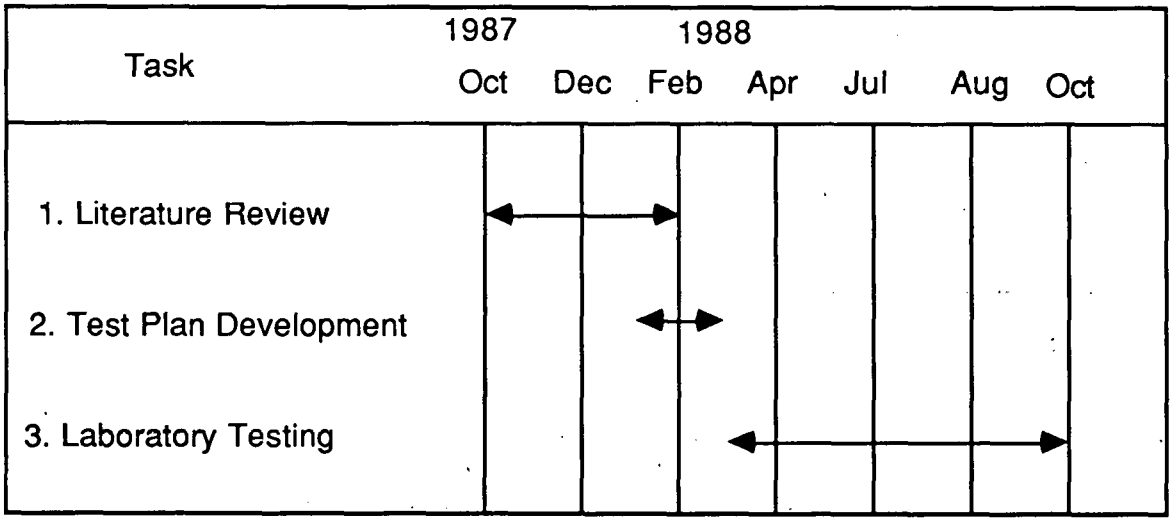

3. OBJECTIVES:

The objective of this program is to investigate process concepts to eliminate 90% of fuel-bound nitrogen, primarily ammonia, in a temperature range of 540° to 870°C from coal gas streams produced by gasification of bituminous coals.

4. BACKGROUND STATEMENT:

In the combustion and gasification of coal, oxides of nitrogen (NO_x) are formed from two sources: fixation of atmospheric nitrogen in high-temperature flames, and oxidation of nitrogen compounds that are part of the coal feedstock. Because U.S. coals contain from 0.5 to 2 wt% nitrogen, the possible contribution of this source to NO_x emissions is not trivial. In the low-oxygen-potential environment near the exit of a gasifier, fuel-bound nitrogen appears largely as ammonia. Removal of ammonia from the hot coal gas will eliminate subsequent production of NO_x from the fuel-bound nitrogen in downstream appliances such as a gas turbine or a molten carbonate fuel cell.

5. PROJECT DESCRIPTION

The program is divided into three tasks:

- Comprehensive review of the literature: Identify and assess the effectiveness of concepts for hot gas ammonia removal. Based on a critical review of this information, catalytic decomposition of ammonia was selected as a process concept that has a significant potential for successful development.

- Development of an experimental test plan: Design a protocol to evaluate the performance of several candidate catalysts selected on the basis of the literature review.

- Catalyst testing: Experimentally screen candidates to identify one superior catalyst. Determine the reaction kinetics of this catalyst to provide a quantitative basis for scale-up of the process.

6. RESULTS/ACCOMPLISHMENTS

LITERATURE REVIEW

Comprehensive surveys of technical, patent, government, and commercial literature were performed by computerized searching of Chemical Abstracts, Energy Abstracts, and Metallurgical Abstracts. For concepts reported before 1967 (the year from which the data bases can be searched by the use of computers) manual scanning of these sources was used. Several hundred document titles relating to potential ammonia removal concepts were found. Based on a critical review of the documents or abstracts, the following concepts were selected for detailed assessment:

- Catalytic decomposition
- Sorption/reaction with solids
- Partial oxidation of ammonia to nitrogen
- Staged combustion processes

Catalytic Decomposition

Ammonia is thermodynamically unstable at hot coal gas cleanup temperatures. Because the decomposition step has a high activation energy, about 114 kcal·mole^{-1}, (Yumura and Asaba, 1981) thermal decomposition cannot be used to decrease the level of ammonia in hot coal gas. However, the use of catalysts will allow attainment of equilibrium levels. Figure 1 illustrates the equilibrium concentration of ammonia in a low-Btu gas stream as a function of temperature and pressure. The calculations indicate that the reactions between various components of the coal gas, such as water gas shift and methanation influence the equilibrium level of ammonia in the coal gas stream. Because the formation of methane decreases the volume of the gas, an increase in the concentration (ppm) of ammonia in the gas phase could occur under equilibrium conditions, as shown in Figure 1.

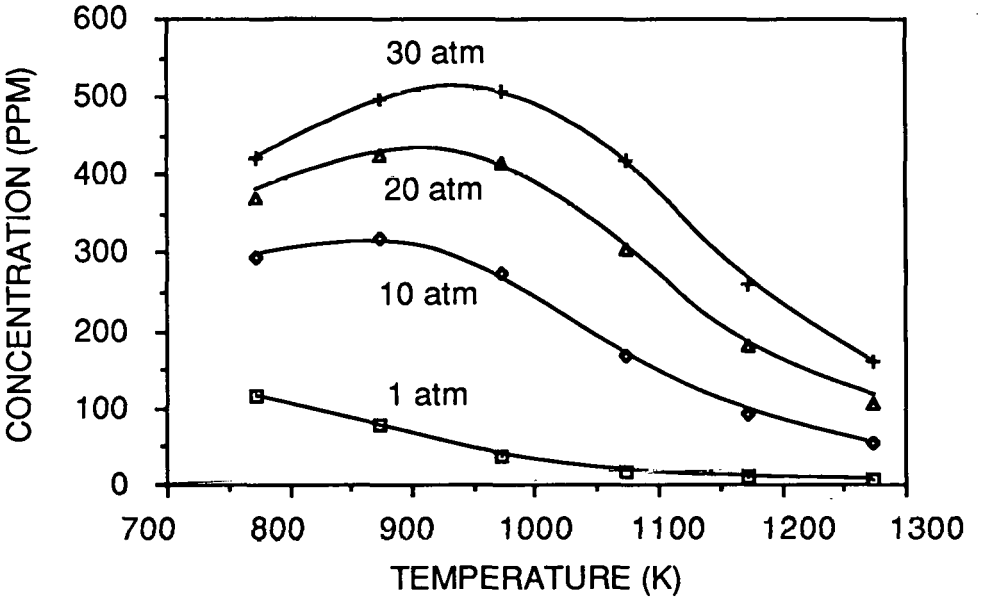

Figure 1. Equilibrium Concentration of NH_3 as a Function of Temperature and Pressure

Largely because of great interest in ammonia synthesis, the reverse reaction, the catalytic decomposition of ammonia has been examined by many investigators over a period of about 50 years. Many of these studies relate to the commercial bulk iron and promoted iron catalysts; however, a significant number of other studies have focussed on alternative catalysts including noble- and base-metals, and oxides. Nearly all published studies suggest that the catalytic decomposition occurs through successive dehydrogenation of surface-adsorbed NH_x species to form nitrogen and hydrogen adatoms. These adatoms recombine to form hydrogen and nitrogen molecules and desorb from the surface. The catalytic activity appears to be related to the strength of the N-metal bond (Tamaru 1980). If this bond is weak, the driving force for N adatom formation on the surface is decreased. Alternatively, if the bond is strong, then nitride formation is favored over nitrogen atom recombination and desorption. Metals such as

Ru, Co, Fe, and Ni with moderate N-metal bond strength are strong candidates to act as catalysts for ammonia decomposition. In general, the rate of decomposition is governed either by (a) the rate of dissociation of NH_3 molecule on the surface, as is the case under high temperature and/or low pressure conditions, or (b) the rate of desorption of nitrogen adatoms, as is the case under low temperature and high pressure conditions.

In addition to good catalytic activity, the resistance of the catalyst toward sulfur poisoning and steam attack must be taken into account. Because chemisorption of H_2S occurs at high-coordination sites where NH_3 chemisorption is also favored, the presence of H_2S in the coal gas could decrease the activity of the catalyst. Steam, at high temperatures, could oxidize the metal and also attack the supports such as alumina. An earlier, unpublished study by Engelhard Corporation found that under hot coal gas conditions, the deterioration of the catalysts under high steam levels is a more serious problem than poisoning by low levels of H_2S. Instead of the alumina support used in that study, high-temperature, steam-resistant supports such as magnesium aluminate are likely to alleviate this problem.

Sorption/Reaction with Solids

By analogy with the removal of H_2S by metal oxide sorbents, ammonia can be removed, in principle, by reaction with a metal or an oxide. Metals such as iron dissolve a moderate amount of nitrogen and form metastable nitrides (Darken and Gurry 1953). The metallurgical process of nitriding steels is conducted in an atmosphere containing NH_3. The solubility of nitrogen in steel increases with temperature and with the amount of alloying elements such as Cr, Mn and V. However, in coal gas containing high levels of steam or H_2S, iron sorbents are not suitable for removal of ammonia because of oxidation or sulfidation of the metal. Similar considerations also apply to reactive metals such as Ti and Zr which have large solubilities for nitrogen.

Reduction of oxides such as TiO_2 by ammonia was also considered. The Gibbs energy changes associated with their reduction by ammonia are more favorable than those for reduction by H_2. For example, the reaction of NH_3 with TiO_2 to form Ti_4O_7 has a standard Gibbs energy change of 0.8 kcal·mole^{-1} at 1000 K in contrast to that of 4.95 kcal·mole^{-1} for the same reaction with H_2. However, equilibrium calculations indicate that the ratio of ammonia to steam in a typical hot coal gas is not sufficiently high for the reduction reaction to proceed.

Reaction with Another Gas

Removal of NO_x by reaction with added ammonia has been proposed as a method for NO_x control in flue gases (Thermal DeNox process). Hence, the reduction in NH_3 levels in the hot coal gas by reaction with added NO was considered as a potentially useful concept. Recent studies of reaction mechanisms (Branch, Miller, and Kee 1979) suggest that the presence of OH radicals is necessary for the intiation of the reaction between NO and NH_3. The concentrations of such radicals are considerably less in hot coal gas than in flue gas. Hence, it appears that the reaction between NH_3 and NO may not be suitable for ammonia removal from hot coal gas.

Staged Combustion Processes

Recently, attention has been focussed on staged homogeneous and catalytic combustion of gaseous fossil fuels as a means of reducing NO_x emission. Because the fuel-bound nitrogen in coal gas is oxidized even at temperatures as low as 800°C, a small reduction in flame temperature is not sufficient to prevent fuel-bound NO_x formation. In simple terms, staged combustion processes use the interaction between NH_x radicals and NO to form N_2 under highly reducing conditions present in the fuel rich primary stage. Any unburnt fuel is then oxidized in the secondary stage where, by dilution with steam or air, the flame temperature is kept relatively low to prevent the formation of thermal NO_x. In a study of the staged combustion of low and medium-Btu coal gases, a significant reduction in the formation of fuel-bound NO_x was observed (Westinghouse Corporation 1982). The level of fuel-bound NO_x decreased at long residence time and a high fuel/air ratio in the primary stage. However, increases in the total pressure or the Btu content of the fuel increased the level of fuel-bound NO_x formed.

Earlier studies (Folsom et al., 1980) of catalytic combustion with noble metal catalysts indicated that fuel-bound nitrogen such as ammonia is readily oxidized to NO_x. However, NO_x formation was reduced under fuel rich conditions when base metal catalysts, such as mixed Cr_2O_3-Co_3O_4, are used (Prasad, Kennedy, and Ruckenstein 1981). Thus, it is possible that a two-stage catalytic combustion system could reduce the formation of NO_x from fuel-bound nitrogen. Because the base metal catalysts are less efficient in the oxidation of hydrocarbons than noble metal catalysts, a two stage catalytic combustion using both base- and noble-metal catalysts is more likely to be successful in reducing the formation of NO_x during combustion of hot coal gas.

In summary, both catalytic decomposition and staged combustion processes have the potential to reduce the emission of fuel-bound nitrogen compounds during the use of coal gases. A process based on catalytic decomposition will be independent of coal gas end use, whereas, staged combustion processes require modification of the combustor and they may affect efficient energy utilization. In view of these considerations, the catalytic decomposition method was selected for further investigation.

TEST PLAN

The experimental protocol for evaluating the efficacy of catalysts for removing ammonia under laboratory-scale conditions involve two phases: (a) a screening study of several catalysts and (b) a detailed kinetic study of a selected catalyst. Initially, in the screening phase of the program, the catalysts will be tested for their activity and durability at 550° and 800°C at atmospheric pressure under low steam-low H_2S, high steam-low H_2S, and high steam-high H_2S conditions. Table 1 lists the gas compositions that will be used in these tests. The catalysts selected include Ni, Ni-Mn, Ni-Ir, Ni-Cu, and Cr_2O_3-CO_3O_4 supported on stabilized alumina, magnesium aluminate spinel (monoliths or pellets), SiC fabric and zinc ferrite. The catalyst that has the superior performance under these conditions will be then subjected to a detailed testing phase. In this phase, the parameters affecting catalyst performance will be varied

systematically to determine a global rate law for the decomposition of ammonia in hot coal gas. The range of test conditions include the following: temperatures from 550° to 870°C, pressures from 1 to 30 atm, NH_3 levels from 500 to 5,000 ppm, H_2S levles from 0 to 3,000 ppm and steam levels from 10 to 30 vol%.

Table 1. Composition of Simulated Coal Gas in Screening Tests

Component	Representative gasifier and Concentration (mole%)		
	Low H_2O-Low H_2S KRW air-blown	High H_2O-Low H_2S GE air-blown	High H_2O-High H_2S Texaco O_2-blown
CO	21.8	7.1	34.5
H_2	13.7	15.7	22.0
CO_2	7.0	12.4	7.0
N_2	39.5	26.5	0.0
H_2O	7.2	27.4	28.7
NH_3	0.5	0.5	0.5
H_2S	0.0001	0.0001	0.3
He*	10.3	10.3	10.3

* He is the diluent in the NH_3-He gas mixture used as a source of NH_3

CATALYST TESTING

Experimental Procedure

The screening tests and most of the experiments in the kinetic study will be performed in a fixed bed reactor made of either 316 stainless steel or 601 inconel alloy. The simulated coal gas mixture is mixed by blending individual components or gas mixtures using mass flow controllers. The rate of ammonia decomposition is determined by gas chromatographic (GC) analysis of ammonia in the feed and the product gas before condensing the steam. In the gas chromatograph, ammonia is separated from the rest of the gas mixture in a Chromosorb 103 column, and is detected using a photoionization detector. This detector has a high sensitivity and a broad dynamic range for NH_3 and H_2S components. It is relatively insensitive to the other components of the coal gas. Because the column can not separate NH_3 and H_2S adequately, H_2S is removed by a copper sponge bed at 150°C in the sample line. Decomposition of NH_3 by copper at this temperature is negligible. This analytical procedure allows rapid (about 10 min) determination of NH_3 in wet coal gas in the range <1 to 5000 ppm. Remaining gaseous components are determined by GC after condensation of steam.

Experimental Results

To date decomposition of NH_3 in simulated coal gas have been determined for two catalysts. The first is a commercial proprietary nickel catalyst on a magnesium aluminate support designed for methanation and steam reforming of hydrocarbons up to a temperature of 900°C. Its excellent resistance to steam at high temperature makes it a suitable candidate for the present

application. The second catalyst is a nickel catalyst (United Catalysts Inc. G-65) modified by SRI by the addition of 1 wt% Ir to increase its resistance to H_2S poisoning. This catalyst has CaO-stabilized alumina as the support.

The rate of decomposition of NH_3 by the $Ni/MgAl_2O_4$ catalyst was found to be very sensitive to the reaction temperature (Figure 2). At 550°C and a space velocity of $3x10^4$ h^{-1}, the percentage of NH_3 decomposed was less than 1% even at low levels of H_2S. However, as the temperature was increased, the conversion increased. The measured activation energy of 23.6 $kcal \cdot mole^{-1}$ is similar to the value reported by Rostrup-Nielsen (1973) for nickel on $MgAl_2O_4$ catalysts. At 800°C, the catalyst exhibited a high activity that was not affected by the presence of steam. In the absence of H_2S, a conversion of about 98 to 99.5% was observed at a space velocity of $1x10^4$ h^{-1} (Figure 3). Addition of 100 ppm of H_2S decreased the conversion to about 90%, but further increases to 3,000 ppm of H_2S did not degrade the activity any further. An examination of the catalyst after about 25 h of testing at 800°C did not show any physical deterioration.

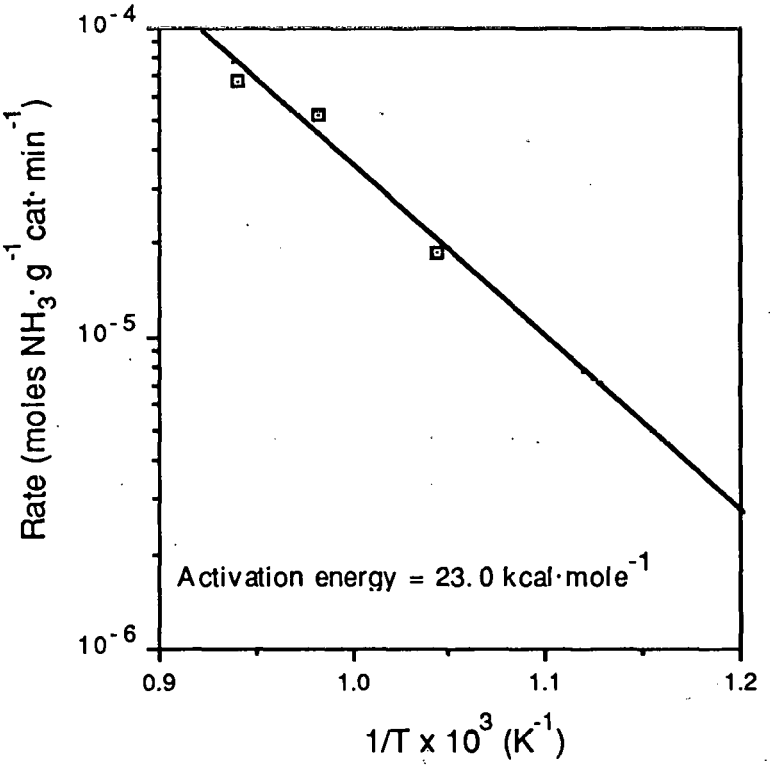

Figure 2. The Rate of Decomposition of NH_3 on a Ni/Magnesium Aluminate Catalyst as a Function of Temperature.

In contrast to the $Ni/MgAl_2O_4$ catalyst, the Ir-promoted Ni catalyst (G-65*) exhibited some activity at 550°C. At this temperaure and a space velocity of $1x10^4$ h^{-1}, a conversion of about 75% was observed in the absence of H_2S, whereas a near-stable conversion of 55% was noted under high steam-low H_2S test conditons (Figure 4). Tests conducted at 800°C indicate that the poisoning of the catalyst by H_2S is reversible at this temperature. The

catalyst exhibited a conversion of about 65%, with a feedstock containing 3,000 ppm of H_2S, at a space velocity (SV) of $1x10^4$ h^{-1}. The conversion increased to about 90% when the feed stock was changed to the high steam-low H_2S composition (Figure 5).

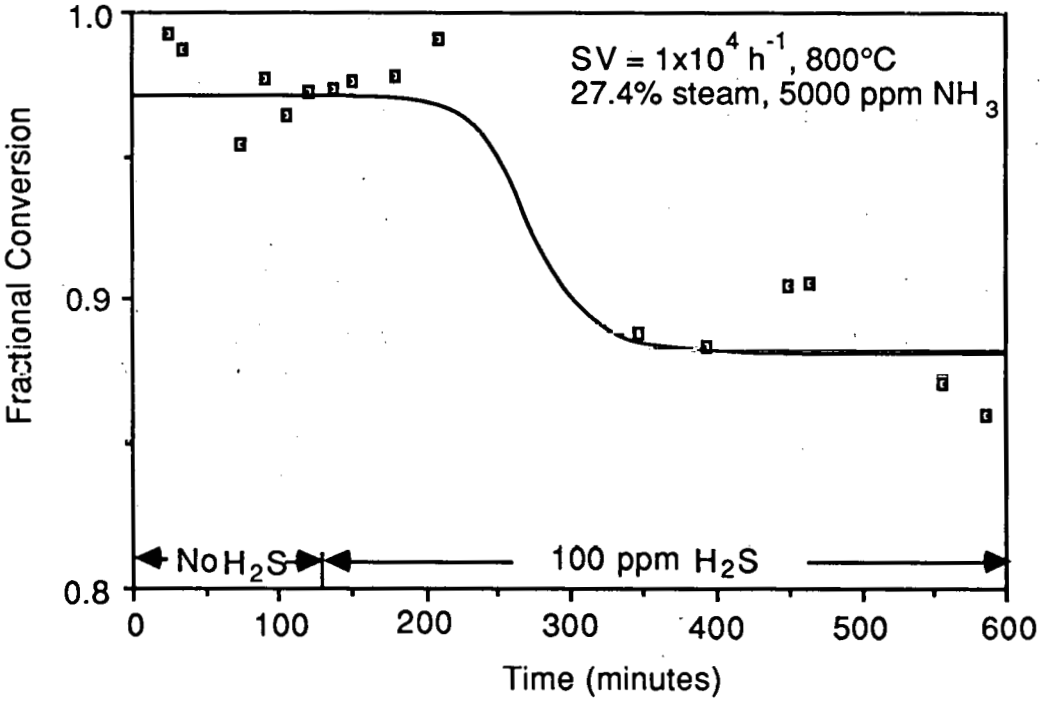

Figure 3. The Conversion of NH_3 by a Ni/magnesium Aluminate Catalyst at 800°C.

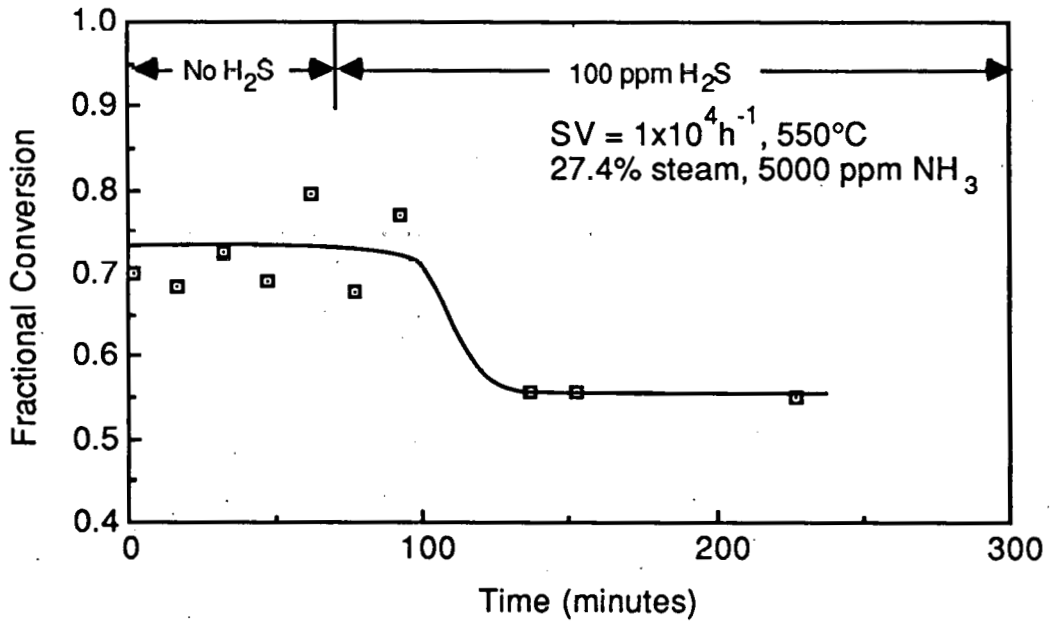

Figure 4. The Conversion of NH_3 by Ir-Promoted Ni Catalyst (G65*) at 550°C.

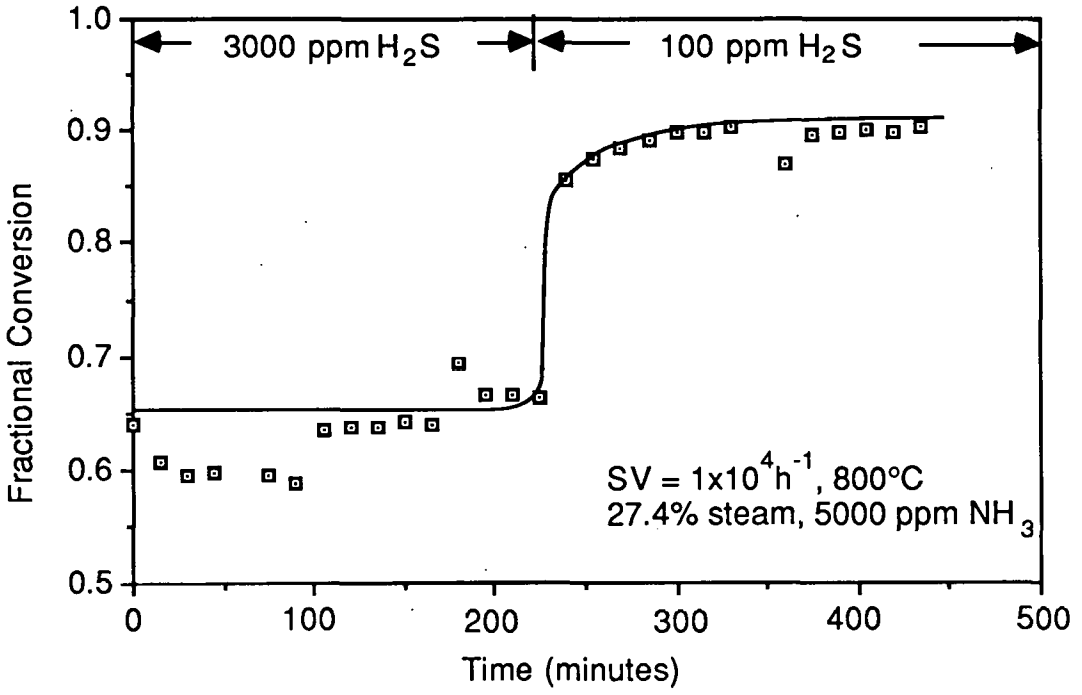

Figure 5. The Conversion of NH_3 by Ir-Promoted Ni Catalyst (G65*) at 800°C.

Summary of Accomplishments

- A comprehensive literature review was performed to identify several potentially useful concepts for the removal of NH_3 from hot coal gas streams. Of these, catalytic decomposition and staged combustion processes have the ability to achieve the present objective. The catalytic decomposition was selected for testing because the process is independent of coal gas end use.

- A test plan has been developed to test the concept of catalytic decomposition in a laboratory-scale fixed bed reactor.

- Screening experiments with supported catalysts are in progress. Nickel-based catalysts appear to be suitable for decomposition of NH_3 in hot coal gas streams. Ammonia conversions of 90% have been observed in feedstocks containing 26% steam and 100 ppm H_2S. Preliminary results indicate that higher amounts of H_2S may not degrade the activity at 800°C.

7. FUTURE WORK:

The future work will include:

- Completion of screening tests with the remaining selected catalysts.
- Review of the results from the screening tests and selection of a catalyst that is superior in activity, tolerance to steam and sulfur, and compatible with hot coal gas cleanup conditions.
- Investigation of the selected catalyst under various conditions of temperature, pressure, gas composition and space velocity to obtain a rate law useful for process scale-up.
- Evaluation of the results and recommendations for futher development of the concept.

8. REFERENCES:

Branch, M.C., Miller, J.A., and Kee, R.J. (1979) Chemical Kinetics of the $NH_3/NO/O_2$ System, Paper presented at the Meeting of Western States Section of the Combustion Institute, Berkeley, CA, October 15, 1979, Paper WSS 79-138.

Folsom, B.A., Clark, W.D., Courtney, C.W., Heap, M.P., and Seeker, W.R. (1980), Proceedings: Fourth Workshop on Catalytic Combustion, Cincinatti, OH, May 1980, EPA 600/9-80-035, pp. 432-455.

Prasad, R., Kennedy, L.A., and Ruckenstein, E. (1981) Oxidation of Fuel Bound Nitrogen in a Transitional Metal Oxide Catalytic Combustor, Combustion Sci. and Technol., 27, pp. 44-54.

Tamaru, K. (1980) New Trends in Chemistry of Nitrogen Fixation, 9, pp. 13-16.

Westinghouse Electric Corporation (1982) Low NO_x Heavy Fuel Combustor Concept Program Phase IA- Combustion Technology Generation: Coal Gas Fuels, Final Report to NASA under contract DEN 3-146, (DOE/NASA/0146-2).

Yumura, M., and Asaba, T. (1981), Rate Constants of Chemical Reactions in the High Temperature Pyrolysis of Ammonia, Eighteenth Symposium (International) on Combustion, The Combustion Institute, Pittsburgh, PA., pp. 863-872.

INJECTION OF DENSELY LOADED FLOWS INTO ENTRAINED-FLOW GASIFIERS

1. CONTRACT: DE-AC21-85MC22064

CONTRACTOR: Science Applications International Corporation
9760 Owensmouth Avenue
Chatsworth, California 91311
818/709-5222

CONTRACTOR PROJECT MANAGER: Dr. Raymond B. Edelman

PRINCIPAL INVESTIGATORS: Dr. Reiner Kollrack, Calvin Morrison, William N. Bragg and Dr. Raymond Edelman

METC PROJECT MANAGER: Leland Paulson

PERIOD OF PERFORMANCE: June 25, 1986 to June 17, 1987

2. SCHEDULE/MILESTONES:

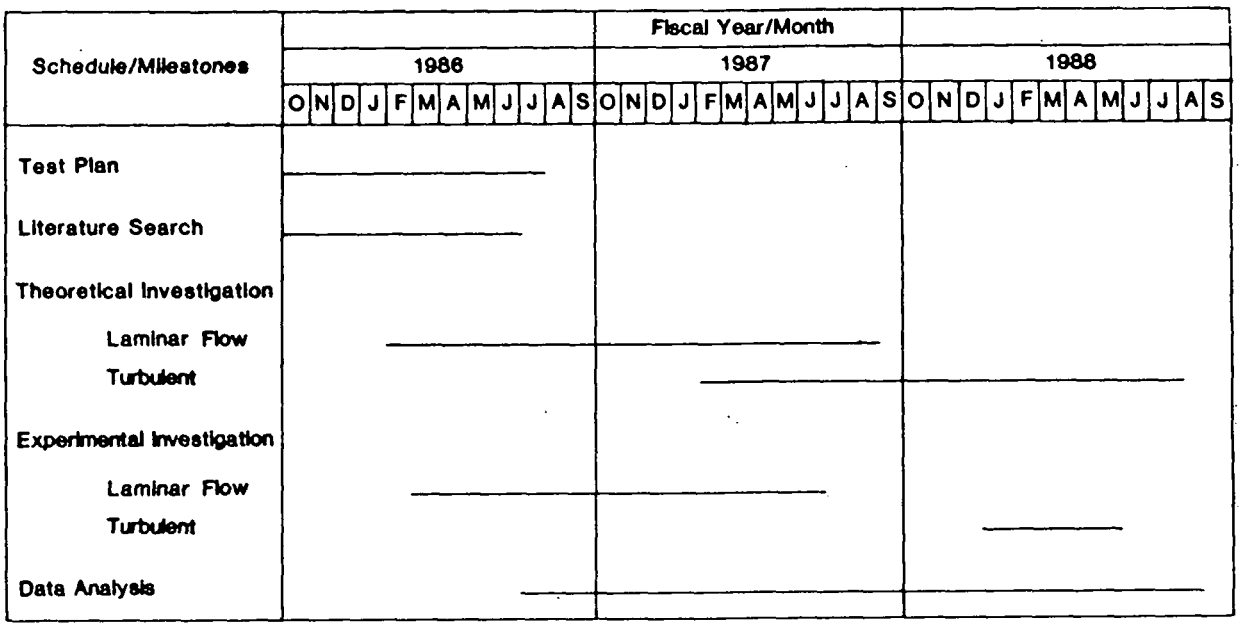

3. OBJECTIVES:

The main objective of this work is to develop a broad understanding of the relevant mixing phenomena for densely laden particle-gas streams injected into quiescent air or moving air streams. A practical application of the results will be the development of improved injection and mixing configurations for entrained-flow coal gasifiers. As a first step, injection of non-reacting particle/air streams into quiescent air is considered.

The specific objective is the development of a model and computer code capable of describing multi-phase laminar and turbulent jet flows, turbulent pipe flows with, and without, swirl and turbulent flows with sudden expansion. Emphasis is directed toward modeling dense loading conditions.

An experimental test facility is constructed to allow velocity and concentration measurements on well defined dense multi-phase flows. "Well defined" implies a known particle distribution, particle size and shape, as well as (perfectly) elastic collision between particles. The purpose of the experimental data is to help validate and refine the current model, as well as to be directly applicable to entrained-flow gasifier designs.

The validated/refined multi-phase flow model will be applied in parametric-type studies to correlate various inlet conditions with resultant mixing rates for different injector configurations.

4. BACKGROUND:

Entrained-flow gasification processes use finely pulverized coal, with particle sizes from 10-100 μm, gasifying it at relatively high temperatures as it is carried through the device in suspension by oxygen or air, steam and product gases. At the high operating temperature of 2500° to 3000° F., essentially all carboneous volatiles such as methane and aromatics are converted to molecular hydrogen, steam, carbon monoxide and carbon dioxide. The absence of methane distinguishes the product gas of entrained-flow gasifiers from the product gas of fixed bed or fluidized bed gasifiers. The atmospheric pressure, dry fed Koppers-Totzek units are the only entrained-flow gasifiers in commercial use (Bodle and Schorg, 1979). Experience with commercial Koppers-Totzek gasifiers shows generally poor carbon utilization with the attendant low thermal efficiency. Coal injectors are crucial to effective operation of entrained-flow gasifiers, largely controlling throughput and significantly affecting conversion efficiency, and therefore, thermal efficiency. This point has been demonstrated by recent applications of rocket injector technology to advanced high throughput entrained-flow gasifiers (Ubhayakar, et al., 1979). A major potential advantage of this technology providing increased mixing and heating rates is higher throughput, partially due to an increased amount and rate of devolatilization. Similarly, poor mixing results in increased reactor residence times and non-uniform coal treatment. Non-uniformity largely controls the amount of unreacted solid carbon exiting the gasifier.

5. PROJECT DESCRIPTION:

A. Theoretical

The current model is based on an Eulerian frame work of equations, treating particle-particle interactions by individual phases instead of individual particles. This model has been developed from a system of instantaneous equations for continuity and momentum for the carrier and dispersed phases, respectively. From these equations, mean momentum and continuity equations are derived. The fluctuating variables such as velocities and volume fractions are subsequently modeled for turbulent flows. In addition, the momentum equation of the carrier phase for turbulent flows is expressed by a two-equation system for the turbulent kinetic energy and its

dissipation rate following the method developed by Elghobashi and Abou-Arab (1983).

Dense loading conditions are characterized by increasing importance of the interaction between various particle phases. Symlal's (1985) treatment of particle-particle momentum exchanges has been adopted for this model. Here, the average distance between particles is reduced by the fact that the effective total volume available for movement of particles takes into consideration the volume of the particles and the void volume of various densely packed structures of these particles. The void volume for densely packed structures is mainly a function of the particle size distribution. Empirical relations for resultant void volumes have been reported by Fodors and Landel (1979).

Another important term in the system of governing equations for turbulent multi-phase flows, which is strongly affected by dense loading conditions, is the Schmidt number for dispersed phases. The expression for the Schmidt number has been expanded to reflect the input of particle-particle collisions for dense loading conditions.

B. Experimental

The apparatus is comprised of an air-particle injection and metering system, a particle recovery system and a Laser-Doppler Velocimeter comprised of an argon-ion laser, TSI dual beam LDV optics with a Bragg cell, forward scatter collection optics, counter processor and a data acquisition system.

Figure 1 shows the four flow configurations that constitute the basis of a stepwise increase in complexity from laminar jet flow to turbulent pipe flow and finally, the inclusion of swirl and sudden expansion. All flows in this report are vertical downward.

6. RESULTS/ACCOMPLISHMENTS

A. Theoretical

Model calculations were first directed toward debugging and refinement of the computer code. Next, inlet loading conditions were varied to test the model applicability to dilute, as well as dense loading conditions. Dilute flow data by Modarress, et al.(1982) were compared to corresponding calculated results to demonstrate the applicability of the model and code to low loading conditions as discussed later on. Considering dense loading conditions for monodispersed laminar vertical downward jet flows, typical axial velocity and concentration profiles are shown in Figures 2a and 2b. The inlet conditions have been chosen for comparison with experimental results. Within the region of dense loading, the particle phase drags the gas phase along. Only where the concentration has decreased below levels typically considered being the borderline

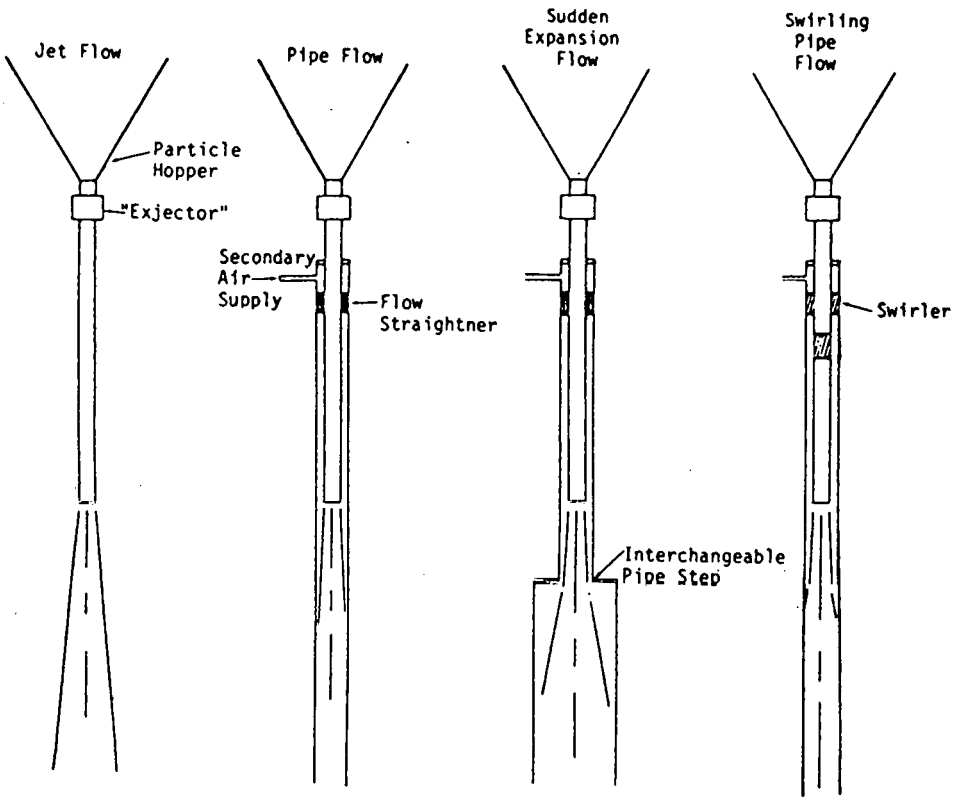

Figure 1: Experimental configurations.

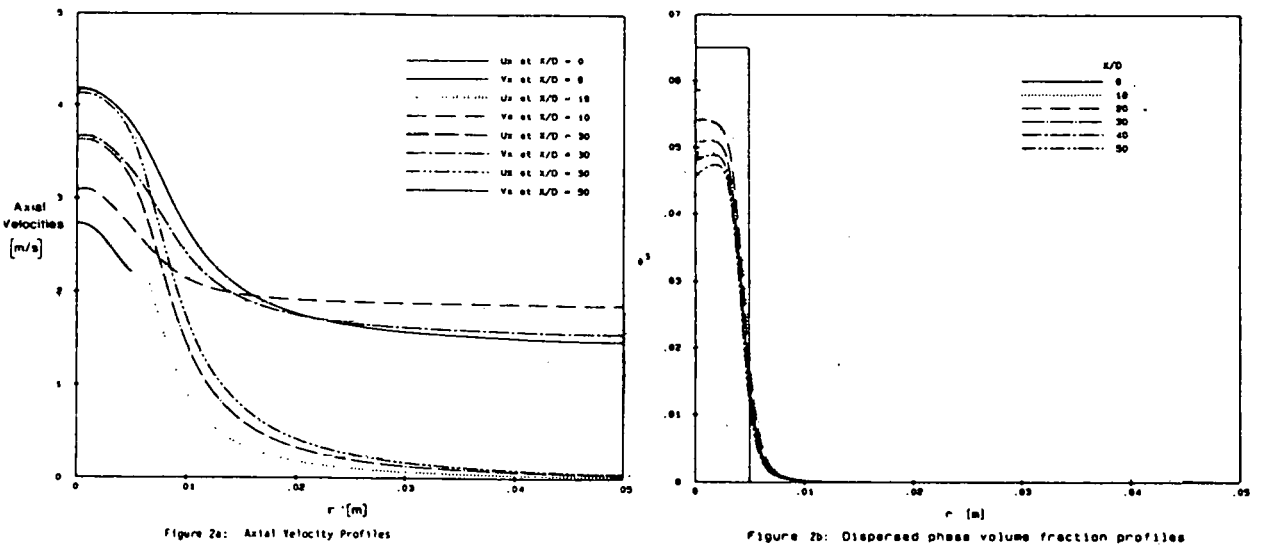

Figure 2a: Axial Velocity Profiles

Figure 2b: Dispersed phase volume fraction profiles

Figure 2: Laminar, monodispersed jet flow.

Nozzle Diameter= 1 cm
Particle Size =200 μm
Particle Volume Fraction=0.065

Particle Density=2540 kg/m^3
Reynolds Number = 800
Viscosity = 1.8 x 10^{-5} kg/ms

between dense and dilute conditions, does the slip between the dispersed and the gas phase increase noticeably. Volume fractions of 0.3 to 0.4% are commonly considered borderline values. The current results for dense multi-phase flows can be best explained by conceptually dividing the flow into three zones

1. Outer Zone showing very low particle densities. This zone is characterized by unilateral gas-particle coupling (governed by the gas). Furthermore, particle-particle interaction (collisions) plays no role. Particles approach the terminal velocity of a single particle in quiescent air.

2. Inner Zone showing high particle loadings. This zone is also characterized by unilateral gas-particle coupling. However, it is governed by the particles. Particles approach free fall velocities and drag the relatively small mass of air along. Particle-particle interactions play a minor role because of the near dynamic equilibrium state that characterizes this zone.

3. Transition Zone, separating the outer from the inner zone. This zone is characterized by a very steep particle concentration gradient. There is bilateral gas-particle coupling. Furthermore, for the inlet condition considered, particle-particle interactions are less important than gas-particle interactions.

The system of laminar governing equations in the current model only contains a single "adjustable" constant mainly covering multiple scattering and fraction of impaction for particle-particle momentum exchanges. Comparisons of calculated multi-phase flow profiles with experimental ones will be used to refine the value of this constant. The treatment of turbulent flows, however, results in a number of constants describing the k-ϵ equation system. In addition, the Schmidt number of the dispersed phase contains a constant α as previously cited. Comparisons of calculated turbulent dilute two-phase flow results with corresponding experimental data serves to obtain an optimized value of the constant α as well as to demonstrate the applicability of the present model to dilute conditions. Figures 3a and 3b show predicted results and experimental data (Modarress, Wuerer and Eloghobashi, 1982) for comparison. The best fit between experimental and calculated data is obtained for $\alpha = 0.05$.

Preliminary dense turbulent multi-phase flow model results are shown in Figure 4. The main feature is a strong dampening effect on the turbulence level in regions of heavy particle loading.

In contrast, the turbulent kinetic energy in the transition and outer zones follow the expected pattern showing an increasing turbulent kinetic energy level due to shear, followed by relatively slow dampening of this level further downstream. The strong turbulence dampening effect in the inner zone, due to high particle con-

Nozzle Diameter = 2cm
Particle Volume Fraction = 3.5×10^{-4}
Particle Density=3.0×10^{3} kg/m^3

Particle Diameter = 200 μm
Reynold Number = 14100
Input Viscosity = 4.5×10^{-2} kg/ms

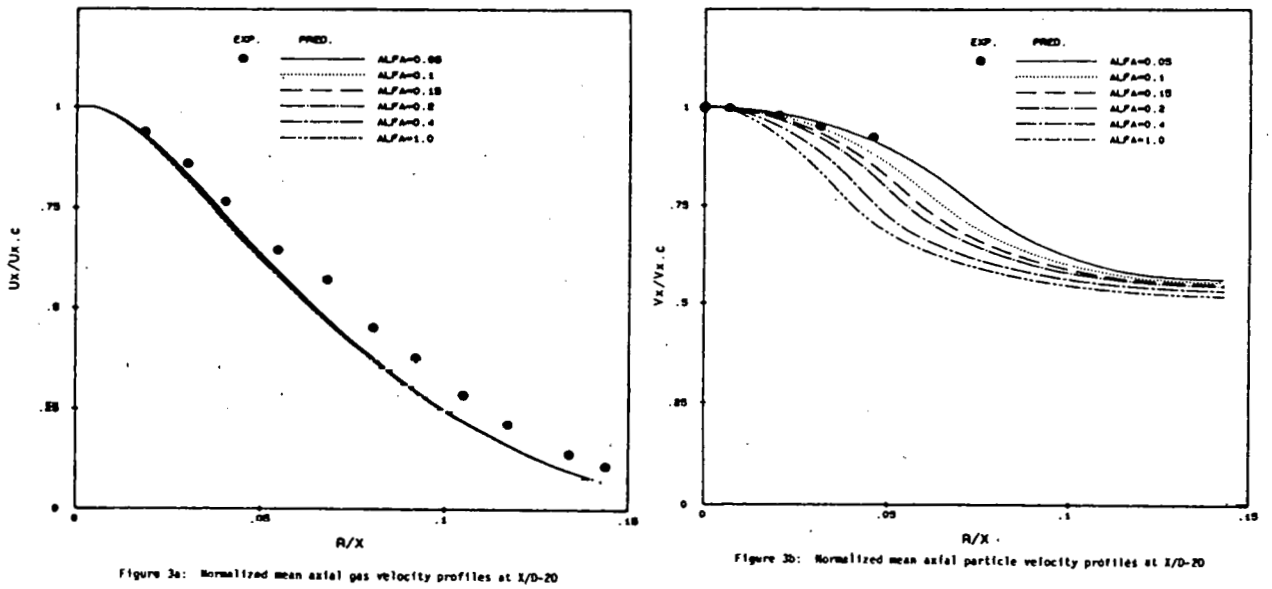

Figure 3a: Normalized mean axial gas velocity profiles at X/D=20

Figure 3b: Normalized mean axial particle velocity profiles at X/D=20

Figure 3: Dilute monodispersed turbulent jet flow.

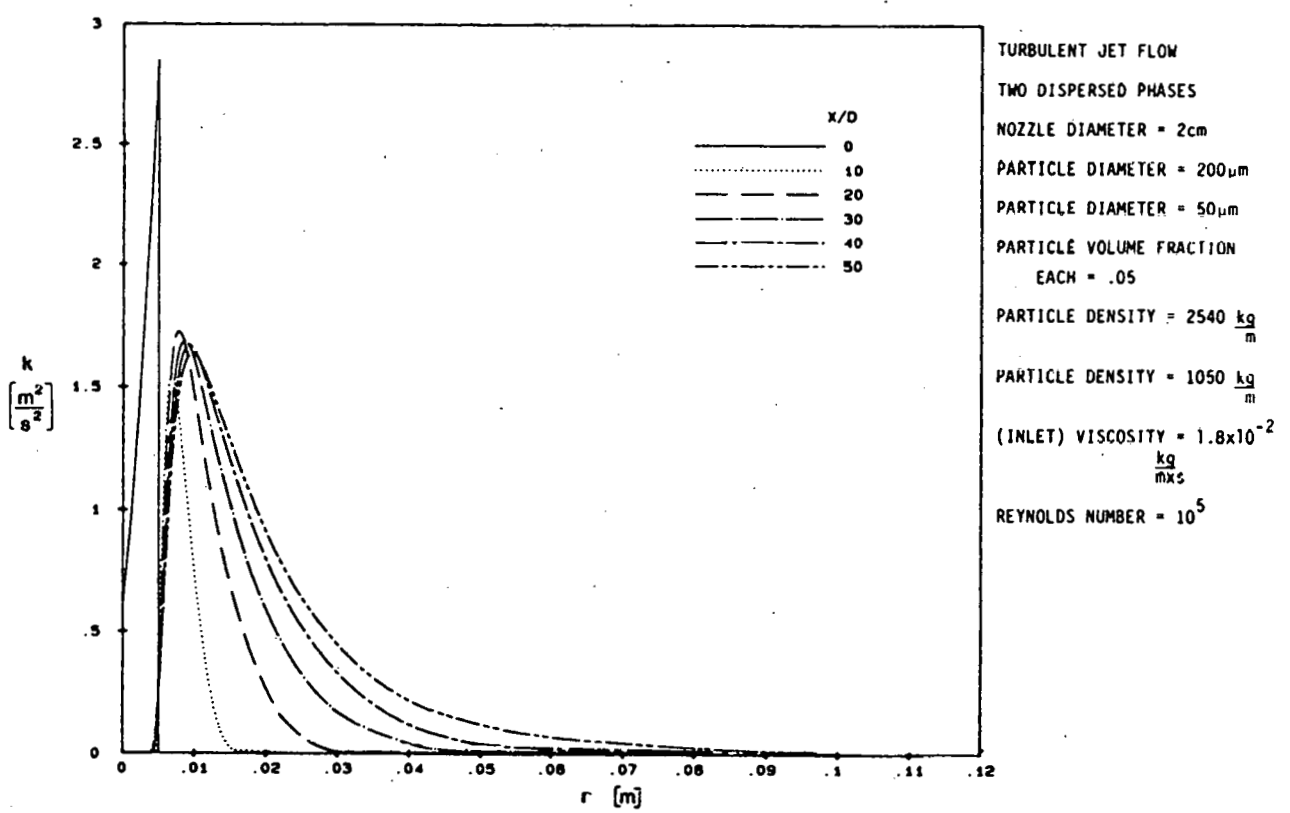

Figure 4: Turbulent kinetic energy profiles at various axial locations.

centrations, indicates that in addition to a "baseline", laminar dense-phase flow has practical implications.

B. Experimental

All measurements on multi-phase flows for this study are being performed at Sandia National Laboratories (Livermore, California). Figure 5 shows two laminar jet flows of equal mass flow rate exiting injectors of different length. The flow from the longer injector displays a coring effect. Potential causes of the coring phenomenon such as electrostatic effects are currently under investigation.

Axial velocity profile measurements for the particle phase are shown in Figure 6, including the corresponding calculated results. The experimental velocity data agree well with the predicted data close to the centerline and in the outer region, while in between, the experimental profile is more spread out than the calculated one. Possible causes for the discrepancy are currently under investigation. Variations of the inlet conditions and nozzle configurations will be applied to test the reproducibility of the test data. In addition, the calculated inlet air velocity and particle concentration profiles will be matched to new data becoming available in the near future.

7. FUTURE PLANS

After completion of the current measurements on laminar and turbulent jet flows, the test plan calls for measurements on turbulent pipe flow with and without swirl and with sudden expansion. In order to handle multi-phase flows with swirl or with sudden expansion, the current parabolic model must be extended to elliptic equations.

Future comparison of experimental data with model results will be used to validate and refine the model in an iterative way as discussed before.

The final task of this contract phase is a parametric-type study of inlet conditions and injector configurations such as upstream versus downstream injection, lateral versus coaxial injection, or swirling versus non-swirling injection.

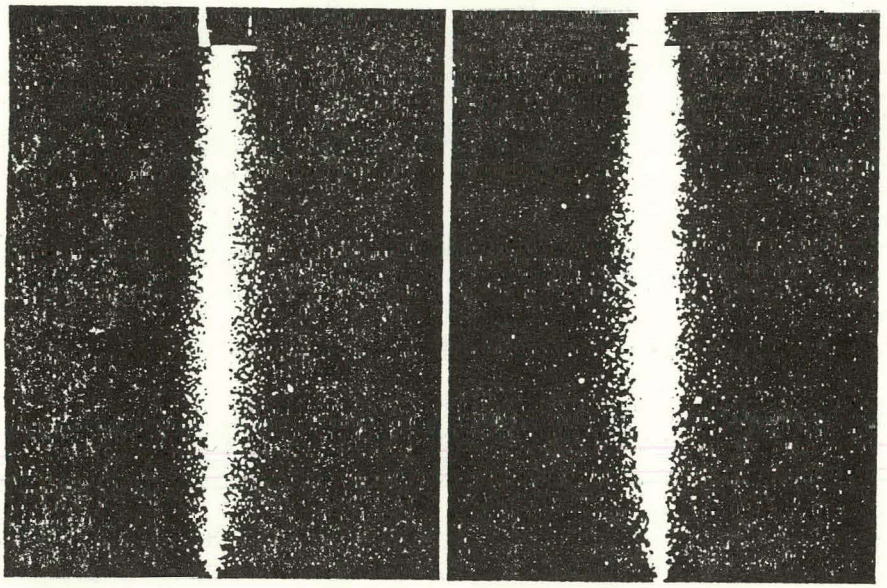

Figure 5: Monodispersed laminar jet flows.

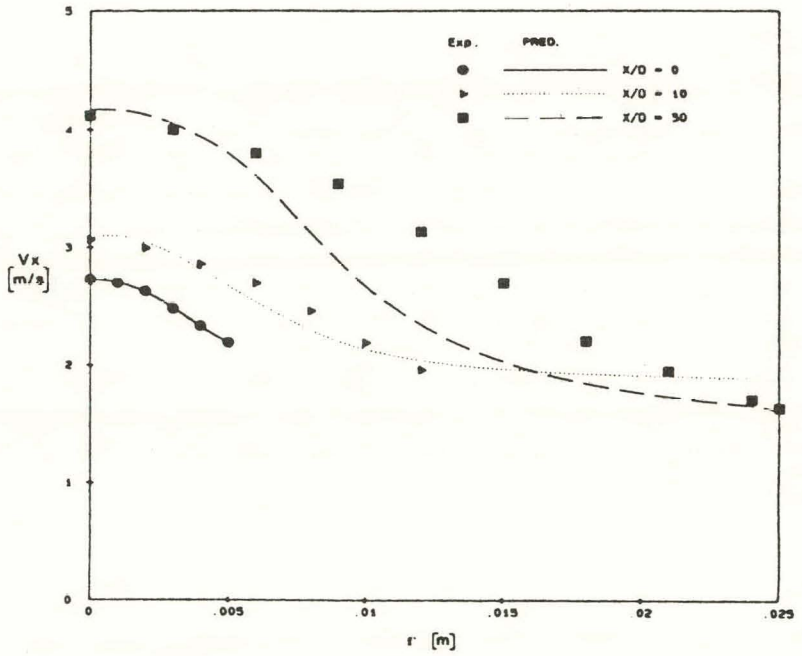

Figure 6: Axial velocity profiles of the particle phase at various downstream positions.

Particle Diameter=165 μm
Particle Density = 250 kg/m^3
Particle Volume Fraction = 0.03

Nozzle Diameter = 1 μm
Reynolds Number = 800
Viscosity = 1.8 x 10^{-5} kg/ms

8. REFERENCES

1. Bodle, W.W. and Schora, F.C., 1979, "Advances in Coal Utilization Technology," Institute of Gas Technology, 11.

2. Elghobashi, S.E. and Abou-Arab, T.W., 1983, "A Two-Equation Turbulence Model for Two-Phase Flows," Phys. Fluids, 25, 931.

3. Fedors, R.F. and Landel, R.F., 1979,"An Empirical Method of Estimating the Void Fraction in Mixtures of Uniform Particles of Different Size." Powder Technology 23, 225.

4. Modarress, D., Wuerer, J., and Elghobashi, S., 1982, "An Experimental Study of a Turbulent Round Two-Phase Jet," AIAA/ASME 3rd Joint Thermophysics, Fluids, Plasma and Heat Transfer Conference, St. Louis, Missouri.

5. Syamlal, M., 1985, "Multiphase Hydrodynamics of Gas-Solids Flow." PhD Thesis, Illinois Institute of Technology, Chicago, Ill.

6. Ubhayakar, S.B., Oberg, C.L., Combs, L.P. and Friedman, J., 1979, "Rocket Reactor Technology Applied to Coal Conversion," Advances in Coal Utilization Technology, Institute of Gas Technology, 407.

ATTRITION AND ENTRAINMENT STUDIES RELATED TO FLUIDIZED-BED COAL GASIFIERS

1. DOE CONTRACT NUMBER: DE-AC21-85MC22061

CONTRACTOR: Institute of Gas Technology
3424 South State Street
Chicago, IL 60616
312/567-3650

PROGRAM MANAGER: Dr. Suresh Babu

PRINCIPAL INVESTIGATOR: Dr. Ted Knowlton

METC PROJECT MANAGER: Dr. W. S. Liou

CONTRACT PERIOD OF PERFORMANCE: July 15, 1985 to July 14, 1987

2. SCHEDULE: See Figure 1.

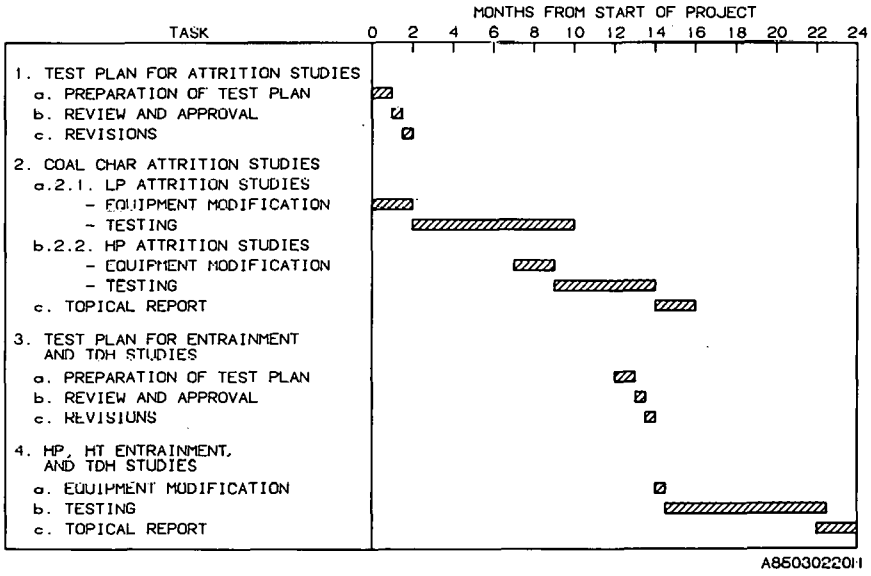

Figure 1. PROJECT SCHEDULE.

3. OBJECTIVES:

The objectives of this program are —

- To determine the relative importance of mechanical, thermal and chemical-reaction attrition of coal chars in a fluidized bed.
- To determine the variation of entrainment rate and transport disengaging height (TDH) of coal char particles as a function of gas density, gas viscosity and gas velocity.

4. BACKGROUND STATEMENT:

In a fluidized bed, interparticle abrasion and collision in the bed or at the grid, thermal shock and chemical reaction lead to the generation of fines which can be carried out of the bed in the exit gas stream. In fluidized-bed gasification process (and in coal conversion processes in general) the generation of carbon and ash fines is one of the major problems that must be addressed. Excessive fines generation results in increased costs for particle collection systems (e.g., in cyclones) and high fines recycle rates. The high recycle rates can impose a significant heat penalty on a process. Therefore, it is desirable to minimize the generation and the subsequent carryover of the coal char fines. To do so, it is necesary to determine the chief causes of attrition and the primary variables affecting the entrainment of fines.

5. PROJECT DESCRIPTION:

The work on this project is divided into four tasks. The titles of the individual tasks are listed below.

Task 1. Test Plan for Coal Char Attrition Studies.

Task 2. Coal Char Attrition Studies.

Subtask 2.1. Ambient Pressure Attrition Studies.
Subtask 2.2. High-Pressure Attrition Studies.

Task 3. Test Plan for High-Pressure, High-Temperature Entrainment Rate and Transport Disengaging Height Studies.

Task 4. High-Pressure Entrainment Rate and Transport Disengaging Height Studies.

In Task 1, a detailed test plan describing the attrition tests to be conducted in Task 2 was sent to DOE for review and approval.

Task 2 consisted of work in two Subtasks. In Subtask 2.1, the effects of gas velocity, system temperature and chemical reaction on the attrition rate of bituminous and lignite coal chars in a fluidized bed was determined. The investigation was conducted in a 6-inch-diameter ambient-pressure fluidization unit. The effect of fluidizing-gas velocity on the attrition rate of two chars at ambient temperature was first determined. Attrition tests were then conducted in the fluidized bed at three temperatures over the temperature range of 70° to 1800°F. Finally, tests were conducted on the same chars with chemical reaction occurring in the fluidized bed. The results from these three sets of tests were then compared to determine the relative importance of mechanical, thermal, and chemical reaction effects on the generation of coal fines in fluidized beds.

In Subtask 2.2, tests were conducted in an 8-inch-diameter, high-pressure fluidized-bed unit to determine the effect of gas density on the attrition rate of lignite and bituminous coal chars. The tests were conducted over the pressure range of 25 to 350 psig.

In Task 3, a detailed test plan describing the entrainment rate and transport disengaging height (TDH) tests to be conducted in Task 4 was sent to DOE for review and approval.

In Task 4, the effects of gas density and gas viscosity on the entrainment rate and the transport disengaging height of bituminous and lignite coal chars in a fluidized bed are being determined. The tests are being conducted in the 8-inch-diameter Advanced Multipurpose Research Reactor (AMRR) over a pressure range of 25 to 350 psia and a temperature range of ambient up to 1600°F.

6. RESULTS/ACCOMPLISHMENTS:

The low-pressure attrition testing in Subtask 2.1 was conducted in the 6-inch-diameter test unit shown in Figure 2 with -20+35 mesh coke breeze

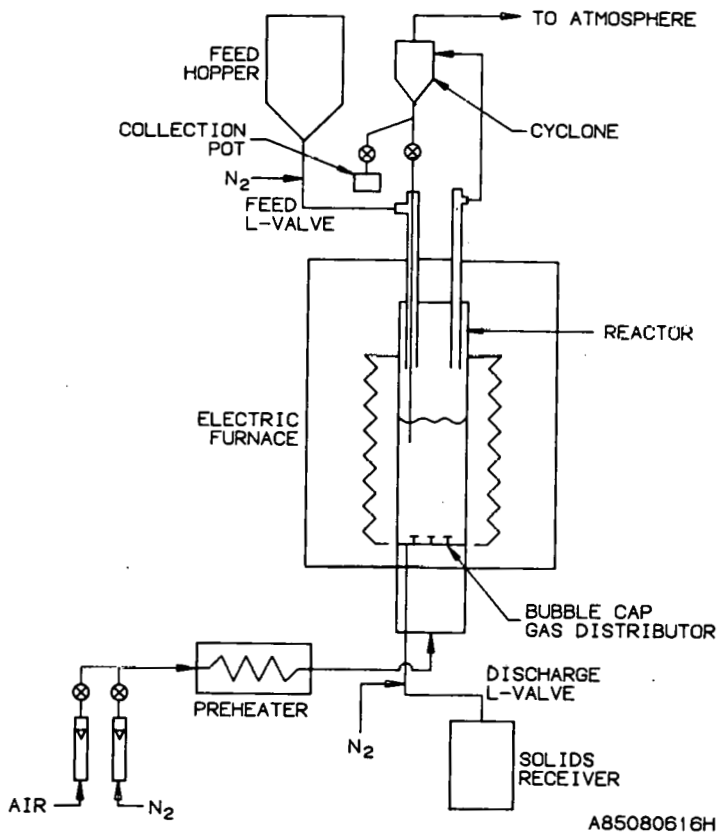

Figure 2. 6-INCH-DIAMETER ATTRITION TEST UNIT.

(a bituminous coal char) and -20+35 mesh lignite char. Attrition tests were conducted to determine the effects of gas velocity, system temperature, and chemical reaction on the rate of fines generation with both types of coal char. The tests without chemical reaction were conducted in a batch mode. In each test, the solids were fluidized for a preselected period of time (usually 1/4 to 3 hours, depending on the rate of fines generation) and then were removed from the unit. The solids were then riffled to obtain a representative bed sample. A particle-size distribution of the bed material was obtained and this sample (plus the other bed material) was returned to the column for the next test. The solids separated by the cyclone were also collected and weighed, but were not returned to the bed. This procedure was repeated until the rate of generation of fines became constant.

The effect of gas velocity on the rate of fines generation in the bed is shown in Figure 3 for -20+35 mesh coke breeze. In this figure, the

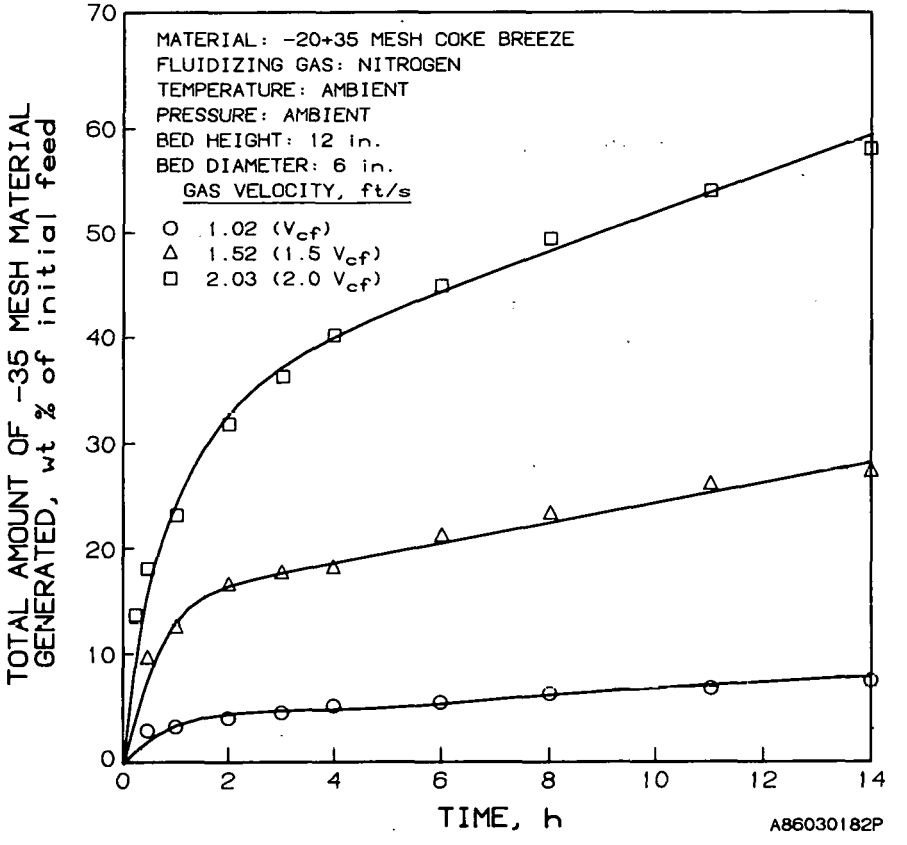

Figure 3. THE EFFECT OF FLUIDIZING GAS VELOCITY ON FINES GENERATION.

cumulative weight percent of fines (defined as the amount of solids generated smaller than 35 mesh) produced is plotted for each superficial fluidizing-gas velocity tested as a function of the time spent in the fluidized bed. The amount of fines produced increased significantly with

the superficial fluidizing-gas velocity due to the increased kinetic energy of the gas jets at the grid and the increased momentum of the particles colliding with each other in the bed.

For all three curves shown in Figure 3, the initial rate of fines production was high, but then leveled off to a relatively constant rate after about three hours of exposure time in the bed. This behavior suggests that the initial attrition rate could be due to the breakage of sharp edges on the char particle which would lead to a rounding of the particles. Photomicrographs of the feed and attrited material support this concept.

Tests to determine the relative amount of char attrition occurring because of 1) turbulence in the fluidized bed, and 2) the gas jets at the grid were conducted in a test column equipped with a porous-plate distributor. With the porous-plate distributor, high-velocity grid jets are not formed. Therefore, the char attrition measured in the porous-plate tests should primarily be the attrition due to the turbulence in the bed.

The results showed that the amount of fines generated in the tests without grid-gas jets was substantially less (approximately an order of magnitude) than the amount of fines generated in the tests with grid-gas jets for both coke breeze and lignite char. The results of the tests showed conclusively that the majority of the coal-char attrition was produced by the grid-gas jets and not by the turbulence in the fluidized bed.

Experiments were also conducted to determine the effect of system temperature on the attrition rate of -20+35 mesh coke breeze and -20+35 mesh lignite char. The effect of system temperature on the fines generation rate of lignite char is shown in Figure 4 at a constant fluidizing-gas

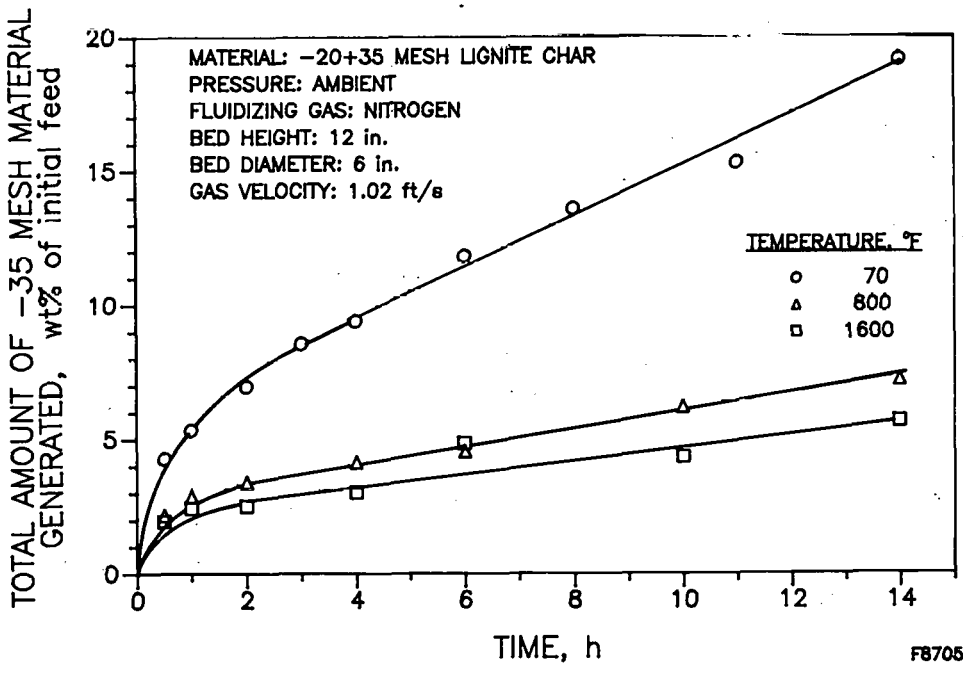

Figure 4. THE EFFECT OF SYSTEM TEMPERATURE ON FINES GENERATION.

velocity of 1.02 ft/s. In this figure, the cumulative weight percent of fines produced at temperatures of 70°, 800°, and 1600°F is plotted as a function of time the solids spent in the bed. The figure shows that the amount of fines generated decreases significantly with increasing system temperature.

The reason for the decrease in the fines generation rate with temperature is that the major source of attrition in the batch attrition tests is the grid-gas jets and grid-gas attrition is proportional to the kinetic energy of the gas jets ($\rho_g U_j^2$). Because the rate of fines generation is proportional to the gas density, when the temperature is increased, ρ_g decreases and the rate of fines generation decreases.

ATTRITION RATE CONSTANTS:

The total attrition rate constant (k_t) in a fluidized bed is defined by the following equation:

$$\frac{dW}{dt} = k_t W \qquad (1)$$

where

$\frac{dW}{dt}$ = the rate at which fines are generated in the fluidized bed, g/h

W = the weight of solids in the bed, gm

k_t = total attrition rate constant, h^{-1}

Integration of Equation 1 leads to the following expression:

$$\ln (100-F) = C - k_t t \qquad (2)$$

where

F = cumulative weight percent of solids converted to fines
$= ([W-W_o]/W_o) \times 100$, %

W_o = initial weight of solids in the bed, g

t = exposure time of solids in the bed, h

C = constant of integration

A plot of ln (100-F) versus t yields a straight line with a slope equal to $-k_t$.

The total attrition rate constant can be partitioned into an attrition rate constant due to the grid-gas jets (k_j) plus an attrition rate constant (k_b) due to turbulence in the bulk of the fluidized bed, or —

$$k_t = k_j + k_b \qquad (3)$$

By subtracting the amount of fines generated in the tests without grid-gas jets (i.e., those generated by the turbulence in the bed) from the total amount of fines generated in the bed, the amount of fines generated by the grid jets was calculated. The attrition rate constant due to the grid jets was then calculated from the rate of fines generated by the grid jets.

The values of the attrition rate constant due to the gas jets at the grid were correlated with both $\rho_g U_j$ (the momentum of the grid-gas jets) and $\rho_g U_j^2$ (the kinetic energy of the grid-gas jets). It was found that k_j correlated better with $\rho_g U_j^2$ than $\rho_g U_j$ for both coke breeze and lignite char.

The expression for k_j for coke breeze was found to be best represented by

$$k_j = 2.6 \times 10^{-8} (\rho_g U_j^2)^{1.4} \quad (4)$$

while the expression obtained for k_j for lignite char was

$$k_j = 6.0 \times 10^{-9} (\rho_g U_j^2)^{1.7} \quad (5)$$

The difference in the two equations is primarily due to the physical properties of each char. More fines were produced in the attrition tests with the lignite char. This is reflected in the higher power on $\rho_g U_j^2$ in Equation 5.

The physical property which appears to best characterize the relative tendency of the chars to attrit, is the Hardgrove Grindability Index (HGI). The HGI is a measure of the relative grindability of a material. The higher the value of the index, the more likely it is that the material will break under impact and/or abrasion. The HGI for lignite char was 64, while that for the coke breeze was 38.

The HGI was incorporated into the rate constant analysis in an attempt to develope an overall equation of k_j which would apply to both chars. Linear regression gave the following equation for k_j —

$$k_j = 2.8 \times 10^{-12} (\rho_g U_j^2)^{1.56} (HGI)^{2.15} \quad (6)$$

This expression correlated the data to within ±30%.

Continuous-char feed attrition tests with chemical reaction occurring in the bed were also conducted with both chars. These tests were conducted at 1600°F with 10% oxygen in the fluidizing gas. For comparison, continuous-feed char tests with no chemical reaction were also conducted at 1600°F with no oxygen in the fluidizing gas. The results of these tests with -20+35 mesh lignite char are shown in Figure 5. The tests with chemical reaction produced more fines per pound of char fed than the tests without chemical rection. From these results it appears that the grid velocity effect becomes more dominant at the higher gas velocities. This can be seen in Figure 5 where the curve for the no-reaction tests approaches the chemical reaction curve at the highest grid-gas kinetic energy value tested.

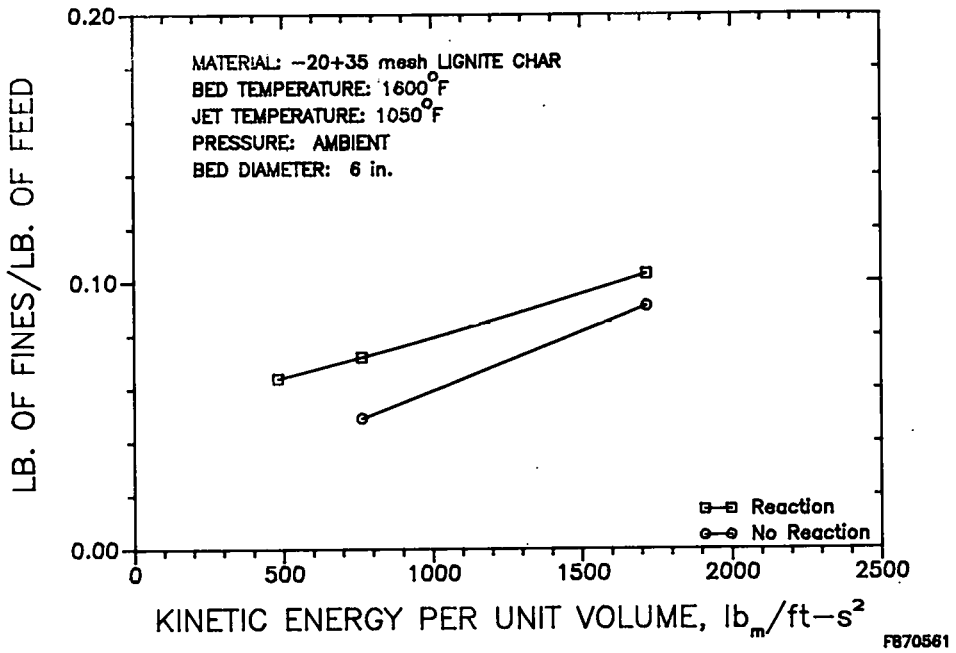

Figure 5. FINES GENERATION WITH AND WITHOUT CHEMICAL REACTION.

The effect of system pressure on the fines generation rate was determined in the 8-inch-diameter AMRR test unit. Tests were conducted at 50, 190, and 365 psia at a system temperature of 1750°F. The fines generation rate was found to increase with system pressure. This was expected since earlier work showed that the fines generation rate in a fluidized bed is proportional to $\rho_g U_j^2$. Because ρ_g increases with pressure, the amount of fines generated should also increase with pressure.

Tests are presently underway in the 8-inch-diameter AMRR fluidization test unit to determine the effects of gas density and gas viscosity on the entrainment rate of coal char from a fluidized bed. Results to date indicate that the entrainment rate increases with both gas density and gas viscosity. This can be seen in Figure 6 in which the entrainment rate of coke breeze material is plotted as a function of superficial fluidizing-gas velocity for several test conditions. The tests were designed to vary gas density at a constant gas viscosity and then to vary gas viscosity at a constant gas density.

7. FUTURE WORK

The work to determine the effects of gas density and gas viscosity on the entrainment rate and transport disengaging height of coal char will be determined in the unique AMRR high-pressure, high-temperature fluidization test facility.

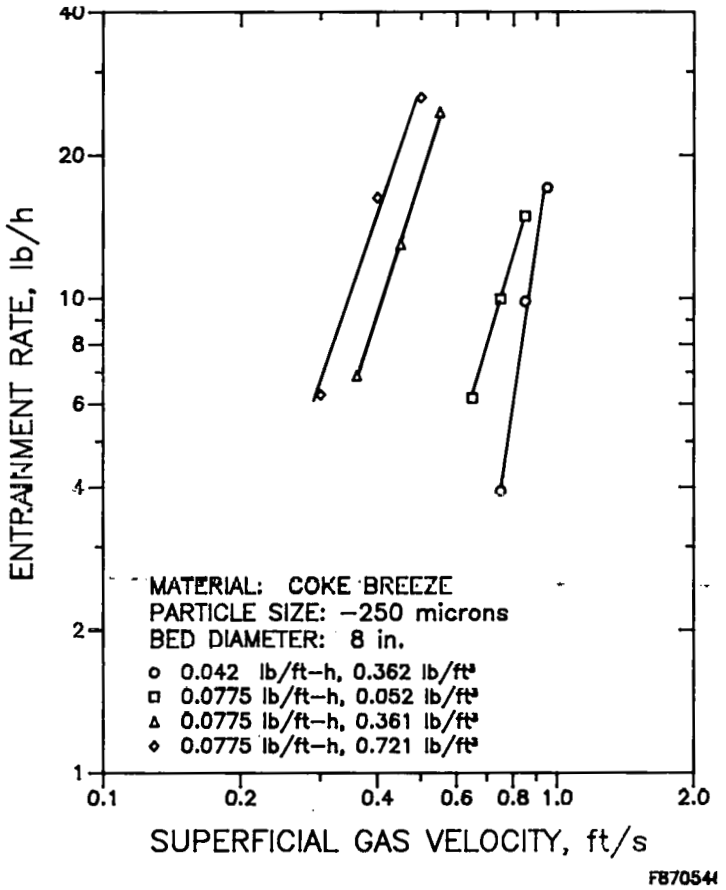

Figure 6. THE EFFECT OF GAS DENSITY AND VISCOSITY ON CHAR ENTRAINMENT RATE.

CONTRACT:	MECHANISMS FOR HOT GAS CLEANUP
CONTRACTOR:	U.S. Department of Energy Morgantown Energy Technology Center P.O. Box 880 Morgantown, WV 26507-0880
METC BRANCH CHIEF:	John J. Kovach
PRINCIPAL INVESTIGATOR:	Jason M. Cook Ranjani V. Siriwardane
METC PROGRAM MANAGER:	Norman T. Holcombe
PERIOD OF PERFORMANCE:	October 1, 1986, to September 30, 1987

ABSTRACT

Calcium-based sorbents are used for sulfur capture in both combustion and gasification applications. A knowledge of the fundamental chemistry of the reactions of sulfur-bearing gases, such as hydrogen sulfide and sulfur dioxide, with calcium-based sorbents is the main goal of this project. Investigations are presently being conducted which will permit the determination of the mechanisms and their kinetics that occur during the initial stages of reactions of these gases with solid surfaces. X-ray photoelectron spectroscopy (XPS) techniques are being used as the main avenue of approach to determining the experimental data that will be used as the means of obtaining a basic chemical understanding. The experiments are conducted over a temperature range of 25° to 1,000° Celsius and are being performed on high purity, single crystal surfaces. Theoretical models which simulate the reactions of sulfur-bearing gases with porous sorbent particles are being used to extrapolate reaction information obtained under high vacuum conditions for comparison with sorbent performance under process conditions. Depth profile studies in conjunction with the XPS experiments on the reacted surfaces will be utilized as the means of determining the depth of penetration of sulfur into the sorbent particle, as well as the penetration depth of the oxygen. The oxidation of the sulfide to the more stable sulfate is important from an environmental viewpoint since the sulfur that remains in the ash that is removed from the bed must be in a stable form for disposal. One project goal is to determine what, if any, environmental problems might result in the disposal of this ash and to determine methods of dealing with them. Additional sulfur utilization data, based upon controllable input parameters (i.e., initial porosity, internal surface area, temperature,

---

This submitted manuscript has been authored by U. S. Government employees acting within their official capacity. On advice from counsel, a transfer of copyright form cannot be executed.

etc.), using micronized calcium oxide and naturally occurring limestones/dolomites may be obtained through the use of a variety of techniques, such as differential flow reactors, packed-bed reactors, and/or volumetric gas sorption systems.

INTRODUCTION

DOE has for some time been involved in the development of both gasification and combustion systems for the conversion of fossil fuels in an environmentally acceptable manner. One of the major concerns of these systems is the efficient and, therefore, cost-effective removal of the sulfur-bearing gases generated during the conversion or combustion process. In the gasification system (fixed bed, fluidized bed, or entrained), the major sulfur-bearing gas phase species is hydrogen sulfide (H_2S), while in the combustion process (entrained or fluidized), the major gas phase sulfur species is sulfur dioxide (SO_2). A promising method currently under investigation at METC is the in-bed capture of H_2S in the stirred fixed-bed gasifier using limestones or hydrated lime. Zinc ferrite has been investigated for the high-temperature removal of H_2S from the gasification stream while it is proposed to recycle the regeneration gases from the zinc ferrite to the system so that sulfur removal can occur without using an external sulfur removal system. In the fluidized-bed combustion system, the limestone reacts with the SO_2 released during the combustion process (1).

The optimization of this process requires a detailed understanding of both the behavior of the calcium-based sorbent at various locations in both the gasification and combustion system and the interaction that occurs between the sorbent and the gases resident within that location. This can be accomplished by using models which take into account temperature, time, etc. It requires, however, accurate reaction rate constants that are dependent upon only a single property, such as pore diffusion or surface reactivity. It is in this area that this project will make its major contribution.

The goals of this project are:

1. Evaluate gas-sorbent models with the goal of determining their usefulness in predicting sorbent behavior within a combustion system.

2. Determine the mechanisms and kinetics of the initial stages of the interactions occurring between sulfur-bearing gases and calcium-based sorbents.

Included in the first goal is the possibility that additional experiments, not related to the second goal, will be needed so as to provide the necessary input parameter information required by the model(s). Also, the need to have information relative to the post-reaction sorbent condition to use as a check on the model(s) will necessitate additional experiments. The most likely area in which these types of experiments will be required will be in the determination of the pore-size distribution and in the determination of its change with respect to reaction conditions.

EXPERIMENTAL METHODS

Two major experimental techniques are being employed in these studies; these include (1) X-ray photoelectron spectroscopy, and (2) volumetric gas sorption. Each of these techniques, along with its advantages and disadvantages, will be discussed separately.

X-ray photoelectron spectroscopy (XPS) is performed by bombarding the surface of a sample with a beam of as many mono-energetic X-rays as possible (2). The usual method of accomplishing this is by using a filter that will adsorb all but the K-α radiation, such as a thin aluminum foil will for either aluminum or magnesium radiation. The X-rays will interact with the surface atoms by inelastically scattering their electrons (mainly their core electrons). The kinetic energies (or, more accurately, the binding energies) of these inelastically scattered electrons provide information not only as to the element but also to its chemical state; the peak's height provides a direct measure of its concentration. Since the gas exposure pressure of the SO_2 in the reactions that are studied by XPS are approximately 10^{-6} Torr (760 Torr = 1 atmosphere), the initial stages of sulfur sorption can be determined by a series of successive exposures which will provide the intensity versus total exposure data that can be used to determine the reaction rate (or more accurately the sticking coefficient and the activation energy) and to provide information as to the surface reaction mechanism. Although the present system can only reach temperatures of 800°C (Celsius), a new probe (that is presently on order) should permit temperatures of 1,200°C to be obtained.

The high vacuum system on which the XPS studies are being conducted is shown in Figure 1. The preparation chamber is used for etching (or removing) unwanted impurities from the surface, evaporating selected impurities onto the surface (such as iron and sodium), and for gas exposures (such as either pure reactant gas or a mixture with oxygen). The preparation chamber will then be evacuated, the gate valve will be opened, and the probe with the sample will be transferred into the detection chamber. The sample end of the probe is resistively heated, thereby permitting the sample to remain at a constant temperature during the course of the experiment. The sample will be placed at the detector's focal point, at which position the kinetic energy measurements will be made. The detector consists of a dual pass, cylindrical mirror analyzer that only permits electrons within a selected range to reach the photoelectron multiplier of the detector.

A volumetric gas sorption system (3) consists, in its simplest case, of a chamber of known volume, a pressure gauge, and a vacuum pump. A sample is placed in the chamber and evacuated (along with any additional pretreatments, such as calcination or dehydration). Then a specific pressure of reactant gas is introduced into the chamber (of known volume) and is allowed to react; the chamber is sealed off during this time. The equilibrium pressure is recorded and a new quantity of reactant gas is introduced into the chamber. This procedure continues until no additional adsorption takes place. This same setup can also be used to make pore volume measurements and BET surface area determinations on the identical samples without any

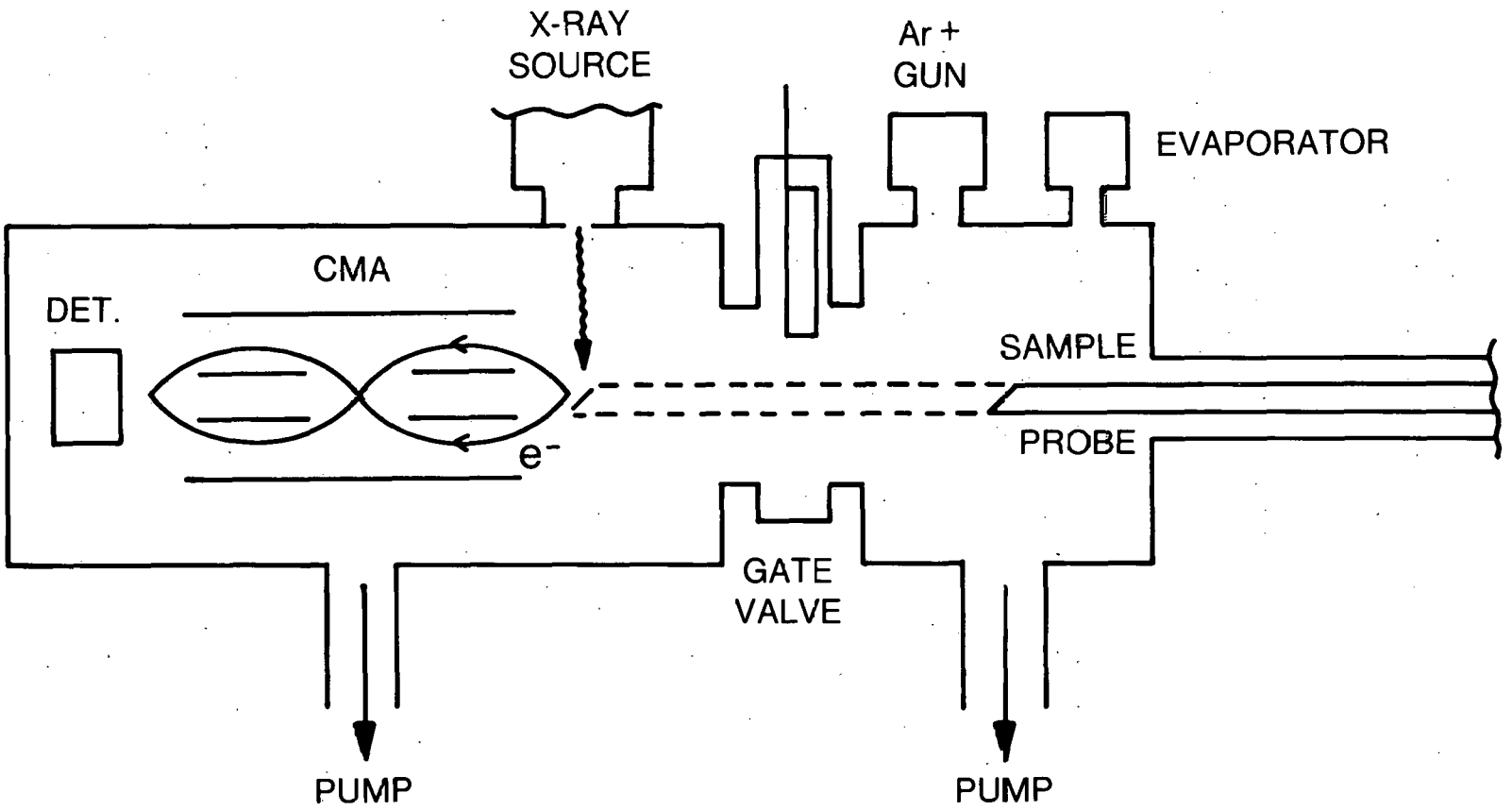

Figure 1. TNB-X System: X-Ray photoelectron spectroscopy system used in the experimental portion of this work showing both the detection chamber on the left and the sample preparation chamber on the right.

possibility of contamination. Therefore, both the calcium utilization and the changes in pore volume and surface area can be determined. As with the XPS system, the volumetric system is designed to be capable of reaching temperatures of 1,200°C.

The volumetric gas sorption system that was designed for this project is shown in Figure 2. The main differences between the system described above and the system shown in Figure 2 are the extra ports for different gases, for the mass spectrometer, etc. The mass spectrometer is required since one of the resultant products of the H_2S reaction with CaO is water (H_2O). Since this reaction creates one H_2O for every H_2S that is formed, the equilibrium pressure should be the same as the initial pressure. Therefore, a mass spectrometer is required to determine the concentrations of each of these two gas species.

MODELING

The best method for predicting either the SO_2 or the H_2S capture utilization of the calcium-based sorbent in either a combustion region or in a region that is downstream from a combustion region is to approximate the adsorption using a model which simulates the system's behavior. Therefore, theoretical models which simulate the reactions of these gases with porous sorbent particles will be evaluated and then utilized to predict sorbent behavior within the various zones or regions of an energy producing system. Although it is possible that additional models could be obtained in the future, at the present time only the following models have been (or are being) obtained and are being evaluated: (1) the Pore-Tree Model developed by Dr. Girard A. Simons of PSI (4), and (2) a grain model developed by Dr. Peter Christman at the University of Texas at Austin (5). A third model that was developed by Dr. Stratis V. Sotirchos of the University of Rochester (6) has been requested and should be ready for operation in the near future. Very brief descriptions of each of these models are as follows:

1. Pore-Tree Model: The model assumes that all pores start large at the surface and branch to smaller and still smaller sizes as they penetrate into the particle(s). The inputs consist of physical data, reaction rates, and process parameters. For each particle, the output provides information as a function of temperature and time concerning calcium utilization, internal and external surface area, and porosity.

2. Random Pore Model: This model, developed by Dr. Christman as part of his Ph.D. work, assumes that no collisions occur among the pores and that a boundary layer resistance exists on the outside of the pellet. The input data also consists of physical data, reaction rates, and process parameters. The outputs for each particle, time, and temperature are similar to the Pore-Tree Model.

3. Pore Plugging Model: Dr. Sotirchos' model provides transient data for a gas-solid reaction where the solid is characterized by an np-modal,

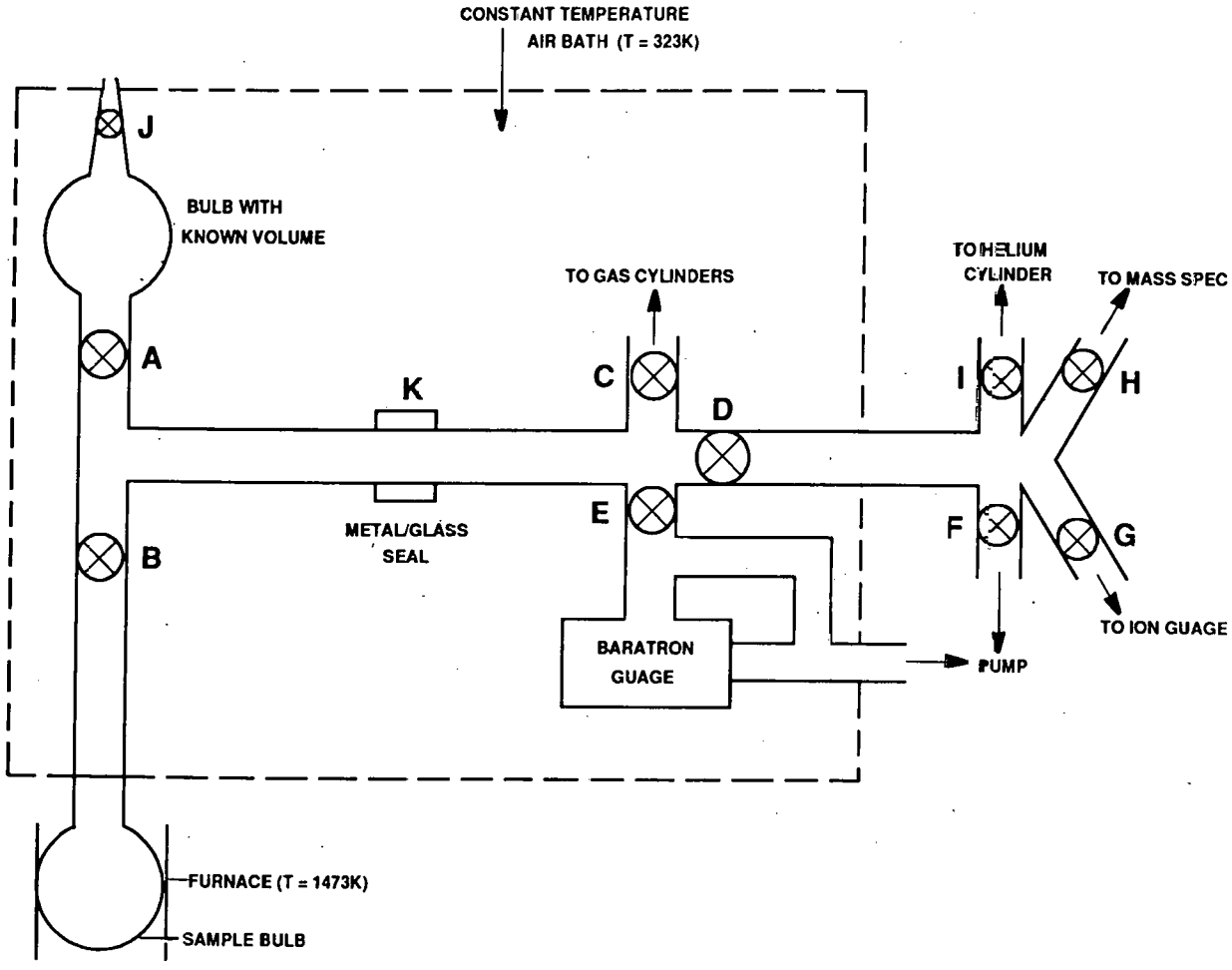

Figure 2. Volumetric Gas Sorption System Schematic showing the reaction chamber on the left (enclosed in a box of constant temperature to eliminate changes in volume) and the connections for gases, gauges, and the mass spectrometer.

discrete pore size distribution. The pores are assumed to be non-intersecting. With the exception of the pore size distribution, the input parameters are similar to the other models.

Several other models (7-9) exist and might be investigated if time and resources permit. Any model that could be successfully utilized for calculations for a bed type of system, such as a fluidized bed system, might also be used for calculations of reactions that occur in an entrained type of system. Due to the short residence times of particles in the combustor of an entrained reactor, the utilization of these models is possible only if the basic chemical reaction rates are known and not included with diffusion and porosity rates.

This is precisely the purpose of much of the work in this project, i.e., the providing of the basic chemical information as separated from the combined chemical and diffusional information. The reactions are being carried out specifically on pure, single crystal surfaces so that only the interactions with the surface layer of atoms and any penetration into and reaction with sub-layers of atoms will be observed. The effect of porosity is thereby eliminated through the simple technique of eliminating all pores.

An example of one of the methods by which the models will be evaluated is as follows: Dr. Christman has taken TGA data on the reaction of SO_2 with calcium sorbents through 600°C (5). He determined that the sorbent product was sulfite. An identical conclusion was reached based upon the work performed at METC. Therefore, the plan is to use the data obtained at METC for the initial stages of the reaction as input to the models in order to predict the behavior that would correspond to the measurements that Dr. Christman reported. A comparison of these results and predictions should permit an evaluation of the models, as well as indicating areas for improvement.

RESULTS AND DISCUSSION

XPS investigations studying the interactions of SO_2 with clean, iron-covered, and sodium-covered surfaces of high purity, single crystals of CaO have been carried out at temperatures of 25°, 100°, 200°, and 400°C (10-11). It was observed (10) that SO_2 reacted with clean and sodium-covered CaO to form sulfite. The addition of sodium to the surface increased the reactivity of the surface permitting a high level of saturation to occur. It was postulated that the sodium atom reacted with a calcium oxygen unit to activate the adsorption of SO_2.

Although SO_2 reacted with iron-covered CaO to form sulfite, it also formed (at higher iron coverages) sulfide (11). This sulfide formation is similar to the behavior that is seen on pure iron foils (12). The sulfide formation can only occur if sufficient iron is present on the surface, i.e., initially for low iron coverages, only sulfite formation is observed.

The addition of oxygen to clean, iron-covered, and sodium-covered single crystal CaO surfaces before the SO_2 exposure occurred generally led to

increased adsorption of the SO_2 (13). Although the preadsorbed oxygen did produce a separate peak on the clean CaO surface, its identification was not possible since it appeared as a side peak on the much larger crystal oxygen peak. However, the form of the sulfur product did not vary from the sulfite that was observed on the non-oxygen treated surfaces. The addition of oxygen onto the clean CaO surface lead to a significant increase (approximately double) in SO_2 adsorption, but the amount of adsorption on the oxygen-treated, sodium-covered surface did not vary from the non-treated surface.

The reactions that occur on the iron-covered surface are substantially different in that the oxygens react with the iron forming iron oxide. This oxidation of the metallic iron caused a significant reduction in the formation of sulfide even though there was an increase in sulfite formation. This indicates that the metallic form of the iron is required for sulfide formation.

The addition of alkalis (14) other than sodium to a single crystal CaO surface showed that a lithium surface was more reactive than was a sodium surface which was more reactive than was a potassium surface; however, each of the atoms led to a promotion in SO_2 adsorption on the surface. Although each of these atoms donate an electron to the substrate to facilitate the reactions between the SO_2 and the CaO surface, the larger size of the size of the ion is apparently a main inhibitor in the reaction. Lithium can settle down into the surface in such a way that the adsorption of SO_2 is not blocked by its presence. The specific sulfur species that was formed deviated from the pure sulfite of sodium in that high levels of potassium produced sulfide in addition to sulfite while high levels of lithium produced sulfide and a species that was neither sulfite nor sulfate. A possible designation for this product is $Li_2S_2O_3$, or some similar compound.

The deposition of alkali halides (14) on a CaO surface appeared to simply provide a physical blockage of the surface with the larger halides providing more blocking that did smaller halides. Therefore, the only sulfur species observed on the surface was sulfite. The extra electron which the alkali atoms would have possessed to donate to the surface is no longer present as it has already been given to the halide. This eliminates any additional excitation of the surface.

The simplest method of determining the kinetics of these surface reactions is by calculating the sticking coefficient (15). Simply, the sticking coefficient is the percentage of impingements on the surface that lead to the reaction under consideration. The overall form of the sticking coefficient is

$$s = s_o \cdot f(\theta) \cdot e^{-E/RT}$$

where s_o is the initial sticking coefficient, $f(\theta)$ is the probability that a collision will take place at an available site based upon the surface coverage θ, E is the activation energy, R is the universal gas constant, and T is the temperature in Kelvin. The form which $f(\theta)$ takes provides

additional information as to the type of reaction that is occurring on the surface, such as one site adsorption with no precursors. For the SO_2 reaction with the clean CaO surface, an initial sticking coefficient of approximately 0.45 was observed with an activation energy of 185 calories. This indicated that over the temperature range of 25° to 400°C, the initial sticking coefficient showed little temperature dependence and that the main factor affecting the rate of adsorption was how rapidly SO_2 could be transported to the surface.

At this time, experimental data has been taken at 800°C but not in sufficient quantities to permit the initial sticking coefficient or the activation energy to be determined. However, some interesting results have been observed. SO_2 reacted with the CaO surface to form sulfite, which decomposed over time to produce sulfide and sulfate. When a mixture of oxygen and SO_2 was reacted with the CaO surface, the length of the exposure was a critical factor. For a short exposure, i.e., a pressure of 10^{-7} Torr for 20 minutes, both sulfide and sulfate were observed, but, for a long exposure, i.e., a pressure of 10^{-7} Torr for 2 hours (120 minutes), only sulfate was observed. This indicated that the SO_2 was initially reacting with the CaO to form sulfite

$$SO_2 \text{ ===> } SO_3 \qquad (1)$$

which then decomposed to form sulfide and sulfite

$$SO_2 \text{ ===> } S + SO_4 \quad . \qquad (2)$$

Finally, in the presence of oxygen, the sulfide was oxidized to sulfate

$$S + O_2 \text{ ===> } SO_4 \quad . \qquad (3)$$

This observation confirms and clarifies previous postulations (5,16-18) and will permit an actual determination of the factors which most directly effect the sulfate formation.

CONCLUSIONS AND FUTURE WORK

Computer simulation or modeling has been determined to be the preferred method of approach to studying the effect of sorbents on sulfur removal from combustion systems. Laboratory results obtained through the XPS measurements, the flow reactor studies, and the volumetric investigations will be used in these models to permit predictions to be made concerning both the fixed-bed gasifier and the entrained combustor bench-scale tests in which METC is also engaged. Several models have been obtained and are presently being evaluated as to their overall usefulness for this purpose.

X-ray photoelectron spectroscopy experiments have been carried out dealing with the reactions of sulfur dioxide with clean, iron-covered, and sodium-covered, single crystal surfaces of calcium oxide over a temperature range of 25° to 400°C. The reaction produces sulfite and, in the case of iron, sulfide. The quantity of reaction can be increased by preadsorbing oxygen

on the surface or by the deposition of other alkali atoms (i.e., lithium or potassium) but is inhibited by the deposition of alkali halides. Sticking coefficient calculations show that the rate of the reaction is mainly dependent upon the speed with which atoms are brought in contact with the surface. Reactions with clean surfaces at 800°C have confirmed that SO_2 reacts to form sulfate which then undergoes dissociation to sulfide and sulfate. Excess oxygen then oxidizes the sulfide yielding a surface that contains only sulfate.

The future direction of these experiments will be directed along the following paths:

1. Obtain and evaluate existing sorption models.

2. Use these models to predict sulfur capture in combustion systems.

3. Extend XPS studies on the reaction of SO_2 with CaO surfaces (including modifications) to 1,000°C.

4. Perform a similar set of XPS investigations for the interaction of hydrogen sulfide with regular and modified CaO surfaces.

REFERENCES

1. This can be readily discerned by reviewing proceedings of METC's cleanup contractors meetings for the past couple of years.

2. An excellent discussion of XPS as well as a fine collection of previous references in the general area of the technique are given in:

   Handbook of X-ray and Ultraviolet Photoelectron Spectroscopy, Ed. by D. Briggs, Heyden & Sons, Inc., New York, 1978.

3. For additional information on surface area and measurement techniques, the following text should assist:

   Adamson, A. W., Physical Chemistry of Surfaces, 3ed., John Wiley & Sons, New York, 1976.

4. Simons, G. A., AIChE Journal 32, p. 1491 (1986).

5. Christman, P. G., "Analysis of Simultaneous Diffusion and Chemical Reaction in the Calcium Oxide/Sulfur Dioxide System," Ph.D. Dissertation, University of Texas at Austin, December 1981.

6. Yu, H. C., and S. V. Sotirchos, AIChE Journal 33, p. 382 (1987).

7. Bhatia, S. K., and D. D. Perlmutter, AIChE Journal 27, p. 224 (1981). AIChE Journal 27, p. 247 (1981).

8. Hartman, M., and R. W. Coughlin, AIChE Journal 22, p. 490 (1976). Ind. Eng. Chem., Process Des. Develop 13, p. 248 (1974).

9. Work by Dr. G. D. Silcox and others as described to me by Dr. D. M. Slaughter, personal communication.

10. Siriwardane, R. V., and J. M. Cook, J. Colloid Interface Sci. 114, p. 525 (1986).

11. Siriwardane, R. V., and J. M. Cook, J. Colloid Interface Sci. 116, p. 70 (1987).

12. Furuyama, M., K. Kishi, and S. Ikeda, J. Elec. Spec. Relat. Phenom. 13, p. 59 (1978).

13. Siriwardane, R. V., J. Colloid Interface Sci. 116, p. 463 (1987).

14. Siriwardane, R. V., J. Colloid Interface Sci. (to be published).

15. Hayward, D. O., and B. M. W. Trapnell, Chemisorption, Butterworths, Inc., Washington, DC, 1964.

16. Hatfield, J. D., Y. K. Kim, R. C. Mullins, and G. H. McClellan, Tennessee Valley Report PB 202 407, June 1970.

17. Lallai, A., G. Mura, A. Viola, and F. Giola, International Chem. Engin. 19, p. 445 (1979).

18. O'Neill, E. P., D. L. Kearns, and W. F. Kittle, Thermochemica Acta 14, p. 209 (1976).

LOW TEMPERATURE, SULFUR TOLERANT, HOMOGENEOUS
CATALYSTS FOR THE WATER-GAS SHIFT REACTION

1. CONTRACT NUMBER: DE-AC21-85MC22065

CONTRACTOR:
SRI International
333 Ravenswood Avenue
Menlo Park, CA 94025
415-859-3465

CONTRACTOR PROJECT MANAGER: Richard M. Laine

PRINCIPAL INVESTIGATORS:
Richard M. Laine
Bernard J. Wood
Gopala N. Krishnan
Jon G. McCarty
Robert H. Schwaar

METC PROJECT MANAGER: Hsiao-Ya L. Lai

CONTRACT PERIOD OF PERFORMANCE: October 1, 1985 to September 30, 1988

2. SCHEDULE/MILESTONES:

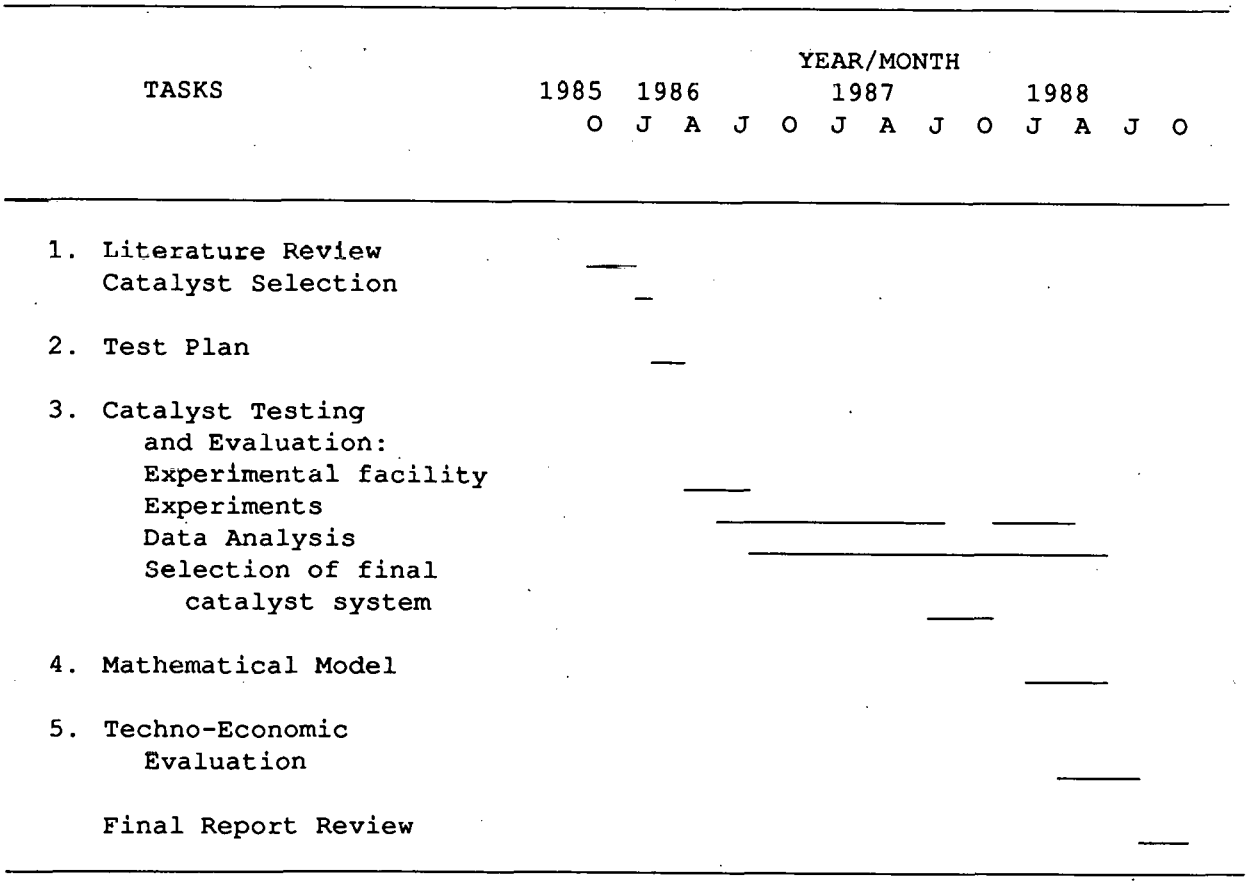

3. OBJECTIVE:

The objective of this project is to identify, prepare, test, characterize, and evaluate a practical, homogeneous catalyst for the production of hydrogen from coal gas by the water-gas shift reaction (WGSR).

4. BACKGROUND STATEMENT:

In long term planning for energy resources and chemical feeedstocks, hydrogen derived from steam gasification of coal may become an important alternative to hydrogen obtained from steam reforming of natural gas. The production of additional hydrogen from syngas by WGSR substantially enhances the yield of this product. Thus, a potentially important route to improving the economy of hydrogen production is to enhance the efficiency of industrial WGSR catalysis.

In current practice, syngas is shifted by passage through two sequential heterogeneous catalytic reactors. The first operates at about 350°C, using an iron-chromia catalyst that is resistant to sulfur poisoning. At this temperature, the equilibrium conversion of CO to H_2 cannot exceed about 85%. To improve CO conversion to >95%, the partially shifted gas, after removal of H_2S and CO_2, is passed through a second reactor containing, typically, a copper/zinc oxide catalyst at 250°C. Finally, the CO_2 produced in the second stage is removed from the product gas.

In contrast, a single homogeneous WGSR reactor can operate at temperatures below 200°C with equilibrium CO conversions to hydrogen exceeding 95%. Thus, provided that the rate of reaction is sufficiently fast under these conditions, as now seems likely, a single, homogeneous WGSR stage could replace the two-stage heterogeneous WGSR system. Furthermore, we have demonstrated in this program that a number of homogeneous WGSR catalysts exhibit high tolerance to sulfur. Consequently, in this process scheme, sulfur removal could be combined with the CO_2 removal step that is situated downstream from the WGSR reactor.

Considering the advantage of high conversions at low temperatures using a catalyst that is sulfur resistant, together with the process simplifications that accompany a single stage reactor, it is evident that the homogeneous catalytic WGSR process offers great potential for significant savings in capital and operating costs. Recently published reports in the scientific and patent literature (Laine and Wilson, 1984) indicate that a number of homogeneous catalytic systems are capable of catalyzing the WGSR with moderate activity. Therefore, we are evaluating the WGSR performance of selected homogeneous catalyst systems with simulated coal gas feedstocks for use in the production of hydrogen from coal gas.

5. PROJECT DESCRIPTION:

TASKS

The research effort is divided into five tasks:

- A comprehensive review of the literature and selection of ten candidate catalysts.
- Development of a catalyst evaluation test plan.
- Testing of candidates to identify one superior catalyst; evaluation of the reaction kinetics of this catalyst.
- Development of a mathematical model that uses the measured rate data to describe the catalytic process.
- Preparation of a techno-economic evaluation of the process.

The first and second tasks have been completed and were described in detail last year (Wood, et al, 1986). The catalyst systems selected for the experimental testing program are listed in Table 1.

Table 1. Selected Homogeneous Catalyst Systems for WGSR

Number	System
1	$Cr(CO)_6$/alcohol base
2	$Mo(CO)_6$/alcohol base
3	$W(CO)_6$/alcohol base
4	$Ru_3(CO)_{12}$/alcohol/hydroxide
5	$Fe(CO)_5/Ru(CO)_{12}$/alcohol/hydroxide
6	Ru/amine
7	Sulfonated rhodium/phenanthroline
8	Ruthenium/phenanthroline
9	Cobalt/phenanthroline
10	Meta-monosulfonated triphenyl phosphine complex of Rh

The test plan (Laine, et al, 1986) includes a screening program to select, from among the ten candidates, a superior catalyst that will be evaluated subsequently in detailed reaction kinetics measurements in a bench scale reactor. These experiments will provide data for the development of a mathematical model of the process and for process economic evaluation.

EXPERIMENTAL PROGRAM

The experimental testing program, using as feed a simulated Texaco oxygen-blown gasifier coal gas in a batch test arrangement, is currently in progress. This program uses a protocol in which the parameters affecting catalyst performance (e.g., solvent, base, temperature, sulfur contaminant level) are varied systematically. The results of each test are assessed promptly so that a decision can be made whether to modify a particular parameter and repeat the test, or reject the specific catalyst in favor of an alternative candidate.

Screening tests are performed in a high-pressure, stirred, batch reactor system, capable of operation at temperatures up to 200°C. The reactor is a PTFE-lined Parr bomb containing a magnetic stir bar. A high pressure sampling system withdraws and analyzes small aliquots of the gaseous contents of the reactor at periodic intervals. Analyses for H_2, CO, and CO_2, and other trace components, are performed by gas chromatography. The system is shown schematically in Figure 1.

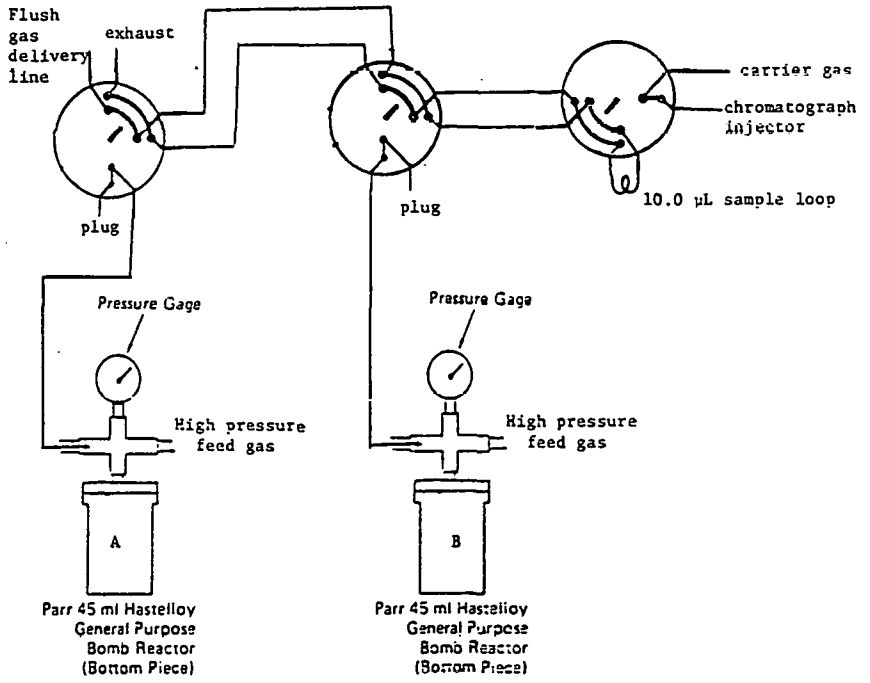

Figure 1. High Pressure, Automatic Sampling, Dual Reactor System

After charging the reactor with measured quantities of the catalyst, solvent, base, and liquid H_2O, (and in many experiments, a quantity of NaHS that provides an equivalent sulfur concentration of 1000 ppm) the vessel is closed, then flushed and pressurized to 350 psi with the simulated coal gas [51.3 CO, 34.8 H_2, 11.1 CO_2, 0.8 CH_4 (mol% dry basis)].

The reactor is then placed in a hot oil bath with a magnetic stirrer, to start the reaction at the desired temperature. During the course of the test the consumption of CO and the formation of H_2 are monitored continually. Typically, the quantity of CO converted to H_2 increases with time at a uniform rate for several hours. These data are used to calculate the initial turnover frequency, TF, defined as the ratio: mole H_2 formed per hour/mole catalyst precursor. At longer times, the partial pressures of H_2 and the other gases reach a steady state condition, usually corresponding to about 85% conversion of the initial charge of CO to H_2. The duration of each experiment is 20 hours.

6. RESULTS/ACCOMPLISHMENTS:

SOLVENT/BASE EFFECTS ON CATALYTIC PERFORMANCE

To date, screening tests have been performed using carbonyl-complex catalysts based on Cr, Fe, Mo, Rh, Ru, and W respectively, in addition to mixed Fe and Ru complexes. Specific complexes have been dispersed in different types of solvent (protic and aprotic) and have been activated by a variety of bases. Significant variations in activity have been observed in many of these cases.

The tri-ruthenium dodecacarbonyl complex is one catalyst that has exhibited generally superior performance among those tested. However, the WGSR activity of this complex, as measured by initial TF, exhibits considerable variation with respect to the reaction environment. For example, the activity increased by more than 400% (from TF = 1.7 to 7.6) when the aprotic solvent triglyme (triethylene glycol dimethyl ether) was substituted for the protic solvent, triethylene glycol. Significant variations in activity were observed also with different bases. At 180°C, in triglyme solvent and with an initial charge of 14 mmol H_2O, the use of 9.2 mmol of N,N,N',N'-tetramethyl-1,6-hexanediamine gave an initial TF = 12.3, in contrast to initial TF = 10.4 with 12 mmol of N-methylpiperidine.

Catalyst activity also depends on the concentration of the amine base. TF values increase with an increase in the amount of amine added to the reactor, all other parameters being constant, as shown in Table 2 for the case of tetramethyl-hexanediamine base in triglyme solvent with an initial charge of 56 mmol H_2O.

Table 2. Effect of Amount of Base on WGSR Activity of $Ru_3(CO)_{12}$

Amount (mmol)	Initial Turnover Frequency (TF)
4.6	23.6
9.2	27.1
13.8	33.0

Results of recent experiments demonstrated that the highest values in Table 2 do not represent upper limits. In duplicate experimental runs in which the reactor was charged with 63.1 mmol of this base, 84 mmol of water, and no organic solvent, an average initial value of TF = 56 was measured. This observation, that an organic solvent is not required to obtain high hydrogen formation rates, provides an additional process simplification with an attendant potential cost saving for the hydrogen plant.

EFFECT OF WATER

The activity of the catalyst is also a function of the concentration of water in the system. Activity increases as the water charge is increased, but appears to reach a maximum value in the vicinity of 84 mmol water, as shown for two catalyst systems in Table 3.

SULFUR TOLERANCE

A number of catalyst systems have been tested for sulfur tolerance by making kinetic measurements with and without added NaHS in an amount equivalent to 1000 ppm H_2S. Measured values of initial TF for the two cases were within the range of experimental error for the following catalysts:

$Cr(CO)_6$, $Mo(CO)_6$, $Ru_3(CO)_{12}$, $Fe(CO)_6/Ru_3(C))_{12}$, $Fe(CO)_6/Rh_6(CO)_{16}$.

These results indicate that the homogeneous WGSR catalysts are highly tolerant toward sulfur impurities.

Table 3. Effect of Water on WGSR Activity at 200°C

Catalyst	Base/Solvent	mmol Base	mmol H_2O	Initial TF
$Ru_3(CO)_{12}$	Tetramethylhexanediamine/ Triglyme	9.2	28	24.2
			56	27.1
			84	29.3
			112	25.9
		13.8	56	33.0
			112	28.9
$Mo(CO)_6$	Potassium Carbonate/ Triethylene glycol	1.1	56	9.6
			84	14.7
			112	14.3

APPROACH TO EQUILIBRIUM CONVERSION

As mentioned earlier, after a period of 10 to 15 hours, the partial pressures of the gaseous components in the batch reactor reached a steady state level, typically indicative of about 85% conversion of the initial charge of CO to H_2. This conversion is less than the equilibrium value calculated on the assumption that all components are in the gaseous state. In fact, of course, the reactor contains a two-phase system in which some species are in the liquid phase, others are in the dissolved state, and the remainder are gases. The partition of gaseous components, especially water, between the gas and liquid phases is unknown. Hence it is impossible to judge, from equilibrium considerations, what represents the limiting factor that determines the observed steady state concentrations. Experimental determination of the ultimate attainable CO conversion to H_2 must await measurements in a continuous-flow reactor.

We have established that the apparent cessation of reaction in these experiments is not due to the deactivation of the catalyst, by performing multiple, successive runs with the same catalyst sample. At the end of 20 hours, the reactor is vented then repressurized with fresh

simulated coal gas. The catalyst system [$Ru_6(CO)_{12}$/amine/triglyme] remained active after 3 runs, with an observed decrease in the initial TF from 13.7 to 6.1. The diminution in activity may be due to loss of water vapor in the venting between runs; no water replenishment was made in the successive recharges.

TECHNO-ECONOMIC CONSIDERATIONS

A preliminary techno-economic analysis (Table 4) that compared the capital costs of 1000-ton/day hydrogen plants using homogeneous and heterogeneous WGSR processes respectively, indicated that the homogeneous catalyst technology could be competitive. In this analysis, the superior durability of the homogeneous catalyst compensated for its higher initial cost, which was balanced also by a somewhat higher capital cost for the heterogeneous process plant. The analysis was based on a turnover frequency of 330 for the homogeneous catalyst, a figure that represents a goal for the experimental program. The assessment used a model that considered only the costs of the catalyst and the reactors, and thus it is subject to later revision.

Table 4. Process Comparison

Item	Homogeneous Catalyst	Heterogeneous Catalyst
Catalyst	$Ru_3(CO)_{12}$ Complex	Fe/Cr_2O_3 High Temp.Stage Cu/ZnO Low Temp.Stage
Turnover Frequency	330 g-mol CO/mol Cat/h	H.T.: 0.52 lb-mol CO/ft^3/h L.T.: 0.19 lb-mol CO/ft^3/h
Initial Cost ($):		
Reactors	940,000	5,600,000
Catalyst	23,000,000	10,200,000
Catalyst Life	Indefinite	4 years
Current Status	Early R & D	Existing Art

SUMMARY OF ACCOMPLISHMENTS

- The tri-ruthenium dodecacarbonyl complex has exhibited superior performance, among the catalyst systems tested. Initial turnover frequencies greater than 50 have been measured in simulated, sulfur-contaminated, coal gas feedstock. The additional increase in activity required to attain the goal of TF = 330 now appears attainable.

- High catalyst activities have been observed in an organic-solvent-free system. The process simplification represented by such a system may offer significant savings in cost.

- Molybdenum hexacarbonyl complex catalyst systems have exhibited turnover frequencies as high as 15. Although this is only about 1/3 the activity of ruthenium, the much lower cost of molybdenum would be a compensating factor in process catalyst selection.

- Many of the tested catalyst systems have exhibited tolerance to contaminant sulfur at the 1000 ppm level.

7. FUTURE WORK:

The catalyst screening task is being continued. Investigation will be made of the effect on catalyst activity of both qualitative and quantitative variations in solvents and bases, in addition to an exploration of simplified, organic-solvent-free systems.

Although base metal catalyst systems have been generally inferior in activity to those using ruthenium, they will not be dismissed. Because of the substantially lower cost of such systems, some sacrifice in activity could be tolerated. Consequently, base metal complexes will continue to be examined during the remainder of the screening task.

The completion of the screening program with the selection of a catalyst for bench-scale investigation is anticipated later this calendar year, as scheduled. The requirements for the bench-scale studies are being discussed in the light of the screening test results in order to anticipate needed equipment and materials. The modeling effort will begin during the bench-scale measurements. The detailed techno-economic evaluation will commence at the completion of the experimental work. No significant changes in the project plan or schecule are expected.

8. REFERENCES:

Laine, R.M., Wood, B.J., and Krishnan, G.N., 1986. Low Temperature, Sulfur Tolerant, Homogeneous Catalysts for the Water-Gas Shift Reaction, Task 2: Test Plan, Topical Report No. 2, Contract No. DE-AC21-MC22065, April, 1986.

Laine, R.M. and Wilson, Jr., R.B., 1984. Aspects in Homogeneous Catalysis, 5, 217-240, (1984).

Wood, B.J., Krishnan, G.N., Schwaar, R.H., McCarty, J.G., and Laine, R.M., 1986. Low Temperature, Sulfur Tolerant, Homogeneous Catalysts for the Water-Gas Shift Reaction, Proceedings of the Sixth Annual Gasification Contractors Meeting, M. R. Ghate and L. A. Baker Jarr, editors, DOE/METC-86/6043, Morgantown, WV, (1986) p. 235.

REMOVAL OF H_2S FROM GASIFIED COAL

1. CONTRACT NUMBER: AA 85 40

CONTRACTOR: Lawrence Berkeley Laboratory
Applied Science Division
University of California
Berkeley, CA 94720

CONTRACTOR PROJECT MANAGER: Dr. Elton J. Cairns

PRINCIPAL INVESTIGATOR: Professor Scott Lynn

METC PROJECT MANAGER: Dr. Lisa A. Jarr

CONTRACT PERIOD OF PERFORMANCE: January 1, 1984 to September 30, 1987

2. SCHEDULE/MILESTONES:

FY 1987-89 Program Schedule

12/86	Solubility studies completed.
12/86	Studies of reaction kinetics at ambient temperature completed.
6/87	Complete corrosion studies.
6/88	Present alternative designs for integrating H_2S removal with hydrogen production from coal gasification.
6/89	Complete study of chemical kinetics at very low concentrations. Complete study of factors controlling crystal-size distribution of sulfur formed by reaction of H_2S and SO_2. Complete study of reactive absorption of SO_2.
9/89	Submit final report on evaluation of H_2S-removal process for treating gasified coal.

3. OBJECTIVES:

The objective of this research program is to develop an improved process for removing H_2S from a variety of coal gases. The process goals are to achieve:

- Reduction of H_2S in the treated gas to very stringent specifications.
- Lower capital and operating costs relative to conventional technology.
- Flexibility of design that permits either very selective H_2S removal or co-absorption and co-production of H_2S-free CO_2 or light hydrocarbons.
- Production of marketable elemental sulfur from the H_2S with minimal release of sulfur compounds to the environment.

4. BACKGROUND STATEMENT:

When coal is gasified most of the sulfur is converted to H_2S and must be removed before the gas can be used either as a fuel or as synthesis gas. The UCB Sulfur Recovery Process (UCBSRP) is being developed as a general method for removing H_2S from gases. The H_2S is absorbed in a polyglycol ether, then reacted in the liquid phase with SO_2 to form sulfur and water. The process allows high specificity and flexibility; H_2S can be reduced to the part-per-million level or below in the presence of CO_2 and the other components of gasified coal. The CO_2 may be left in the original gas stream or it may be co-absorbed and recovered as a separate, sulfur-free product. The process thus has application both to syngas and hydrogen production from O_2-blown gasifiers and to power production using an air-blown gasifier.

The development of this process has been divided into a number of tasks:

- To determine the solubilities of H_2S, SO_2, CO_2, CH_4 and other hydrocarbon gases, water and sulfur in the organic solvent as functions of pressure, temperature, and solvent composition.
- To determine the effects of temperature and solvent composition on reaction kinetics.
- To investigate the suitability of steel and other materials of construction for this system.
- To determine the parameters controlling the crystal size distribution of sulfur so that crystals of 100 micrometers or greater will be formed in the process.
- To determine the parameters controlling reactive absorption of hydrogen sulfide by solutions containing sulfur dioxide.
- To set up a computer model of this process to aid in its evolution.
- To compare the anticipated costs of this process with those of conventional technology.

6. RESULTS/ACCOMPLISHMENTS:

PROCESS CONFIGURATIONS

High H_2S Selectivity

Figure 1 shows a flowsheet for the UCBSRP in a configuration that gives maximum selectivity for H_2S removal. This result is achieved as follows: In the primary absorber H_2S is removed primarily by physical absorption. The stream of solvent leaving the absorber is nearly saturated with all of the components of the gas being treated. A water wash at the top of the primary absorber prevents loss of solvent vapor in the treated gas.

Most of the solvent stream leaving the primary absorber then enters a reactor/crystallizer that operates at the pressure of the primary absorber. A second

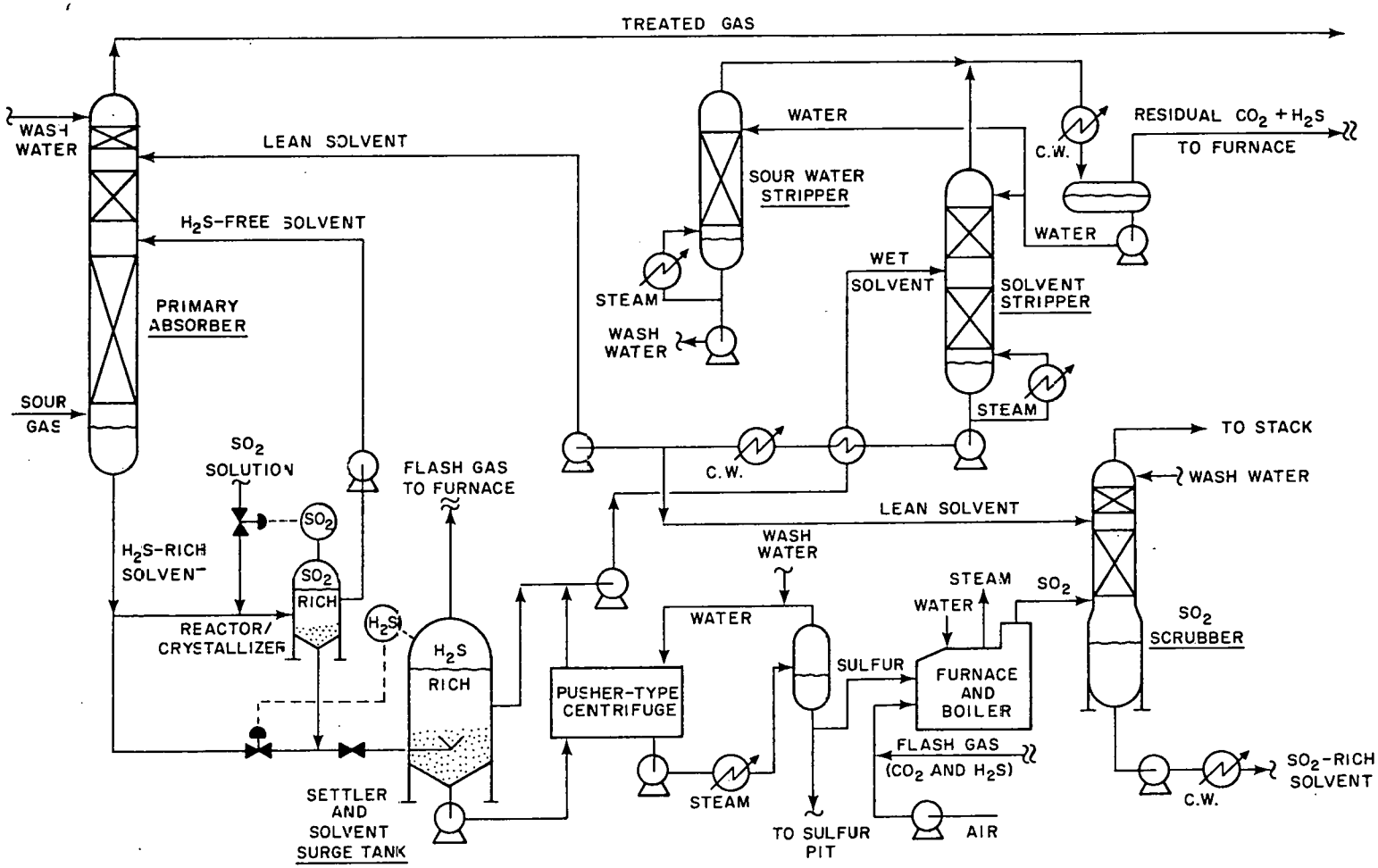

Figure 1 H_2S-Selective Process.

solvent stream containing SO_2 is metered into the same reactor at a rate that keeps the SO_2 content within the reactor a few percent above stoichiometric relative to the H_2S. (It is necessary to have an excess of one reactant or the other in each reactor to avoid excessive reactor volumes and the need for highly precise reactor control.) A clarified overflow from the SO_2-rich reactor is pumped to the primary absorber. This solvent stream has been completely freed of its H_2S content but is still saturated with respect to the other components in the gas being treated in the primary absorber. The net co-absorption of these other gas components (such as CO_2) is thus kept quite small and the effective selectivity for H_2S is of the order of 50. The SO_2 content of this solvent stream, although low, provides a chemical enhancement for the absorption of the H_2S at that point in the primary absorber to facilitate meeting very stringent H_2S specifications in the treated gas. (The temperature in the primary absorber is high enough to prevent precipitation of the sulfur formed by this reaction. Not shown in Figure 1, to avoid clutter, is provision for cooling both reactor/crystallizers with cooling water so that the solvent is sub-saturated in sulfur at all other points in the system.)

The underflow from the SO_2-rich reactor carries the sulfur and water formed in the reaction between H_2S and SO_2. The flow of this stream is sized to keep the water content of the solvent from exceeding 5% and is directly proportional to the rate of H_2S removal - - the flow will typically be about 10% of the total flow of solvent through the primary absorber. Sufficient H_2S-rich solvent, from the primary absorber, is added to the stream to leave a small excess of H_2S after all of the residual SO_2 has reacted. This stream is then flashed to atmospheric pressure in the settler/surge tank. The off-gas from this flash could be recompressed and returned to the inlet of the primary absorber, but more commonly it will simply be vented to the sulfur furnace.

The sulfur made in the process forms a slurry in the underflow from the surge tank. The sulfur is recovered and washed in a centrifuge. In most cases about one-third of the sulfur will be burned in the furnace to make the SO_2 needed in the process. Unless the concentration of H_2S in the gas entering the primary absorber is quite low, the energy recovered in the waste-heat boiler will supply and perhaps exceed the energy required by the process. The furnace is operated under sulfur-rich conditions, with the excess sulfur being condensed in an economizer and recycled to the burner, to prevent SO_3 formation in the combustion gas.

The overflow streams from the surge tank and the centrifuge are combined and sent to the solvent stripper. Boiling most of the water out of the solvent provides a stripping vapor that also removes unreacted H_2S and co-absorbed gases such as CO_2 from the solvent. The condensate from the stripper is used for wash water in the absorbers and centrifuge after passing through the sour water stripper. The net water of reaction is suitable for use as boiler feed water. The vent gas from the stripper is combined with the flash gas from the settler/surge tank and may be sent to the furnace.

Most of the solvent leaving the solvent stripper is used in the SO_2 scrubber where it absorbs the SO_2 from the combustion gas leaving the furnace. The SO_2 content of this solvent is nil, and hence the SO_2 content of the stack gas leaving the scrubber can readily be reduced to the part-per-million level. The solubility of SO_2 in the solvent is quite high, so the concentration of

the solution leaving the scrubber will typically be about 10% SO_2 by weight. The remainder of the solvent from the solvent stripper is sent to the primary absorber, where it prevents loss of SO_2 in the treated gas.

Co-Absorption and Recovery of Other Gases

Figure 2 shows a process configuration suitable for removing and recovering one or more components (in addition to the H_2S) from the gas being treated. An example would be the removal of CO_2 from a synthesis gas ahead of a shift reactor in a process for producing hydrogen. The operation of this process is identical to that described above in many respects. It differs as follows:

At the bottom of the primary absorber is a short section in which much of the H_2 and CO are stripped from the solvent. The stripping gas is obtained by a partial flash of the solvent immediately downstream of the primary absorber. Most of the H_2S-rich solvent stream leaving the flash drum, together with a controlled flow of SO_2 solution, enters an SO_2-rich reactor. The pressure of the SO_2-rich solvent stream is reduced in stages (only two are shown) to about one atmosphere. The off-gas from each stage is recompressed to the pressure desired for the CO_2 product and is contacted with a small amount of neat solvent to remove traces of SO_2, then washed with water to recover solvent vapor. For the case shown, in which a high degree of CO_2 removal is not required, clarified H_2S-free solvent from the atmospheric flash can be pumped directly back to the primary absorber.

As in the flow configuration designed for high H_2S selectivity, the sulfur and water formed in the reaction are conveyed out of the last SO_2-rich reactor in a stream that is rendered H_2S-rich with by-passed H_2S solution. As before, the flow of this stream is proportional to the rate of sulfur production.

CURRENT STATUS OF PROJECT TASKS

Solubility Studies

The solubility studies are complete. The solubilities of H_2S, SO_2, CO_2, propane and butane were measured in several polyglycol ethers as functions of temperature and pressure. The data are correlated well by Henry's Law. Sulfur solubilities were measured in the same solvents and the effect of water content on all solubilities was determined.

Reaction Kinetics

Ambient-temperature kinetics studies have been completed. The reaction is first-order with respect to both H_2S and SO_2 concentrations. A very effective family of catalysts (heterocyclic aromatic nitrogen compounds) has been identified. A catalyst concentration of less than 1 wt % is sufficient to ensure 99+ % reaction in a residence time of one minute. Still to be determined are the effect of temperature on reaction kinetics and verification that the reaction order persists at very low concentrations of H_2S and SO_2.

Corrosion Studies

Corrosion studies were performed by submerging metal coupons half way in a

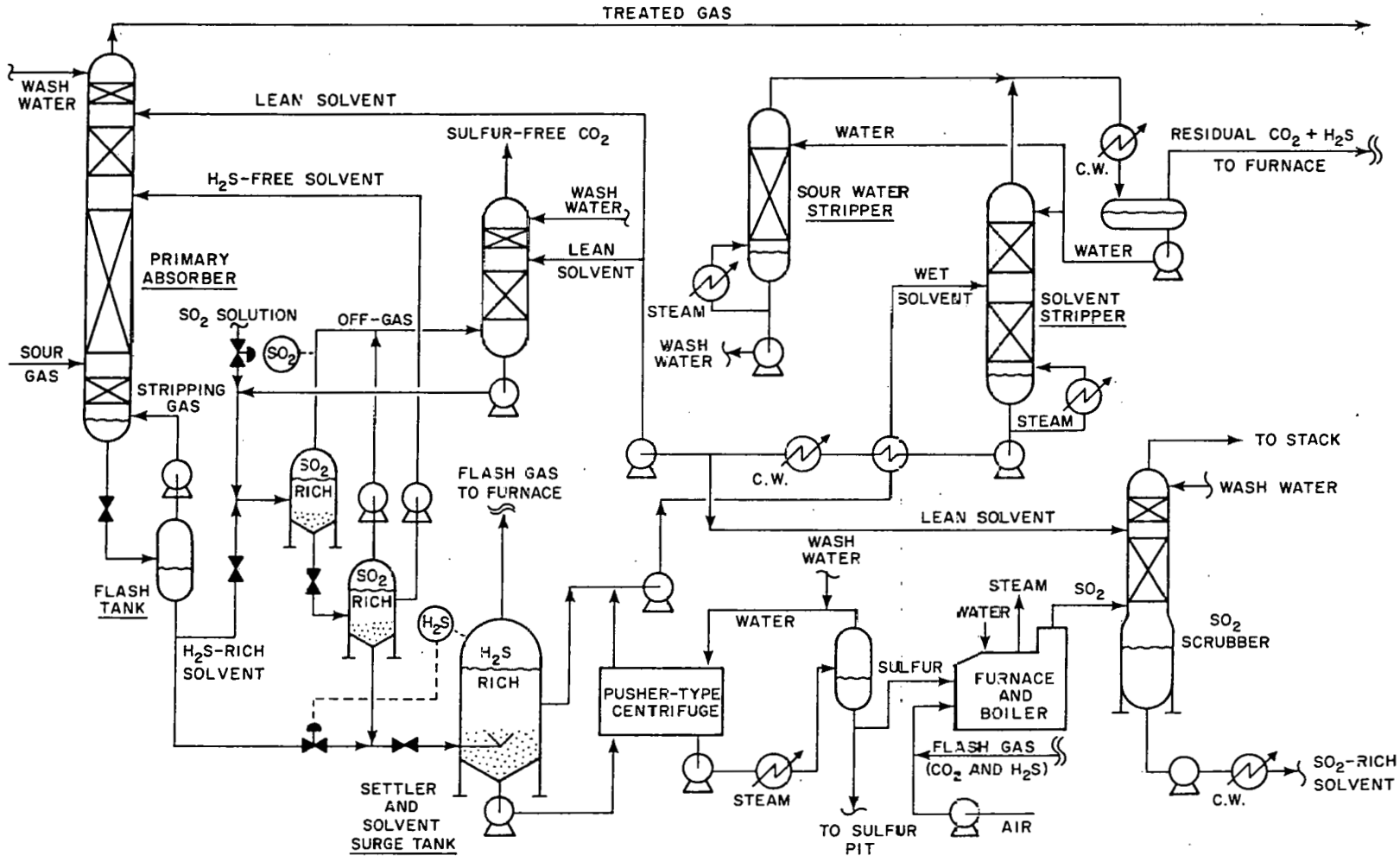

Figure 2 Co-Absorption Process.

solution of H_2S or SO_2 in a glycol ether. To make the system as corrosive as possible, the solvent was a mono-ether (which is also an alcohol) and sulfur and water were added in concentrations twice (or greater) those encountered in the process. The exposure was carried out for three successive 20 to 30-day periods at each temperature. Table 1 shows the corrosion rates observed.

Table 1 Corrosion Rates of Steels in Process Solutions.

	MEASURED RATES AND CONDITIONS *		
Metal	SO_2: @ 100°C	@ 120°C	H_2S @ 150°C
Carbon Steel	0.6	1.7	0.05
304 Stainless	0.7	1.5	0.02
316 Stainless	1.3	4.8	0.01

* Mils/year in diethylene glycol methyl ether, 5% H_2O, saturated with sulfur, 50 - 100 psi gas pressure.

Since 60°C is the maximum temperature at which SO_2 is present (outlet of the SO_2 absorber), carbon steel and 304 and 316 stainless steels should corrode at rates much less than 1 mil/year (0.02 mm/yr) under all process conditions.

Sulfur Crystallization

A major potential advantage of the UCB Sulfur Recovery Process is the purity of the crystalline sulfur that is produced. To realize this advantage fully, one must produce relatively large (100+ micrometers) sulfur crystals. The sulfur crystallizes from solution both as a result of cooling and as a result of chemical reaction between H_2S and SO_2. In the former casewhich is being studied first, the degree of supersaturation is relatively low because the solubility of sulfur in the solvent varies only a few grams per liter over the temperature range of interest. A substantially higher concentration of sulfur can result from the chemical reaction.

The crystallizer consists of a well-stirred 2-liter vessel. Hot saturated feed enters at the top, and the vessel walls are cooled. Cold effluent exits at the bottom of the vessel as a sulfur/solvent slurry. The solids residence time is the same as that of the liquid. During a run a sample of the effluent slurry is collected by diverting the entire effluent stream momentarily into a flask. The size distribution of the sulfur crystals is then determined by sedimentation analysis, an example of which is shown in Figure 3.

Preliminary data obtained with this system are shown in Table 2. Five runs were made where the liquid residence time was varied from 2.80 to 5.10 mins. The feed solution was saturated with sulfur at 50° $\pm$ 1°C, then heated to 52° $\pm$ 1°. The crystallization temperature was held constant at 32° $\pm$ 2°. As expected, the mean particle diameter increases with increasing residence time. The similarity of the results for runs 4A and 4B shows the reproducibility of the sedimentation analysis. Comparing the results of runs 2 and 3 shows the variation between runs with similar operating conditions.

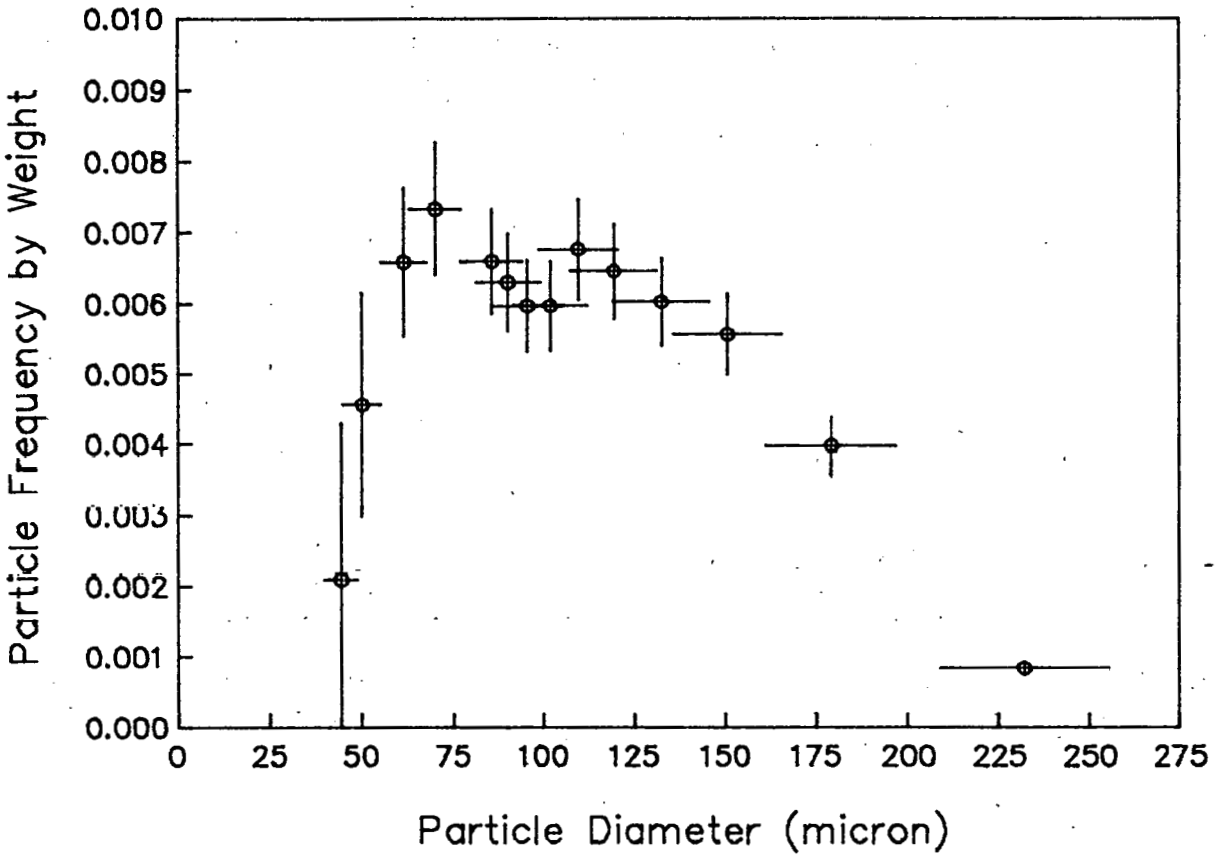

Figure 3 Crystal-Size Distribution by Sedimentation Analysis.

Table 2 Variation of Average Crystal Size with Residence Time.

Run	Residence Time (min.)	Mean Diameter (microns)
1	5.10 ± 0.18	110 ± 6
2	3.64 ± 0.13	101 ± 6
3	3.64 ± 0.13	82 ± 5
4A	2.80 ± 0.10	84 ± 5
4B	2.80 ± 0.10	74 ± 5

Gas Absorption with Chemical Reaction

Tray efficiency data are needed for two process situations. In one, H_2S at very low concentration is being absorbed by a chemically reactive solution of

SO_2. This condition obtains near the top of the primary absorber. In the other, gaseous SO_2 in the low parts-per-million concentration range is absorbed by lean process solvent. This condition corresponds to the top of the SO_2 absorber. Both are of interest because one wishes to effect very stringent sulfur removal with the UCBSRP. The equipment for this project consists of a single seive tray (or section of packed column) placed in a test section of a closed flow loop through which a gas stream can be circulated. A stream of solvent from a feed tank passes through the test section and is collected at the outlet. The H_2S or SO_2 content and the flow of both the gas and the liquid streams entering and leaving the test section can be monitored under steady-state conditions. Murphree tray efficiencies (or over-all mass-transfer coefficients) are determined from the mass balances and the solubility data mentioned above.

The results of an initial set of experiments measuring SO_2 absorption are shown in Table 3. Four absorption runs were performed at 41°C with inlet gas-phase SO_2 concentrations varying from 230 ppm to 1850 ppm. Gas-phase SO_2 concentrations were measured by a pulsed fluorescent SO_2 analyzer and liquid-phase concentrations were measured by titration.

Table 3 SO_2 Absorption by Triglyme at 41°C and 126 kPa.

Inlet ppm	Outlet ppm	X_{out}	E_{mv}
230	165	0.00044	0.84
640	550	0.00087	0.29
1175	950	0.0017	0.38
1850	1600	0.0038	0.47

At the low liquid-phase concentrations (less than 0.028 M SO_2 in triglyme) of these runs the titrations were not accurate, and large errors occurred in the mass balance between the gaseous SO_2 fed to the absorber and the SO_2 absorbed by the solvent. Investigation showed that the titrations yielded inaccurate results, so the outlet liquid-phase concentration of SO_2 (x_{out}) necessary for calculating the Murphree tray efficiency (E_{mv}) was calculated from the difference between the inlet and outlet gas concentrations and the inlet liquid concentration. The efficiency of 84 percent for the lowest-concentration run is probably a spurious result since all previous runs have shown E_{mv} in the 30 to 50 percent range as do the runs at higher concentration shown above.

7. FUTURE WORK:

EXPERIMENTAL STUDIES

Reaction Kinetics

The interpretation of the experiments in which H_2S is absorbed by dilute solutions of SO_2 depends upon knowledge of the reaction-rate constant at

absorber conditions. These conditions are both more dilute and at a higher temperature than those of the earlier kinetics experiments, which were run to obtain design data for the reactor/crystallizers. A spectrophotometric technique is being developed for this new study.

Sulfur Crystallization

The crystallizer is being modified to incorporate crystal size classification. In the new flow scheme, a portion of the effluent that overflows the top of the crystallizer will be pumped up an elutriation tube attached to the bottom of the vessel. Large-diameter crystals with a terminal settling velocity equal to or greater than the fluid velocity in the tube will fall down the tube and into a sample chamber. The hot feed will be injected in the lower portion of the crystallizer, into a fluidized bed of larger crystals. This will produce a supersaturation zone in the vicinity of the largest crystals, providing more crystal growth and less nucleation than in the current design. The expected increase in crystal size results from increasing the residence time in the crystallizer of the solids relative to the liquid.

Gas Absorption with Chemical Reaction

Future work will include development of an analytical technique for measuring very low concentrations of SO_2 in the process solvents using UV spectroscopy. Data obtained for absorption of H_2S enhanced by the presence of SO_2 in the solvent will be used to develop a model that incorporates the reaction kinetics work described above.

Computer Modelling and Process Evaluation

A computer model that simulates all of the unit operations in the process is operational and facillitates process synthesis for specific applications. This calculational tool was used in the economic evaluation of one application of the process where there was found to be a reduction of about one-third in capital investment and a substantial improvement in operating costs relative to conventional technology (see Section 8 below). The same approach will be used to evaluate and further refine the process configurations shown in Figures 1 and 2 for the purification of hydrogen derived from gasified coal. This study will include consideration of the energy efficiency involved in integrating the UCBSRP with the process of producing hydrogen from coal-derived synthesis gas.

8. ARTICLES AND PRESENTATIONS:

Demyanovich, R.J. and Lynn, S. 1987. Vapor-Liquid Equilibria of Sulfur Dioxide in Polar Organic Solvents. I&EC Research 26 548.

Lynn, S., Neumann, D.W., Sciamanna, S.F., and Vorhis, F.H. 1986. A Comparison of the UCB Sulfur Recovery Process with Conventional Sulfur Recovery Technology. Presented at Boston Meeting, AIChE, August, 1986.

Neumann, D.W. and Lynn, S. 1986. Kinetics of the Reaction of H_2S and SO_2 in Organic Solvents. I&EC Proc. Des. & Dev. 25 248.

GAS SEPARATION BY PRESSURE SWING ADSORPTION FOR PRODUCING HYDROGEN FROM COAL

1. CONTRACT NUMBER: DE-AC21-85MC22060

CONTRACTOR:
State University of New York
Department of Chemical Engineering
Buffalo, New York 14260
(716) 636-2519

PRINCIPAL INVESTIGATOR: Ralph T. Yang

METC PROJECT MANAGER: Lisa A. Jarr

PERIOD OF PERFORMANCE: May 17, 1985 - November 16, 1987

2. SCHEDULE/MILESTONE:

Test Plan	June 1985 - September 1985
Equilibrium Adsorption	
Equipment Construction	June 1985 - October 1985
Pure Gases	September 1985 - May 1986
Mixtures	November 1985 - June 1987
Diffusivities in Zeolite	
Equipment Construction	June 1985 - November 1985
Diffusivity Measurement	November 1985 - June 1987
Zeolite PSA Cycles	
Equipment Construction	June 1985 - September 1985
PSA Cycles for Binary to Five-Component Mixtures	October 1985 - June 1987
Modeling	October 1985 - November 1987
Computer Software for Zeolite PSA Models and Final Report	July 1987 - November 1987

3. OBJECTIVES:

The objective of this contract is to develop a zeolite pressure swing adsorption (PSA) process to be used for the production of hydrogen from coal gasification products. The objective is illustrated in Fig. 1, which clearly shows the advantage in process simplicity for PSA over the conventional process.

4. BACKGROUND STATEMENT:

Low-energy, economical gas separation processes are required as alternatives to energy-intensive and costly technologies such as cryogenic distillation and wet scrubbing for gasification products to produce hydrogen from coal. Gas separation and acid gas removal processes currently constitute a significant fraction of the total cost of hydrogen production from coal. SUNY (Buffalo) has demonstrated that PSA processes using activated carbon offer the potential for an economic separation of

HYDROGEN FROM COAL

CONVENTIONAL:

NEW(DOE):

Figure 1. Comparison of Schemes for Hydrogen Production from Coal.

hydrogen from gas mixtures similar in composition to gasification products. Adsorption of gases on zeolites, as compared to activated carbon, have higher selectivities toward certain gases, and give better separations and products of higher purity. High-purity hydrogen (99.999%) is required by an increasing number of industries such as electronics, semiconductors and metal treating industries. Such a high-purity hydrogen can only be produced by using zeolite as the sorbent.

The commercial PSA process for hydrogen purification is illustrated in Fig. 2. It is not feasible to use this PSA process for bulk separation, that is, for feed mixtures containing less than 50% H_2 (by vol.). A typical coal gasification product contains 20-30% H_2. Thus, this project aims at developing PSA cycles for producing hydrogen at purities in the range of 99.0 - 99.999% from coal gasification products.

5. PROJECT DESCRIPTION:

For the purpose of understanding and modeling the PSA separation, information must be gathered on the thermodynamic (equilibrium adsorption isotherms) and transport (diffusivities) properties. Therefore, the project encompasses the following four major tasks:

- To measure equilibrium adsorption of pure-component and mixtures of gases on zeolite sorbent. The gases are H_2, CO, CH_4, CO_2 and H_2S. The sorbent is 5A zeolite. The temperatures are 23 and 100°C and the total pressure range is 0 - 1000 psia.

- To measure diffusivities of the above-mentioned gases in 5A zeolite.

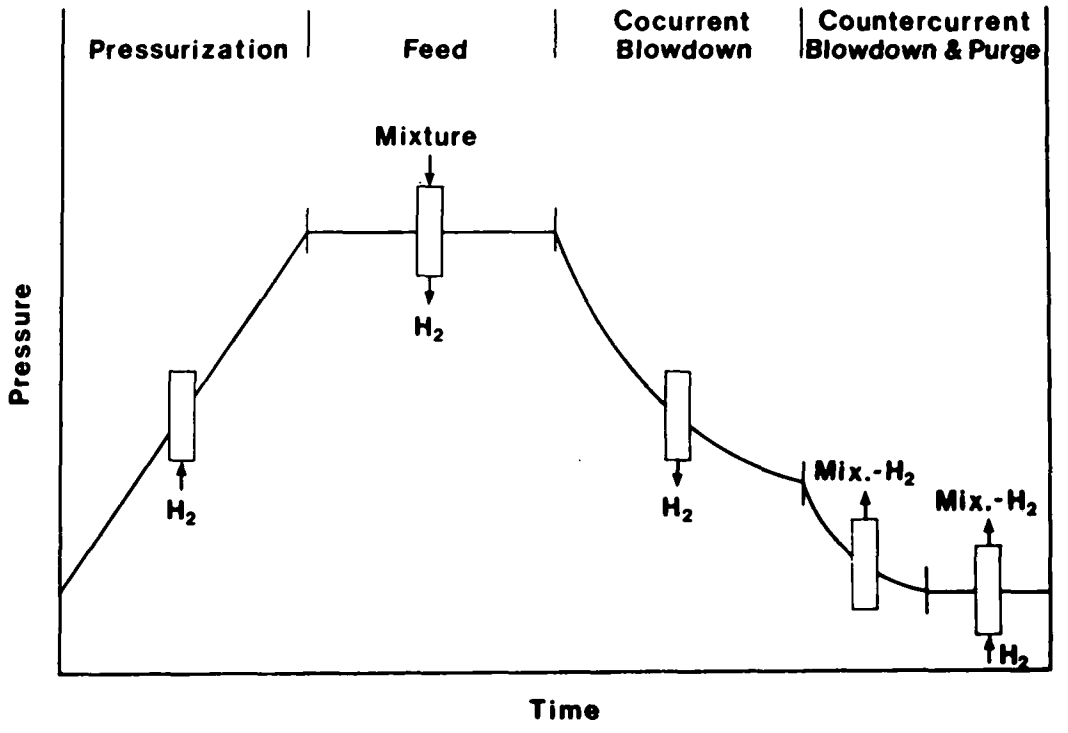

Figure 2. PSA Cycle for Hydrogen Purification.

- To carry out experiments on PSA cycles using 5A zeolite as the sorbent for separating coal gasification products, to determine the most efficient PSA cycles, and to determine the optimal PSA cycle conditions for the best separations.

- To develop mathematical models for the PSA cycles which can be used for design, control, and scale-up.

6. RESULTS/ACCOMPLISHMENTS:

EQUILIBRIUM ADSORPTION

Equilibrium adsorption of mixtures of H_2, CO, CH_4, CO_2 and H_2S on 5A zeolite has been measured at 20°C to 100°C at total pressures below 800 psig. A complete database has been established for mixtures ranging from binary to five-component. Approximately 120 sets of mixture data were gathered in this program. In general, the ideal adsorbed solution theory (IAS) does not correlate the data well. The data were correlated more satisfactorily by the loading ratio correlation (LRC), which is used for PSA process design and modeling purposes.

DIFFUSIVITIES IN ZEOLITE CRYSTALS

Diffusivities of the five aforementioned gases in zeolite 4A and 5A crystals have been measured, at 20 and 100°C.

NEW PSA PROCESSES

New PSA processes have been developed for separating coal gasification products into either a high-purity hydrogen (over 99.999%) or a clean (H_2S-free) synthesis gas (H_2 + CO). A five-component gas mixture simulating Texaco gasifier product was used in the experiments. The gas mixture contained: H_2(36.0%), CO(50.0%), CH_4(0.8%), CO_2(12.0%) and H_2S(1.2%). The two PSA cycles developed for high-purity H_2 production are:

Cycle A

Step I	H_2 Pressurization, 4 min.
Step II	Adsorption, 4 min.
Step III	Cocurrent Blowdown, 4 min.
Step IV	Countercurrent Evacuation, 4 min.

Cycle B

Step I	H_2 Pressurization, 4 min.
Step II	Adsorption, 4 min.
Step III	Cocurrent Blowdown, 4 min.
Step IV	Countercurrent Evacuation, 2 min.
Step V	Countercurrent Vacuum Purge, 2 min.

The cycles for producing H_2S-free synthesis gas are:

Cycle C

Step I	Feed Gas Pressurization, 4 min.
Step II	Cocurrent Blowdown, 4 min.
Step III	Countercurrent Evacuation, 4 min.

Cycle D

Step I	Feed Gas Pressurization, 4 min.
Step II	Adsorption, 4 min.
Step III	Cocurrent Blowdown, 4 min.
Step IV	Countercurrent Evacuation, 4 min.

Typical experimental results for H_2 production from Texaco gasifier products by cycles A and B are shown, respectively, in Tables 1 and 2. Both cycles were able to produce a five-nine purity hydrogen. Cycle B differed from cycle A in the additional vacuum purge step. This step caused a smaller breakthrough of CO and CH_4 toward the end of Step III, and hence a higher hydrogen purity in Step III. The product recovery and feed throughput in both cycles were high as compared with commercial PSA processes for H_2 purification.

Table 1. H_2 Production from Texaco Gasifier Product Using Cycle A. Feed P = 200 psig, End P of Step III = 15 psig, End P of Step IV = 7.8 psia. (Sorbent: 5A zeolite, 510 g; All Vol. in STP)

Step	Time, s	Flow Rate, ℓ/min	Effluent Composition, mol %				
			H_2	CO	CH_4	CO_2	H_2S
II	270	1.25	99.999+	0.000	0.000	0.000	0.000
	330	1.25	99.999+	0.000	0.000	0.000	0.000
	390	1.25	99.999+	0.000	0.000	0.000	0.000
	450	1.25	99.999+	0.000	0.000	0.000	0.000
III	510	1.76	99.999+	0.000	0.000	0.000	0.000
	570	1.83	99.999+	0.000	0.000	0.000	0.000
	630	1.77	99.999+	0.000	0.000	0.000	0.000
	660	1.67	99.057	0.943	0.000	0.000	0.000
	690	1.47	83.763	16.225	0.012	0.000	0.000
IV	750	2.78	13.002	66.361	0.986	17.907	1.744
	810	1.41	6.146	73.503	1.116	17.587	1.648
	870	0.76	3.882	75.375	1.127	17.814	1.802
	930	0.62	1.354	77.148	1.127	18.369	2.002

Step	Total Effluent, ℓ/cycle	Average Effluent Composition, mol %				
		H_2	CO	CH_4	CO_2	H_2S
II	5.00	99.999+	0.000	0.000	0.000	0.000
III	6.41	97.378	2.620	0.002	0.000	0.000
IV	5.57	8.726	70.600	1.054	17.865	1.755
Product Recovery, %		83.54	95.90	99.80	99.99+	99.99+

Feed Amount = 8.20 ℓ/cycle, H_2 Used in Step I = 8.78 ℓ/cycle.

Typical results for clean syngas production are shown in Tables 3 and 4 for, respectively, Cycles C and D. Both cycles produced an H_2S-free syngas and the product recoveries for both H_2 and CO were high. Cycle D differed from Cycle C in the additional feed step (Step II in Cycle D). From Tables 3 and 4 it is seen that the additional feed step substantially increased the feed throughput while not affecting the product purity and recovery.

Two types of PSA models have been developed: equilibrium model and bidisperse pore diffusion model. In the equilibrium model, all mass transfer resistances are neglected. The bidisperse pore diffusion model include the diffusion resistances in both crystals and binder in the zeolite pellets.

7. FUTURE WORK:

The project is being successfully drawn to a conclusion. The remaining effort will be the completion of PSA parametric experiments and the mathematical models.

Table 2. H_2 Production from Texaco Gasifier Product Using Cycle B. Feed P = 200 psig, End P of Step III = 15 psig, End P of Step IV = 7.8 psia. (Sorbent: 510 g 5A zeolite; All Vol. in STP).

Step	Time, s	Flow Rate, ℓ/min	Effluent Composition, mol % H_2	CO	CH_4	CO_2	H_2S
II	270	1.25	99.999+	0.000	0.000	0.000	0.000
	330	1.25	99.999+	0.000	0.000	0.000	0.000
	390	1.25	99.999+	0.000	0.000	0.000	0.000
	450	1.25	99.999+	0.000	0.000	0.000	0.000
III	510	1.78	99.999+	0.000	0.000	0.000	0.000
	570	1.93	99.999+	0.000	0.000	0.000	0.000
	630	1.80	99.999+	0.000	0.000	0.000	0.000
	660	1.80	99.999+	0.000	0.000	0.000	0.000
	690	1.71	98.464	1.536	0.000	0.000	0.000
IV	750	2.87	16.730	62.842	0.965	17.689	1.774
	810	1.41	7.405	72.292	1.162	17.386	1.755
V	870	1.02	8.730	71.947	1.144	16.503	1.676
	930	1.04	20.208	63.646	1.043	13.496	1.607

	Purge H_2, ℓ/min
870	0.19
930	0.21

Step	Total Effluent, ℓ/cycle	Average Effluent Composition, mol % H_2	CO	CH_4	CO_2	H_2S
II	5.00	99.999+	0.000	0.000	0.000	0.000
III	7.22	99.715	0.285	0.000	0.000	0.000
IV	6.34	13.940	66.540	1.051	16.743	1.726
Product Recovery, %		71.08	99.38	99.99+	99.99+	99.99+

Feed Amount = 8.49 ℓ/cycle, H_2 Used in Step I = 9.62 ℓ/cycle.

Table 3. Synthesis Gas Production from Texaco Gasifier Product Using Cycle C. End P of Step I = 200 psig, End P of Step II = 1 psig, End P of Step III = 9.3 psia. (Sorbent: 510 g 5A zeolite; All Vol. in STP).

Step	Time, s	Flow Rate ℓ/min	Effluent Composition, mol % H_2	CO	CH_4	CO_2	H_2S
II	270	5.45	81.335	18.427	0.238	0.000	0.000
	330	3.07	19.295	79.286	1.419	0.000	0.000
	390	2.27	8.334	90.090	1.576	0.000	0.000
	450	0.84	2.957	95.521	1.522	0.000	0.000
III	510	1.02	0.724	34.920	0.629	56.001	7.726
	570	0.83	0.340	37.515	0.621	56.149	5.357
	630	0.78	0.098	45.918	0.625	48.907	4.452
	690	0.69	0.000	50.176	0.623	45.436	3.765

Step	Total Effluent, ℓ/cycle	Average Effluent Composition, mol % H_2	CO	CH_4	CO_2	H_2S
II	11.63	45.048	54.048	0.904	0.000	0.000
III	3.32	0.330	41.323	0.625	52.176	5.546
Product Recovery, %		99.79	82.08	83.52	99.99^+	99.99^+

Feed Amount = 14.95 ℓ/cycle.

Table 4. Synthesis Gas Production from Texaco Gasifier Product Using Cycle D. End P of I and Feed P = 200 psig, End P of III = 1 psig, End P of IV = 9.8 psig. (Sorbent: 510 g 5A zeolite; All Vol. in STP).

Step	Time, s	Flow Rate, ℓ/min	Effluent Composition, mol %				
			H_2	CO	CH_4	CO_2	H_2S
II	270	1.40	66.388	33.000	0.505	0.107	0.000
	330	1.35	63.574	35.702	0.536	0.188	0.000
	390	1.31	60.914	38.349	0.560	0.177	0.000
	450	1.31	59.758	39.508	0.597	0.137	0.000
III	510	3.78	57.084	42.082	0.670	0.164	0.000
	570	3.59	38.796	59.997	0.958	0.249	0.000
	630	3.25	18.385	80.020	1.224	0.371	0.000
	690	1.44	10.836	87.314	1.243	0.580	0.000
IV	750	1.86	4.253	32.006	0.560	56.789	6.392
	810	1.07	0.055	28.209	0.593	64.894	6.249
	870	0.83	0.037	30.702	0.567	62.448	6.246
	930	0.57	0.000	32.858	0.628	60.290	6.224

Step	Total Effluent, ℓ/cycle	Average Effluent Composition, mol %				
		H_2	CO	CH_4	CO_2	H_2S
II	5.37	62.728	36.572	0.549	0.151	0.000
III	10.26	35.689	63.043	0.974	0.294	0.000
IV	4.33	1.847	30.430	0.579	60.337	6.307
Product Recovery, %		98.97	87.72	85.43	98.36	99.99^+

Feed Amount = 21.76 ℓ/cycle.

GAS SEPARATION USING ION EXCHANGE MEMBRANES FOR PRODUCING HYDROGEN FROM SYNTHESIS GAS

1. DOE CONTRACT NUMBER: DE-AI21-86MC23120

   CONTRACTOR: National Bureau of Standards
   Center for Chemical Engineering
   Boulder, CO 80303-3328

   CONTRACTOR PROGRAM MANAGER: Dr. Richard D. Noble

   PRINCIPAL INVESTIGATORS: Dr. Richard D. Noble

   METC PROJECT MANAGER: Lisa A. Jarr

   CONTRACT PERIOD OF PERFORMANCE: May 26, 1986 to May 26, 1988

2. SCHEDULE/MILESTONES:

Legend: ∇ Task Initiated
Δ Task Completed
O Major Reports

Schedule of Performance			Months from Start
Task	Subtask	Title	2 4 6 8 10 12 14 16 18 20 22 24
1		Test Plan	∇—Δ
2		Facilities Construction	
	2.1	Safety Modifications	∇—Δ
	2.2	Fabrication of New Membrane Cell	∇—Δ
3		Membrane Testing	
	3.1	Membrane Preparations and Configuration	∇———Δ
	3.2	Shift Products Separation	∇———Δ
	3.3	Gasifier Products Separation	∇———Δ
4		Mathematical Modeling	
	4.1	Modification of Existing Models	∇——Δ ∇——Δ
	4.2	Comparison with Experimental Results	∇———Δ
		Comprehensive Topical Report	O——O

3. OBJECTIVES:

   - Evaluate candidate facilitated transport ion exchange membrane systems.
   - Study the effect of membrane performance due to feed gas concentration, carrier chemistry, pressure, and temperature.
   - Develop mathematical models, as needed.

4. BACKGROUND STATEMENT:

The most widely used method for producing H_2 is steam reforming of CH_4. The production costs are very sensitive to feedstock (CH_4) costs. Production of H_2 from coal is projected to become economical when the CH_4 price reaches $7.00/MMBTU (Bartis and Marks, 1984). The Energy Information Administration indicates that this will occur in the period between 1990 and 1995. Thus, it is appropriate at this time to conduct research which has the best opportunities for reducing H_2 production costs from coal gasification.

High temperature coal gasifiers have the most favorable conditions for H_2 production. Uniform high temperatures in fluidized-bed and entrained-flow gasifiers cause cracking of hydrocarbons to occur. Also, oxygen reacts with the devolatilization products to produce H_2, CO, and CO_2.

It is also desirable to maximize CO production. CO can be converted to H_2 using the water gas shift reaction. Figure 1 shows a block flow diagram for a typical entrained-flow process. Table 1 gives typical gasifier exit mole fractions for two different gasifiers.

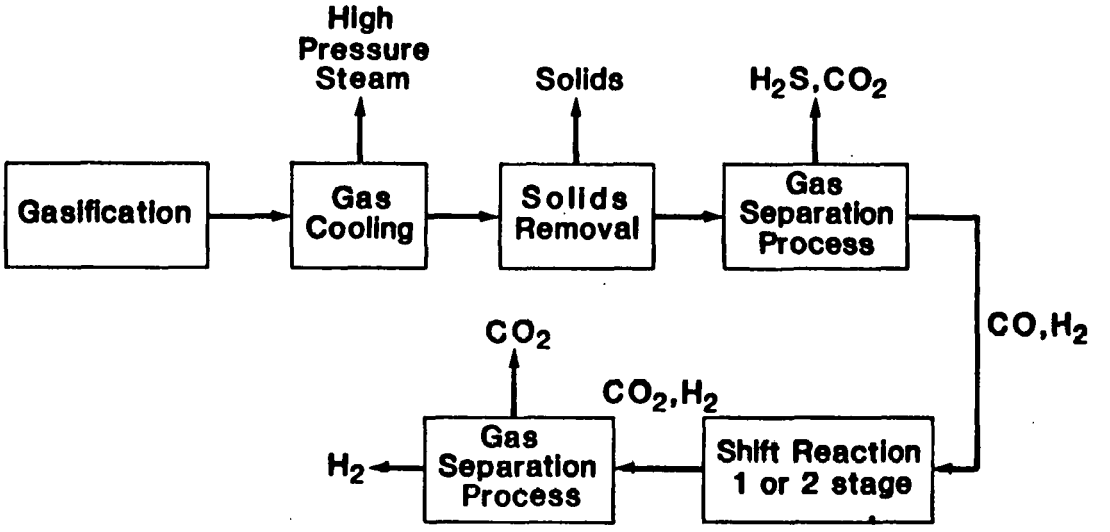

Figure 1. Block Diagram of Entrained-Flow Coal Gasification Process to Produce H_2.

Table 1. Gasifier Exit Mole Fractions.

Gasifier	CO_2	H_2S	CO	H_2
Koppers-Totzek (GKT)	.061	.006	.434	.187
Texaco	.102	.01	.41	.298

Bartis and Marks have identified low energy separation processes such as membranes as a key research opportunity in reducing capital and operating costs and hence the H_2 production costs. They state that technical improvements in gas separation could lead to production cost reductions of 15 to 20 percent. Referring to figure 1, there are two points at which gas separations are required. CO_2 and H_2S must be removed from the gas stream after gasification and prior to the shift reaction. This separation step prevents sulfur poisoning of the shift catalysts and maximum H_2 production from the shift reaction. The second gas separation occurs after the shift reaction. CO_2 must be removed from the product stream to produce high purity H_2.

This approach has the advantage that high and low temperature sulfur sensitive catalysts can be used for the shift reaction. A staged shift sequence can be used. An initial step at high temperature can allow for steam recovery. A second shift step at low temperatures can follow where the equilibrium favors H_2 production.

A second approach is to immediately shift the gasifier products and then separate the CO_2 and H_2S from the H_2. This approach required highly sulfur resistant and more costly catalysts. The disadvantage of this approach is that the product gas contains several percent CO which must be removed by pressure swing adsorption or methanation.

The use of membrane separations for the gas separation processes described above is an area deserving special attention because of its great potential for low capital cost and energy efficiency. A membrane process could theoretically separate a binary mixture reversibly, and therefore consume only the minimum work to accomplish the separation. The implicit simplicity and energy efficiency of membrane processes have stimulated basic and applied research for many years. To date, few membrane processes other than reverse osmosis and nitrogen separation from air have demonstrated any industrial utility primarily because of the problems of speed and selectivity in separation. The diffusion coefficient of most molecules is so low that exceedingly thin membranes must be constructed to produce industrially acceptable fluxes. These thin polymer membranes may have fabrication and mechanical integrity problems. Selectivity has usually been poor in membrane systems unless the mixture components are radically different, as in desallination.

An example of selectivity problems is worth discussing at this point. As described above, a critical separation step is the separation of CO_2 and H_2. Commercially available polymer membranes, such as the Monsanto Prism system, cannot separate these gases very well. The permeability (product of diffusivity and solubility) for each gas is approximately equal; therefore, a separation is difficult.

An alternative approach to developing high performance membranes is to use liquids as membrane materials, and incorporate in the liquids materials which will chemically augment or facilitate the transport of one component across the membrane. Facilitated transport in liquid membranes employs a reversible chemical reaction. The liquid membrane

contains a mobile carrier species which remains in the membrane phase. At one interface, the membrane phase contacts the phase rich in the permeant species (extract phase). The carrier reacts with the permeate to form a complex. The complex diffuses to the opposite boundary where the reverse reaction takes place. This frees the permeate into the permeate-lean phase (receiving phase). In this way, a very selective separation with corresponding high fluxes can be achieved. The overall mass transfer rate in a facilitated transport system is not determined by equilibrium between the fluid phase and the membrane phase. Instead, the transport process is established by a coupling of diffusion and the complexation reaction rate. Also, the separation takes place without the large energy consuming step of a phase change (i.e. distillation) or a large pressure drop (i.e. polymeric membranes).

Liquid membranes for gas separations have typically been prepared by immobilizing the solvent-carrier solution in a thin support. Two primary problems are associated with immobilized liquid membranes (ILMs): loss of solvent and loss or deactivation of the carrier. Solvent loss occurs when solvent evaporates or is forced from the support pore structure by large transmembrane pressures. Carrier loss can occur when solvent in the feed stream condenses on the feed due to a pressure gradient which would leak out the carrier. The passage of one or more pore volumes of solvent through the membrane would drastically reduce carrier concentration. Irreversible side reactions of the carrier with impurities in the gas stream could lead to deactivation or breakdown of the carrier.

A promising solution to the problems with ILMs has been to use ion exchange membranes as a support for complexation agents. A cationic or anionic carrier is exchanged into an appropriate nonporous ion exchange membrane to form the facilitated transport membrane. This configuration has the advantage that the carrier cannot easily be forced out of the support since the carrier is retained by strong electrostatic forces. Carrier concentrations can be increased because the concentration is limited by ion exchange sites and not by physical solubility. Ion exchange membranes provide longer operating lifetimes in adverse conditions where conventional ILMs may be subject to carrier or solvent loss. Ion exchange membranes also have the benefit of greater mechanical strength. Previous work with ion exchange membranes for CO_2 and H_2S separation have shown that the ion exchange configuration is superior to the ILM, even at equivalent thicknesses.

The real potential of facilitated transport membranes is to improve the selectivity of the separation without sacrificing high fluxes. The importance of our previous work (Way et al., 1987; Way and Noble, 1987)is that we have demonstrated experimentally that a reactive ion exchange membrane can be highly selective for CO_2 and H_2S over hydrocarbons and still have high fluxes. In addition, our understanding of the transport mechanisms involved has enabled us to simulate our experimental data theoretically which is necessary for scale-up and design.

The separation problems associated with the production of H_2 via coal gasification are the removal of CO_2/H_2S and the separation of a CO_2/H_2 gas mixture. We have demonstrated expertise with facilitated transport membranes for CO_2 and H_2S. As stated above, the CO_2/H_2 separation is difficult using a polymer membrane because of selectivity limitations. Therefore, facilitated transport is an ideal novel approach to improve the economics of H_2 production.

We have been successful in transferring the technology we have developed to industry. The DOE is in the process of filing a patent application for our work. We have made presentations at several national meetings (AIChE, ACS) and there has been very strong industrial interest in our work from DuPont, Dow, Union Carbide, Airco, Air Products, Bend Research, and SRI International.

5. PROJECT DESCRIPTION:

The overall goal of the proposed work is to demonstrate the use of facilitated transport membranes in the production of hydrogen from synthesis gas. The objectives of the project are as follows:

1. Evaluate the feasibility of candidate facilitated transport liquid membranes for application to the H_2 recovery process.

2. Determine the effect of pressure, temperature, feed gas concentration, carrier chemistry, and membrane configuration on the performance of facilitated transport liquid membranes for the separation of CO_2, CO, H_2S, and H_2.

3. Determine the lifetime of promising membranes for the separations described above.

4. Develop mathematical models for the prediction of experimental results, scale-up, process design, and optimization of a membrane-based separation scheme for producing H_2 from coal.

5. Perform a preliminary process design and economic analysis to demonstrate the feasibility of using membrane technology in coal gasification processes to produce H_2 from coal.

The scope of work below outlines our plans to complete these objectives over a three year period. The DOE will evaluate the progress made after 22 months to determine if the work planned for the third option year should be funded.

6. RESULTS/ACCOMPLISHMENTS:

Two ion-exchange films have been studied. The first film is a perfluorosulfonic acid ionomer. A polybenzimidizole (PBI) film was also used. Both films are cationic. Sodium was exchanged into each film to study the basic permeability of the membrane. Sodium does not react with

the gases studied. Ethylenediamine (EDA) was exchanged into each film to form a reactive membrane since EDA reacts with both CO_2 and H_2S.

Pure H_2 fluxes were measured using the perfluorosulfonic acid ionomer in the EDA form. For feed gases consisting of 25 and 50 mole % H_2, the H_2 fluxes were 3.19×10^{-10} and 6.58×10^{-10} gmol/cm^2.s, respectively. A H_2/CO_2 selectivity experiment was also performed. For a 50/50 mole % feed gas, the CO_2 flux was 2.75×10^{-9} and H_2 flux was 2.20×10^{-10} gmol/cm^2.s. This corresponds to a CO_2/H_2 separation factor of 12.5. This is significant since a commercial polysulfone hollow fiber system has a H_2/CO_2 separation factor of 2.7.

The PBI film was used in the sulfonated form. The major problem with this film was the tendency to lose water. This water loss led to a reduction in flux for both CO_2 and H_2. For example, for a 40% CO_2 feed, the flux went from 2.7×10^{-9} to 1.3×10^{-9} gmol/cm^2.s over a period of four days using the Na form. The EDA form did facilitate CO_2 transport, although the data was very scattered. In general, the CO_2 flux was a factor of 10 or better using the EDA form compared to the Na form. For

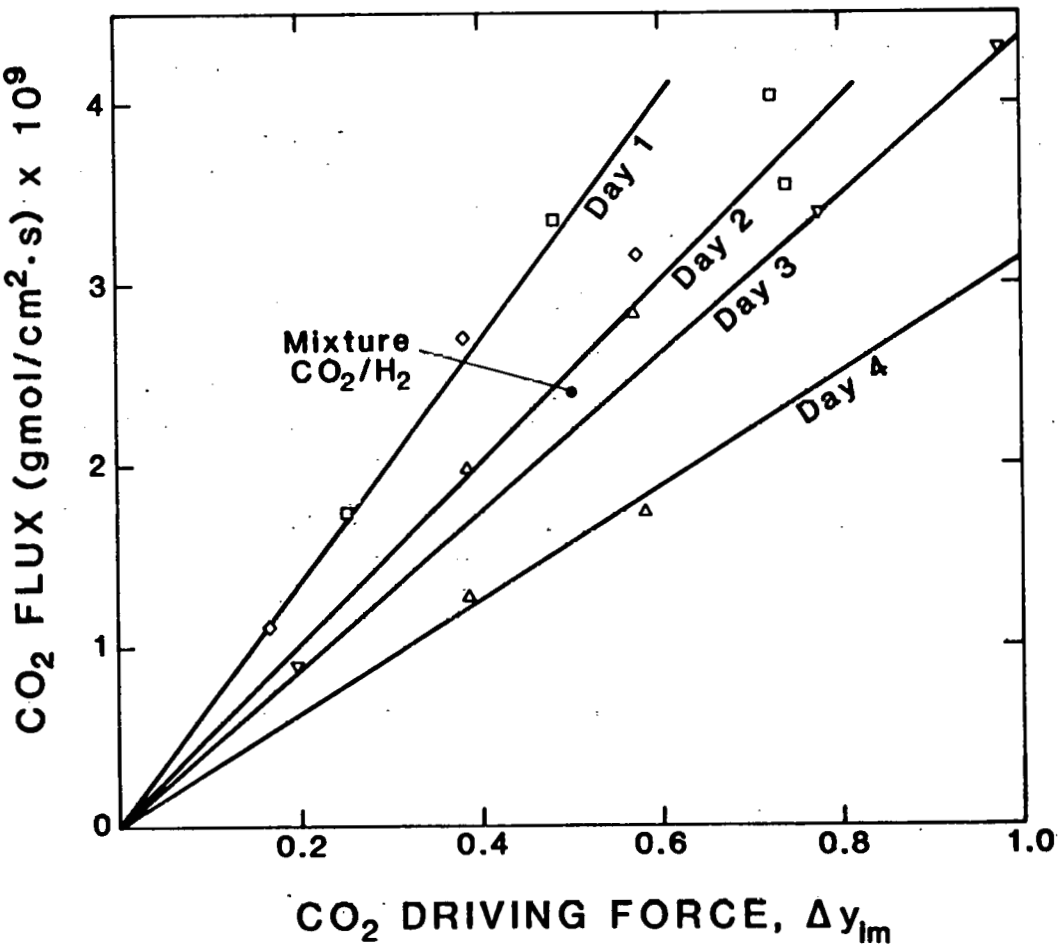

Figure 2. CO_2 Flux vs. Driving Force for PBI Membrane.

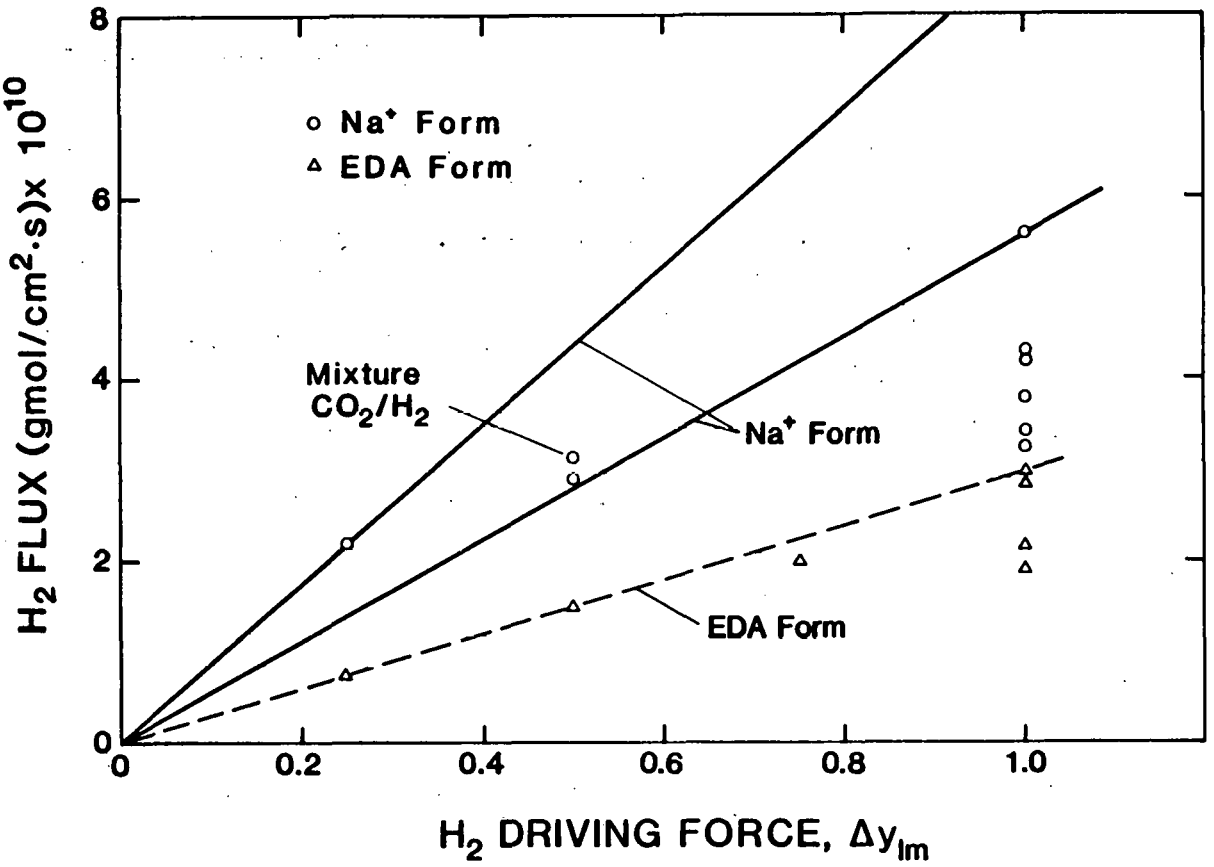

Figure 3. H_2 Flux vs. Driving Force for PBI Membrane.

H_2 the EDA form produced a lower flux than the Na form. This effect could be explained by the higher ionic strength and, therefore, lower solubility of H_2 in the EDA form. For a 100% H_2 feed, the EDA form produced a flux of 3.0×10^{-10} gmol/cm^2.s and the Na form produced a flux of 4.3×10^{-10} gmol/cm^2.s.

A structural analysis of the PBI film was done. Using elemental analysis and IR spectra, it was determined that the ion-exchange site density was less then reported by the manufacturer. This result indicates that the film cannot support as much EDA as originally indicated.

It has been decided to discontinue the studies of the PBI film due to the problems stated. The perfluorosulfonic acid ionomer will be used in future experiments.

ACCOMPLISHMENTS

- Structural analysis of PBI film was done using elemental analysis and IR spectra.
- CO_2 and H_2 flux measurements were done using both a perfluorsulfonic acid and a polybenzimidizole ionomer film.
- CO_2/H_2 separation factor of 12.5 was measured for the perfluorosulfonic acid ionomers in the EDA form.
- Construction and testing of a smaller membrane cell for use with thinner films.

7. FUTURE WORK:

- CO_2/H_2 and H_2S/H_2 binary mixture measurements using the perfluorosulfonic acid ionomer.
- Measurements at ambient conditions and temperatures up to 120°C and pressures up to 5 atm.

8. REFERENCES:

1. Bartis, J. T. and Marks, L. S., "Technical Evaluation and Systems Analysis of Hydrogen Production from Coal," final report for DOE Contract No. DE-AP21-84MC02159 (1984).
2. Way, J. D., Noble, R. D., Reed, D. L., Ginley, G. M., and Baker, L. A., "Facilitated Transport of CO_2 in Ion-Exchange Membranes," AIChE J. 33, 480-487 (1987).
3. Way, J. D. and Noble, R. D., "Hydrogen Sulfide Facilitated Transport in Perfluorosulfonic Acid Membranes," in 'Liquid Membranes: Theory and Applications,' R. D. Noble and J. D. Way, eds., ACS Symposium Series, in press (1987).

SEPARATION OF GAS MIXTURES BY SUPPORTED COMPLEXES

1. FTPA NUMBER: 10581

CONTRACTOR: Pacific Northwest Laboratory
P.O. Box 999
Richland, WA 99352

CONTRACTOR PROJECT MANAGER: Michael A. Lilga

PRINCIPAL INVESTIGATORS: Michael A. Lilga
David A. Nelson
Richard T. Hallen

METC PROJECT MANAGER: Dr. H. L. Sophie Lai

CONTRACT PERIOD OF PERFORMANCE: 1 October 1986 through 30 September 1987

2. SCHEDULE/MILESTONES:

TASK	PROJECT MONTH (FY 1987) O N D J F M A M J J A S
A. Establish Kinetic Parameters	
1. Determine Equilibrium Constants	Δ
2. Determine Kinetics of H_2 Uptake	Δ
3. Determine Kinetics of H_2 Release	Δ
B. Improvement of H_2 Uptake	
1. Prepare Substituted Cr Complexes	Δ
2. Determine Equilibrium and Kinetics of H_2 Binding	Δ
C. Membrane Attachment	
1. Prepare Ionic Chromium Complex	Δ
2. Screen Reactivity with H_2	Δ
3. Economic Evaluation	Δ

3. OBJECTIVES:

The objective of this project is to prepare and investigate coordination complexes that can be used to selectively separate gases from mixtures. Recent research has focused on hydrogen separation. Specific goals are to prepare inexpensive complexes that either react reversibly and specifically with H_2, or reversibly incorporate H_2 into a substrate at rates that are fast enough to be useful in a H_2 separation system.

4. BACKGROUND STATEMENT:

The selective separation or purification of gases, especially hydrogen and CO, is highly desirable in processes utilizing product gas from coal gasification. However, gas separation is one of the most difficult and energy intensive processes encountered. The development of new and innovative methodologies to selectively and efficiently separate specific gas components from mixed-gas streams could significantly reduce the cost and complexity of product gas production and processing. For example, gasification with air could be substituted for oxygen gasification as is now used for the generation of synthesis gas. In addition, the selective separation of H_2 from synthesis gas could make coal an attractive future source of H_2 for use as a fuel or chemical feedstock.

The Pacific Northwest Laboratory (PNL) is examining transition-metal complexes as selective agents for the separation of syngas components from gas mixtures. Transition-metal complexes are known which react reversibly with gases such as H_2, CO, O_2, and CO_2. This reversible binding can be used to transfer the gas from a region of high partial pressure to a region of lower partial pressure. The selectivity of transfer is determined primarily by the selectivity of the metal in binding a specific gas. The nature of the ligands surrounding the metal has a large influence on the selectivity and reversibility of gas binding. We have successfully used ligand modification to prepare complexes that have improved properties for H_2 or CO binding and, therefore, separation.

The use of transition-metal complexes to separate syngas components was previously demonstrated by us using a dimeric palladium complex as a carrier in a two-column absorber/stripper bench-scale apparatus (Lyke, et al, 1986). While the concept was successfully demonstrated, the cost of palladium required for long-term operation was prohibitive. Cheaper complexes were subsequently studied, leading to the development of chromium complexes, discussed below, which reversibly bind H_2. The use of less expensive complexes in this type of system should significantly reduce the initial capital outlay for a gas separation unit.

An alternative method of minimizing costs is to incorporate the metal complex within an immobilized liquid membrane; i.e., utilize the metal complex as a reactive carrier in facilitated transport. In this application, the amount of complex necessary is much less than in the two-column system. In addition, the separation selectivity and permeability of the solvent-sorbed membrane can be greatly enhanced when a metal complex is present as a transport agent. The result could be an efficient and selective methodology for gas separation.

5. PROJECT DESCRIPTION:

The current project centers on the preparation and characterization of complexes that can be used to separate H_2 from gas mixtures. Of interest are complexes which are inexpensive and reversibly bind H_2. In

particular, dimeric complexes of chromium, $[(C_5H_4R)Cr(CO)_3]_2$ (R=H, CO_2CH_3, alkyl), are being studied in this project. The basic methodology used is to prepare various derivatives containing substitution on the cyclopentadienyl ligand and screen these derivatives for reversible reaction with H_2. Once reversibility is achieved, kinetic and equilibrium data will be collected to fully characterize the system and possibly elucidate the effects of substituents on H_2 binding.

Also of interest are complexes which reversibly and catalytically incorporate H_2 into an organic ketone substrate. A Rh/Sn complex which reversibly hydrogenates/dehydrogenates cyclohexanone will be discussed. While Rh is not inexpensive, it is present in very low concentration and represents a potentially inexpensive yet selective H_2 separation method.

6. RESULTS/ACCOMPLISHMENTS:

The reaction of H_2 with $[CpCr(CO)_3]_2$, where Cp is cyclopentadienyl (eq. 1), has been reported previously. Fischer (1955, 1963) found that the reaction occurs at 70°C and 150 atm H_2 to afford the monomeric hydride

$$[CpCr(CO)_3]_2 + H_2 \rightleftharpoons 2\ CpCr(CO)_3H \qquad (1)$$

complex $CpCr(CO)_3H$. The monomeric chromium hydride rapidly evolves H_2 when heated to 80°C, its melting point.

The literature appears to indicate that H_2 uptake is difficult but that H_2 loss is relatively easy. It was of interest therefore to prepare more active derivatives that more readily bind H_2. Substitution of a carbonyl ligand is one method to make the complex more reactive. Phosphite substitution of $[CpCr(CO)_3]_2$ has been studied by Muetterties and coworkers (Goh, et al., 1979). Addition of two equivalents of $P(OMe)_3$ to a solution of $[CpCr(CO)_3]_2$ affords $[CpCr(CO)_2(P(OMe)_3]_2$. This complex reacts cleanly with 1 atm H_2 at 20°C to give the monomeric hydride, $CpCr(CO)_2(P(OMe)_3)H$. The increased reactivity was suggested to be a result of increased steric bulk at the metal centers which tends to weaken the Cr-Cr bond. Cleavage of the metal-metal bond generates reactive coordinately unsaturated fragments. The reversibility of the hydrogen addition was not determined but the ease of the virtually quantitative H_2 uptake suggests that the $P(OMe)_3$ ligand is too bulky for easy reversal. A ligand of intermediate bulk, such as an alkyl isocyanate, is expected to result in intermediate reactivity.

In order to study the reaction of H_2 with the chromium complexes, a pressure reaction vessel containing either a high pressure UV/Vis or an IR spectrometer cell was constructed. The UV/Vis cell contains sapphire windows and the IR cell contains ZnS windows, rated to 1000 psi. A reaction occurring in the vessel can be monitored by tipping the entire apparatus to fill the spectrometer cell and placing it into the spectrometer.

Our investigation has demonstrated that the reaction of H_2 with $[CpCr(CO)_3]_2$ is much more facile than previously reported. At 10 atm

and room temperature, the reaction is complete before a spectrum can be taken. This dimer is found to react with 1 atm H_2 slowly at room temperature but faster at 65°C, reaching completion in 0.5 hours. Regeneration to the extent of about 5% can be achieved by heating to 100°C for 2 hours. H_2 is rapidly lost upon photolysis, however, CO is also lost and an inactive complex is formed.

In order to improve regeneration, i.e., H_2 production, a derivative was prepared containing the electron withdrawing $-CO_2CH_3$ group on the cyclopentadiene ring (Macomber, et al, 1983). It was reasoned that electron withdrawing groups could increase the strength of the metal-metal bond and make formation of the dimer complex more favorable. The substituted dimer complex reacts readily with 1 atm H_2 at room temperature with an apparent half life of 0.5 h. This activity is about the same as for the unsubstituted complex. Regeneration appears to be easier for the substituted complex, however, with about a 10% conversion at 90°C after two hours. Thus, electron withdrawing groups seem to favor regeneration.

The regeneration is still difficult for these complexes, presumably because the reaction is bimolecular. It is expected that vast improvement may be accomplished by linking the two cyclopentadiene ligands together with an alkyl chain, thereby making regeneration unimolecular. Work is currently underway to prepare these complexes and study their reactions with H_2.

A $RhCl_3/SnCl_2/LiCl$ catalyst system was examined which dehydrogenates alcohols such as isopropanol and butanol. Previous results indicated the possibility of an equilibrium between the alcohol, the related ketone, and hydrogen. Catalysis of this equilibrium within an immobilized liquid membrane could give a highly selective hydrogen separation system. Low molecular weight alcohols and ketones, however, suffer from high vapor pressures and slow dehydrogenation and hydrogenation rates at their maximum usable temperatures.

Less volatile alcohol/ketone systems were studied. As a result, higher temperatures and faster rates were obtainable. Hydrogenation and dehydrogenation processes were studied separately using a reaction flask connected to a simple gas buret. Cyclohexanol is found to dehydrogenate cleanly to cyclohexanone and H_2 at 110°C to 170°C. If the atmosphere over the reaction is swept with N_2, H_2 evolution continues. If the system is purged with H_2, an uptake of gas is noted, indicating that hydrogenation is taking place. The cyclohexanone concentration in the equilibrium mixture is very low, i.e., the equilibrium lies well toward cyclohexanol. The cyclohexanol/cyclohexanone system was cycled through three dehydrogenation/hydrogenation procedures over the course of one week at 150°C without serious loss of catalyst activity or substrate decomposition.

7. EVALUATION OF POTENTIAL FUTURE PLANS:

Future research will entail a study of the alkyl-bridged cyclopentadiene chromium complexes. These complexes are thought to be excellent candidates for rapid, reversible H_2 binding. These complexes are also amenable to additional ligand substitution to further improve H_2 binding. The effects of ligand substitution will be examined in a kinetic study of selected complexes.

Chromium complexes are relatively inexpensive to prepare and as a result could be used for gas separation using an absorber/stripper system. Additionally, the results of this research are directly applicable to the use of coordination complexes as reactive carriers within facilitated transport membrane systems. The advantage of facilitated transport with coordination complexes depends upon the dramatic increase in selectivity due to the complexes combined with the selectivity of specific solvents (immobilized liquid membranes). Since gas separations by membranes are inherently low energy processes, the development of highly selective systems would be very significant for coal gasification and product gas processing.

8. REFERENCES

E. O. Fischer, Inorg. Synth., 1963, 7, 136.

E. O. Fischer, W. Hafner and H. O. Stahl, Z. Anorg. Allgem. Chem., 1955, 282, 47.

L. Y. Goh, M. J. D'Aniello, S. Slater, E. L. Muetterties, I. Tavanaiepour, M. I. Chang, M. F. Fredrich, and V. W. Day, Inorg. Chem., 1979, 18, 192.

S. E. Lyke, M. A. Lilga, D. A. Nelson, B. R. James and C. L. Lee, I & EC Product Res. Develop., 1986, 25, 522.

D. W. Macomber and M. D. Rausch, Organometallics, 1983, 2, 1523.

MEASUREMENT OF ALKALI VAPORS IN PFBC PROCESS STREAM AND THEIR REMOVAL WITH A FIXED GRANULAR-BED SORBER

1. FTPA NUMBER: ANL 49701 (B&R AA-05-10)

CONTRACTOR: Argonne National Laboratory
9700 South Cass Avenue
Argonne, IL 60439

CONTRACTOR PROJECT MANAGERS: Dr. Michael Petrick
Dr. Martin J. Steindler

PRINCIPAL INVESTIGATORS: Dr. Sheldon H. D. Lee
Dr. Kevin M. Myles

COLLABORATING INVESTIGATORS: Dr. William J. Haas and Mr. D. E. Eckels, Ames Laboratory

METC PROJECT MANAGER: L. Megan Day

PERIOD OF PERFORMANCE: October 1, 1986 to September 30, 1987

2. SCHEDULE/MILESTONE

1987 Program Schedule

	O	N	D	J	F	M	A	M	J	J	A	S
PFBC/Alkali Sorber Testing												
-Quantify alkali vapor concentration and demonstrate sorber.											|--	
-Install and test candle filter assembly.			|----------	----------	----------	----------	----------	----------	----------	----------	----------	----------
-Modify gas stream sampling line.								|-------	-------	-------	-------	-------
Calibration of Ames Alkali Analyzer and Batch-Type APST		|----------	----------	----------	----------	----------	----------	----------	----------	----------	----------	----------
Lab Testing for Studying Alkali Vapor Capture by Stainless Steel Gas Sampling Line			|----------	----------	----------	----------	----------	----------	----------	----------	----------	----------

3. OBJECTIVES:

The objectives of this work are to critically measure the alkali-vapor (Na and K) concentration in a pressurized fluidized-bed combustion (PFBC) process stream on a real-time, on-line basis and to demonstrate a fixed granular-bed sorber for the control of alkali vapors from the actual PFBC process stream.

4. BACKGROUND STATEMENT:

Alkali-metal compounds, such as chlorides and sulfates of sodium and potassium, present in the process stream of coal combustion could cause hot corrosion of a gas turbine. Spacil and Luthra[1] predict that the quantity of alkali vapor in the PFBC process stream could be up to two orders of magnitude greater than the current industrial gas-turbine specification limit of 0.024 ppmW. In contrast, the recent calculations by Scandrett and Clift[2] suggest that, if the aerosol alkali particulate could be removed, the residual alkali vapor in the process stream would be less than the limit. Measurements of the alkali vapor in a PFBC process stream have been made by several institutions and found to be in the order of 0.1 to 10 ppmW. A conventional batch-type extraction of the flue gas, followed by the analysis of the condensate, was used in these measurements. It was not until recently that a real-time, on-line alkali analyzer was developed and tested in the gas stream of both coal gasification and combustion.[3]

A fixed granular-bed sorber is being developed at Argonne National Laboratory (ANL) for the control of the alkali vapor in a PFBC process stream. After an extensive screening study, activated bauxite was found to be the most effective sorbent in capturing the NaCl, KCl, and K_2SO_4 vapors that were doped into a simulated PFBC gas stream.[4] Activated bauxite was also demonstrated to be easily and effectively regenerated for reuse by a simple water-leaching process.[5] The effectiveness of activated bauxite for alkali-vapor capture has been confirmed by others.[6]

5. PROJECT DESCRIPTION:

This project supports the DOE/METC Fossil Energy Program for the development of PFBC technology. To achieve the objectives of this project, a high-temperature, high-pressure alkali sorber has been designed, fabricated, and installed onto the ANL laboratory-scale 15.2-cm-dia (6-in.-dia) PFBC facility (PFBC/alkali sorber facility). The specifications and the detailed engineering design, as well as a process description of the entire PFBC/alkali sorber facility, were presented previously.[7] The real-time alkali concentrations (sodium and potassium) in the process stream are measured by an Ames on-line alkali analyzer[3] for both the sorber-inlet and sorber-outlet gas streams. In addition to the Ames alkali analyzer, a batch-type alkali and particulate sampling train (APST) is installed as a back-up for the analysis of both alkali vapor and particulate in the sorber-inlet gas stream. The APST is designed on the basis of a cold-trap condensation method.

Six test series have been completed in the PFBC/alkali sorber facility, and the test results[7-9] indicated that the alkali vapor concentrations in the PFBC process stream measured by the batch-type APST are at least an order of magnitude greater than the values measured by the Ames alkali analyzer. The source of this analytical discrepancy needs to be sought. The test results also show that the fate of the NaCl vapor being injected into the PFBC process stream was complicated by the presence of high ash loading (on the average of 500 ppmW) in the process stream and the use of a long (about 6.5-m) stainless steel sampling line that could capture the NaCl vapor under the test conditions. The high dust loading in the process stream also affects the gas sampling and its analysis.

6. RESULTS/ACCOMPLISHMENTS

Three experimental activities have been proceeding during this year: (1) laboratory calibration of the Ames alkali analyzer and the batch-type APST, (2) laboratory study on alkali-vapor capture by stainless steel, and (3) modification of the PFBC/alkali sorber to reduce particulate loading in the PFBC process stream. Results of each activity are as follows:

LABORATORY CALIBRATION OF AMES ALKALI ANALYZER AND BATCH-TYPE APST

The objective of this activity is to simultaneously calibrate both the Ames alkali analyzer and the batch-type APST for the determination of the accuracy of their alkali measurements for a gas stream that contains controlled amounts of NaCl and KCl vapors. To achieve this objective, a pressurized stainless steel alkali-vapor generation unit was constructed and integrated with the Ames alkali analyzer and the APST, as shown schematically in Figure 1.

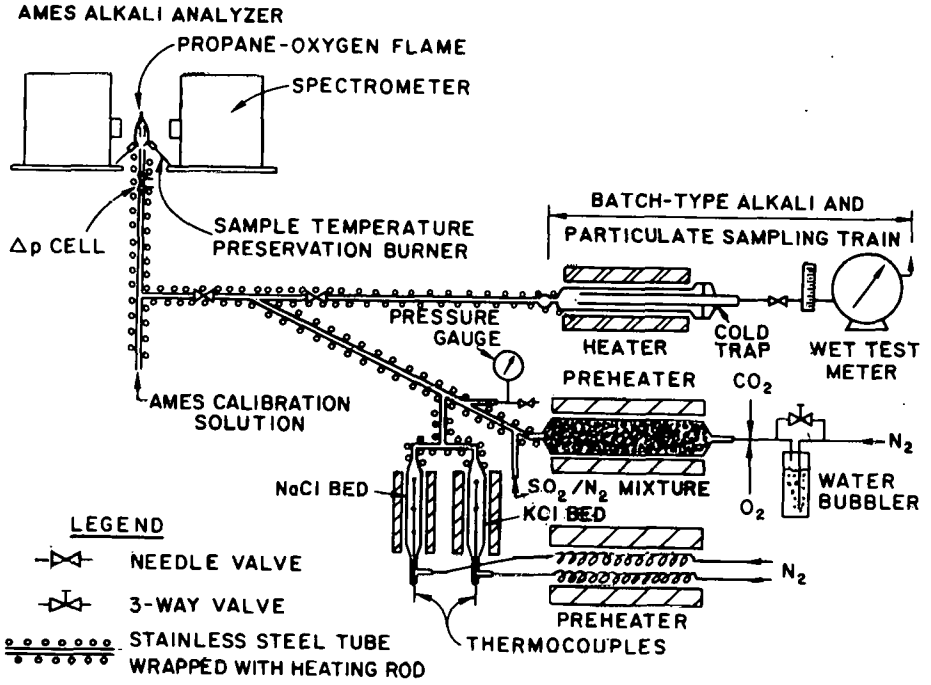

Figure 1. Schematic of Pressurized NaCl-KCl Vapor Generation Unit Integrated with Ames Alkali Analyzer and Batch-Type APST

The unit shown in figure 1 is entirely constructed with 304 stainless steel material. NaCl and KCl vapors are generated by introducing preheated nitrogen streams through beds (2.54-cm ID, 12.7-cm long) of granular NaCl and KCl that can be separately maintained at a controlled temperature. The vapors are mixed with a preheated diluent gas stream, and the mixture is passed through a section of 66-cm-long 304 stainless steel tubing (for improving the mixing). The flow is then split, with a

fraction flowing to the Ames alkali analyzer and another fraction to the APST. The length of the flow path from the salt bed to the Ames analyzer is the same as that of the APST. The flow rate of the gas stream entering into the flame of the Ames analyzer burner is measured by the ΔP cell, and the flow to the APST is monitored by a flowmeter and measured by a wet-test meter. To prevent the condensation of the NaCl and KCl vapors on the gas transport line, the temperature of the entire gas transport line is always maintained higher than that of the salt beds.

A series of high-pressure tests was conducted to measure both NaCl and KCl vapors transported in either a N_2 gas stream or a simulated PFBC gas stream that contains 3.0% O_2, 16.5% CO_2, 0.12% H_2O vapor, 470 ppmV SO_2, and the balance N_2. For each gas stream condition, the background concentration with no alkali vapor present in the gas stream was first established, and then alkali vapors were introduced into the gas stream.

Alkali Background Measurement

The background alkali concentrations were measured with no alkali vapor being introduced into the gas stream. The purpose of these measurements was to establish the alkali blanks of the batch-type APST.

The background sodium and potassium concentrations in the nitrogen gas stream were measured by the Ames alkali analyzer to be <5 ppbW. In contrast to this, the background alkalis measured by the APST during the same measuring periods were 30-50 and 20-30 ppbW for sodium and potassium, respectively. The alkali blanks for the APST can reasonably be estimated from these high-pressure background measurements to be, on the average, 40 $\pm$ 30 and 30 $\pm$ 20 ppbW for sodium and potassium, respectively. Within the limits of the experimental and analytical errors, these alkali blanks are considered to be reasonably good for a batch-type sample extraction technique.

Alkali-Vapor Measurement by Ames Alkali Analyzer and APST

After the completion of the alkali background measurements, alkali vapors were generated by passing a 1 L/min nitrogen stream into the NaCl and KCl salt beds, which were separately controlled at a constant temperature. As shown in Fig. 1, the vapors were immediately diluted with a preheated nitrogen gas stream or a simulated PFBC gas stream. The diluted stream was transported and later was split to provide a 6 L/min flow into the flame of the Ames alkali analyzer and a 3 L/min flow into the APST for the measurement of the alkali vapors. Measurements were made under both 2.5 and 9.2 atm absolute (22 and 120 psig) system pressures. Results of these measurements are tabulated in Table 1.

As shown in Table 1, the alkali vapor concentrations measured by the Ames alkali analyzer have a wide range of precision; the average coefficient of variation of the measured concentrations varies from a few percent to about 30%. As compared to the theoretically calculated alkali vapor concentrations, the measured concentrations by the Ames alkali analyzer also have a wide range of accuracy. It varies from a few percent up to a

Table 1. Alkali Vapor Concentration Measured by Ames Alkali Analyzer and Batch-Type Alkali and Particulate Sample Train (APST) as Compared to the Theoretically Calculated Concentrations

Measurement No.	Type of Gas Stream	System Pressure Abs. atm.	Measurement Period	Average Salt Bed Temperature[a] °C		Theoretical Alkali Concentration[b] ppbW		Measured Average Alkali Vapor Concentration, ppbW			
								Ames Analysis[c]		APST Analysis[d]	
				NaCl	KCl	Na	K	Na	K	Na	K
PAVC-1-2	N_2	2.5	11/21/86 1701-1801	641±9	582±32	200±60	230±180	150±20	150±10	50±40	220±40
-3	N_2	2.5	11/21/86 1805-1908	641±9	580±32	200±60	210±170	170±20	130±10	120±30	180±40
-6	N_2	9.2	11/22/86 1615-1715	690±5	620±31	230±40	200±150	120±30	80±20	50±50	190±60
-7	N_2	9.2	11/22/86 1740-1840	690±6	622±31	240±30	220±160	190±20	120±10	150±50	80±60
PAVC-2-5	N_2	9.2	12/17/86 2239-2339	713±1	664±22	460±20	620±350	1200±400	450±40	130±40	270±40
-6	N_2	9.2	12/18/86 1659-1809	717±2	670±23	500±20	740±430	840±40	580±10	160±40	270±40
-7	SFG[e]	9.2	12/18/86 1852-1952	715±3	668±23	430±30	640±380	310±50	290±20	140±40	210±40
-8[f]	SFG	9.2	12/18/86 2054-2154	713±3	666±24	300±20	460±280	250±50	250±40	110±20	160±20

[a] An average of two temperatures. One was measured inside the salt bed at 2 54 cm below the top of the bed; the other was measured outside the salt bed container (2.54-cm-ID stainless steel pipe) near the top of the bed. Both temperatures were found to affect the measured alkali vapor concentration in the gas stream.

[b] Calculated on the basis of equilibrium vapor pressures of the salt beds controlled at the average salt bed temperature.

[c] An average of values measured during each entire measuring duration. Measurement was made for every 2-4 minutes.

[d] Values have been corrected for the alkali blanks of the APST.

[e] SFG represents a simulated PFBC gas stream containing, on the average, 3.0% O_2, 15 5% CO_2, 0.12% H_2O, 470 ppmV SO_2, alkali vapors, and the balance N_2.

[f] The total flow rate of this measurement was 12 L/min, as opposed to 9 L/min used in the rest of the measurements.

factor of two. The measured concentrations are mostly lower than their corresponding theoretical concentrations. The capture of the alkali vapors by the heated stainless steel transport line could partially account for these observed lower concentrations. The extent of alkali vapor capture by the heated stainless steel transport line needs to be better defined.

In these two series of measurements, the Ames alkali analyzer was calibrated on a daily basis. Under the same calibration conditions, the alkali intensities measured from a calibration solution could also vary up to a factor of two from day to day. Based on these alkali-vapor measurement studies, the accuracy of the Ames alkali analyzer can be reasonably estimated to be on the order of a factor of two.

Also shown in Table 1 are the results obtained from measurements with the APST conducted during the same measuring periods as the Ames alkali analyzer. These results have been corrected for the alkali blanks discussed previously. The average sodium and potassium vapors measured by the APST are generally in the same order of magnitude as those measured by the Ames alkali analyzer. For the first series of measurements (PAVC-1 series), the alkali vapors measured by both the Ames alkali analyzer and the APST are in reasonably good agreement. For the second series of measurements (PAVC-2 series), the concentrations measured by the APST are consistently about 50% lower (except for sodium concentrations of (PAVC-2-5 and -6, for which the Ames results are questionable) than those of the Ames results. Apparently, an unknown loss of alkali vapors occurred during this series of measurements. The source of this loss is not known. Despite this finding, the results of the first series of measurements, which show reasonably good agreement with the Ames analysis, provide an encouraging indication of the capability of the APST for the measurement of alkali vapors.

In order to double-check the chemical form of alkali vapors being transported and collected on the cold trap of the APST, the cold-trap solutions collected from the PAVC-1 series were analyzed for chloride ion. The results indicate that the alkali vapors transported in the nitrogen gas stream and later captured by the cold trap are present as chlorides. Our earlier studies showed that, in the simulated PFBC gas stream, the alkali chloride vapors were captured by the cold trap essentially as a form of sulfates. Sulfate could be formed by the reaction of chloride vapor with SO_2 in the gas phase and subsequently captured by the cold trap. It could also be a product of the reaction between the captured chloride (on the cold trap) and the SO_2 that continuously flows through the cold trap during the entire measuring period.

ALKALI-VAPOR CAPTURE BY STAINLESS STEEL

In our earlier laboratory tests, NaCl vapor was observed to be captured by a stainless steel tubing when it was heated up to >750°C.[9] The extent and behavior of this alkali vapor capture at the simulated PFBC gas stream conditions (in terms of temperature, pressure, and gaseous composition) are yet to be determined. The objectives of this activity are (1) to

measure the rate of alkali-vapor capture by a heated stainless steel and to screen a suitable material for use as a gas sampling line and (2) to obtain a better understanding on the capture behavior and mechanism.

To achieve the first objective, a thermogravimetric analysis (TGA) set-up is being used to measure the weight change of a stainless steel coupon when it is exposed in the alkali-vapor bearing gas stream at high temperatures. This TGA study will be continued to test different types of stainless steel and super-alloy. The rate of alkali-vapor capture will be established and used as a comparison criterion for the selection of material to be used as a sampling line in the PFBC/alkali sorber facility.

To achieve the second objective, the experimental set-up shown in Figure 1 is also being used to study the alkali-vapor capture by, and release from the heated stainless steel gas transport line under conditions closely simulating the PFBC process stream. A series of tests has been conducted under the system pressure of 9.2 atm absolute and temperatures between 850 and 950°C for the 304 stainless steel gas transport line (in Fig. 1). The Ames alkali analyzer was used to continuously monitor (1) the sodium and potassium concentrations when the NaCl-KCl-vapor-bearing nitrogen gas stream or the NaCl-KCl-vapor-bearing simulated PFBC gas stream was flowing through the line and (2) the subsequent release of both sodium and potassium from the stainless steel line when the alkali-vapor-free nitrogen or the alkali-vapor-free simulated PFBC gas stream was transported through the line. Some significant observations obtained from this series of alkali-vapor capture and release studies are summarized as follows:

As shown in Figure 2, the NaCl and KCl vapor concentrations were fairly constant at average concentrations of 840 ppbW for Na and 570 ppbW for K in the nitrogen carrier gas stream during the time period between 1639 and 1810 of December 18, 1986. These concentrations immediately reduced to the average concentrations of 320 and 290 ppbW for Na and K, respectively, as soon as the nitrogen carrier gas stream was replaced with a simulated PFBC carrier gas stream (containing 3.3% O_2, 17.4% CO_2, 0.14% H_2O vapor, 540 ppmV SO_2, alkali vapor, and the balance N_2) at the time 1817. At this time, temperatures of both NaCl and KCl beds were maintained constant, indicating that the drop in alkali concentrations cannot be attributed to a drop in the salt bed temperature. In a separate study, the alkali (Na and K) concentrations measured by the Ames alkali analyzer were found not to be affected by the gaseous composition of the gas stream entering into the flame of the analyzer; therefore, this >50% drop in alkali concentration indicated a substantial capture of both vapors by the stainless steel line when the vapors were transported in the simulated PFBC gas stream. Figure 2 also shows that, at the time 2200, the switch of the simulated PFBC carrier gas stream to a nitrogen gas stream bearing 0.14% H_2O vapor caused a preferential increase in potassium concentration (38% increase in potassium as compared to 17% increase in sodium), and that both sodium and potassium concentrations immediately increased to substantially higher average concentrations of 700 and 510 ppbW, respectively, as soon as the water vapor was eliminated from the nitrogen carrier gas stream. Due to a slightly lower (7°C) salt bed temperature, these concentrations are slightly lower than those (480 and 570 ppbW for Na and K, respectively) measured previously under a similar nitrogen gas stream during the time 1639 and 1810.

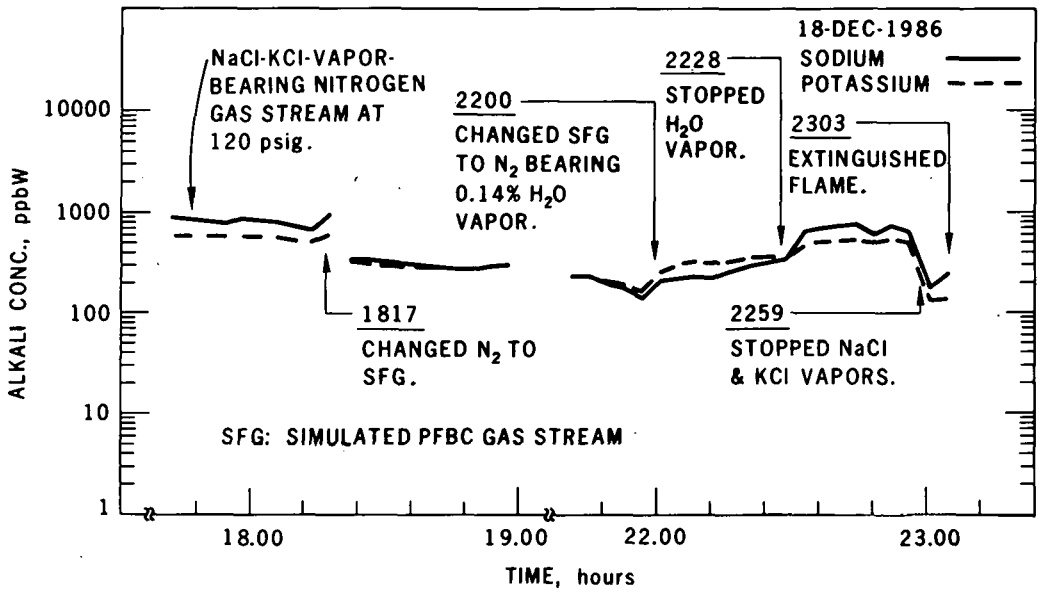

Figure 2. Measured Sodium and Potassium Concentrations in the Gas Stream Showing the Capture of Alkali Vapors in the Simulated PFBC Gas Stream by Heated Stainless Steel.

Previous study in this work showed that, after having been exposed to the NaCl-vapor-bearing nitrogen gas stream (250-320 ppbW sodium) for about an hour, the heated (>750°C) stainless steel continuously released sodium into the NaCl-vapor-free nitrogen gas stream at a level of <10 ppbW.[9] The extent of this alkali release was much greater during this series of tests, as shown in Figure 3. Figure 3 clearly shows that, after having been exposed for 3 h to the nitrogen gas stream that contains 0.4-2.2 ppmW Na (as NaCl vapor) and 0.4-1.5 ppmW K (as KCl vapor), the heated (850-950°C) stainless steel gas transport line continuously released 45-50 ppbW Na and 25-30 ppbW K into the alkali-vapor-free N_2 gas stream. Surprisingly, the amounts of alkalis released from the line quickly increased to the ranges of 220-280 ppbW Na and 180-240 ppbW K when the alkali-vapor-free simulated PFBC gas stream was flowing through the line. This alkali release continued for several hours. Similar behavior was observed when the line was exposed to the Nacl-KCl-vapor bearing simulated PFBC gas stream.

In order to study the effect of each gas component in the simulated PFBC gas stream on the release of the captured alkalis from the heated stainless steel, each gas component was eliminated one at a time from the simulated PFBC gas stream and the change in the amount of alkali release was measured. Results showed that the amount of alkali (Na and K) release was not affected by the elimination of SO_2, O_2, and CO_2 in the simulated

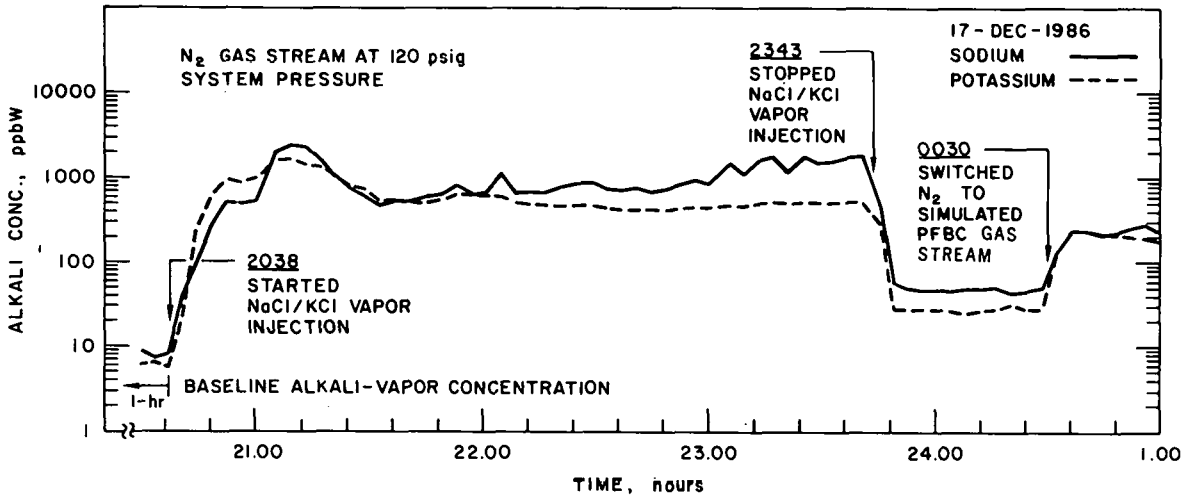

Figure 3. Measured Sodium and Potassium Concentrations in the Gas Stream Showing Alkali Release from a Heated Stainless Steel Previously Exposed to NaCl-KCl-Vapor-Bearing N_2 Gas Stream.

PFBC gas stream. However, the removal of water vapor from the gas stream immediately caused a sharp drop in the amount of alkali release - sodium dropped from 150 to 45 ppbW and potassium dropped from 90 to 12 ppbW. The amount of alkali release immediately increased and then decreased to the previous values by reintroducing the simulated PFBC gas stream and then the nitrogen gas stream bearing no H_2O vapor.

To further verify these observations, we introduced one component at a time into the nitrogen carrier gas stream and examined the effect of each added component on the alkali release. Results of this study showed that the addition of 17.4% CO_2, 3.3-15% O_2, and 540-1500 ppmV SO_2 into the nitrogen gas stream did not have any obvious effect on the alkali release from the heated stainless steel. However, the addition of 0.14% water vapor immediately caused greater than 5 times increase in both sodium and potassium release, as observed previously.

MODIFICATION OF PFBC/AKLAKI SORBER TO REDUCE PARTICULATE LOADING IN PFBC PROCESS STREAM

In this activity, the alkali sorber vessel was modified by replacing the existing secondary and tertiary cyclones with three 6-cm OD, 4-cm ID, 31-cm long, high-temperature SiC candle filters, as shown schematically in Figure 4. The filters are supplied by the Industrial Filter and Pump Manufacturing Company, Cicero, IL. A hot commissioning of these candle

filters has been successfully completed under the test conditions shown in Table 2. During the steady-state test period (5 h), two particulate-loading measurements were made for the filter inlet gas stream and three measurements made for the filter outlet gas stream. Results of these measurements showed that the average particulate loading of the PFBC process stream exiting from the first-stage hot cyclone was about 1340 ppmW. This process stream entered into the alkali sorber vessel where the candle filters are housed. After passing through the filters, the process stream entered into the head space of the sorber vessel where the clean process stream was sampled for its particulate loading. The particulate removal efficiency of the filters calculated on the basis of the first particulate loading measurement in the filter outlet gas stream was 80%. For this measurement, some particles were clearly observed being collected on the filter paper used for the particulate sampling. The efficiency was quickly increased to 97 and 98% for the next two measurements. Viewing under the microscope showed that the filter papers of these two measurements were as clean as the fresh paper, except for some rust contamination of the filter paper caused by the sampler.

During the 5-h hot commissioning test, the candle filters had been pulse-cleaned once using the in-line pulse-cleaning nitrogen supply. This pulse cleaning was conducted after the candles operated for 2.5 h. No visual system upset was observed due to this pulse cleaning.

After the test, the upper surface of the tube sheet, where the filter outlet gas stream exits, was very clean. This observation is in contrast to the ash accumulation of up to several centimeters thickness, which was observed previously when the secondary and tertiary cyclones were used. As expected, the inlet side of the candle filter was totally covered with about 1-mm-thick fly ash; however, the outlet side of the candle filter was visually very clean, indicating that no fly ash had penetrated through the filter. Also, no visual damage or crack was observed on the candle filters.

SUMMARY

Three activities have been proceeding during this year with the objective of overcoming the difficulties encountered in our effort to measure the level of alkali vapor in the PFBC process stream. Results and accomplishments achieved from these activities can be summarized as follows.

In the first activity, the Ames alkali analyzer and the batch-type APST were calibrated with controlled amounts of NaCl and KCl vapors transported in the pressurized (9.2 atm absolute) simulated PFBC gas stream. The Ames alkali analyzer had an alkali measurement precision varying from a few percent to about 30%, and its accuracy was estimated to be on the order of a factor of 2. An alkali blank of the APST was measured to be 40 $\pm$ 30 and 30 $\pm$ 20 ppbW for sodium and potassium, respectively. The alkali vapor concentration measured by both the Ames alkali analyzer and the APST were in reasonably good agreement.

The second activity involved determining the extent and behavior of the alkali-vapor capture by the heated stainless steel gas transport line.

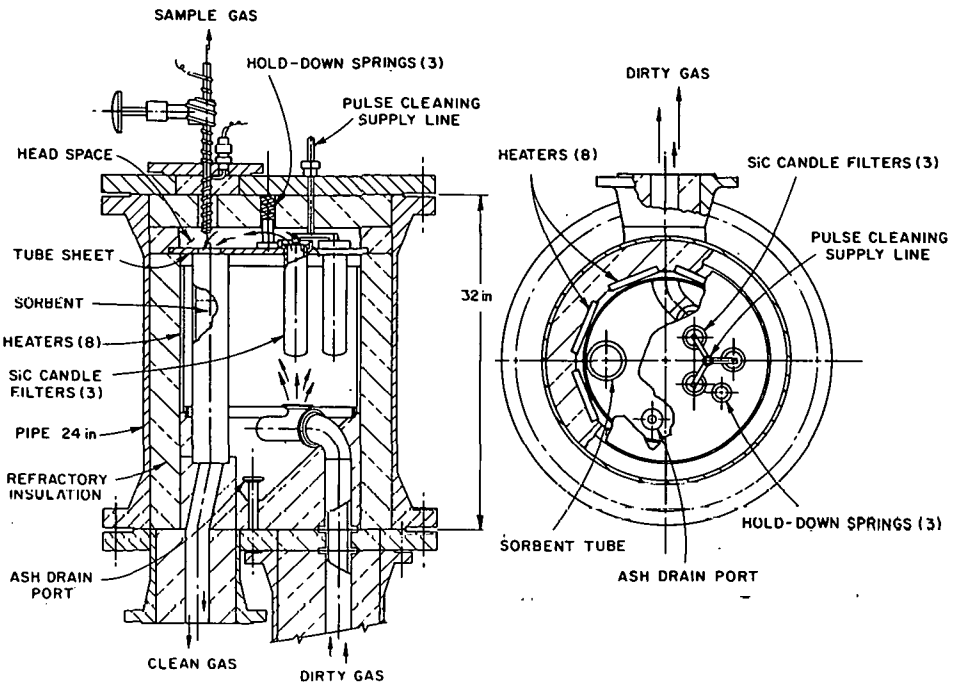

Fig. 4. Alkali Sorber Vessel Showing the Installation of SiC Candle Filters

Table 2. Nominal Operating Conditions of the PFBC/Alkali Sorber for the Hot Commissioning of the Candle Filters

Combustor	
Coal:	Sewickley seam, Pittsburgh, PA
Sorbent:	Tymochtee dolomite, Huntsville, OH
Average Bed Temperature:	900-925°C
System Pressure:	9.2 atm absolute (120 psig)
Fluidizing Velocity:	1 m/s
Alkali Sorber Vessel	
Sorber Bed Material:	None
Sorber Vessel Interior Temperature:	850°C
No. of Candle Filters:	3 (6-cm OD, 4-cm ID, 31-cm long)
Filtration Face Velocity:	1.55 cm/s
Pulse-Cleaning:	In-line N_2 gas at 14.6 atm absolute (200 psig)
Gas Stream Analysis	
Particulate Loading:	Batch-type particulate sampler for both dirty and clean gas streams

The 304 stainless steel line, which was maintained at temperatures of 850-950°C, was found to appreciably capture both NaCl and KCl vapors transported through the line in a pressurized (9.2 atm absolute) N_2 gas stream. This capture was significantly enhanced when the vapors were transported in a simulated PFBC gas stream, primarily due to the presence of water vapor in the gas stream.

The captured alkali was found to reversibly release to the alkali-vapor-free gas stream. The simulated PFBC gas stream showed much greater scouring power (5 to 10 times) than the N_2 gas for the enhancement of the release of the captured alkalis. The water vapor was shown to be the essential component that accounts for this greater scouring power. The nitrogen gas stream that contains water vapor had the same extent of scouring power as the simulated gas stream.

In the third activity, the secondary and tertiary cyclones in the alkali sorber vessel of the PFBC/alkali sorber facility were replaced with three high-temperature SiC candle filters. The hot commissioning test of the filters successfully demonstrated their high efficiency for the removal of fly ash. With this significant achievement, the sampling of the PFBC process stream for alkali-vapor measurement will become much more reliable. The complication caused by the presence of fly ash in the process stream should be eliminated. However, the alkali-vapor capture by the heated stainless steel sampling line is still a challenging problem that remains to be solved.

EVALUATION OF POTENTIAL FUTURE PLANS

The mechanism of the alkali-vapor capture and its release is not clear at this stage. Studies will be continued to gain this understanding. The TGA work will also be continued to measure the rate of alkali-vapor capture and to screen a suitable material (with little or no alkali-vapor capture) for use as a sampling line. Before this material can be identified, an alternative is to shorten the sampling line so that the alkali-vapor capture by the line will be minimized. To achieve this, the existing sampling line of the PFBC/alkali sorber unit (a total of about 25-ft long) will be removed, and the Ames alkali analyzer will be positioned right on the top of the alkali sorber vessel. Our preliminary layout shows that by doing so, the sampling line can be shortened to 2-3 ft long. After the establishment of a reliable analytical technique, the testing of the PFBC/alkali sorber will be continued to measure the level of alkali vapor in the PFBC process stream generated from the combustion of several different ranks of coal and simultaneously to demonstrate the removal of the alkali vapor by a fixed granular-bed sorber of activated bauxite.

ACKNOWLEDGMENTS

The authors wish to express their appreciation to K. J. Jensen, I. M. Fox, F. L. Williams, and E. A. Huff of the Analytical Chemistry Laboratory, ANL, for their assistance with the chemical analyses. Technical assistance has also been given by F. G. Teats, R. Benson, L. Ruppert, and H. Myers of the Chemical Technology Division, ANL.

8. REFERENCES

1. Spacil, H. S. and K. L. Luthra. 1982. "Volatilization/Condensation of Alkali Salts in a Pressurized Fluidized Bed Coal Combustor/Gas Turbine Combined Cycle." J. Electrochem. Soc., Vol. 129, No. 9, pp. 2119-2126, September.

2. Scandrett, L. A. and R. Clift. 1984. "The Thermodynamics of Alkali Removal from Coal-Derived Gases." J. Inst. Energy, Vol. 57, No. 433, pp. 391-397, December.

3. Haas, W. J., Jr., D. E. Eckels, S. H. D. Lee, and R. F. Henry. 1985. "Recent Developments and Observations Pertinent to Real-Time Monitoring of Alkali Concentrations in Hot Gas Streams from Fluidized Bed Combustion of Coal." Proc. of DOE Fifth Annual Contractors' Meeting on Contaminant Control in Coal-Derived Gas Streams, May 7-9, Morgantown, WV., pp. 493-512.

4. Lee, S. H. D., and I. Johnson, 1980. "Removal of Gaseous Alkali Metal Compounds from Hot Flue Gas by Particulate Sorbents." J. Eng. Power, ASME Trans., Vol 102, pp. 397-402.

5. Lee, S. H. D., S. D. Smith, W. M. Swift, and I. Johnson. 1981. "Studies of the Regeneration of Activated Bauxite Used as Granular Sorbent for the Control of Alkali Vapors from Hot Flue Gas of Coal Combustion." Argonne National Laboratory Report ANL/CEN/FE-81-1, May.

6. Luthra, K. L., and O. H. LeBlanc. 1981. "Alkali Removal from Hot Combustion Gases by Adsorption." General Electric Company Report No. 81CRD170, August.

7. Lee, S. H. D., R. F. Henry, and K. M. Myles, 1984. "Control of Alkali Vapors by a Granular-Bed Sorber." Proc. of DOE Fourth Annual Contractors' Meeting on Contaminant Control in Hot Coal-Derived Gas Stream," May 15-17, Morgantown, WV, pp. 28-40. K. E. Markel, ed., DOE/METC-85-3, December.

8. Lee, S. H. D., R. F. Henry, W. I. Wilson, K. M. Myles, W. J. Haas, Jr., and D. E. Eckels. 1986. "Measurement of Alkali Vapors in PFBC Flue Gas and Their Control by a Granular-Bed Sorber." Proc. of the Fifth Annual Contractors' Meeting on Contaminant Control in Hot Coal-Derived Gas Streams, May 7-9, 1985. Morgantown, WV. pp. 513-528, DOE/METC-85/6025.

9. Lee, S. H. D., K. M. Myles, W. J. Haas, Jr., and D. E. Eckels, 1986. "Measurement of Alkali Vapors in PFBC Flue Gas and Their Removal with a Fixed Granular-Bed Sorber." Proc. of the Sixth Annual Contractors' Meeting on Contaminant Control in Coal-Derived Gas Streams, June 4-5, Morgantwon, WV, pp. 58-77, DOE/METC-86/6042.

A STUDY OF HIGH TEMPERATURE REMOVAL OF ALKALI IN A PRESSURIZED GASIFICATION SYSTEM

1. CONTRACT NUMBER: DE-AC21-83MC20050

CONTRACTOR: Westinghouse R&D Center
1310 Beulah Road
Pittsburgh, PA 15235
412-256-2250

CONTRACTOR PROJECT MANAGER: Dennis M. Bachovchin

PRINCIPLE INVESTIGATORS: D. M. Bachovchin
M. A. Alvin

METC PROJECT MANAGER: L. Megan Day

PERIOD OF PERFORMANCE: September 30, 1983 through October 31, 1986

2. SCHEDULE/MILESTONES:

Milestone	Completion Date
Identify fabrication process and economics	9/84
Acquire commercial pellets	1/85
Determine emathlite composition	6/84
Project stable gettered phases	9/84
Evaluate getter kinetics, mechanism	3/86
Develop kinetic model	9/85
Evaluate gettering at low composition	8/86
Determine ultimate reaction product	2/86
Prepare fixed bed test equipment	3/85
End test operation	2/86
Data analysis	3/86
Performance Projections	9/86

3. OBJECTIVES:

The overall objective of this work is to develop, to a point of readiness for scale up to pilot plant level, a specific concept for removal of alkali metal vapors from hot gases. This concept, which is applicable to gasification and FBC systems, is to pass the gases through a fixed bed of emathlite, a natural clay, with which the alkali reacts irreversibly. The bed material is replaced annually. Specific goals, corresponding to program tasks, include:

- Identify a commercial process for fabrication of getter pellets and examine processing costs.

- Determine the mechanism, stoichiometry, and kinetics of the gettering reaction in laboratory studies, to provide the data for reactor scale-up.

- Determine the capacity of the emathlite for sodium gettering, particularly in the presence of low concentrations of sodium vapor.

- Demonstrate the concept by testing fixed beds (~ 10 kg) of getter pellets exposed to alkali-laden combustion gases. Show that the laboratory kinetic data can be used to design fixed bed getter reactors.

4. BACKGROUND STATEMENT:

Westinghouse began work on the alkali gettering concept in 1978. That DOE-sponsored work (Mulik, et al, 1980, Mulik, et al., 1983) formed the basis of the current work.

Thermodynamic equilibrium studies were made that served to identify mineral classes that could possibly be good getters.

Two test units were built for examination of getter materials. The first was a unit in which several getter pellets could be exposed, usually for six hours, to various gases containing 80 ppm NaCl or KCl at 11 atm and 800 to 900°C. This unit was valuable in screenings of a large variety of potential getter materials, because of the high salt concentration and the capability of testing a number of different pellets at once. Atomic Absorption (AA) was used to measure extent of gettering.

The second unit was the double-balance thermogravimetric analysis (TGA) unit. In this unit, salt is evaporated from a balance-supported vessel into a carrier gas that flows past a balance-supported getter pellet at another temperature. Thus both salt concentration and getter weight gain can be continuously determined. Typical conditions are 1 atm, 850 to 900°C, and 1 to 10 ppmv, with exposure times of around 100 hr. The following major test series were run on the TGA: testing for more accurate comparison of potentially good getters identified with the bench-scale unit; a detailed examination of activated bauxite gettering; and an examination of emathlite gettering.

Another phase of the earlier work was a chemical engineering assessment of getter reactor performance. Several getters and reactor schemes were examined. Kinetic expressions and reactor sizing expressions were developed.

The main conclusions from this previous work were:

- Emathlite was identified as a leading getter material. It is a natural fuller's earth that is inexpensive, has high capacity for sodium, and binds sodium irreversibly.

- The packed bed is the preferred contacting scheme. The slow kinetics make a long solids residence time necessary to obtain acceptable getter utilization, and countercurrent, non-backmixing contacting is needed for complete gas cleaning.

The present work constitutes an effort to further develop our understanding of the process.

5. PROJECT DESCRIPTION:

GETTER FABRICATION STUDIES

Work under this task was described in more details earlier (Bachovchin and Alvin, 1985a, Bachovchin, et al., 1985b). A commercial process for the manufacture of emathlite pellets, based upon water slurrying and extrusion, was identified. The process flow diagram, equipment list, material balance, and cost analysis were developed. The cost of pellets produced by a dedicated plant and the cost of purchased pellets were related to production level.

Pellets that had been commercially made with this process were acquired for laboratory testing.

GETTER REACTION MECHANISM DEFINITION

We have previously shown that sodium is incorporated into an insoluble glass phase encapsulating the emathlite pellet and that chlorine is not picked up. The overall rate is governed by diffusion across this glass layer.

We determined the stoichiometry of the reaction product. X-ray diffraction analysis showed substantial quantities of $Na_2(SiO_2)_2$ were present in the acid leachates of TGA-tested pellets. The sodium to silicon ratio is important since it determines the ultimate capacity of emathlite as a sodium getter.

A series of 16 TGA tests were made to identify the reaction mechanism and kinetics. Most of these used pellets made by dry-pressing in the laboratory. Three TGA tests were made on gettering by commercially made (by California Pellet Mill Inc.) emathlite pellets. In each of these tests a pellet was exposed to a sequence of NaCl and water vapor combinations. The results showed again that water vapor is necessary, although it does not show up in reaction stoichiometry. In these tests we also showed that temperature has no effect on the kinetics over the range of 1048 to 1173K.

A kinetic model was developed (Bachovchin and Alvin 1985c). The single particle gettering rate is given by:

$$\frac{dm}{dt} = \frac{2\pi(R+L)DC}{\ln\left(\frac{R}{\sqrt{R^2 - \frac{m}{\pi LF}}}\right) + \frac{D}{K_g R}} \qquad (1)$$

where

m	=	moles Na per pellet
t	=	time, hr
R	=	pellet radius, m
L	=	pellet length, m
D	=	experimental glass-phase diffusion constant, m^2/hr
C	=	bulk gas NaCl concentration, mol/m^3
K_g	=	gas-phase mass transfer coefficient, m/hr
F^g	=	pellet capacity, mol Na/m^3 of pellet

For pellets made in the laboratory, the TGA data are fit by D=0.23 and F=15,300, while for the commercially prepared pellets the best parameter values were D=0.013 and F=15,300. The difference in the capacity parameter F is solely due to the different dry pellet densities. The reason for the difference in the diffusion-related kinetic constant D is not known, but is probably related to pellet structural differences.

GETTER CAPACITY MEASUREMENTS

A previously assembled long-term test reactor has been used to study gettering at low concentrations. The test program is summarized in Table 1.

Table 1. Long-Term Exposure Tests

Test	Run Length, hr	Gas NaCl Conc., ppm	wt% Na
background	-	-	0.09
4	120	3.5	0.98
6	768	0.58	0.35
7	1464	0.69	2.49
8	2875	0.26	1.27
9	1506	0.15	0.36
10	1464	~10,000	19*
11	4368	0.02	0.18

* (18.8 wt% Na, 27.6 wt% Si)

The tests have been made using laboratory pellets at 1123K and 1 atm., except that Test 11 used a commercial pellet. The results of tests 4 through 9 and 11 indicate continued getter activity at low concentrations. Rates are proportional to alkali concentration and follow the kinetics of Equation (1), using the parameters appropriate to pellet type.

Test 10 was intended to be a high concentration long-term test to get a highly converted pellet. Because of gas recirculation in the reactor the concentration was much higher than anticipated and produced completely converted material, with a net Na/Si ratio of 0.83:1 ($Na_2Si_2O_5$ with some SiO_2), confirming the final mole ratio capacity.

BENCH SCALE PROCESS DEVELOPMENT UNIT STUDIES

An existing high-temperature, high-pressure test facility with equipment for dust feed was fitted with an alkali getter bed as shown in Figure 1.

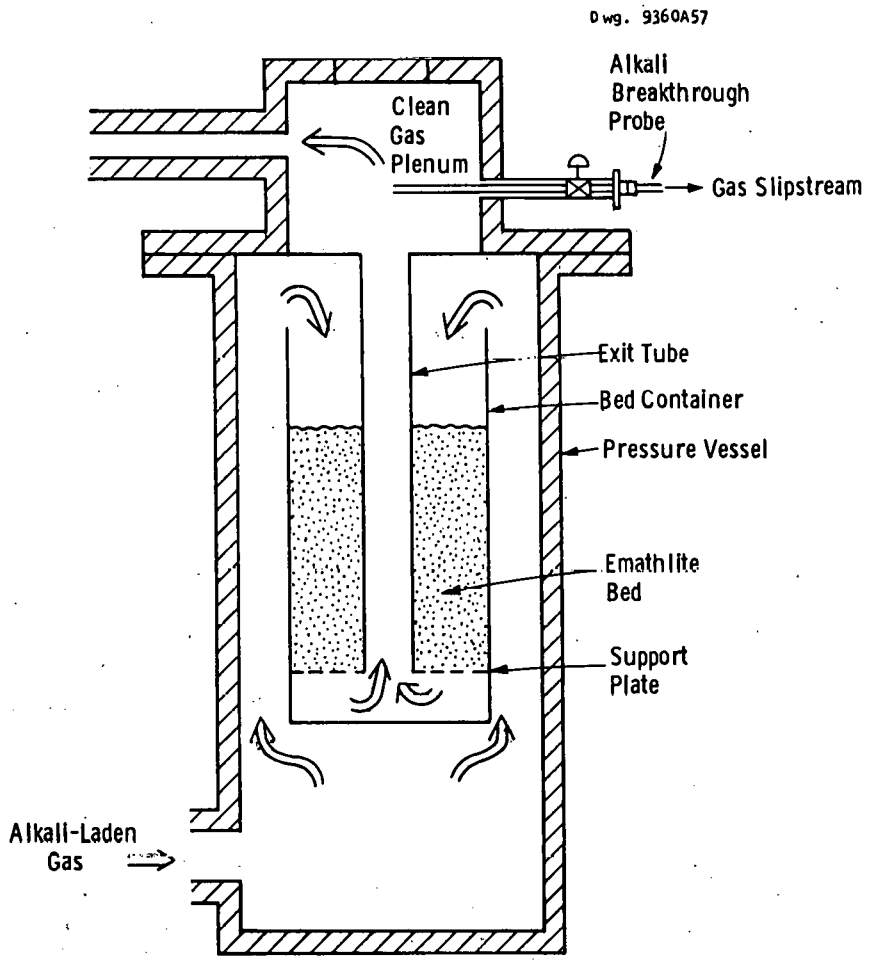

Figure 1. Packed Bed Assembly

The high temperature was maintained by burning methanol in air. Sodium chloride was introduced by dissolving it in the fuel, which contained several percent water. Alkali breakthrough was measured with a removable probe through which a portion of the off-gas was purged and in which the salt condenses. Periodically the probe was removed and rinsed, with the rinse analyzed for sodium with an ion-selective electrode.

A series of five tests, using commercial pellets, was run on this facility, as summarized in Table 2.

After each of the first three tests, pellets were analyzed for sodium content as a function of position in the bed.

Test 1 was a shakedown test with only a shallow bed of pellets. Test 2 was a repeat, but with maximum bed depth in the apparatus. In both cases alkali breakthrough and pellet analyses were consistent with reactor kinetics based on Equation (1). The high pressure drop increase in Test 1 was caused by the accumulation of rust flakes from the wall of the container on the upper surface of the bed. There was little container wall above the bed in Test 2.

Test 3 was made with larger pellets. Although dust was fed (at ~100 ppm in the gas for 47 hr) there was no pressure drop increase. The observed breakthrough and pellet conversions were again in accord with the kinetic model. Note that alkali breakthrough rose during the test due to the lower activity of the large pellets. Also more alkali was picked up by pellets near the bed exit, because more alkali survived the bed inlet section.

Tests 4 and 5 were made with the intent of higher dust feed rates to evaluate possible bed plugging. However, dust feeder performance allowed lower feed rates than wanted. The gettering kinetics of Tests 4 and 5 were consistent with earlier results.

This fixed-bed test sequence demonstrated that the TGA determined kinetics can be used to size fixed beds, and that the beds can remove alkali to low concentrations. Note that in a commercial application a deeper bed can be used to achieve virtually complete removal for a desired bed life. The beds were not plugged when dust was fed, although more severe dust loadings are needed to simulate long-term exposure.

PERFORMANCE PROJECTIONS

A fixed bed reactor kinetic model (Bachovchin, et al., 1986) was developed based on the kinetic mechanism identified in the TGA tests (Equation 1). The observed rates in the fixed bed tests were better fit by using a value of the diffusion kinetic constant of $_3D=0.004$ m^2/hr, with the capacity parameter remaining at 15,300 mol/m^3. The reason for the lower rate constant is not known, but possible explanations include mutual obstruction of pellet surfaces by packed pellets or a lower rate

Table 2. Summary of Fixed Bed Tests

Test	1	2	3	4	5
Duration, hr	102	85	98	46	29.5
Pellet diameter, cm	0.64	0.64	1.27	1.27	0.64
length, cm	1.3	1.3	2.8	2.8	1.3
Bed depth, cm	13	40	40	40	40
Bed area, cm^2	314	314	314	314	314
Bed weight, kg	4.0	12.2	11.9	11.8	12.7
Velocity, cm/s	37-43	43-49	38-47	46-47	46-47
Temperature, K	1106-1133	1080-1174	1030-1165	1141-1159	1142-1168
Pressure, kPa	1140-936	1140	1136-1074	1134	1127
Bed ΔP, kPa					
start	2.9	4.3	3.0	2.7	3.2
final	58	10.4	3.0	3.9	4.8
Salt concentration, ppm					
in	12	10	10	10	10
out	~2	~0.2	0.3-2	0.7-1.1	0.3
Dust feed, g	0	0	696	950	200
Pellet analyses, wt% Na					
inlet	4.2	3.1	0.95		
outlet	2.3	0.32	0.40		

in an oxidizing environment. In any case, the actual performance of a commercial fixed bed will be dominated by the capacity factor F, since pellets will remain exposed long enough to be substantially converted.

Using the lower kinetic constant and the fixed bed kinetic model we performed calculations to characterize fixed bed sorbent bed designs. Table 3 summarized these calculations, indicating bed (pressure vessel) volume and sorbent (emathlite) requirements as functions of pellet size and desired bed life. These calculations assume a 10 ppmv inlet concentration at 10 atm, and an outlet concentration at 10 atm, and an outlet concentration rising to 0.01 ppm, at the end of the stated bed life.

Table 3. Sorbent Bed Design Characterization

Pellet Diameter, cm	Bed Life, hr	Bed Volume, $m^3/(m^3$ gas/hr)	Sorbent Consumption, g/m^3 gas	Bed Depth,* m
1.2	4000	0.0022	0.325	3.5
1.2	7000	0.0029	0.244	4.6
0.6	4000	0.0011	0.167	1.8
0.6	7000	0.0016	0.133	2.5

* At a gas velocity of 1500 m/hr

Based on these calculations and on the pellet costs earlier developed, we projected the cost of pellets versus level of production in terms of the number of 100 MWe gasification plants served. Table 4 summarizes for one particular pellet size and bed life, i.e., for one sorbent consumption rate from Table 3.

Table 4. Emathlite Pellet Cost*

Emathlite Facility	Production Level	Emathlite Pellet Cost $/Ton Coal
Dedicated	For 1 Plant	1.11
	For 10 Plants	0.17
	For 100 Plants	0.06
Toll	For 1 Plant	0.45
	For 10 Plants	0.31
	For 100 Plants	0.17

* 0.6 cm diameter pellets, 7000 hr bed life

6. RESULTS/ACCOMPLISHMENTS

The most significant findings of this work are:

- A commercial pelletization process and economics have been identified.
- Gettering occurs by formation of a glass from gaseous sodium and from the silica in emathlite. The glass is predominantly $Na_2Si_2O_5$, establishing ultimate getter capacity.
- Gettering kinetics are determined by the rate of diffusion across the product glass layer. Kinetic constants have been determined.
- The kinetics observed in the TGA studies, in the long-term low concentration tests, and in the fixed-bed tests are consistent.
- Kinetics are insensitive to temperature over the range of interest.
- There are no capacity limitations at low gas-phase alkali concentrations due to sorption equilibria. Rate is proportional to concentration.
- No operational problems such as pellet attrition or bed plugging occurred in the packed bed tests.

7. EVALUATION OF POTENTIAL FUTURE WORK:

Work under this contract has been completed. The alkali gettering concept with regard to sodium, has been defined and demonstrated. Several areas of investigation would be useful to complete the understanding needed for scale-up of the concept:

- Laboratory examination of gettering of other salts (e.g., KCl).
- An assessment of gettering economics.
- A comparison with other methods of prevention of hot corrosion.
- Scale-up testing at a gasification and/or PFBC pilot plant.

A major data deficiency impairing scale-up design is the lack of knowledge of vapor-phase (and particulate-phase) alkali emissions rates. The size of the fixed bed should be proportional to the alkali concentration, which must, therefore, be more accurately known for economic and reliable design.

8. REFERENCES:

Bachovchin, D. M., and M. A. Alvin, 1985a. Paper presented at the Fifth Annual Contractor's Meeting on Contaminant Control in Coal-Derived Gas Streams, Morgantown, WV.

Bachovchin, D. M., M. A. Alvin, and E. A. DeZubay, 1985b. Simultaneous High-Temperature Removal of Alkali and Particulates in a Pressurized Gasification System, Fifth Quarterly Report, Prepared for DOE by Westinghouse R&D, Pittsburgh, PA, October 1984-December 1984. Contract #DE-AC21-83MC20050.

Bachovchin, D. M., and M. A. Alvin, 1985c. Simultaneous High-Temperature Removal of Alkali and Particulates in a Pressurized Gasification System, Eighth Quarterly Report, Prepared for DOE by Westinghouse R&D, Pittsburgh, PA, July-September 1985.

Bachovchin, D. M., M. A. Alvin, E. A. DeZubay, and P. R. Mulik, 1986. "A Study of High Temperature Removal of Alkali in a Pressurized Gasification System", Final Technical Report, Prepared for DOE by Westinghouse R&D, Pittsburgh, PA, DOE/MC/20050-2226.

Mulik, P. R., M. A. Alvin, and D. M. Bachovchin, 1983. High-Temperature Removal of Alkali and Particulates in a Pressurized-Gasification System, Final Report, Prepared for DOE by Westinghouse Research and Development Center, Pittsburgh, PA, April 1981-July 1983, DOE Contract No. DE-AC21-81MC16372.

Mulik, P. R., D. F. Ciliberti, M. A. Alvin, and D. L. Keairns, 1980. Simultaneous High-Temperature Removal of Alkali and Particulates in a Pressurized Gasification System, Final Report, Prepared for DOE by Westinghouse Research and Development Center, Pittsburgh, PA, October 1978-October 1980, Contract DE-AC21-78ET11026.

THE PRESENT AND FUTURE OF GAS SUPPLIES

Luncheon Speech, June 18, 1987
William F. Morse, Vice President of Research, Columbia Gas

Thank you very much for the opportunity to be with you today. The subject of my talk, The Present and Future of Gas Supply, is one that seems at times like a never-ending soap opera. However the consequences are more serious and important, at least to some of us.

My comments will be those of a technology manager. One that has been frustrated by the ups and downs of the development of a synthetic fuels industry in the United States. It started with direct involvement in coal, oil, shale, and heavy oil gasification research back in the late '50s as a member of A.G.A.'s research staff, and has continued ever since, both in regard to industry/ government activities as well as our own in-house projects.

Looking backward and forward, it is clear to me that synthetic natural gas will never compete economically with natural gas as long as "conventional" natural gas is readily available. The issue is when will we start "running out" of "conventional" natural gas?

Let's examine the past. The history of natural gas is loaded with bad political and regulatory decisions which have given very false signals to technologists in the field of synthetic fuels.

The unrealistically controlled, low price of gas at the wellhead resulting from the 1954 Supreme Court decision in the famous Phillips case, which interpreted the 1935 Natural Gas Act, set the stage for the reduced drilling for gas which resulted in the shortage of available natural gas starting in the late 1960's. Severe shortages hit in 1976-1977. Gas at the wellhead was deregulated in a complex fashion to some degree in 1978. As a result, drilling dramatically increased, as did prices, and an excess gas "bubble" was created which still exists. Prices are now temporarily quite low. However, the sale of gas continues to decrease. There are various reasons. The high prices of the early '80s caused much more conservation than was anticipated. There is still room for more conservation, especially in the industrial market. Gas historically competed on low cost. End use gas technology reflects this in that the efficiency and performance of gas equipment is often inadequate with the higher prices that now prevail. New equipment is reducing consumption in existing markets. Also, competition is increasing.

What happened as a result of the political actions taken is now rather obvious. How could so many poor decisions be made, resulting in so many needless disruptions and ups and downs? I'll let you answer that, but you might start by considering what happens when the short term emphasis and overreaction of the political process takes over under the guise of protecting the public. Further, the majority of the decision makers had a very limited understanding of the supply and economics of natural gas. Although it might appear so, Washington is not the home of the leading geologists and petroleum engineers.

One of the interested groups that suffered during the course of events I just described was the synthetic fuels advocates. They too miscalculated the role of synthetic gas and, most particularly, its timing. Those involved in synthetic fuels also had very little background and understanding about natural gas. They, as did the politicians and regulators, and yes, many gas industry representatives, did not understand the exploration and production of oil and gas.

Let me ask you some questions. Your competition is natural gas. As you prepare your plans, proposals, budgets, etc., are you comfortable with the competitive position and timing of your programs? Is this the time to propose a pilot plant or project scaleup? Should more time be spent at the basic research or laboratory level? Can your concept have an impact?

It is easy to analyze the past, although many seem doomed to repeat history. What about the future? I will not make a forecast at this time, but I do wish to make a point about forecasting. Do you ever notice how many forecasts are made by non-experts, people who do not have personal and direct experience in the subject. Most forecasts are a simple projection of the recent past. Two data points and a ruler, and one is ready to give a luncheon talk. This is particularly true about energy forecasting because the implications are so broad, so many interests are involved, and so many forecasts are made.

Yes, the price of natural gas will go up in the near future, and yes, there is plenty of gas still available at less than the price of synthetics. In fact, we will never run out of natural gas as far as you and I are concerned. The price of conventional gas will go up because we are drilling deeper, further offshore, smaller and more difficult to find formations, and further away, such as Northern Canada, Alaska, and the Arctic. Increasingly coming into the picture will be unconventional sources, and please remember that there are no hard lines separating conventional and unconventional resources. Unconventional sources typically include the Devonian shales of Appalachia, tight Western sands, the geopressured zones of the southwest, coal bed methane, etc. These represent almost unlimited resources.

So the real question is not when will we run out of gas, but rather when will the price rise to the point synthetics and renewables can compete.

I would like to refer you to one set of forecasts, not necessarily from the standpoint of touting their quality but rather the source. I'm referring to the biennial supply forecasts of the A.G.A. Supply Committee. I'm holding copies of the 1983 and 1985 reports, and there will be another one this year. There is also a counterpart, the Demand Committee Study, which is produced biennially also, in the alternate years. These studies represent a consensus of gas industry management. That in itself doesn't make it right, but it does represent the current thinking of many decision makers. They directly and indirectly support and use what you are trying to accomplish. It is easy reading. I suggest you do so.

The Supply forecasts discuss and quantify all current and potential sources of gas -- conventional and unconventional natural gas, synthetic gas, and renewable gas. The '83 Survey suggests two to twelve 250 million cu.ft. per day coal gasification plants by the year 2000. The '85 Survey report indicates one to two such plants and five to ten plants by 2010. For comparison purposes, the

Great Plains plant produces about 125 million cu.ft. per day. You would need about 350 Great Plains plants to supply the natural gas supplied today.

It sounds in some respects that I'm painting a negative picture for synthetics. But there is one key which is very critical. That is lead time. The time to bring a new synthetic gas process from the inception of the idea, through the lab, PDU, pilot plant, semi-works plant, and first full scale plant is well over ten years if everything goes well -- particularly funding. If there is an opportunity in the year 2000 for large scale, 250 million cu.ft. day plants, then it is probably already too late for the first installations for the major process concept any of you might propose.

If we wait until the need for synthetic gas is obvious, then it is too late. What we are failing to do, as experts in the field, is to convey within the political process the need for a large, orderly RD&D synthetic gas program and, most importantly, that the implementation of that program be under the control of technologists. The latter is particularly difficult because a major source of the funding will have to, and should, be from the Federal Government.

The past administration wanted to electrify the nation because we had run out of gas. This administration wants to shut down DOE research in regard to fossil fuels. Funds for an orderly program are available within the current budget. All that has to be done is correct the obviously excessive allocation of funds to nuclear energy.

We are all too familiar with a recent major attempt experiment which was a disaster -- the Synthetics Fuels Corporation. The funding was provided, but the operation became a political nightmare. Before that, A.G.A. and OCR put together a major coal gasification program but it supported every scheme in sight to get political support.

The selection of those synthetic process concepts which should receive major funding is difficult at best. In the past, which Congressional District got the pilot plant was more important than technical and cost issues. We technologists have got to be more assertive in these matters. That is true in the U.S. of more than just synthetic fuels. We have to learn to operate inside the political process, not outside of it. Sure, the exercise is not as nice and neat as it should be. But we have to share the blame for past fiascoes. If you allow major technology programs and processes to be picked by Congressmen, lawyers, and accountants, I say good luck!!

In some way or another, we must convince the nation of the need for a synthetic gas program, intelligently timed, with major Federal Government funding, and with major gas industry involvement from a management and funding standpoint. In doing this, we must have proper procedures to evaluate and select the best projects. That means some way to protect ourselves from all the poorly thought out schemes which have always plagued such awards because of the legal and political pressures brought to bear. This cannot be done without strong and sound technical input. One cannot expect non-technologists to make the right decisions.

In summary, the following must be considered in establishing and conducting an orderly, efficient, economical, and timely synthetic gas development program.

1. You, the technologists, must become more involved in the total activity. We must work within the system. We will never be given a blank check. But, the technology based and affected decisions must be made by technologists.

2. Timing is very critical. We have had too many false starts.

3. Understand the competing alternatives. Remove your blinders. Understand the competition.

Thank you for your attention.

A NOVEL APPROACH TO HYDROGEN RECOVERY, STORAGE, AND TRANSPORT

1. CONTRACT NUMBER: DE-AC21-84MC23287

CONTRACTOR: United Technologies Research Center
Silver Lane
East Hartford, CT 06108
(203) 727-7224

CONTRACTOR PROJECT MANAGER: Dr. Madhav Ghate

PRINCIPAL INVESTIGATORS: Nicholas L. Krascella

METC PROJECT MANAGER: Lisa A. Jarr

CONTRACT PERIOD OF PERFORMANCE: February 20, 1987 to December 20, 1988

2. SCHEDULE/MILESTONES:

1987 Program Schedule

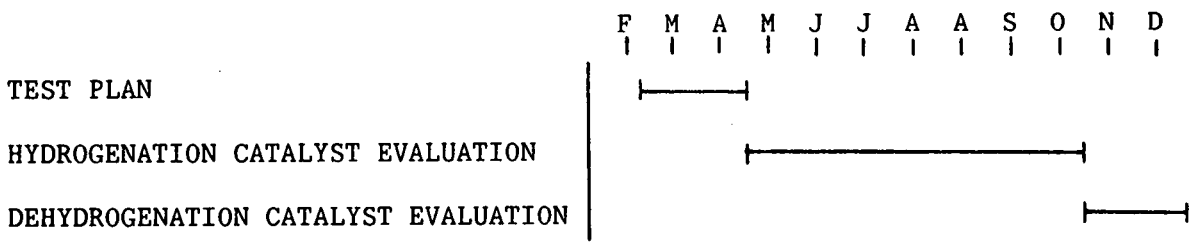

3. OBJECTIVES:

The objective of this contract is to demonstrate, on a laboratory scale, the selective recovery of hydrogen from a mixed gas stream typical of coal gasification system, or initial stage fiber membrane separator output via the hydrogenation-dehydrogenation reactant pair. Experimental results obtained in this investigation will provide a data base for a preliminary engineering-economic assessment of the organic hydride recovery, storage, and transport system and will serve as a basis for comparison with respect to state-of-the-art recovery, storage, and transport technology.

4. BACKGROUND STATEMENT:

Recently, United Technologies Research Center (UTRC) has been exploring the catalytic hydrogenation of aromatic hydrocarbons for the recovery of hydrogen from gas mixtures containing as contaminants CO, CO_2, and CH_4. In this concept, hydrogen can be selectively removed from the gas mixture, conveniently recovered as pure hydrogen stored and transported as an ambient temperature liquid hydride, and using a single chemical system. The transporting system (Kesten and Haught 1984) derives from

chemical heat pipe technology conceived and developed at UTRC (Kesten, Boedeker, and Couch 1983) and (Kesten and Haught 1986). The recovery of hydrogen from the organic hydride (Kesten 1986) is a particularly efficient one in which the catalytic combustion of some of the hydrogen is used as the source of heat for the dehydrogenation reaction (Kesten 1969) and (Marteney and Kesten 1981).

A large number of aromatic hydrocarbon/cycloparaffin reaction systems -- benzene/cyclohexane, toluene/methylcyclohexane, naphthalene/tetralin, and tetralin/decalin lend themselves to the removal, storage, and transport of hydrogen as an organic hydride. In the toluene/methylcyclohexane system, the reactions occur over a reasonable temperature range, are easily catalyzed, are readily reversible, exhibit little potential for side reactions (Seery and Colket 1985), are conducted in the gas phase at atmospheric pressure, and simple condensation of the organic reactants permit separation of contaminant gases or hydrogen.

The key steps in the chemical system for liquid hydride recovery, storage, and transport of hydrogen are shown in Fig. 1 and are based on temperatures derived from equilibrium calculations. In Step 1, hydrogen and toluene enter the catalytic hydrogenator at a temperature of approximately 120 C and react to form methylcyclohexane with the liberation of about 17 Kcal/mole hydrogen. If gas mixtures rather than pure hydrogen are introduced into the hydrogenator, the hydrogen is

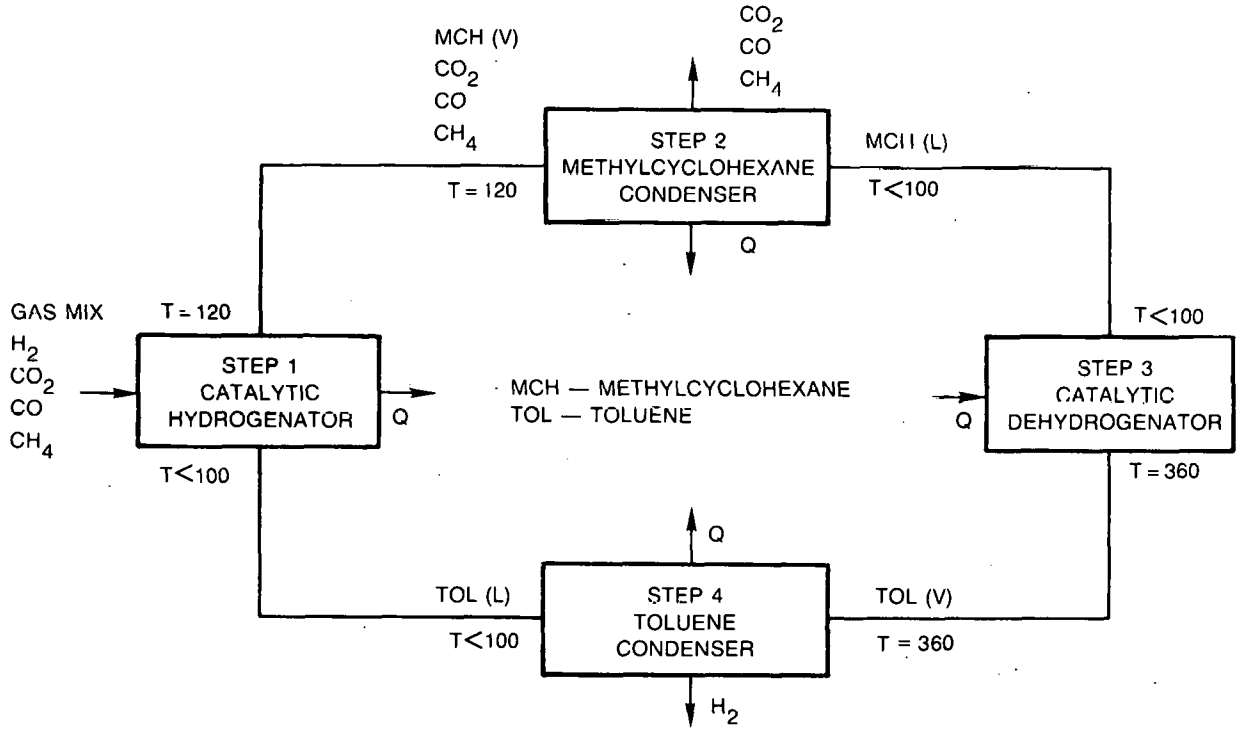

Figure 1. System for H_2 Recovery; Storage and Transport

selectively separated from the contaminant gases by the hydrogenation reaction. In Step 2, the effluent gases pass through a condenser, are cooled below 100 C, condensing the methylcyclohexane to a liquid for storage and/or transport. In the case of process gas input, the hydrogen component is separated from the contaminant gases. In Step 3 the liquid methylcyclohexane, stored at or transported to the user site, is vaporized and heated to about 360 C in the catalytic dehydrogenator where it is converted to toluene and hydrogen with the absorption of approximately 17 Kcal/mole hydrogen. In Step 4 the toluene and hydrogen mixture is cooled to a temperature below about 100 C to condense the toluene and separte the hydrogen for utilization. The liquid toluene is then transported to the hydrogenator for recycle.

The toluene/methylcyclohexane chemical system binds three moles of hydrogen per mole of methylcyclohexane and provides a hydrogen storage density of 3 pounds/ft^3. As shown by the data of Table 1, the liquid hydride storage density exceeds all but liquid hydrogen, and both liquid hydrogen and the only other system of competitive storage density cryoabsorption, require the establishment and maintenance of cryogenic temperatures with their associated equipment and energy costs. Toluene and methylcyclohexane are each stable liquids at ambient temperatures and have boiling points of 111 and 100 C and freezing points of -95 and -126 C, respectively. Thus with the liquid organic hydride system, conventional facilities can be used for storage and transport, without the necessity for refrigeration or auxiliary heating. Further, the toluene/methylcyclohexane liquid hydridge system consists of gases and liquids, eliminating the problems associated with solids while facilitating the transfer, handling, and separation of the system components.

Table 1. Hydrogen Storage Capabilities

Storage Medium	H_2 Density (lbs/ft^3)
Liquid Organic Hydride (TOL/MCH)	3.0
Compressed Gas (2900 psi)	1.1
Liquid Hydrogen	4.4
Metals Hydridges (Iron Titanium)	1.0
Cryoabsorption	2.5
Glass Spheres	0.8

The long-term value of this storage system obviously depends on the extent to which undesired side reactions can be avoided. Experiments at UTRC have investigated the hydrogenation of toluene to methylcyclohexane over a Pt/Rh catalyst, varying the temperatures and pressures (residence times) and examining the degree of reaction and extent of side reactions. The experiments were conducted over a temperature range of 55 to 150 C and a pressure range of 100 to 840 Torr. For the experiments, hydrogen and toluene were passed as mixed gases over a Pt/Rh catalyst supported on an alumina substrate. The experiments have demonstrated conditions of complete reaction, with degradation products from side

reactions below the limit of gas chromatograph detectability (less than 30 ppm). Quantitative measurements have determined a reaction rate under these conditions of 1.5×10^{-2} moles toluene/gm cat-hr (Seery and Colket 1985).

Similarly, hydrogenation of toluene was conducted statically in the liquid phase under high pressure over Pt/Pd, Ni, Ni/Cu, and Pt catalysts using a Parr bomb. Hydrogenation of toluene to methylcyclohexane proceeded rapidly to completion in the liquid phase at a variety of temperatures. Loss of catalyst activity in the presence of impurities was observed to be readily and repeatedly reversed.

Initial hydrogenation experiments with gas contaminants (79% hydrogen, 2% carbon monoxide, 17% carbnon dioxide, and 2% methane) showed rapid deactivation of the Pt/Rh catalyst with negligible hydrogenation of the toluene. However, the catalyst activity was readily restored by purging with hydrogen at the operating temperature. Subsequently, investigations were conducted with hydrogen and individual reformer gas constituents to determine the deactivation source. Methane in concentrations up to 10% exhibited no adverse effect on the hydrogenation reaction. Carbon monoxide in concentrations up to 1% and carbon dioxide in concentrations up to 10% also did not appreciably affect the conversion reaction.

5.0 PROJECT DESCRIPTION

A critical element in the development of the liquid hydride concept for the recovery of H_2 from a contaminated gas mixture such as the effluent stream from a coal gasifier, or a fiber membrane separator used for the partial separation of hydrogen, centers on the development of suitable hydrogenation catalysts which can tolerate reasonable concentrations of contaminants without appreciable deactivation. Materials or combination of materials will be selected as candidates for tolerant hydrogenation catalysts. Three of the candidate catalysts will be evaluated experimentally as possible hydrogenation catalysts using the toluene/methylcyclohexane system. Initial testing will be conducted with pure hydrogen to establish baseline hydrogenation data for comparison with similar data obtained in subsequent tests with hydrogen contaminated with various concentrations of CO, CO_2, H_2S, and CH_4 individually and in combination. The experimental parameters to be examined in these tests are: catalyst bed temperature, reactant flow rate, reactant gas composition, and stoichiometry (H_2/toluene). The experimental results will provide data on the effect of contaiminants for the selected catalysts in terms of conversion yield, overall reaction rates, and the extent of degradation product formation.

Ideally, use of a single catalyst configuration for both the hydrogenation and dehydrogenation reactions is desirable from the standpoint of simplicity and reduced inventories of expensive materials. However, different catalysts may be required to provide acceptable reaction rates at minimum hydrogenation and dehydrogenation temperatures and to minimize formation of degradation products. The potential dehydrogenation catalysts will be experimentally evaluated over a range of temperatures. One of the catalysts would be selected from those

hydrogenation catalysts previously examined; the other two will be selected from known dehydrogenation catalyst configurations reported in the current literature. The tests results will provide conversion yields, overall reaction rates, and the extent of degradation product formation as a function of catalyst loading, reactant flow rate, and catalyst bed temperature.

6.0 RESULTS/ACCOMPLISHMENTS

This program was initiated on February 20, 1987. To date, a test plan has been formulated and a number of contaminant tolerants hydrogenation catalyst have been identified. In addition, the hydrogenation reactor system has undergone minor modifications to facilitate operation and has been loaded with a Pt/Rh catalyst for the initial hydrogenation studies.

7.0 FUTURE WORK

Future studies under the current contract involve open-loop performance test using both a catalytic hydrogenator and a catalytic dehydrogenator to demonstrate concept feasibility and to provide basic data for a preliminary systems analysis of the concept.

8.0 REFERENCES

Kesten, A. S.: Low-Energy Method for Freeing Chemically Bound Hydrogen, Patent No. 4,567,033, January 28, 1986.

Kesten, A. S.: Analytical Study of Catalytic Reactors which Promote Endothermic Reactions of Hydrocarbon Fuels. Presented at the AIAA 4th Thermophysics Conference, San Francisco, CA, 1969.

Kesten, A. S., L. R. Boedeker and H. T. Couch: A Self-Driven Chemical Heat Pipe. Heat Recovery Systems, Volume 3, pg. 311, 1983.

Kesten, A. S. and A. F. Haught: Gas Transporting System, U.S. Patent No. 4,478,814 (1984).

Kesten, A. S. and A. F. Haught: Self-Driven Chemical Heat Pipe. U.S. Patent No. 4,346,572 (1982).

Marteney, P. J. and A. S. Kesten: Kinetics of Surface Reactions in Catalytic Combustion. Presented at the 18th Symposium on Combustion, The Combustion Institute, 1981.

Seery, D. J. and M. B. Colket, III: The Catalytic Hydrogenation of Toluene: Temperature and Residence Time Effects. Presented at the 2nd International Symposium on Hydrogen Produced from Renewable Energy, Cocoa Beach, Florida, October 1985.

HYDROGEN RECOVERY BY NOVEL SOLVENT SYSTEMS

Contract Number DE-AC21-87MC23292

Contractor The Research Foundation of C.U.N.Y.
on behalf of The City College of C.U.N.Y.
1515 Broadway
New York, NY 10036

Contractor Project Manager Dr. Zvi Ludmer

Principal Investigator Professor Reuel Shinnar

METC Project Manager Lisa A. Jarr

Period of Performance February 3, 1987 - February 2, 1989

Schedule/Milestone

Literature survey	February 1988
Test Plan	May 1987
Design and Construction of Experimental Apparatus	February 1988
Screening Tests	February 1989
Preliminary Economic Evaluation	February 1989
Comprehensive Topical Report	February 1989

OBJECTIVES

The objective of this work is to develop a novel method for purification of hydrogen from coal-derived synthesis gas. The study involves the search for suitable mixtures of solvents for their ability to separate the hydrogen from the coal derived gas stream in significant concentration near their critical point of miscibility. The properties of

solvent pairs identified will be investigated in more detail to provide data necessary for economic evaluation and process development.

BACKGROUND STATEMENT

In hydrogen production, separation of hydrogen from the other contituents of raw syngas is expensive and highly energy intensive. A novel, cheaper and less energy intensive process could here lead to substantial cost reduction. We propose to do this by finding radically improved solvents for extraction processes. One needs to find solvents with a greater power of solution and higher selectivity that can be regenerated with lower energy consumption. To achieve this, a solvent would have to operate between $20^{o}C$-$80^{o}C$ and exhibit a strong dependence of gas solubility on temperature.

In a recent study we have suggested that a novel class of solvents should have these desired properties. It was found that mixtures of solvents near their critical point of miscibility exhibit strongly improved solvent properties. Solubility for certain compounds strongly increases near the critical composition point. This is similar to the well-known super critical extraction with fluids at their gas liquid critical point, but has considerable advantages over it as there is no need for high pressure [Paulaitis, 1983, Penninger et al., 1985]. This research could also have impact on other areas of fossil fuel technology.

PROJECT DESCRIPTION

Based on theoretical considerations we have recently shown that the solubility ($\bar{n}$) of a solid in a binary mixture close to its immiscibility critical point has the following form [Ludmer, Shinnar and Yakhot, 1987].

$$(\bar{n}) = \exp(b\tau^{3\nu-\gamma} - 6\alpha^2 c^2 \tau^{3\nu-\gamma-2\beta})/T^2 \qquad (1)$$

where $\tau = \frac{T-T}{T_c}$; $c = \bar{x} - \bar{x}_c$ $T_c = T_c(c=0)$;

$\bar{X}_c$ denotes the critical composition and b and α are only weak functions of temperature. According to the theory of critical phenomena the following identity holds (Landau and Lifshitz, 1983):

$$3\nu - \gamma - 2\beta = 0 \qquad (2)$$

and thus the coefficient of c^2 in equation (1) can be assumed to be independent on τ. From equation (1) it is also clear that at the critical composition (c=0) the solubility ($\bar{n}$) has a maximum value. Figure 1 describes the solubility of anthracene in the binary solution mixtures of methanol and hexane. The observed maximum in solubility in the vicinity of the critical composition is in agreement with the above theoretical consideration. Similar results were also observed with other systems.

Based on our previous studies we have reason to believe that some binary solution mixtures in the vicinity of their immiscibility critical

---

Figure 1. Enhanced solubility of anthracene in binary mixtures of methanol (M) and hexane (H). CST is around 34°C. C.C. denotes critical composition.

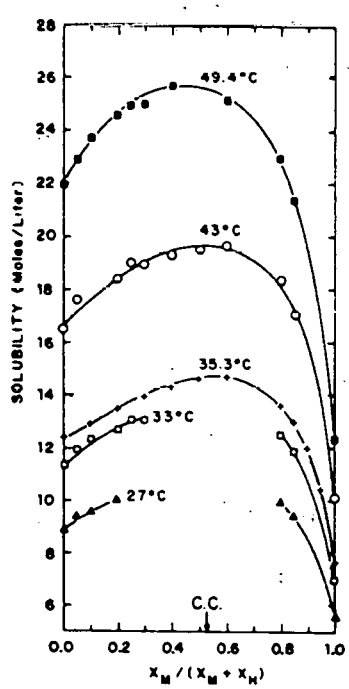

---

point will have promising properties as regard

to their selective solubility of the syn-gas components. Our primary goal, based on theoretical considerations, will be to identify the various solvent mixtures, and to determine the solubility of the various individual syn-gas components[CH_4, H_2S, CO_2 and CO]. Figures 2-5 describe schematically four types of immiscibility curves. Solvent mixtures with a lower critical point are very good candidates for our approach.

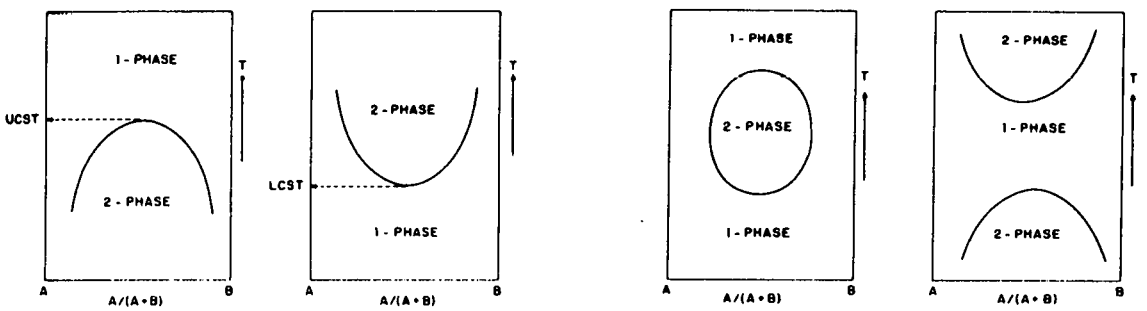

Figures 2-5. Schematic presentation of various types of miscibility curves. Examples: #2 (hexane, methanol), #3 (water, lutidine), #4 (water, nicotine), #5 (cyclohexane, polystyrene).

ACCOMPLISHMENTS

We are presently working on the design of the experimental test facility. The experimental set-up will consist of a transparent mixing chamber and a magnetic pump for vapor circulation. Analysis will be performed of both the vapor and the liquid phases, by means of gas chromatography (GC). In order to improve the analysis both the vapor and the liquid phases will be circulated via 6 port GC sampling valves. Following the screening tests promising binary mixtures will be further investigated. The solubility of the individual syn-gas components will be studied as a function of temperature and pressure. Finally based on the solubility information a process design studies and preliminary cost estimate will be performed. The purpose of which will be to establish the

best process option that would lead to a significant improvement and cost reduction for hydrogen separation.

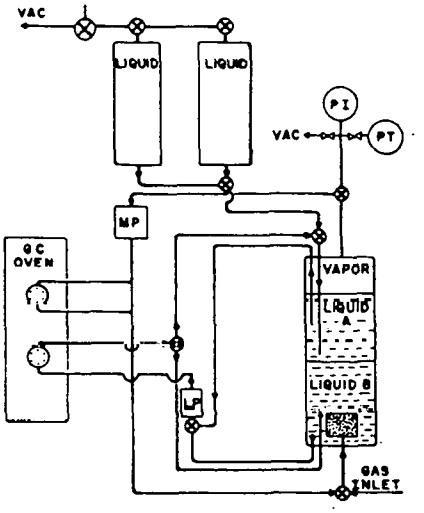

Figure 6. Proposed experimental set-up for gas solubility studies.
LP, MP Liquid and vapor recirculating pumps, respectively, PI - Pressure indicator, PT - Pressure transducer, GC - Gas chromatograph.

FUTURE WORK

Assembly of the presently planned test facility and perform test experiments. Based on theoretical considerations various binary solvent mixtures will be selected. The solubility of the syn-gas components will be investigated close to the immiscibility critical point of the binary solution mixtures.

REFERENCES

Ludmer, Z., R. Shinnar and V. Yakhot, "Solubility in Binary Mixtures at the Immiscibility Critical Point," AIChE Journal, 1987.

Landau, L.D. and E.M. Lifshitz, "Statistical Physics," Pergamon Press, Oxford (1983).

Paulaitis, M.E. et al., "Supercritical Fluid Extraction," Rev. Chem. Eng. 1, 179 (1983).

Paulaitis, M.E., J.M.L. Penninger, R.D. Gray, Jr. and D. Phillip, Eds., "Chemical Engineering at Supercritical Fluid Conditions," Ann Arbor Sci. Pub. (1983).

Penninger, J.M.L. et al., eds., "Supercritical Fluid Technology," Elsevier (1985).

LOW COST HYDROGEN/NOVEL MEMBRANE TECHNOLOGY FOR HYDROGEN SEPARATION FROM SYNTHESIS GAS

1. CONTRACT NUMBER DE-AC21-85MC22130

CONTRACTOR: Membrane Technology and Research, Inc.
1030 Hamilton Court
Menlo Park, CA 94025
(415) 328-2228

PRINCIPAL INVESTIGATORS: Richard Baker
Hans Wijmans
Ingo Pinnau
Daryl Roberts

METC PROJECT MANAGER: Lisa Baker-Jarr

CONTRACT PERIOD OF PERFORMANCE: September 30, 1985 - September 30, 1988

Task 1. Literature survey
Task 2. Test plan
Task 3. Laborary experiments
- 3.1 Prepare high performance membranes
- 3.2 Construct membrane modules
- 3.3 Evaluate membrane modules
- 3.4 Perform module system studies

Task 4. Mathematical model
Task 5. Economic cvaluation
Task 6. Preparation of reports

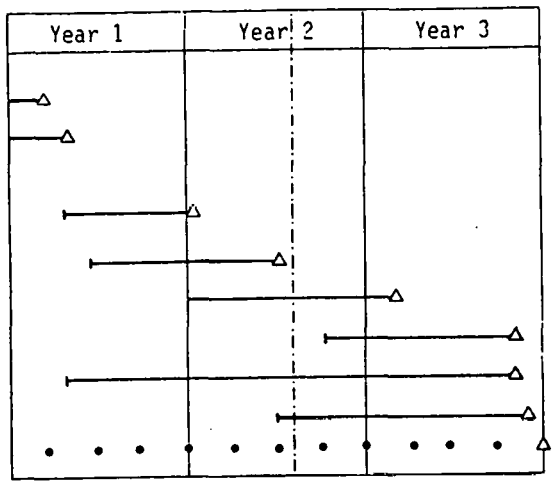

3. OBJECTIVE:

The separation of hydrogen from synthesis gas is a major cost element in the manufacture of hydrogen from coal. Separation of these gases by membranes is a alternative technique that is still largely unexplored and that could offer substantial cost savings. The objective of this program is to develop membranes suitable for these separations and demonstrate their applicability with small spiral-wound modules on model gas mixtures representative of those found in synthesis gas processes.

4. BACKGROUND STATEMENT:

There are three opportunities for membrane separation in the production of hydrogen from coal:

- The separation of hydrogen from carbon monoxide before the shift reactor.
- The separation of hydrogen from carbon dioxide and hydrogen sulfide after the shift reactor.
- The separation of hydrogen from nitrogen after the acid gas removal in an air-blown gasification process.

Model coal gasification schemes incorporating membranes in these three steps are shown in Figure 1.

5. PROJECT DESCRIPTION:

As an initial step in our program, a review of polymer permeability data, either available in the literature or obtained at MTR, was performed. Based on this initial screening, two polymers were selected for membrane development work:

- Poly(etherimide) for the separation of hydrogen from nitrogen and from carbon monoxide.
- Poly(ether-ester-amide) for the separation of hydrogen sulfide and carbon dioxide from hydrogen.

(a) Carbon Monoxide from Hydrogen and Carbon Dioxide

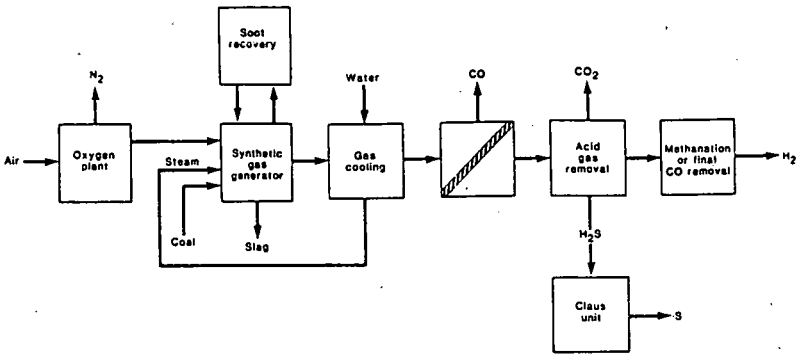

(b) Hydrogen from Hydrogen Sulfide and Carbon Dioxide

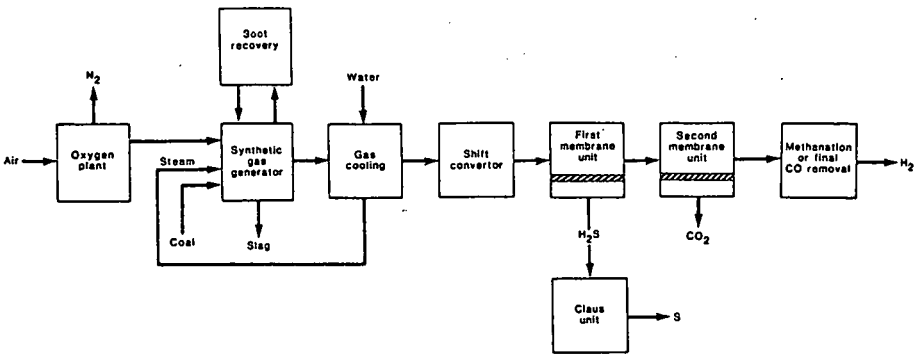

(c) Hydrogen from Nitrogen, Carbon Monoxide, and Carbon Dioxide

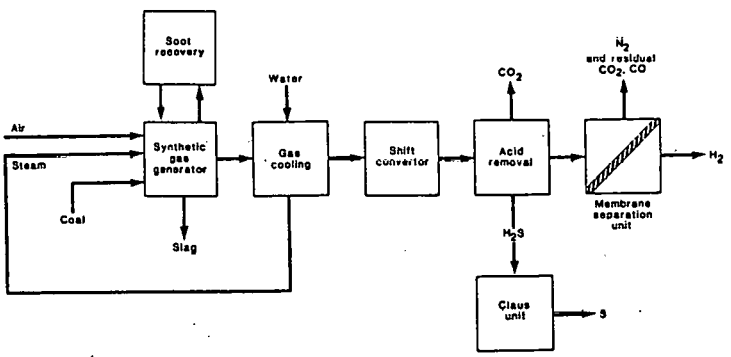

Figure 1. Examples of synthesis gas membrane separation processes.

After characterizing the membrane properties of relatively thick (20-50 μm) films, we concentrated on fabricating asymmetric or composite ultrathin high-performance membranes. Asymmetric or composite ultrathin membranes in which the permselective layer is on the order of 0.5- to 1.0-μm-thick are required if usefully high membrane fluxes are to be obtained. The dense permselective layer is formed on the surface of a much thicker microporous support layer. The microporous support provides the mechanical strength required without altering the flux and selectivity of the permselective layer. A schematic diagram of a composite ultrathin membrane is shown in Figure 2.

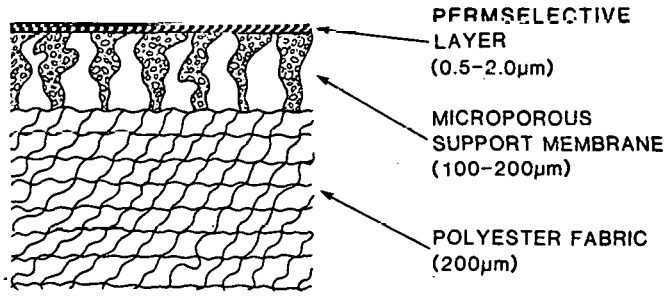

Figure 2. Cross-section of composite membrane.

6. RESULTS/ACCOMPLISHMENTS:

POLY(ETHERIMIDE) MEMBRANES

The properties of the poly(etherimide) membranes are summarized in Figure 3. As shown, these membranes are extremely permeable to hydrogen compared to nitrogen and carbon monoxide. Poly(etherimide) membranes would, therefore, be most suitable for these separations. Poly(etherimide) is a tough, high-melting polymer. We have shown that the membranes maintain their desirable selectivity properties at temperatures in excess of 90°C. Membrane selectivity for gas mixtures is also essentially independent of feed gas composition, as the results in Figure 4 show.

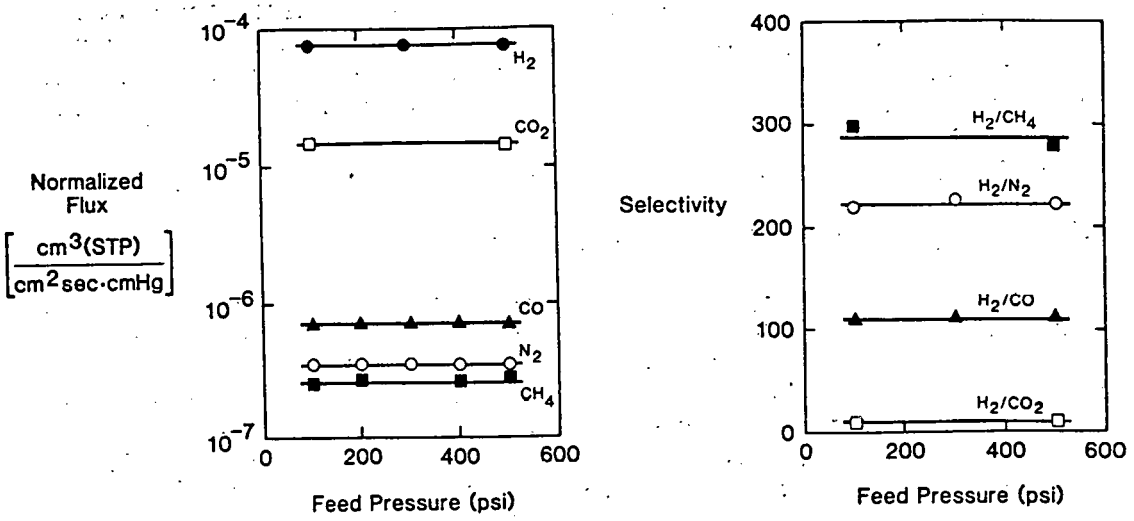

Figure 3. Normalized fluxes and selectivities of poly-(etherimide)/polydimethylsiloxane composite membranes as a function of feed pressure. Temperature: 25°C.

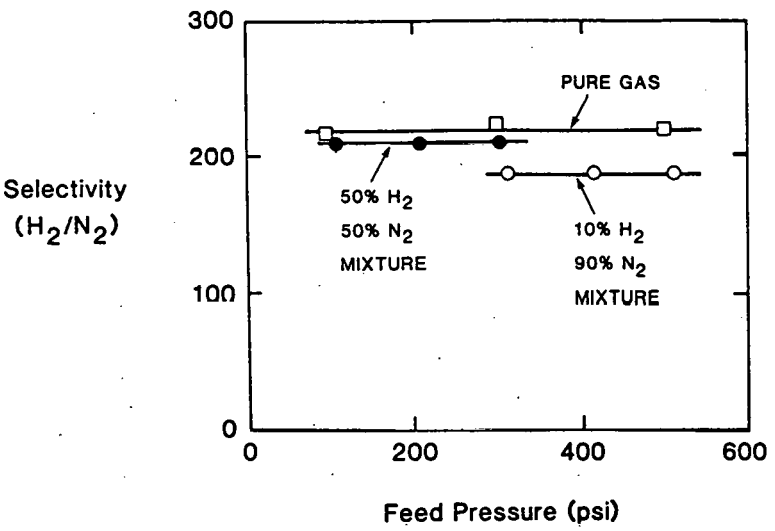

Figure 4. Hydrogen over nitrogen selectivity of poly-(etherimide)/polydimethylsiloxane composite membranes as a function of feed pressure. Temperature: 25°C.

The membranes have been fabricated into continuous rolls of flat-sheet membranes and as hollow fibers. Currently, we favor hollow-fiber membranes because it is easier to fabricate poly(etherimide) membranes into defect-free high-surface-area modules as hollow fibers, rather than as spiral-wound flat-sheet membrane modules.

POLY(ETHER-ESTER-AMIDE) MEMBRANES

Poly(ether-ester-amide) membranes are extremely selective for carbon dioxide, compared to other gases, as the data in Figure 5 show. Thus, these membranes are most suited to the separation of carbon dioxide from hydrogen/methane/nitrogen mixtures. Based on data on pure gases a carbon dioxide/hydrogen selectivity of greater than 10 would be expected. With gas mixtures, plasticization of the membrane by carbon dioxide lowers the selectivity to between 7 and 8. This mixed gas selectivity is lower than the pure gas selectivity, but still much higher than almost all other polymeric membranes.

We have fabricated these poly(ether-ester-amide) films into spiral-wound membrane modules and tests with these modules are now underway.

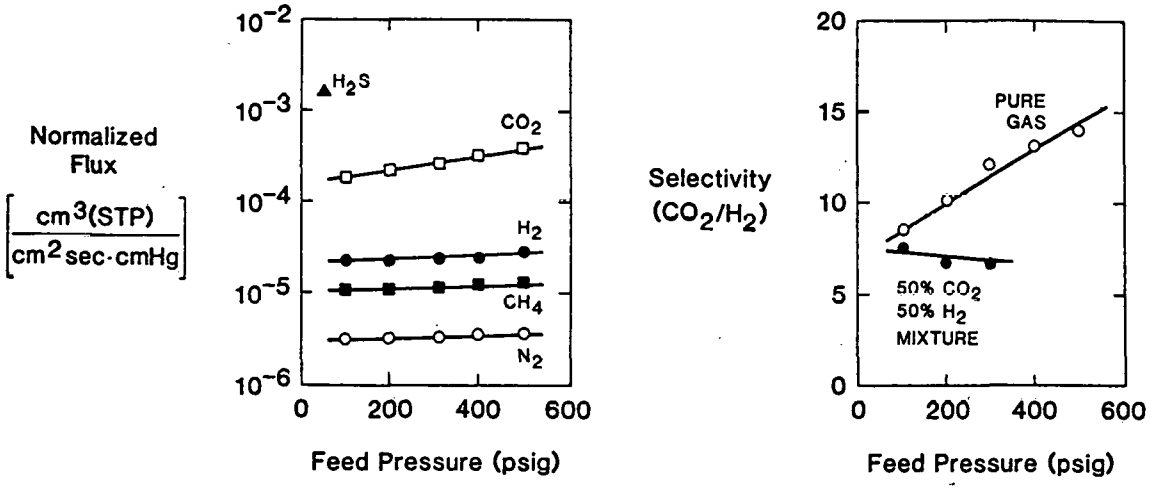

Figure 5. Normalized fluxes and selectivities of poly-(ether-ester-amide) composite membranes as a function of feed pressure. Temperature: 25°C.

MATHEMATICAL MODEL

In addition to these experimental studies, SRI International has developed computer models for use in evaluating the performance of different membrane systems. The codes address:

- Cross-flow Membrane Module Performance
- Counter-current Membrane Module Performance
- Reciprocating Compressor Design
- Discounted Cash Flow Analysis

Flow sheet programs have been developed which combine a number of the above codes to evaluate the performance and economics of an entire process.

7. FUTURE PLANS

The following tasks will be performed in the final year of the program:

- Construct membrane modules
- Evaluate modules with gas mixtures
- Complete mathematical model
- Perform economical analysis of membrane systems for production of hydrogen from coal.

ADVANCED STUDIES OF THE BIOLOGICAL CONVERSION OF SYNTHESIS GAS TO METHANE

1. CONTRACT NO. DE-AC21-86MC12181

CONTRACTORS: Board of Trustees
University of Arkansas
Fayetteville, AR 72701
(501) 575-4951

CONTRACT PROJECT MANAGER: J. L. Gaddy

PRINCIPAL INVESTIGATORS: E. C. Clausen
J. L. Gaddy

METC PROJECT MANAGER: W. S. Liou

CONTRACT PERIOD OF PERFORMANCE: September 29, 1986 - September 28, 1989

2. SCHEDULE/MILESTONES:

1986-87 PROGRAM SCHEDULE

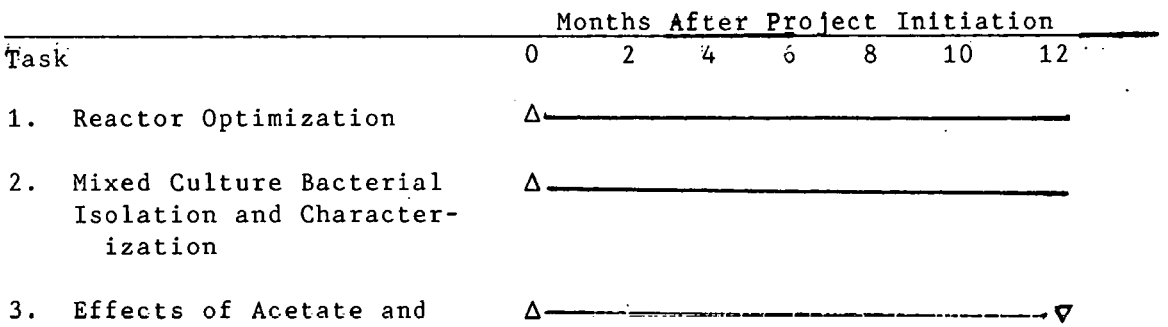

Δ - Initiate Specific Task

∇ - Complete Specific Task

3. OBJECTIVE:

The objective of this project is to obtain fundamental data to allow optimization of the biological system for producing methane from coal-derived gas. Studies involving reactor and culture optimization and reactor design and scale-up will be performed during the contract period.

4. BACKGROUND STATEMENT:

The technical feasibility of the biological conversion of coal synthesis gas to methane has been demonstrated in the University of Arkansas laboratories. Several microorganisms have been identified as having commercial potential for producing methane. These include a mixed culture of partially identified bacteria; P. productus, which produces acetate, a methane precursor; and Methanothrix sp., which produces methane from acetate. These cultures have been used in mixed reactors and immobilized cell reactors to achieve total CO and H_2 conversion in a retention time of less than two hours, quite good for a biological reactor. The cultures carry out the conversions at ordinary temperatures and pressures, without sulfur toxicity. This contract addresses the further development of this technology through culture and reactor optimization, definition of mass transfer and kinetic parameters for scale-up and concept demonstration.

5. PROJECT DESCRIPTION:

The contract is organized into seven tasks to be completed in a three year period.

- Optimization of the conditions and reactor type for each culture. Selection of the best systems for scale-up and prolonged demonstration.
- Continued search for improved cultures through isolation and identification of microorganisms in the mixed culture and microorganisms to convert CO and H_2 directly into methane.
- Determine the pressure limitations and acetate toxicity of various microorganisms to further reduce reactor volume by operation at higher pressures.
- Confirm sulfur toxicity limits of the microorganisms in continuous culture.
- Determine mathematical relationships to define the mass transfer and kinetic coefficients of the reactions.
- Bench-scale operation to demonstrate the optimal performance and culture stability over prolonged continuous operation.
- Develop computer simulation models to predict the economics of these processes and identify sensitive parameters for further concentrations.

The results from this research program should lead to the development of a simple and economical process alternative to high temperature, high

pressure shift conversion and methanation in producing methane from coal synthesis gas. Cultures that operate in ordinary temperature and pressure, with retention times of only a few minutes for complete conversion to methane, will be developed. Inexpensive reactors that maximize cell density and conversion without agitation are under study. Mass transfer and kinetic parameters for scale-up of PDU and commercial units will be developed.

6. RESULTS/ACCOMPLISHMENTS:

The following results were obtained during the first 8 months of the contract period. As is shown in the Program Schedule, the research effort during this time period has been concerned only with Tasks 1, 2, and 3.

° Optimized growth and media conditions for P. productus, the organism found most suitable in converting CO to methane precursors. Very low levels of amino acids or soybean hydrolyzate may be used to replace expensive yeast extract as essential nutrients.

° Determined product yields and effects of acetate and CO on substrate uptake and product formation for P. productus: $Y_{X/CO}$ = 1.5 g cell/mol CO and $Y_{AcH/CO}$ = 0.25 mol acetate/mol CO. No inhibition was found at a dissolved CO tension of 1.7 atm or an acetate concentration of 30 g/L.

° Performed continuous culture experiments with P. productus using continuous gas and liquid feed. Performance at or very near complete mass transfer-limited operation was obtained. Significant improvements over previous studies with batch media exchange were made.

° Experimental techniques both in batch and continuous culture for the determination of kinetic and stoichiometric parameters have been developed for all biological cultures.

° The effects of CO, H_2, agitation and pressure on the mixed culture were defined. The most significant results are that methane formation from CO_2 and H_2 is mass transfer-limited, while methane formation from acetate is not affected by agitation.

° The mixed culture has been observed to contain significant populations of P. productus, Methanosarcina and Methanothrix. A co-culture containing these species from pure cultures has been successfully utilized for methane production from synthesis gas.

° The effects of pressure, acetate and CO on methanogens has been determined. It has been found that while high total pressure is not deleterious to performance, increased CO partial pressure in the gas phase negatively affects methane production.

The results of these studies will be essential in optimizing the culture and reactor system. Future work during the contract period will focus on determining reaction kinetics and miss transfer relations in preparation for reactor scale-up and bench-scale process tests. An economic evaluation of all the process technology will be made to aid

in design and scale-up decisions.

7. FUTURE WORK:

Future work during the remainder of 1987 will concentrate on completing Tasks 1, 2, and 3: reactor optimization, mixed culture isolation and characterization, and the effects of acetate and increased pressure on methanogenesis. Task 3 is scheduled for completion in October 1987, and Tasks 1 and 2 are scheduled for completion in March 1988. The remaining four tasks will be initiated during 1988 and 1989 as scheduled.

BIOLOGICAL GASIFICATION

1. CONTRACT NUMBER: DE-AC21-87MC23285

CONTRACTOR: Atlantic Research Corporation
5390 Cherokee Avenue
Alexandria, Virginia 22312

PROGRAM MANAGER: (Contractor) Dr. Daman S. Walia

PRINCIPAL INVESTIGATOR: Dr. Jenefir D. Isbister

METC PROJECT MANAGER: Dr. Wen-Shou Liou

CONTRACT PERIOD OF PERFORMANCE: June 1987 - June 1989

2. SCHEDULE/MILESTONES

1987 Program Schedule

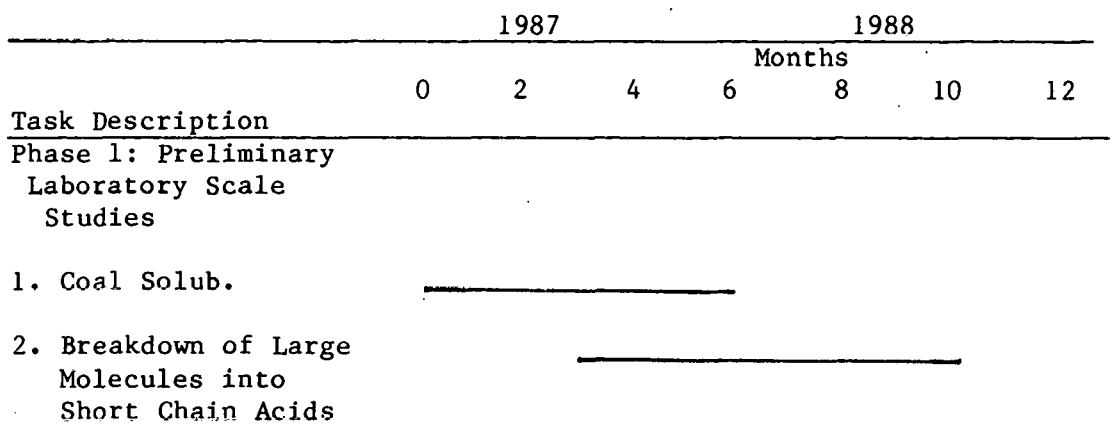

3. OBJECTIVES:

This project addresses the program area of Fundamentals of Coal Gasification Chemistry/Coal Derived New Fuel Forms. The program has three specific objectives:

- To demonstrate on a laboratory scale the microbial conversion of three coals (North Dakota Lignite, Wyodak subbituminous and Ohio bituminous) to methane.
- To demonstrate the microbial conversion of coal to methane in a continuous bench-scale process.
- To develop design criteria for pilot-scale and economic analysis for full-scale microbial coal to methane conversion units.

This research project has as its ultimate goal the development of an efficient, economical microbial process for conversion of undesirable coals to a clean fuel, methane.

4. BACKGROUND STATEMENT:

The United States has coal reserves capable of supplying energy for several hundred years, however many coal seams in this country are not used because the coal has undesirable characteristics such as low heating value and high sulfur content. The development of an economical process in which a clean, easily used fuel is derived from such coals would be of great economic benefit to many coal mining regions as well as to the United States as a whole. Coal gasification processes have been developed although, in general, gasification processes are expensive and the final cost of the methane produced from coal is not competitive with current prices for natural gas and/or oil. Production of a clean, economical fuel from our vast coal reserves would be of great benefit to the U.S. in maintaining good environmental quality, maintaining a high standard of living and in gaining energy independence by decreasing the need for foreign oil imports.

5. PROJECT DESCRIPTION:

Five technical tasks will be implemented to address the objectives of this project. The overall process concept is presented below in Figure 2. Coal (lignite, subbituminous, bituminous) will be treated chemically or microbially to produce water soluble products suitable for further aerobic bioconversion to lower molecular weight products which can in turn serve as feedstock for anaerobic conversion to methane.

The first of the five tasks will evaluate two approaches to conversion of three coals of varying rank into liquid products. One approach will use chemical/thermal softening techniques to break the cross linked coal matrix into high molecular weight liquids. A second approach will use an unique consortium of fungi and bacteria isolated by Atlantic Research to break down the coal macromolecular structure with resulting liquid products. The aqueous soluble products from chemical/thermal softening and from the microbial solubilization will be characterized and comparisons will be made with respect to molecular weight of products and extent of coal depolymerization by each treatment.

Three coals will be used in this program, a North Dakota lignite, a Wyoming subbituminous and an Ohio bituminous coal. Each of the coals will be pulverized and ground to a D_{80} of 100 mesh prior to tratment using the chemical/thermal procedures or the microbial solubilization proccdures.

Microbial solubilization of coals using the ARC consortium has been demonstrated, although the process is slow. Optimization of the conversion of coal to liquid is a goal of this subtask. Variables to be studied include nutrients, pH, and temperature.

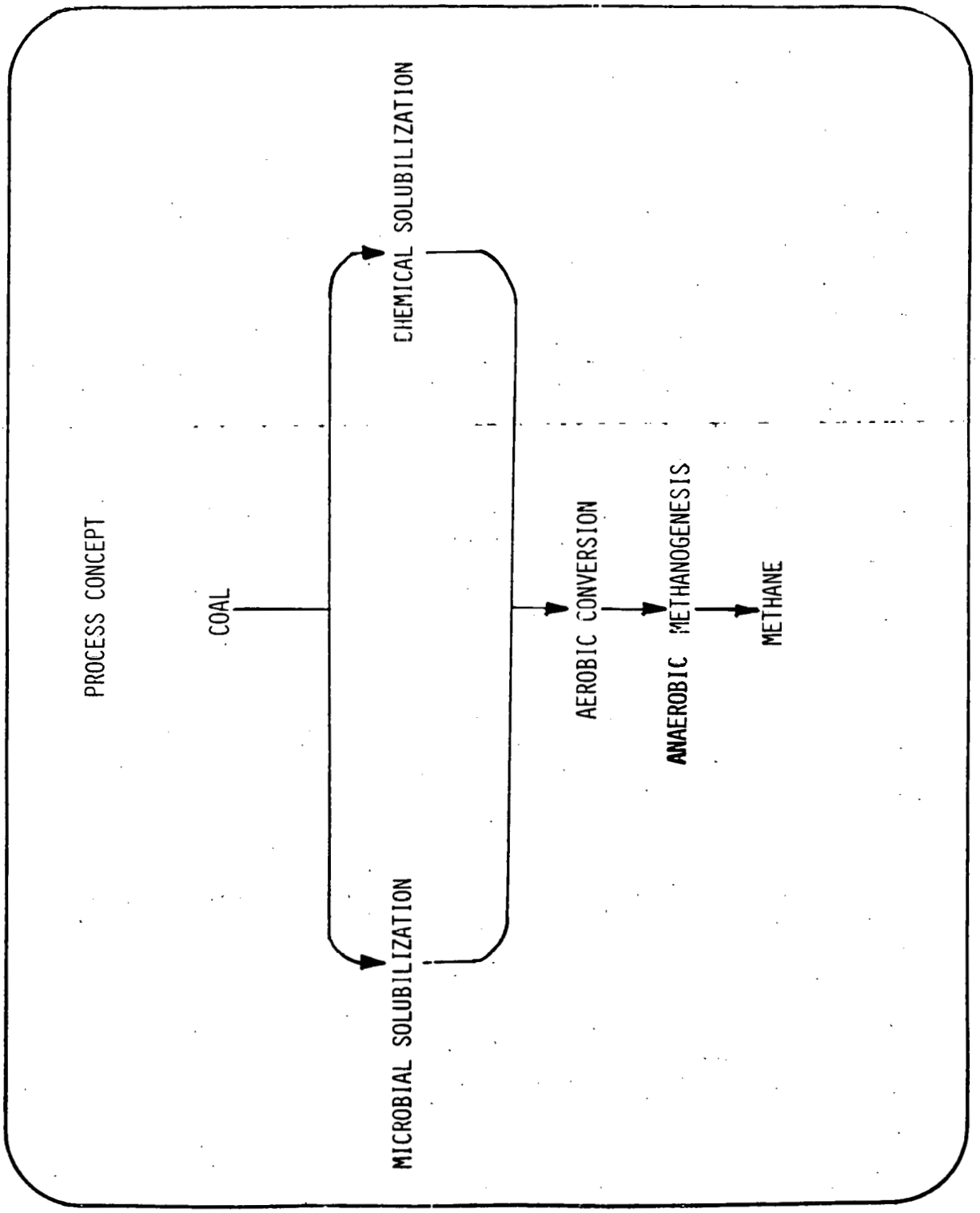
PROCESS CONCEPT
COAL
CHEMICAL SOLUBILIZATION
MICROBIAL SOLUBILIZATION
AEROBIC CONVERSION
ANAEROBIC METHANOGENESIS
METHANE

Figure 2

The soluble products from chemical/thermal and microbial treatments will be measured for total organic matter solubilized, molecular weight ranges for the products and susceptibility to further microbial biodegradation. Products will be lyophylized and monitored for total mass, Btu, elemental content and acid number. Gel permeation chromatography will be used to determine the molecular weight distributions of the solubilized coal. Some of the lower molecular weight products will be derivatized by methylation or silylation for analysis by gas chromatography-mass spectometry.

Analysis of the time required for solubilization, projected costs for solubilization, quantity of lower molecular weight compounds and quantity of impurities present in product-containing liquids will be used to select the treatment most suited for coal processing to supply liquid products for Task II.

Task II will address breakdown of the liquid products obtained in Task I to short chain acids and/or alcohols. The best aerobic microbial population(s) for further conversion of the organic coal digests will be selected and the effects of nutrient addition for rapid, efficient bioconversion of the digests will be evaluated. The products from aerobic bioconversion of the digest will be surveyed for molecular weight range(s), for preliminary indentification and/or characterization and for suitability as a feedstock for anaerobic conversion to methane based on the following analyses:

- o Quantitation of biomass
- o Identification of major microorganisms present
- o Molecular weight profiles of meidum using gel permeation chromatogrpahy
- o Elemental analysis of the freeze dried products
- o Derivatization of selected product fractions followed by GC/MS analysis.

Task III will address the anaerobic biological conversion of aerobicaly produced substrates to methane. Each of the coals will be pretreated using the procedure selected in Task I to yield the most desirable feedstock for aerobic microbial conversion to short chain acids and/or alcohols. Methanogenic cultures will be stabilized in laboratory digestors using synthetic sewage sludge feedstocks. After stable conditions have been achieved and biomass concentrations are adequate for rapid methane production, digests from each of the lignite, subbituminous and bituminouus coals will be introduced into fermentors as feedstocks for methane production. Parameters to be monitored for each fermentor include the following:

- o pH
- o Alkalinity
- o Ammonia
- o COD (feed, effluent)
- o Gas production
- o Gas quality

Task IV will demonstrate the processes developed in the preceding tasks. The process is envisioned as a continuous unit, or a continuous batch unit, for production of methane from coals. Each unit process will consist of four subunits. A proposed schematic for a coal to methane unit is presented in Figure 3. The first unit will be an aerobic bio-disc or chemical softening apparatus. The bio-disc was selected as a proposed process unit because extracellular enzymes produced by microorganisms attached to the large surface areas in the bio-disc are continuously secreted into the medium. The rotating disc provides agitation and aeration as the coal feed enters the biological unit. As the coal moves from stage to stage within the first unit, it is solubilized and the soluble products are removed as aqueous overflow with ash removed through a bottom drain. A second sub unit is also an aerobic bio-disc in which the effluent or product from aerobic bioconversion of the soluble coal products is routed through a molecular weight cutoff ultrafiltration unit of selected size. This allows for larger molecular weight products to be recycled to the second stage bio-disc for further size reduction while providing the permeate containing the lower moelcular weight substrates to the anaerobic bio-disc for conversion to methane. Off-gases from the anaerobic bio-disc will be collected by displacement of water to obtain a volume reading on the gaseous product. Gas quality will be determined by sampling of the gas produced for analysis by a Varian Gas Chromatograph equipped with a thermal conductivity detector and a Carbosieve S-II column.

Analysis of coal conversion to methane will include the following tests:

- o Rate and efficiency of liquefying coal
- o Rate of formation and quality/quantity of low molecular weight acids and alcohol from solubilized coal
- o Rate and purity of methane formation from low molecular weight compounds
- o Overall rate and purity of methane production from feed coal.

Parameters measured will include percent total carbon converted to product, acid number for low molecular weight products and purity of methane generated.

Based on data obtained from the continuous coal to methane unit, a continuous pilot scale unit will be designed. This unit will process 1000 lb of coal per day for production of methane. Tankage, plumbing, electrical controls, layout for construction and costs for construction will be included. Preliminary economics for a plant to process 100 TPH of coal will be presented.

6. RESULTS/ACCOMPLISHMENTS:

Three North Dakota lignite coals and a Wyodak subbituminous coal have been selected for use in this project and are currently available

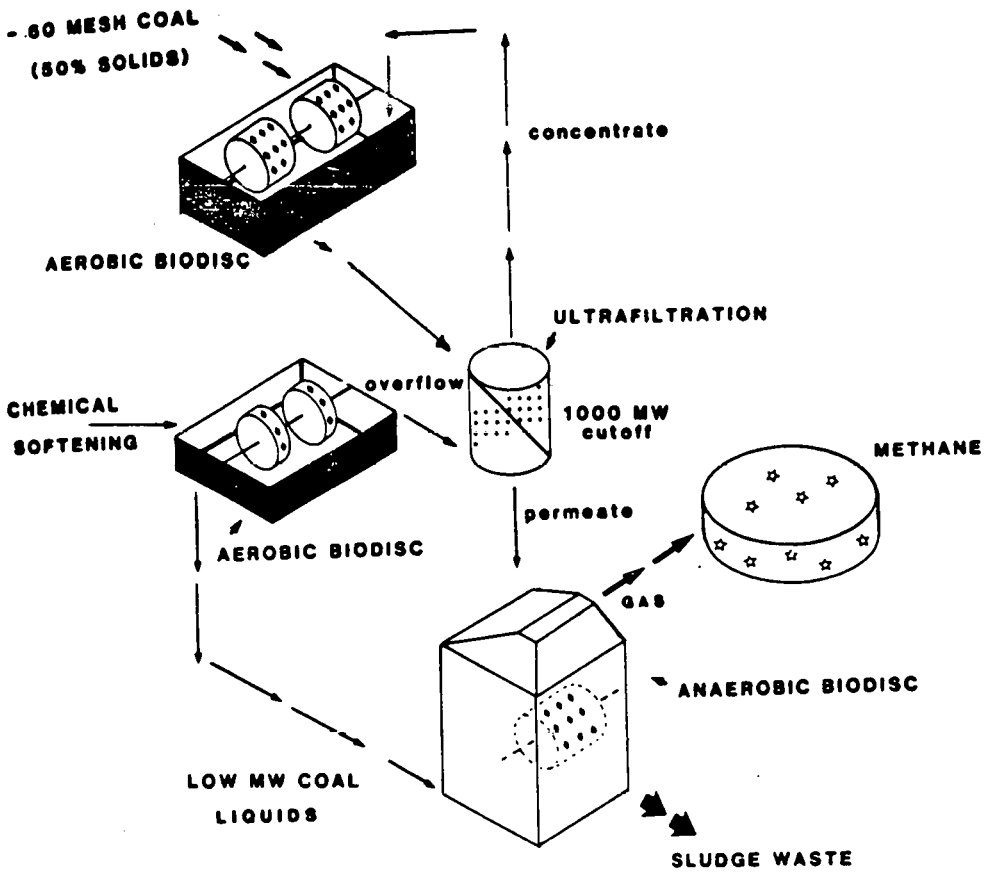

Figure 3. SCHEMATIC OF CONTINUOUS COAL TO METHANE UNIT

in-house. A bituminous coal will be selected and ordered if a suitable coal is not available in the ARC sample collection.

Preliminary studies to evaluate a variety of chemical and thermal treatments have been initiated. Alkali solubilization appears to be enhanced in the presence of sodium bicarbonate and ethanol. One of the lignites will be selected for all future work on lignite coals based on organic conversion to soluble products.

As a measure of solubilization, a constant weight of coal is pretreated and suspended in a constant volume of liquid at pH 11 prior to autoclaving. After cooling, the pH of the resulting liquid is monitored and separation of the liquid from the solids accomplished by centrifugation. The supernatant fluid is diluted as appropriate and OD_{450} is measured for a relative value of solubilization. Many aromatic compounds absorb light strongly at a wavelength of 450 nm, thus spectrophotometric measurements can be used as a relative determination. Samples are diluted with distilled water to produce solution concentrations resulting in an OD_{450} of ≤ 1.0. The OD_{450} is directly proportional to the relative concentrations of products absorbing at this wavelength.

A microbial consortium isolated by Atlantic Research is currently being evaluated for solubilization of lignite and subbituminous coals. Relative extent of solubilization is monitored using the spectrophotometric method discussed above. Relatively rapid and efficient solubilization has been achieved when the lignite and subbituminous coals are pretreated with nitric acid for one hour before microbial treatment is initiated. Optimization of this process is underway.

7. EVALUATION OF POTENTIAL FUTURE PLANS

Selection of the best treatment of coal for efficient, rapid conversion to liquid products will be followed by optimization of the selected process for each of the coals; lignite, subbituminous and bituminous. Efforts are underway to determine molecular weight ranges for soluble products, to characterize products by solubility and by derivatization of some products.

Tests to evaluate inhibitory effects of soluble coal derived products will be initiated in the near future. Aerobic and anaerobic cultures will be monitored for inhibition by the soluble products and eventually for the capacity to bioconvert these products to desired feedstock(s) for methane production.

PROCESS DEVELOPMENT UNIT FOR COAL GASIFICATION
TIED TO REGENERATIVE HOT GAS CLEANUP

1. GRANT NUMBER: DE-FG21-87MC24138

RECIPIENT: Calderon Energy Company
P. O. Box 126
Bowling Green, Ohio 43402
419/352-4631

RECIPIENT'S PROJECT MANAGER: Albert Calderon

PRINCIPAL INVESTIGATORS: Robert Duthie
Karl Polen
Albert Calderon

METC PROJECT MANAGER: L. Megan Day

PERIOD OF PERFORMANCE: February 26, 1987 to November 25, 1988

2. SCHEDULE/MILESTONES:

1987-1988 Program

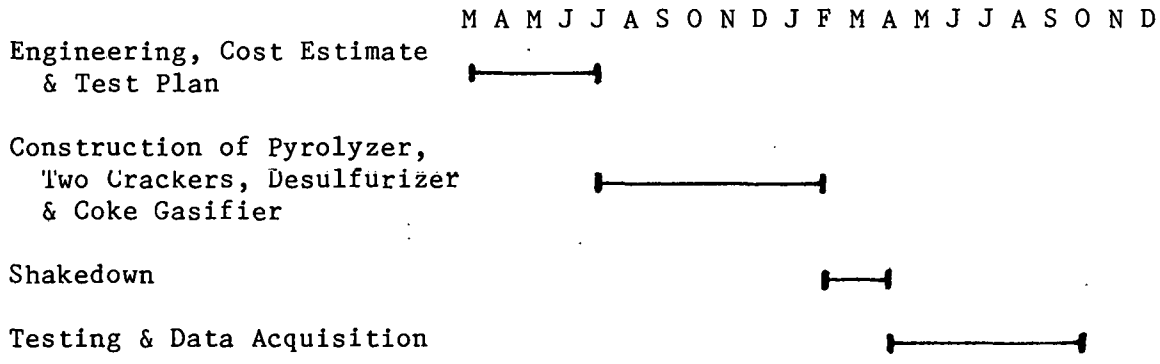

3. OBJECTIVES:

The generic problem being addressed by this grant project is the utilization of coal with any sulfur content in an economical, environmentally acceptable manner. The proposed solution is a new and unique proprietary coal gasification process which is modular in configuration.

The purpose of this project is to demonstrate the operation of a commercial scale process module. This includes the engineering, construction and operation at a feed rate of 50 tons per day of high-sulfur (3.2% S) caking coal. The module will operate continuously at pressure (350 psi) and be integrated with its proprietary hot gas cleanup system

to yield clean gases free of tars and compounds of sulfur and particulate matter. The complete coal conversion system consists of:

- A charging mechanism which accepts run-of-mine coal (ROM).
- A heated vertical pyrolysis tube which removes tars and other volatiles, and agglomerates coal fines.
- Air-blown char gasification with a water-quenching lock hopper for slag removal.
- Separate production of the rich pyrolysis gas and the lean gas from char gasification.
- Hot gas cleanup in which tars are cracked and sulfur and alkali metals are removed in regenerative hot sorbent beds.
- Sorbent regeneration to recover byproduct sulfur.
- Disposal of inactive sorbent, alkali metals and coal ash as an inert slag.

4. BACKGROUND STATEMENT:

The Calderon process for the gasification of coal and its application to combined cycle power generation as illustrated in Figure 1 differs from the currently demonstrated IGCC technologies in that:

- Air rather than oxygen is employed in the gasification.
- The product gases are treated hot and dry for removal of sulfur, and the hydrocarbon constituents are converted to CO and H_2.
- Minimal quantities of steam are produced. Substantially all of the energy output is in the form of hot pressurized product gas.
- Waste water treatment facilities are not needed.

5. PROJECT DESCRIPTION:

GASIFICATION PROCESS

The design of this process incorporates flexibility to accomodate different run-of-mine coals and conversions of such coals to gas and to char via pyrolysis. The char is in turn gasified with air.

The mechanical configuration and operation of specific process components are as follows:

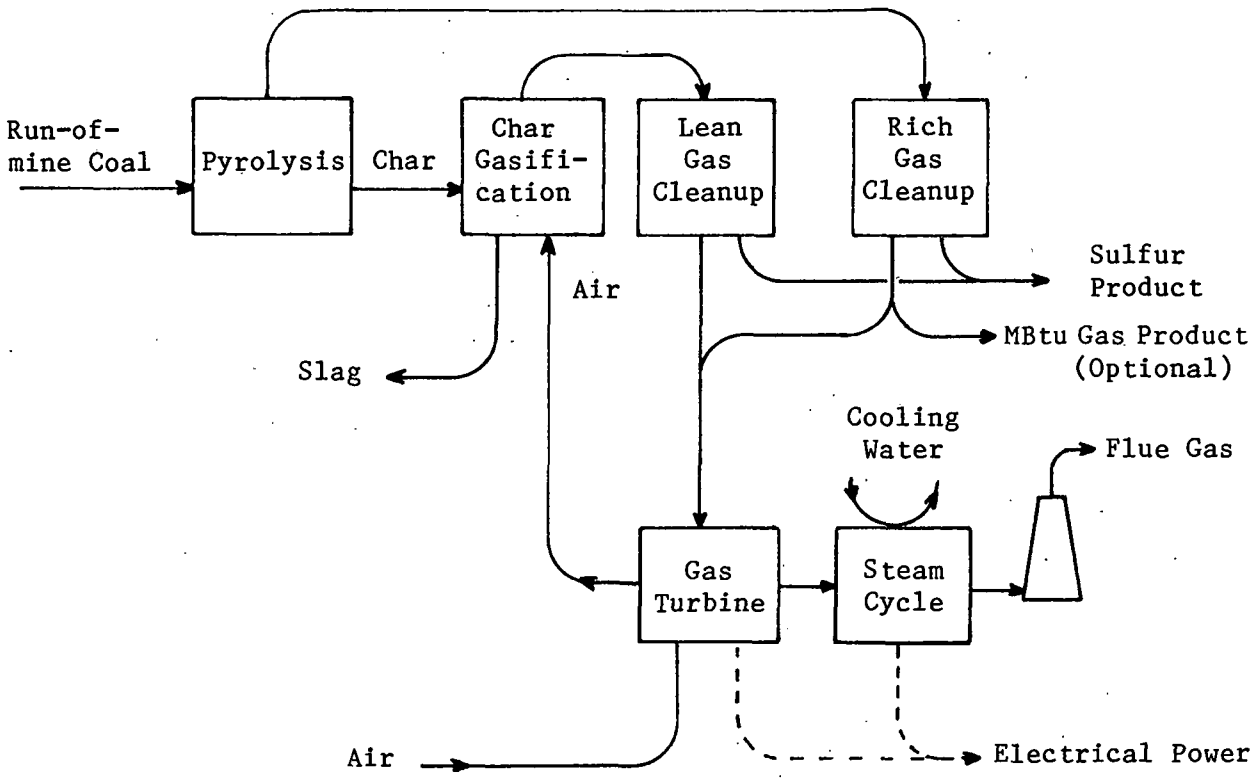

Figure 1. Calderon Gasification Combined Cycle Power Generation

Coal Pyrolysis

The coal is force fed to the bottom of a vertical tubular pyrolyzer and moves upward, first through an unheated section and then through a heated section. The gas produced, containing water evaporated from the coal and its coking products (predominantly tars, CH_4, CO, and H_2), escapes upwards through fissures in the coking coal. The hot char leaves the top of the pyrolyzer in the form of an agglomerated friable mass. The char discharges as broken porous lumps into the char gasifier. Heat to raise the feed coal to pyrolysis temperature is supplied to the pyrolyzer by directing a portion of the hot gas effluent (lean gas) from the char gasifier.

Char Gasification

The broken char enters the top of the char gasifier and is rapidly further heated in the upper portion of the bed by contact with the exiting gasifier product gas and then reacts in the lower portion

of the gasifier with the feed air. The ash content of the char is melted to a fluid slag which drains from the bottom of the gasifier. The gasification rate is controlled to balance the char made by the addition rate of the air.

Hot Gas Cleanup

The rich gas from the pyrolyzer is admitted through a rich gas cracker containing a sorbent bed. The bed and the gas are heated in order to crack the hydrocarbons and to desulfurize the rich gas in one step.

The cracker employed for treating the lean gas is arranged in the same way as the rich gas cracker. In the event separation of the lean and rich gas is not required, the two gases are combined and passed through a single cracker.

Sulfur Recovery (Cracker Regeneration)

During regeneration the treating gas flow through the bed is reversed employing air which reacts with sulfur compounds to liberate SO_2. The carbon from the cracked hydrocarbons is removed by oxidation with SO_2 and by partial oxidation with the air to form CO. Such carbon oxidation yields the sulfur in elemental form.

The liberated sulfur leaves the top of the bed as a vapor mixed with CO and N_2 and is recovered by condensation. The tail gas is recycled to the lean gas cracker. Regeneration is carried out slightly above the operating cracker pressure in order to recycle the tail gas.

Integrated With Combined Cycle

The primary interaction between the gas turbine and its steam cycle and the Calderon Gasification process lies in the potential use of the turbine air compressor to supply (with additional compression) the air for the char gasification. The gas supplied to the gas turbine from the gasification will be hot and dry (likely at a temperature of 900° F) and may require steam addition for NOx control.

Thermal Efficiency

Based on an illustrative material and energy balance for gasification a projected performance for a suitably integrated combined cycle system is very favorable when compared to other gasification processes.

6. ACCOMPLISHMENTS:

Bechtel National, Inc., San Francisco, California, has been selected to do the process design and equipment specification. Alliance Machine Company, Alliance, Ohio, has been selected to carry out the balance of plant design and provide procurement and erection services. The module will be built and operated at Alliance Machine for a period of at least six months.

7. POTENTIAL FUTURE PLANS:

It is believed that this process can demonstrate cost-effective production of clean fuel gas from run-of-mine high sulfur coal. In addition, the separate production of a syngas (rich pyrolysis gas) offers an option for co-production of chemicals, methanol or synthetic natural gas. With this dual capability the process is expected to find application for both retrofit and new plant applications. The lean gas from the char gasification has a reduced heat content resulting from the air blown gasification but is still a suitable high temperature pressurized clean fuel for power generation.

For retrofit/repowering application to existing pulverized coal-fired power plants, cost savings are expected to entirely support the cost of the new gasification facilities. Sources of savings include:

- Replacement of low sulfur coal with a cheaper high sulfur coal fuel.
- Elimination of facilities such as:

  -Coal grinding and pulverizing

  -Fly ash removal and handling

  -Ash damage to boiler tubing

  -Flue gas scrubbing.
- Increased overall fuel efficiency.

For new installations, the Calderon gasification process is expected to show a significant advantage in both operating efficiency and capital cost over the current oxygen blown gasification systems as well as advanced direct coal combustion technologies employing non-regenerative sulfur removal, such as fluidized beds.

The planned demonstration and development program may offer a solution to the "Acid Rain" problem at no net cost to the utilities or the rate payers with the capability of co-producing clean liquid fuel (methanol) as a byproduct.

EXPANSION OF HIGH-TEMPERATURE, HIGH-PRESSURE DATA SET FOR COAL GASIFICATION

1. CONTRACT NUMBER: DE-AC21-84MC 21376

CONTRACTOR: The Pennsylvania State University
Fuel Science Program
University Park, PA 16802
(814) 865-6511

CONTRACTOR PROJECT MANAGER: Robert G. Jenkins

PRINCIPAL INVESTIGATORS: Robert G. Jenkins
Alan W. Scaroni

METC PROJECT MANAGER: Wen-Shou Liou

CONTRACT PERIOD OF PERFORMANCE: September 1984-December 1987

2. SCHEDULE/MILESTONES:

Derivation of Test Plan	October 1984-December 1984
Equipment Modifications	January 1985-June 1985
Generation of Base Data	July 1985-September 1986
Generation of Supporting Data	July 1987-November 1987

3. OBJECTIVES:

The primary objective of this project is to provide a complementary study to those being undertaken by METC and Advanced Fuels Research Corp. in the area of high-temperature, high pressure coal devolatilization/gasification. This study will extend the data base into shorter residence times (< 1 s) to investigate the effect of pressure on the initial stage of coal devolatilization. The effects of rank, pretreatment and gaseous atmosphere on coal devolatilization under pressure will also be investigated.

4. BACKGROUND STATEMENT:

An understanding of the fundamental and interrelated processes of coal devolatilization and char reactivity is essential in order to advance gasification technologies. Data are needed on the effect of coal properties and operating variables on the devolatilization/gasification behavior of coals under conditions similar to those in advanced-concept gasifiers, typically a high-temperature and high -pressure environment for entrained coal particles. Models for coal devolatilization/gasification are needed in order to predict the behavior of coals in advanced-concept gasifiers.

5. PROJECT DESCRIPTION:

A set of weight loss and product distribution data, which directly overlaps those generated by METC and AFR has been generated for residence times from 1-3 seconds, pressures between 100-900 psig, and temperatures up to 1100°C. Relevant chemical and physical analyses of the devolatilization products; char, condensibles and gases, have been performed. A meaningful comparison of results generated in the extended and supporting

studies, which have no direct overlap, can be made based on this set of data. The combined study extends the data generation into shorter residence times (< 1s) which are not available in the METC gasifier. Many of the important devolatilization/gasification phenomena take place within this short time period. The effects of rank, coal pretreatment and gaseous atmosphere on coal devolatilization are being investigated in the supporting studies. A comprehensive global kinetic model for devolatilization of the coals is being produced.

6. RESULTS/ACCOMPLISHMENTS:

A reactor system, which is capable of subjecting pulverized coal particles to temperatures and pressures up to 1100°C and 1000 psig, respectively, for a range of residence times is being used in this study. It's operating principle and procedure have been described elsewhere (Jenkins and Scaroni 1986).

Four coals, lignite, sub-bituminous, and high and low volatiles bituminous are being investigated. Proximate and ultimate analyses of two of the raw coals are shown in Table 1. Devolatization experiments with the Montana Rosebud sub-bituminous coal were performed at a temperature of 1189 K, applied N_2 pressures of 100-900 psig and residence times between 0.1 to 1.7 seconds.

The effect of residence time on weight loss and condensibles yield is shown in Figures 1 and 2, respectively. The weight loss of the Montana Rosebud coal increased steadily with increasing residence time and reached a maximum at 1.0 second. At higher pressures (178, 309, and 530 psig) the increase in weight loss with increasing residence time was more regular than at the lower pressure (100 psig). The decrease in condensibles yield with increasing residence times followed an opposite trend to the weight loss, the minimum yield being at 1.0 second. The effect of pressure on weight loss for devolatization at 1189 K, 0.3-1.0 seconds residence time and up to 900 psig applied N_2 pressure is shown in Figure 3. At short residence times (0.3 and 0.5 seconds) increasing pressure reduced the weight loss, but the weight loss increased slightly after going through a minimum at 178 psig at the longer residence time (1.0 second). The effect of pressure on condensibles yield at 1189 K, 0.3-1.0 seconds residence time and applied pressure up to 900 psig is shown in Figure 4. The condensibles yield increased significantly with pressure up to 178 psig for all residence times and, with the exception of the short residence time (0.3 sec), continued to increase at a slower rate with increasing pressure. Solomon et al. (1986) reported similar condensibles yields for the same coal at 1089 K and 0.47 seconds residence time. Sundaram et al. (1983) also observed an increase in condensibles yield from a sub-bituminous coal with increasing He pressure.

The effect of pressure on the C/H ratio of the condensibles and char produced upon devolatilization is shown in Figures 5 and 6, respectively. As indicated in Figure 5, the C/H ratio of the condensibles remained relatively constant except at 0.3 seconds residence time where a significant drop occurred at 178 psig. Figure 6, however, indicates a signficiant drop in C/H ratio of the char as pressure increases. The C/H ratio of the 0.3 second residence time char decreased from over 1.8 at 100 psig to below 1.4 at 178 psig then showed no significant change. The C/H ratio dropped gradually from over 2.2 at 100 psig to 1.8 at 900 psig for the char produced at 1.0 second. The reduction in carbon content increased with decrease in residence time. Sundaram et al. (1983) reported that the total carbon conversion went through a maximum before decreasing with increasing pressure for the devolatilization of a sub-bituminous coal under inert gas pressures (Ar, He, and N_2) in an entrained flow furnace. The effect of pressure on the yield and composition

of gaseous products is presented in Figure 7 and 8, respectively. The trend for total gas yield is consistent with the effect of pressure on weight loss and condensibles yield by comparing Figures 3, 4, and 7. In general, the total gas yield dropped significantly from 100 to 178 psig then increased slightly with increase in pressure. Solomon et al. (1986) reported a similar trend. At the short residence time (0.3 seconds), the CO and CO_2 yields increased with increasing pressure while the CH_4 yield decreased. Increasing pressure reduced the CH_4 yield as has been reported by Serio et al. (1983). For higher than 0.3 seconds residence time, the concentration of gaseous products decreased in the following order: CO, CO_2, CH_4, C_2H_4 and C_2H_6. This is in agreement with data of Sundaram et al. (1983) and that of Serio et al. (1983) for the hydrocarbon gases.

Devolatilization experiments on the Illinois No. 6 coal were performed at a temperature of 1189K, pressure of 309 psig N_2, and residence times between 0.5 to 1.7 seconds. The effect of residence time on weight loss and condensibles yield is shown in Figure 9. It can be seen that weight loss during devolatilization increased steadily with increasing residence time, while the condensibles yield was in the opposite direction. For example, the weight loss at 0.5 seconds was about 25% and increased to close to 50% at 1.7 seconds, the corresponding condensibles yields at these two residence times were over 20% and close to 10%, respectively. It is apparent that significant amounts of condensibles are generated and can be extracted at the short residence time (0.5 seconds). However, at longer times (> 0.8 seconds) the amount of condensibles is reduced, possibly due to mass transfer limitations in this highly coking bituminous coal. It is widely believed that mass transfer plays a significant role in determining the devolatilization behavior of bituminous coal under pressure (Suuberg 1985).

7. FUTURE WORK

The study will be extended into the effects of coal rank, coal pretreatment and gaseous atmosphere on devolatization behavior. Analysis of the data from both the combined and supporting studies will be performed. The project will be concluded by generation of a global kinetic model for devolatization/gasification of the coals used in this study.

8. REFERENCES

Jenkins, R. G. and Scaroni, A. W., Proceedings of the Sixth Annual Gasification Contractors Meeting, DOE /METC 86/6043, 1986, pp. 171-181.

Tsai, C. Y., An Experimental Investigation of the Initial Stages of Pulverized Coal Combustion, *Ph.D. Thesis*, The Pennsylania State University, 1985.

Solomon, P. R., Serio, M. A. and Hamblen, D. G., Proceedings of the Sixth Annual Gasification Contractors Meeting, DOE/METC 86/6043, 1986, pp. 171-181.

Sundaram, M. S., Steinberg, M., and Fallon, P. T., *Preprints, Div. Fuel Chem., Am. Chem. Soc.*, Vol. 28, No. 5, 1983, pp. 106-129.

Serio, M. P., Solomon, P. R. and Heninger, S. G., *Preprints, Div. Fuel Chem., Am. Chem. Soc.*, Vol. 31, No. 3, 1986, pp. 210-221

Suuberg, E. M., Mass Transfer Effects in Devolatization of Coals: A Review of Experimental Evidence and Models, *Chemistry of Coal Conversion* (Ed., Schlosberg, R. H.) Plenum Press, New York, 1985, pp. 67-117.

TABLE 1
Characteristics of the Coals used in This Work

Analysis (wt%)	Coals	
	Montana Rosebud[a] (subbituminous)	Illinois #6[a] (H.V.B)
Proximate		
Moisture	—	—
Ash	9.7[b]	11.1
Volatile Matter	42.7	42.2
Fixed Carbon (by diff.)	47.6	46.7
Ultimate		
Carbon	74.3[c]	73.9
Hydrogen	6.0	5.1
Nitrogen	1.0	1.4
Sulfur	1.5	4.2
Oxygen (by diff.)	16.9	15.4

[a]Provided by METC
[b]Dry basis
[c]Dry ash free basis

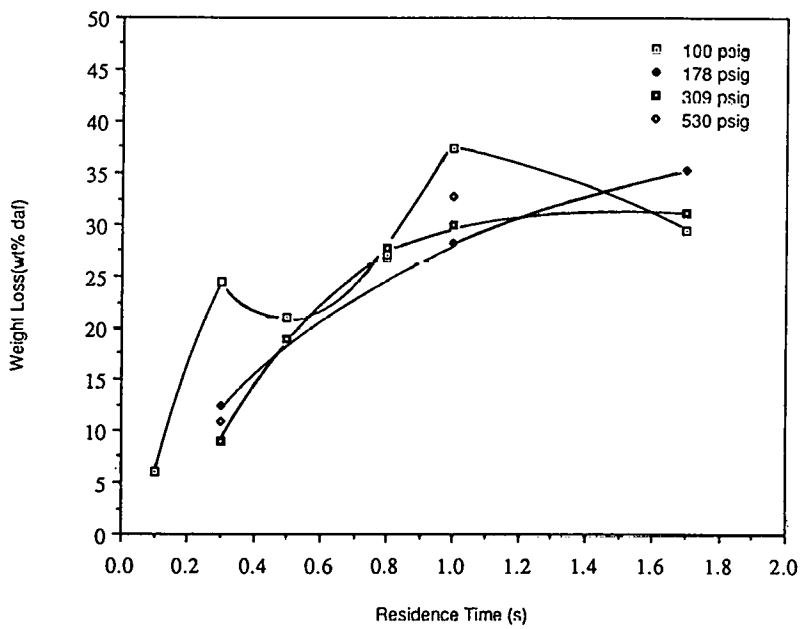

Figure 1. Effect of Residence Time on Devolatilization Weight Loss of Montana Rosebud Coal at 1189 K.

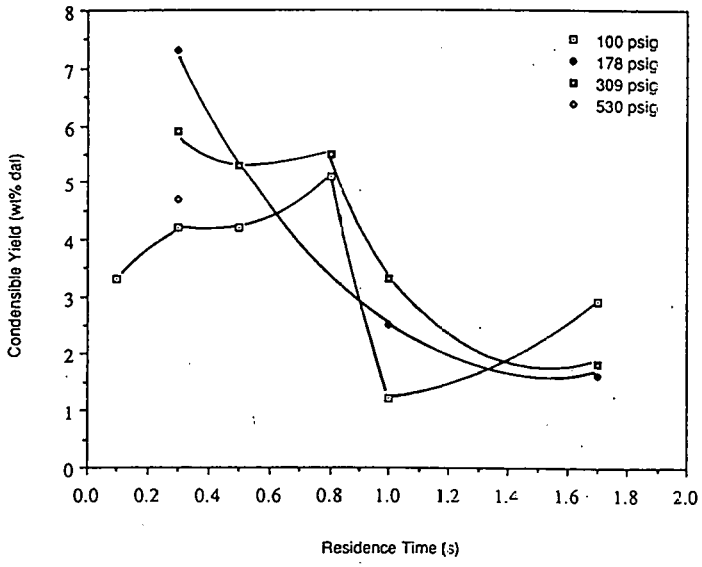

Figure 2. Effect of Residence Time on Devolatilization Condensible Yield from Montana Rosebud Coal at 1189 K.

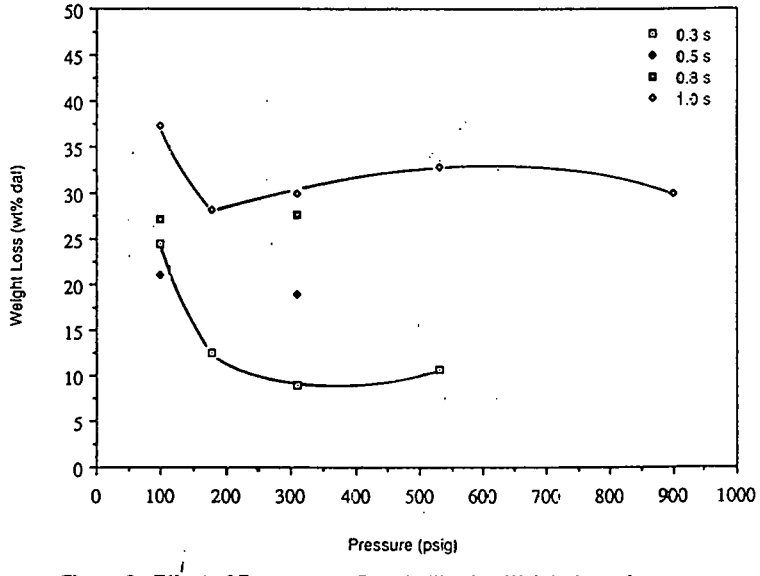

Figure 3. Effect of Pressure on Devolatilization Weight Loss from Montana Rosebud Coal at 1189 K.

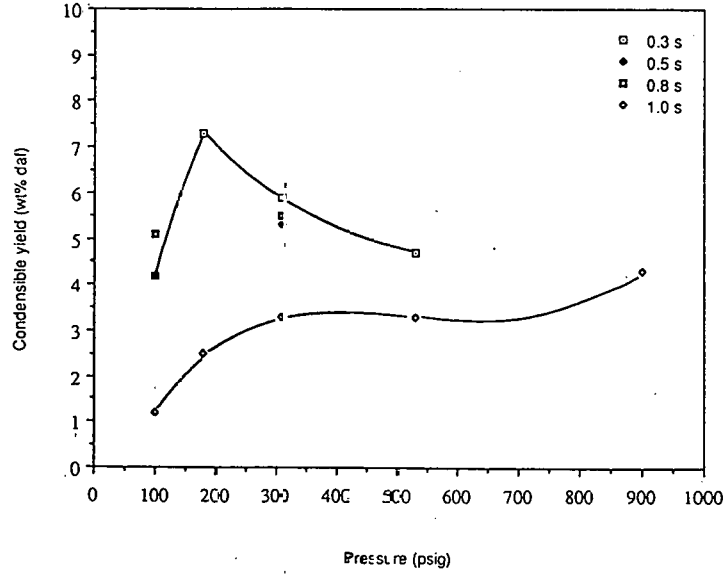

Figure 4. Effect of Pressure on Devolatilization Condensible Yield from Montana Rosebud Coal at 1189 K.

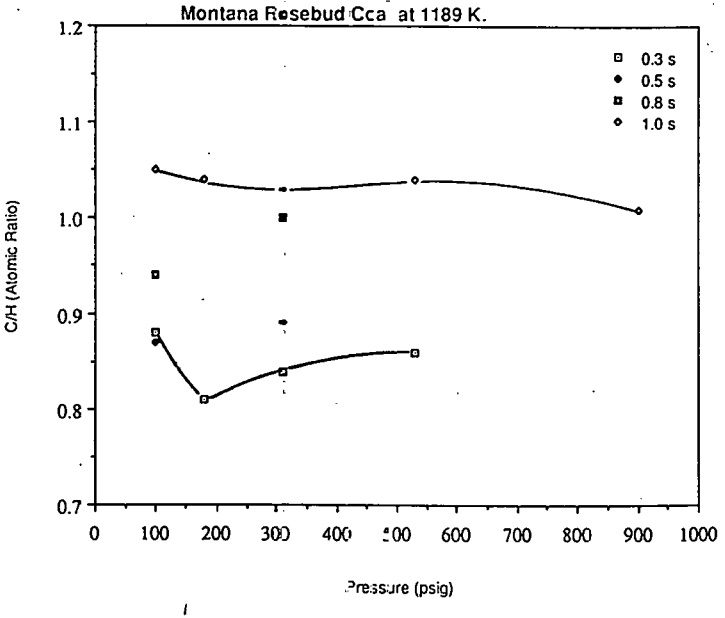

Figure 5. Effect of Pressure on C/H Ratio of Condensible from Devolatilization of Montana Rosebud Coal at 1189 K.

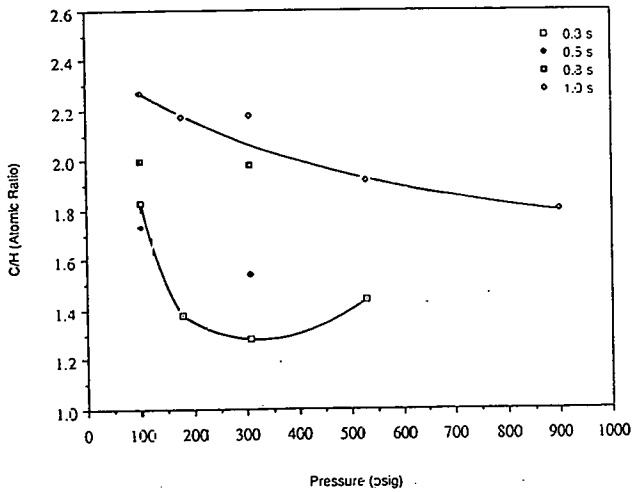

Figure 6. Effect of Pressure on C/H Ratio of Char from Devolatilization of Montana Rosebud Coal at 1189 K.

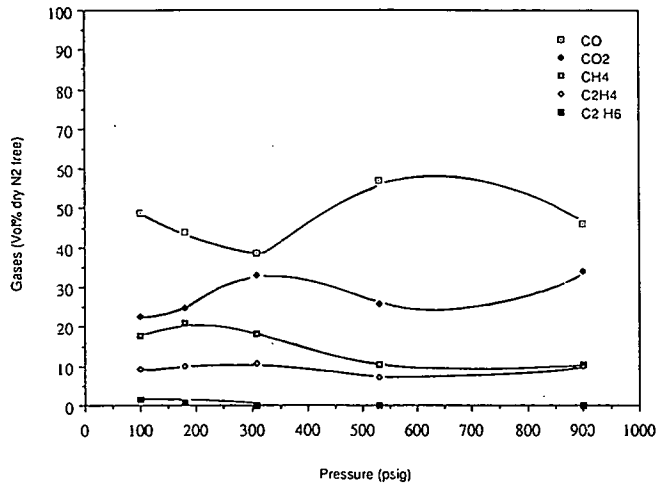

Figure 8. Effect of Pressure on Devolatilization Gas Composition from Montana Rosebud Coal at 1189 K and 1.0 s.

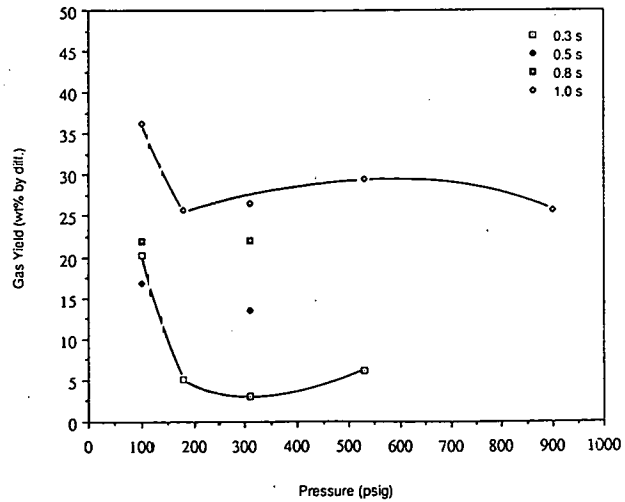

Figure 7. Effect of Pressure on Devolatilization Gas Yield from Montana Rosebud Coal at 1189 K.

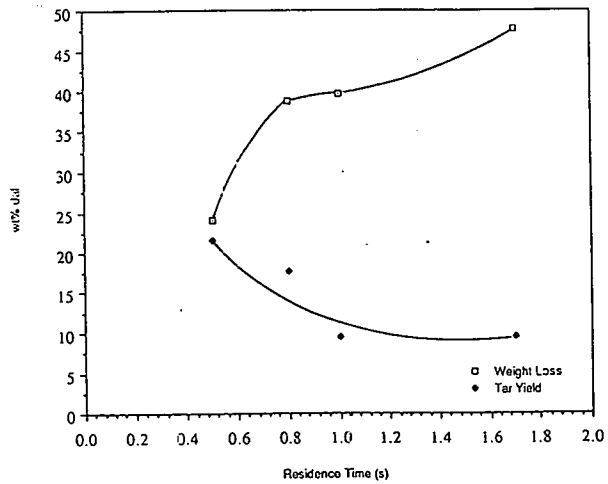

Figure 9. Effect of Residence Time on Devolatilization Weight Loss and Condensible Yield of Illinois No. 6 Coal at 1184 k and 309 psig Nitrogen.

EXPANSION OF HIGH-TEMPERATURE, HIGH-PRESSURE DATA SET FOR COAL GASIFICATION

1. **CONTRACT NUMBER:** #DE-AC21-84MC21004

CONTRACTOR:

Advanced Fuel Research, Inc.
87 Church Street
East Hartford, CT 06108
(203) 528-9806

PROGRAM MANAGER (CONTRACTOR): Peter R. Solomon

PRINCIPAL INVESTIGATORS:

Michael A. Serio
David G. Hamblen

METC PROJECT MANAGER: Justin L. Beeson

CONTRACT PERIOD OF PERFORMANCE: September 28, 1984 to September 28, 1987

2. **SCHEDULE/MILESTONES:**

1987 PROGRAM SCHEDULE

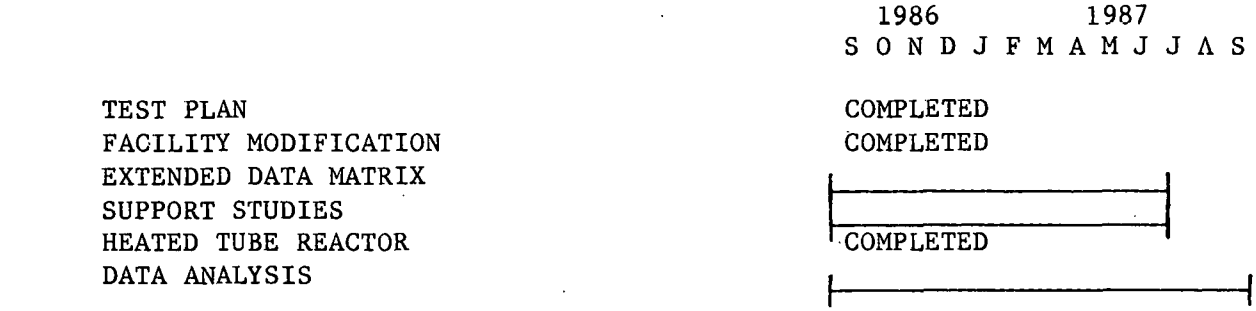

3. **OBJECTIVES:**

The program has three major objectives: 1) Determination of chemical kinetic rates for pyrolysis and CO_2 gasification. 2) Investigation of the relationship between char reactivity and char formation conditions, particularly with regard to heating rate and pressure. 3) Investigation of the effect of high temperature and high pressure on pyrolysis and gasification reactions.

4. **BACKGROUND STATEMENT:**

This project is complementary to one being conducted at METC with the Advanced Gasification Facility (AGF) entrained reactor and at Penn State using the same coal (Montana Rosebud subbituminous). It partly overlaps and extends the programs at these facilities. The ultimate goal of the combined programs is to supply a data base, understanding and predictive capability which can lead to improved gasification systems.

5. **PROJECT DESCRIPTION:**

A test plan was formulated which overlapped and extended the METC AGF matrix. The plan includes two composite factorial data matrices, one tailored to CO_2 gasification, the other to devolatilization studies. The

effects of particle size, heating rate, and reactive gas were studied along with temperature and pressure. The plan also included supporting studies to provide baseline (1 atm. pressure) data on the thermal and optical properties, pyrolysis kinetics, and char reactivity for Montana Rosebud subbituminous coal. Selected studies were done on a Kentucky No. 8 bituminous coal. Four different reactor systems are being used: 1) high pressure entrained flow reactor (HPR), 2) atmospheric pressure entrained flow reactor (EFR), 3) heated tube reactor (HTR), 4) thermogravimetric analyzer/evolved gas analyzer (TGA/EGA). The latter three facilities include in-situ FT-IR diagnostics. The high pressure reactor system has been modified to allow experiments up to 500 psig.

6. RESULTS AND ACCOMPLISHMENTS:

Pyrolysis Kinetics and Product Yields 1 atm Pressure - First, a series of baseline kinetic pyrolysis experiments was performed in the HTR and TGA/EGA at one atmosphere pressure with the Montana Rosebud coal which included material balances, particle temperature measurements, and thermal and optical property measurements (Solomon, et al., 1986a; Serio, et al., 1987a). The results of the temperature measurement experiments were simulated with a model to obtain the pyrolysis kinetic parameters for major product evolution (Solomon, et al., 1986a, Serio, et al., 1987a). The kinetic rate for overall mass loss was consistent with values determined for coals of lower, higher and similar rank in our other programs.

Pyrolysis Kinetics and Product Yields at High Pressure - A set of pyrolysis data was obtained for three size cuts of Montana Rosebud coal at pressures of up to 400 psig. The most significant effect of increased pressure was to slightly decrease yields of most hydrocarbon volatiles, including tar. The effects of pressure were found to be dependent on the temperature level. A heat transfer model was developed for the HPR to model the particle time-temperature history, which was a modification of one developed previously for the atmospheric pressure entrained flow reactor (EFR). As a first approximation, it was assumed that the one atmosphere kinetics were valid. The simulations were generally in good agreement with the data except for products influenced by secondary reactions (Serio, et al., 1986). Our conclusion is that primary pyrolysis kinetics are substantially independent of pressure.

Char Reactivity Studies - One of the goals of the program is to determine the effects of char formation conditions, including pressure and heating rate, on char reactivity. Toward this end, a number of chars generated in experiments in the HPR, HTR, EFR, and TGA/EGA, have been analyzed by a newly-developed non-isothermal technique (Solomon et al., 1986b). The results for several Montana Rosebud chars are shown in Fig. 1. The data on this plot represent excursions in total pressure, heating rate, final temperature, and residence time. The final temperature was found to be the most important variable followed by residence time, pressure, and heating rate (Serio, et al., 1987b). The pressure series is indicated by the open squares of Fig. 1. There does appear to be a countervailing trend of T_{cr} vs H content when compared to the rest of the data. This will also be the subject of additional investigation.

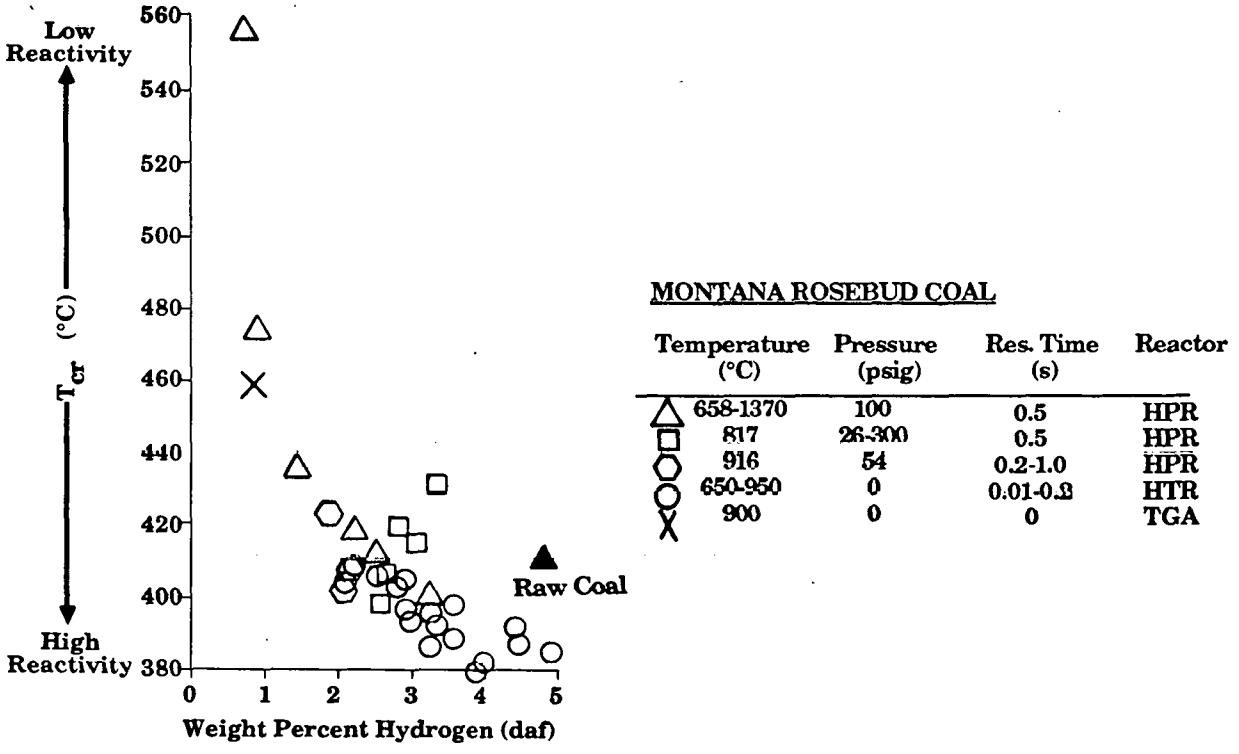

Figure 1. Variation of Reactivity with the Hydrogen Concentration for Chars from Montana Rosebud Coal Formed Under a Wide Range of Conditions.

Effect of Pressure on Tar Yields and Molecular Weight Distributions - The effect of pressure on the yield and molecular weight distribution of tar has been modeled using a combined Functional Group/Depolymerization, Vaporization, Crosslinking (FG/DVC) model developed under Contract No. DE-AC21-85MC22050 (Solomon, et al., 1987a, 1987b).

The model accounts for both internal and external mass transport limitations on tar escape. Higher external pressure reduces the escape rate of tar. The tar molecules break into smaller pieces which consume larger amounts of donatable hydrogen per unit mass of tar. This reduces the tar average molecular weight and the tar yield, since the amount of donatable hydrogen is limited. In addition, the opportunity for repolymerization via crosslinking reactions increases. Some examples of these effects and comparisons of model predictions with the literature are shown in Figs. 2 and 3.

Figure 2 shows fair agreement between data and theoretical predictions of the effect of pressure on the tar molecular weight distribution. Figure 3 shows good agreement between model predictions and the data of Anthony, et al., (1974), on pressure effects on total volatiles yield and the data of Suuberg, et al., (1978) for tar yield.

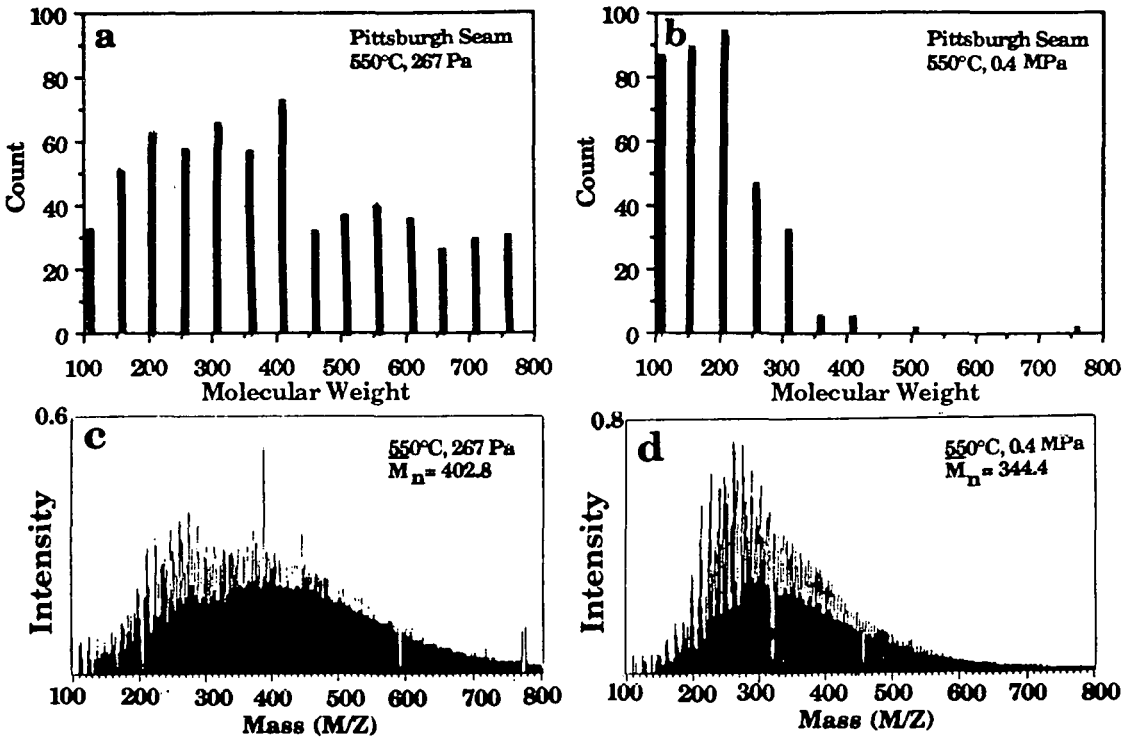

Figure 2. Comparison of Predicted (a and b) and Measured (c and d) Tar Molecular Weight Distribution for Pyrolysis of a Pittsburgh Seam Coal in a Heated Grid Apparatus at a Heating Rate of 600°C/sec to 550°C. Figure a and c Compare the Prediction and the Measurement at 267 Pa. Figure b and d Compare the Prediction and Measurement at 0.4 MPa.

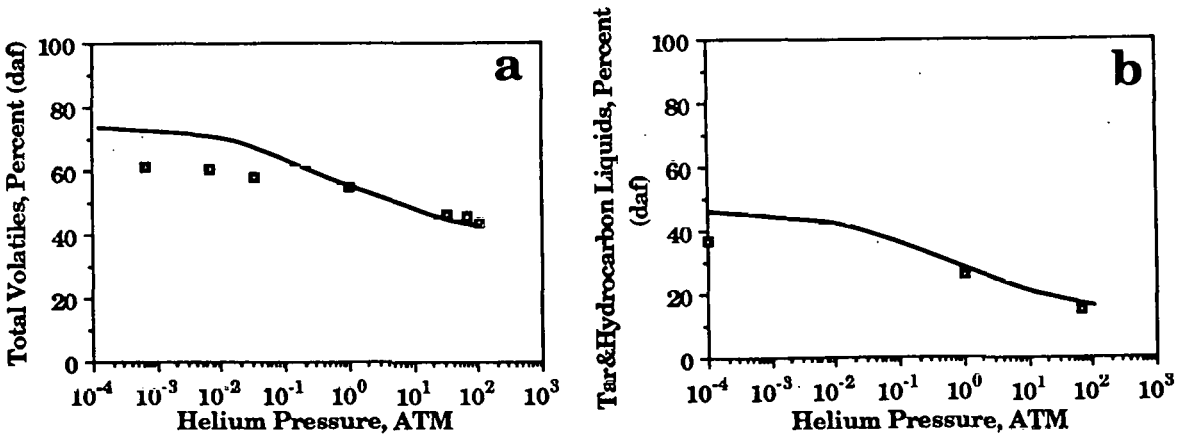

Figure 3. Comparison of Measurement and Prediction of Product Yields as a Function of Pressure. a) Volatiles vs Pressure (data from Anthony, et al., 1974) and b) Tar Plus Liquids vs Pressure Data from Suuberg, et al., (1979).

Summary of Accomplishments

- Performed a series of pyrolysis kinetic experiments from 1 to 30 atm pressure with the Montana Rosebud coal.
- Made O_2 and CO_2 reactivity measurements on chars formed over a wide range of temperatures, heating rates, and pressures.
- Demonstrated that a combined DVC/FG model could accurately predict variations of tar yield and molecular weight distributions with pressure.

7. FUTURE WORK:

- Conduct CO_2 gasification tests on previously formed chars.
- Further investigate effects of char formation conditions, especially pressure and mineral content, on reactivity towards O_2 and CO_2.
- Application of combined FG/DVC model to predict tar formation and yields from pyrolysis experiments with Montana Rosebud coal.

8. REFERENCES:

Anthony, D.B., Howard, J.B., Hottel, H.C., and Meissner, H.P., 15th Symp. (Int) on Combustion, the Combustion Inst., Pittsburgh, PA p 1303, (1974).

Serio, M.A., Hamblen, D.G., Markham, J.R., Solomon, P.R., Energy and Fuel, **1**, (2), 138, (1987a).

Serio, M.A., Solomon, P.R., and Suuberg, E.M., "Variations in Char Reactivity with Coal Type and Pyrolysis Conditions", accepted for Presentation at the 1987 Int. Conf. on Coal Science, The Netherlands, (Oct. 26-30, 1987b).

Serio, M.A., Solomon, P.R., and Heninger, S.G., ACS Fuel Chem. Prepr. **31**, (3), 210, (1986).

Solomon, P.R. and Serio, M.A., "Evaluation of Coal Pyrolysis Kinetics" presented at the NATO Workshop on "Fundamentals of Physical-Chemistry of Pulverized Combustion", Les Arcs, France, (1986).

Solomon, P.R., Hamblen, D.G., Carangelo, R.M., Serio, M.A., and Deshpande, G.V., "Models of Tar Formation During Coal Devolatilization", Combustion and Flame, to be published, (1987a).

Solomon, P.R., Hamblen, D.G., Carangelo, R.M., Serio, M.A, and Deshpande, G.V., "A General Model of Coal Devolatilization", ACS Div. of Fuel Chem. Preprints, **32**, (1987b).

Solomon, P.R., Serio, M.A., Carangelo, R.M., and Markham, J.R., Fuel, **65**, 182, (1986a).

Solomon, P.R., Serio, M.A., and Heninger, S.G., ACS Div. of Fuel Chem. Preprints, **31**, (3), 200, (1986a).

Suuberg, E.M., Peters, W.A., and Howard, J.B., in Thermal Hydrocarbon Chemistry, (A.G. Oblad, H.H. Davis, and R.T. Eddinger, Eds.), Adv. in Chem. Series, **183**, pp 239-257, Am. Chem. Soc., Washington, DC (1979).

ADVANCED GASIFICATION ENTRAINED REACTOR

Larry A. Bissett
Morgantown Energy Technology Center

Figure 1. Objectives/Background.

Devolatilization and associated phenomena occur in nearly all coal conversion processes, but are particularly important in entrained gasification due to the small particle sizes, high temperatures, and short residence times involved. Existing data are often contradictory and basic reaction mechanisms and kinetics remain poorly understood. Further experimental work should improve modeling capabilities and could lead to process improvements.

Objectives

- **Determine the effects of coal gasification environment on product yields over broad range of reaction conditions**
- **Advance the understanding, development, and modeling of gasification technology**

Background

- **Complex reaction phenomena remain poorly understood**
- **Broad range study needed to detect reaction mechanism changes and integrate other related investigations**
- **METC's operating parameter range unique**

METC 86-509-7 BE5

Figure 2. Technical Approach

The reactor has broad operational capabilities and is uniquely characterized by a gas-solid mixing section which, in combination with highly preheated gases, results in high particle heating rates. Instead of having coal type as a variable, a comprehensive test program was pursued on one coal employing a statistical experimental design. This has enabled the use of regression modeling and statistical analyses of the test data. Experimental trends identified by this approach are being compared to predictions from the PCGC-2 computer code and will hopefully lead to code improvements. The code is also being used to estimate experimental gas and particle residence times.

Technical Approach

Equipment

- **Unique reactor**
  - — **Rapid gas-solid mixing**
  - — **High particle heating rates**
  - — **Broad operational ranges**

Experimental

- **Comprehensive test program on one coal**
- **Statistical experimental design**

Modeling

- **Regression and statistical analyses of test data**
- **Comparison of trends with PCGC-2 predictions**
  - — **Gas and particle residence times**
  - — **Validation and improvements**

METC T87-1219-1 BE8

Figure 3. Reactor Aspects.

The entrained reactor is a muffle tube design in which argon is used to essentially balance pressure across the high-purity alumina parts. Heat is furnished by six computer-controlled, graphite-element, low-voltage electric heaters. A unique feature is the combined use of a turbulent mixing zone with a laminar-like reaction zone. Cold nitrogen injected through a probe within the reaction tube is used to quench the total reaction mixture and control residence time.

Reactor Aspects

- **Muffle tube design with pressure balance**
- **Reaction tube - 3'' I.D. x 4' long**
- **6 graphite element resistance heaters**
  - **— Computer controlled**
  - **— 230 KVA total**
- **Turbulent mixing zone; laminar reaction zone**
- **Quench probe for residence time control**

METC 86-509-2 BE5

Figure 4. Advanced Gasification Entrained Reactor.

Reactant gases are fed and highly preheated along the horizontal axis of the reactor and coal, conveyed by argon, is introduced from the top of the vertical axis through a water-cooled feed tube. A unique mixing configuration, located at the junction of the horizontal and vertical axes, turbulently combines the hot reactant gases with the coal and subsequently transitions the mixture to a laminar-like flow as it downwardly enters the reaction tube. Thermocouples are used to measure heater and reaction temperatures. Layers of solid and porous graphite are used to insulate the water-cooled pressure shell.

Advanced Gasification Entrained Reactor

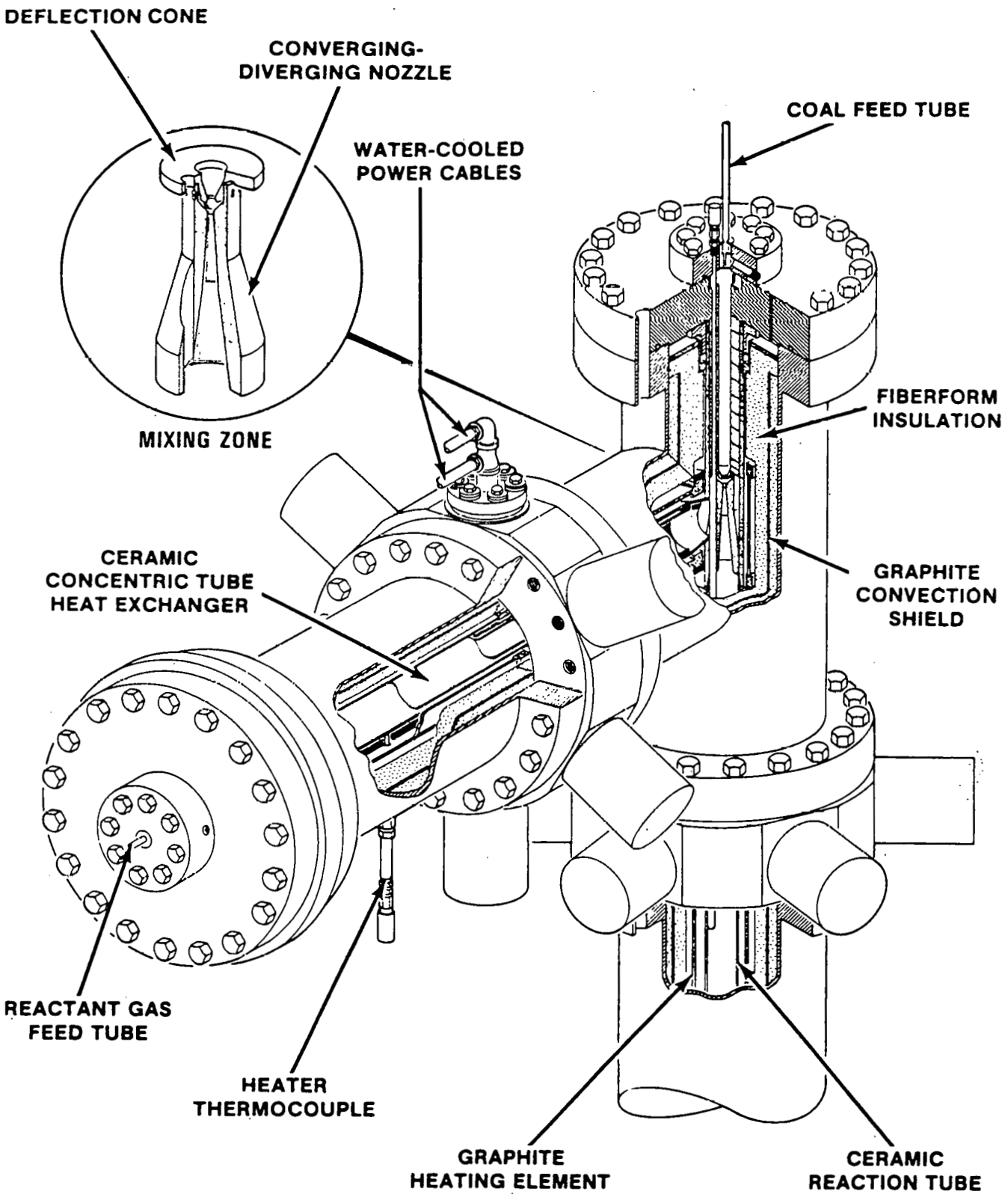

Figure 5. Concentric Tube Mixing Configuration.

The mixing configuration is a two-piece construction in which coal is fed down the center and hot reactant gases are fed through an annulus formed by an extension of the coal feed tube and the throat of the mixing nozzle. Mixing is encouraged by maintaining the annular gas velocity approximately 5 to 10 times higher than the coal feed velocity. The mixed flow transitions to laminar-like as it diverges. A ceramic protection tube passes through small openings in the mixing configuration and houses thermocouples used to measure reaction temperatures.

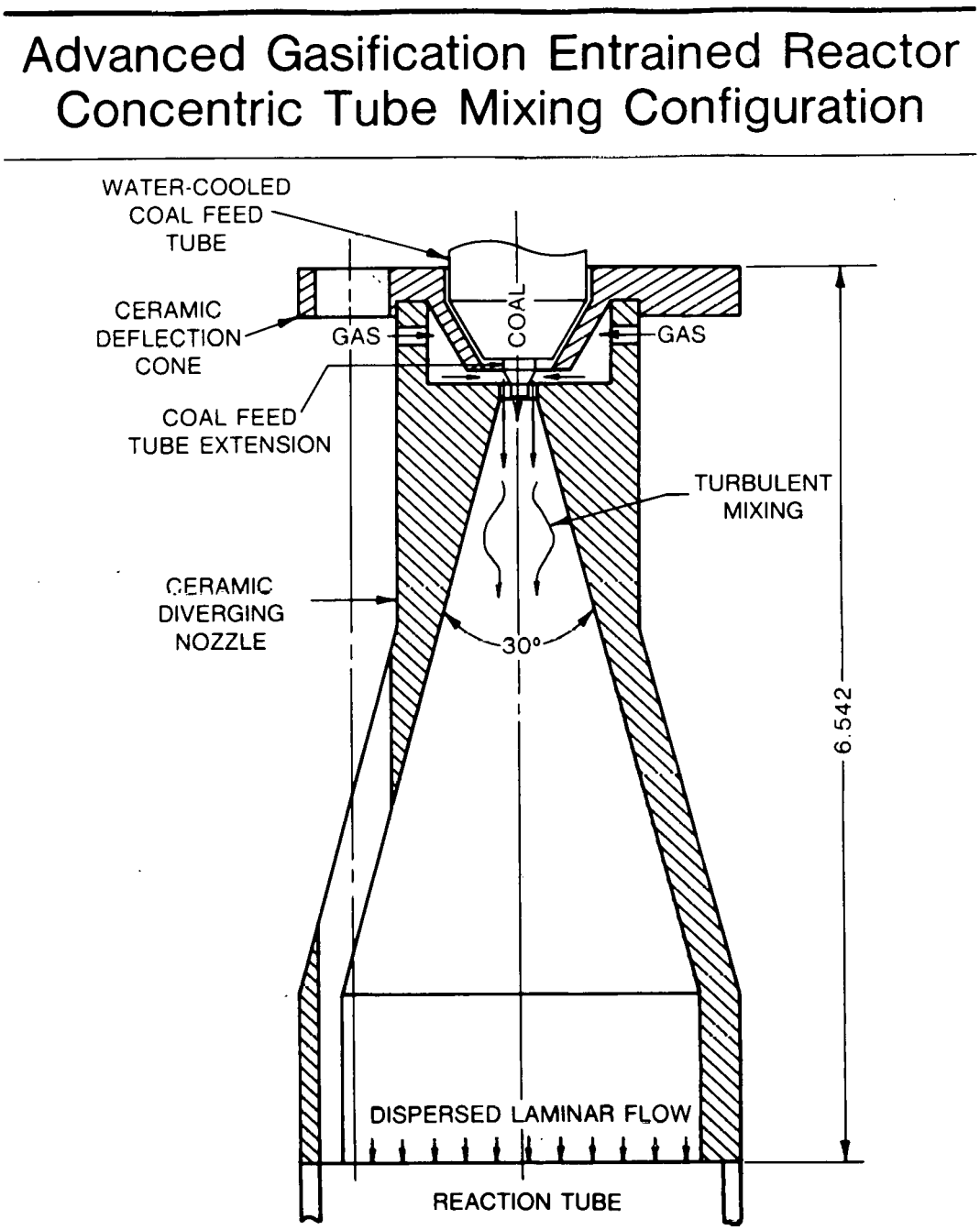

Figure 6. Major Test Classes.

A comprehensive test program with Montana Rosebud subbituminous coal is being conducted. The program is organized into three major test classes to study nitrogen, steam, and carbon dioxide environments, and an additional class to investigate char gasification reactions. The classes are further subdivided into test series to study the effects of temperature, pressure, residence time, and particle size. The Class 3 nitrogen-coal and the Class 4 steam-coal tests have been completed.

Montana Rosebud Coal Test Program
Major Test Classes

Class	Description	Purpose
3	N_2 - Coal	Product Yields in Inert Environment (Composite Factorial)
4	Steam-Coal	Product Yields in Reactive Environment (Composite Factorial)
5	Steam-Char CO_2 - Char	Char Reaction Rates (Select Conditions)
6	CO_2 - Coal Steam/Inert-Coal	Product Yields in Reactive Environments (Select Conditions)

METC 85-564-03 BE5

Figure 7. Composite Factorial Variable Levels.

Within the major test classes, a composite factorial experimental design is used to investigate the effects of reaction temperature, pressure, and gas residence time. This design enables a wide range of conditions to be studied with a comparatively small number of tests and permits the use of response surface and statistical techniques for data analyses. Uniform variable spacing is used for testing and analyzing to help ensure that each test point carries about the same weight. Some theoretical considerations are incorporated into the variable levels to facilitate regression modeling.

Montana Rosebud Coal Test Program
Composite Factorial Variable Levels

Variable	Levels				
METC Test Code	1	2	3	4	5
Factorial Code	−2	−1	0	1	2
Temperature, °F (X_1)	1500	1681	1898	2165	2500
Pressure, PSIG (X_2)	100	178	309	530	900
Residence Time, Sec (X_3)	2.19	3.20	4.68	6.84	10.00

Temperature = Reciprocal Level Spacing

Pressure and Residence Time = Logarithmic Level Spacing

METC 85-564-02 BE5

Figure 8. Graphical Representation.

The central composite factorial design consists of three types of tests which can be graphically represented by a pair of nested cubes. The center test point is the middle level of each variable and is represented by the common center of the cubes. The six axial test points at the centers of the outer cube faces are maximum and minimum levels combined with center point levels. The eight factorial test points at the corners of the inner cube are all combinations of intermediate levels. Thus, a test matrix consists of 15 different test conditions. The center point test is usually repeated at least three times to determine experimental variation.

Composite Factorial Experimental Design
Graphical Representation

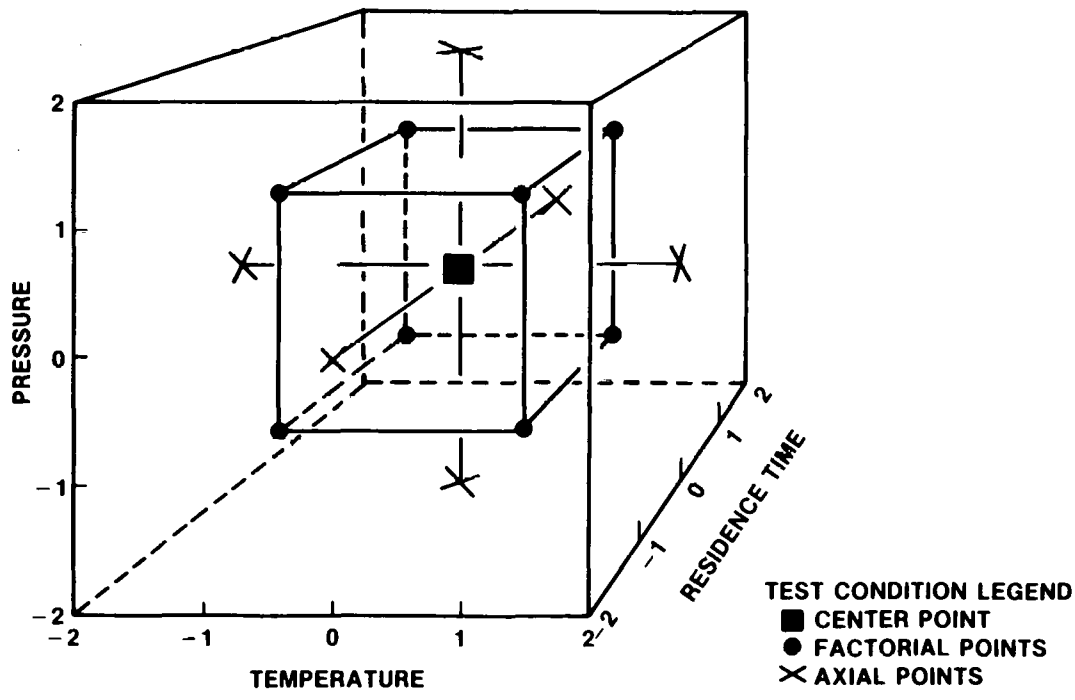

METC A-85-734-01 BE7-85

Figure 9. Regression Model Prediction For Elemental Retention in Char Versus Reaction Temperature

Quadratic response surface models are used to analyze the product yield and composition data as functions of the reaction conditions. When statistically significant, these regression models are used to predict trends. This figure shows regression model predictions for elemental retentions as a function of reaction temperature at the experimental center point pressure and residence time conditions for the steam-coal tests. At the lowest temperature, the relative order of the retentions is very similar to those in the nitrogen-coal tests except for sulfur, which had a much higher retention (approximately 70 percent) in the nitrogen-coal tests. In contrast to the tests at pyrolysis conditions, heterogeneous reactions occurred to a substantial degree in the steam-coal tests, and consequently, all retentions decreased with temperature. The models predict that nearly all the coal reacted in under 5 seconds at 2,000 degrees Fahrenheit.

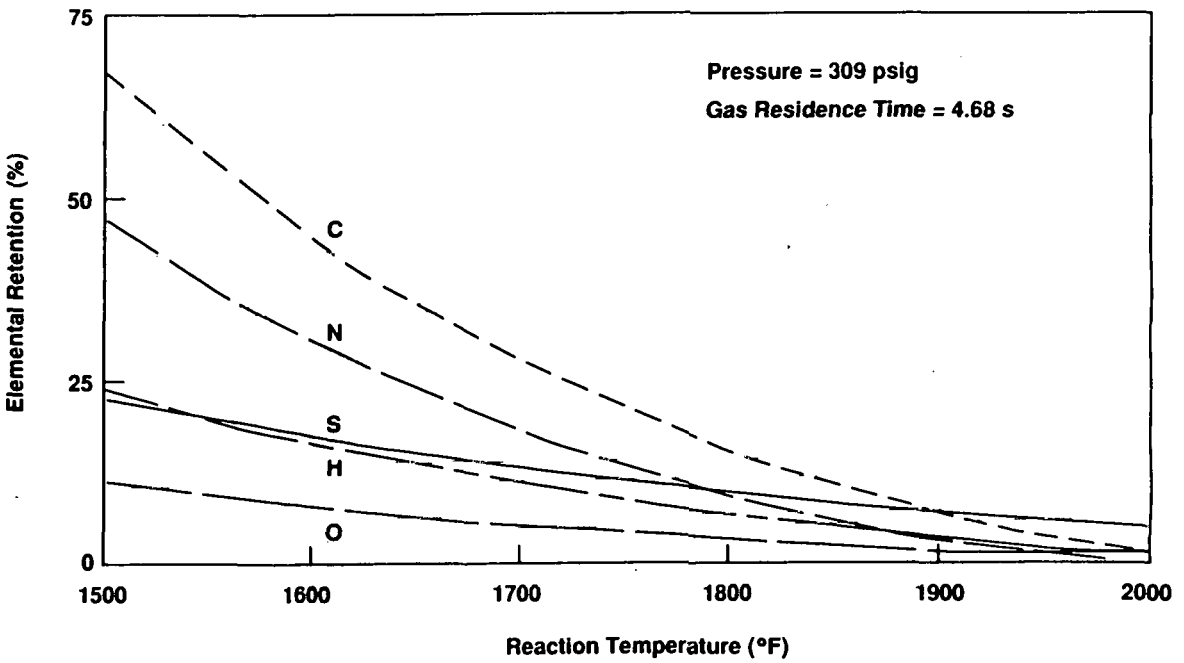

Regression Model Prediction for Elemental Retention in Char Versus Reaction Temperature, Class 4A Steam-Montana Rosebud Coal Tests, METC Advanced Gasification Facility Entrained Reactor

I87-1219-C BE8

Figure 10. Regression Model Prediction For Carbon Retention in Char Versus Gas Residence Time.

This figure shows the predicted variation in carbon retention with residence time at various reaction temperatures for the steam-coal tests. As expected, the model predicts that at any residence time level, carbon retention decreases (or conversely, carbon conversion increases) at higher reaction temperatures. The effect of temperature becomes less pronounced at the longer residence times due to the more extensive conversion that has already occurred. Because the coal reactivity was so high in these tests, nearly complete conversion always occurred in the higher temperature tests, and consequently, elemental retention trends at temperatures above about 2,000 degrees Fahrenheit could not be adequately represented by the quadratic response surface models.

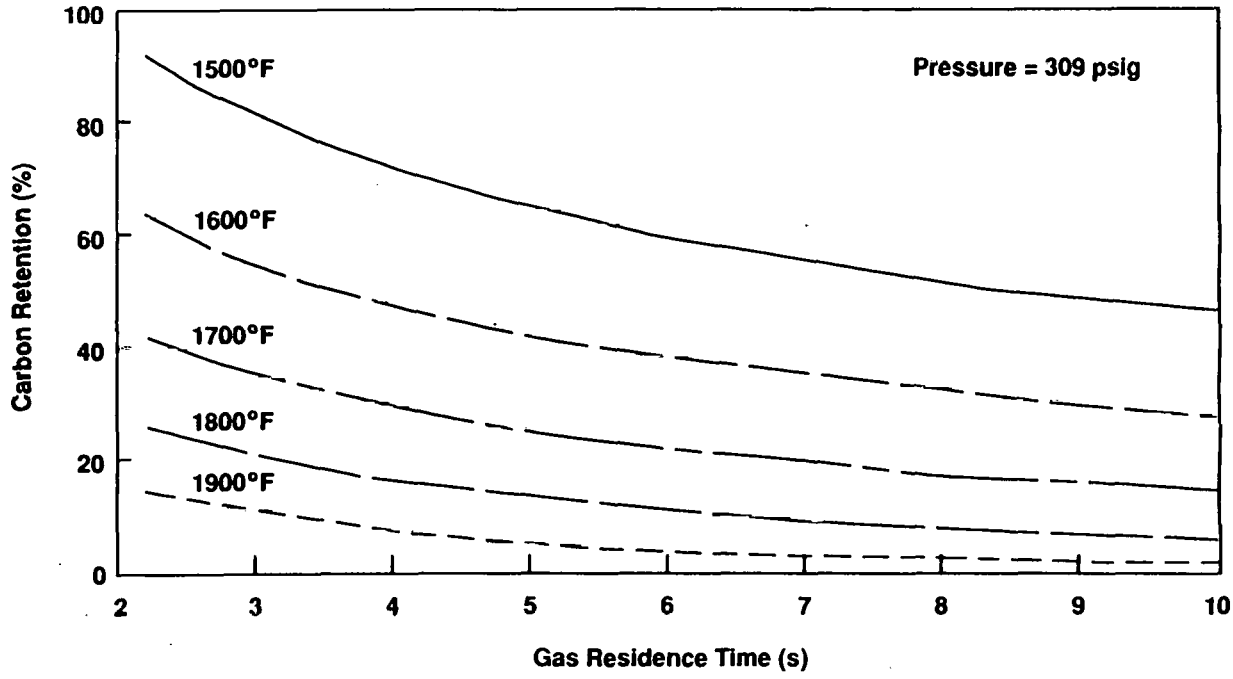

Regression Model Prediction for Carbon Retention in Char Versus Gas Residence Time, Class 4A Steam-Montana Rosebud Coal Tests, METC Advanced Gasification Facility Entrained Reactor

I87-1219-B BE8

Figure 11. Arrhenius Plot For Carbon Conversion Based on Regression Model Prediction For Various Carbon Retention Intervals.

The regression model for carbon retention in char for the steam-coal tests was used to estimate the activation energy for the steam-carbon gasification reaction as it occurred in the tests. This was done by first computing first-order rate constants at various temperatures from the regression model prediction for carbon retention versus residence time. A linear fit of these rate constants in an Arrhenius plot was then made to determine activation energy. Initial efforts to correlate the rate constants over a carbon retention range of 70 to 10 percent were unsuccessful due to nonlinearity in the resulting Arrhenius plot. Therefore, rate constants over smaller retention ranges were used. This approach, shown by the figure, resulted in satisfactory linearity and indicated that activation energy increased from 40 kcal/mole at low conversion levels to 53 kcal/mole at high conversion levels. Although not well quantified, it is generally accepted that activation energy increases with particle burnout, as is shown by this approach. Coal chars are also expected to have lower activation energies relative to pure carbons due to higher reactivities. Typical activation energies cited in the literature for the steam-carbon reaction are in the 60-70 kcal/mole range.

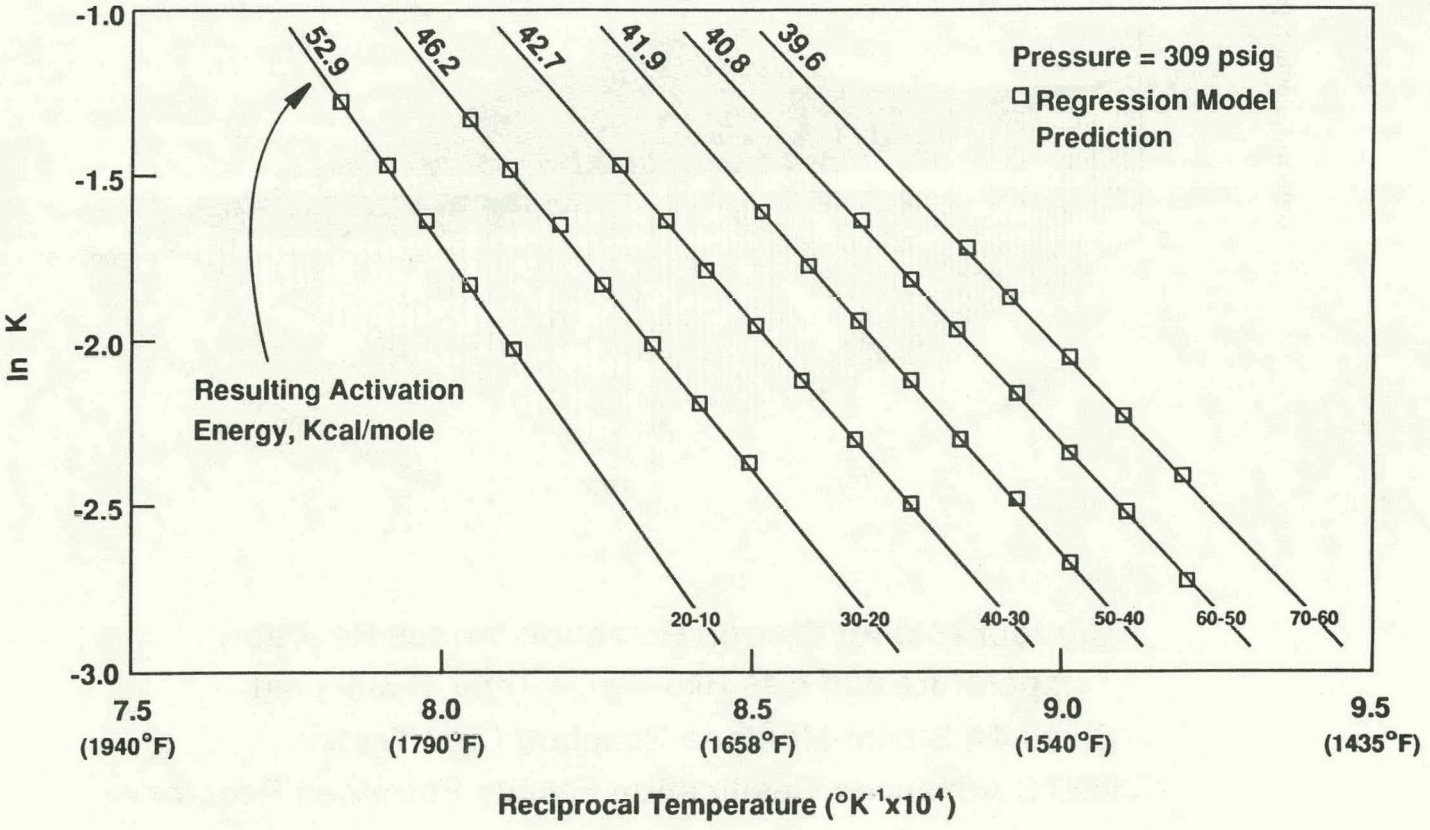

Arrhenius Plot for Carbon Conversion Based on Regression Model Prediction for Various Carbon Retention Intervals, Class 4A Steam-Montana Rosebud Coal Tests, METC Advanced Gasification Facility Entrained Reactor

I87-1219-A BE8

Figure 12. Contour Plot For Carbon Retention in Char Versus Reaction Temperature and Gas Residence Time.

In the regressional analyses, when there is more than one reaction variable with statistically significant predicted effects, the regression model can justifiable be used to generate 3-dimensional contour plots. This figure illustrates the predicted carbon retention at the center point pressure condition of the experimental design. Contour plots help to visualize the general behavior of a model. For instance, this plot shows that in the steam-coal tests, the sensitivity of carbon retention to residence time at the lowest temperature was small compared to the sensitivity to temperature at the shortest residence time.

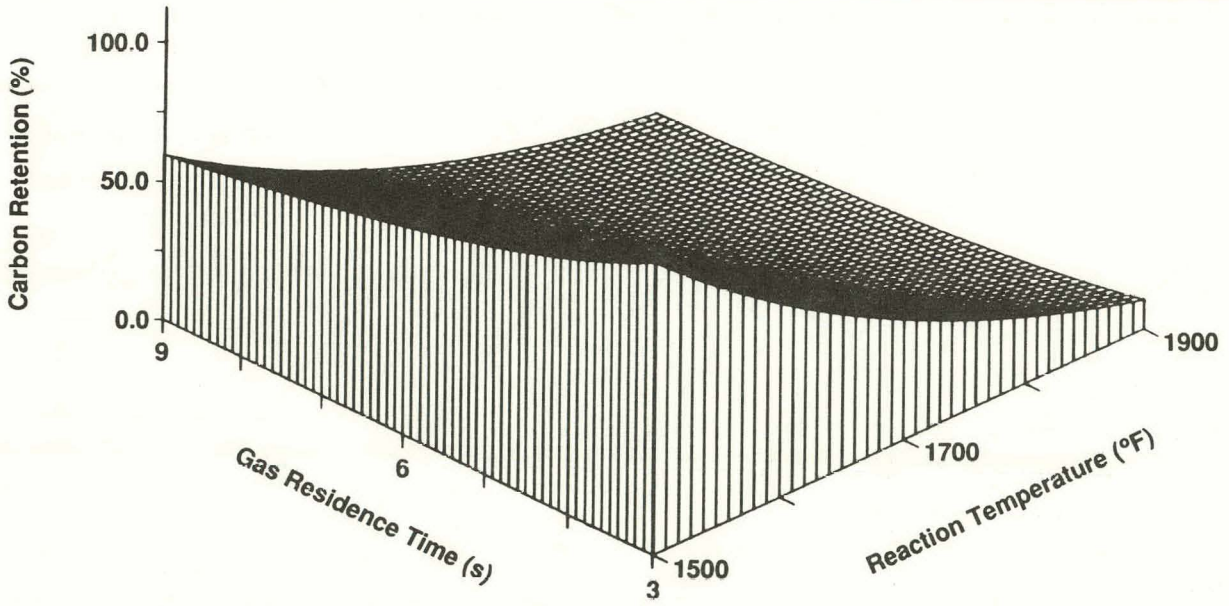

Contour Plot for Carbon Retention Versus Reaction Temperature and Gas Residence Time at 309 psig, Class 4A Steam-Montana Rosebud Coal Tests, METC Advanced Gasification Facility Entrained Reactor

I87-1219-D BE8

Figure 13. Recent Conclusions and Observations.

As for the nitrogen-coal tests, the regressional analyses of the steam-coal test data showed that reaction temperature had the most effect on product yields and compositions. As expected, due to the occurrence of more reactions, considerably more residence time effects were evident in the steam test data compared to the nitrogen test data. Except for several polycyclic aromatic compounds, there were no significant predicted pressure effects. Although the reasons for this are unclear, the high steam partial pressures used in the experiments may have been a contributing factor. The molecular weight spectrum of polycyclic aromatic compounds, or tar species, was similar to that in the nitrogen-coal tests, but total yields were nominally only one-fourth as much. A short test series was conducted in which char, generated at the center point test condition in nitrogen, was reacted in steam. By comparison of the carbon-steam reaction rate constants in the coal and char tests, there was no striking evidence of "early-time" enhanced reactivity in the coal tests, as was expected, but the data are still being evaluated. Preliminary inspection of the carbon dioxide-coal test data indicates that coal ractivity was less than in steam, and that carbon dioxide may have significantly affected the behavior of hydrogen in the system, perhaps beyond just the effect of the water-gas shift reaction alone. This is supported by the consistent lack of detectable hydrogen in the product gas and evidence in some of the lower temperature tests of some particle agglomeration reminiscent of bituminous coal behavior.

Recent Conclusions and Observations

Conclusions From Steam Tests (Compared to Nitrogen Tests)

- Temperature effects again most important
- Considerably more residence time effects
- No significant predicted pressure effects
- Similar tar spectrum but with reduced yields
- No evidence of "early-time" enhanced char reactivity

Observations From Carbon Dioxide Tests

- Coal reactivity less than in steam (expected)
- Carbon dioxide may be significantly altering hydrogen behavior (unexpected)
  - — No hydrogen detected in product gas
  - — Some particle agglomeration reminiscent of bituminous coal behavior
  - — Possibly improved hydrocarbon yields
  - — More than just water-gas shift reaction effects?

METC T87-1219-2 BE8

Figure 14. Future Plans.

The planned test program with Montana Rosebud subbituminous coal has essentially been completed. Regressional analyses of the carbon dioxide-coal test data and the exercise of interrelating the regression models from the three composite factorial test series must still be done. Activities to simulate the reactor with the PCGC-2 computer code will continue, and reaction chemistry improvements based on the experimental data will be incorporated into the code as warranted. Experimentally, if the feasibility to test with bituminous coal is demonstrated, steam and carbon dioxide composite factorial test series with Illinois No. 6 are planned so comparisons with the subbituminous coal results can be made. In addition, exploratory concept tests using select gaseous reactants, special reaction conditions, or different heating methods to reduce process severity and favor specific products may be attempted.

Future Plans

Experimental

- Complete subbituminous coal test program
- Conduct composite factorial tests with bituminous coal
- Conduct exploratory concept tests
  - — Reduce severity and increase efficiency

Modeling

- Interrelate regression models from composite factorial tests
- Continue using and upgrading PCGC-2 model to simulate reactor

Reporting

- Complete analyses and reporting of subbituminous coal test data
- Report on PCGC-2 modeling activities and changes

METC T87-1219-3 BE8

SIDESTREAM ZINC FERRITE REGENERATION TESTING

Thomas Grindley
Morgantown Energy Technology Center

FIGURE 1. Objective and Background

It has been known for some years that large potential economic gains can be gained by high-temperature purification of the product of coal gasification for use by gas turbines, fuel cells, etc. An attempt is being made to lay the experimental foundation to bring the technology to fruition. This is being done by development of regenerable solid sorbents from laboratory scale through sidestream testing and process development.

Objective

- **Gasification Island**
  - **— Hot gas cleanup key link between gasifier and gas turbine heat engine**
  - **— Sulfur removal to ∼ 10 ppm**
- **Molten Carbonate Fuel Cells**
  - **— Zinc ferrite sorbents initial step in cleanup process**
  - **— Sulfur removal requirement to less than 1 ppm**

Background

- **Conventional coal gas cleanup by water quench and liquid absorption processes inefficient and costly**
- **System studies indicate large potential efficiency and cost gains for hot gas cleanup**
- **Research and development into hot gas cleanup not brought to fruition**

METC 86-369-1 BE4 T87-1202-1 B8

FIGURE 2. Zinc Ferrite

A key factor in the development of hot gas cleanup technology is considered to be a regenerable, high-temperature desulfurization sorbent. Zinc ferrite has been selected for detailed study. This sorbent is typically made in the form of cylindrical extrusions from finely divided zinc oxide and iron oxide ingredients together with inorganic binders and modifiers. The zinc and iron oxides combine to form zinc ferrite in which the zinc is widely dispersed within the spinel crystal structure.

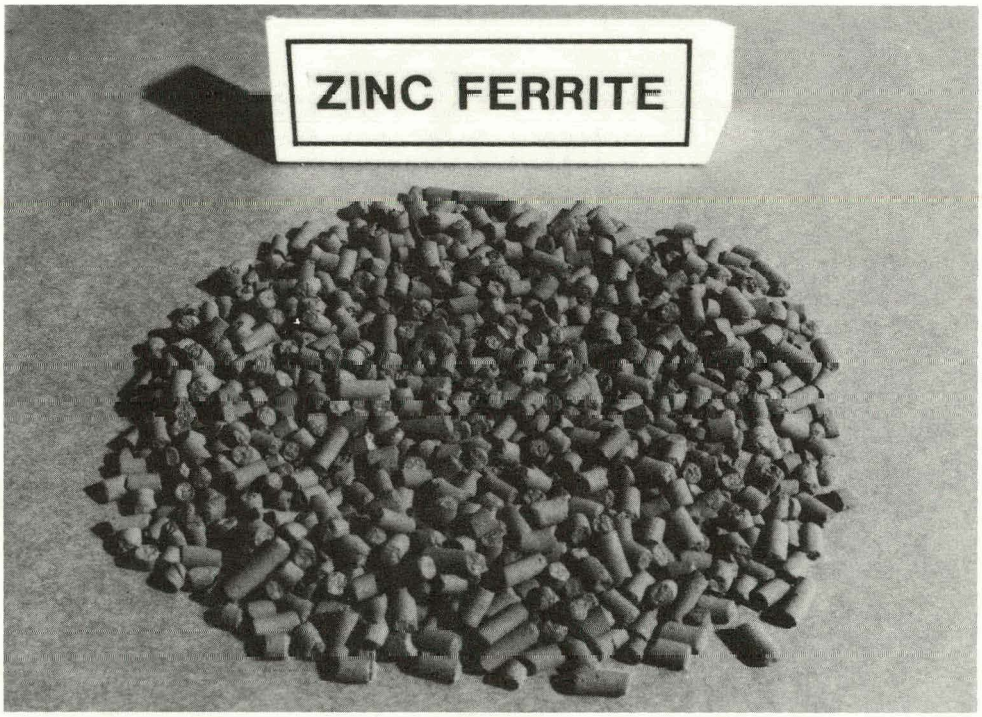

FIGURES 3-7. Test Units

A laboratory-scale unit, essentially consisting of a 2-inch diameter fixed-bed, low-pressure, stainless steel or quartz reactor, has been used to screen and parametrically evaluate numerous sorbents for their ability to desulfurize simulated hot coal gas and to be regenerated.

Sorbents identified through lab-scale testing have been evaluated in a sidestream unit consisting of a 6-inch diameter fixed-bed, high-pressure Incoloy 800H reactor. These tests have determined the ability of the sorbents to function in actual hot coal gas from fixed- and fluid-bed gasifiers.

Test Units

- 6-inch diameter fixed-bed reactor unit tested on gasifier sidestreams
  - — METC 24 T/D fixed-bed gasifier
  - — METC 150 lb/hr fluid-bed gasifier
- 2-inch diameter fixed-bed lab-scale unit for parametric studies

METC 86-369-3 BE4

Lab-scale Desulfurization Unit

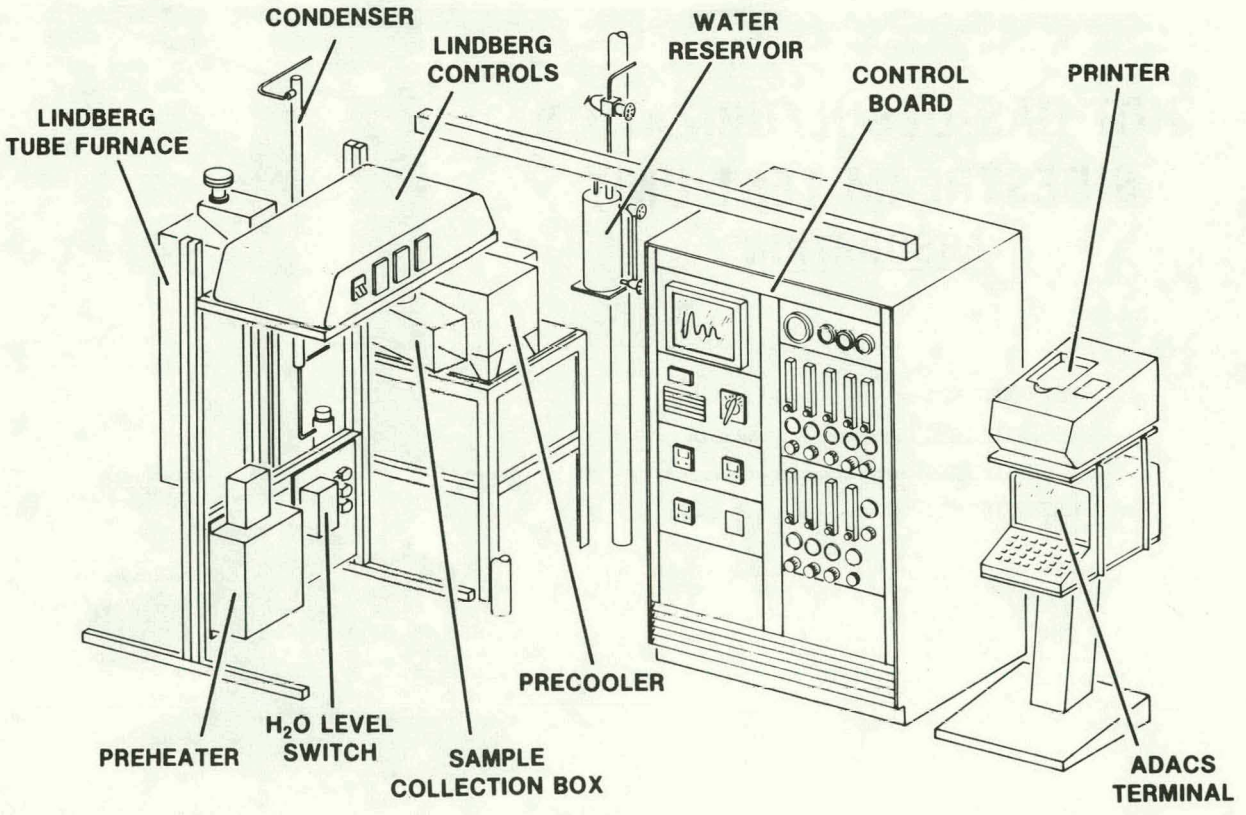

EG&G A-85-435-08

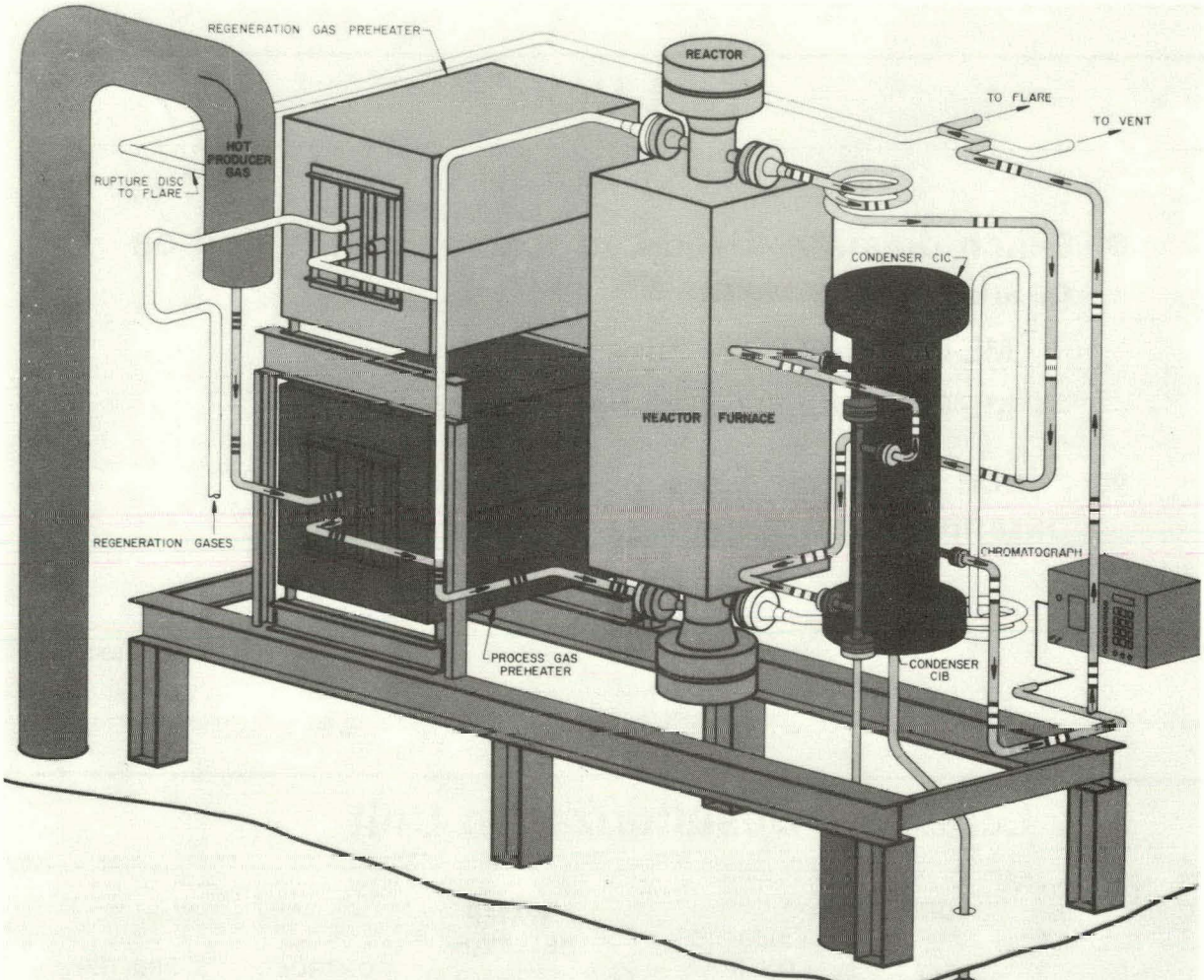

HOT GAS DESULFURIZATION SIDESTREAM TEST UNIT

ABSORPTION

LEGEND

- HOT PRODUCER GAS WITH SULFUR
- HOT PRODUCER GAS WITHOUT SULFUR
- COOLER PRODUCER GAS WITHOUT SULFUR
- COLD PRODUCER GAS WITHOUT SULFUR

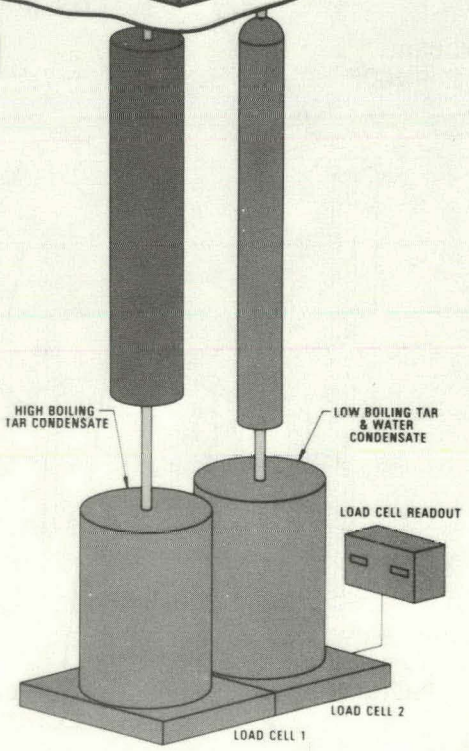

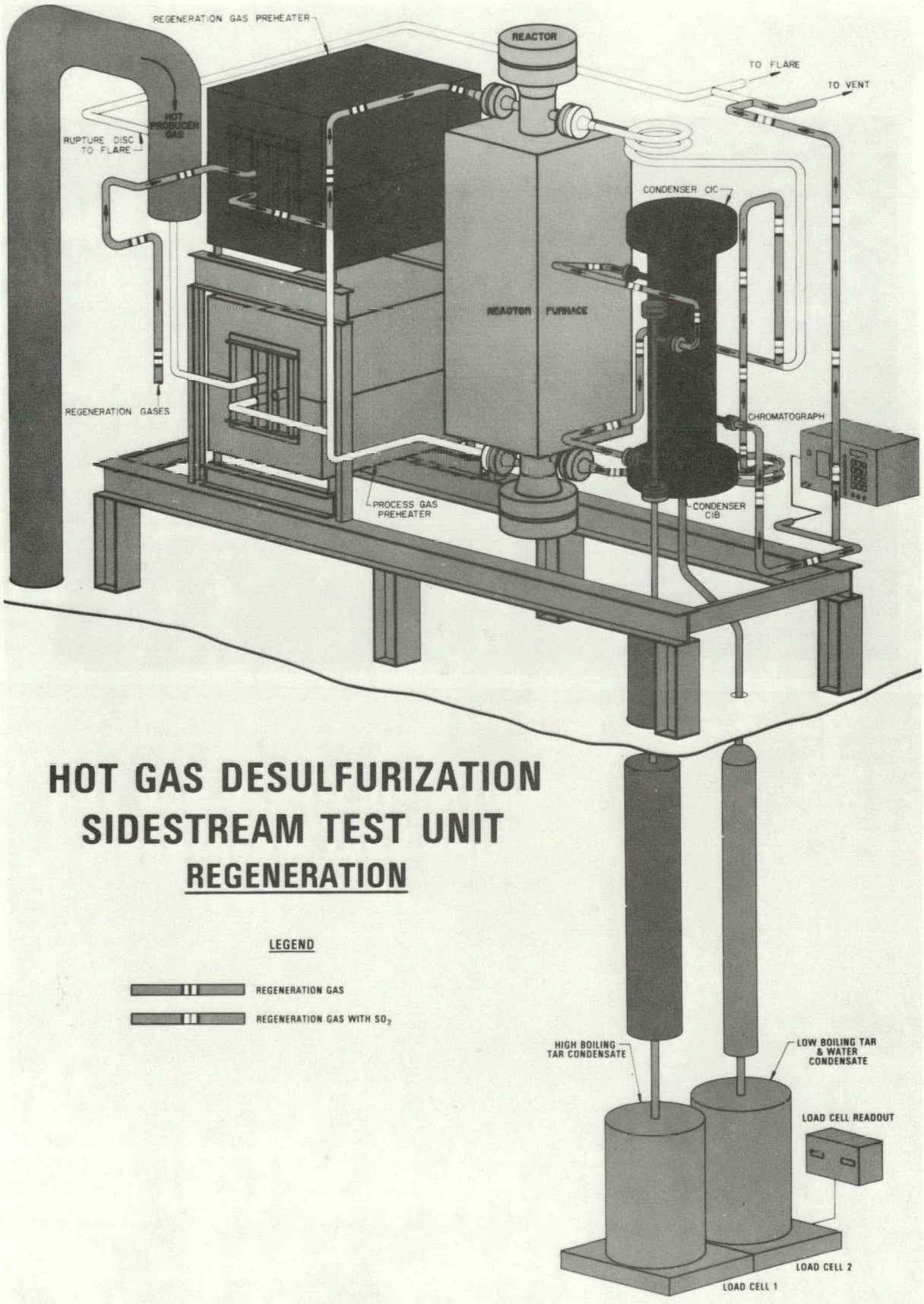

HOT GAS DESULFURIZATION SIDESTREAM TEST UNIT

REGENERATION

LEGEND

REGENERATION GAS

REGENERATION GAS WITH SO_2

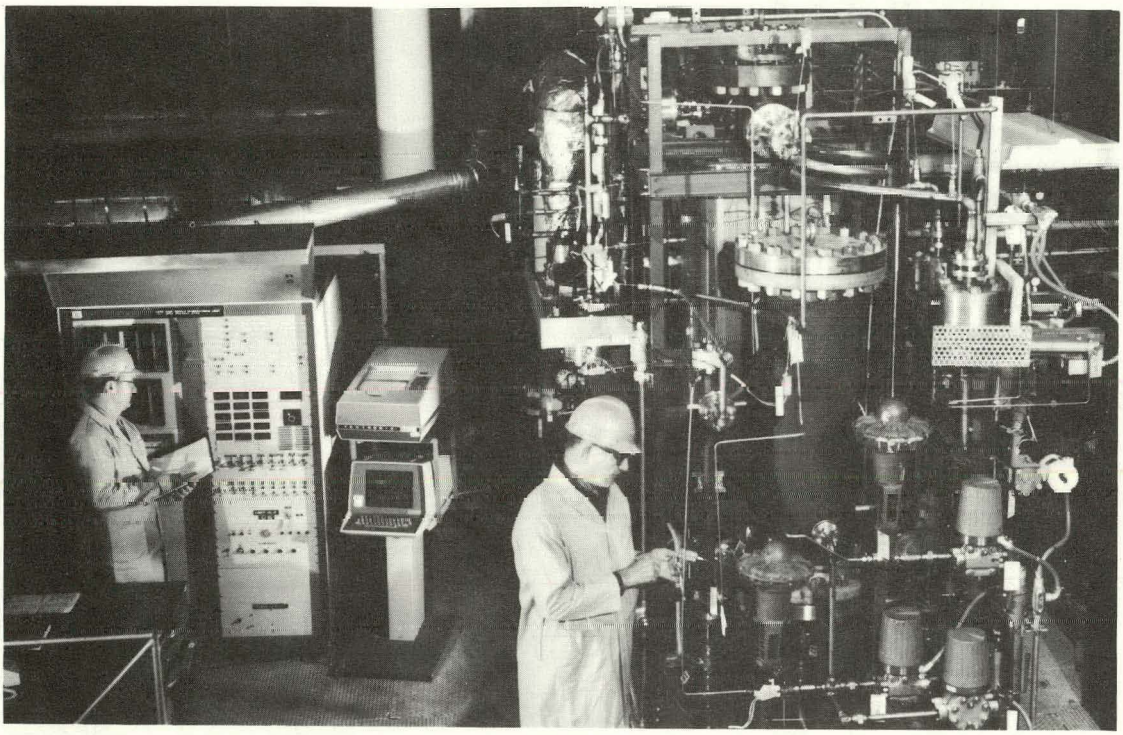

FIGURES 8-10. Summary of Tests

The activities carried out with the lab-scale and sidestream units are summarized in itemized form. These activities have been reported in detail in METC publications.

Summary of Tests
Lab Scale Unit

- **Completed screening tests of several zinc oxide based sorbents**
  - **Regenerable zinc ferrite sorbent developed**
- **Performance of zinc ferrite evaluated parametrically**
  - **Various simulated gases (KRW, Lurgi)**
  - **Pressures from 0 to 25 psig**
  - **Temperatures from 400 to 1500°F**
  - **Regeneration with steam/air by volume from 1/1 to 3/1**
- **Measured residual sulfates in regenerated sorbents**
- **Completed support tests for design of process developmental unit**
- **Determined ability of sorbents to remove hydrogen chloride and ammonia from hot simulated gases**

METC T87-1202-3 B8

Summary of Tests
Sidestream Unit with Fixed-Bed Gasifier

- Completed 500 hours on-line with zinc ferrite
  - 13 desulfurization runs
  - 9 regeneration runs
- Unit operated at:
  - 100-300 psig
  - 1000-1300°F
  - Steam/air: 0.2 to 0.4 wt/wt
- Gas derived from
  - Pittsburgh bituminous
  - Kittaning bituminous
  - Indian head lignite
- Air and oxygen blown gasification

METC T87-1202-2 B8

Summary of Tests
Sidestream Unit with Fluid-Bed Gasifier

- Completed 800 hours testing with zinc ferrite
  - 22 sulfidation runs
  - 16 regeneration runs
- Test parameters:
  - 200-300 psig
  - 1000-1200°F sulfidation
  - Montana Rosebud coal
  - Air blown gasification
  - T and P effects on regeneration
  - Multiple sorbent formulations
- Studied sorbents for enhanced durability
- Supported design of larger scale development unit
- Studied combined oxidation/reductive regeneration

FIGURE 11. Zinc Ferrite Sulfidation

Hydrogen sulfide breakthrough plots for the lab-scale, fixed-bed reactor are shown through three cycles of desulfurization of simulated air-blown coal gas with a zinc ferrite sorbent. It is evident that, after successive regenerations, the sorbent retains both its ability to lower H_2S concentration to less than 10 ppm, and its sulfur loading capability before breakthrough.

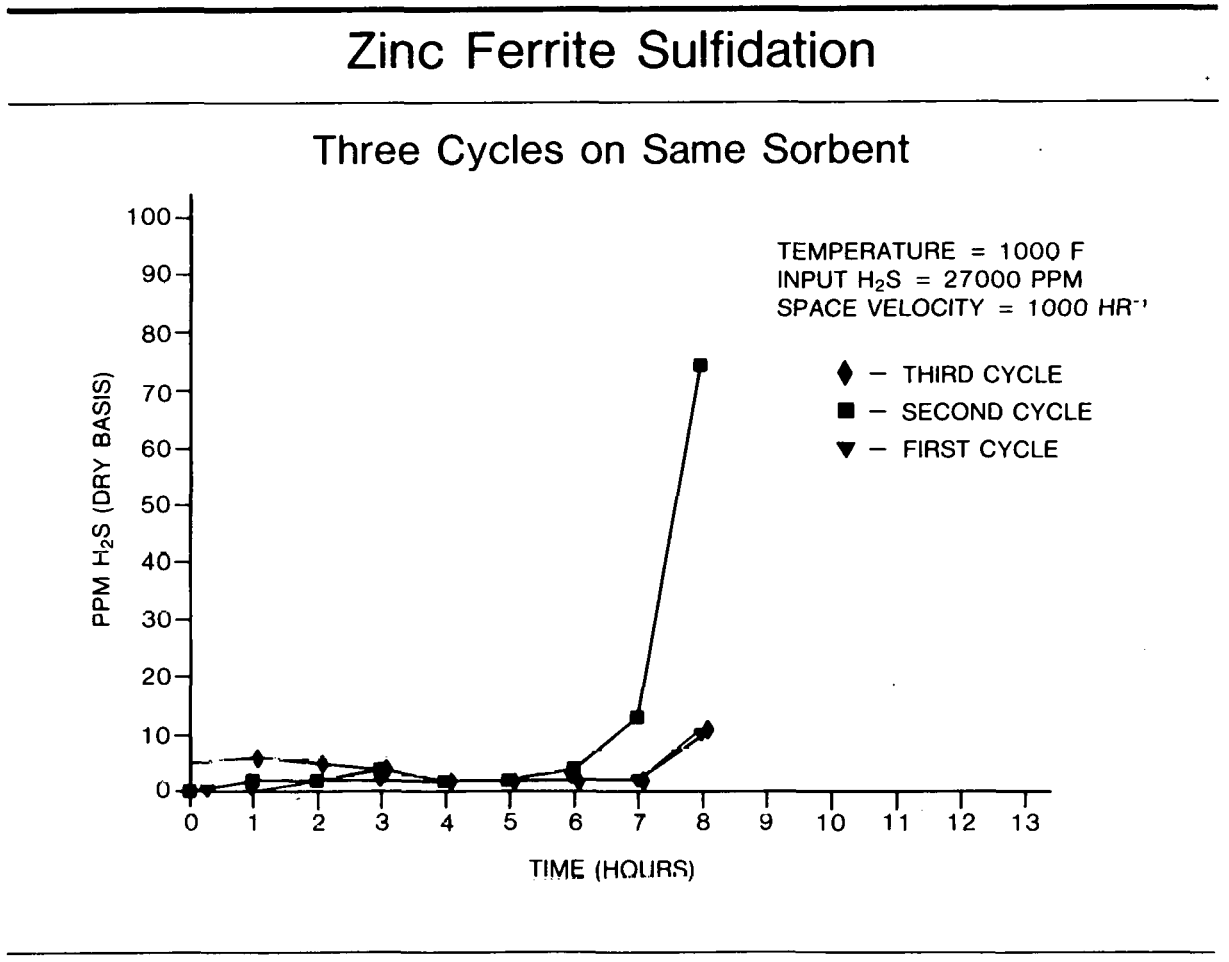

FIGURE 12. Zinc Ferrite Sulfidation Lab-Scale Unit Tests

Hydrogen sulfide breakthrough plots are shown at four temperatures for the desulfurization of simulated air-blown coal gas by zinc ferrite sorbent. The gas composition is the same as that in the KRW process development unit. The plots indicate that sulfur absorption before breakthrough declines when the temperature exceeds 1,200°F. This is attributed to the formation of wustite in the sorbent.

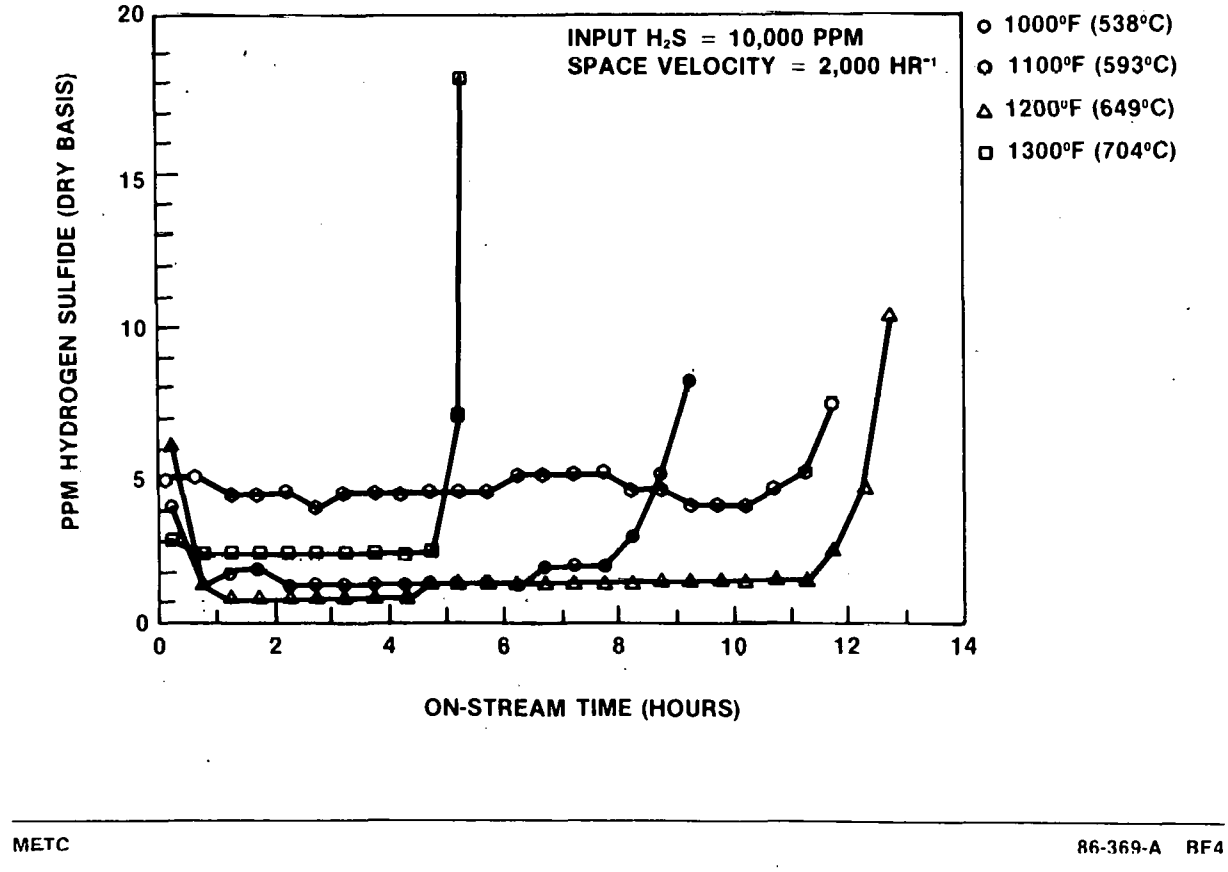

FIGURE 13. Major Findings

Major findings in the project are itemized. The present status is that zinc ferrite sorbents have demonstrated sufficient promise to justify process development with fixed- and fluid-bed gasifiers. It is expected that desulfurized gas from the process will be combusted in gas turbine trials.

Major Findings

- Sorbent capable of removing H_2S and COS to <10 ppm through multiple cycles
- Inorganic binders e.g. bentonite improve sorbent durability
- Sorbent most suitable for 1,000 - 1,200°F operation
  - — Reactivity declines at low temperature
  - — Wustite forms at high temperature
- Excessively reducing gas causes detrimental formation of wustite
- Both oxidative and reductive regeneration required

METC T87-1301-1 BE8

FIGURE 14. Future Plans

The lab-scale and sidestream desulfurization units will be utilized principally in support of process development for high-temperature coal gas desulfurization. This will involve modification to the lab-scale unit for operation at pressures to 450 psig and installation of a second reactor in the sidestream unit to study tar, chloride, and ammonia removal.

Fluid-bed operation and study of novel sorbents are also planned for the lab-scale unit.

Future Plans

- **Sidestream Unit**
  - **Study of tar, chloride and ammonia removal from hot gas**
  - **Evaluation of novel sorbents**
  - **Study of partition of contaminants between gas and particulates**

- **Lab-Scale Unit**
  - **Study of oxidative and reductive regeneration at pressure**
  - **Fluid-bed operation at pressure**
  - **Support studies for process design**

METC T87-1247-1 BE8

METC FIXED-BED GASIFIER

Kalman Pater
Morgantown Energy Technology Center

FIGURE 1. METC FIXED-BED GASIFIER AND GAS CLEANUP SYSTEM

The Morgantown Energy Technology Center (METC) fixed-bed gasification and gas cleanup system is an integrated test facility that is focused on the METC stirred, fixed-bed gasifier with both air- and oxygen-blowing capabilities. The installation includes a novel "dry-tar" gas cleanup system that sequentially removes contaminants in separate manageable effluent streams. This enhances their further treatment, disposal, or recycling. A major feature of the cleanup system is a first-of-its-kind pressurized Holmes-Stretford desulfurizer plant. The system has been successfully demonstrated on a broad spectrum of U.S. coals from western subbituminous through the highly caking eastern bituminous variety. The system has recently been modified to support development of "hot gas" cleanup technology. Key issues being addressed are gasifier in-bed sulfur capture, on-line zinc ferrite absorbers to remove H_2S, and recycle of the SO_2 laden absorber regeneration gases to the gasifier for reaction with the ash and discharge in a stable form.

FIGURE 2. METC FIXED-BED GASIFIER

The METC gasifier is a Wellman-Galusha type that has been extensively modified to operate at pressures up to 300 psi. The 42-inch diameter unit can process up to 48 tpd of coal into nominally 300 Btu/scf gas when oxygen blown, or 150 Btu/scf when air blown, at production rates up to 180,000 scfh. It is equipped with a deep-bed stirrer for processing highly caking coals. The stirrer arms traverse a helical path through the bed, breaking agglomerations and void formations to ensure bed uniformity. Thermocouples mounted in the stirrer arms provide data to locate the transition between the ash and combustion zones resulting in stable ash level control.

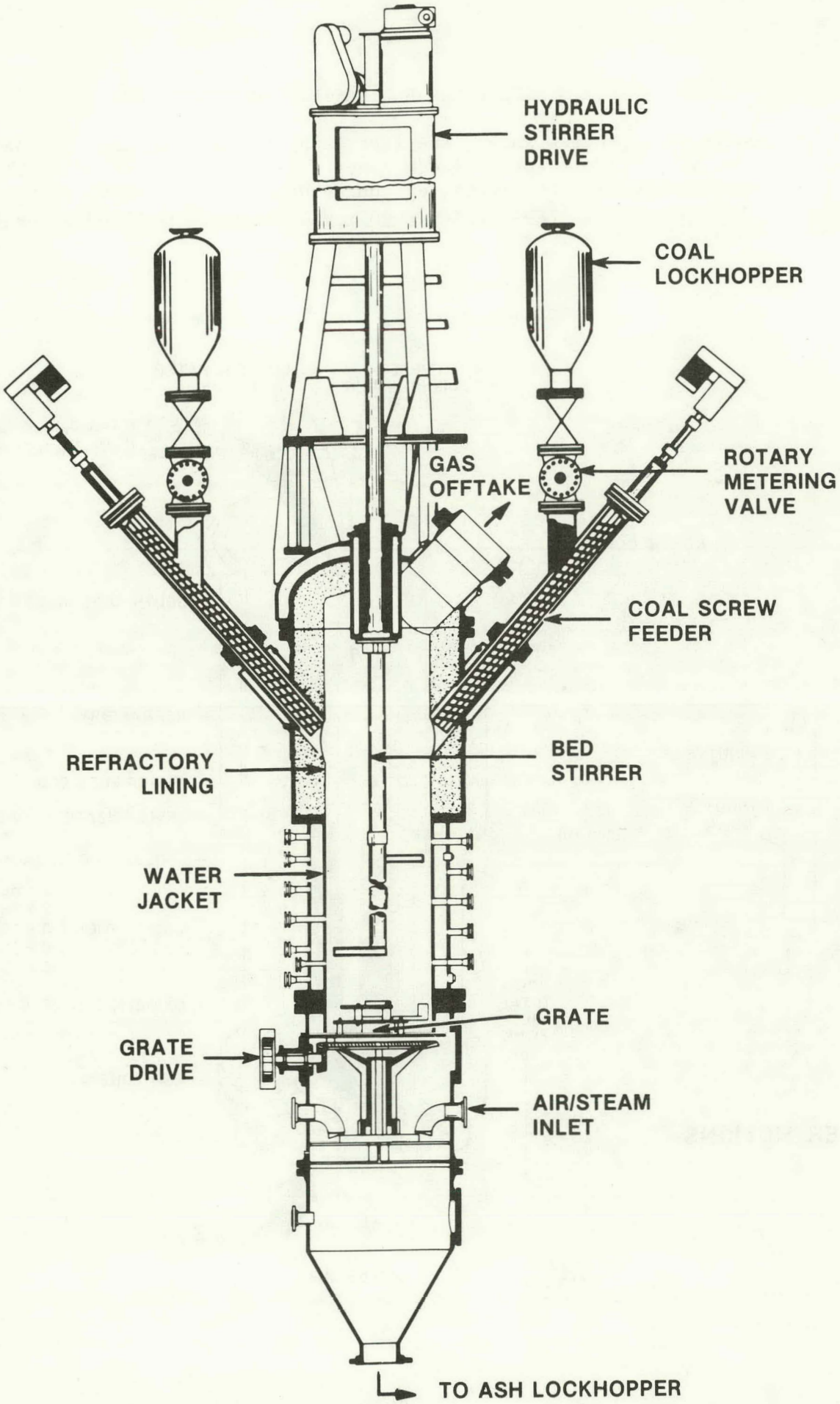
HYDRAULIC
STIRRER
DRIVE
COAL
LOCKHOPPER
GAS
OFFTAKE
ROTARY
METERING
VALVE
COAL SCREW
FEEDER
REFRACTORY
LINING
BED
STIRRER
WATER
JACKET
GRATE
GRATE
DRIVE
AIR/STEAM
INLET
TO ASH LOCKHOPPER

FIGURE 3. METC FIXED-BED GASIFIER REACTION ZONES

In the counterflow process shown, the last thing the hot exiting gas contacts is the relatively cold, volatile-laden upper fuel bed. Consequently, the gas stream contains significant amounts of contaminants, including coal dust, condensable tars and oils, light hydrocarbons, water, ammonia, phenols, sulfur gases, and alkali metals.

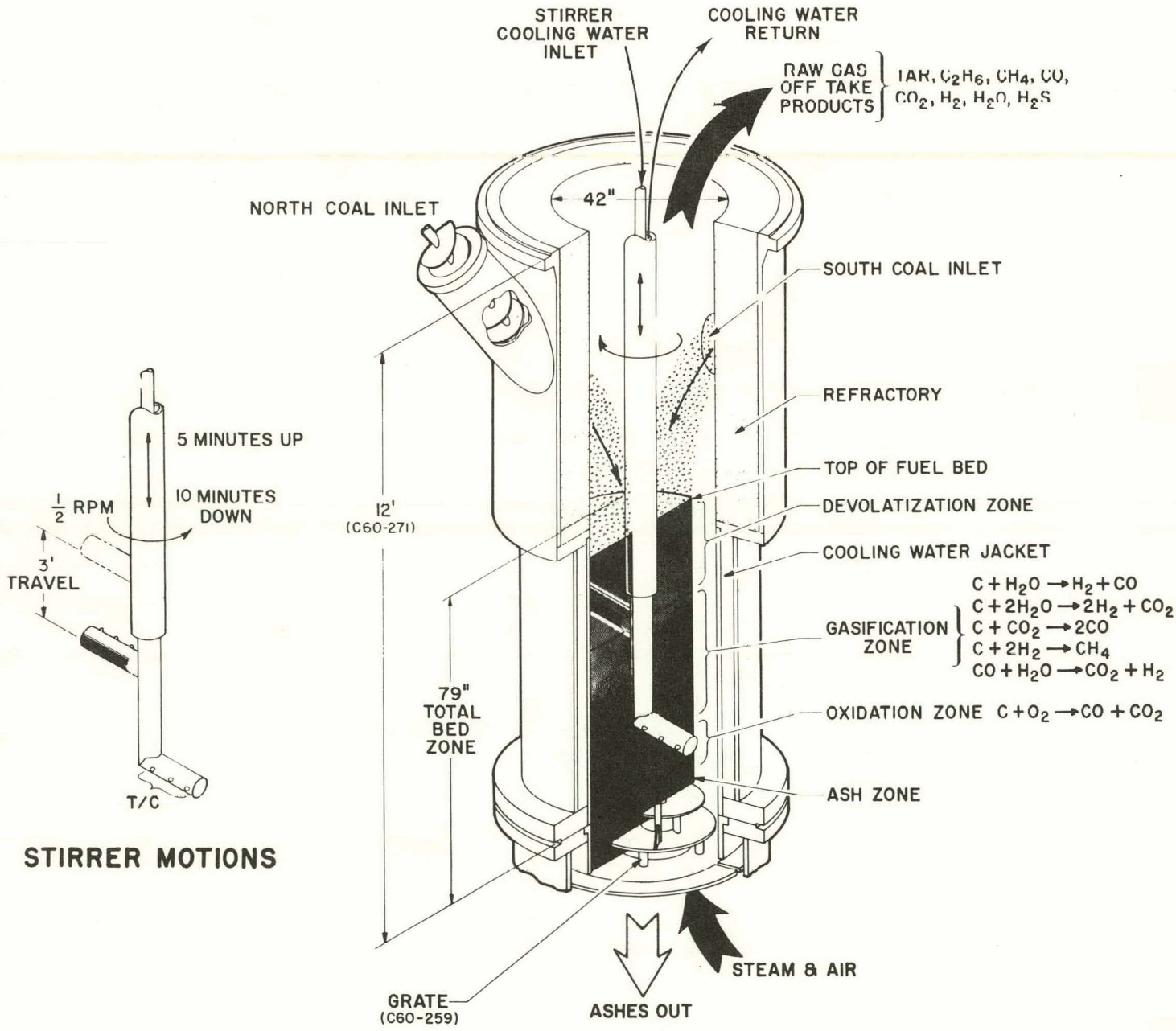

Test Run 106

Objective: To Determine Capability of Lump Limestone (3/8" x 1/4")
To Remove Sulfur in METC's Fixed-Bed Coal Gasifier

Operating Conditions*	Baseline**	Ca/S=1**	Ca/S=2**	Ca/S=1, Fe/S=0.5**
Coal Feed Rate, lb/hr***	2,260	2,172	2,364	2,317
Steam Feed Rate, lb/hr	1,898	1,911	1,891	1,900
Air Feed Rate, lb/hr	4,791	4,800	4,775	4,750
Gasifier Pressure	199	199	197	198
Gasifier Exit Temperature, Deg. F	1,082	1,168	1,086	1,163
Gas Production, Wet, scfh	136,430	129,639	128,458	132,392
Gas Composition, Dry, Vol. %				
H2	19.7	19.2	20.2	19.7
CO2	12.1	12.8	12.7	13.0
CO	17.6	17.3	16.7	16.9
N2	45.1	45.7	45.2	45.2
CH4	3.5	3.3	3.4	3.5
Totals (expressed as H2S)	0.494	0.405	0.402	0.422
% H2O in Gas	21.2	16.6	16.7	18.5
Heating Value of Gas, Btu/scf	173.5	180.9	179.3	178.9
Sulfur Capture Efficiency, %				
Gas Basis	1.5	6.3	14.7	9.8
Ash Basis	2.4	4.3	4.8	4.4

*Average parameters over a test period.

** "Baseline" means no added limestone or iron oxide.
Numbers are expressed as nominal molar ratios.

*** 1" x 3/8" washed Arkwright coal, S=2. 18% (~ 50% pyritic sulfur).

C87-1251-2 BE8

Evaluation of Sulfur Capture Results

- Possible reasons for low capture efficiency during Run 106
  - Sorbent particles too large and not well-dispersed
  - Sorbent calcines after bulk of coal sulfur is released
  - Sorbent sinters before extensive capture can occur
- Reasons to expect better overall capture in future tests
  - Use of smaller, more dispersed particles
  - Use of hydrated lime instead of limestone
  - Dravo-Wellman results and others substantiate this expectation
  - Offgas sulfur will be recycled to gasifier bottom

METC C87-1251-1 BE8

Accomplishments

- Processed wide spectrum of U.S. coals
- Demonstrated system reliability, highly automated system control and sophisticated instrumentation
- Unique ash level control system
- Performed environmental characterization of the work place and process streams
- Demonstrated tar/fines utilization
- Demonstrated operability on run-of-mine coal
- METC dry-tar gas cleanup system demonstrated as viable alternative to conventional quench technology
- Developed gasifier models and completed ASPEN simulation

METC 86-528-2 BE5

Integrated Gasifier/Hot Gas Clean-Up Concept

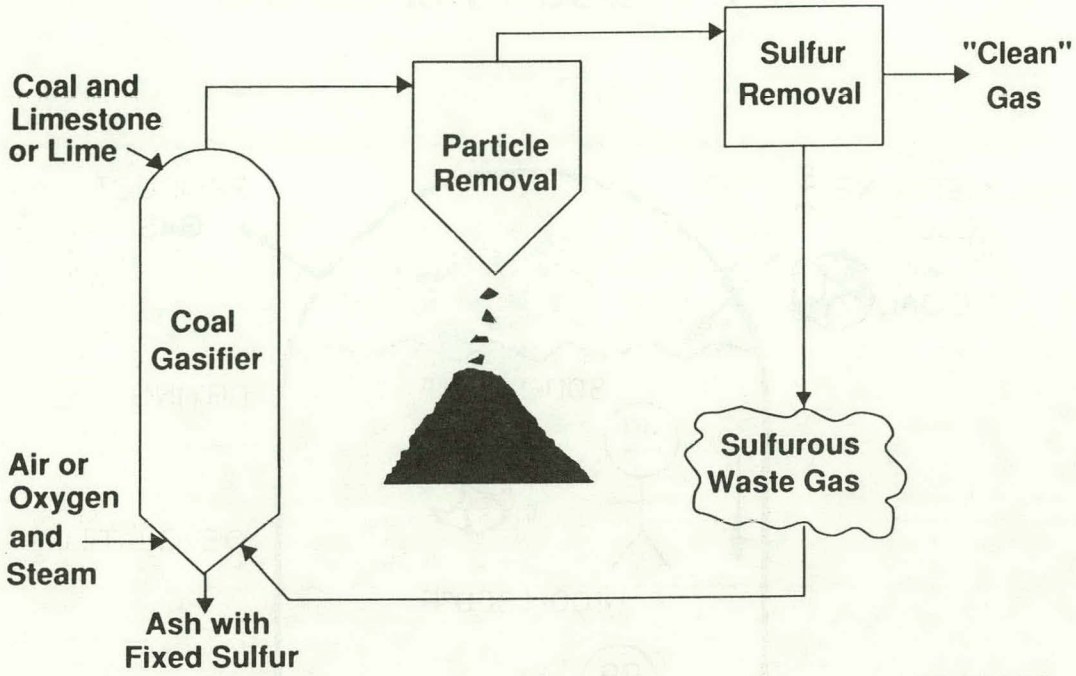

C87-1251-B BE8

Fixed-Bed Gasification

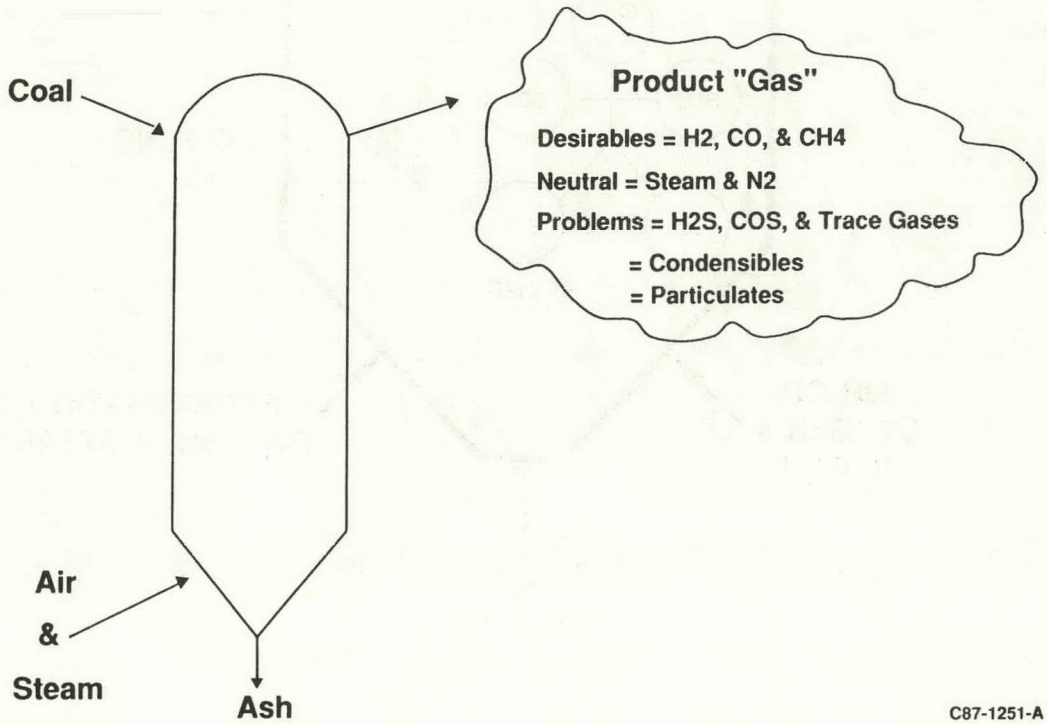

C87-1251-A BE8

Key In-Bed Phenomena

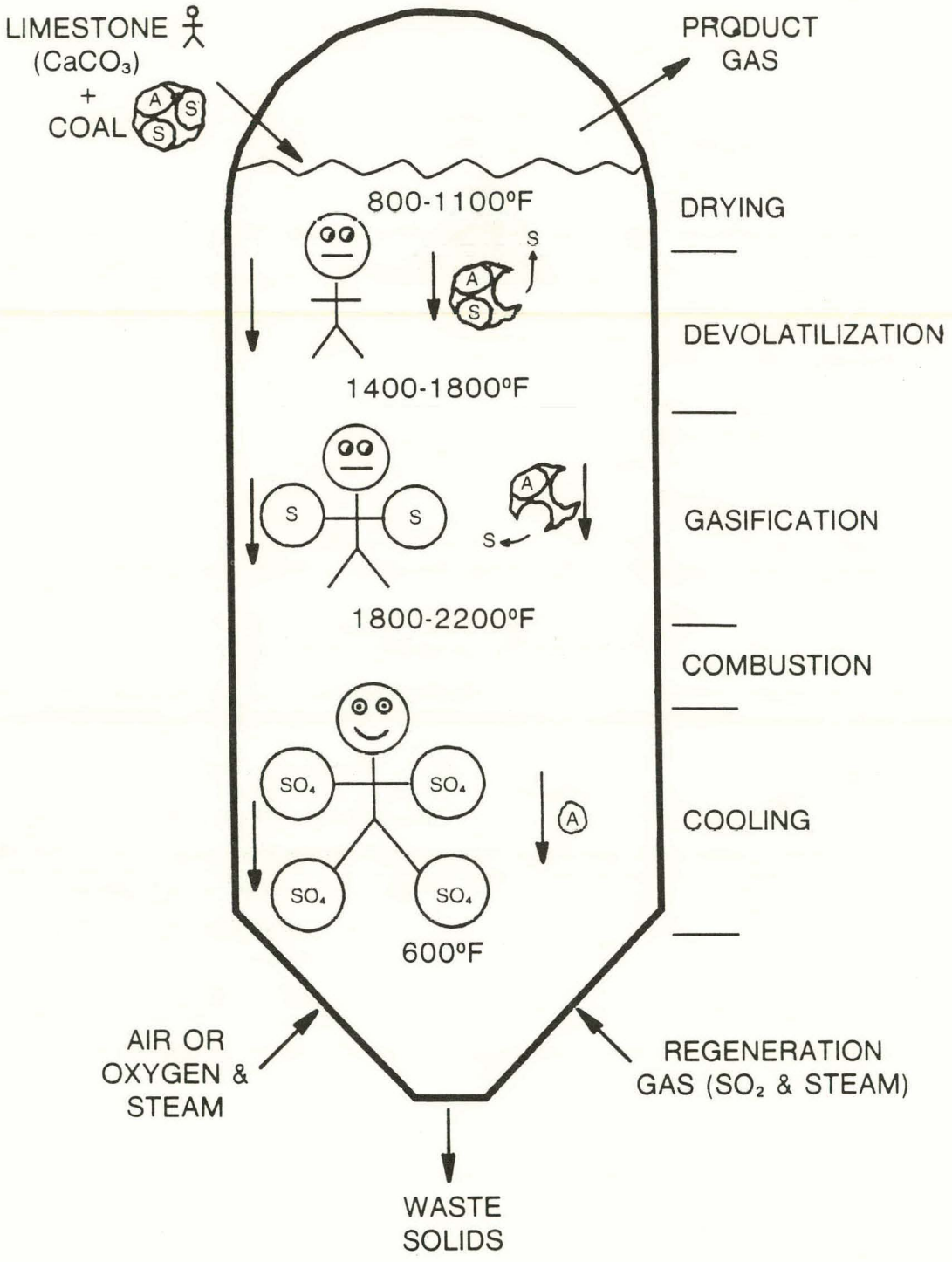

I87-366-F B3

Gasifier Feedstock Preparation Alternatives

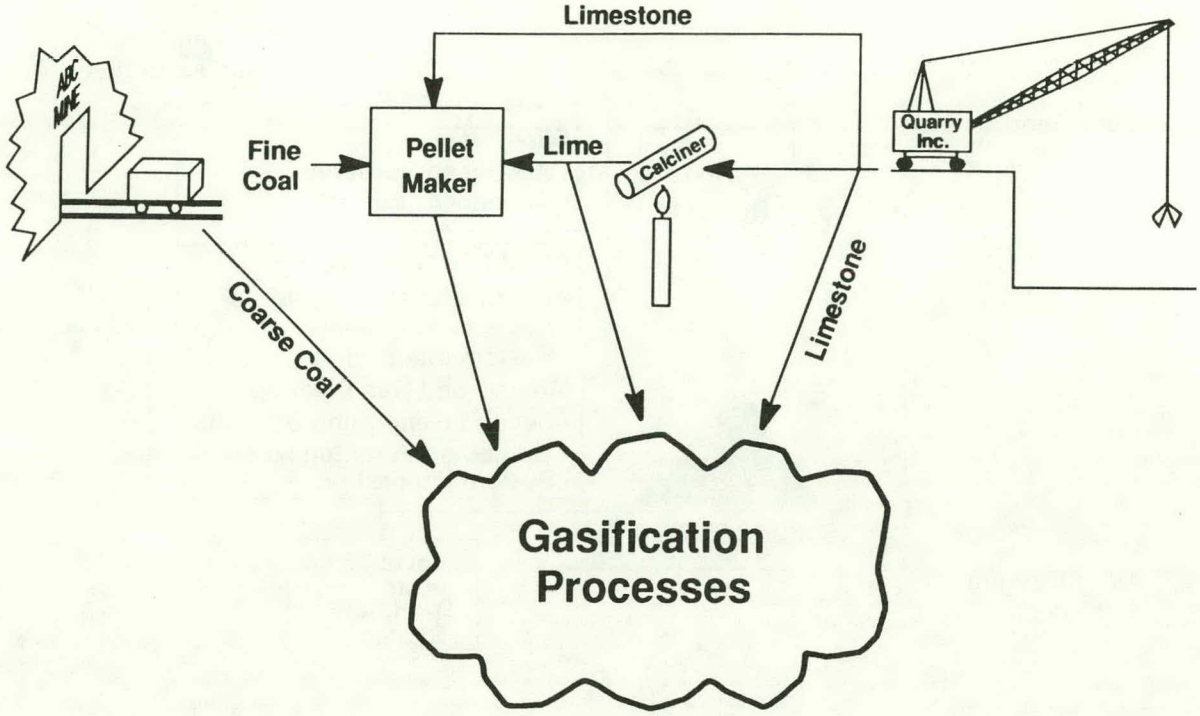

I87-1251-E BE8

Fixed-Bed Gasification Testing Summary

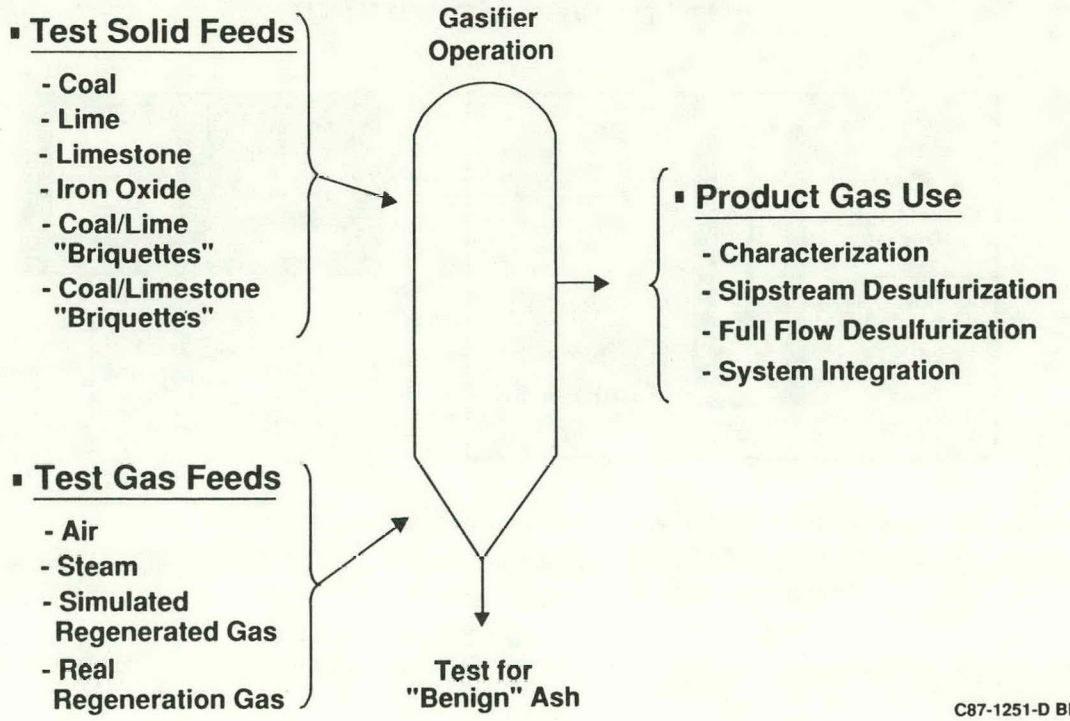

C87-1251-D BE8

Summary of Gasification Island System Support Testing

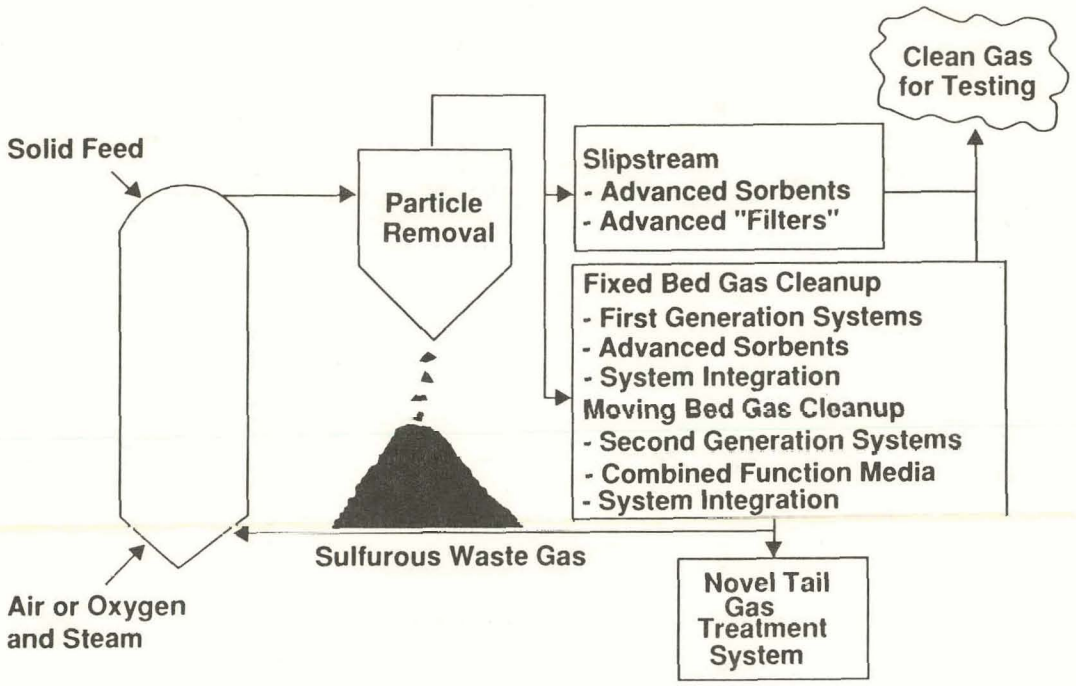

C87-1251-C BE8

Gasification Island and Gas Turbine System for Power Generation

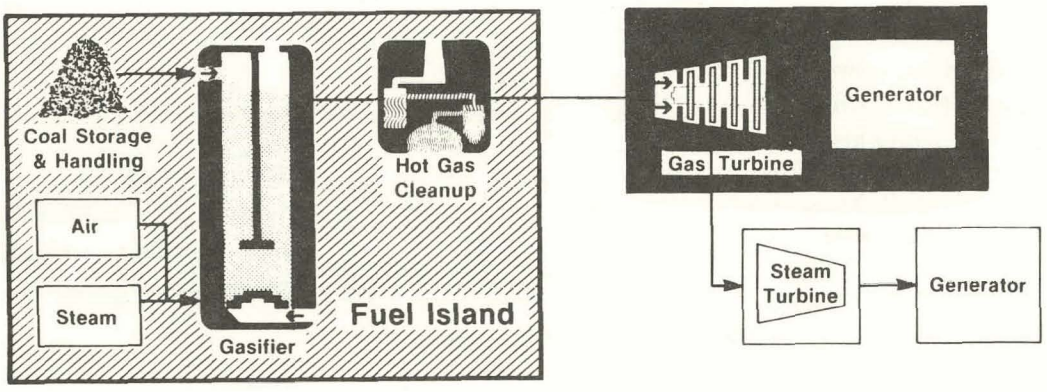

Size - > 50 MWe →
Cost - $800 to $950 per kW
Efficiency - 35 to 44 percent
Heat rate - 9,800 to 7,800 Btu per kW-hr

86-398-D D4

Why Gasification Island?

- A very simple/low cost system
  - — Minimal hardware
  - — Factory built/rail shippable components
  - — Standardized design
    - Minimizes engineering cost on repeat orders
- Flexible
  - — Applies to all coal ranks
  - — Total or minimal integration with rest of system
    - Retrofit applications
- Superior environmental performance
  - — Potentially a dry process
- Mechanisms to increase exports
  - — Equipment & coal
- Provides utilities with a new technological path
  - — High efficiency/low capital cost systems
  - — Ideal for 50-100 MW capacity increments

METC 86-528-5 BE5

METC Advanced Hot Gas Clean-up System

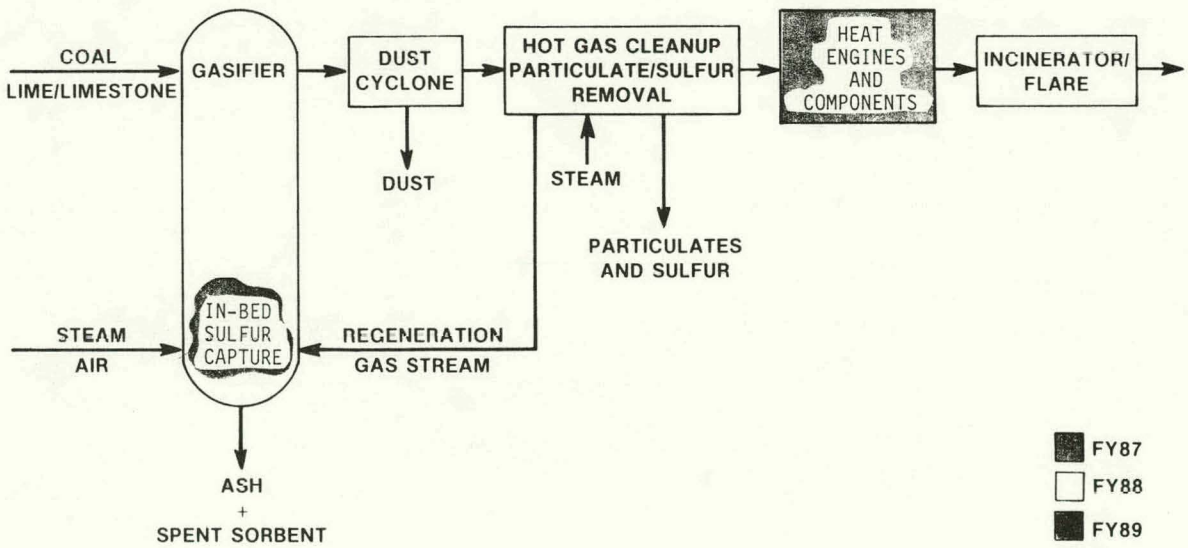

— NEAR ZERO WASTEWATER EFFLUENT
— NEARLY AUTOMATIC/HIGHLY FLEXIBLE OPERATIONAL CONTROL

METC 86-528-A BE5

Near Term Project Plans

FY 87

- Conduct in-bed sulfur capture testing
  - Lump limestone/coal mixture
  - Hydrated lime/coal briquette
  - Pulverized limestone/coal briquette
  - SO_2 recycle in all sorbent tests
- Design full flow hot gas desulfurizer (FFHGD)
  - Zinc ferrite based

FY 88

- Procurement and installation of FFHGD

FY 89

- FFHGD testing

METC C87-1251-2 BE8

A MECHANISTIC STUDY OF THE ENERGETIC HETEROGENEITY OF COAL CHARS

1. CONTRACT NUMBER: DE-AC21-87MC23284

CONTRACTOR: BROWN UNIVERSITY
Division of Engineering
Chemical Engineering Program
Box D
Providence, Rhode Island 02912

CONTRACTOR PROJECT MANAGER: J.M. Calo

PRINCIPAL INVESTIGATOR: J.M. Calo

METC PROJECT MANAGER: H.-Y. L. Lai

CONTRACT PERIOD OF PERFORMANCE: April 1987 - April 1989

2. SCHEDULE/MILESTONES:

1987 Program Schedule

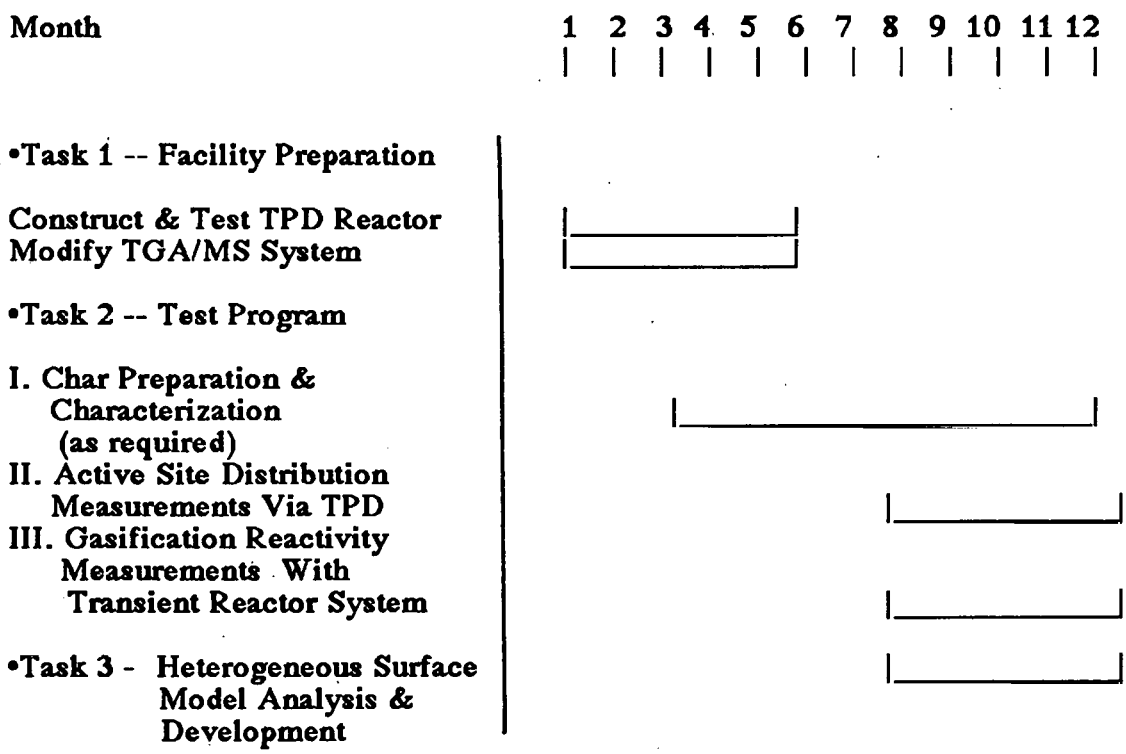

3. OBJECTIVES:

The objective of this contract is to examine the relationships between the energetic heterogeneity of coal char surfaces and gasification reactivity. The results of this study will help answer questions such as whether surface heterogeneity can be optimized to enhance char reactivity, thereby helping to make future coal gasifiers more efficient.

4. BACKGROUND STATEMENT:

All published steady-state rate forms for carbon gasification are based on the concept of a homogeneous surface (i.e., equivalent active centers or sites), in spite of the fact that many carbons and chars have been shown to possess a distinct energetic distribution of active sites. Recently, we have shown (Calo and Perkins 1987) that energetic heterogeneity of coal char surfaces can significantly affect gasification reactivity. Among the questions that naturally arise is whether coal char surfaces can somehow be optimized for enhanced reactivity due to this effect. This cannot be assessed currently since there is virtually no information regarding what form(s) distributions of surface heterogeneity may assume in coal chars, and how pretreatment conditions and subsequent surface evolution affect them.

5. PROJECT DESCRIPTION:

TPD/MS STUDIES

The project involves both experimental and analytical components. The basic experimental approach involves the application/adaptation of temperature-programmed desorption/mass spectrometry (TPD/MS) of surface species formed upon exposure of well-characterized coal char samples to adsorbent gases.

The TPD/MS technique involves the measurement of species in the gas phase resulting upon heating a solid adsorbent sample in a programmed fashion (usually linear). The resultant desorption spectra usually consist of one or more peaks. The shapes of these peaks and the positions of the peak maxima with respect to temperature are related in a fundamentral manner to the desorption process and to the energetics of the adsorbed precursor surface species.

In the current project, char surface heterogeneity will be determined primarily using oxygen chemisorption, followed by TPD. As a result of previous work in our laboratory (Suuberg et al. 1986, Wojtowicz et al. 1987), we have developed a fundamental understanding of the interaction of molecular oxygen with char surfaces. Oxygen adsorbs as atoms onto carbon surfaces, rapidly converting to surface oxides. TPD of these surface oxides results in the evolution of CO and CO_2, depending upon desorption conditions.

TPD spectra will be obtained under a variety of conditions. The primary variables of interest are total exposure and partial pressure of adsorbate, temperature, heating rate, and extent of burnoff. Underlying all these, of course, are the primary variables of char type and pyrolysis regimen. These spectra will be examined for the classical features of peak temperature dependence on surface coverage, multi-peaking, skewness, etc., in order to provide clues as to candidate active site distribution models. Based upon these observations, a model discrimination study will be conducted to determine the most appropriate models. One basic distinction that is hoped to be established, with respect to char type and treatment, is whether there are multiple functional group and/or site

combinations with different rates of desorption, or whether there is basically a single functional group and/or site combination whose rate of decomposition is a distributed function (e.g., linear, Gaussian, or Poissonian).

CHAR REACTIVITY/ACTIVE SITE CONCENTRATION VIA TRANSIENT KINETIC TECHNIQUES

As a result of previous work (Sy and Calo 1983; Calo et al. 1985), we have developed a transient kinetic technique to measure the reactivity of chars and to decouple the intrinsic rate constants and the effective active site concentration (see Sy and Calo 1983 for details). Therefore, the resultant multiparameter fit of the transient CO_2 gasification data, in terms of an appropriate HSM (to be determined in the current work), yields directly C_t, the effective active site concentration under actual gasification conditions. This latter value is then available for direct comparison to the corresponding value found via the TPD measurements. In this manner, the fraction of the active site distribution, as determined by low temperature O_2 chemisorption/TPD, actually involved during gasification can be determined. This fraction and its behavior are currently completely unknown.

The potential of this approach is quite significant. If, for example, the active site distributions determined by TPD are found to correlate gasification reactivity well, and, as suspected, the pre-exponential factor of the gasification rate constant is found to be relatively constant with respect to char type, then it will be possible to predict gasification reactivity *a priori* from simple TPD measurements only.

DEVELOPMENT OF HETEROGENEOUS SURFACE MODEL(S) [HSM(s)]

The general development of HSMs requires consideration of the sensitivity of observed gasification rates to intrinsic kinetic mechanisms and active site distributions. Even if the oxygen-exchange mechanism for CO_2 gasification is found to be applicable to the data for all the chars under the conditions of the present work (see section 6. RESULTS/ ACCOMPLISHMENTS below) the assumption of uniform surface heterogeneity, which results in Eq. (1), may not. In any case, the general form of the HSM is independent of these restrictions. Therefore, based on the results of the experimental portion of the proposed work, it may be necessary to investigate other intrinsic kinetic mechanisms, and/or, more probably, different active site distributions.

6. RESULTS/ACCOMPLISHMENTS:

A HSM has been developed for CO_2 gasification, based upon the oxygen-exchange mechanism and an assumed linear energetic distribution of active sites. Basically, surface heterogeneity is taken into account by dividing the surface into a number of individually uniform, normalized elements *ds*, describing the surface coverage on these locally homogeneous surface elements in accordance with the kinetic mechanism, and then averaging the reactivity over the entire surface upon assuming an active site distribution. The result of this procedure for the oxygen-exchange mechanism anfd a linear energetic distribution of active sites is:

$$W = (\Omega/\delta)\sqrt{\xi}\tan^{-1}[\sqrt{\xi}(1 - e^{-\delta})/(\xi e^{-\delta} + 1)] \qquad (1)$$

where: W = surface-averaged, specific gasification rate; $\xi = a_{12}P_{CO2}/[1+a_{-12}P_{CO}]$;

$a_{12}=k_1^o/k_2^o$; $a_{-12}=k_{-1}^o/k_2^o$; $k_i=k_i^o\exp[-\delta s]$, where the k_i are the rate constants for the oxygen-exchange model (i.e., k_1, k_{-1}, and k_2), and $E_i=E_i^o \pm \delta RTs$ (+ for adsorption and - for desorption steps) are the corresponding activation energies; and $\Omega=k_2^o C_t$.

It can be shown that this expression reduces to all of the steady-state CO_2 gasification kinetics rate forms that have appeared in the literature, even with the arbitrarily imposed restrictions of the oxygen-exchange mechanism and uniform active site distribution. For example, for the case of $\delta \rightarrow 0$:

$$\lim_{\delta \rightarrow 0} W = \Omega a_{12} P_{co2} / [1 + a_{-12} P_{co} + a_{12} P_{co2}] \qquad (2)$$

which is the most frequently applied rate form in the literature for the Boudouard reaction, especially at near-atmospheric pressures. Therefore, for small enough δ (i.e., a homogeneous surface) this expression applies for all values of ξ.

Sample plots of Eq. (1) are presented in Figure 1a with δ as a parameter.

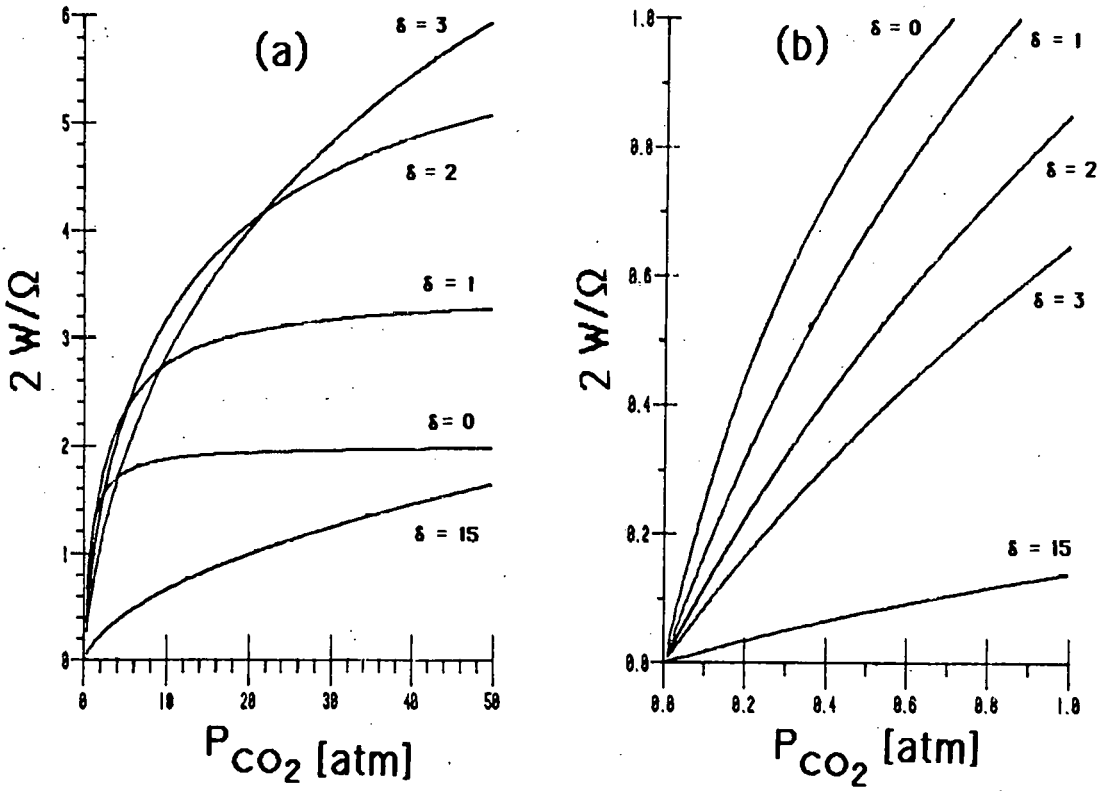

Figure 1. Plots of Eq. (1) showing the variation of W with P_{co2} with δ as a parameter. The values of the model constants are P_{co}=0.2 atm; a_{12}=2.0 atm^{-1}; and a_{-12}=2.0 atm^{-1}. Figure 1b is a magnified view of the lower lefthand corner of Figure 1a, showing the behavior of W as a function of P_{co2}<1 atm.

As can be seen, increasing surface heterogeneity (i.e., δ) initially enhances, and ultimately inhibits the specific gasification rate. This is attributable to the fact that the HSM actually decreases the inhibition effect of CO_2 relative to that for a homogeneous surface. It can be easily shown that W exhibits a maximum for $\delta\varepsilon[0,\infty]$ only for $\xi\geq 1$, which occurs at increasingly larger values of δ as ξ increases above unity. The parameter δ serves as a kind of "scale factor" on W, enhancing it when when $\xi>1$ and $\delta<\delta_{max}$, and diminishing it for $\xi\leq 1$, and for $\delta>\delta_{max}$ when $\xi>1$. In Figure 1b, which is a magnification of the lower lefthand corner of Figure 1a, it is shown that increasing δ monotonically inhibits the gasification rate for $\xi<1$ (e.g., for low P_{CO2}).

It is also worth noting that the curves presented in Figure 1 are all qualitatively similar, and, therefore, it is not surprising that heterogeneous behavior can easily be mistaken for homogeneous behavior. The degree of surface heterogeneity of a char can be assessed only via measurements of specific gasification rates relative to some reference, nearly homogeneous material, and/or via separate active site energy distribution measurements. Indeed, surface heterogeneity is quite probably primarily responsible for the relatively large variations in rate parameter and activation energy values, as well as various alternative mechanistic interpretations of rate data that have been reported in the literature for the Boudouard reaction.

7. FUTURE WORK:

Since this is a new project, the experimental effort is not yet fully underway. A search for a postdoctoral research associate to "spearhead" the experimental work is currently ongoing, and it is expected that the successful candidate will begin work on the project this summer. The most immediate objective is to construct and develop the TPD/MS apparatus and begin the corresponding studies.

8. REFERENCES:

Calo, J.M. and M.T. Perkins, "A Heterogeneous Surface Model for the Steady-State Kinetics of the Boudouard Reaction," *Carbon* **77**, 322 (1987).

Calo, J.M., R. Ganapathi, and S.E. Ellison, "Transient Kinetic Studies of Char-Gas Reactions: Steam Gasification," *ACS Div. Fuel Chem. Prepr.* **30**, 294 (1985).

Suuberg, E.M., M. Wojtowicz, and J.M. Calo, "Oxygen Chemisorption as a Tool for Characterizing 'Young' Chars,", *ACS Div. Fuel Chem. Prepr.* **31**, 186 (1986).

Sy, O. and J.M. Calo, "Transient Kinetic Studies of Char-Gas Reactions," *ACS Div. Fuel Chem. Prepr.* **28**, 6 (1983).

Wojtowicz, M., J.M. Calo, W. Lilly and E.M. Suuberg, "Low Temperature Reactivity of Chars Towards Oxygen," to be presented at the 18th Biennial Conference on Carbon, Worcester, MA, July 19-24, 1987.

FUNDAMENTAL FLUIDIZATION RESEARCH PROGRAM AT MORGANTOWN ENERGY TECHNOLOGY CENTER

Joseph S. Mei
Thomas W. Keech
Thomas J. O'Brien
Morgantown Energy Technology Center

ABSTRACT

The Morgantown Energy Technology Center, Office of Fossil Energy, U.S. Department of Energy, is conducting extensive fluidization research in support of various Fossil Energy Programs. Despite the widespread application of fluidized-bed reactors, the basic understanding of the fluidization phenomena is imprecise and based on a "guess and try" approach. The METC fluidization research program was initiated in early 1986 with the objectives of providing in-depth, validated data and developing a comprehensive predictive capability. These will increase the understanding of fluidization processes and provide a sound basis for the design of fluidized-bed reactors for fossil energy applications. The fluidization research program is focused on the specific fluidized-bed technology needs identified in the Advanced Coal Technology Programs for the three major technology areas, coal combustion, coal gasification, and oil shale retorting. The initial program implementation will focus on the test facility development, novel instrumentation development, along with modification of existing models. The salient design features of the test facilities, which include a 1-foot diameter atmospheric fluidized-bed cold model and a 2-foot diameter pressurized fluidized-bed warm model, are described. The initial experiments to be conducted in the 1-foot unit to characterize the flow regimes and their transitions are discused. Several novel instrumentation developments, which will provide better techniques to measure local bed voidage and solid circulation patterns, are presented. Extensions of comprehensive mechanistic fluidized-bed code are also described. These include implementation of an improved gas/solid drag law, a realistic granular phase stress tensor, and the ability to describe a particle size distribution. This code has now been used to simulate many fluidization phenomena, most recently, particle segregation.

OBJECTIVE

- PROVIDE IN-DEPTH, VALIDATED DATA ON FLUIDIZATION PHENOMENA
- DEVELOP A COMPREHENSIVE PREDICTIVE CAPABILITY IN TERMS OF NUMERICAL MODELS AND ENGINEERING CORRELATIONS

BACKGROUND

- BASIC UNDERSTANDING OF FLUIDIZATION PHENOMENA REMAINS IMPRECISE AND FAR FROM COMPLETE
- METC FLUIDIZATION RESEARCH PROGRAM BASED ON IDENTIFIED NEEDS FOR THE THREE MAJOR TECHNOLOGIES: COAL COMBUSTION, COAL GASIFICATION, AND OIL SHALE RETORTING

FIGURE 1. OBJECTIVES AND BACKGROUND

Despite the widespread application of fluidized-bed reactors, the basic understanding of the fluidization phenomena is imprecise and based on a "guess and try" approach. The METC fluidization research program was initiated in early 1986 with the objectives of providing in-depth, validated data and developing a comprehensive predictive capability. The fluidization research program is focused on the specific fluidized-bed technology needs identified for coal combustion, coal gasification, and oil shale retorting.

****
* EXPERIMENTATION *
****

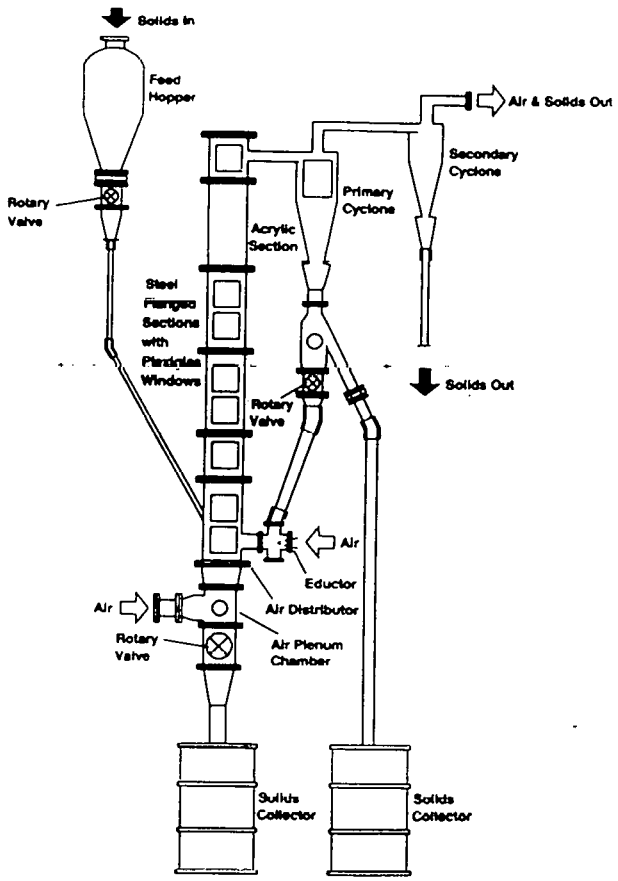

FIGURE 2. 30 CM DIAMETER ATMOSPHERIC FLUIDIZED BED COLD MODEL

The atmospheric pressure, ambient temperature, 30 cm diameter unit will be initially used to conduct the initial broad range of experiments for flow regime characterization. The cold unit consists of five flanged sections, four 1.2 m long sections and one 0.6 m long section. Three of the 1.2 m long sections are carbon steel with transparent plexiglas windows. The other 1.2 m long section is transparent acrylic plastic. Instrumentation ports are located vertically 10 cm apart. Entrained particles are captured by a primary and secondary cyclones. The particles from the primary cyclone can be recycled to the bed or removed from the fluidized-bed system. The cold unit is capable of operating at a superficial velocity up to 7 m/sec and is equipped with continuous solids feed/withdrawal system. This cold unit is currently under shakedown.

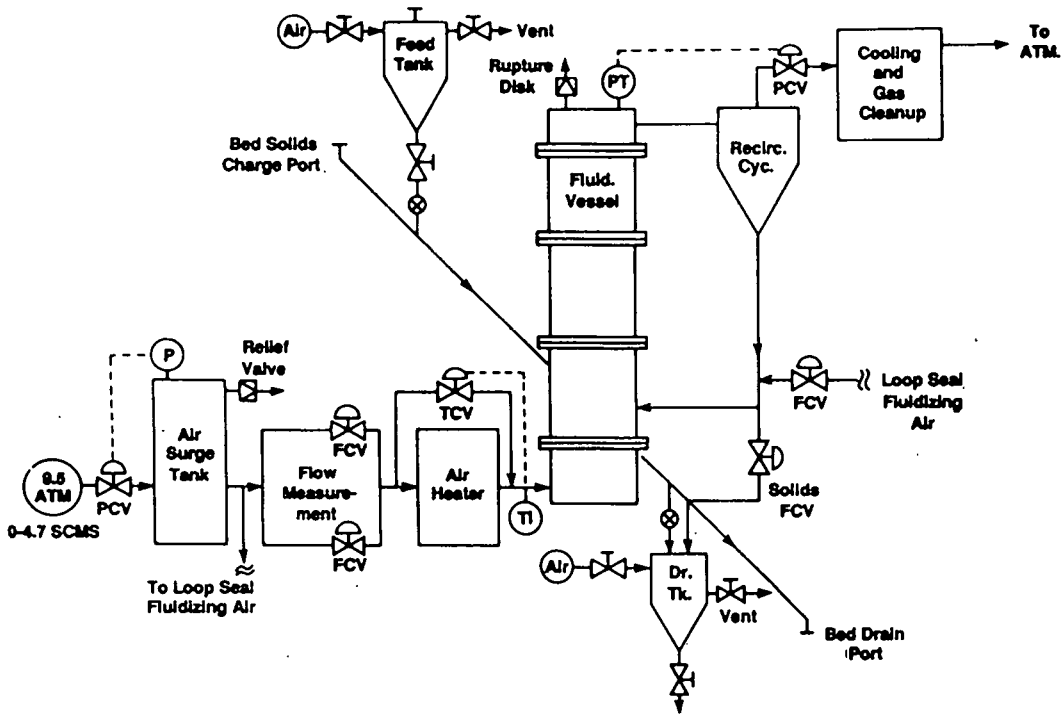

FIGURE 3. SIMPLIFIED PROCESS FLOW DIAGRAM FOR THE 60 CM DIAMETER PRESSURIZED FLUIDIZED BED WARM UNIT

The 60 cm diameter pressurized fluidized-bed warm unit is constructed from carbon steel and has four interchangeable 2.4 m long sections, a 0.9 m long top section, and 0.9 m long bottom section. Instrumentation ports and sight glasses are vertically located on each section. This unit is equipped with a batchwise continuous solids feed and a continuous withdrawal systems. Bed materials are fed into the fluidized-bed from a feed hopper. Air and entrained particles leaves the main vessel and enters a gravity settler, then enters the primary and secondary cyclones, and finally air exits through a fabric filter dust collection system. This pressurized unit is capable of operating at 8 atmosphere, 645 K, and at superficial velocity up to 6 m/sec. This warm unit will be initially used to determine the effects of gas density and viscosity on flow regimes and their transitions. Later, the unit will be used to provide experimental data for gas/solid mixing and circulation patterns, and heat and mass transfer. This 60 cm diameter pressurized unit is currently being designed.

Design Parameter	Parameter Value											
Bed Material Shape	Spherical				Cylindrical				Irregular			
Bed Material Density	Nylon 1140 kg/m^3		Glass 2500 kg/m^3		Light		Heavy		Light		Heavy	
Bed Material Size	3180 μM	760 μM	3180 μM	4760 μM	SM	LG	SM	LG	SM	LG	SM	LG
Static Bed Height	Low (1.5), High (3.5), and Height Providing Constant Bed Weight Regardless of Bed Particle Characteristics											
Pressure (psig)	20	60	20	60	20	60	20	60	20	60	20	60
Temperature (°F)	300	70	650	70	High	70	High	70	High	70	High	70

INDEPENDENT VARIABLES	DEPENDENT VARIABLES	MEASURED VARIABLES
Particle Density	Min Fluidization Velocity	Bed Pressure Drop
Particle Size	Min Bubbling Velocity	Bed Voidage
Particle Shape	Transition Velocity between	Bed Expansion
Static Bed Height	* Bubbling/Slugging	
Bed Pressure	* Slugging/Turbulent	
Bed Temperature	* Turbulent/Fast fluidization	

FIGURE 4. TENTATIVE EXPERIMENTAL TEST MATRIX FOR FLOW REGIMES CHARACTERIZATION

A full factorial statistical design experiment will be conducted in both the 30 cm diameter atmospheric fluidized-bed cold model and the 60 cm diameter pressurized fluidized-bed warm model to characterize flow regimes as well as their transitions. For the tests to be conducted in the 30 cm diameter cold unit, two particles densities and two monoparticle sizes will be investigated for each different shape. For each combination, test will be performed for three static bed heights. The test series using the 60 cm diameter pressurized warm unit, however, will include two pressures, three bed temperatures, three particle shapes, two particle densities, two monoparticle sizes, and three static bed heights.

****
*INSTRUMENTATION *
****

- **Multi-electrode capacitor array for bed density display**
  - 3-DIMENSIONAL
  - 16 ELECTRODES
  - 100 IMAGE FRAMES PER SECOND
- **Radio frequency transmitter tracking for the investigations of solids movement**
  - SMALL TRANSMITTER
  - TEN POSITION-DETERMINING RECEIVERS
  - 3-COORDINATE POSITION TRACKING
  - 100 POSITION MEASUREMENTS PER SECOND
- **Particle impact probe for particle collision force/VELOCITY measurement**
  - **Fast response**
  - **High sensitivity**

FIGURE 5. INSTRUMENTATION CONCEPTS FOR FLUIDIZATION RESEARCH

The objective of the instrumentation development effort is to provide the fluidization research program with unique sensors, instrumentation systems, and measuring techniques required to quantify those parameters which characterize the flow regimes, the gas and solid interactions and circulation patternsm and the heat transfer mechanisms. Initial focus of instrumentation development will be aimed at understanding the fundamental mechanisms of fluidization processes. Three instrumentation concepts have been established to provide support for the integrated tasks of the fluidization program. These three instrumentation concepts together with their salient features are described in this figure.

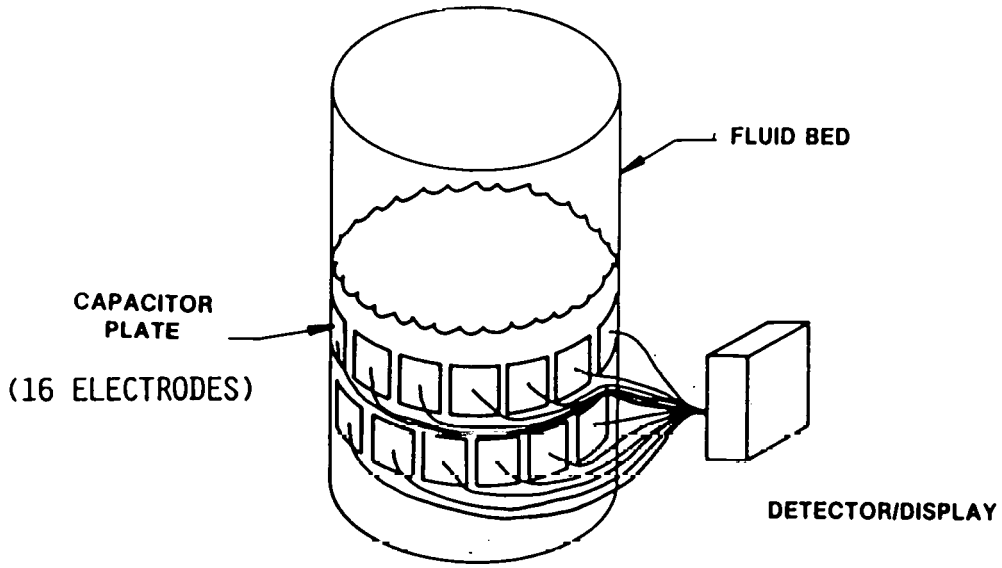

FIGURE 6. MULTI-ELECTRODE CAPACITANCE IMAGING SYSTEM

The multi-electrode capacitance density imaging system provides dynamic 3-dimensional fluidized bed voidage images by means of the transformation of capacitance measurements across the bed into density maps at high image fram rates.

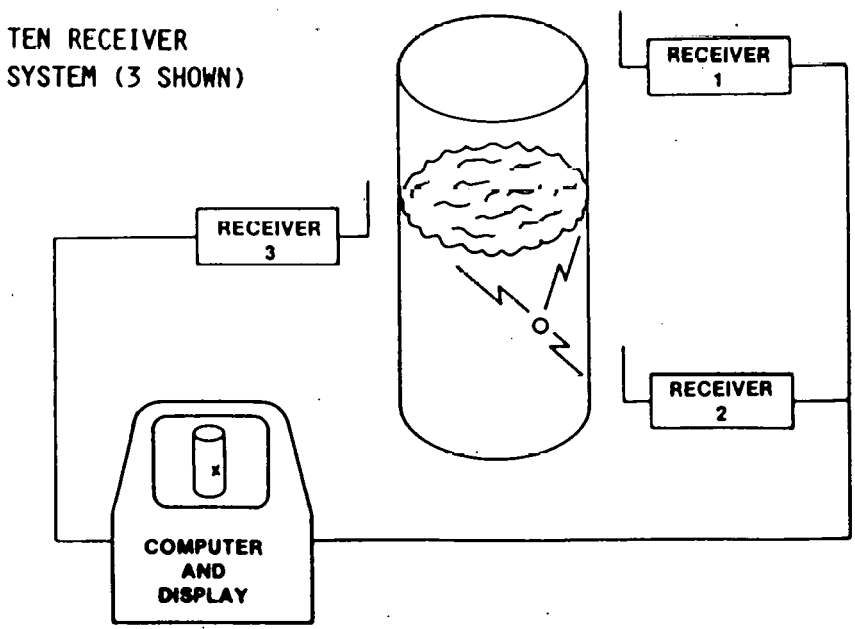

FIGURE 7. RADIO TRANSMITTER/RECEIVERS PARTICLE TRACKING SYSTEM

The radio transmitter/receivers particle tracking system estimates 3-coordinate positions of a bed-particle-sized transmitter from differences of arrival (TDOA) of the transmitted wave to ten receivers placed around the fluidized-bed and operates at 100 position computations/second.

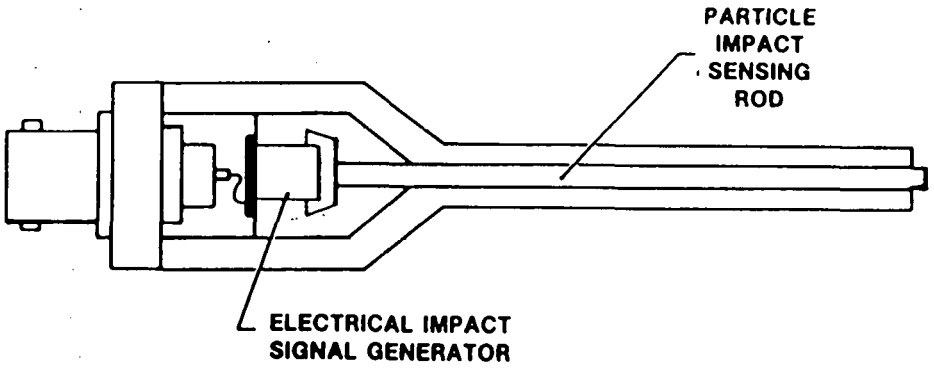

FIGURE 8. PARTICLE IMPACT PROBE

The particle impact probe is designed to experimentally determine particle forces/velocities in the fluidized bed. A particle impact at the probe tip will deform the sensing elemtnt and the electrical transducer (attached to the sensing element) will convert the deformation to a voltage proportional to the kinetic energy of the particle.

****
* MODELING *
****

Computer Simulation Conditions:

Fluidizing Medium:	Air
Particle Shape:	Glass Beads
Particle Diameter:	0.046 cm
Particle Density:	2.48 gm/cc
Initial Void Fraction:	0.42
Jet Velocity:	36.4 cm/sec
Grid Velocity:	18.2 cm/sec

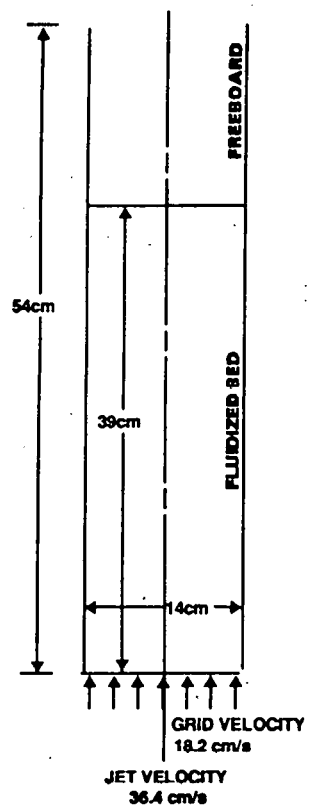

FIGURE 9. COMPUTER SIMULATION CONDITIONS FOR THE DYNAMICS OF A BUBBLE IN A FLUIDIZED BED

Bubbles in a fluidized bed reactor were simulated using a multiparticle computer code which was developed here at METC. This figure presented the conditions assumed for the simulation of bubbles as well as the granular phase.

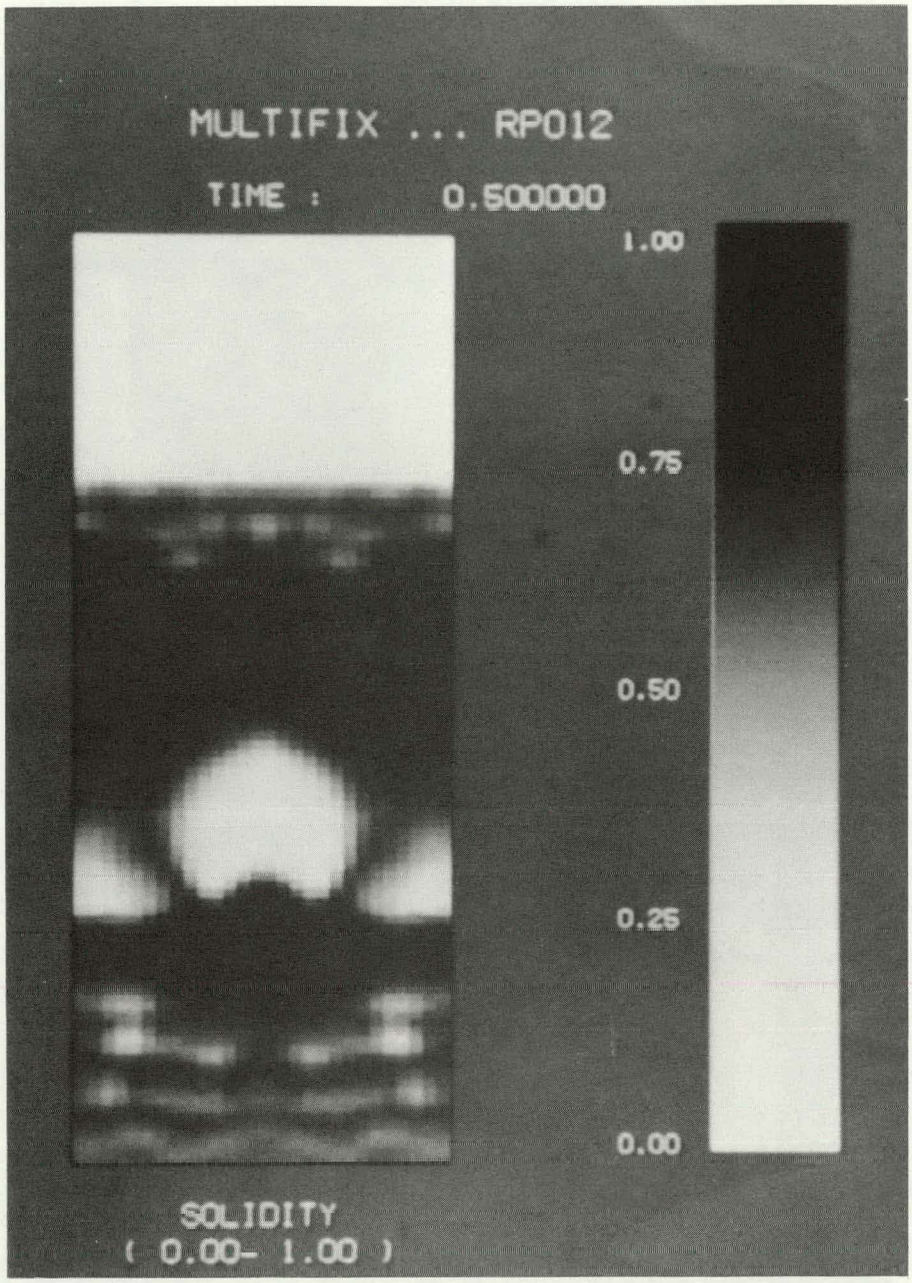

FIGURE 10. GRANULAR CONCENTRATION ABOUT A BUBBLE

The light/dark scales proportional to the concentration of the granular material(solidity). The white regions(freeboard and bubble interior) have a solidity of ≈ 0.0; the darkest regions have a solidity of ≈ 0.8, typical of bed at minimum fluidization.

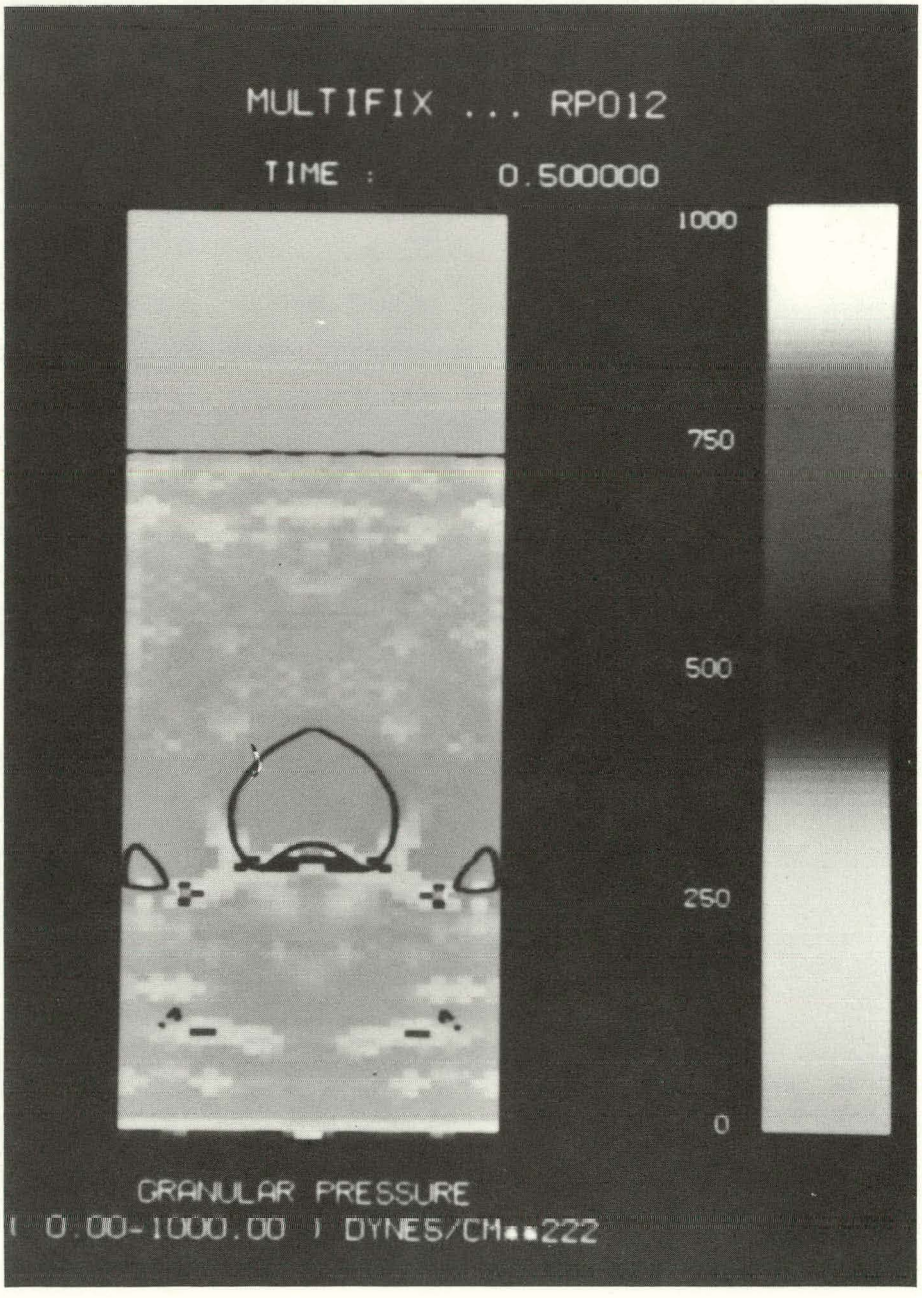

FIGURE 11 A. GRANULAR PRESSURE IN A BUBBLING FLUIDIZED BED

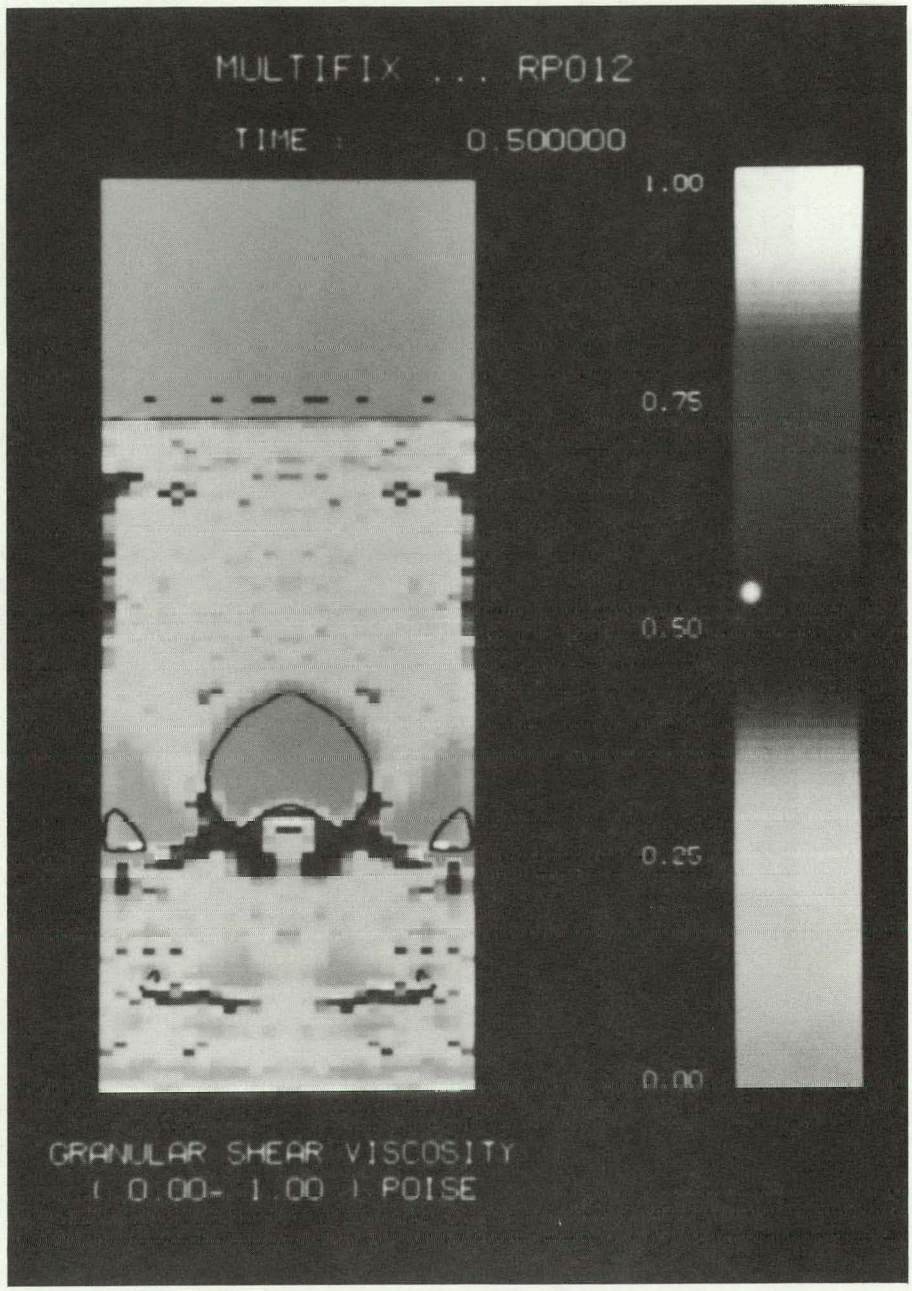

FIGURE 11 B. GRANULAR SHEAR VISCOSITY IN A BUBBLING FLUIDIZED BED

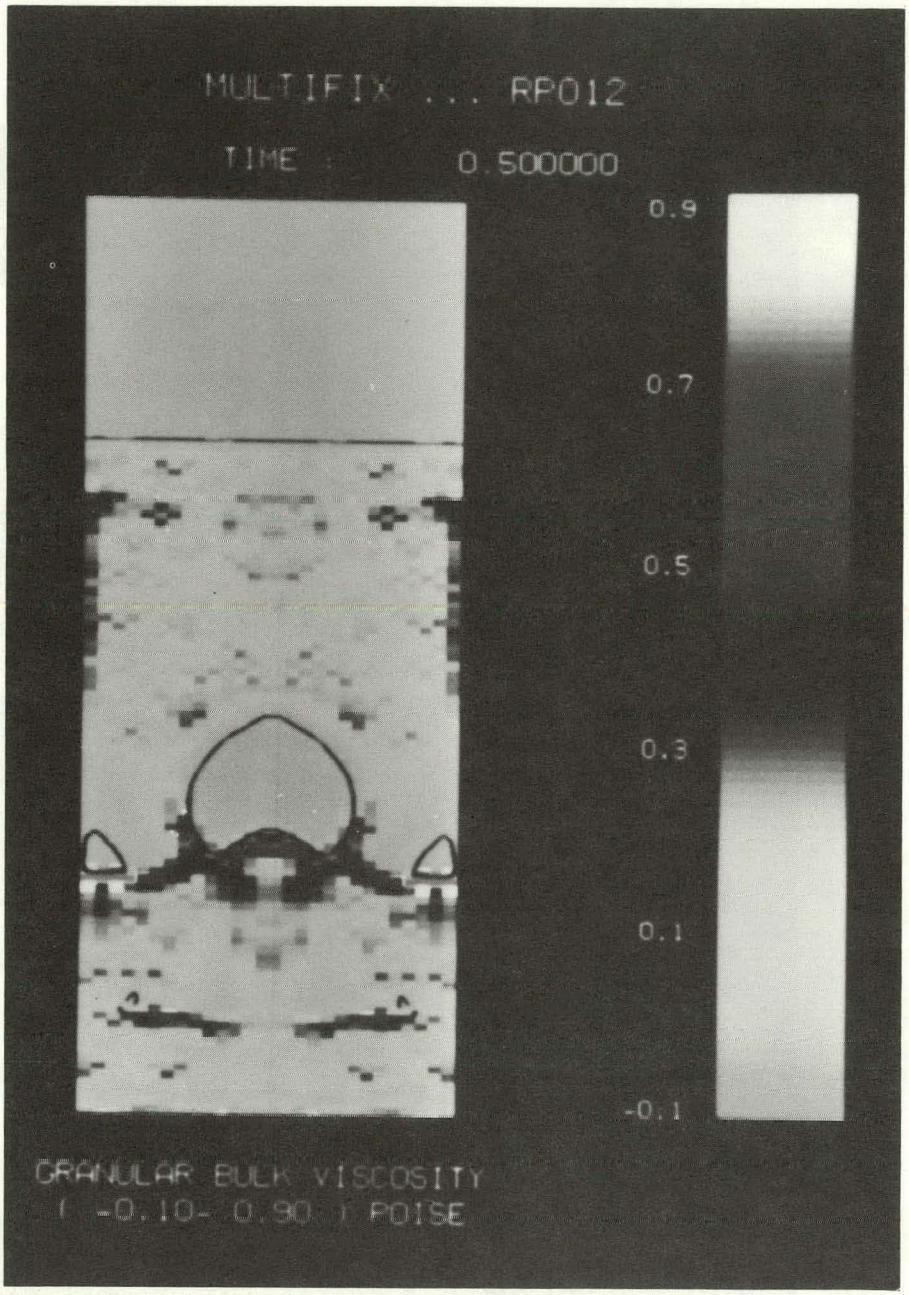

FIGURE 11 C. GRANULAR BULK VISCOSITY IN A BUBBLING FLUIDIZED BED

Although particle/particle interactions are seldom considered in fluidized beds, they must be included in order to simulate bubble dynamics. These interactions give rise to a stress in the granular phase. These figures, with the same bubble outlined, show how the stress in the granular phase (granular pressure, shear viscosity, and bulk viscosity) is distributed during the passage of a bubble.

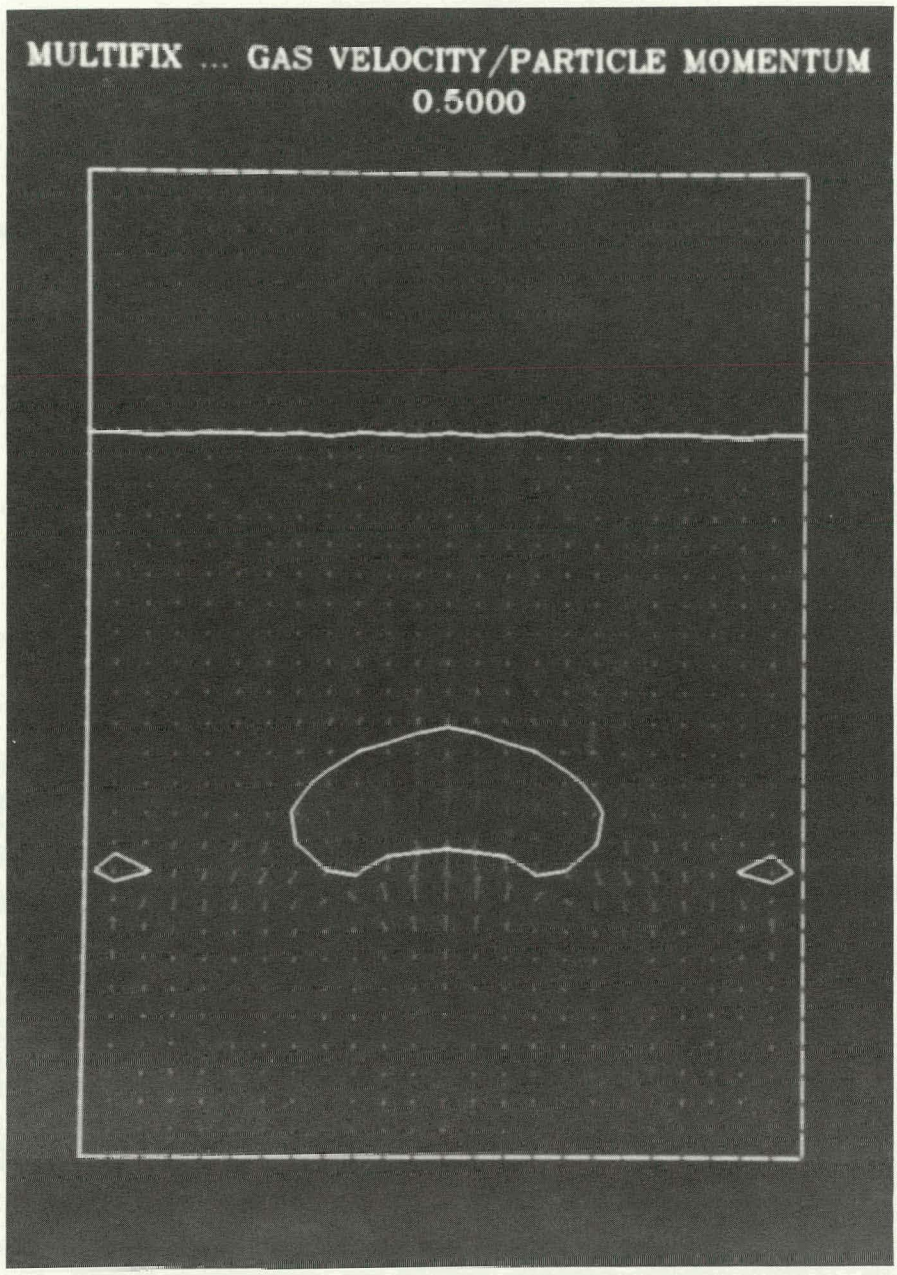

FIGURE 12. GAS/SOLID VELOCITIES IN A BUBBLING FLUIDIZED BED

The red(green) arrows show the direction and magnitude of the velocity of the gas(granular) phase. Gas bipassing the bed, through the bubble is easily seen as the long, red arrows inside the bubble. The rapid granular motion in the wake of the bubble shown by the long, green arrows below the bubble contour. This contour, drawn at a solidity of 0.8, outlines the dominate features of the more detailed solidity figure. Notices that the bubble has the characteristic spherical cap/wake form.

DEVELOPMENT OF A NOVEL NESTED-FIBER FILTER CONCEPT FOR HIGH-TEMPERATURE AND HIGH-PRESSURE PHYSICAL CLEANUP

1. CONTRACT NUMBER: DE-AC21-86MC23251

CONTRACTOR: Battelle Columbus Division
505 King Avenue
Columbus, Ohio 43201-2693
614/424-6424

CONTRACTOR PROJECT MANAGER: Mr. Robert D. Litt

PRINCIPAL INVESITGATOR: Mr. H. Nicholas Conkle

METC PROJECT MANAGER: Mr. Thomas P. Dorchak

PERIOD OF PERFORMANCE: October 1, 1986 to September 30, 1988

2. SCHEDULE/MILESTONES:

Design Alternatives Evaluation	Complete
Cold Model Testing	June 1987 to November 1987
Hot Model Testing	November 1987 to June 1988

3. OBJECTIVES:

The project objective is to develop a gas-filtration system capable of operating at high temperatures and pressure (HTHP) for use in IGCC and PFBC applications. Such systems will require efficient particulate removal at temperatures over 980 C (1800 F) and pressures of 10 to 30 atmospheres.

4. BACKGROUND STATEMENT:

The Nested Fiber Filter (NFF) system is based on the concept of a nest of needle-like fibers made from an alloy suited for the application. Filter action results from particle matter forming dendritic, or chain-like, particulate matter structures on the surface of the fibers as illustrated in Figure 1. The program will address the following three important experimental issues:

- How well does the fiber filter remove particulate matter in realistic environments?
- How difficult is the separation of particulate matter from fibers?
- What is the effect of temperature and pressure on operation?

Battelle developed the concept of using nested fibers for a high-temperature filter as part of an internal design study. Baseline experiments were conducted to determine the technical feasibility of the system. Particulate capture levels over 99.9 percent with 5 micron particles at 230 mm (9.3 in.) water pressure drop were achieved. A system for implementing the concept of nested fibers for use as a high-temperature filter was desired

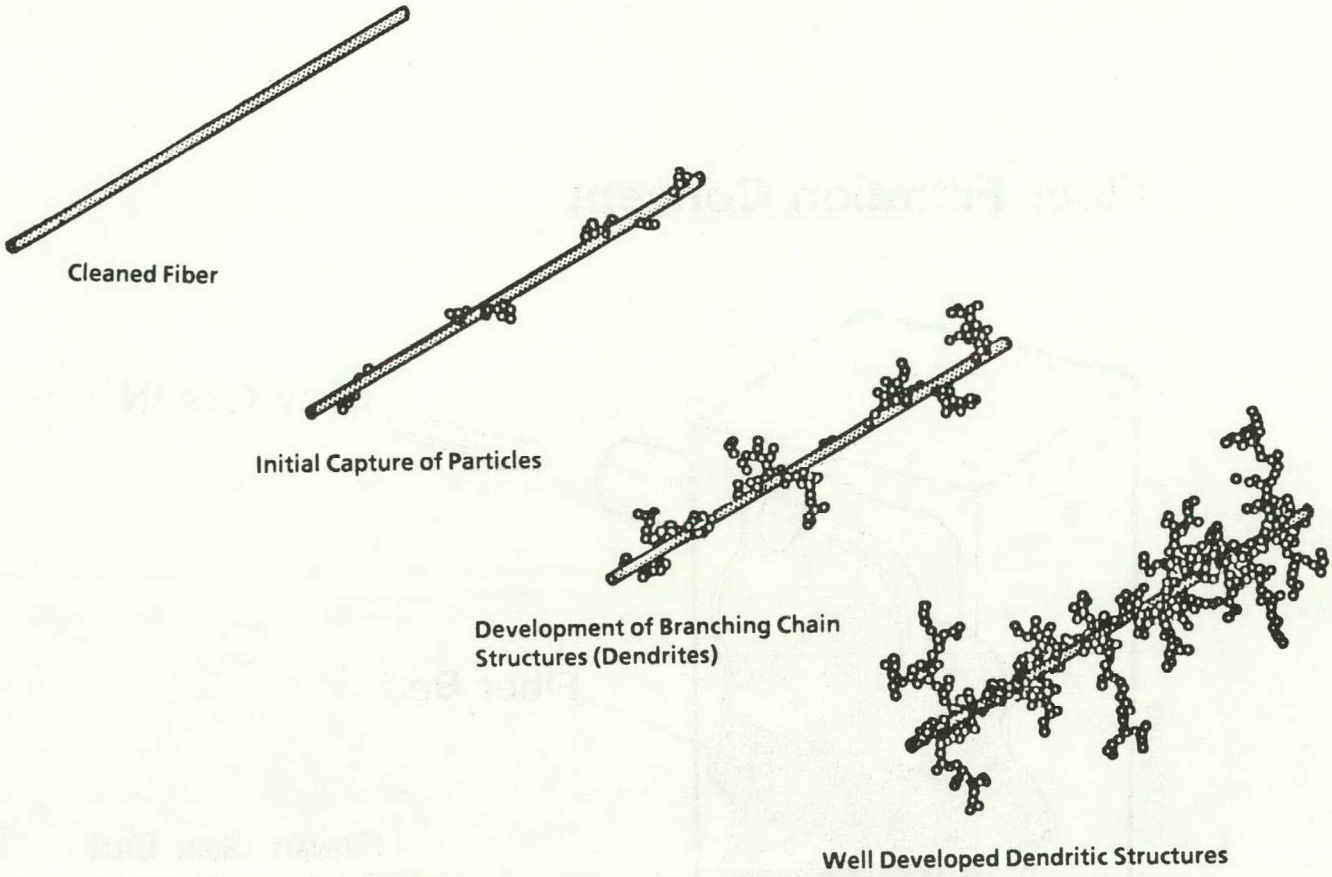

Figure 1. Formation and Growth of Dendrites on an Individual Fiber.

for integration with advanced power systems. This program is directed towards developing a system for implementing the nested-fiber filter concept into a workable system at HTHP. The general process concept is illustrated in Figure 2.

The major advantages of the NFF system include high throughput, high efficiency, low pressure drop, and compact equipment.

5. PROJECT DESCRIPTION:

Three tasks are planned to complete the Phase I Assessment effort. They provide a direct progression from prior work accomplished at Battelle through generating data on a complete bench-scale system. The three tasks are:

Task 1 - Design Alternatives
Task 2 - Cold Model
Task 3 - Hot Model.

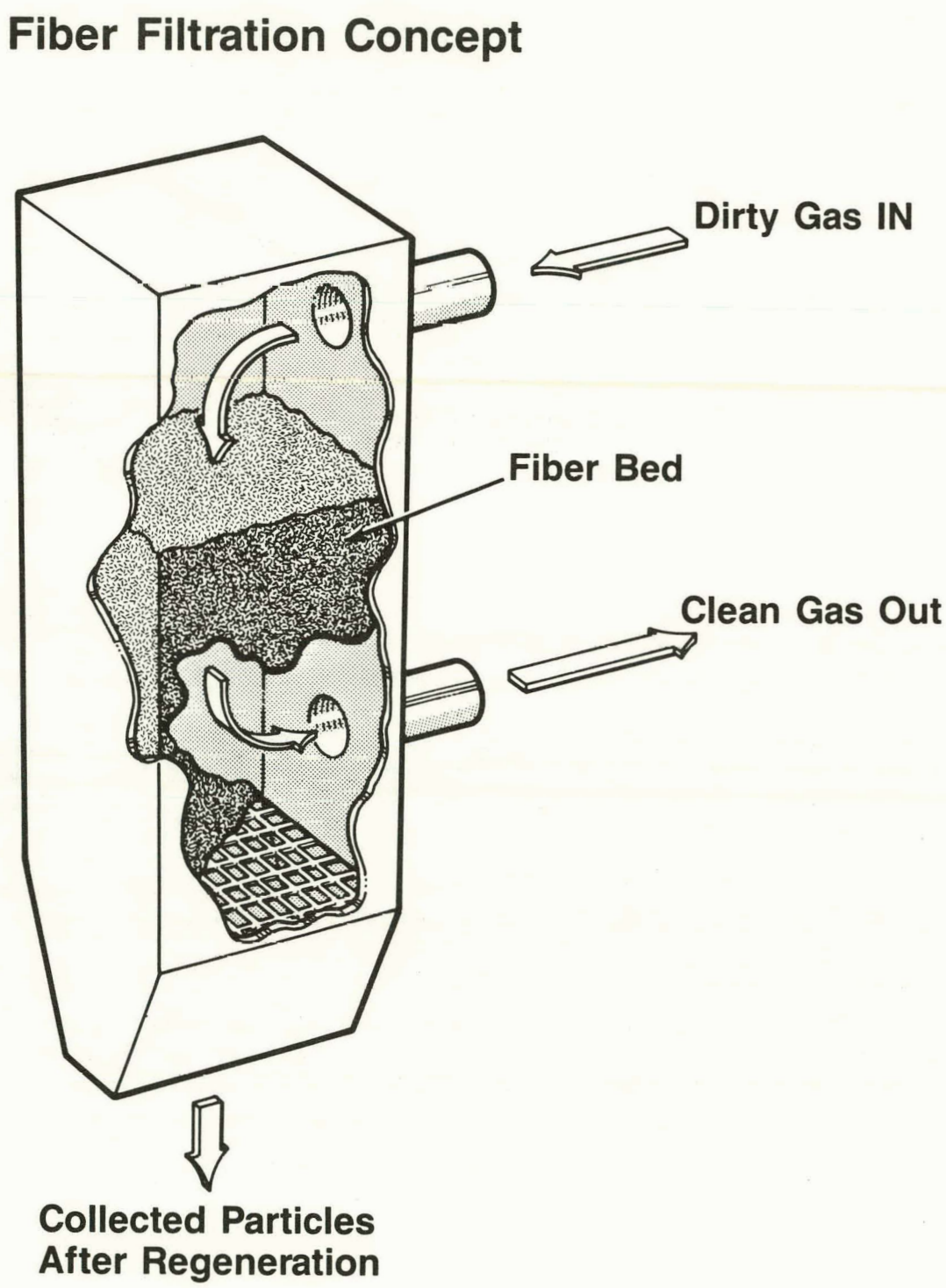

Figure 2. Fiber Filter Concept.

The first task, Design Alternatives (completed in February, 1987) provided a better mechanistic understanding of fiber filtration, explored how the mechanical functions within the NFF could be achieved, allowed selection of the best candidate system, and produced initial test plans for conducting the cold- and hot-model experiments.

The second and current task, Cold Model, involves design, construction and testing of a bench-scale, cold model NFF. Currently an atmospheric pressure module and a high-pressure test unit are under construction with shakedown and testing scheduled to commence in June, 1987.

The third task, Hot Model, will serve to verify that the high performance efficiencies achievable at ambient conditions can also be achieved at elevated temperatures and pressures. For this task, a high-temperature bench-scale test module will be constructed and evaluated.

6. RESULTS/ACCOMPLISHMENTS:

- Evaluated dendritic capture mechanisms and projected the performance under HTHP operating conditions.
- Generated and evaluated alternative design configurations for HTHP applications and selected the most promising configuration for experimental testing and evaluation.
- Designed a low-pressure test module and filter cleaning chamber, and a high-pressure test module capable of operating at elevated temperatures.
- Developed a detailed cold-model test plan.
- Initiated construction of the test modules and modification to an existing test facility.

7. FUTURE WORK:

After the Phase I program, an optional Phase II Mechanical Development phase may be authorized to explore more thoroughly the capabilities of NFF. Upon completion of the Assessment phase, and the Mechanical Development phase, if authorized, the process will be subjected to an Engineering Assessment in the final phase of this contract.

Application of the NFF to particulate control from conventional coal-fired boilers is also of interest.

THROWAWAY PROCESSES FOR TREATMENT OF REGENERATION TAIL GASES

1. CONTRACT NUMBER: DE-AC21-86MC23086

CONTRACTOR: Arthur D. Little, Inc.
Acorn Park
Cambridge, MA 02140
(617) 864-5770

CONTRACTOR PROJECT MANAGER: Lawrence R. Woodland

PRINCIPAL INVESTIGATORS: Dr. Itamar Bodek
Lawrence R. Woodland

METC PROJECT MANAGER: Thomas P. Dorchak

CONTRACT PERIOD OF PERFORMANCE: September 30, 1986 to May 29, 1988

2. SCHEDULE/MILESTONES:

1987 Program Schedule

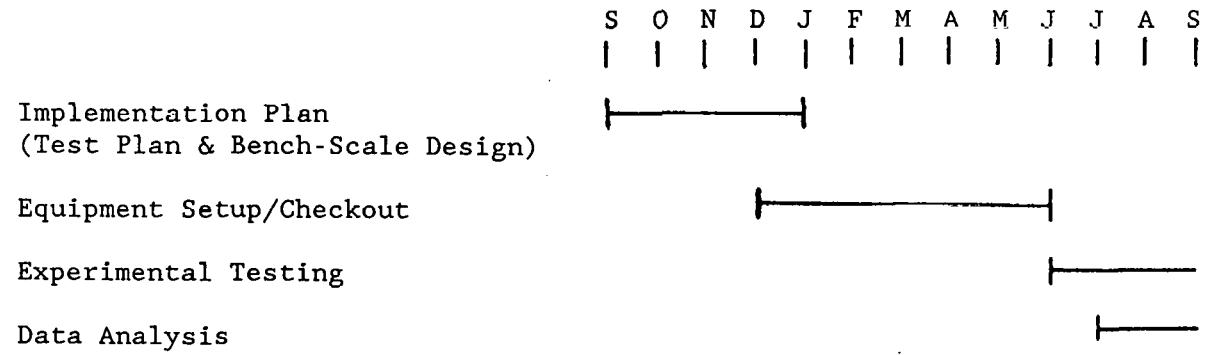

3. OBJECTIVES:

The goal of this program sponsored by the Morgantown Energy Technology Center (METC) is to evaluate processes for treating the regeneration tail gas from a high-temperature desulfurization process (zinc-ferrite process) used in coal gasification applications. METC has sponsored the development of an elemental sulfur recovery process which has proven to be technically practical, but appears economically unattractive. The primary objective of this test program is the demonstration on a bench-scale of an energy-efficient, non-recovery process that can treat this offgas stream, while producing environmentally acceptable waste products.

A second objective of this test program is to collect sufficient data to allow incorporation of the test results into a conceptual full-scale design for comparing the economics of the non-recovery processes with the recovery processes under development.

4. BACKGROUND STATEMENT:

There are a number of flue gas desulfurization (FGD) processes being used commercially for treatment of flue gas from pulverized coal-fired boilers that could be used for removal of sulfur dioxide from the desulfurization reactor regeneration tail gas. The more common of these commercial FGD systems are as follows:

Wet Scrubbing	"Dry" (Spray Dryer) Absorption
Lime	Sodium (Soda Ash or Nacholite)
Limestone	Lime
Soluble Alkali (Sodium Base)	Limestone
Dual-Alkali (Sodium/Lime)	

The wet scrubbing systems are usually higher in efficiency (and cost) than are the newer spray dryer absorber systems in which a water slurry of alkali is injected into the flue gas and the dried sorbent product collected in a baghouse. A simplified block flow diagram showing the relationship between the hot gas desulfurization system and the proposed FGD process tail gas cleanup system is presented below:

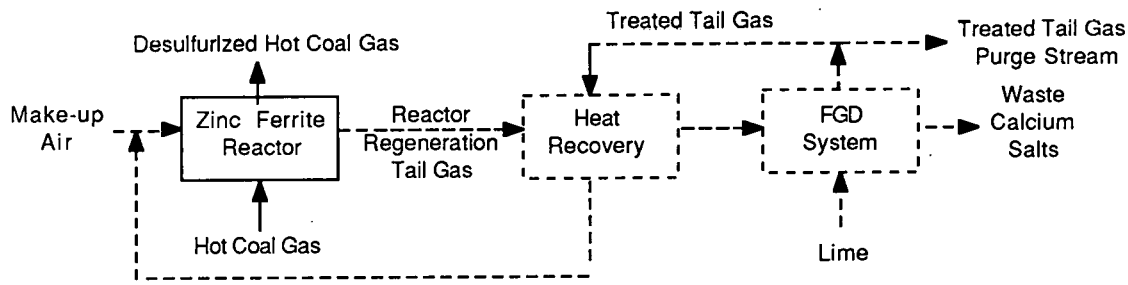

During the hot coal gas desulfurization cycle, the zinc-ferrite mixed oxide reacts with hydrogen sulfide in the gas stream to form mixed sulfides and water vapor. When the zinc ferrite bed in the reactor becomes saturated with sulfur, the bed is taken off-line and regenerated using makeup air (for oxygen) and recycled treated tail gas, consisting primarily of nitrogen and water vapor, as diluent.

A typical composition range of the regeneration tail gas which results from passage of the air/diluent mixture through the desulfurization reactor is as follows:

Nitrogen and/or steam	88.0 to 97.5 volume %
Sulfur Dioxide (SO_2)	2.5 to 12.0 volume %

Because of the large quantity of nitrogen and/or steam diluent required in the regeneration process to control temperature, there is a great incentive to recycle it back to the regeneration system after SO_2 removal. However, the SO_2 would have to be removed to sufficiently low levels, say 100 ppm, to avoid sulfation of the hot gas desulfurization sorbent in the regeneration step. Where possible, heat recovery from the hot regeneration tail gas should be practiced. In the above diagram recovered heat is shown being used to reheat the recycled treated tail gas.

5. PROJECT DESCRIPTION:

The two FGD process concepts which will be investigated in the bench-scale test program are the spray drying and dual-alkali processes. Although these two technologies have already been demonstrated on commercial and/or pilot plant scale for coal-fired generating stations, they are presently operated under much different conditions than required for this application. They are normally used for much lower sulfur dioxide concentrations; and in most cases, at lower temperatures and atmospheric pressure.

The spray drying process was selected for evaluation since it is potentially the least expensive of the FGD processes and SO_2 removal efficiencies of up to 90% have been achieved in commercial systems. The dual-alkali system was chosen as the wet FGD system to be tested since it can achieve very high SO_2 removal efficiency (over 96%) and does not experience the scrubber pluggage problems encountered with lime or limestone systems. In the dual-alkali system, a soluble alkali (sodium salt) solution is used for the sulfur dioxide absorption. The spent soluble alkali solution is then regenerated with lime, producing a waste calcium salt, and the sodium solution recycled to the absorber. For the dual-alkali system, only the SO_2 absorption step will be tested, since the regeneration step has been well characterized in commercial practice.

Each of the two (bench-scale) scrubbing systems will consist of two parts: (1) a synthetic tail gas system to supply a heated mixture of nitrogen and sulfur dioxide to the scrubbing system, and (2) the scrubbing system itself. Table 1 summarizes the test conditions that will be used with each of the two bench-scale scrubbing systems.

Table 1. Test Run Conditions for Bench-Scale Tail Gas Treatment

Type of Alkali	Alkali/SO_2 Ratio or Na^+ Concentration	Inlet SO_2 Concentration (%)	L/G or Contact Time	Pressure (psig)	Active Trays	Inlet Temp (^oF)
1.0 Dual Alkali			L/G			
Na_2SO_3	0.5 N	3,6,12	30,60,120	0.5	6	400
Na_2SO_3	0.49 N	3,6,12	30,60,120	0.5	6	400
NaOH	0.01 N					
Na_2SO_3	1.0 N	3,6,12	30,60,120	0.5	6	400
Na_2SO_3	0.5 N	3,6,12	30,60,120	0.5	4	400
Na_2SO_3	0.5 N	3,6,12	30,60,120	15	6	400
Na_2SO_3	0.5 N	3,6,12	30,60,120	15	4	400
2.0 Spray Dryer			Contact Time			
Lime	2.0:1	1.5	40 seconds	0.5	--	1000
Soda Ash	1.2:1	1.5	40 seconds	0.5	--	1000

A schematic of the dual-alkali bench-scale FGD system is shown in Figure 1.

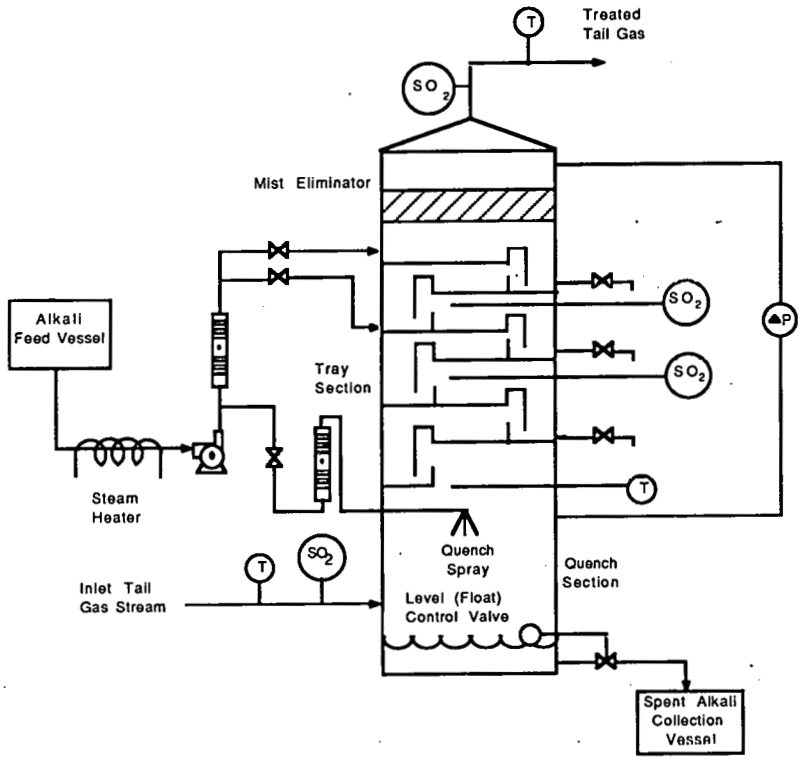

Figure 1. Schematic of Dual-Alkali FGD Absorber System

The bench-scale dual-alkali absorber system will be operated over the range of scrubbing liquor to gas ratios (L/G) and inlet gas concentrations listed in Table 1. The scrubbing efficiency of each individual tray (as well as overall system efficiency) will be measured by means of gas sampling ports located between each tray and the number of operating trays varied from four to six by changing the tray to which the scrubbing solution is introduced. The quench spray section of the absorber will be used primarily to cool the incoming gas stream, but its contribution to sulfur dioxide removal efficiency will also be determined.

A pilot plant spray dryer unit (as depicted in Figure 2) will be rented from a commercial spray dryer manufacturer for use in the bench-scale testing of this process.

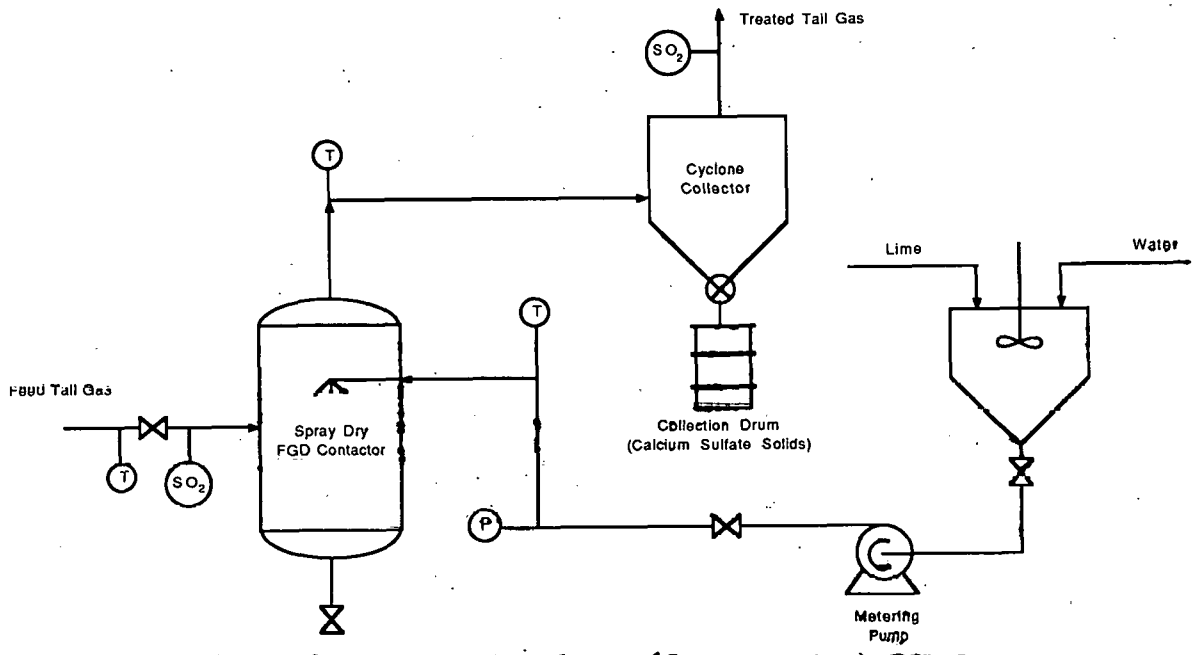

Figure 2. Schematic of Dry (Spray Drying) FGD System

6. RESULTS/ACCOMPLISHMENTS:

- o The Implementation Plan (Test Plan and Detail Design Plan) have been completed and accepted by METC.
- o The bench-scale synthetic tail gas supply and dual-alkali systems have been fabricated and installed and are ready for testing.

7. FUTURE WORK:

Bench-scale testing of the dual-alkali system will be initiated to investigate the parameters listed in Table 1. When testing of the dual-alkali system is completed (in early September 1987), the spray drying system will be installed and tested until the end of November 1987. Following completion of the data analysis for the two processes, estimated capital and operating costs will be prepared for comparison with sulfur recovery processes.

8. REFERENCES:

VanNess, R.P, L.R. Woodland and E.D. Gibson, Full-Scale Dual Alkali FGD Demonstration at Louisville Gas and Electric Company. EPA-600/7-83-039. August 1983.

SORBENT-BASED RECOVERY OF SULFUR FROM REGENERATION TAIL GASES

1. CONTRACT NUMBER: DE-AC21-86MC23260

CONTRACTOR: Research Triangle Institute
Research Triangle Park, NC 27709
(919) 541-6255

CONTRACTOR PROJECT MANAGER: Santosh K. Gangwal

PRINCIPAL INVESTIGATORS: Scott M. Harkins
Santosh K. Gangwal

METC PROJECT MANAGER: T. P. Dorchak

PERIOD OF PERFORMANCE: September 16, 1986 to September 15, 1988

2. SCHEDULE/MILESTONES

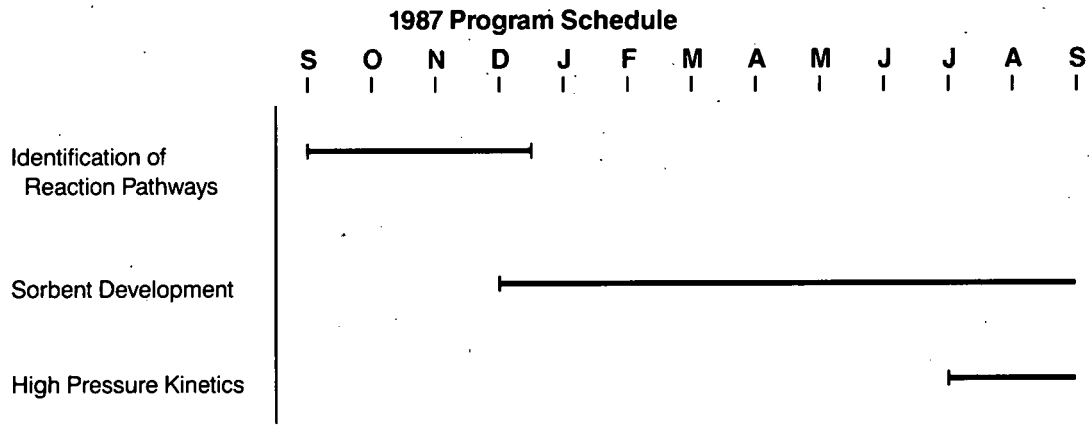

3. OBJECTIVES

This project is to develop a process for the conversion of hot gas desulfurization off-gases containing approximately 1% SO_2 to a suitable Claus plant inlet gas containing 10 to 50% H_2S at high pressure and temperature. The process will employ a regenerable alkali metal based sorbent with appropriate structural integrity, reactivity, capacity, and mechanical strength.

4. BACKGROUND STATEMENT

In recent years, METC has developed and advanced a hot gas desulfurization concept based on a regenerable zinc ferrite sorbent. The potential benefit of hot gas cleanup is most significant when the clean gas is used in a fuel cell or turbine since the sensible heat of the gas can be recovered. Figure 1 is a simplified representation of hot gas cleanup systems currently under development by METC. The zinc ferrite process for hydrogen sulfide removal adsorbs H_2S onto the zinc ferrite,

which is then regenerated by a dilute oxygen containing stream. This produces a hot regeneration tail gas containing 1-3% SO_2 with the balance being inerts (steam or nitrogen) which must be disposed of in an environmentally acceptable manner.

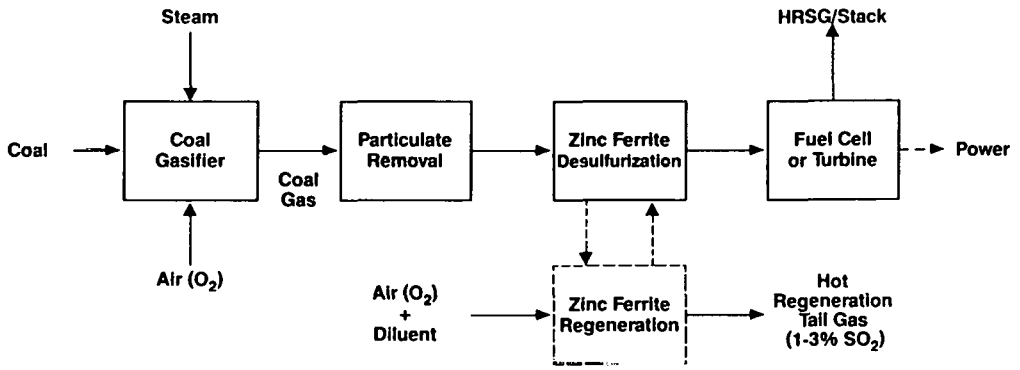

Figure 1. High Temperature Desulfurization.

One attractive option for the disposal of the tail gas is recovery of elemental sulfur from the gas by the Claus process. This process is much cheaper to apply to gases containing high concentrations of H_2S than to dilute streams. The process investigated by this project would take the waste regeneration tail gases from the zinc ferrite (or similar process) and produce a 10-50% H_2S gas stream at elevated temperatures (675-725°C) and pressures (150-400 psig) suitable for elemental sulfur recovery by the Claus process.

Figure 2 shows the proposed process. A regenerable alkali based metal sorbent is used to remove the SO_2 at 650-725°C from the regeneration tail gas. The cleaned tail gas can then be recycled to regenerate additional zinc ferrite. The alkali sorbent is then regenerated with hot coal gas (or H_2) at 700-725°C to produce a hot H_2S-containing gas suitable as a Claus plant feed.

The preparation of the sorbent follows from Beinstock et al. (1961, 1964, 1967) at the U.S. Bureau of Mines for the removal of SO_2 from combustion flue gases. The sorbent is being developed to have greater structural integrity, reactivity, capacity, and mechanical strength. Enhancement of these properties is believed to be necessary for successful application of the sorbent.

5. PROJECT DESCRIPTION

Samples of the proposed alkali metal-based sorbent were prepared very early in the program, and these were tested in a bench-scale apparatus to demonstrate that the process was worthy of further investigation. The possible reactions between the sorbent during sulfidation and regeneration were thermodynamically studied to both verify process feasibility and to examine possible thermodynamic limitations of the process. Current research is focusing on the development of a superior sorbent with suitable properties for use in the process. After producing a successful "base" sorbent, variations of the base sorbent proce-

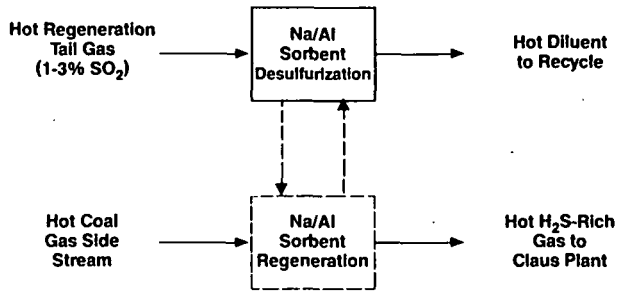

Figure 2. High Temperature Regeneration Tail Gas Treatment.

dure are being examined to produce a sorbent which is best suited to the process. The reactivity, capacity, and structural integrity of several sorbent variations will be examined, and the most suitable sorbent selected for further testing.

The technical feasibility of using the alkali metal-based sorbent to remove SO_2 from hot gas regeneration off-gases and produce a suitable feed gas stream to a Claus plant has been demonstrated with both preliminary bench scale tests and a thermogravimetric reactor at atmospheric pressure. The sorbent pellets produced were extrudates 1/16" dia. x 1/8" long. The pellets showed surface areas of 10 m^2/g and crush strength of 5 lb/mm. The pellets were initially tested in a Dupont 951 thermogravimetric analyzer. This allowed the weight of the sorbent to be measured as it was alternately exposed to 1% SO_2 in N_2 (for sulfidation) and H_2 for regeneration. Figure 3 shows the weight changes of a sorbent sample during sulfidation and regeneration at 700 °C. The weight gain of the sorbent in SO_2 was nearly 20% and there was excellent repeatability of the sulfidation and regeneration during the cycles. The sulfidations were not complete when the sorbent was regenerated, indicating that the material has a higher capacity than 20%. The rapid rates of sulfidation and regeneration indicate the high reactivity of the sorbent.

The alkali sorbent has also been tested in a bench-scale reactor system shown in Figure 4. The outlet gas concentrations were measured by two gas chromatographs (GC). One GC analyzed the fixed gases present while the other GC was devoted exclusively to measurement of H_2S in the outlet gas. This system exposed 50 cm^3 of sorbent pellets in a fixed bed of sulfidation and regeneration gases. Several samples of the sorbent were produced in reduced and sulfided forms using this system for detailed analytical/physical characterization. A typical cycle for the experiment was to first activate the sorbent in H_2 (700 °C), sulfide the sorbent in 2% SO_2 in N_2 (700 °C), followed by sorbent regeneration in either simulated clean coal gas or hydrogen (700 °C). The sulfidation and regeneration cycles were then repeated.

The bench-scale tests demonstrated that the process was technically feasible at 700 °C using the proposed sorbent. The sorbent completely removed SO_2 to the detection limit of the GCs and had a demonstrated capacity of up to 40% by weight SO_2. The observed concentrations of

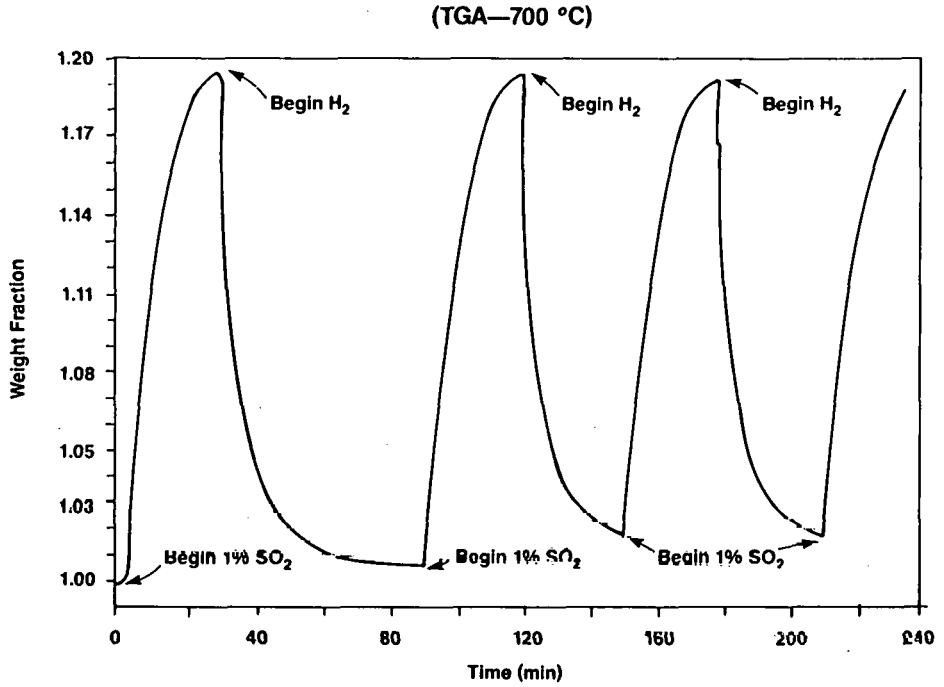

Figure 3. Sorbent Sulfidation/Regeneration Cycles.

H_2S in the regeneration gas were 16-60%, showing that the sorbent can be regenerated to produce feed gas suitable for a Claus plant. Crush strength tests of the sorbent test samples indicate that the sorbent maintained its structural strength through 4 sulfidation/regeneration cycles. It was discovered that high concentrations (>50%) of steam at 700 °C in the sulfidation gas may deactivate the sorbent. Deactivation was not observed at 340 °C. The regeneration of the sorbent in both hydrogen and clean coal gas was demonstrated.

6. RESULTS/ACCOMPISHMENTS

- The technical feasibility of a process concept based on a sodium/aluminum sorbent for recovery of elemental sulfur from regeneration tail gases has been demonstrated.
- The sorbent was demonstrated to absorb up to 40% by weight SO_2 at 700 °C and could be regenerated through multiple cycles with reducing gas to produce a H_2S-rich gas containing up to 60% H_2S.
- The sorbent extrudates retained structural integrity, strength, reactivity, and capacity following multicycle testing.

7. FUTURE WORK

Current work involves the preparation of an enhanced sorbent material. Several variations in the sorbent preparation procedure are being employed to produce a sorbent with enhanced reactivity, capacity, and structural properties. The reactivity and capacity of prepared sorbents will be measured using a thermogravimetric reactor while crush

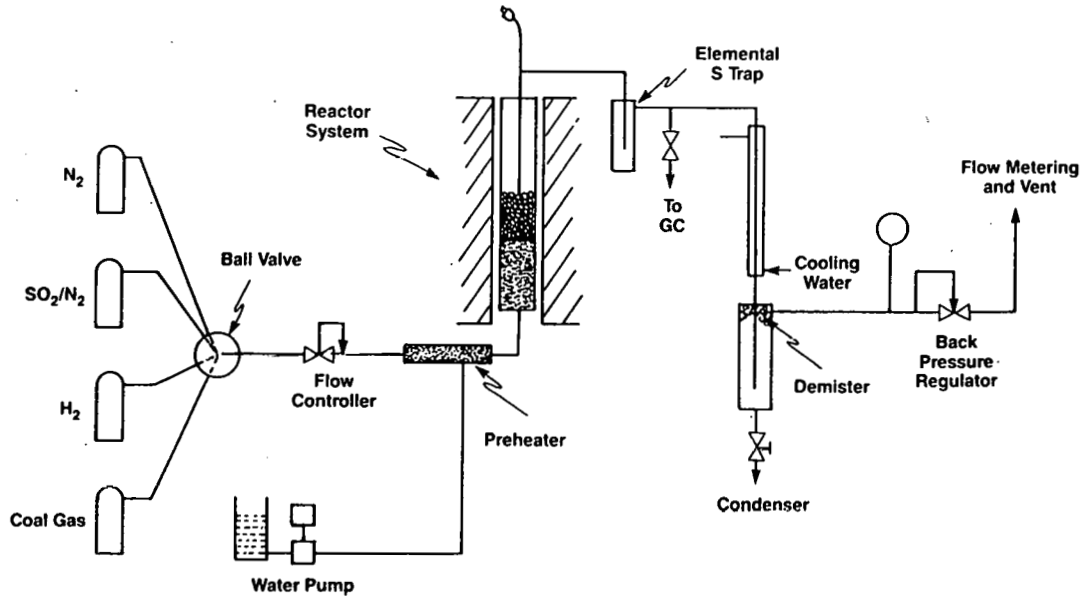

Figure 4. Sorbent Test Apparatus.

strength will be measured as an indication of structural integrity. The sorbent samples prepared using the bench scale apparatus and sorbents prepared by varying the preparation procedure will be characterized by several methods, including: Inductively Coupled Plasma (ICP, for Na and Al), crush strength (ASTM D-4179), X-ray diffraction (for chemical phases), mercury porosimetry (pore volume distribution), BET surface area, Differential Thermal Analysis (DTA, for chemical compounds), sulfur and carbon analysis, Scanning Electron Microscopy (SEM), ESCA, and Nuclear Magnetic Resonance (NMR). Once the most appropriate sorbent is identified, a large batch of the sorbent will be prepared for high-pressure kinetics measurements and additional bench-scale test. In summary, we will precisely identify the sorbent reactions, develop an enhanced sorbent, develop a reproducible sorbent preparation procedure, study high-pressure sorbent kinetics, and demonstrate sorbent performance with high-pressure bench-scale tests.

8. REFERENCES

Beinstock, D., J. H. Field, and J. G. Myers, Bureau of Mines, Dept. of Investigations, 5735, PB 192542 (1961).

Beinstock, D., J. H. Field, and J. G. Myers, Bureau of Mines, Dept. of Investigations, 7021, PB 192544 (1967).

Beinstock, D., J. H. Field, and J. G. Myers, J. of Eng. for Power, 7353 (1964).

MODELING HYDRODYNAMIC MIXING IN PROCESS DESIGN AND DEVELOPMENT OF FLUIDIZED BED GASIFIERS

1. CONTRACT NUMBER: DE-AC21-85MC22062

CONTRACTOR: University of Massachusetts
Amherst, MA 01003

METC SECTION/BRANCH CHIEF: M.R. Ghate

PRINCIPAL INVESTIGATOR: T.R. Blake

METC PROJECT MANAGER: L.A. Jarr

CONTRACT PERIOD OF PERFORMANCE: October 1, 1985 - September 30, 1988

2. SCHEDULE/MILESTONES:

TASK	MONTHS FROM START OF PROJECT 0 6 12 18 24 30 36
I. Develop a reactor specific version of CHEMFLUB	----------
II. Incorporate correlations in software for minicomputer	----------
III. Model cold flow fluidization	----------
IV. Model high temperature reactor environment	-------

3. OBJECTIVES:

In this project, models for hydrodynamic mixing in fluidized beds are to be used in a representative process design and development scenario for the KRW gasifier.

The particular emphasis in this study is upon the use of two modeling approaches: the dimensional analysis and scaling of fluidization data, and the finite difference hydrodynamic model CHEMFLUB. Predictions of hydrodynamic mixing in the KRW reactor are made.

Further, the relative value and practicality of the two different models for predicting hydrodynamic mixing is to be assessed.

4. BACKGROUND STATEMENT:

The hydrodynamic computer model CHEMFLUB incorporates an implicit finite difference technique for solving the "first principles" equations describing gas and particle dynamics in a fluidized bed (Blake and Chen (1981)). CHEMFLUB can be used to predict the hydrodynamic mixing in the bed, such as jet penetration, bubble motion, particle entrainment, and

particle circulation. Also, the finite difference computational zones provide a numerical "construction" of a wide variety of reactor geometries because the walls, injectors, etc., are resolved incrementally through these computational zones.

The CHEMFLUB model was developed under USDOE Contract EX-76-C-01-1770, and it is documented by Chen (1981) and Chen, et. al (1981). There have been additional projects, cf. Goldman (1984) and Padhye (1984), which were sponsored by the USDOE (Contracts DE-AC21-82MC19265 and DE-AT21-82MC11284 T049), to assess the physicochemical and the numerical aspects of CHEMFLUB.

Another practical and important modeling technique for the prediction of hydrodynamic mixing in fluidized beds is that of dimensional analysis and scaling. Such dimensional analysis is a useful design protocol and has been extensively used in the correlation and extrapolation of hydrodynamic phenomena from existing data.

There have been studies, cf. Zenz (1983) and Blake, et. al (1985), where dimensional analysis and scaling has been used to develop correlations of fluidization data (USDOE Contracts DE-AC21-80MC14141 and DE-AC21-81MC16440). Additional research on dimensional analysis and the correlation of fluidization data is presented by Fitzgerald, et. al (1982), Glicksman (1984), and Blake (1986).

5. PROJECT DESCRIPTION:

This modeling of hydrodynamic mixing in the KRW gasifier should be a prototype for future design work. Such modeling is needed to assist in the design of coal gasifiers where hydrodynamic mixing, associated with fluidization, dominates the performance of the reactor. The information to be obtained in this study should, first, define those design issues which can be addressed through the application of these models and, second, indicate the relative advantage of each modeling approach for predicting the influence of hydrodynamic mixing on reactor performance.

The application and assessment of the two modeling approaches to fluidization in gasifier design involves four tasks. Briefly, these tasks are:

I. Develop a KRW-reactor specific version of the CHEMFLUB model through the modification of the hydrodynamic constitutive equations, and the chemistry of the gasification reactions. The version of CHEMFLUB which is being used in the study is an axisymmetric version which has been used by METC and which is most appropriate to the quasi-axisymmetric geometry of the KRW reactor.

II. Incorporate fluidization correlations in software appropriate for interactive use on a DEC VAX minicomputer with the VMS operating system. This software will include available dimensionless correlations and associated data bases on jet penetration, solids circulation, particle

entrainment, particle segregation, bubble motion, heat transfer, and mass transfer.

III. Apply CHEMFLUB and the correlations to cold flow fluidization measurements in order to verify these models and, also, to use the models to assess the applicability of the experimental results. The CHEMFLUB model is designed to represent the gas dynamics, the solid particle motion and the coupled influences of chemistry and mixing for time scales of the order of the gas residence time in the reactor. The correlations also provide a description of such fluidization phenomena, and represent an alternative design technique for characterizing the nature of hydrodynamic mixing in the fluidized bed. It is essential that the application, of either of these modeling approaches to a new design, be verified in a scaled hydrodynamic environment through comparison with flow visualization data.

IV. Use CHEMFLUB and the correlations to investigate the hot reactor environment of the KRW gasifier and determine the influence of high temperature and pressure on hydrodynamic mixing. These calculations will be for time scales associated with gas residence time in the reactor, but they will be used to assess the coupling of hydrodynamic mixing with reactor operability and reactor performance. These analytical results will be compared with available data on high temperature and high pressure fluidization.

The accomplishment of these tasks by the University is being assisted by the Westinghouse Corporate R&D Center and by S-CUBED; the research at these corporations is being performed under subcontract to the University.

6. RESULTS/ACCOMPLISHMENTS

- Analyzed the data base from the KRW 3 m diameter cold flow rig, and compared measurements with existing correlations.

- Modified subroutines in the CHEMFLUB finite difference hydrodynamic model.

- Used CHEMFLUB to simulate fluidization in the KRW rig, and in the Westinghouse 30 cm diameter cold flow rig. These calculations were compared with the observed experimental conditions.

- Studied the evolution of bubbles arising from fluidization produced by a uniform grid in beds comparable to the size of the Westinghouse and KRW configurations. These predictions appear to be the first such calculations of nonlinear instabilities leading to bubble formation. A comparison with bubbles created by a central jet is obtained.

Dr. W.C. Yang of Westinghouse contributed to the identification and interpretation of the data from the cold flow experiments. Mr. J.W. Pritchett of S-CUBED developed and implemented important modifications in the CHEMFLUB subroutines.

7. EVALUATION OF POTENTIAL AND FUTURE PLANS:

The relative value and practicality of the two different modeling approaches, finite difference hydrodynamical modeling, and dimensional analysis and scaling of fluidization data, will be assessed. Therefore, this study will provide a needed application and evaluation of these modeling approaches within the context of a specific process design scenario. Such modeling should be a prototype for future design of fluidized bed gasifiers where hydrodynamic mixing, associated with fluidization, dominates the performance of the reactor.

Some preliminary conclusions have been made on the relative advantage each modeling approach for predicting hydrodynamic mixing in process design. For example, the finite difference model is the preferable approach when the geometry and flow conditions are more complicated than the data base which establishes the correlation. This situation arises in the KRW configuration when the prediction of jet penetration height is needed. That jet is influenced by the gas flows through two or more concentric injectors and by the very large gas flows through the annulus and the conical grid. Typically, most data on jet penetration is for simpler flow configurations.

However, it is also important to realize that both the constitutive equations and the numerical algorithms which are used in such finite difference models are often limited in applicability. This means that for the immediate future, such models must be considered to be research rather than design tools. In the present study, it was necessary to modify CHEMFLUB to obtain simulation of the KRW cold flow environment.

Some specific comparisons between the CHEMFLUB model and the correlations are:

jet penetration - CHEMFLUB provides a better prediction of the KRW experiments than the correlation,
bubble geometry - CHEMFLUB predicts a longer and narrower bubble than in the KRW experiments (correlation does not exist),
bubble velocity - correlation provides better representation of the KRW experiments than CHEMFLUB, but correlation requires specification of bubble size,
characteristic frequency - CHEMFLUB gives excellent prediction of low frequencies at higher elevations in KRW rig but does not predict the high frequencies at lower elevations.

The efficacy of finite difference hydrodynamic models, such as CHEMFLUB, depend on the development of sophisticated constitutive equations for describing the particle - particle and particle - gas forces. It is our view that the predictions by CHEMFLUB would be improved if the model included such equations. It is also our view that there is insufficient fundamental data upon which to judge sophisticated constitutive equations.

In the next year of this study, the major research effort will be on the development and application of correlations of fluidization data for

cold flow and hot reactor environments. Also, some limited applications of CHEMFLUB to the KRW cold and hot reactor environments will be made.

8. REFERENCES:

Blake, T.R. (1986), "On the Continuum Theories of Fluidization with Application to the Interpretation of Data," SIAM National Meeting, July, Boston.

Blake, T.R., and P.J. Chen (1981), ACS Symposium Series, 168, p. 157.

Blake, T.R., M.R. Webber, P.B. Sunderland, E. Randall, C.Y. Wen and C.A. Ku (1985), "Hydrodynamical Basis for Scaling Fluidization Data on Jet Penetration and Mixing Relevant to Fluidized Bed Gasifiers," USDOE Report DOE/MC/16440-1937.

Chen, P.J. (1981), "Computer Modeling of Coal Gasification Reactors, Volume I," USDOE Report DOE/ET/10242-T1 (Vol. 3)

Chen, P.J., G.P. Schneyer, E.W. Peterson, T.R. Blake, J.L. Cooke and D.H. Brownell, Jr. (1981), "Computer Modeling of Coal Gasification Reactors, Volume III," USDOE Report DOE/ET/10242-T1 (Vol. 1)

Fitzgerald, T.J., D. Bushnell, S.D. Crane and Y.C. Shieh (1982), "Testing of Cold Scaled Bed Modeling for Fluidized Bed Combustors," Final Report on USDOE Contract DOE/PC/30218-T2.

Glicksman, L.R. (1984), "Scaling Relationships for Fluidized Beds," Chem. Engr. Sci., 39, No. 9, p. 1373.

Goldman, A.L. (1984), in Proceedings, Fourth Annual Advanced Gasification Contractors Meeting, Eds. M.R. Ghate and H.L. Lai, USDOE Report DOE/METC/85-2.

Padhye, A.R. (1984), ibid.

Zenz, F.A. (1983), "State of the Art Review and Report on Critical Aspects and Scaleup Considerations in the Design of Fluidized Bed Reactors," USDOE Report DOE/MC/14141-1304.

NOVEL CONCEPTS OF SYSTEM ASSESSMENT IN COAL GASIFICATION

Contract Number DE-AC21-86MC23280

Contractor CUNY Research Foundation of New York
Department of Chemical Engineering
The City College of New York

Contractor Project Manager Professor Reuel Shinnar

METC Project Manager Wen Liou

Period of performance October 1, 1986 - September 30, 1989

Objectives

The objective of this task is to assess the impact of the end use and total system design on the economically desirable operating conditions and design properties of gasifiers. It is also intended to investigate novel system configurations that will improve the performance and cost of the total system, and inquire what gasifier properties lead to better overall system properties. Two related problem areas were chosen for this study, which are:

A) Assessment of gasifier requirements for generation of electricity from coal in combined cycle power plants that have

1) very low emissions and acceptable disposable solids
2) high thermal efficiency
3) lower investment costs and suitability for modular construction
4) the ability to produce liquid hydrocarbons by mild gasification

Special emphasis will be given to study the applicability of fluid bed gasifiers and in particular airblown fluid bed gasifiers for this purpose.

B) Study the potential of a slagging and a fluid bed gasifier for hydrogen production with the coproduction of methane and mild gasification products. Assess the impact of novel separation processes on the overall cost and performance of such a system as well as on conventional hydrogen plants from coal.

Background

Role of System Assessment in Coal Gasification

Most studies dealing with the evaluation of coal gasification processes focus solely on the gasifier itself and its performance. There is, however, a need to look more closely at the total system in several ways. Characteristics of the gasifier dominate and influence the choice of the downstream technology, and thereby the cost and thermal efficiency of the total system. Thus, for example, an indirect liquefaction plant utilizing a gasifier with a low H_2/CO ratio benefits from a technology that can utilize the syngas without shift (1). On the other hand, if the gasifier has a high H_2/CO ratio a different choice for indirect liquefaction will be optimal for the total system.

But the opposite is also true. The application strongly affects the choice of the gasifier, and so can other developments. For example, the optimal requirements of a gasification plant for a combined cycle power plant integrated with a gasifier are different from a fuel-gas gasifier. Thus, in a plant when the main product is fuel or syngas, sensible heat at the gasifier outlet is only valuable if it can be used for feed preparation (steam and oxygen). Any excess is either of no value or limited value. The penalty is much lower in a combined cycle power plant complex as the heat can be integrated into the electricity generation. Similarly, the latent heat of excess steam has no value in a fuel gas gasifier but its value in a combined cycle power plant depends on the availability of hot gas cleanup. If hot gas cleanup is available, the pressurized steam contained in the gas can be expanded in the turbine and is therefore a valuable component of the product gas, whereas in the absence of hot gas cleanup, its latent heat is mostly a penalty as it is expensive to condense steam from a dilute stream. The impact of gasifier properties is therefore a two-way street that is also affected by separation technology. One has therefore to understand the total system and the way different process components interact with each other in order to design a system which has the desirable characteristics with minimum cost and high thermal efficiency.

A thorough understanding of the total system will strongly increase the chance for a successful commercialization. The goal of this study is to apply this to two applications of gasification technology and investigate the implication of the total system's demand in gasification technology and on the chance of successful commercialization.

Project Description

The commercial applications to be studied are:

a) A combined cycle power plant using an airblown fluidized bed gasifier with in-bed desulphurization and hot gas cleanup. An overall flow schematic is given in Fig. 1.
b) A combined cycle power plant similar to Figure 1 but integrating a mild devolatiliation stage coproducing mild gasification liquids in a power plant.
c) A novel scheme of hydrogen production from coal with coproduction of either SNG, or SNG and mild gasification products.

Work till now has concentrated on item a and is going to be discussed in the

following.

Achievements Till Now

Airblown fluidized bed gasifiers for power generation in a combined cycle power plant.

Power plants are the most important near term application of coal gasification (2). This application is attractive today due to its competitive cost and low emissions. One demonstration plant, "the Cool Water Project," has been operating successfully for the last two years with good results, and other projects are under way (3).

One promising approach is based on a fluid bed gasifier. A schematic description of this project is given in Fig. 1. The coal is gasified with air and steam in a fluid bed in the presence of limestone or dolomite which captures 90% of the sulfur. The hot gas is first cooled by either quench of heat transfer to about 1000°F, passed through a ceramic filter and then through a hot gas cleanup unit developed in Morgantown. The hot gas is then fed to a combined cycle gas turbine. Steam for the gasifier is either generated in the product gas cooler or in the ash oxidizer. The hot ash containing the dolomite is fed to a fluid bed oxidizer which also combusts the unconverted carbon from the fluid bed.

Such a system has several potential advantages over oxygen blown gasifiers.

1) The oxygen plant is eliminated.
2) It is suitable for low grade coal.

The elimination of the oxygen plant could lead to lower investment costs and also higher thermal efficiency, which ultimately would be the main advantage of such a system. About 20% of the total power output in "Cool Water" goes to the oxygen plant. The challenging system problem is: can this energy be saved

In the absence of hot gas cleanup the advantage of using air is quite small both in cost and thermal efficiency. This is due to two reasons.

o Use of air increases the sensible heat of the gas and reduces cold gas efficiency. If this sensible heat is used solely for steam generation it reduces the output of the gas turbine thereby reducing the thermal efficiency. This reduces the gain in net thermal efficiency that results from the elimination of the oxygen plant.

o The cost of H_2S removal depends on total gas throughput and therefore increases for airblown gasification.

Hot gas cleanup partially removes the first disadvantage as the gas including the nitrogen is fed hot (1000°F) to the turbine. This also allows to utilize the unconvertable steam for expansion in the turbine, and therefore also removes the penalty from unconverted steam. Our evaluation will therefore assume that it is not necessary to cool the gas to low temperature to remove H_2S from the gas (4,5).

The scheme in Fig. 1 removes also some of the inherent disadvantages of fluid beds which are:

1) Conversions above 90% are hard to achieve in the present design of fluid bed gasifiers whereas entrained bed gasifiers or a BGC Slagger achieved 98% carbon conversion. In Fig. 1 the unconverted carbon including fines formed would be converted in the fluidized bed oxidizer which is similar to a fluidized bed boiler.

2) Fluidized bed gasifiers require dilution of the oxygen with either steam or nitrogen. Here, the nitrogen does not cause any penalty, whereas in a fuel gas application excess steam results in a large penalty.

The scheme in Fig. 1 also has some disadvantages which have to be minimized. Here, proper system analysis can play an important role.

The most important are related to hot gas cleanup. Present methods of hot gas cleanup do not ultimately result in elemental sulfur, but in $CaSO_3$ which has to be oxidized and disposed together with the ash and a large excess of lime or dolomite. Sulfur is much easier to dispose and can be sold. One standard giga watt power plant would generate 2 million tons a year of the ash-gypsum lime mixture. It would be highly desirable to find some uses for these materials. The second penalty is due to the fact that to be disposable as solid waste, the calcium sulfite requires oxidation to sulfate. This requires a separate oxidizing unit thereby complexing the system. On the other hand, this also solves two of the problems of fluid beds.

The addition of lime strongly improves the operation of a fluid bed with Eastern coal. In fact, it is essential for successful operation at elevated pressures, at least in present designs. We will discuss this

later. The oxidizing stage also allows combustion of the unconverted carbon, which probably would have been required anyway.

The first question that arises is what are the penalties we pay for the use of air. The total minimum amount of oxygen is exactly the same for both systems. Use of oxygen eliminates the nitrogen feed to the gasifier and therefore in higher BTU content of the fuel gas. For present gas turbines ($2100^{o}F$) this has no advantage as long as the BTU content of the gas is above 80 BTU/SCF. If the turbine temperature increases this also increases the minimum heat content of the fuel gas.

This, however, puts a constraint on the design of the gasifier. We note immediately that we cannot design the gasifier without taking into account turbine properties.

There is another aspect of the same problem, namely, how much heat is taken out of the gasifier feed and converted to steam or lost as low grade heat. Heat taken out as steam such as by cooling the gases before cleanup shift energy from the gas turbine to the steam cycle, which has a lower efficiency expecially at the size of such a unit does not allow a complex steam cycle. Cooling the gases also leads to large heat losses.

Operating Map of Gasifier

To understand this problem better, we need to understand the operating constraints of the gasifier. To do so, we evaluated the available pilot plant results for an airblown KRW gasifier, and tried to project its operation in a large scale plant. To do so, we used a kinetic model for such a gasifier developed under the previous contract (2). This model reasonably predicts the effect of changes in operating parameters in the present pilot plant. Typical pilot plant results are given in Table 1.

The first results of this evaluation are summarized in Figs. 2-4 where we give the results of the model computations for the case without dolomite. In Fig. 2 we plot carbon conversion versus gasifier bed temperature. The main operating parameters at our disposal are air-to-coal ratio, steam-to-air ratio, bed height and coal feed rate. In Fig. 2 bed height is fixed to a bed weight of 200 lb/ft^2 and instead of coal feed rate we fix the gas velocity at bed exit to 2 feet/second. In a design the main constraint in throughput is the gas velocity as high gas velocity causes excessive elutriation. The 2 feet/second limit is based on KRW experience. The

oxygen-to-coal ratio and steam-to-air ratio are given as operating lines in the plot. We plot the molar ratio of oxygen-to-coal instead of air-to-coal as this is stochiometrically easier to interpolate.

The results indicate that at those conditions an airblown conversion above 90% requires an oxygen-to-coal ratio of close to .45 equivalent to an R_c-R value of zero. Higher oxygen values would improve conversion but at the expense of the heating value of the gas.

To interpret the permissible operating range, we need to look at Fig. 3 where we give the BTU content of gas as a function of the operating conditions. The BTU content is based on total wet gas as the steam is not condensed in this scheme. We note that steam-to-oxygen ratios should be below unity. This means that operating temperatures should preferably be above 1900°F. Now the coal assumed the plot (Pittsburgh No. 8) could agglomerate at high temperatures, unless an additive such as calcium carbonate is added. Lime used as a desulfurization agent allows operation at 2000°F. It reduces the carbon content of the bed, but compensates for this by catalyzing the gasification reaction. The overall results are quite similar to Fig. 2 and 3. Fig. 4 gives the impact of bed height. Increasing bed height increases the carbon content, and allows a higher conversion at a given operating temperature. However, we have no data at higher bed heights to confirm this prediction.

In Fig. 4 the contact efficiency of the bed was assumed to be independent of bed height, which is true for most turbulent beds. We don't have data for the projected operating conditions to confirm that the bed is turbulent. In many fluid beds contact efficiency decreases with bed height. Our system analysis will therefore be based on the base case in Fig. 2 modified for limestone addition.

Effect of Steam Balance

Steam is an important medium in the combined cycle plant to utilize energy that is not utilized in the gas turbine. It can also be used to increase the function of total energy used in the gas turbine. Two examples were preliminary analyzed till now.

a) Use of steam versus recycle gas in the gasifier.

A gasifier operating at 2000° with an oxygen-to-carbon ratio of .45 or larger requires addition of steam (about one to two moles of steam per mole oxygen). Steam or recycle gas is also required for the agglomeration zone. In the presence of hot gas cleanup steam has a significant advantage over recycle gas as it enters the gasifier replacing excess air. It also increases the rate of gasification whereas recycle gas decreases it. Recycle gas has to be cooled in a steam generator thereby reducing the advantage of the hot gas cleanup. Quantitative results are going to be provided in the final report.

b) Use of Quench versus a Boiler to Cool the Product Gas.

For hot gas cleanup this gas has to be cooled from 2000°F to 1000°F. Present system designs also use a valve in front of the turbine which demands a gas temperature below 1200°F. This cooling can be done by either injecting water or using a waste heat boiler. In the presence of hot gas cleanup, quenching with water has an advantage over a waste heat boiler. It reduces investment cost. It eliminates the waste heat boiler and reduces the size of the steam cycle. It also reduces the size of the compressor as now less excess air is needed to give a given combustor temperature. Similar arguments apply to the use of steam instead of recycle gas. However, the amount of steam that can be used for quench strongly depends on the BTU content of the gas.

Totally relying on quench at a gasifier temperature of 2000°F is onlyfavorable if the wet BTU content of the gas is kept above 130 BTU/SCF. Even then it drops to 90 BTU/SCF. However, even if quench is only used partially, it achieves part of the above goals. The amount quench that can be used depends on the BTU content of the wet gas or in other words on operating conditions in the gasifier and on the flame temperature of the gas turbine itself, as the latter limits the amount of steam dilution permissible. This illustrates the strong need for a total system approach in the design and development of the gasifier itself.

Future Work

Presently, the operating maps are modified to include operation with lime. We are also preparing operating maps that give the thermal efficiency

of the gasifier in a way that is useful for judging system performance. In a combined cycle power plant, it is important to supply the maximum amount of energy to the power plant and this can therefore serve as a criterion for optimizing gasifier operation.

The goal in the first stage is to relate thermal efficiency and cost to operating and design parameters in a single model in a way similar to what we did with coal gasification for fuel and syngas. These results will then be used in two ways. It will lead to suggestions for commercialization and will also serve as basis for a system assessment of the novel schemes mentioned in the project description.

References

1) Shinnar, R.and Kuo, J.N., "Gasifier Study for Mobil Coal to Gasoline Processes," T-E 2766-13 (1978).

2) Halow, J.S. (1985), Power Generation Through Coal Gasification, J. + ASME/I Power Generation Conference, Milwaukee, WI, October 1985.

3) EPRI, "Coal Water Coal Gasification Program: Fourth Annual Progress Report," EPRI AP-4832, October 1986.

4) Stone and Webster Engr. Co., (1977), "Comparative Evaluation of High and Low Temperature Gas Cleaning for Coal Gasification Combined-Cycle Power Systems," EPRI-AF-416.

5) Shinnar, R., "Hot Gas Cleanup for Fuel Gas - Incentives for Development," (1980), DOE Report

6) Shinnar, R., Avidan, A.I. and Weng, L., "Evaluation of Fluidized Bed Coal Gasification Present Status and Future Development Problems," Final Report, for the period September 1, 1985 - September 15, 1986. DOE, DE-AC-21-84M-C21259.

Table 1 FLUIDIZED BED GASIFIER PDU

AIR-BLOWN PGH#8 + DOLOMITE

		TP-036-4		
Steady State		4A	4B	8B
Temperature	(°F)	2022	2028	1958
Pressure	(psia)	230	230	230
Dolomite	(lb/lb maf)	0.42	0.51	0.29
Fines Elutriation	(lb/lb maf)	0.30	0.30	0.21
Bed Linear Gas Velocity	(ft/sec)	1.34	1.44	1.82
Coal Throughput	(lb maf/hr/ft^2)	174	190	241
Steam	(lb/lb maf)	0.29	0.26	0.32
Air/Coal	(lb/lb maf)	4.14	4.10	3.88
Oxygen/Coal	(lbmol/lbmol)	0.440	0.436	0.435
Recycle Gas + Purge With Dolomite Transp.Gas	(lb/lb maf)	2.56	2.54	2.81
Recycle Gas + Purge Without Dolomite Transp.Gas	(lb/lb maf)	1.52	1.59	2.07
Carbon Conversion X %		84.8	85.8	79.2
R = O_2 / (C*X)		0.519	0.509	0.549
Rc - R		-0.041	-0.040	-0.119
Cold Gas Efficiency	(% feed)	64.7	65.5	52.6
Cold Gas Efficiency	(% converted)	73.7	73.8	62.7

Fig.1 COMBINED CYCLE POWER PLANT WITH FLUIDIZED BED GASIFIER

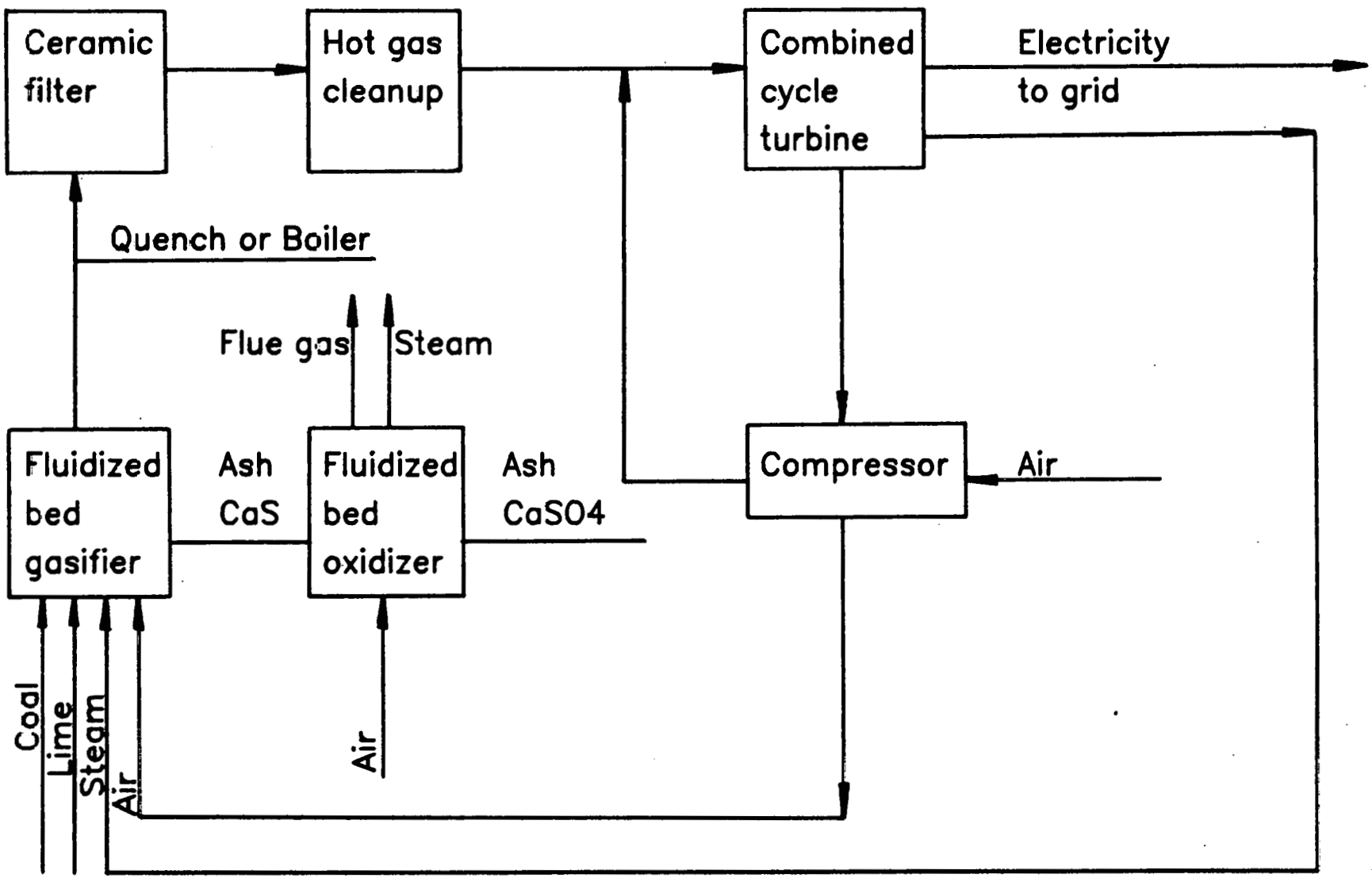

Fig. 2 OPERATING MAP OF AIR-BLOWN GASIFIER

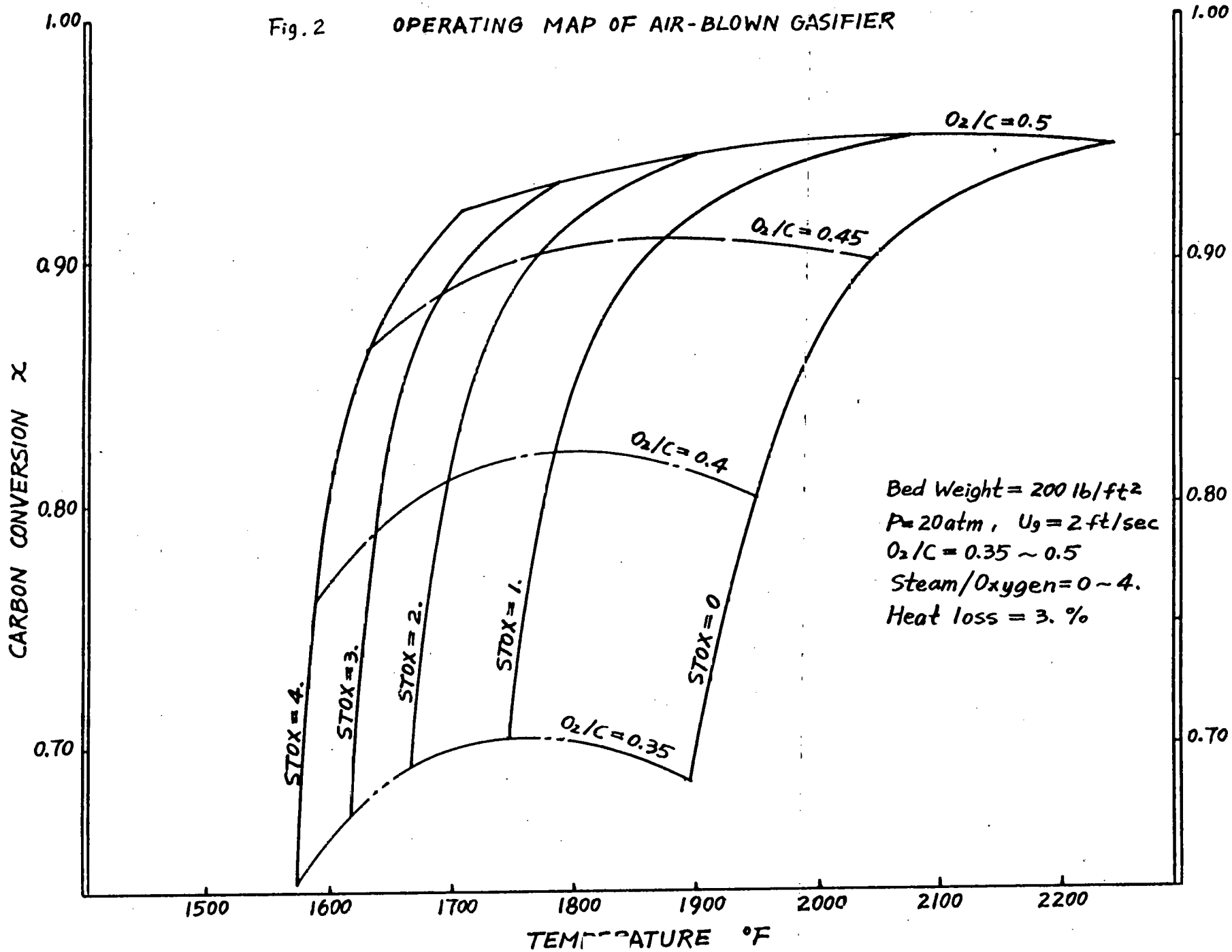

Fig. 3 AIR-BLOWN GASIFIER OPERATING MAP

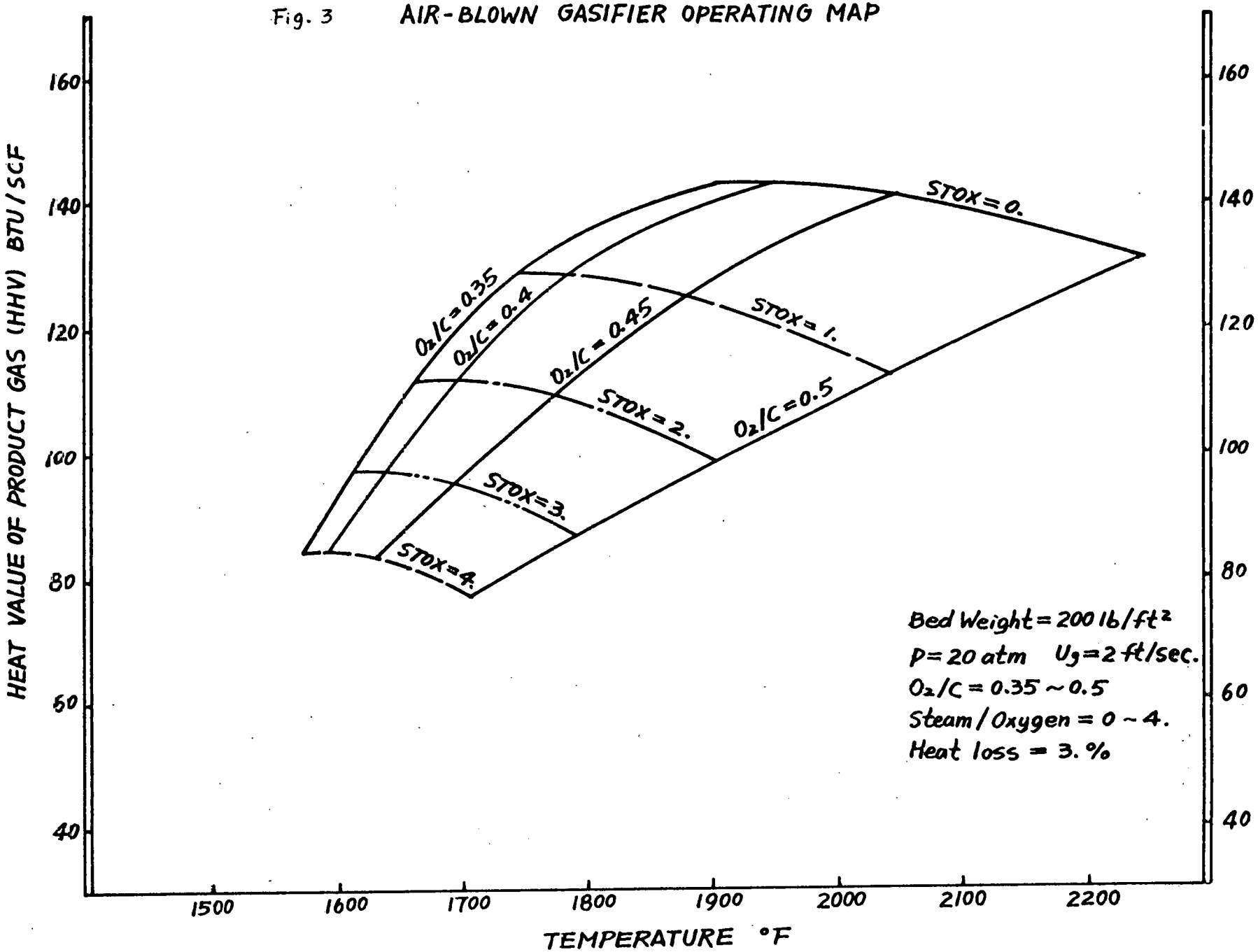

DEVELOPMENT OF A HOT GAS CLEANUP SYSTEM

1. CONTRACT NUMBER: DE-AC21-85MC22144

CONTRACTOR: Institute of Gas Technology
3424 S. State St.
Chicago, IL 60616

CONTRACTOR PROJECT MANAGER: Gerald L. Anderson

PRINCIPAL INVESTIGATORS: Gerald L. Anderson
F. Otis Berry

METC PROJECT MANAGER: V. P. Kothari

PERIOD OF PERFORMANCE: October 1, 1985 to September 30, 1987

2. SCHEDULE/MILESTONES:

Program Schedule

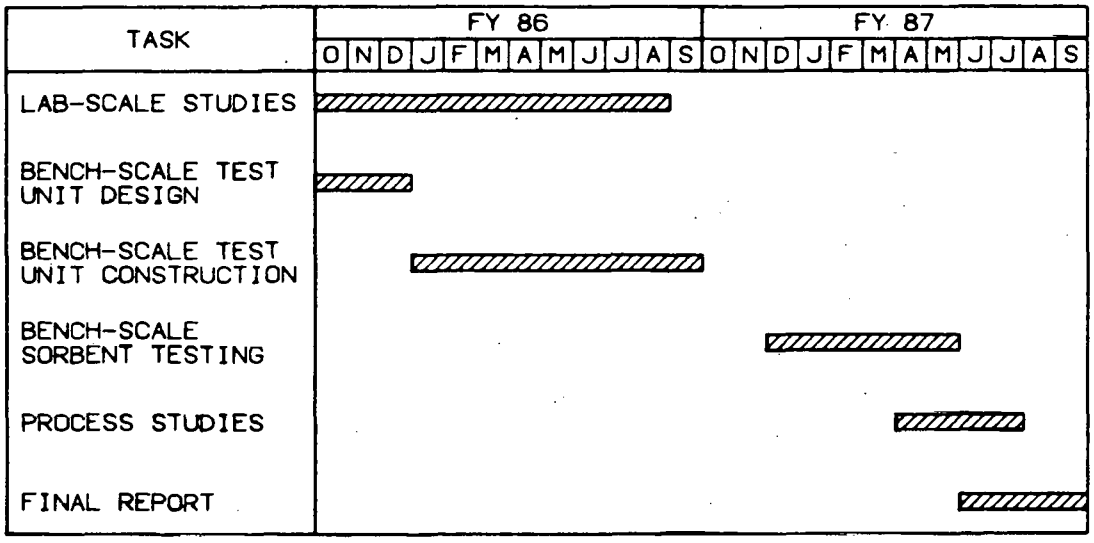

3. OBJECTIVE:

The overall objective of this program is to develop means to remove reduced sulfur-containing compounds (e.g., H_2S and COS) and HCl from hot coal-derived fuel gases for use in advanced power plants such as integrated coal gasification-combined cycle power plants and coal gasification-molten carbonate fuel cell power plants.

4. BACKGROUND STATEMENT:

Numerous studies have been performed comparing different approaches to integrating coal gasifiers with electric power production technologies

Department of Energy
Morgantown Energy Technology Center
P.O. Box 880
Collins Ferry Road
Morgantown, West Virginia 26505

E R R A T A

DOE/METC-87/6079, Vol. 2
(DE87006496)

PROCEEDINGS OF THE SEVENTH ANNUAL
GASIFICATION AND GAS STREAM CLEANUP SYSTEMS
CONTRACTORS REVIEW MEETING

June 1987

Figure 4 of "Novel Concepts of System Assessment in Coal Gasification" is on page 644.

We apologize for any inconvenience this may have caused.

such as gas turbines and molten carbonate fuel cells (King, 1976; Westinghouse R&D Center, 1983; Blecher, 1984; Robson, 1984). Each of these studies concluded that, if the fuel gas from the gasifier could be cleaned at an elevated temperature, the cost of electricity from the plant could be significantly lowered.

For many years, IGT has been exploring a process concept for removing reduced sulfur-containing compounds from 1000° to 1200°F coal-derived fuel gases. The process, known as the mixed metal oxide process, uses a mixture of metal oxide-containing sorbents that react with the sulfur-containing compounds. Reactions are of the type —

$$MO + H_2S = MS + H_2O \quad (1)$$

$$MO + COS = MS + CO_2 \quad (2)$$

where MO is a metal oxide and MS is its corresponding metal sulfide. The metal oxide-containing sorbents currently being explored for the process are 1) a zinc oxide-on-zinc aluminate sorbent and 2) a cobalt titanate-on-titania sorbent.

A simplified diagram of the fuel gas desulfurization part of the process is shown in Figure 1. The two sorbents mentioned above are segregated into separate beds. The sulfur-containing fuel gas first comes into contact with the cobalt titanate-containing sorbent where more than 67% of the fuel gas sulfur is removed. The partially desulfurized fuel gas then comes into contact with the zinc oxide-containing sorbent where the sulfur content of the fuel gas is reduced to less than 20 ppm(v).

The unique feature of the IGT process is in the regeneration. As shown in Figure 2, the fuel gas sulfur is recovered as elemental sulfur rather than SO_2 or H_2S and there is no tail gas from the process. Regeneration of the mixture is performed with pure O_2 and a recirculating stream of SO_2. The O_2 regenerates the zinc oxide-containing sorbent by the reaction —

$$ZnS + 3/2\ O_2 = ZnO + SO_2 \quad (3)$$

The SO_2 from this reaction is then combined with the recirculating stream of SO_2 to regenerate the cobalt titanate-containing sorbent. The reaction is —

$$Co_9S_8 + 9/2\ SO_2 + 9\ TiO_2 = 9\ CoTiO_3 + 25/4\ S_2 \quad (4)$$

The recirculating stream of SO_2 is required because reaction 4 is thermodynamically limited. The product gas contains both elemental sulfur and SO_2. The elemental sulfur is removed from the SO_2 by cooling and condensation and the SO_2 is recycled back to the cobalt titanate bed undergoing regeneration.

Under DOE contract DE-AC21-82MC19403 (Anderson, 1985), IGT began work on the cobalt titanate-containing sorbent. Proof-of-concept studies were

Fig. 4 OPERATING MAP OF AIR-BLOWN GASIFIER

IMPACT OF BED WEIGHT ON CARBON CONVERSION

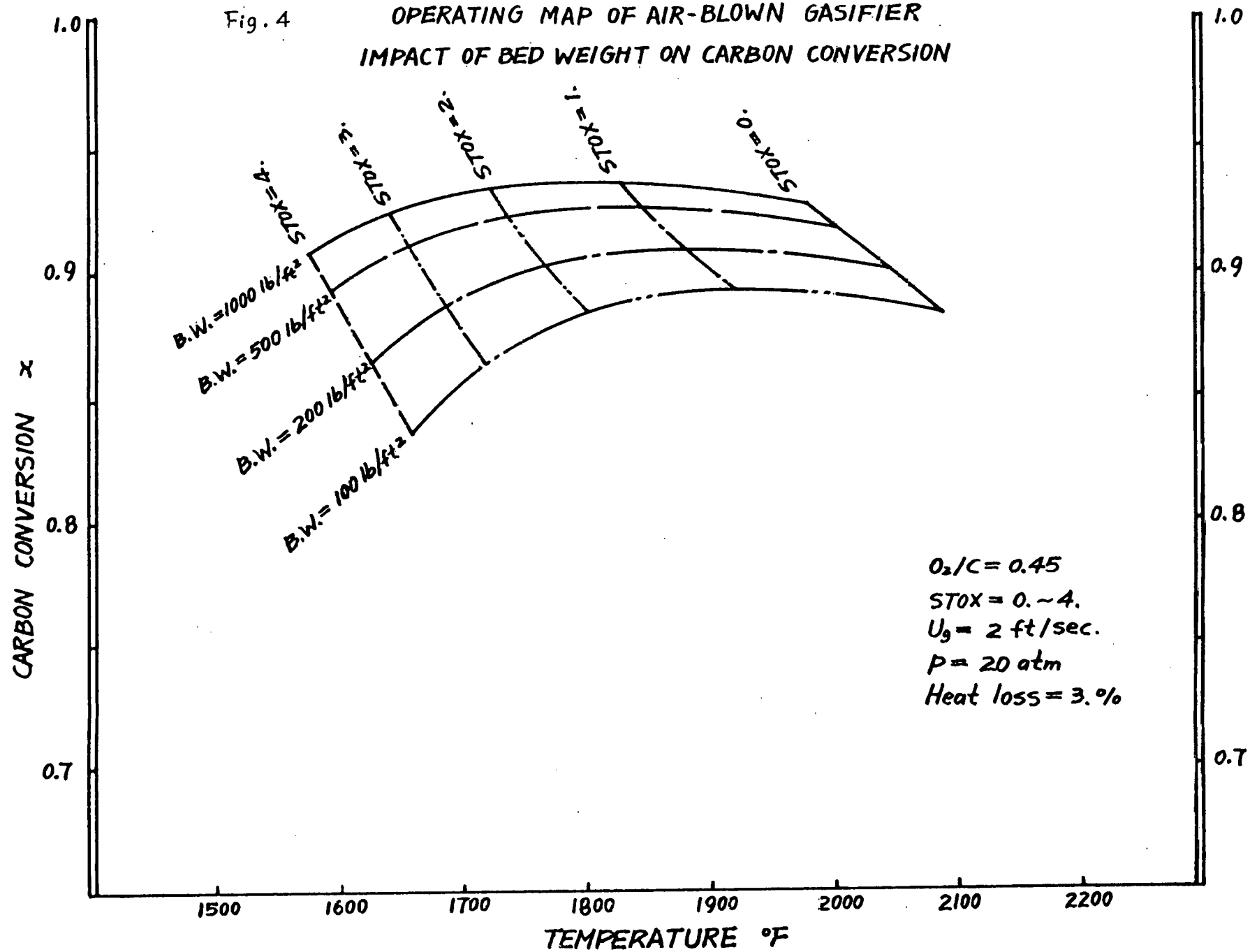

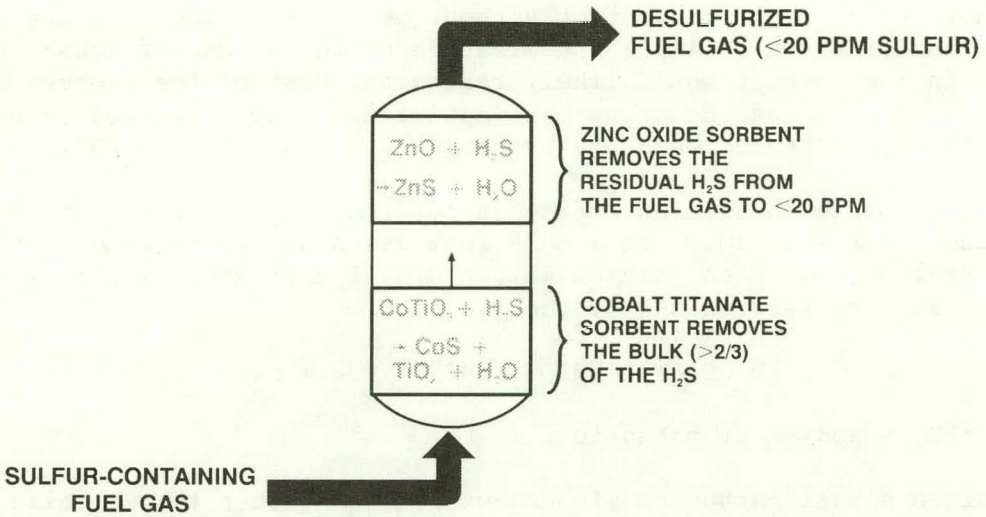

Figure 1. Fuel Gas Desulfurization With IGT Mixed Metal Oxide Process

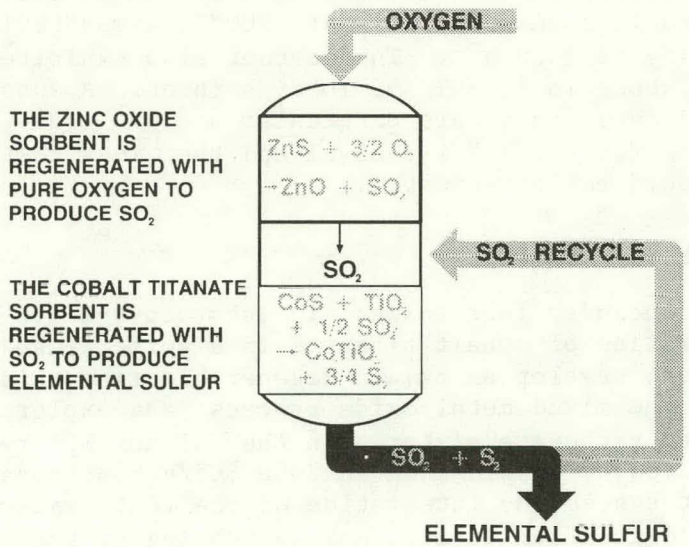

Figure 2. Sorbent Regeneration — Mixed Metal Oxide Process

conducted on a 100% cobalt titanate-containing sorbent and the cost of the process was estimated. The analysis indicated that the mixed metal oxide process would likely cost about $436/kW of installed power plant capacity and would contribute about 38 mills to the cost of each kWh of output if the proof-of-concept sorbent were used. However, the analysis also indicated that simple optimization of the amount of cobalt titanate used in the sorbent would likely reduce the cost of the process by 50% and that a combination of sorbent optimization and improved sorbent reactivity might decrease the process cost by as much as 75%.

IGT also began to develop a process for removing HCl and other trace contaminants from 1000° to 1200°F fuel gases under the same contract. The process, based on using a molten alkali carbonate mixture within a solid matrix, removes HCl by the reaction —

$$M_2CO_3 + 2\ HCl = 2\ MCl + CO_2 + H_2O \qquad (5)$$

where M is sodium or potassium.

A molten alkali carbonate mixture was chosen rather than a solid alkali carbonate for three reasons. First, a molten alkali carbonate mixture can reduce the HCl content of the fuel gas to a much lower value than a solid. Second, a molten melt was expected to be more reactive than a solid. Finally, the molten carbonate mixture was expected to remove other trace contaminants from the fuel gas such as volatile trace metals that a solid would not.

Preliminary tests on the concept were conducted with a sorbent containing the eutectic alkali carbonate mixture 50% Na_2CO_3/50% Li_2CO_3. The sorbent was able to reduce the HCl content of a simulated fuel gas from 300 ppm(v) to less than 1 ppm(v) at 1200°F, atmospheric pressure and a space velocity of 1000 h^{-1}. The sorbent also exhibited an HCl removal capacity of about 16 lb HCl/100 lb of sorbent. A subsequent cost study, however, indicated that this particular sorbent would probably be too costly to use for total HCl removal and that less costly molten carbonate mixtures should be investigated.

5. PROJECT DESCRIPTION:

The program includes four tasks: 1) laboratory-scale studies to optimize the concentration of cobalt titanate in a sorbent used in the mixed metal oxide process; develop an oxygen regenerable zinc oxide/zinc aluminate sorbent for the mixed metal oxide process; and explore the use of less costly molten carbonate mixtures in the IGT hot HCl removal sorbent, 2) construction of a skid-mounted 3000 SCF/h bench-scale hot gas cleanup process test system, 3) integration of the test system with a 6-inch fluidized-bed gasifier at IGT, and 4) testing of the IGT processes with actual hot coal-derived fuel gases in the new bench-scale unit.

6. RESULTS/ACCOMPLISHMENTS:

During the past year, several of the above tasks have been completed. These are 1) optimization of the concentration of the cobalt titanate in the cobalt titanate sorbent, 2) exploration of the potential to use less costly molten carbonates in the IGT hot HCl removal process, and 3) construction of the 3000 SCF/h skid-mounted bench-scale test system. In addition, preliminary studies have been completed on the impact of recent work on the cost of the IGT processes.

Optimization of the Cobalt Titanate Sorbent

Optimization of the concentration of cobalt titanate in the mixed metal oxide cobalt titanate sorbent was performed by conducting a series of tests with several cobalt titanate-on-titania sorbents. Sorbents containing 50%, 25%, and 10% cobalt titanate, were prepared as 3/16 inch by 3/16 inch pellets from cobalt and titania powders.

Each of the sorbents was tested in a 2-inch OD, 3/4-inch ID refractory-lined fixed-bed test system shown in Figure 3. Sulfidation was conducted at 1200°F and 250 psig with a simulated coal gas containing approximately 20 mol % H_2, 15% CO_2, 10% CO, 15% H_2O, 5000 ppm(v) H_2S and, the balance N_2. Regeneration was conducted at 1600°F and atmospheric pressure with a variety of N_2/SO_2 mixtures.

Each sorbent was sulfided and regenerated at least three times. The relevant data from the sulfidation runs is provided in Figure 4. This figure shows the effect of space velocity on the useful sulfur removal capacity of each sorbent. The useful sulfur removal capacity is the average sulfur loading in the sorbent bed at breakthrough. Breakthrough for the cobalt titanate sorbent is defined as the instant when the product gas H_2S concentration exceeds 1/3 the feed concentration. Therefore, for a fuel gas containing 5000 ppm(v) of H_2S, breakthrough occurs when the H_2S concentration of the product exceeds 1600 ppm(v).

As expected, an increase in the concentration of cobalt titanate in the sorbent increases its useful sulfur removal capacity at a fixed operating space velocity. At an operating space velocity of 2000 h^{-1}, the useful sulfur removal capacity of the 50% cobalt titanate sorbent is about 7 lb/100 lb of sorbent, whereas the useful capacities of the 25% cobalt titanate and 10% cobalt titanate sorbents are about 4.2 and 1.2 lb/100 lb, respectively.

Data from regeneration of the sorbents is shown in Figure 5. The downward trend with increasing SO_2 partial pressure indicates that, at 1600°F, elemental sulfur production is nearly equilibrium controlled. The overall reaction is —

$$Co_9S_8 + 9\ TiO_2 + 9/2\ SO_2 = 9\ CoTiO_3 + 25/4\ S_2 \qquad (6)$$

Under equilibrium control, elemental sulfur production would be inversely proportional to the SO_2 partial pressure to the 0.28 power. The curve

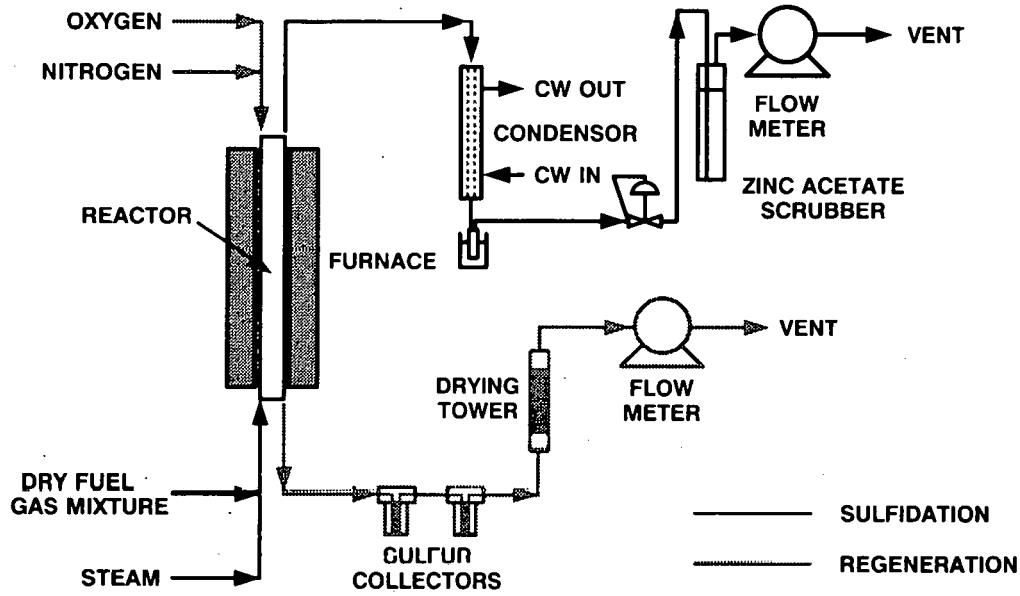

Figure 3. Laboratory-Scale Desulfurization Sorbent Test Unit

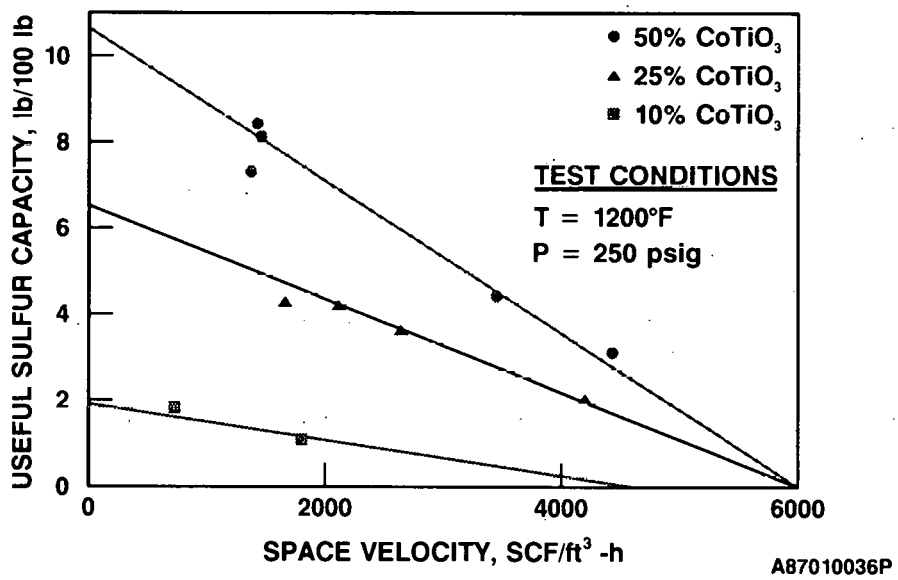

Figure 4. Useful Sulfur Capacity of Cobalt Titanate Sorbents

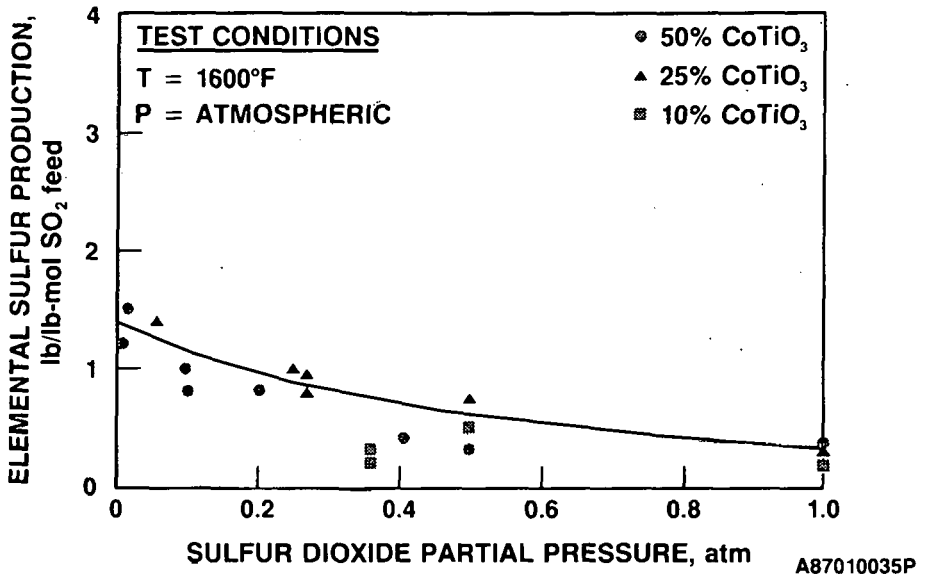

Figure 5. Regeneration Data — Cobalt Titanate Sorbents

that is drawn in Figure 5 is inversely proportional to the SO_2 partial pressure to the 0.4 power.

With the experimental laboratory-scale data, the impact of cobalt titanate concentration on process cost was estimated. It was determined that a cobalt titanate concentration of 50% by weight was optimum, provided the life of the sorbent is independent of composition. Assuming a life of 1 year, the relative sulfur removal cost of each sorbent is given in Table 1. These relative costs reflect only the sorbent replacement cost and the capital cost associated with the vessel housing the cobalt titanate sorbent. The costs do not include any costs associated with the zinc oxide sorbent or regeneration equipment and assume that the vessel is sized for an 8 hour sulfidation period followed by a less-than-8-hour regeneration period.

As can be seen in Table 1, sorbent replacement and vessel costs for the 50% cobalt titanate sorbent contribute $277/ton of removed sulfur. On the other hand, these items contribute $340/ton and $526/ton for the 25% and 10% sorbents, respectively. Not shown in the table are the equivalent costs for a 100% cobalt titanate sorbent. This sorbent, tested under a previous contract, would contribute over $700/ton of removed sulfur.

With the selection of a 50% cobalt titanate/50% titania sorbent as the elemental sulfur producing sorbent in the mixed metal oxide process, a new overall cost for the process was estimated. As shown in Table 2, the capital cost of the mixed metal oxide process using the 50% cobalt titanate sorbent is about $288/kW for a 100 MW coal gasification/molten carbonate fuel cell power plant and the impact on the cost of electricity is 20.3 mills/kWh. These represent decreases of 34% and 47%, respec-

Table 1. Effect of Cobalt Titanate Concentration on Sulfur Removal Cost

SORBENT COMPOSITION	ESTIMATED SULFUR REMOVAL COST*
50% $CoTiO_3$	277
25% $CoTiO_3$	340
10% $CoTiO_3$	526

* $/TON OF REMOVED SULFUR WITH SORBENT LIFE OF ONE YEAR

Table 2. Estimated Cost of IGT Mixed Metal Oxide Process

ASSUMPTIONS

SORBENT LIFE:	1 YEAR
SORBENT COST:	$1.18/LB (ZINC): $6.90/LB (COBALT)
CYCLE TIME:	16 HOURS

CAPITAL COST*	$288/kw
CONTRIBUTION TO COE*	20.3 mills/kwh

*100 MW COAL GASIFICATION/MCFC PLANT

tively over earlier projections on the process using a 100% cobalt titanate sorbent. However, these projected costs are still subject to considerable uncertainty. The process cost is quite sensitive to sorbent life, which has been assumed to be 1 year and the process cost assumes that an oxygen regenerable zinc oxide sorbent can be developed. Both of these assumptions need to be verified.

Testing of Alternative Hot HCl Removal Sorbents

To explore the use of less costly molten carbonate mixtures in the IGT hot HCl removal sorbent, a series of tests were conducted with prototype sorbents incorporating the following carbonate mixtures —

- 50% Na_2CO_3/50% Li_2CO_3
- 70% Na_2CO_3/30% Li_2CO_3
- 90% Na_2CO_3/10% Li_2CO_3
- 95% Na_2CO_3/5% Li_2CO_3
- 33% Na_2CO_3/33% K_2CO_3/34% $BaCO_3$

The prototype sorbents were prepared by combining each mixture with 40 volume percent MgO powder, which serves as the solid matrix for the molten mixture. The mixture was then extruded and sintered. The physical size of the prototype sorbents was about 1/8 inch diameter by 1/8 inch long.

Of the five mixtures listed above only three are completely molten at 1200°F: the 50% Na_2CO_3/50% Li_2CO_3 mixture, the 70% Na_2CO_3/30% Li_2CO_3 mixture, and the 33% Na_2CO_3/33% K_2CO_3/34% $BaCO_3$ mixture. The 90% Na_2CO_3/10% Li_2CO_3 and the 95% Na_2CO_3/5% Li_2CO_3 mixtures are only 33% and 16% molten at 1200°F, respectively. The reason they were selected was because they have higher theoretical capacities for HCl removal and are less costly than the other sodium/lithium mixtures. The one concern was that they might be considerably less reactive because they are not completely molten.

The prototype sorbents were tested in a 1-inch OD fixed-bed reactor system as shown in Figure 6. The reactor was made of quartz and the tubing, condensors and heat exchangers external to the reactor were made of either teflon or vycor.

The tests were conducted at 1200°F and atmospheric pressure. A simulated fuel gas containing about 25% H_2, 25% CO, 20% CO_2, 30% H_2O, and 300 ppm(v) of HCl was used in all tests. The amount of sorbent used in each test was 40 grams and the fuel gas flow rate was fixed at 7.4 standard liters/ minute providing a space velocity of about 10,000 h^{-1} for all tests.

The results of the tests are shown in Figure 7. All five of the sorbents exhibited good reactivity toward HCl. As expected the sorbent containing the 50% Na_2CO_3/50% Li_2CO_3 mixture was the most reactive. It reduced the concentration of HCl in the simulated fuel gas from 300 ppm(v) to 0.06 ppm(v). However, it also has the lowest HCl removal capacity and is the most expensive of the five tested.

Of the five sorbents tested, the ones containing 95% Na_2CO_3/5% Li_2CO_3 and 33% Na_2CO_3/33% K_2CO_3/34% $BaCO_3$ are the most economical. Although they are not the most reactive, they have larger capacities and are less costly than the more reactive mixtures containing large concentrations of Li_2CO_3.

A summary of the projected costs for the five HCl removal sorbents is shown in Table 3. As can be seen, the 95% Na_2CO_3/5% Li_2CO_3 and the 33% Na_2CO_3/33% K_2CO_3/34% $BaCO_3$ mixtures decrease the cost of HCl removal via the IGT concept from \$7.63/lb of removed HCl to less than \$3.33/lb, a decrease of over 56%. However, even \$3.33/lb of removed HCl is still

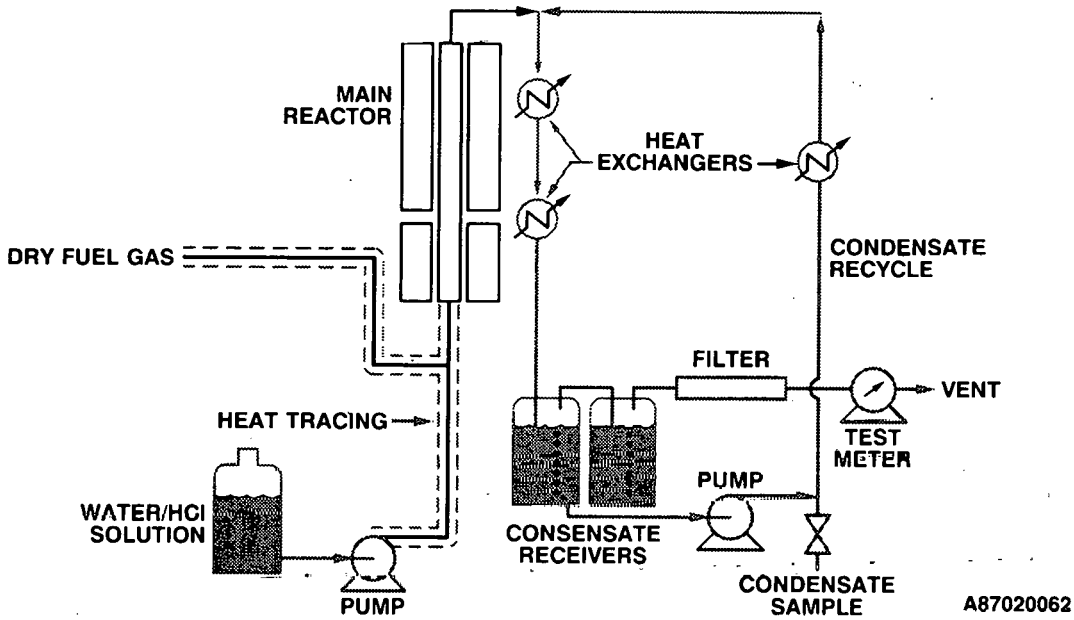

Figure 6. Laboratory-Scale HCl Removal Test Unit

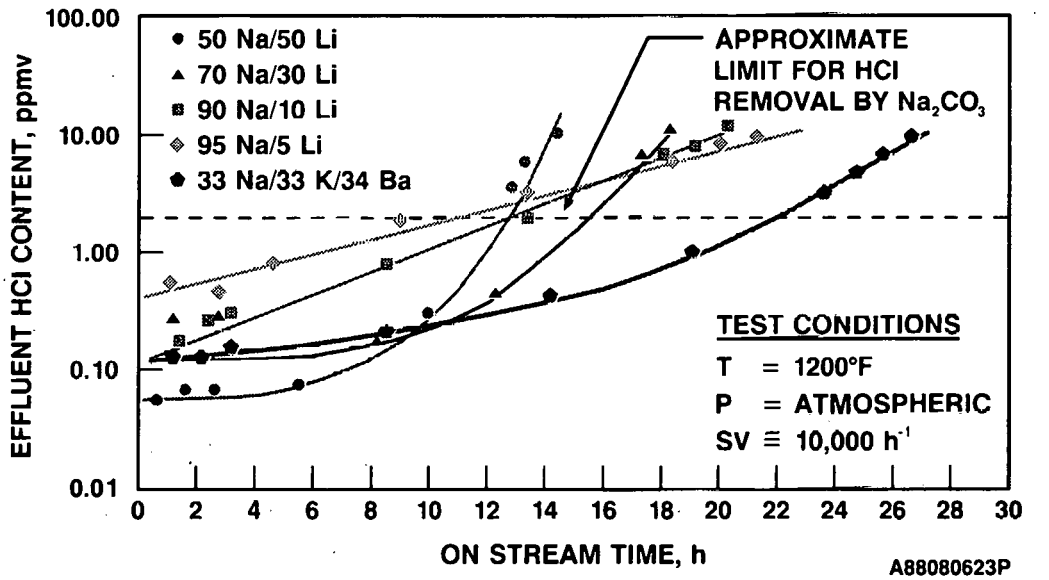

Figure 7. Hot HCl Removal Sorbent Breakthrough Curves

Table 3. Comparison of HCl Removal Costs by Prototype Sorbents

SORBENT MIXTURE	SORBENT COST $/LB	REMOVAL CAPACITY LB HCl/LB	PROCESS COST $/LB HCl
50% Na/50% Li	0.70	0.111	7.63
70% Na/30% Li	0.57	0.118	6.13
90% Na/10% Li	0.45	0.135	4.46
95% Na/5% Li	0.42	0.176	3.25
33% Na/33% K/34% Ba	0.50	0.196	3.33

probably larger than would be realized using a sorbent prepared from a naturally occurring sodium carbonate-containing material such as nahcolite. The one advantage that the IGT sorbent might have is its ability to remove other trace contaminants from the fuel gas that might prove deleterious to a gas turbine or a fuel cell, but this remains to be proved.

Construction of a Bench-Scale Hot Gas Cleanup Test Unit

The final major accomplishment during the past year has been the construction of an integrated bench-scale hot gas cleanup test unit for testing the IGT hot gas cleanup processes with actual coal-derived fuel gases. The unit, which is skid-mounted for easy transport, is presently attached to a 6-inch fluidized-bed gasifier located at IGT's Energy Development Center.

A simplified schematic diagram of the unit is shown in Figure 8. The unit is designed to handle up to 3000 SCF/h of hot coal-derived fuel gas at a pressure up to 300 psig and a temperature up to 1400°F. The unit contains a high temperature, high-pressure particulate removal system and provisions for testing a regenerable bulk sulfur removal sorbent such as the mixed metal oxide sorbents, a hot HCl removal sorbent and a trace contaminant removal sorbent.

The particulate removal system in the unit employs four silicon carbide candle filters. Each candle is 39 inches in length and 2.36 inches in diameter. The wall thickness of each candle is 0.39 inches and the average pore size is 3 microns. Each candle also has a separately actuated blow back line for cleaning.

For testing IGT's mixed metal oxide process, the unit contains a 20-inch OD, 6-inch ID, 107-inch high vessel which will house up to 1 cubic foot of sorbent. The inner tube is schedule 40, alonized Incoloy 800. Provisions for regenerating the sorbents are also included. Preheaters

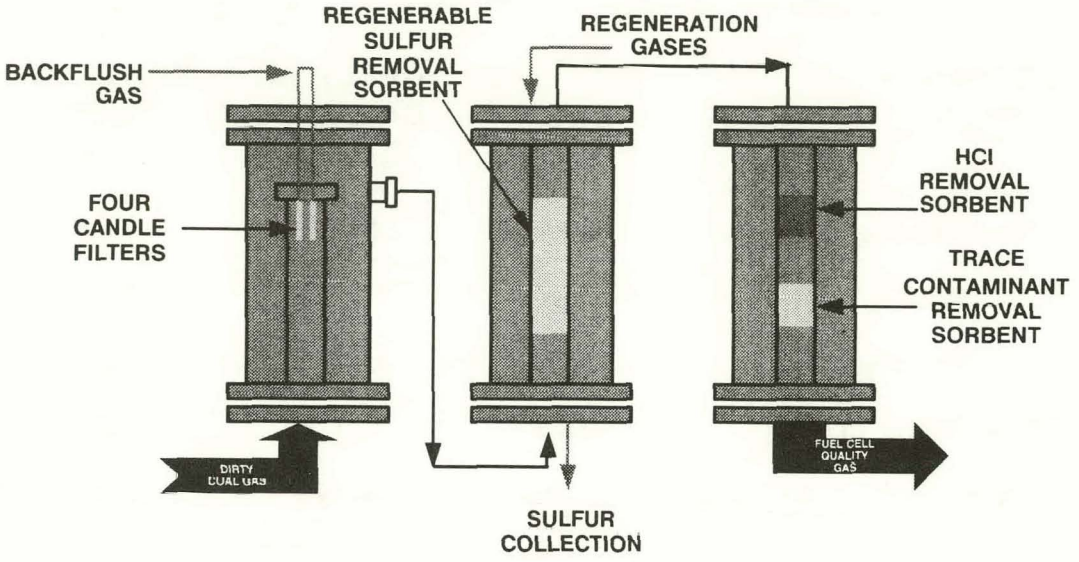

Figure 8. Simplified Schematic-Bench-Scale Hot Gas Cleanup Unit

and flow controllers exist for feeding O_2, SO_2, and N_2 to the sorbent bed and a two-stage elemental sulfur collection system is included for recovery of elemental sulfur from the product gas. However, no provision has been made to recycle SO_2 after elemental sulfur recovery. The SO_2 is supplied from cylinders containing liquid SO_2.

A separate 20-inch OD, 6-inch ID, 107-inch high vessel will house both an IGT hot HCl removal sorbent and a trace contaminant removal sorbent such as being developed by Energy Research Corporation, Danbury, Conneticut. The vessel will house up to 1/2 cubic foot of each material. In addition, a gas sample point between the two beds will permit independent assessment of the performance of each sorbent.

In addition to normal gas analysis points before and after each major operation, the unit has specially designed gas sampling points for monitoring alkali in the gas stream.

At present, most of the unit has been checked out, but some shakedown testing of the unit remains. It is anticipated that bench-scale testing could commence as early as September of this year.

7. FUTURE WORK:

During the remainder of this program, work that is planned includes 1) completing laboratory-scale studies on a new zinc oxide/zinc aluminate

sorbent for the mixed metal oxide process, 2) conducting bench-scale studies, and 3) updating the estimated cost of using the IGT processes in advanced power plant applications. After this program, plans are to continue to explore potential means of reducing the cost of IGT's hot gas cleanup technology and to continue testing the technology with simulated and actual coal derived-fuel gas to the extent possible. One of the greatest uncertainties in not only IGT's mixed metal oxide process, but other similar processes is the life of the sorbents. The cost of the process is highly dependent upon sorbent life and therefore this needs to be estimated with some reasonable precision for decision-making purposes. For example, extending the life of the sorbents in the mixed metal oxide process from 1 year to 2 years decreases the cost of the process by about 13%. Just the opposite occurs if the life of the sorbents is only 6 months rather than 1 year.

8. REFERENCES:

Anderson, G. L., et al., "Development of a Hot Gas Cleanup System for Integrated Coal Gasification/Molten Carbonate Fuel Cell Power Plants," Final report prepared for U.S. DOE/METC as an account of work performed under contract no. DE-AC21-82MC19403, Document No. DOE/MC/19403-1816, October 1985.

Blecher, W. A. and Robson, F. B., "Assessment of Fuel Gas Cleanup Systems." Paper presented at the 183rd National ACS Meeting, Division of Fuel Chemistry, 1984.

King, J. J., "Energy Conversion Alternatives Study — United Technologies Phase II Final Report." Report prepared for the National Aeronautic and Space Administration under NASA Lewis Research Center Contract NA53-29586, 1976.

Robson, F. B., "Comparison of Hot and Cold Gas Cleaning in Coal Gasification for Combined-Cycle Power Generation." Paper presented at the 183rd National ACS Meeting, Division of Fuel Chemistry, 1984.

Westinghouse R&D Center, "Evaluation of Gasification and Gas Cleanup Processes for Use in Molten Carbonate Fuel Cell Power Plants." Final report for the U.S. DOE/METC under contract no. AC21-81MC16220, 1983.

SULFUR RECOVERY FROM HOT COAL GAS DESULFURIZATION PROCESSES

1. CONTRACT NUMBER: DE-AC21-84MC21097

CONTRACTOR: The Ralph M. Parsons Company
100 West Walnut Street
Pasadena, CA 91124

PROGRAM MANAGER: Dr. J. B. O'Hara

PRINCIPAL INVESTIGATORS: Dr. J. B. O'Hara
T. K. Chow
J. E. Findley

METC PROJECT MANAGER: S. J. Bossart

CONTRACT PERIOD OF PERFORMANCE: October 1, 1984 to April 15, 1987

2. SCHEDULE/MILESTONES:

MILESTONE	DATE COMPLETED
Selected Preferred Technology	February 1985
Completed "Scouting" Reaction Tests	April 1985
Defined Experimental Test Plan	April 1985
Defined Experimental Test Facility	June 1985
Start of Experimental Program Authorized	October 1985
Experimental Program Ended	December 1986
Conceptual Design/Economic Evaluation Completed	April 1987
Final Report Draft Completed	April 1987

3. OBJECTIVE:

The project objective was to define the preferred technology and projected economics for recovery of salable elemental sulfur, in an environmentally acceptable manner, from regeneration offgases produced in hot coal gas desulfurization processes.

4. BACKGROUND STATEMENT:

A high potential version of the METC Hot Gas Cleanup Program consists of high temperature chemisorption of sulfur compounds on a chemically active solid sorbent such as zinc ferrite. The sulfided sorbent can be regenerated for reuse by contact with an air-diluent mixture at 1000-1350°F to produce a regenerator offgas containing 1.5 to 5.0 mole percent SO_2. For environmental reasons, this offgas must be processed to eliminate the SO_2 before being released to the atmosphere. This project defines procedures, and projected economics, for converting the SO_2 to salable elemental sulfur.

5. PROJECT DESCRIPTION:

Major project tasks included preferred process selection, experimental testing, conceptual designs and economic evaluation. The results of each of these activities are described below.

PREFERRED PROCESS SELECTION

Regenerator operation for a two-vessel fixed-bed hot gas desulfurization is quasi-continuous and can result in transients for offgas total flow rate and SO_2 concentrations. Fluidized bed or multi-vessel fixed bed configurations are examples of regeneration systems that will minimize such transients.

Sulfur recovery complexes containing three types of processing units were considered for treating the regenerator offgas. These included (1) SO_2 concentration/purification (C/P), (2) SO_2 reduction/sulfur production (R/P) and (3), tail gas treatment to ensure meeting environmental emission standards. Figure 1 depicts the production of elemental sulfur from regenerator offgas using these process units.

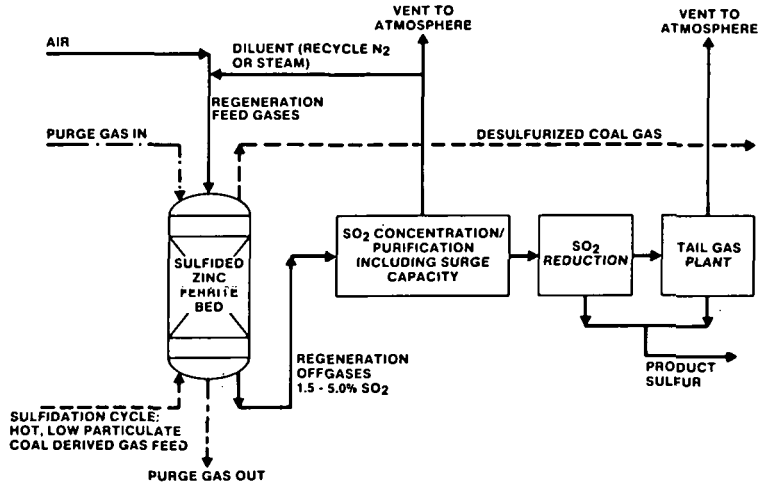

Figure 1. Primary Process Units, Sulfur Recovery from Regenerator Offgases.

The SO_2 C/P unit will significantly increase the SO_2 concentration and reject impurities prior to feed to the SO_2 reduction/sulfur production unit. It will also provide surge capacity between a quasi-continuous desulfurizer regenerator and a continuous sulfur producing plant.

Candidates were screened to define the preferred technologies to achieve the project objectives. The 11 candidates for SO_2 concentration/ purification, six for SO_2 reduction/sulfur production and five for tail gas treatment are listed in Tables 1, 2, and 3, respectively. These candidates can be combined in 300-plus combinations of regenerator offgas-to-sulfur configurations.

Table 1. SO_2 Concentration/Purification Process Candidates.

1. Wellman-Lord
2. Modified Citrate
3. Flakt-Boliden Citrate
4. Magnesia Slurry Scrubbing
5. Shell/Universal Oil Products Copper Oxide Adsorption
6. Westvaco Activated Carbon
7. Lugas
8. Bergbau Forschung, Dry Absorption Process
9. Union Carbide Amine Process (UCAP)
10. Ammonia-Ammonium Bisulfate (ABS)
11. Ionics Electrolyte Regeneration

Table 2. SO_2 Reduction/Sulfur Production Candidates.

1. RESOX
2. Allied
3. Beavon Sulfur Removal (BSR)/Stretford (BSRP)
4. Augmented Claus
5. Citrate
6. Phosphate

Table 3. Tail Gas Process Candidates.

1. BSR/Claus
2. BSR/Methyl/Diethyl Amine (MDEA)
3. BSR/Stretford (BSRP)
4. BSR Selectox
5. Incineration Plus Recycle Incinerate to SO_2 Concentration/Purification Process

The characteristics of each of the separate candidates were tabulated and analyzed using the Table 4 Process Selection criteria. Inputs to the tabulations included direct contact with process owners, literature searches using the DOE/RECON data base, and other published material. The analysis resulted in definition of a "short list" consisting of the 11 candidate configurations shown in Table 5. The short list included one SO_2 concentration/purification candidate, four SO_2 reduction/sulfur production candidates, and five tail gas candidates.

The Wellman-Lord SO_2 concentration/purification process was selected based on its performance characteristics and the experience gained from 30-plus commercial units. It absorbs SO_2 in an aqueous sodium sulfite solution to form sodium bisulfite, which in turn is decomposed in a double effect evaporator to liberate the SO_2 and regenerate sodium sulfite. Surge capacity can be supplied by storing the aqueous sodium bisulfite solution.

Table 4. Process Selection Criteria.

Factor	Weight, %
Process Simplicity	5
Reliability	12
Capability to Respond to Transient Operations	10
By-Product Credit	5
Environmental Factors Including Waste Disposal	15
Thermal Efficiency	5
Preferential Use of Coal as Energy Source and Raw Material in Preference to Oil or Natural Gas	5
Capital Costs	13
Operating Costs	12
Commercial Status	18
Total	100

SO_2 reduction/sulfur production candidates included RESOX, Allied, Beavon Sulfur Recovery Process (BSRP) and Augmented Claus. The RESOX reduction is accomplished by high temperature contact with coal, preferably anthracite. Allied uses high temperature catalytic reduction by methane. BSRP consists of catalytic conversion of all sulfur species to hydrogen sulfide (H_2S) followed by conversion of the H_2S to sulfur in a Stretford plant. The Augmented Claus Process consists of high temperature homogeneous reduction of SO_2 by synthesis gas (syngas) components H_2 and CO followed by additional sulfur production in a Claus unit. The Claus tail gas is incinerated to convert residual sulfur species to SO_2 and the incinerate is then recycled to the Wellman-Lord absorber.

Candidate process groupings 1, 2, and 4 shown in Table 5 each included Wellman-Lord SO_2 C/P units to concentrate/purify all of the SO_2 contained in the regenerator offgas prior to supply of the SO_2 feed to the reduction units. Because the BSRP unit can perform well with a dilute 1 percent SO_2 feed, the Case 3 unit contained a W-L point capacity capable of processing only 10 percent of the regenerator offgas (to minimize variations of feed concentrations to the downstream BSRP). Preliminary conceptual designs plus key heat and material balance factors were developed for each group.

Preliminary estimates were developed for fixed capital investments (FCI) and operating costs for each of the 11 short list candidate cases. A contingency was included for the FCI based on commercial experience, state of development, type of processing (e.g., gas, liquid, or solid processes) and the judged capability of the process owners to assure successful design and startup. Prior background data for pioneer plant performance developed by the Rand Corporation (Merrow 1981) were also used as guidelines to establish contingencies. A contingency was included to

Table 5. Summary of Eleven "Short-List" Configurations.

Candidate Process Grouping Number	Case No.	SO_2 Recovery/ Concentration Process	SO_2 Reduction/ Production Process	Tail Gas Process
1	1A	Wellman-Lord	RESOX	BSR/Claus
	1B	Wellman-Lord	RESOX	Recycle to W-L
	1C	Wellman-Lord	RESOX	BSR/MDEA
	1D	Wellman-Lord	RESOX	BSR/Stretford
2	2A	Wellman-Lord	Allied (2 Claus Stages)	None
	2B	Wellman-Lord	Allied (2 Claus Stages)	Recycle to W-L
	2C	Wellman-Lord	Allied (3 Claus Stages)	None
3	3	Wellman-Lord	Beavon Sulfur Removal (BSR)	Stretford
4	4A	Wellman-Lord	Augmented Claus	BSR/Selectox
	4B	Wellman-Lord	Augmented Claus	BSR/Stretford
	4C	Wellman-Lord	Augmented Claus	Recycle to W-L

recognize uncertainty associated with combining multiple separate plant units to form a sulfur recovery complex performing the three separate process functions illustrated in Figure 1.

Table 6 summarizes the relative rankings for FCI and operating costs for each of the candidate groupings. These preliminary economic estimate rankings were used as one input to the selection process.

Each of the ten Table 5 process selection criteria was independently assessed by three evaluators for each of the 11 short list candidates. The evaluation results were totaled. The results of these evaluations were reviewed to assess the consistency of the evaluation results with the data and perceptions generated during the course of the work. The results of the evaluation are summarized in Table 7.

Case 3 and 4C results were further compared. The preliminary estimates indicated that the Augmented Claus and BSRP technologies each offered potential for low cost sulfur production. The Case 3 technology is the more mature of the two, with more than 50 commercial plant credits.

The decision was made to experimentally investigate the Augmented Claus scheme (Case 4C) and develop subsequent conceptual design/economic evaluations for further comparison with the Case 3 BSRP technology.

Table 6. Rankings[1] for Fixed Capital Investment and Operating Costs, Short List Candidates.

Case No.	Battery Limits Fixed Capital Investment Including Contingency	Operating Cost
1A	8	8
1B	6	9
1C	11	11
1O	10	10
2A	3	4
2B	7	7
2C	5	5
3	4	1
4A	2	3
4B	9	6
4C	1	2

[1]Number 1 is estimated lowest cost and 10 is highest cost.

Table 7. Process Configuration Ratings. Reference: Table 5 Process Selection Criteria.

Ranking	Case	Relative Score
1	3	1.0
2	4C	0.90
3	4A	0.85
4	2B	0.81
5	2C	0.81
6	4B	0.80
7	1B	0.73
8	1A	0.73
9	1D	0.65
10	1C	0.62
11	2A	*

*Did not meet environmental limits

EXPERIMENTAL TESTING

Because 30-plus Wellman-Lord, 800-plus Claus, and multiple thermal incineration plants have been operated commercially, the Augmented Claus

(Case 4C) experimental tests were restricted to the SO_2 direct reduction step. Simulations of chemical reaction thermodynamic equilibrium results for reduction of SO_2 using variations in reaction parameters were developed and analyzed to guide experimental testing. Independent variables were concluded to be temperature, SO_2 concentration, mole ratio reductant/SO_2 (H_2+CO/SO_2), reductant composition (mole ratio H_2/CO), space velocity, pressure, and water concentration. The conclusion was to include the first five variables listed above in process optimization analysis. Simulation results indicated that the reaction yields and SO_2 conversion were insensitive to pressure over the 0 to 80 psig range. Results indicated higher sensitivity to feed moisture content; the intent therefore was to conduct tests with moisture content controlled over a narrow range to minimize its impact on the reaction.

Key dependent variables were judged to include percent SO_2 conversion, sulfur yield, H_2S yield, mole ratio H_2S/SO_2, H_2 conversion, and CO conversion. The H_2S/SO_2 ratio is important because the product of the direct reduction serves as feed to a Claus unit where additional sulfur is produced by the reaction:

$$2H_2S + SO_2 = 3/_2S_2 + 2H_2O \qquad (1)$$

A series of scouting experiments was conducted to determine (1) the ability of chemical reaction thermodynamic equilibrium simulation results to predict plant performance and (2) minimum reaction temperatures to achieve equilibrium. The experiments tested homogeneous, uncatalyzed reaction by injecting a syngas mixture into a continuous SO_2 stream. The target reaction variables were:

Temperature:	Variable over the range of 1200-1950°F (649-1066°C)
Reductant Ratio:	Mole Ratio H_2+CO/SO_2 = 2.0-2.3
Space Velocity (at standard conditions):	2000-3000 hr^{-1}
Reductant Composition Mole Ratio H_2/CO:	1.6
SO_2 Feed Concentration:	99 mole percent

Figure 2 is a sketch of the scouting test apparatus used by subcontractor Institute of Gas Technology (IGT). Thermocouples were used to monitor the temperatures of the feed gas streams and the reaction zone. Sulfur and water were removed in a packed condenser at the outlet of the reactor. Effluent gas was collected in a sample bomb that had been evacuated and filled with nitrogen. The gas samples were analyzed for SO_2, H_2, CO, CO_2, H_2S and COS. The composition of the reactor exit gas was calculated from carbon and sulfur balances based on the inlet gas feed rates and compositions plus composition of the dry effluent gas.

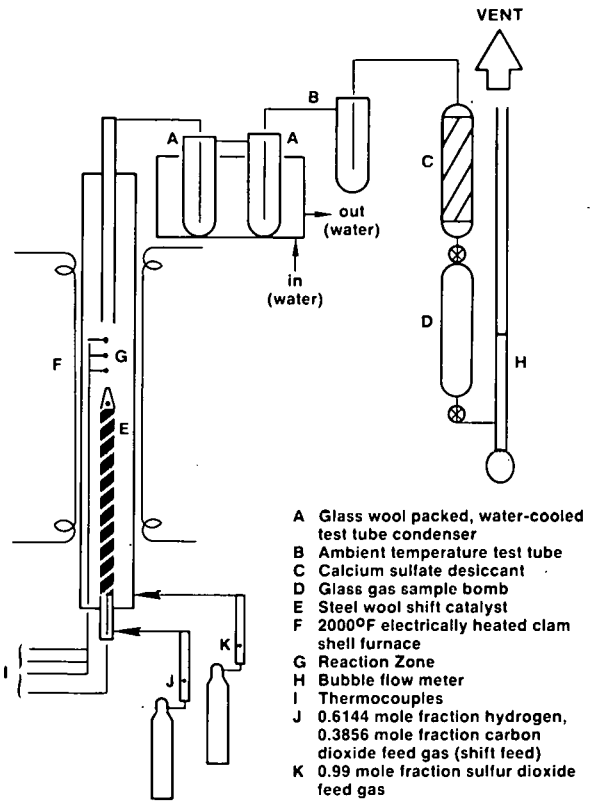

Figure 2. Sketch, Scouting Experiment Apparatus.

The equilibrium product compositions were calculated using the results of the reaction simulation model and the experimentally measured approach to equilibrium for SO_2 conversion expressed as

$$\frac{(C_{so_2})\ exptl}{(C_{so_2})\ equil}$$

Where: (C_{so_2}) exptl = Percent CO_2 conversion calculated from scouting experiment results.

(C_{so_2}) equil = SO_2 conversion predicted by chemical reaction thermodynamic equilibrium simulation.

The fractional approach to SO_2 equilibrium is shown in Figure 3. The results indicate that equilibrium conversion of SO_2 was achieved at 1950-2000°F (1066-1093°C) and that the approach to equilibrium drops to approximately 20% at 1200°F (649°C). At 1950°F (1066°C) the measured product concentrations of sulfur, H_2O and SO_2 coincided well with the predicted equilibrium, recognizing the nature of the experimentation. The comparisons, however, were less favorable for CO_2, H_2, CO, H_2S, and COS.

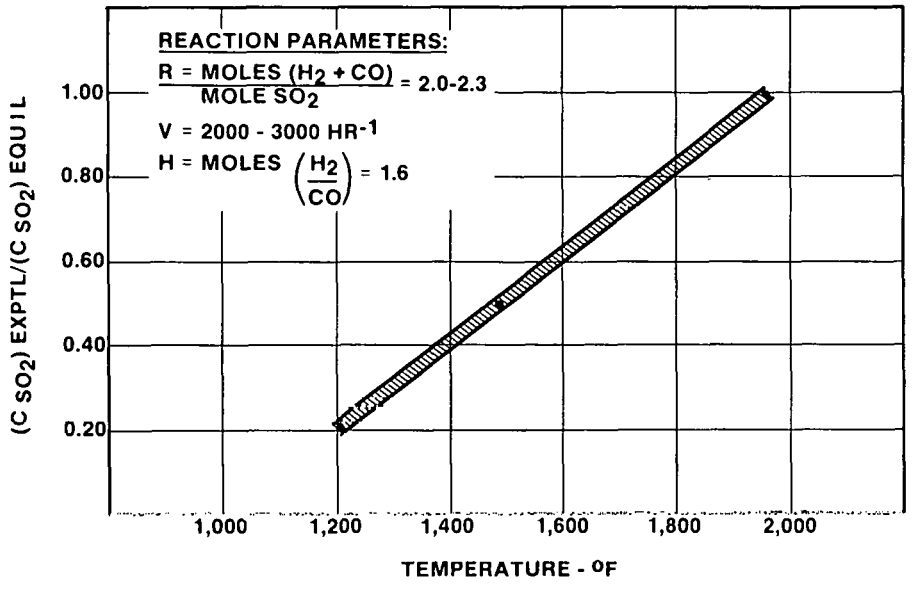

Figure 3. SO_2 Conversion Approach to Equilibrium as a Function of Temperature.

The indication that equilibrium conversion will be achieved at space velocities of 2000-3000 hr^{-1} and temperatures of 1950-2000°F, plus the availability of a computerized equilibrium reaction simulator, provided the basis for assessing industrial plant performance for the technology.

Subcontractor IGT also attempted to obtain experimental data for a half factorial experimental design to quantitatively define the effects of temperature, SO_2 concentration, space velocity, mole ratio reductant to SO_2, and mole ratio of H_2/CO on yields and conversions. Unfortunately, this attempt was unsuccessful, primarily because of materials of construction and material balance problems.

CONCEPTUAL DESIGNS

Conceptual designs were developed for the Case 4C Augmented Claus and Case 3 BSRP-based technologies to serve a 100 MW (megawatt) Molten Carbonate Fuel Cell Power Plant. Simplified block flow diagrams to illustrate the key process units are presented in Figures 4 and 5. Each of the designs included a Wellman-Lord unit. Key heat and material balance information and unit production capacities provided the basis for estimation of capital investment and operating requirements.

Preliminary designs and economic assessments were also developed for two modifications of the Case 4C configuration. The objective was to determine the impact of SO_2 C/P capacity on economics. The modifications consisted of:

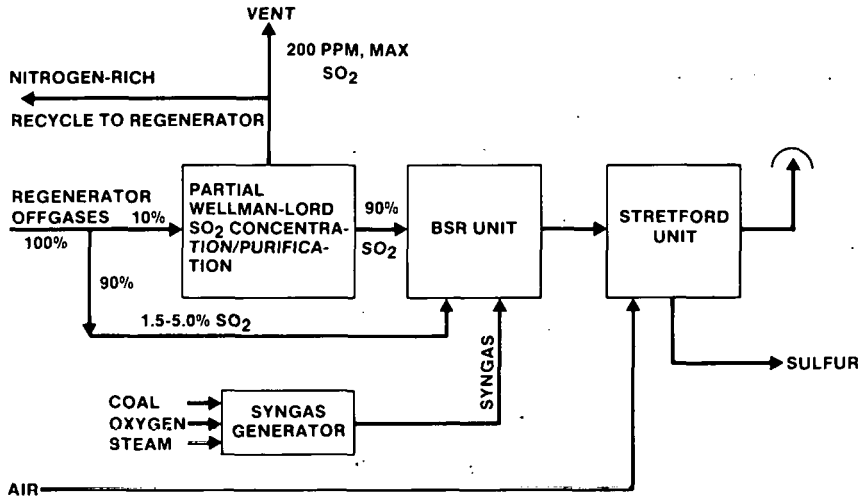

Figure 4. Block Flow Diagram, Case 3
BSRP-Based Plant.

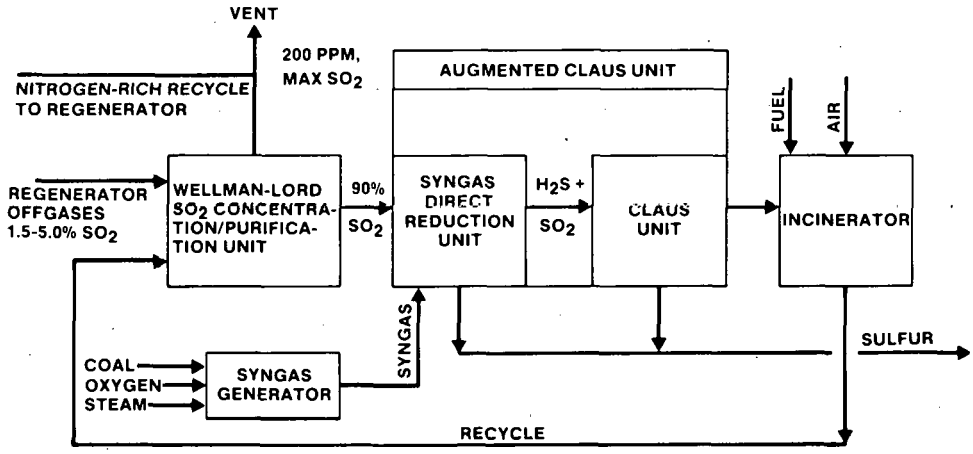

Figure 5. Block Flow Diagram, Case 4C
Augmented Claus-Based Plant.

1. Case 4C': Twenty-five percent of the regenerator offgas is processed in the Wellman-Lord C/P unit prior to feed to an Augmented Claus unit and incineration/recycle to a Wellman-Lord C/P unit. Seventy-five percent of the feed offgas by-passes the Wellman-Lord unit and is fed directly to the Augmented Claus unit.

2. Case 4C": The regeneration offgas is fed directly to the Augmented Claus unit. A BSRP unit treats the Claus tail gas before venting to the atmosphere.

ECONOMIC EVALUATION

Electric Power Research Institute (EPRI 1986) procedures were used to develop the economic evaluations. Key economic estimates generated included Levelized Busbar Costs (LBC), Total Capital Requirements (TCR) and Operating Costs (OC). The LBC reflects the contributions of both capital burdens and operating expenses to the estimated Mills/kWh costs to be incurred to incorporate the sulfur cleaning system in a coal gasification/electrical power production complex. Table 8 compares the LBCs, Capital Requirements, and operating costs for the two prime cases, 3 and 4C, as well as the Case 4C modifications 4C' and 4C".

Table 8. Economic Comparison.

Item	Case 3	Case 4C	Case 4C'	Case 4C"
10-Year Levelized Busbar Cost, $\frac{\text{Mills}}{\text{kWh}}$	19.3	24.3	24.0	18.7
Process Capital - $/kW	147.0	208.0	238.0	200.0
Total Capital Requirement - $/kW	280.0	374.0	424.0	376.0
Fixed Operating Cost, 1st Year $\frac{\$}{\text{kW-Yr}}$	9.6	12.7	16.7	12.3
Net Variable Operating Cost, 1st Year $\frac{\$}{\text{kW-Yr}}$	32.5	36.7	24.6	12.8
Total Net Operating Cost $\frac{\$}{\text{kW-Yr}}$	42.1	49.5	41.2	25.1

The LBCs are essentially equal for the BSRP (Case 3) and the Augmented Claus receiving its feedstock directly from the desulfurizer regenerator (Case 4C"). The estimated total capital requirement for the BSRP is 25 percent lower than for Case 4C" while the total net operating costs are about 65 percent higher.

The BSRP LBC is 25 percent less than that of the Case 4C Augmented Claus which includes a full-capacity Wellman-Lord Plant.

6. RESULTS/ACCOMPLISHMENTS

1. Procedures have been defined for production of elemental sulfur from the SO_2 content of desulfurizer regenerator offgas.

2. BSRP and Augmented Claus were defined as preferred technology for production of elemental sulfur from regenerator offgas.

3. Experimental data was obtained indicating that the homogeneous uncatalyzed reduction of SO_2 by synthesis gas components achieves chemical reaction thermodynamic equilibrium at temperatures in the range of 2000°F at atmospheric pressure.

4. The economics of production of sulfur from regenerator offgas has been estimated using Electric Power Research Institute procedures. Estimated costs are in the 15-25 mills/kWh range.

5. A procedure for selection of preferred technology from multiple candidates was defined and implemented.

6. An experimental design to define the effect of five independent variables on dependent variable results such as yields and conversions was developed. Methods of analyzing and correlating the data were described.

7. Limited test results indicate that alonized stainless steel may be a satisfactory material of construction for reduction of SO_2 by syngas at temperatures and pressures in the range of 2000°F and near-atmospheric pressure, respectively.

7. EVALUATION OF POTENTIAL FUTURE PLANS

There are no current plans to continue or extend this METC-sponsored project.

8. REFERENCES

EPRI. Tag™: Technical Assessment Guide, Volume 1, EPRI P-4463-SR. Palo Alto: Electric Power Research Institute, 1986.

Merrow, E. W., et al. Understanding Cost Growth and Performance Shortfalls in Pioneer Process Plants. Santa Monica: The Rand Corporation, 1981.

KRW Process Development Coal Gasification/Hot Gas Cleanup

Contract Number:	DE-AC21-84MC21063
Contractor:	KRW Energy System, Inc. Madison, Pa. 15663-0334 (412) 722-6033
Contractor Project Manager:	Dale K. Schmidt
Principal Investigators:	Kevin J. Smith Gaurang B. Haldipur Jim L. Lucas
METC Project Manager:	Justin L. Beeson
Period of Performance:	August 1, 1984 through September 30, 1987

1.0 Schedule/Milestones

External desulfurization testing with zinc ferrite has been conducted at KRW since July of 1986. To date four tests have been completed and four additional tests are scheduled for the rest of 1987. A variety of test conditions have been studied as outlined below:

- Fixed bed geometries,
- Space velocity/linear velocity effects,
- Inlet sulfur gas concentration effects,
- Dust loading impact on pressure drop and sorbent utilization,
- Recycle and gasifier disposal of regeneration tail gas, and
- Control of zinc ferrite regeneration.

All testing has utilized zinc ferrite extrudate material manufactured by United Catalysts, Inc. Testing yet to be done in 1987 will continue with external desulfurization in the polishing mode, evaluate upstream filtration of fines, demonstrate the recycling of zinc ferrite regeneration tail gas to the in-bed gasifier to consume SO_2, and evaluate the use of zinc ferrite pellet material manufactured by AMAX. The ultimate goal is to show 99.9% desulfurization with removal of sulfur from the integrated system through the ash/spent limestone withdrawal stream of the gasifier.

2.0 Objectives

The goal of the technology development at KRW is to provide the electric utility industry with an advanced technology for integrated combined cycle power plants that has a low installed cost, a competitive heat rate and cost of electricity, and superior environmental acceptability and can be added in managable increments. The specific objectives of the Waltz Mill Process Development Unit (PDU) operation are: 1) to demonstrate operability of two complementary hot gas sulfur removal systems: gasifier "in-bed" desulfurization with a once-through calcium based sorbent and "external bed" desulfurization utilizing a regenerable zinc ferrite sorbent, 2) to demonstrate hot particulate collection/removal technology, and 3) to characterize levels of particulate, ammonia, alkali, and sulfur emissions from coal gasification as necessary to meet the requirements for power generation and environmental standards.

3.0 Background Statement

The KRW technology is a fuel island concept consisting of a second generation fluidized bed gasification process operating in an air-blown mode with hot gas integrated desulfurization and hot gas particulate cleanup followed by a combined cycle power block. Integrated desulfurization couples the benefits of in-bed desulfurization (limestone addition to the gasifier bed) with the polishing capability of an external bed of zinc ferrite sorbent. These types of plants are targeted to achieve a 30 percent lower electricity cost than conventional coal plants with flue gas desulfurization (Pitrilo, 1986).

4.0 Project Description

The KRW gasification process is a pressurized fluidized bed operating at temperatures upto 2000 °F. Coal (-6 mesh), limestone, and air are fed into the bottom of the gasifier through a central feed tube while agglomerated ash, spent sorbent, and sulfur are removed at the gasifier bottom. Figure 1 is an illustration of the integrated the KRW process development unit as it currently exists.

Coal is rapidly devolatilized in the gasifier combustion zone and the residual char is gasified by steam in the upper region of the fluidized bed. The sorbent mixes with the char in the fluidized bed. Depending on gasifier conditions the calcium based sorbent can calcine from carbonate to oxide. Hydrogen sulfide produced during the gasifiication process, reacts with the calcium oxide (or carbonate) to form calcium sulfide. The coal ash undergoes partial melting and sintering in the combustion region causing fine ash particles to agglomerate. The calcium sulfide mixes with the agglomerated ash near the bottom of the fluidized bed where this mixture is defluidized, cooled, and removed through a rotary feeder. The spent sorbent can be oxidized after removal from the gasifier vessel to form a sulfated material for conventional landfill.

During integrated desulfurization operation, 70 to 95% of the sulfur cleanup is accomplished with the calcium based sorbent in the gasifier bed. Hot particulates are captured with a cyclone and recycled to the gasifier through a dip-leg and non-mechanical valve assembly. Indirect cooling of the product gas exiting the gasifier with water jacketed piping for control of deposition has been discontinued. However, temperature limits of particulate removal devices downstream of the primary cyclone require cooling of the product gas to between 1200 and 1300 °F. This is accomplished with direct injection of liquid water immediately downstream of the primary cyclone at an appropriate rate to achieve the necessary inlet temperature for the secondary particulate removal device. The secondary fines removal device can be either a barrier filter or a high efficiency cyclone. The fines collected by the secondary collection device are quenched by a venturi scrubber and removed from the system and dewatered by a filter press.

The balance of sulfur removal occurs in the external bed of zinc ferrite sorbent. The regenerable dry sorbent of zinc ferrite provides the capability of removing virtually all of the sulfur compounds at gas temperatures from 1000 to 1200 °F. Hot and clean fuel gas can can be delivered from the the fuel island that is well below environmental emission and turbine limits. Regeneration tail gas from a regenerating bed of zinc ferrite is recycled to the gasifier where sulfur compounds in the tail gas are removed by the limestone. This combined feature allows the degree of sulfur removal to be tailored to site specific attainment requirements.

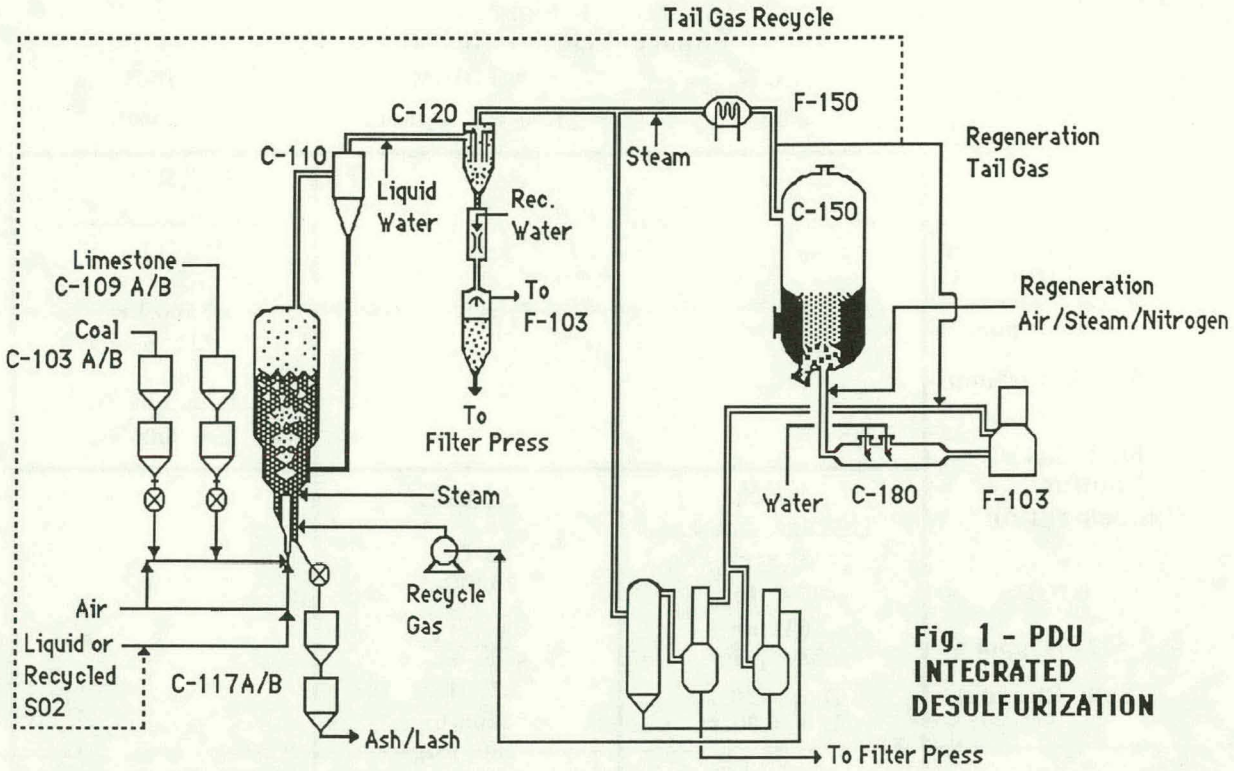

Fig. 1 - PDU INTEGRATED DESULFURIZATION

Reaction chemistry for the two desulfurization processes are well documented and can be reviewed in the attached references.

5.0 Results/Accomplishments

5.1 Technology Issues (External Desulfurization)

Technology issues for both bulk and polishing modes of desulfurization which are to be addressed by large scale testing of zinc ferrite are 1) sulfur removal potential, 2) sulfur sorption capacity at sulfur breakthrough (200 ppm), 3) tolerance for dust, 4) avoidance of sorbent phase transformation, and 5) gas contacting and temperature distribution effects. Technology issues surrounding air/steam rgeneration of sulfided zinc ferrite are: 1) efficiency of sorbent regeneration, 2) byproduct sulfate formation and handling techniques, 3) regeneration tail gas disposal in the gasifier, and 4) accumulated fines removal and/or consumption .

To date five cycles (one cycle is defined as one sulfidation and one regeneration) over four tests have been conducted with external bed desulfurization since July of 1986. A total of 600 hours of operation (sulfidation and regeneration) has been accumulated on the the external desulfurizer using zinc ferrite manufactured by United Catalyst, Inc. Two different fixed bed geometries, 4.5 ft. ID by 6 ft. long and 2 ft. ID by 6 ft. long, have been used which resulted in gas hourly space velocity (GHSV) of 800 hr^{-1} and 3600 hr^{-1} respectively. Fresh zinc ferrite sorbent was charged to the external desulfurizer after the reactor volume was reduced. Both space velocities where achieved using full net product gas flow from the gasifier. Other variations of conditions include primary desulfurization (total inlet sulfur concentration ≈ 4000 ppm), polishing sulfidation (total inlet sulfur concentration ≈ 1000 ppm), and inlet gas with and without fines loading.

Figure 2 is a test matrix of KRW testing of fixed bed desulfurization using zinc ferrite compared to other bench and pilot scale work with respect to varying GHSV over a range of inlet sulfur concentration of the inlet gas.

Figure 2
Space Velocity (SCFH/Cu. Ft.)

Fuel Gas Sulfur Concentration	LOW < 1000	MEDIUM 1000 < X < 2000	HIGH > 2000
LOW < 1500 ppm (Polish Cleanup)			**KRW (Runs 4 & 5)** .08 - .12% S 1.2 fps 3600/hr 230 psig D = 2.00 ft. L = 6.00 ft.
HIGH > 1500 ppm (Bulk Cleanup)	**KRW (Runs1,2,&3)** .25 - .45% S* 0.26 fps 641/hr 230 psig D = 4.50 ft. L = 6.00 ft.	**AMAX** 1.0 % S 3 fps 2000/hr **METC** .5 - .9% S .23 fps 2000/hr 280 psig	

Other variations of testing, not illustrated by the test matrix , have also been investigated and concern inlet fines loading to zinc ferrite and recycle of regeneration tail gas back to an "in-bed" gasifier. Table 1 summarizes those variations of operation conducted to date with zinc ferrite desulfurization.

Table 1 - Summary of External Bed Desulfurization Configuration

Test	Date	Bed Geometry	Desulfurization Mode	Particulate Cleanup	Tail Gas Recycle
TP-37-1	7/86	4.5' Dia by 6'L	Bulk	Sintered Metal Filter	No
TP-37-2	9/86	4.5' Dia by 6'L	Bulk	Sintered Metal Filter	No
TP-37-3	12/86	4.5' Dia by 6'L	Bulk	High Efficiency Cyclone	Yes
TP-37-4	4/87	2.0' Dia by 6'L	Polish	High Efficiency Cyclone	Yes
TP-37-5	6/87	2.0' Dia by 6'L	Polish	Ceramic Candle Filter	Yes

5.2 Desulfurization Performance

Gas cleanup potential of zinc ferrite in the PDU has been clearly demonstrated with achievement of near equlibrium concentrations of H_2S and COS (<10 ppm) in the exit gas. The larger fixed bed volume was designed for bulk desulfurization of air-blown produced gas assuming ultimate sulfur loading of the zinc ferrite in excess of 25 wt.%. Breakthrough time for the design condition was estimated to be ~90 hours. Breakthrough of sulfur was not achieved during the first two cycles due to upstream particulate removal limitations, however, desulfurization performance in terms of lowest concentration of H_2S and COS exiting zinc ferrite was achieved. Actual maximum sulfur sorption capacity of the sorbent was measured in excess of 30 wt. % during cycle 3. Although cycle 3 had similar GHSV to previous cycles it was the first to allow a small amount c fines loading in the inlet gas to reach the fixed bed. The pressure drop steadily increased throughout the sulfidation run. H_2S and COS concentration of the gas exiting the desulfurizer was slightly higher than

experienced during the previous two cycles. The Figure 3 illustrates H_2S concentration of the gas exiting the desulfurizer as well as at the reactor center line and wall with respect to time. After about 60 hours into the run, the reaction front can be clearly seen to pass through the elevation where the centerline and wall measurements are located (~2/3 of the length of bed).

Figure 3
TP-037-3
Desulfurization Run #3
C-150 H2S Concentration

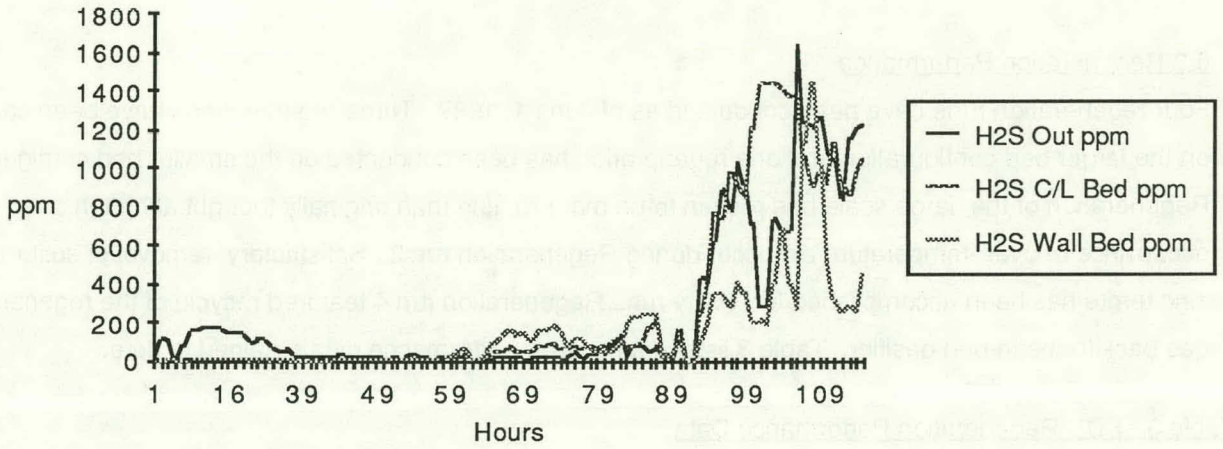

Prior to Desulfurization run 4, the external desulfurizer reactor volume was reduced and fresh zinc ferrite sorbent was charged to the vessel. Desulfurization runs 4 and 5 were conducted with absolute gas flowrates similar to run 3 but with two significant differences. First, fuel gas produced from an in-bed gasifier/desulfurizer was supplied to the external desulfurizer and therefore had significantly lower H_2S and COS concentrations. Second, in anticipation of the lower sulfur loading of the inlet gas, the fixed bed volume was reduced such that the diameter was reduced to 2 feet in diameter while maintaining a 6 feet bed height. The consequence of these changes were increased superficial velocity, increased GHSV, and increased pressure drop across the bed. This operating condition resulted in significantly shorter breakthrough times, poorer desulfurization performance, and lower measured sulfur loading of the zinc ferrite after breakthrough occurred (~19 wt. %). Subsequent testing will attempt to isolate potentially confounding effects of fines accumulation in the fixed bed (which may cause gas bypassing) from increased superficial velocity and GHSV.

Table 2 is a summary of desulfurization performance obtained to date from zinc ferrite testing on the PDU.

Table 2 - PDU Desulfurization Performance Summary

Desulfurization Run	1	2	3	4	5
Max. S Loading , wt.%	N/A	29	31	N/A	19
Radial Temp. Gradient ,°F	275	300	560	100	200
Axial Temp. Gradient, °F	75	50	100	70	50
Gas Inlet Temp. ,°F	1075	1050	1160	1060	1090
GHSV, hr^{-1}	565	788	794	2800 - 3600	1900 - 3300
Superficial Vel., fps	0.17	0.256	0.25	0.83 - 1.25	0.6 - 1.2
ΔP, psi	1.1	0.8	2.94 - 6.56	1.22 - 5.4	1.55 - 6.14
Operating Pressure, psi	223	210	230	221	190
(H_2S+COS) inlet, ppm	3500	3500	3900	650 - 1200	800 - 1300
(H_2S+COS) outlet, ppm	11 - 20	2 - 10	20 - 40	54 - 200	52 - 200
Duration, hours	47	80	116	31	37

N/A = Not Available

5.3 Regeneration Performance

Four regeneration runs have been conducted as of June 1, 1987. Three regenerations have been conducted on the larger bed configuration and one regeneration has been conducted on the smaller bed configuration. Regeneration of the large scale has proven to be more routine than originally thought although one occurrance of over -temperature did occur during Regeneration run 3. Satisfactory removal of sulfur from the zinc ferrite has been accomplished for every run. Regeneration run 4 featured recycle of the regeneration tail gas back to the in-bed gasifier. Table 3 lists regeneration performance data obtained to date.

Table 3 - PDU Regeneration Performance Data

Regeneration Run #	1	2	3	4
ΔT Rise, °F	75	400	336	350
Inlet Gas Temperature, °F	1075	940	1024	1000
Pressure, psig	223	245	230	245
O_2 Conc. Inlet, Vol. %	0 - 0.6	0.8 - 2.6	1.0 - 2.6	1.0 - 2.0
Duration, hours	75	42	144	28

Although steps were taken to minimize iron sulfate formation during regeneration by limiting oxygen concentration of the inlet gas to 2 volume %, there is evidence of its existence after regeneration is completed. Initiation of the subsequent sulfidation run revealed reduction of iron sulfate which produces SO_2 and generates heat due to the exothermic nature of this reaction and the reduction of hematite to magnetite. The Figures 4 and 5 illustrate the increased production of SO_2 and resulting increased temperature respectively which occurred in the transition from Regeneration run 4 to Desulfurization run 5.

5.4 Consumption of Simulated Recycle SO_2 by the In-Bed Gasifier

Two set points conducted during TP-037-4 demonstrate consumption of controlled amounts of synthetic SO_2 fed to the in-bed gasifier/desulfurizer . The conditions were chosen to simulate recycle of tail gas from a regenerating bed of zinc ferrite which contain primarily SO_2 and steam. Preliminary estimates from these runs indicate that about 88 % of the "recycled" SO_2 was consumed by the in-bed gasifier. Table 4 lists preliminary

data obtained from these two set points.

Table 4 - Preliminary SO_2 Consumption Data from TP-37-4

Set Point	Sulfur(from SO_2) (lbs/hr)	Sulfur (Coal) (lbs./hr)	Total Sulfur In (lbs./hr)	Total Sulfur Out(gasifier exit) (lbs./hr)
1A	0	24.33	24.33	7.6
1B	9.97	24.33	34.30	8.8

Figure 4
TP-037-4
SO2 Stack Emission
Beginning of Desulfurization #5

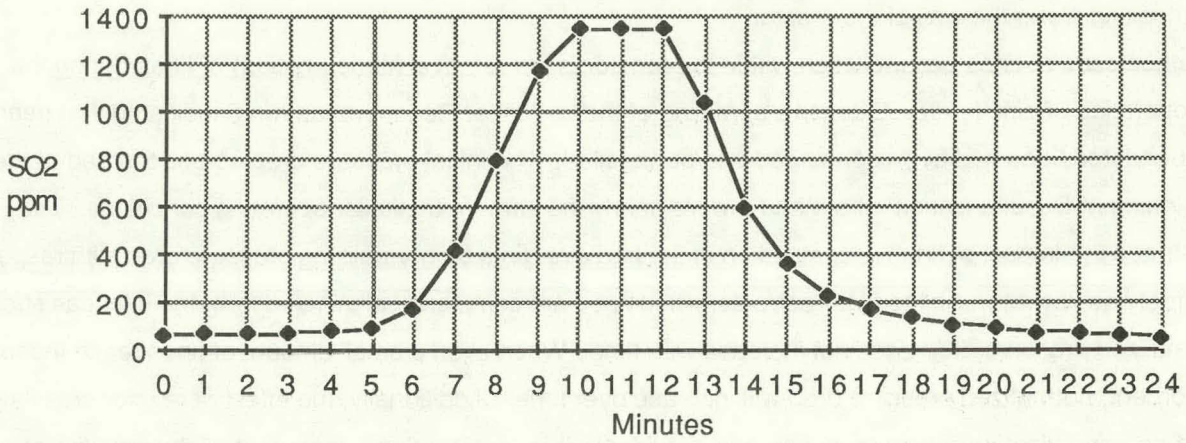

Figure 5
TP-037-4
Temperature Rise of Sulfate/Hematite Reduction
Beginning of Desulfurization #5

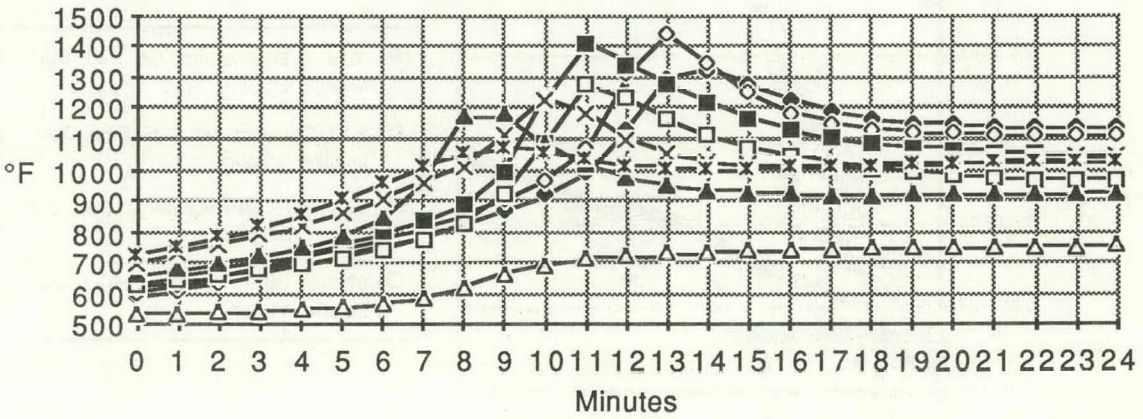

5.5 Impact of Fines Accumulation

As previously mentioned, Desulfurization runs 3 through 5 were conducted with a high efficiency cyclone used as the upstream particulate clean-up device instead of a sintered metal barrier filter. In this mode of operation the fines loading of the fuel gas supplied to the external desulfurizer was around 6 grains/ACF or 9 ppm. Isokinetic sampling upstream and down stream of the desulfurizer indicate that most of the fines blow through the sorbent bed. However, continuously increasing pressure drop across the fixed bed indicate that fines accumulation is occurring. The rate of increase in pressure drop is not alarming but is steady. In Desulfurization run 3 with the larger reactor diameter the rate of increase in pressure drop was much slower and there appeared to be little if any impact on desulfurization performance. Because Desulfurization runs 4 and 5 were conducted with an 80% smaller reactor cross-sectional area, pressure drop increased at a faster rate than in previous runs. What is not clear at this point is the relative contribution of fines accumulation in the packed bed to the poorer desulfurization performance of the latter two runs. Gas chromatograph sampling of the centerline of the middle section of the fixed bed reacor indicated much lower H_2S and COS concentration than that of the fuel gas which had exited the reactor. Our preliminary assessment is that about 10 to 20 % of the fuel gas is channelling along the wall of the reactor.

Another issue of fines accumulation within the reactor is the removal (consumption) of fines during the regeneration of zinc ferrite. Extensive sampling of the bed after Regeneration run 3 indicated that nearly all of accumulated fines had been consumed and/or expelled. The initial pressure drop across the bed at the beginning of Desulfurization runs 4 and 5 were nearly the same with similar operating conditions. The Figure 6 illustrates the impact of fines accumulation in the bed over time by normalizing pressure drop with respect to the fuel gas flowrate. As the plot illustrates, when fines are completely eliminated from the inlet gas stream the normalized pressure drop does not increase with time. When even a small amount of fines reach the fixed bed of sorbent, normalized pressure drop will increase over time. Additionally, the effect of reactor cross-sectional area on normalized pressure drop increase is evident. It is encouraging to note that all the desulfurization runs begin at around the same normalized pressure drop. This indicates that fines removal took place to a significant degree during the previous regeneration.

Figure 6
Effect of Fines Loading on Normalized Pressure Drop in ZnFe System

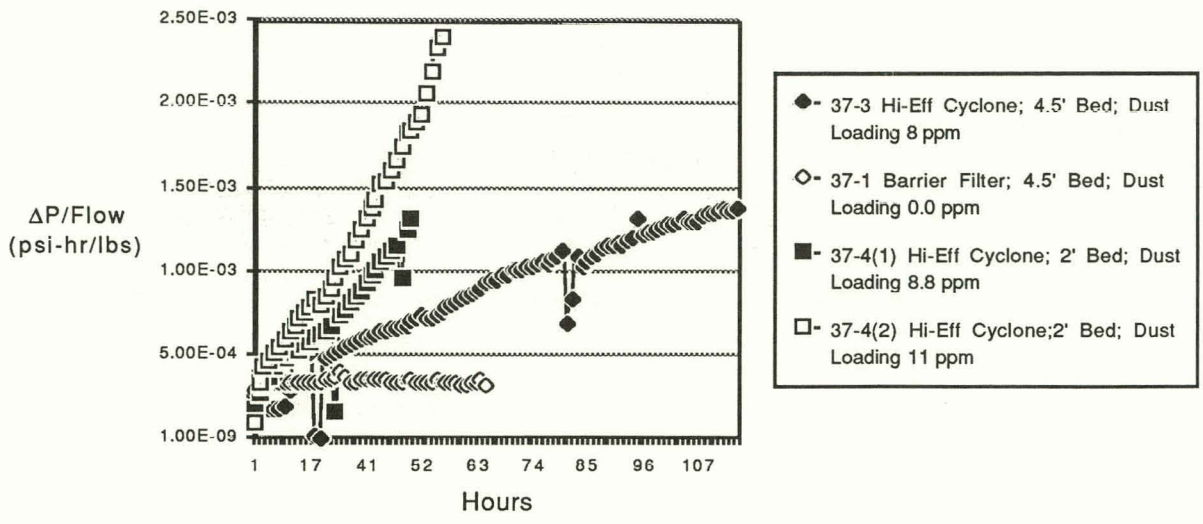

6.0 Future Work

Future work in this contract will involve characterization of an alternate zinc ferrite sorbent (AMAX) especially in the polishing mode, assess polishing mode desulfurization with no fines loading in the inlet fuel gas, trace component analysis of fuel gas exiting zinc ferrite desulfurization, and investigate transient behavior of the integrated gasification/desulfurization system. This will involve four additional tests to be conducted in CY 1987.

8.0 References

Rath, Larry K. and Smith, Kevin J., August 1987, 22nd IECEC Conference , Advanced Coal Gasification Combined-Cycle Generation Using the KRW Gasifier-Recent Pilot Plant Results and Commercialization Efforts.

Schmidt, D. K., et al, June 1986, Sixth Annual DOE Gasification Contractors Meeting, DOE/METC-86/6043, pp. 255 - 264.

Pitrilo, A. A., February 1986, Keystone Energy Futures Project, U.S. Department of Energy, Morgantown Energy Technology Center, A View of the Future Technical Choices of the Utility Industry -- Power and Fuel Mix Alternatives.

DESIGN STUDIES FOR HOT GAS CLEANUP SYSTEM IN A LOAD FOLLOWING MODE

1. CONTRACT NUMBER — DE-AC21-86MC22247

CONTRACTOR: — General Electric Corporate Research and Development
Schenectady NY 12301
(518) 387-6413

CONTRACTOR PROJECT MANAGER: — Daniel P. Smith

PRINCIPAL INVESTIGATORS: — Dr. Eli Gal
Dr. Charles S. Cook
Anthony H. Furman

METC PROJECT MANAGER: — S.J. Bossart

PERIOD OF PERFORMANCE: — August 26, 1986 to August 25, 1987

2. SCHEDULE/MILESTONES

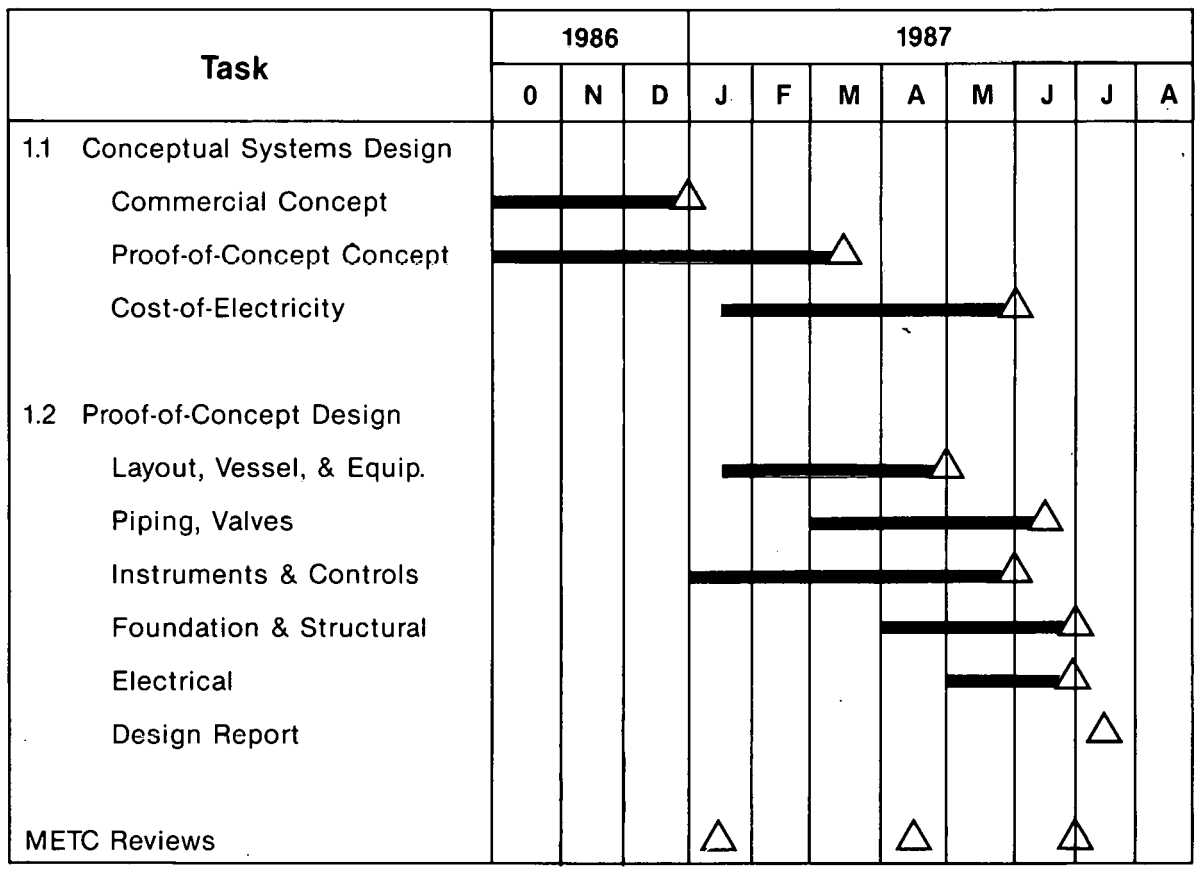

3. OBJECTIVES

The objective of this project is to apply hot gas desulfurization technology to a simplified IGCC system operated in a load following mode. "Simplified IGCC" refers to an electric power generation system consisting of a fixed bed, air blown, dry ash coal gasifier, hot fuel gas desulfurization, and a steam-injected aircraft-derivative gas turbine (Cook 1987). This system has been shown to offer significant reductions in complexity and cost over conventional IGCC systems while providing plant heat rates of less than 9500 Btu/kWh (Corman 1986). A conceptual system design has been developed for a commercial-scale 50 MW electric power generation system based on the simplified IGCC concept. An adaptation of the hot gas desulfurization portion of that design is being developed for installation on an existing air-blown fixed bed gasification facility for proof-of-concept testing. The design characteristics to be evaluated in the proof-of-concept system test include:

- Operation at gasifier pressure and temperature (300 psia, 1100°F).
- Achievement of greater than 90% overall sulfur removal efficiency.
- Reduction of particulate concentration to levels acceptable for gas turbine and NSPS requirements.
- Minimization of net consumption of sorbent material.
- Production of an SO_2-rich regeneration tail gas stream that can be economically treated.
- Demonstration of projected economical operation in a commercial-size system.
- Generation of a database for a commercial-scale system design.

The design includes a complete engineering package for construction of the proof-of-concept system including process flow diagrams, vessel designs, piping and instrumentation diagrams, general arrangement drawings, and equipment specifications. Design studies will address the impact on the cost-of-electricity of this design concept by comparison to previous studies of other coal-to-electricity systems.

4. BACKGROUND

Fuel gas derived from medium- to high-sulfur coals contains 1000 to 6000 ppm of sulfur compounds, mainly in the form of H_2S and COS. These compounds react with metal oxides (MO) under reducing conditions to form metal sulfides (MS):

$$MO + H_2S \rightarrow MS + H_2O. \quad (1)$$

The metal sulfides can be regenerated in a reaction with oxygen to form metal oxides and sulfur dioxide:

$$MS + 1.5O_2 \rightarrow MO + SO_2. \quad (2)$$

The sulfur dioxide can then be treated separately to produce elemental sulfur, sulfuric acid, or a disposable or saleable calcium sulfate. Depending on the metal oxide and the regeneration conditions, the oxidation may be accompanied by some undesirable metal sulfate formation:

$$MS + 2O_2 \rightarrow MSO_4. \quad (3)$$

In the early 1970s DOE-METC began developing, in their programs and those of their contractors, the use of various metal oxides for the process of desulfurization of hot coal-derived fuel gas. Initially iron oxide was chosen as the most promising because of its low-cost, high sulfur loading capacity and high sulfur removal efficiency. A systems evaluation study on the use of fixed beds of pelletized iron oxide in a 500 MW_e IGCC power plant was conducted by Air Products Company under DOE contract (Joshi et al., 1979). The study assumed reduction of H_2S to below 600 ppm (80 to 90% removal) and found hot gas cleanup feasible and economical for the assumptions used.

A process based on high-temperature cleanup using pulverized iron ore has been developed in Japan by IHI (Sugitani et al., 1985). In the IHI process the sulfur from a 900°F coal gas is absorbed in a two-stage fluidized bed where 95% removal efficiency is achieved. Regeneration is done in a separate two-stage fluidized bed using diluted air as the regeneration gas.

As moisture content of the gas increases, sulfur removal efficiency of iron oxide decreases to an unacceptable level. In the early 1980s, a mixed metal oxide (zinc ferrite, $ZnFe_2O_4$) replaced iron oxide as a leading hot desulfurization sorbent because of its ability to yield high sulfur removal efficiency regardless of the moisture content of the coal gas. The search for superior sorbents continues, and the possible use of oxides of copper, aluminium, molybdenum, titanium and others is being examined.

A system that includes a moving bed absorber and a moving bed regenerator containing a regenerable zinc ferrite in the form of cylindrical or spherical pellet sorbent is the basis for the present design work. The system design can be suitable, with minor modifications, for other metal oxides as well. The attractive features of zinc ferrite for use as a sorbent material for air blown gasifier fuel gas desulfurization are:

- Removal of H_2S and COS in coal-derived fuel gas to a level of about 10 ppm can be achieved (Grindly, 1982, 1983, 1984, 1985 and 1986; Jha, 1986).
- Complete sulfidation results in a sulfur loading capacity of 0.4 lb sulfur per 1.0 lb of zinc ferrite and can be achieved for absorption in the temperature range of 700 to 1400°F. (Harrison, 1985, 1986; Kim, 1987)
- Very narrow reaction zones can exist at operating conditions of interest for absorption and regeneration (Grindly, 1984; Jah, 1986).
- Under moderate reducing conditions like those existing in fuel gas from a Lurgi air blown gasifier, the hematite (Fe_2O_3) is reduced to magnetite (Fe_3O_4), rather than to other reduced iron oxide forms, which cause irreversible sorbent damage. (Lamoreaux, 1986; Harrison, 1985)

Multicycle operation is essential for minimization of net sorbent consumption and can be achieved by maintaining proper temperature and gas composition. To ensure efficient and effective utilization of the sorbent, the system design should address the following issues:

- More than 700,000 Btu/lb mole of sulfided zinc ferrite are generated during regeneration. That heat must be removed since irreverisble sintering and plugging of pores occurs in zinc ferrite pellets at pellet temperatures in excess of 1500°F. (Harrison, 1986)

- Initial regeneration of sulfided zinc ferrite is very fast, resulting in a significant temperature difference between the pellet and the regenerating gas (Kim, 1987). The temperature difference is a function of the gas inlet temperature and its oxygen content, and should be considered in the temperature control to ensure that pellet temperature does not exceed the 1500°F limit.
- Regeneration at temperatures below 1200°F results in the formation of $ZnSO_4$. Sulfate formation increases at lower temperature, higher pressure, and in the presence of SO_2 and O_2 in the regeneration gas. The sulfate decomposes quickly above 1200°F. (Krishnan, 1985; Harrison, 1986; Kim, 1987). To minimize sorbent sulfate content, the regenerated material should be discharged from the regenerator at temperatures higher than 1200°F.
- Sulfate decomposition occurs at temperatures lower than 1200°F when a sulfate-containing sorbent is exposed to coal gas (Krishnan, 1985; Harrison, 1986). The effluent contains SO_2 and H_2S, which contaminate the coal gas.
- Elemental zinc may be formed under reducing conditions and at temperatures in excess of 1200°F (Flytzani-Stephanopoulos 1985).

5. PROJECT DESCRIPTION

A novel hot coal gas cleanup concept has been developed by GE. Based on this concept, a hot coal gas cleanup system has been designed for installation in the Process Evaluation Facility at the GE Research and Development Center in Schenectady, N.Y. This facility contains an existing air blown, fixed bed gasifier that produces approximately 10,000 lb/h of coal gas at 1000 to 1200°F and 300 psi. Using Illinois #6 coal, the coal gas contains 5000 to 12000 ppmw of particulates and 3000 to 5000 ppmv of sulfur in the form of H_2S and COS. Particulates and typical gas compositions are given in Tables 1 and 2, respectively.

The hot coal gas cleanup system consists of high-efficiency cyclones to collect entrained particles, a moving bed absorber containing zinc ferrite sorbent to remove sulfur compounds, a moving bed regenerator to regenerate the sulfided sorbent, a regeneration gas recycle system and a solids transport system. A schematic diagram of the hot coal gas cleanup process is given in Figure 1.

Table 1. Ultimate Analysis of Particles Entrained From GE-CRD Gasifier.

	as received	dry
% Moisture	0.49	X.XX
%Carbon	84.01	84.42
% Hydrogen	1.16	1.17
% Nitrogen	1.14	1.15
% Chlorine	0.03	0.03
% Sulfur	1.24	1.25
% Ash	11.50	11.56
% Oxygen (diff.)	0.43	0.42
Total	100.00%	100.00%

Table 2. Typical Composition of Coal-Derived Fuel Gas from GE-CRD Gasifier.

Component	Concentration, %vol
H_2O	29.56
N_2	31.7
H_2	15.8
CO_2	11.2
CO	7.9
CH_4	3.2
Tars	0.04
H_2S	0.4
NH_3	0.2
Total	100.00

FINES REMOVAL

Entrained fine particles from the gasifier are removed in the primary cyclone shown in Figure 1. The cyclone is a commercial GE Environmental Systems, Inc. product with high efficiency designed to operate at 300 psi and 1200°F. The cyclone has been operated in the PEF for more than 200 hours and has demonstrated 98% particulate removal efficiency. Particle concentration downstream of the cyclone was reduced to 100 to 200 ppmw. Particle size distribution before and after the cyclone is given in Figure 2. It is estimated that 70 to 90% of the remaining particulate matter entering the absorber will be captured by the bed, reducing particle concentration to below 50 ppmw. A small amount of zinc ferrite fines will be entrained from the absorber and collected in a secondary cyclone. The high efficiency secondary cyclone will effectively capture most of the high-density zinc ferrite dust (S.G. = 5.3) and will practically eliminate all fines larger than 5 μm. Entrained particles from the regenerator will be captured in a bagfilter located upstream of the recycle compressor. Larger fines, -14 mesh, will be sieved on a screen at the regenerator sorbent outlet.

ABSORBER

The absorber is the intermittently moving bed reactor shown schematically in Figure 1. The sulfur-laden coal gas from the primary cyclone (stream A1) enters the absorber through a gas manifold at its bottom and flows upward countercurrent to the moving bed of zinc ferrite pellets.

The sulfur compounds, mainly H_eS, in the coal gas react with the sorbent according to:

$$ZnO + H_2S \rightarrow ZnS + H_2O \quad (4)$$

$$Fe_3O_4 + 3H_2S + H_2 \rightarrow 3FeS + 4H_2O. \quad (5)$$

The coal gas leaving the absorber (stream A2) is expected to contain less than 10 ppmv of H_2S and COS. One to four percent of the total sulfur in the coal is bound in long chain organic tar vapor and is not removed by the zinc ferrite bed. The sulfur bound in the tar vapor may be reduced by higher temperature operation of the gasifier.

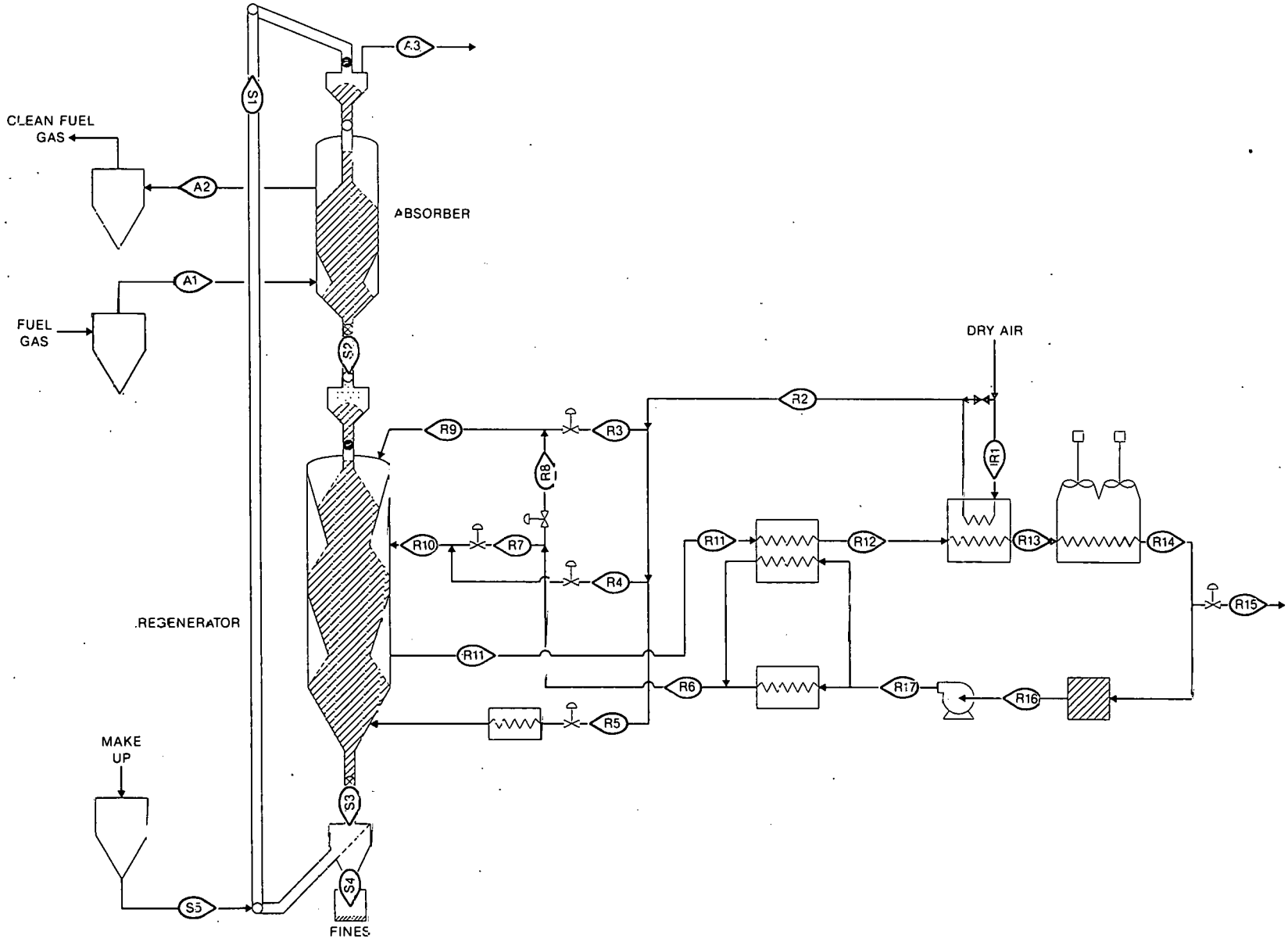

Figure 1. Hot coal gas cleanup system for Process Evaluation Facility.

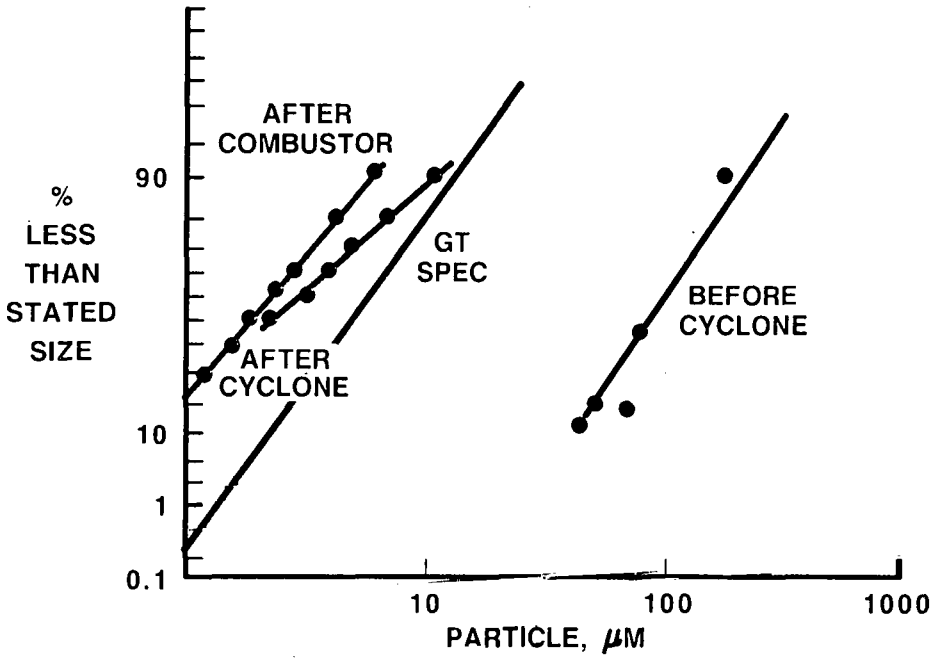

Figure 2. Particle size distibution from Process Evaluation Facility.

The absorber bed is stationary at low H_2S outlet concentration in stream A2, and it starts moving upon H_2S breakthrough. The H_2S breakthrough signal activates the rotary valve at the bottom of the absorber. The rotary valve feeds sulfided sorbent from the bottom of the absorber into the lockhopper (LH2), causing the bed and the reaction zone to move downward by gravity. The displaced sulfided zinc ferrite is replaced by regenerated sorbent from the top lockhopper (LH1).

When regenerated zinc ferrite sorbent is loaded into lockhopper LH1, a slip stream of coal gas (stream A3) is activated. Stream A3 reduces the hematatite to magnetite and decomposes any zinc sulfate residual from the regeneration step according to:

$$3Fe_2O_3 + H_2 \rightarrow 2Fe_3O_4 + H_2O \quad (6)$$

$$2ZnSO_4 + 5H_2 \rightarrow ZnO + ZnS + SO_2 + 5H_2O \quad (7)$$

Stream A3 flows through the top lockhopper (LH1) until a complete sulfate decomposition, detected by low SO_2 concentration, is achieved. The amount of sulfate in the regenerated zinc ferrite depends on the quality of the regeneration step, and is expected to be very small to nil in the current system.

REGENERATOR

The ability to regenerate and recycle the sorbent is essential for economically viable hot coal gas desulfurization. The regeneration step is a highly exothermic oxidation process requiring careful temperature control. Too high a temperature (above 1500°F) sinters and destroys the sorbent structure and reduces its ability to absorb sulfur in consecutive absorption steps. Low temperature (below 1200°F) results in sulfate formation and a lower sulfur removal efficiency.

In order to effectively control the reaction and achieve a complete regeneration, the reactor is divided into three zones (see Figure 1). As the sorbent moves down the

reactor zones, the reaction proceeds in a controlled atmosphere with oxygen concentration as low as 1% in the initial stage and as high as 21% in the final stage. Sorbent movement in the regenerator is controled by the rotary valve at its bottom, which is activated when lockhopper LH2 is full and has been depressurized and purged. The chemical reactions in the regenerator are:

$$ZnS + 2FeS + 5O_2 \rightarrow ZnO + Fe_2O_3 + 3SO_2 \rightarrow ZnFe_2O_4 + 3SO_2 \quad (8)$$

$$ZnO + SO_2 + 0.5O_2 \rightleftarrows ZnSO_4. \quad (9)$$

Reaction 9 is reversible and favors the formation of sulfate at low temperatures in the presence of oxygen. Zinc sulfate is formed in the initial stage of regeneration, but decomposes under the high-temperature, low oxygen concentration conditions at the lower end of the second-stage of regeneration.

First-Stage Regeneration

Sulfided zinc ferrite is fed from lockhopper LH2 to the top of the first stage of regeneration where partial oxidation of up to 30% of the sulfided sorbent occurs. The sorbent moves down the reactor in cocurrent flow with the regeneration gas. The inlet temperature of the regeneration gas (stream R9) is 750 to 900°F and contains 1 to 2.5% oxygen and 10 to 12% sulfur dioxide, with the balance being nitrogen. The regeneration gas flows downwards from the top of the regenerator into the second-stage regeneration zone. During sorbent feeding to the regenerator, the oxygen concentration of stream R9 is maintained at a 1 to 1.5% level, and it increases gradually to about 2.5% by increasing the air (stream R3) to recycle gas (stream R8) ratio. Oxygen concentration is controlled to maintain a maximum outlet gas temperature of 1250°F. Under these conditions no thermal damage occurs to the sorbent, even when its temperature exceeds that of the gas by up to 250°F. The relatively low temperature in the first regeneration stage results in the formation of some sulfate. This sulfate decomposes at the higher temperature in the second regeneration stage.

Second-Stage Regeneration

The second stage of regeneration is the stage where 70 to 75% of the regeneration occurs. The sorbent and the regeneration gas (stream R10), mixed with the gas stream from the first stage, flows cocurrently downwards into the third and final regeneration stage. The inlet temperature of the regeneration gas (stream R10), is 750 to 900°F, and it contains 4 to 5% oxygen and 10 to 12% SO_2, with the balance nitrogen. The oxygen concentration is controlled by the ratio of air (stream R4) to recycle gas (stream R7) to maintain a maximum temperature of 1450°F in the bed. The recycle flow rate is controlled to maintain less than 1% oxygen concentration at the gas outlet from the second regeneration stage. The high outlet temperature of the gas and sorbent at the bottom of the second stage ensures complete sulfate decomposition.

Third-Stage Regeneration

The third and final phase of regeneration is done at the lower end of the reactor where dry air at 600 to 800°F (Stream R5) flows countercurrent to the sorbent. Stream R5 cools the sorbent to a temperature acceptable for downstream equipment in the range of 800 to 1000°F, purges the SO_2-rich gas, and ensures complete regeneration. The outlet gas streams from the second and third regeneration stages mix to form the recycle gas stream (R11).

REGENERATION GAS RECYCLE

The regeneration gas recycle system is shown in Figure 1. It operates in a closed loop with dry air as an input (stream R1) and an SO_2-rich gas (stream R15) as a product output. The regeneration gas recycle loop is designed as an internal diluent that reduces the oxygen concentration in the air to the desired levels without the use of costly externally provided diluents such as steam or nitrogen. Using recycle rather than external inert diluent also enriches the SO_2 concentration of the product stream to as high as 13%.

The heat exchangers in the recycle loop are designed to control the temperature of the regenerator inlet streams (R5, R9, and R10). The gas cooler removes the heat generated during the regeneration reaction by cooling the recycle gas stream (R14) to about 200°F. In a commercial system, the gas cooler will be replaced by a steam generator. In the proof-of-concept design, the recycle compressor operates at low temperature, and a regenerative gas heat exchanger reheats the compressed gas (stream R17).

OPTIMIZATION OF REGENERATION GAS RECYCLE

Lowering the temperature of the regenerator inlet gas streams R9 and R10 is highly desired. Lower inlet gas temperatures, T_{IN}, allow a higher temperature increase (1500°F − T_{IN}) and, as a result, a higher oxygen concentration, a lower dilution-to-air ratio and an overall lower rate of recycle. For example, lowering T_{IN} from a temperature of 950°F to a temperature of 750°F reduces total recycle flow rate by about 30%. The lower flow rate allows size reduction of the regenerator vessel, heat exchangers, valves and pipes, and recycle compressor by the equivalent percentage and reduces the power consumption of the recycle compressor. In previously proposed schemes, gas inlet temperatures had to be kept high (above 1000°F) to minimize sulfate formation and to ensure complete oxidation. In the present design, because the sorbent is heated by the heat of reaction as it moves down the regenerator, the zinc sulfate is initially formed but decomposes as the equilibrium shifts from the right to the left side of Equation 9.

The amount of sulfate formed at low regeneration temperature can be deduced from thermal gravimetric analysis experiments. In the experiment shown in Figure 3, a sulfided zinc ferrite pellet reacts with a 10% SO_2, 4% O_2, 86% N_2 gas at 850°F. Under these conditions, oxidation of the metal sulfide occurs simultaneously with zinc sulfate formation. The weight of the pellet decreases initially because of the oxidation reaction but levels off after about 60 minutes at point 1, when the weight loss by oxidation is equal to the weight gain by sulfate formation. At point 1, the gas temeprature is increased to 1400°F while oxygen is simultaneously eliminated from the gas stream. The temperature increase causes an immediate reduction in the weight of the pellet because of zinc sulfate decomposition to point 2. No weight change is observed in the following 30 minutes, indicating absense of sulfate in the sorbent and absense of reactive component in the gas stream. At point 3 (about 90 minutes after the start of the experiment) oxygen is added to the gas stream, causing a continuation of the regeneration to completion after 200 minutes, with no apparent formation of additional sulfate.

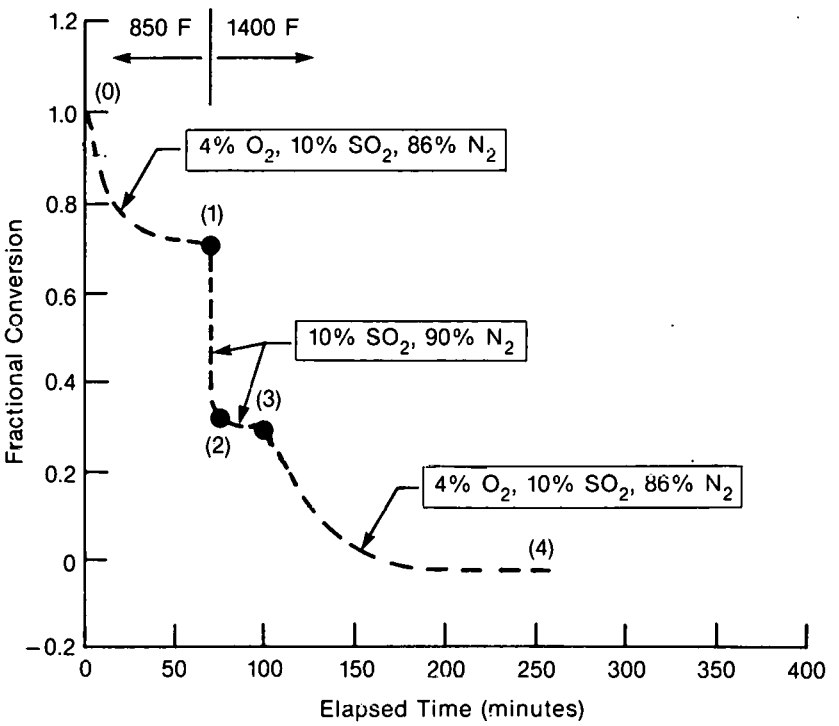

Figure 3. Single-pellet thermal gravimetric analysis — sorbent regeneration.

As described above, lowering the regeneration gas inlet temperature reduces capital and operational costs of the system; however, the following constraints limit the reduction:

- Gas temperature should be sufficiently high to start the oxidation reaction. Once heat is generated, the reaction becomes autocatalytic, with the accelerated rate controlled only by the oxygen concentration.
- Extreme temperatures, i.e., overcooling and overheating, reduce the mechanical strength of the sorbent and its ability to maintain integrity over multiple absorption-regeneration cycles.

SOLID TRANSPORTATION

The sorbent moves down the reactors and lockhoppers by gravity. The bed movement is controlled by the rotary valves at the bottom of each reactor. A vibrating 14-mesh screen is installed at the bottom of the regenerator to classify and remove small particles from the system. The vibrating screen feeds a single bucket elevator with a transport volume similar to that of the lockhoppers. The bucket is insulated to minimize heat losses and pellet cooling during the sorbent transportation. The elevator lifts the regenerated sorbent and discharges it to the top lockhopper (LH1).

PROOF-OF-CONCEPT SYSTEM DESIGN

The proof-of-concept system is designed to be incorporated in the existing GE Process Evaluation Facility. The facility includes a 24 ton/day, dry ash, fixed bed coal gasifier, fines removal cyclone, and full flow turbine combustion system.

The moving bed, hot H_2S removal system is designed to be housed in an 85 ft tall steel structure to be erected adjacent to the gasifier tower, as shown in the elevation view in Figure 4.

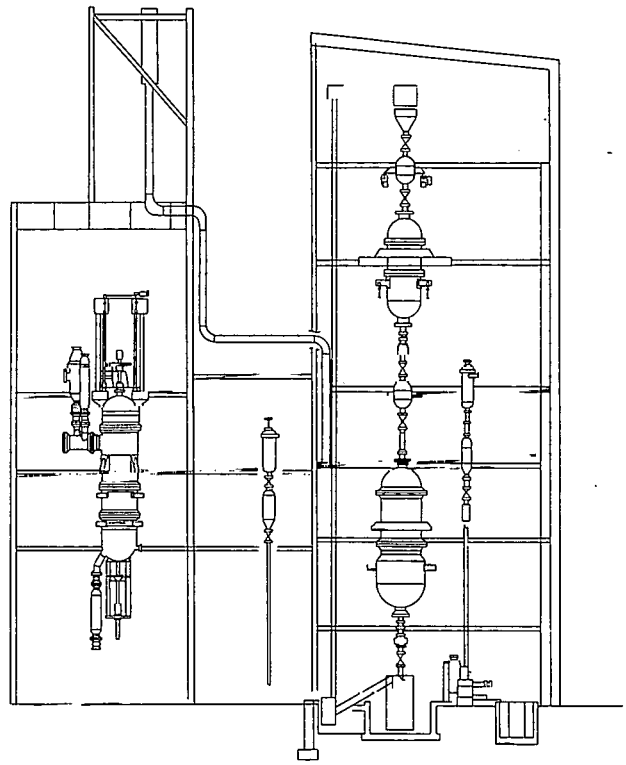

Figure 4. Process Evaluation Facility general arrangement — elevation view.

The absorber and regenerator vessels are shown in outline form in Figures 5 and 6. The vessels are constructed as flanged pressure vessels with internal refractory lining and removable metal cones to provide gas distribution and maintain the proper reaction zones within the vessels. Extensive sampling and instrumentation access has been provided for system characterization. The vessels are mounted on trolley rails to permit splitting of the vessels at the flanges and horizontal roll-out of vessel sections for inspection or modification.

The entire system has been designed to permit detailed characterization of the operation and performance of each of the components within the system. The sampling locations planned within the system are shown in Figure 7.

SORBENT SPECIFICATIONS

The sorbent used as a base for the current pilot design is zinc ferrite in a form of cylindrical or spherical pellets containing up to 20% inert binder material. Power plant systems and operating cost analyses can be used to show that the sorbent's useful life should exceed 100 absorption-regeneration cycles. This means that, for the moving bed system, up to one percent of the sorbent stream can be lost through attrition, entrainment, fines separation and loss of chemical reactivity. Gentle, staged regeneration, as designed here with temperatures not exceeding 1450°F, should maintain a reasonable reactivity over many cycles. The design allows sorbent sulfur capacity to drop

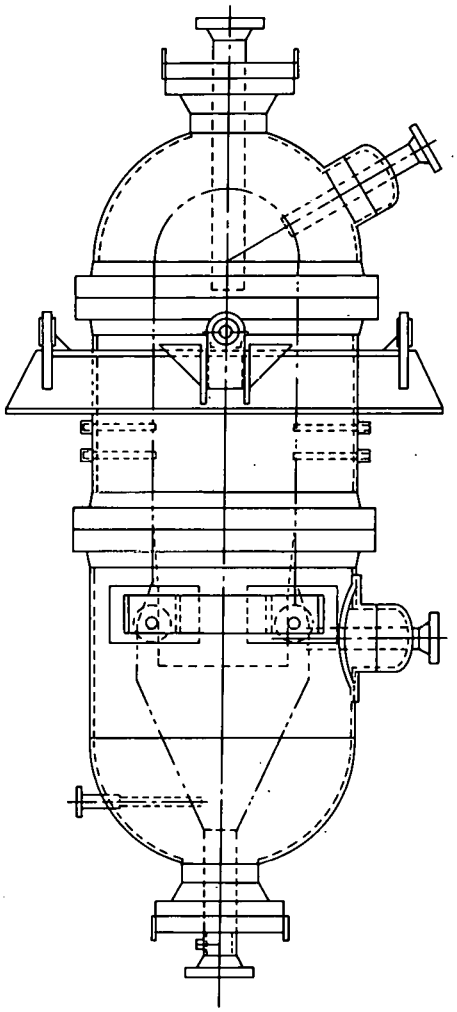

Figure 5. Moving bed, hot H_2S absorber.

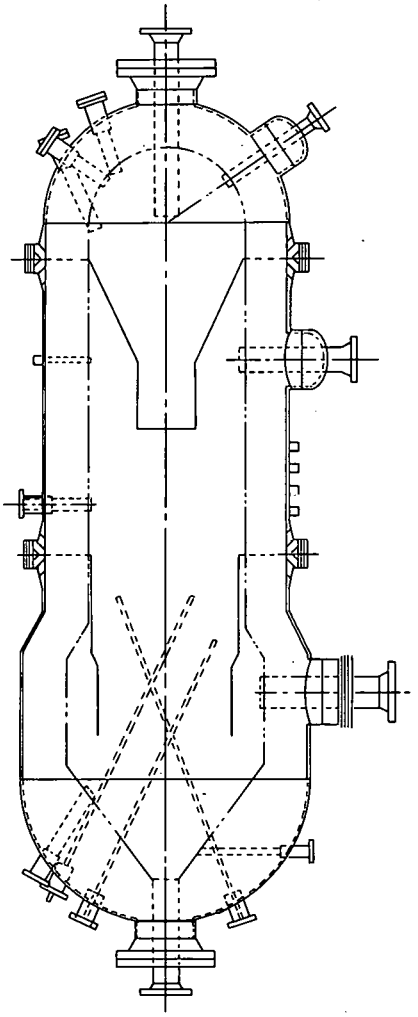

Figure 6. Moving bed, hot H_2S regenerator.

from the theoretical 40% to about 15% by weight before it is designated as chemically useless.

Physical strength and resistance to attrition and breakdown are essential for minimizing sorbent losses and preventing damage to downstream equipment. Early zinc ferrite sorbents developed by United Catalysts, Inc. for DOE-METC contained only small amounts of binders and were relatively soft and weak. Later sorbents with higher content of binders are significantly stronger at the expense of some insignificant loss of reactivity. GE is continuing to work with potential zinc ferrite suppliers to develop an improved sorbent. The main goal of this effort is to develop a physically strong yet chemically reactive sorbent that keeps its integrity after many absorption-regeneration cycles. New sorbents are tested for crush strength, attrition rate in a rotating cylinder and H_2S absorption rate in a thermal gravimetric analyzer. Sorbent acceptance criteria for the moving bed application have been developed. Three sorbent samples have been identified to date as acceptable and more samples will be tested.

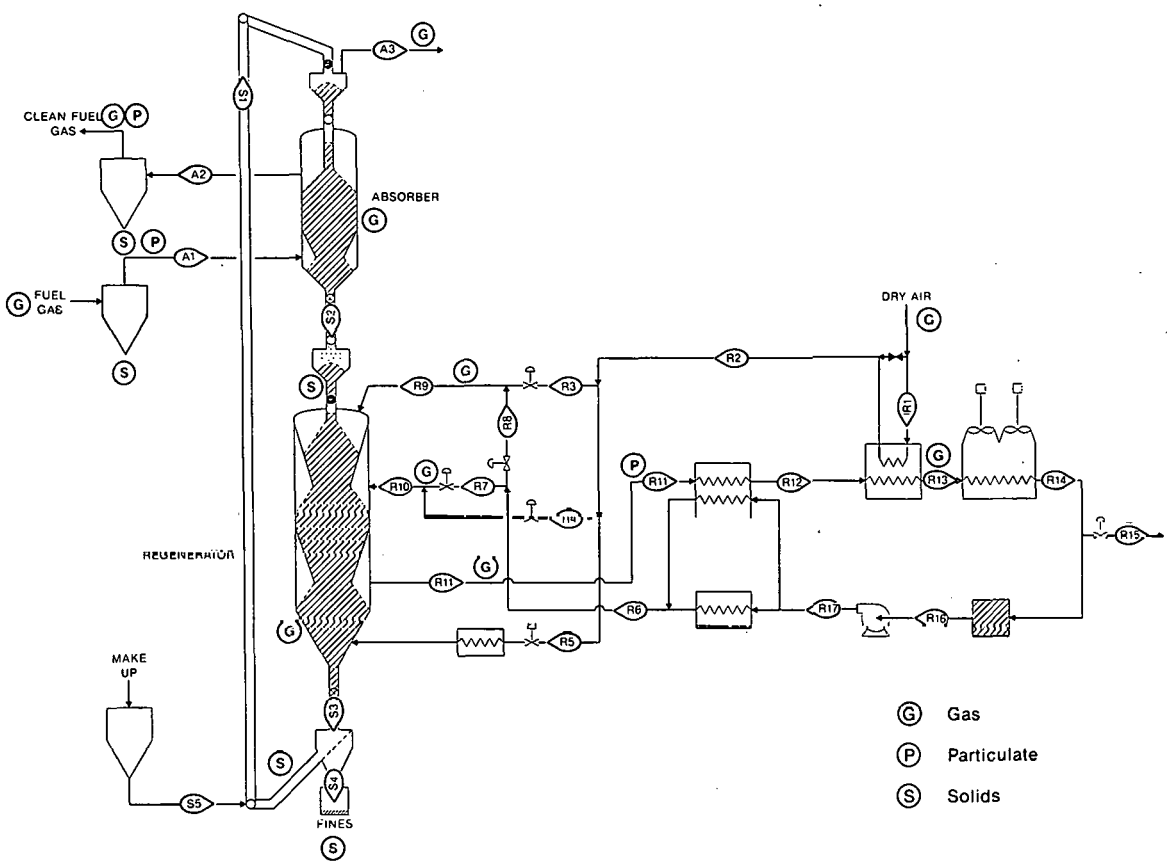

Figure 7. Hot coal gas cleanup system for Process Evaluation Facility.

6. ACCOMPLISHMENTS

- Completed conceptual design of 50 MW simplified IGCC system with fixed bed, air blown, dry ash gasifier; moving bed hot H_2S removal system; and steam-injected aircraft-derivative gas turbine.
- Completed conceptual design of proof-of-concept scale, moving bed hot H_2S removal system for installation in the Process Evaluation Facility with fixed bed gasifier and turbine simulator.
- Developed detailed design of proof-of-concept system including layouts and general arrangements; vessel designs; piping and valving specifications; instrument and control systems; and site civil, foundation, and structural drawings.
- Prepared equipment specifications for purchase of all required equipment and components for proof-of-concept system.
- Initiated design of alternate pressurized regeneration system applicable for tail gas injection into gasifier for in-bed sulfur capture.
- Defined sorbent physical and process requirements and selected candidate sorbent materials based on measured experimental data.

7. FUTURE WORK

The design package for the proof-of-concept adaptation of the moving bed hot H_2S removal system will be completed. This package will contain all drawings and design information required to procure, install, and start the system incorporated into the existing Process Evaluation Facility. A design report will be prepared documenting the design and the design basis. Included in the design report will be identification of instrumentation and measurements required for assessment of the system performance during operation and recommended operating procedures for the system.

A pressurized regeneration variation of the design will be produced to allow evaluation of tail gas recycle to a fixed bed gasifier with in-bed sulfur capture.

Economic assessment of the moving bed, hot H_2S removal system will be made and compared to previous studies of alternative coal-based power generation systems. Performance estimates for commercial IG-STIG power plants using this desulfurization system will be made and cost-of-electricity will be projected.

8. REFERENCES

"Hot Gas Cleanup for Electric Power Generating Systems." May 1986. DOS/METC-86/6038, U.S. Department of Energy, Morgantown Energy Technology Center, Morgantown, WV.

Cook, C.S., J.C. Corman, M.W. Horner, R.J. Payzer. March 1987. "Simplified IGCC: Integrated Steam Injected Gas Turbine (IG-STIG)," *Pacific Coast Electrical Association Annual Engineering and Operating Conference,* Irvine, CA.

Corman, J.C. March 1986. "Simplified IGCC," *13th Energy Technology Conference and Exposition (ET '86),* Washington, DC.

Corman, J.C., and R.P. Shah. August 1986. "Performance Characteristics of a Simplified IGCC System," *21st Intersociety Energy Conversion Engineering Conference.*

Corman, J.C. Sept. 1986. "Systems Analysis of Simplified IGCC Plants," Topical Report DOE/MC/14928-13, September 1986.

Flytzani-Stephanopoulos, M., G.R. Gavalas, S.S. Tamhankar, and P.K. Sharma. 1985. "Novel Sorbents for High-Performance Regenerative H_2S Removal," Final Report DOE/MC/20417-1898, 1985.

Grindley, T., and G. Steinfeld. 1982. "Development and Testing of Regenerable Hot Coal Gas Desulfurization Sorbents," *Second Annual Contractors' Meeting on Contaminant Control in Hot Coal-Derived Gas Streams,* Report DOE/M ETC/82-47.

Grindley, T., and G. Steinfeld. 1983. "Zinc Ferrite Hydrogen Sulfide Absorbent," *Third Annual Contractors' Meeting on Contaminant Control in Hot Coal-Derived Gas Streams,* Report DOE/METC/84-6.

Grindley, T., and G. Steinfeld. 1984. "Testing of Hydrogen Sulfide Absorbent in a Coal Gasifier Sidestream," *Fourth Annual Contractors' Meeting on Contaminant Control in Hot Coal-Derived Gas Streams*, Report DOE/METC/85-3.

Grindley, T., S.S. Kim, E.E. Gorski, and G. Steinfeld. 1985. "Aspects of the Design of a Process Development Unit for High-Temperature Coal Gas Desulfurization," *Fifth Annual Contractors' Meeting on Contaminant Control in Coal-Derived Gas Streams*, Report DOE/METC-85/6025.

Harrison, D.P., G.D. Focht, L. Sa, and P.V. Ranada. 1985. "Structural Changes in Metal Oxide Hot Coal Gas Desulfurization Sorbents," *Fifth Annual Contractors' Meeting on Contaminant Control in Coal-Derived Gas Stream*, Report DOE/METC-85/6025.

Harrison, D.P., P.V. Ranade, G.D. Focht and L.N. Sa. 1986. "Structural Changes in Metal Oxide Hot Coal Gas Desulfurization Sorbents," *Sixth Annual Contractors' Meeting on Contaminant Control in Coal-Derived Gas Stream*, Report DOE/METC-86/6042.

Jha, M.C., M.T. Hepworth and L.K. Baltich. 1986. *Enhanced Sorbent Durability for Hot Coal Gas Desulfurization*, Final Report DOE/MC/21168-2023.

Jha, M.C., M.T. Hepworth, W.E. Smith, R.E. Doane, L.K. Baltich. 1986. "Enhanced Sorbent Durability for Hot Coal Gas Desulfurization," *Sixth Annual Contractors' Meeting on Contaminant Control in Coal-Derived Gas Stream*, Report DOE/METC-86/6042.

Joshi, D., J.H. Olson, M.L. Hayes and V. Shah. 1979. *Hot, Low-Btu Producer Gas Desulfurization in Fixed Bed of Iron Oxide - Fly Ash.* Final Report. DOE Contract No. EF-77-C-01-2757.

Kim, B.M., and R. Ayala. 1987. *Hot Hydrogen Sulfide Removal Process Modeling and Experimental Analysis*, Final Report prepared for Niagara Mohawk Power Corp. by Corporate Research and Development, General Electric Company. 87SRD006.

Krishnan, G.N., G.T. Tong, R.H. Lamoreaux, R.D. Brittain, and B.J. Wood. 1985. "A Study of Sulfate Formation During Regeneration of Zinc Ferrite Sorbents," *Fifth Annual Contractors' Meeting on Contaminant Control in Coal-Derived Gas Streams*, Report DOE/METC-85/6025.

Lamoreaux, R.H., R.D. Brittain and D.L. Hildenbrand. 1986. "Solid Phase Boundaries in Coal Gas Desulfurization by Zinc Ferrite," *Sixth Annual Contractors' Meeting on Contaminant Control in Coal-Derived Gas Stream*, Report DOE/METC-86/6042.

Sugitani, S., J. Nakai, S. Nishizaki, T. Watanabe and M. Tsunasawa. 1985. "Research and Development of a Hot Gas Desulfurization Process," Ishikawajima-Harima Heavy Industries Co., Ltd. (IHI), Tokyo, Japan. 1985.

ENHANCED DURABILITY AND REACTIVITY FOR ZINC FERRITE DESULFURIZATION SORBENT

1. CONTRACT NUMBER: DE-AC21-86MC23172

CONTRACTOR: AMAX Research & Development Center
5950 McIntyre Street
Golden, Colorado 80403-7499
(303) 279-7636

CONTRACTOR PROJECT MANAGER: Dr. Mahesh C. Jha

PRINCIPAL INVESTIGATORS: Ms. Linda K. Baltich
Mr. Mark H. Berggren
Professor Douglas P. Harrison
(Louisiana State University)

METC PROJECT MANAGER: Mr. Suresh C. Jain

CONTRACT PERIOD OF PERFORMANCE: October 1, 1986 to July 31, 1988

2. SCHEDULE/MILESTONES:

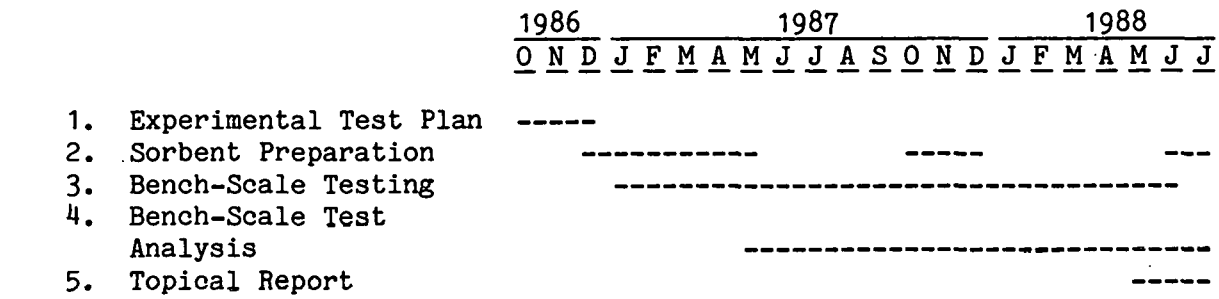

3. OBJECTIVES:

The prime objective of this project is to identify and investigate methods for enhancing the durability and reactivity of the zinc ferrite desulfurization sorbent. The enhancement is to be judged by comparing the reactivity and durability of the sorbents prepared and tested in the program against two base case samples.

The objective will be accomplished by preparing a large number of sorbent samples representing modified chemical compositions and agglomeration and induration procedures. Selected samples that meet the requirements of the physical characteristics will be used in sulfidation/regeneration tests to determine their reactivity. These sorbent samples will be characterized before and after testing to determine their durability. The resulting data will be analyzed to categorize the sorbents and establish the chemical composition and agglomerating and induration procedures that result in the most reactive and durable sorbent.

4. BACKGROUND:

Integrated gasification combined cycle (IGCC) technology appears to be one of the most efficient methods of generating electric power from coal. The process economics can be further improved if the physical and chemical cleanup of the gas stream is performed at high temperature and high pressure before the gas enters the turbine. Desulfurization of the hot coal gas is important for both protection of gas turbine components and compliance with environmental regulations. Hot coal gas desulfurization is even more critical for more advanced and potentially more efficient energy generation concepts such as the molten carbonate fuel cell (MCFC).

Work performed by the Morgantown Energy Technology Center (METC) has demonstrated that a regenerable zinc ferrite sorbent can be used for desulfurization of hot coal gas to a few ppm H_2S level (Grindley and Steinfeld 1983). The overall desulfurization reaction can be represented by the following equation:

$$ZnO{\cdot}Fe_2O_3 + H_2 + 3\ H_2S \rightarrow ZnS + 2\ FeS + 4\ H_2O \qquad (1)$$

The sulfided sorbent can be regenerated by oxidizing the sulfides according to the overall reaction:

$$ZnS + 2\ FeS + 5\ O_2 \rightarrow ZnO{\cdot}Fe_2O_3 + 3\ SO_2 \qquad (2)$$

Steam is used, along with air, to limit the rise in temperature caused by this extremely exothermic reaction. The gas stream can be treated by one of several processes available for sulfur dioxide control. The objective is to recover sulfur in an environmentally acceptable, saleable, or readily disposable form.

The main advantages of using zinc ferrite, in comparison to other metal oxides, are that it permits desulfurization to a few ppm H_2S level and its sulfur sorption capacity is high. Theoretically, 100 grams of pure zinc ferrite can capture 40 grams of sulfur at saturation.

During the course of cyclic sulfidation and regeneration, the zinc ferrite sorbent experiences severe chemical, physical, and thermal changes. There are concerns that these changes will ultimately deteriorate the performance of the sorbent. Laboratory and bench-scale test results have shown that the sulfur sorption capacity of zinc ferrite decreases significantly as the number of cycles increases (Jha, Hepworth, and Baltich 1986).

To minimize the cost of hot coal gas desulfurization, it is important that the sorbent be durable and reactive for as long as possible. This will not only cut down the cost of the sorbent itself but also the cost associated with filling the reactor with fresh sorbent and disposal of the used sorbent.

5. PROJECT DESCRIPTION:

The project is divided into five tasks listed under schedule/ milestones. There is a provision for Task 6 (option) to perform additional testing.

The project objective will be accomplished by a systematic investigation of the sorbent preparation process variables that affect the reactivity and durability of the sorbents. For the purpose of the present program, the reactivity of the sorbent is defined in terms of:

- Kinetics of sulfidation in a single particle TGA apparatus.
- Sulfur sorption capacity at breakthrough in an 18-inch fixed bed.
- Sulfur sorption capacity at near saturation.

The durability of the sorbent may be defined as its ability to maintain the following in repeated cyclic (10 cycles) use:

- Physical characteristics such as crush strength, attrition strength, size, and surface area.
- Chemical characteristics such as sulfur sorption capacity.

6. RESULTS/ACCOMPLISHMENTS:

Progress made in completing various tasks is discussed below, along with the results obtained to date.

TASK 1. EXPERIMENTAL TEST PLAN

This task has been completed. A detailed test plan was prepared discussing how various tasks will be performed and why. The plan calls for bench-scale testing of 15 sorbent samples for 10 cycles under fixed sulfidation and regeneration conditions. Two of the 15 samples have been designated as base case sorbent samples. These sorbents are Sample No. T-2465 (zinc ferrite extrudes produced by United Catalyst Incorporated) and Sample No. 1094-59 (zinc ferrite pellets prepared by AMAX Research & Development Center under a previous METC contract, DE-AC21-84MC21168). Sample 1094-59 is similar to sample 1094-63 produced by AMAX for KRW Energy Systems. The preparation procedures and characteristics of the AMAX samples are described in detail in the final report on the above-mentioned contract (Jha, Hepworth, and Baltich 1986). Thirteen other sorbent samples will represent different preparation conditions in terms of chemical composition, agglomeration procedure, and induration conditions.

Based on past experience, the following primary variables have been selected for a systematic investigation:

- Iron oxide type -- catalyst or pigment grade.
- ZnO/Fe_2O_3 stoichiometric ratio -- 0.8 or 1.0.

- Binders -- 2, 5, or 10 percent bentonite with or without an organic binder (0.5 percent Methocel for extrudes, 2 percent starch for pellets).
- Shape -- Cylindrical extrudes or spherical pellets.

A statistically designed (partial factorial) test matrix covering 24 runs is planned to investigate these variables in various combinations. The sorbent samples produced during these runs are divided into subsamples and indurated under different conditions (0.25, 2, or 4 hours at 1,500, 1,700, or 1,900°F) to determine the optimum indurating conditions. Samples prepared under these optimum conditions are tested for their physical characteristics, and their reactivity is tested through single particle kinetic studies at Louisiana State University.

Samples selected on the basis of physical characterization and single particle kinetic study results will be subjected to 10 cycles of testing in the bench-scale reactor. Analyses of these bench-scale test results will help determine the levels of the primary variables that result in the most durable and reactive sorbent. Next, some secondary variables will be investigated to further improve the quality of the sorbent. At this stage, it is planned to investigate partial substitutions (copper and manganese for zinc and iron) and the addition of catalysts or modifiers (molybdenite and sodium carbonate) as secondary variables. There are indications that these additives might improve the reactivity and durability of the zinc ferrite sorbent.

TASK 2. SORBENT PREPARATION

The main raw materials used in preparation of the sorbents are:

- Catalyst-grade iron oxide, L-2796 (UCI).
- Pigment-grade iron oxide, Bayferrox 645T (Mobay Chemical).
- Zinc oxide, AZO-77 (ASARCO).
- Bentonite (Western), Methocel (Dow), starch (Kingsford).

A bench-scale disc pelletizer and a bench-scale extruder are used to prepare sorbent samples in kilogram quantities. The samples are dried and indurated in electric ovens and muffle furnaces. Details of raw material characteristics and sorbent preparation procedures have been presented before (Jha, Hepworth, and Baltich 1986, Jha 1986).

Bulk density of indurated sorbent samples is measured by determining the weight of sorbent pellets or extrudes required to fill a graduated cylinder of dimensions similar to that of the bench-scale reactor (2-inch diameter, 1-liter capacity). Crush strength is measured using a Chatillon compression tester following ASTM procedure D 4179-82, which is acceptable for the spherical pellets but not for the cylindrical extrudes. However, in lack of any other standard procedure, METC and its contractors continue to use this procedure.

Loss on attrition is determined by tumbling the sorbent pellets or extrudes in a rotating drum following ASTM procedure D 4058-81. Specific surface area is measured by the BET method using a Quantachrome Quantasorb system. Mercury porosity measurement is to be made on selected samples only by an outside laboratory (Coors).

The samples selected for the multicycle bench-scale test program are also subjected to chemical analysis (zinc, iron, and any other element of interest) and mineralogical analysis (zinc ferrite, zincite, hematite, and any other phases).

To date, 27 samples have been prepared in the pellet form and 25 samples have been prepared in the extrude form. They represent 10 of the 24 runs planned (see Task 1) in terms of chemical composition and agglomeration procedures and up to six induration conditions for each formulation. Table 1 summarizes the preparation conditions and physical characteristics of these sorbent samples.

In general, a higher induration temperature resulted in stronger sorbents with greater bulk density. For comparable induration conditions, the extrudes have significantly higher bulk density and crush strength. The difference in bulk density is probably due to two reasons. First, the high pressure used in extrusion results in denser particles with less porosity and specific surface area. Secondly, the extrudes pack tighter than the pellets. The higher crush strength is most likely due to the larger surface area that contacts the two plates of the testing machine.

TASK 3. BENCH-SCALE TESTING

This task is divided into two parts:

- Single particle kinetic studies.
- Bench-scale multicycle test program.

Progress made under each part is discussed below.

Single Particle Kinetic Studies

These studies are being performed at the Chemical Engineering Department of Louisiana State University under a subcontract. The objective is to screen a large number of samples for their relative reactivity. One and a half cycles of testing (sulfidation-regeneration-sulfidation) are performed using a thermogravimetric analysis (TGA) apparatus used in other related METC work (Harrison 1986). Based on the stoichiometry of Reaction 1, a 13.3 percent weight gain is expected if pure zinc ferrite is completely sulfided.

The standard procedure is to subject the sorbent to a reducing gas (10.9 percent H_2, 26.0 percent H_2O, 16.8 percent CO, 4.6 percent CO_2, and 41.7 percent N_2) for 30 minutes. Then, H_2S is introduced at such a flow rate that its concentration is 2.7 mole percent. This high concentration

Table 1. Preparation Conditions and Physical Characteristics of Sorbents Produced.

Pellet Formulations						Range of Physical Characteristic Values[a]		
Run No.	Fe_2O_3 Grade	ZnO/Fe_2O_3 Ratio	% Bentonite	% Starch	Number of Sorbents Tested[a]	Bulk Density, kg/l	Crush Strength, pounds	Loss on Attrition, %
2[b]	Pigment	0.8	2	0	6	0.85 - 1.53	3.8 - 40.3	10.2 - 76.7
3[c]	Catalyst	1.0	2	0	6	0.95 - 1.27	6.8 - 21.5	24.5 - 42.8
5	Catalyst	0.8	2	2	5	1.03 - 1.34	14.5 - 32.8	8.4 - 18.7
19	Catalyst	1.0	10	0	5	0.95 - 1.13	10.2 - 20.8	22.8 - 36.5
21	Catalyst	0.8	10	2	5	0.90 - 1.11	5.7 - 21.2	19.9 - 42.4
Base Case	1094-59					1.01	5.1	--

Extrude Formulations						Range of Physical Characteristic Values[a]		
Run No.	Fe_2O_3 Grade	ZnO/Fe_2O_3 Ratio	% Bentonite	% Methocel	Number of Sorbents Tested[a]	Bulk Density, kg/l	Crush Strength, pounds	Loss on Attrition, %
1	Catalyst	0.8	2	0	5	1.12 - 1.36	29.4 - >50	5.7 - 11.9
4	Pigment	1.0	2	0	5	1.13 - 1.50	24.2 - >50	4.9 - 18.2
7	Catalyst	1.0	2	0.5	5	1.15 - 1.62	31.8 - >50	6.8 - 15.5
9	Catalyst	0.8	5	0	5	1.23 - 1.74	>50	5.7 - 10.8
15	Catalyst	1.0	5	0.5	5	1.20 - 1.68	36.8 - >50	5.3 - 11.7
Base Case	T-2465					1.31	30.2	11.2

[a] After induration for 15 minutes to 4 hours at temperatures from 1,500 to 1,900°F.
[b] Sorbent P5 (see Figure 2) was prepared as part of Run No. 2.
[c] Sorbent P11 (see Figure 2) was prepared as part of Run No. 3.

allows fast sulfidation to a near constant weight. After purging, the sorbent is regenerated with 4 percent O_2, 66 percent N_2, and 30 percent H_2O until its weight stabilizes. (All gas compositions are in mole percent.)

Figure 1 presents the results for base case sorbents T-2465 and 1094-59. Sulfidation for the tests shown was performed at 550 and 650°C, whereas regeneration was performed at 700°C. The results show that the sulfidation temperature did not significantly affect the kinetics of sulfidation. The rate of sulfidation appears to be somewhat faster for 1094-59 in comparison to T-2465. Also, the sulfidation rate during the second cycle was only slightly lower than the rate during the first cycle.

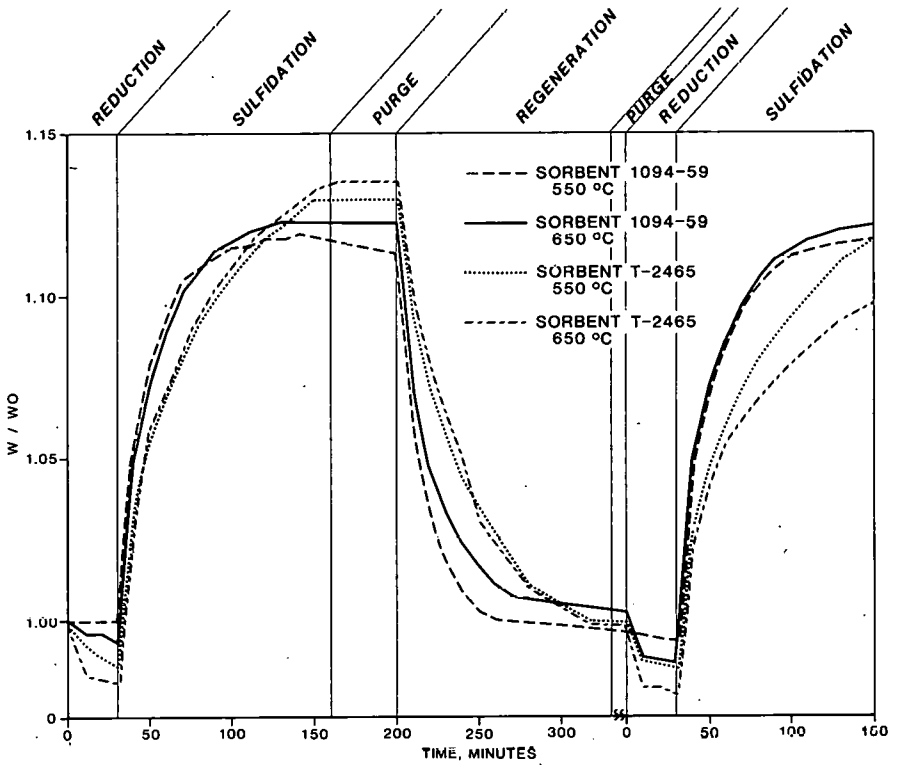

Figure 1. Single particle kinetic study results on base case samples T-2465 and 1094-59 at sulfidation temperatures of 550 and 650°C.

A sulfidation temperature of 550°C will be used during the rest of the program. Figure 2 shows the results for two of the new sorbent samples, P5 and P11 prepared under the present program. Both sorbents showed somewhat faster kinetics of sulfidation than the base case sorbents.

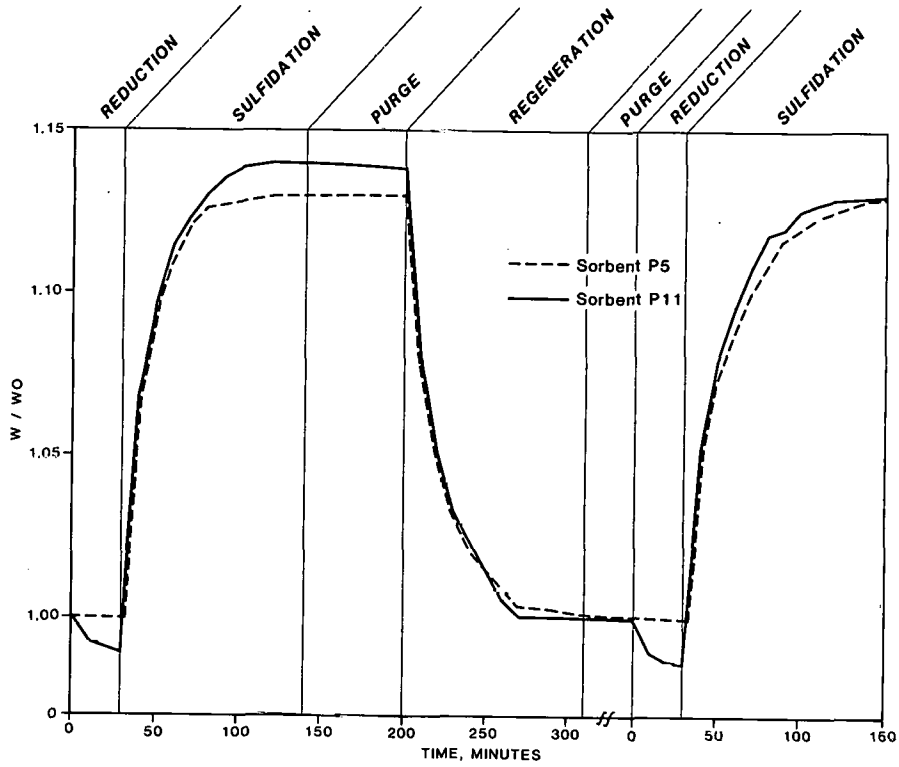

Figure 2. Single particle kinetic study results on samples of new sorbents, P5 and P11, at a sulfidation temperature of 550°C.

Bench-Scale Multicycle Test Program

In this program, sorbents will be tested for 10 cycles. During the first 9 cycles, sulfidation is stopped at breakthrough (200 ppm H_2S in the exit gas), the reactor is purged with nitrogen, and the sorbent regenerated. During the 10th cycle, sulfidation is continued to saturation (H_2S concentration in the exit gas close to the concentration in the feed gas). The sorbent bed is removed from the reactor, and samples from the top, middle, and bottom are analyzed.

The apparatus used for the sulfidation/regeneration studies is shown in Figure 3. It consists of a 2-inch diameter reactor inside a split furnace. The sorbent is filled in the reactor to a height of about 18 inches. This corresponds to a sorbent bed volume of about 1 liter. A MINC-11 computer is used for data acquisition.

During the sulfidation cycle, a simulated coal gas upflows through the reactor at 550°C at a space velocity of 2,000 bed volumes (STP)/hour. The composition of this gas is the same as that used in single particle kinetic studies except that it contains only 1 mole percent H_2S. For regeneration, a 92:8 steam/air mixture is used to maintain the bed temperature in the 700 to 750°C range. The mixture flows down through the reactor at a space velocity of about 2,500 bed volumes (STP)/hour.

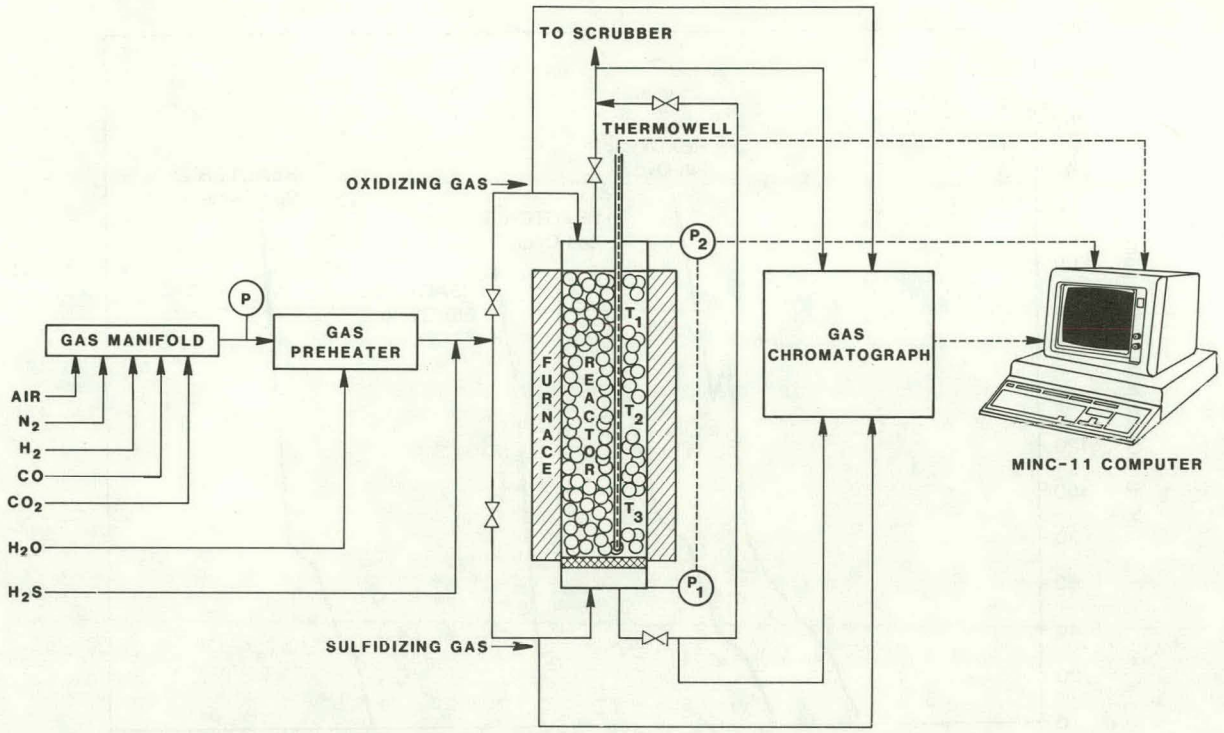

Figure 3. Schematic diagram of the bench-scale desulfurization reactor system.

Two similar reactor systems are set up in the AMAX laboratory. For base case sorbent T-2465, both reactors were used. Figure 4 shows the breakthrough curves for the 2nd and 9th cycles. By knowing the flow rate of the gas, its H_2S content, and the time to breakthrough, the amount of sulfur captured at breakthrough is calculated. This is reported as the sulfur sorption capacity of the sorbent as weight percent of the sorbent (i.e., grams of sulfur captured by 100 grams of sorbent). Table 2 presents these data for all 10 cycles.

Table 2. Sulfur Sorption Capacity of Base Case Sorbent T-2465 at Breakthrough.

	Sulfur Sorption Capacity, Weight Percent of Sorbent									
Reactor	Cycle 1	Cycle 2	Cycle 3	Cycle 4	Cycle 5	Cycle 6	Cycle 7	Cycle 8	Cycle 9	Cycle 10
Left	13.7	28.6	26.3	24.0	22.2	22.6	22.2	20.2	20.4	22.3
Right	8.8	16.3	13.2	19.3	21.6	14.3	15.6	14.7	13.4	14.2

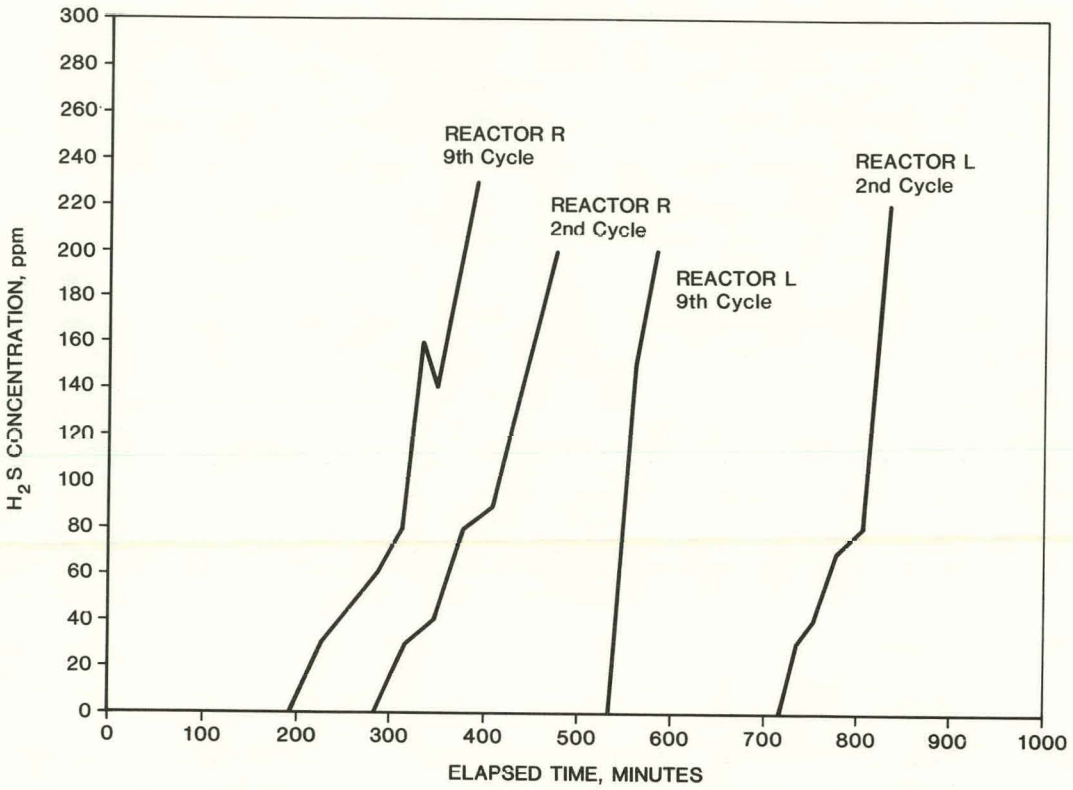

Figure 4. Breakthrough curves for base case sorbent T-2465.

Some drop in sulfur sorption capacity from the 2nd to the 9th cycle is not uncommon for the sorbents and is, in fact, part of the measure of their durability. The difference in performance between the left and right reactor may be due to a difference in packing or reactor temperature profile, although the same procedures were used. This reasoning is also supported by the fact that during the final (10th) cycle in which sulfidation was continued to saturation, the sulfur sorption capacities were found to be similar, 35.8 and 35.9 percent respectively, although the time to reach it was different at 2,473 and 2,287 minutes, respectively.

Tests are currently in progress on the second base case sorbent sample, 1094-59, and sample P11 produced in the present program.

TASK 4. BENCH-SCALE TEST ANALYSIS

At the conclusion of a test series, samples of sorbent are removed from the top, middle, and bottom of the reactor. They are submitted for:

- Chemical Analysis: Zinc, iron, and sulfur.
- Physical Characterization: Bulk density, crush strength, attrition resistance, and specific surface area.
- Mineralogical Analysis: X-ray diffraction and electron microprobe.

These data, along with sulfur sorption capacity, are used to determine the relative reactivity and durability of the particular sorbent.

As of this time, only chemical analyses are available for the three samples of base case sorbent T-2465 removed from the top, middle, and bottom of both reactors. They were all very consistent at 23.5 percent zinc and 40.5 percent iron. Sulfur analysis varied between 29.9 and 31.1 percent, without showing any definite trend. Allowing for 2 percent inert bentonite in the sorbent, sulfur analysis would have been 34.6 percent at 100 percent sulfur saturation.

These results for sorbent T-2465 are in good agreement with the results obtained with the same sorbent at METC and KRW Energy Systems. They show very good reactivity at about 88 percent theoretical capacity for sulfur capture. The physical appearance of the sorbent indicated very good durability. The drop in sulfur sorption capacity at breakthrough during the 10 cycles of testing is noticeable, and it is an objective of the present program to improve the sorbent performance in this respect also.

7. FUTURE WORK:

An iterative approach will be used for sorbent development. Work will continue on the preparation, characterization, and testing of zinc ferrite sorbent samples as planned under Task 1. The test analyses performed under Task 4 will help to establish the best primary variables for preparation of zinc ferrite sorbents with enhanced reactivity and durability. Secondary variables will then be investigated to obtain further improvements.

8. REFERENCES:

Grindley, T. and Steinfeld, G., "Zinc Ferrite Hydrogen Sulfide Absorbent", in Proceedings of Third Annual Contractors Meeting on Contaminant Control in Hot Coal-Derived Gas Streams", K. E. Markel (Editor), DOE/METC/84-6 (CONF-8305112) (DE 84000216), Morgantown Energy Technology Center, Morgantown, West Virginia, 1983, pp. 145-171.

Harrison, D. P., "Structural Changes in Metal Oxide Hot Coal Gas Desulfurization Sorbents", in Proceedings of the Sixth Annual Contractors Meeting on Contaminant Control in Coal-Derived Gas Streams", K. E. Markel and D. C. Cicero (Editors), DOE/METC-86/6024 (CONF-860648) (DE 86001088), Morgantown Energy Technology Center, Morgantown, West Virginia, 1986, pp. 221-230.

Jha, Mahesh C., "Enhanced Sorbent Durability for Hot Coal Gas Desulfurization", op. cit., pp. 231-243.

Jha, M. C., Hepworth, M. T., and Baltich, L. K., Enhanced Sorbent Durability for Hot Coal Gas Desulfurization, Report DOE/MC/21168-2023, Final Report to DOE/METC on Contract DE-AC21-84MC21168, AMAX Extractive Research and Development Center, Golden, Colorado, March 1986.

HIGH-TEMPERATURE SOLID OXIDE ELECTROLYTE FUEL CELL POWER GENERATION SYSTEM

1. CONTRACT NUMBER: DE-AC21-028OET-17089

2. CONTRACTOR: Research and Development Center
Westinghouse Electric Corporation
Pittsburgh, Pennsylvania 15235
(412) 256-1903

CONTRACTOR PROJECT MANAGER: A. R. Jones

PRINCIPAL INVESTIGATORS: Thomas E. Lippert
Wayne L. Lundberg
W. Jerry Parker

METC PROJECT MANAGER: Charles M. Zeh

CONTRACT PERIOD OF PERFORMANCE: March 7, 1986 through April 30, 1989
(MOD A030)

2. SCHEDULE/MILESTONES:

1987 Schedule

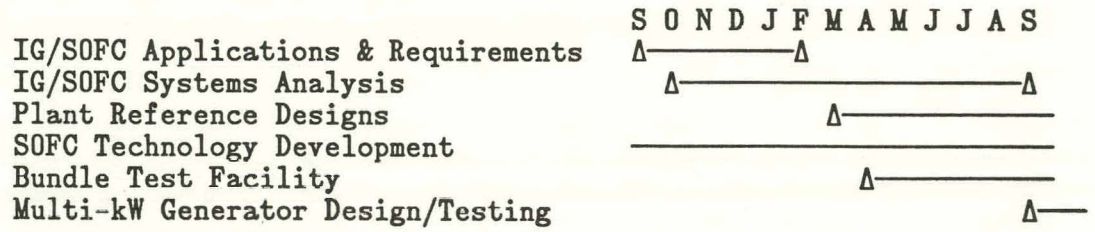

3. OBJECTIVES:

The work described represents one task of the contract. The purpose of this task is to establish developmental goals for the Solid Oxide Fuel Cell (SOFC) technology based upon the requirements of commercial power generation systems. Systems analysis and conceptual design studies are being conducted to define candidate Integrated Gasification, Solid Oxide Fuel Cell (IG/SOFC) power cycle arrangement, plant and component design requirements and economic goals for central station utility applications.

4. BACKGROUND STATEMENT:

Solid oxide fuel cells are electrochemical devices that operate at temperatures that approach 1100°C to directly produce electricity from coal fuel gas and exhaust gases that are 600-900°C suitable for bottoming cycles. The cells readily conduct oxygen ions from an air electrode (cathode), where they are formed, through a solid electrolyte to a fuel electrode (anode), where they react with the carbon monoxide (CO),

hydrogen (H_2) and methane (CH_4) contained in the coal gas to deliver electrons and produce electricity. Figure 1 illustrates the design of the state-of-the-art SOFC developed by Westinghouse. It features a thin porous air electrode made of modified lanthanum manganite that is overlaid onto a porous, calcia-stabilized zirconia support tube. A gas-tight electrolyte of yttria-stabilized zirconia, (approximately 50 mm thick) covers the air electrode, except in an area of about 9 mm wide along the entire active cell length. This strip of exposed air electrode is covered by a thin, dense layer of magnesium-doped lanthanum chromite. This layer, termed the cell interconnection, serves as the electric contacting area to an adjacent cell or to a power contact. The fuel electrode is a nickel-zirconia cermet and is about 150 mm thick and covers the electrolyte surface except in the vicinity of the interconnection.

Cell construction is tubular with one end closed. For cell operation, air is introduced to the fuel cell air electrode through an injector tube that is positioned within the cell, Figure 2. The air is discharged from the injector tube near the closed end of the fuel cell, flows through the annular space formed by the cell and coaxial injector tube. Fuel flows on the outside of the cell. At the open end of the cell, the oxygen depleted air stream exits the cell and is combusted with the partially depleted fuel stream. Typically, 40 to 85% of the fuel is utilized (reacted) in the active fuel cell section.

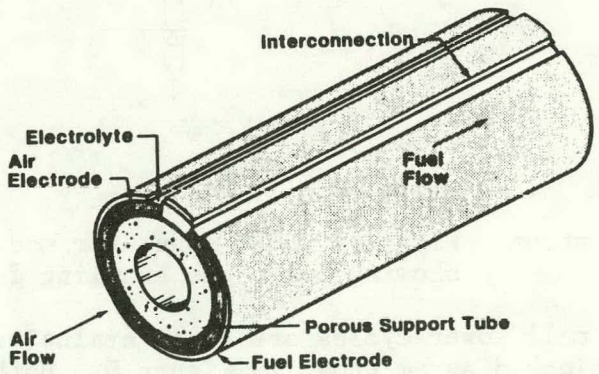

Figure 1. Design of a single solid oxide fuel cell.

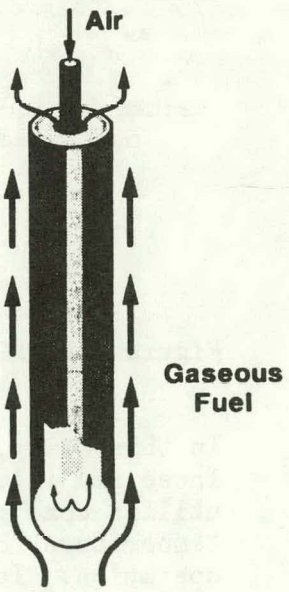

Figure 2. Schematic showing fuel and air flow paths in SOFC.

To construct an electric generator, the individual cells are bundled into an array of series-parallel electrically connected tubes to form a semi-rigid structure that is a basic generator building block, Figure 3. The individual bundles are arrayed in series to build generator voltage and form submodules. Submodules are further combined in either parallel or series connections to form generator modules. Figure 4 illustrates the overall construction of a commercial scale fuel cell module that would contain 10,000 or more cells and produce about 3.5 MWe electric. In a 250 MWe coal gasification central power station, between 30 to 40 such fuel cell modules would be used.

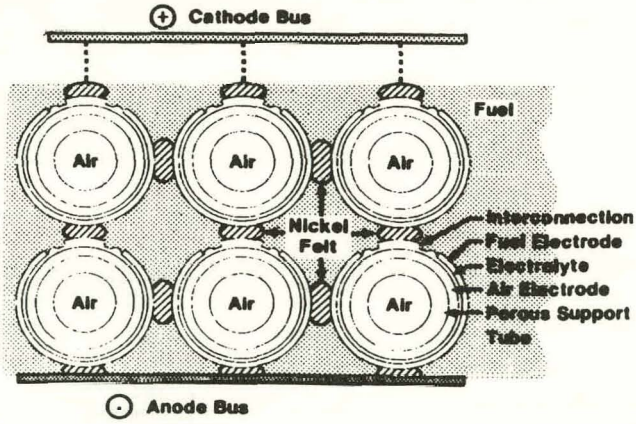

Figure 3. SOFC Bundle Configuration

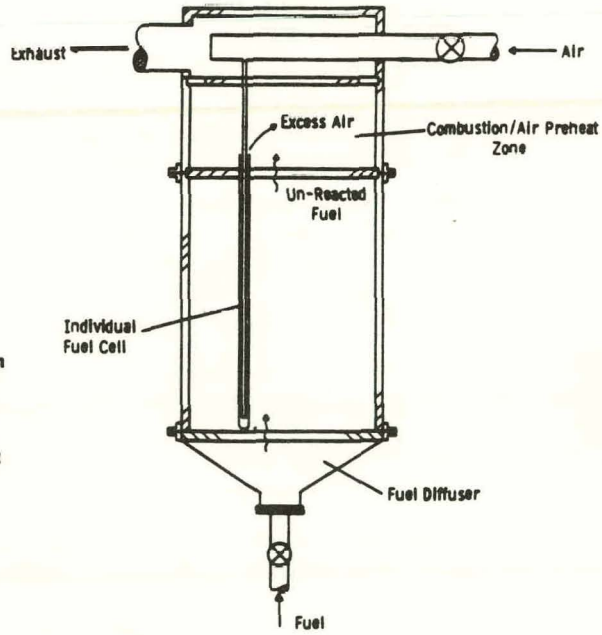

Figure 4. SOFC generator module showing basic gas handling features

In this study, two basic fuel cell power cycles are being evaluated. These are illustrated in the block diagram shown in Figure 5. Both cycles utilize coal gasification and hot gas cleanup to produce a high temperature, high pressure fuel gas suitable for solid oxide fuel cell operation. In one approach, the fuel cell is operated at atmospheric pressure and is directly coupled to a heat recovery steam generator power plant. In the second approach, the fuel cell is operated at high pressure. In this case, combustion gases exiting the SOFC unit are exhausted to a gas turbine combined cycle system. Both approaches provide power cycles that result in plant heat rates less than 7500 Btu/kWh and represent power generation systems that should enhance the use of coal gasification technology for electric utility and industrial applications.

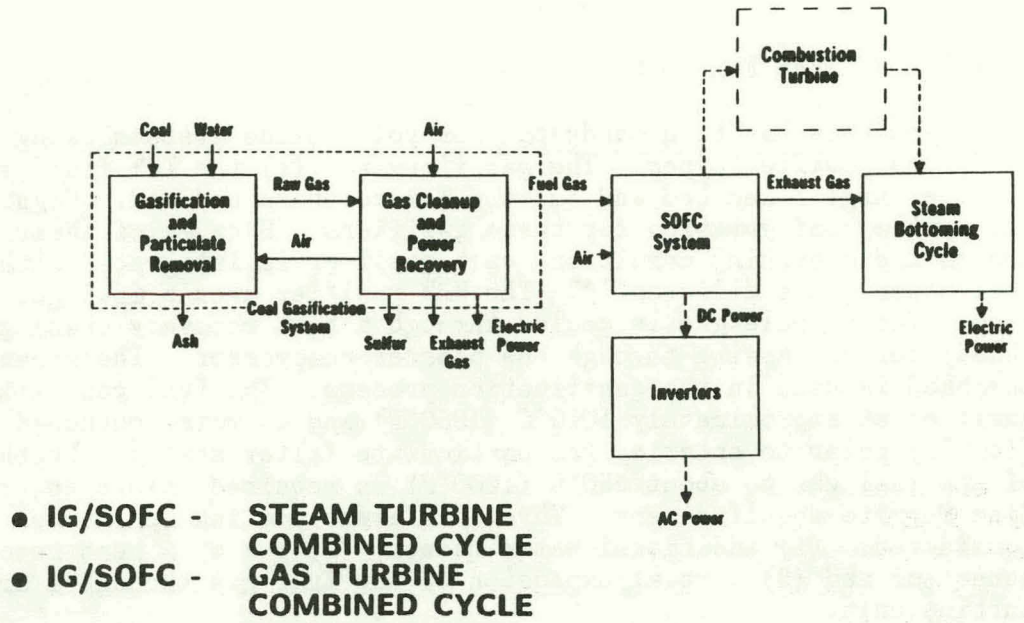

Figure 5. Schematic of coal fueled SOFC power plant configurations

5. PROJECT DESCRIPTION:

APPLICATIONS AND USER REQUIREMENTS

Nine candidate applications ranging from large central station coal based utility plants, repowering, dispersed power generation and industrial cogeneration have been identified for mature-market SOFC power systems (1). These various applications were then prioritized through a review process that included participation of EPRI and eight different electric-gas utility companies representing a cross section of today's industry. The review focused on needs expected to materialize in the late 1990's, timing that is consistent with SOFC commercial development. All the utilities responding identified as a high priority the coal based central station application in the 250 MWe range as an appropriate system for conceptual design. This reflects the predicted ability of SOFC combined cycle systems to operate at low heat rates and the projected need for baseload capacity in the late 1990 - early 2000 time frame. Potential applications that may be earlier that were selected include repowering of existing oil, gas and coal fired power plants in the 150 - 300 MWe range and the application of small (<50 MWe) modular systems suitable for dispersed power generation or as building blocks to existing systems. On the basis of this review, a coal-based (gasification) central station has been selected as the focus for systems analysis and conceptual design.

GASIFIER SYSTEMS FOR SOFC

Cycle analysis has been conducted for solid oxide systems using three different gasifier types. The gasifiers are (a) the KRW fluidized bed, (b) the Lurgi fixed bed and (c) the Texaco entrained bed. Figure 6 shows the system configuration for these gasifiers. Because of their respective design and operating condition, each gasifier is integrated with the fuel cell power cycle differently. The KRW gasifier uses a fuel gas recycle loop. The recycle gas is cooled through a heat recovery steam generator (HRSG) before passing through the booster compressor. The steam raised in the HRSG is used in the gasification process. The fuel gas exits the gasifier at approximately 1010°C (1850°F) and is water quenched to 870°C (1600°F) prior to entering the particulate filter system. Further cooling of the fuel gas to about 650°C (1200°F) is required before entering the Zinc Ferrite desulfurizers. Three different cooling approaches were considered: (1) additional water quench, (2) use of a heat recovery steam generator and (3) partial expansion of the fuel gas through a small gas turbine unit.

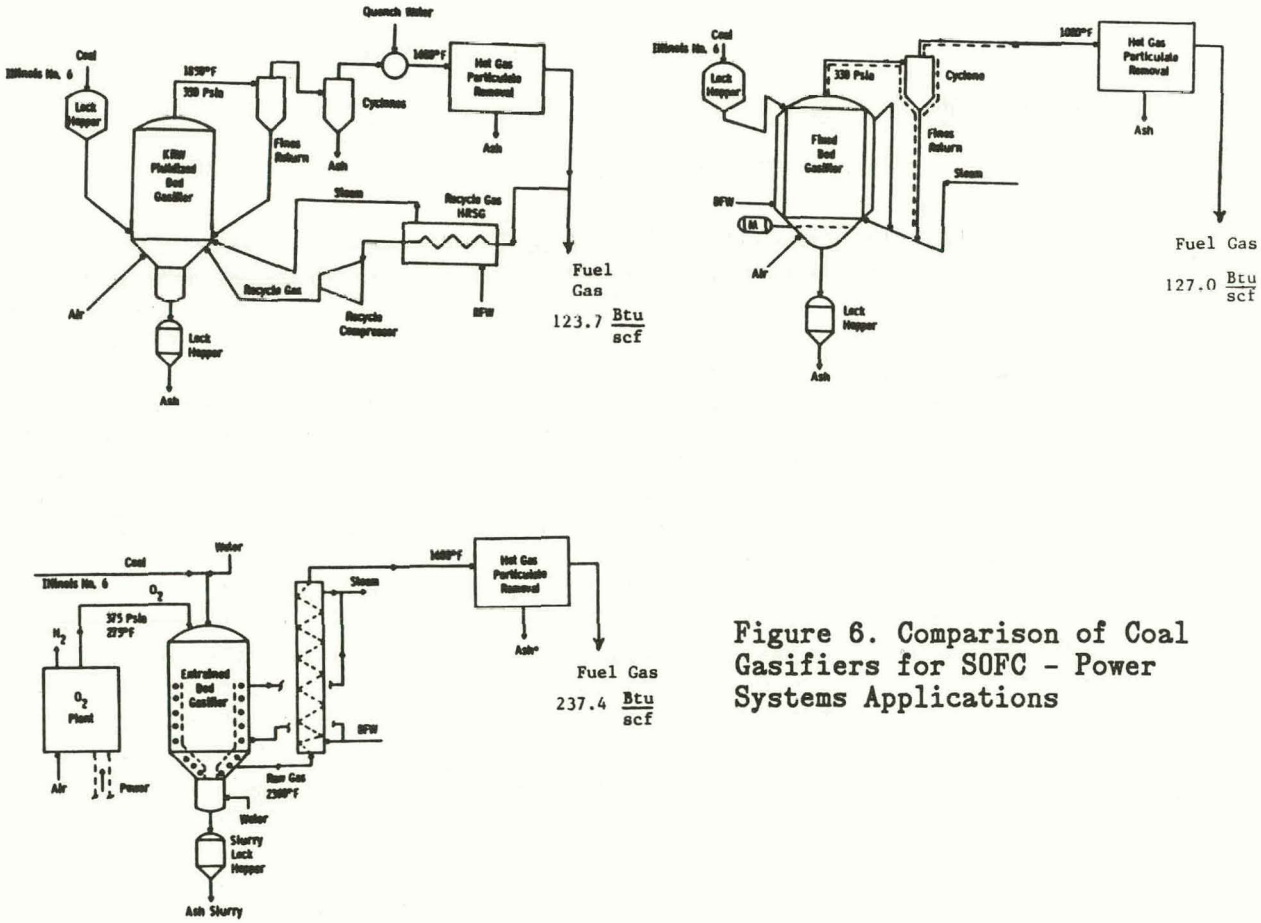

Figure 6. Comparison of Coal Gasifiers for SOFC - Power Systems Applications

In the Lurgi design, no recycle fuel gas system is used and the steam for the gasifier is supplied from the steam plant bottoming power cycle. The fuel gas temperature exiting the gasifier is approximately 538°C (1000°F) and is sufficiently low that no additional cooling is needed prior to entering the gas cleaning systems. Since both the KRW and Lurgi are air blown gasifiers, an air compressor unit is provided as part of the power cycle system.

The Texaco gasifier uses oxygen for gasification and an air separation plant is provided. Steam for the gasification process is provided via the coal/water slurry that is fed directly into the gasifier.

The raw fuel gas exiting the gasifier is at about 1260°C (2300°F) and is cooled prior to entering the particulate filter and desulfurizer by passing through a heat recovery steam boiler that is integrated with the steam turbine power cycle. The Zinc Ferrite system is assumed to remove sufficient H_2S from the fuel gas to achieve a 10 ppm H_2S outlet concentration.

POWER CYCLE FOR IG/SOFC STEAM TURBINE COMBINED CYCLE

The cycle diagram given in Figure 7 shows the power cycle component arrangement for the KRW/SOFC Steam Turbine combined cycle plant. In this arrangement, the high pressure, high temperature (871°C, 22 atm) fuel gas from the gasifier is expanded to lower the fuel gas temperature prior to desulfurization. Net electrical power is produced which represents 15 to 20 percent of the plant output. The fuel gas exits the expander at about 594°C (1100°F) and 5.2 atm. After desulfurization, the fuel gas is further expanded to near ambient pressure and a temperature of about 420°C (785°F). The power from this turbine is used to drive the gasifier two-stage air compressor.

The front-end arrangement of the power cycle for the Lurgi and Texaco gasifiers differs from that of the KRW. For the Lurgi system with the lower fuel gas temperatures, no further fuel gas temperature conditioning is needed prior to desulfurization. Following desulfurization, the gas is expanded to near ambient pressure in a turbocompressor arrangement that also produces net electrical power. Similarly, for the Texaco system that uses a heat recovery steam generator to cool the fuel gas, no additional fuel gas temperature control would be required prior to the desulfurizer. After the desulfurizers, the fuel gas is expanded to near ambient pressures through a gas turbine generator unit. For this case, however, there is no air compressor unit since an air separation plant is utilized.

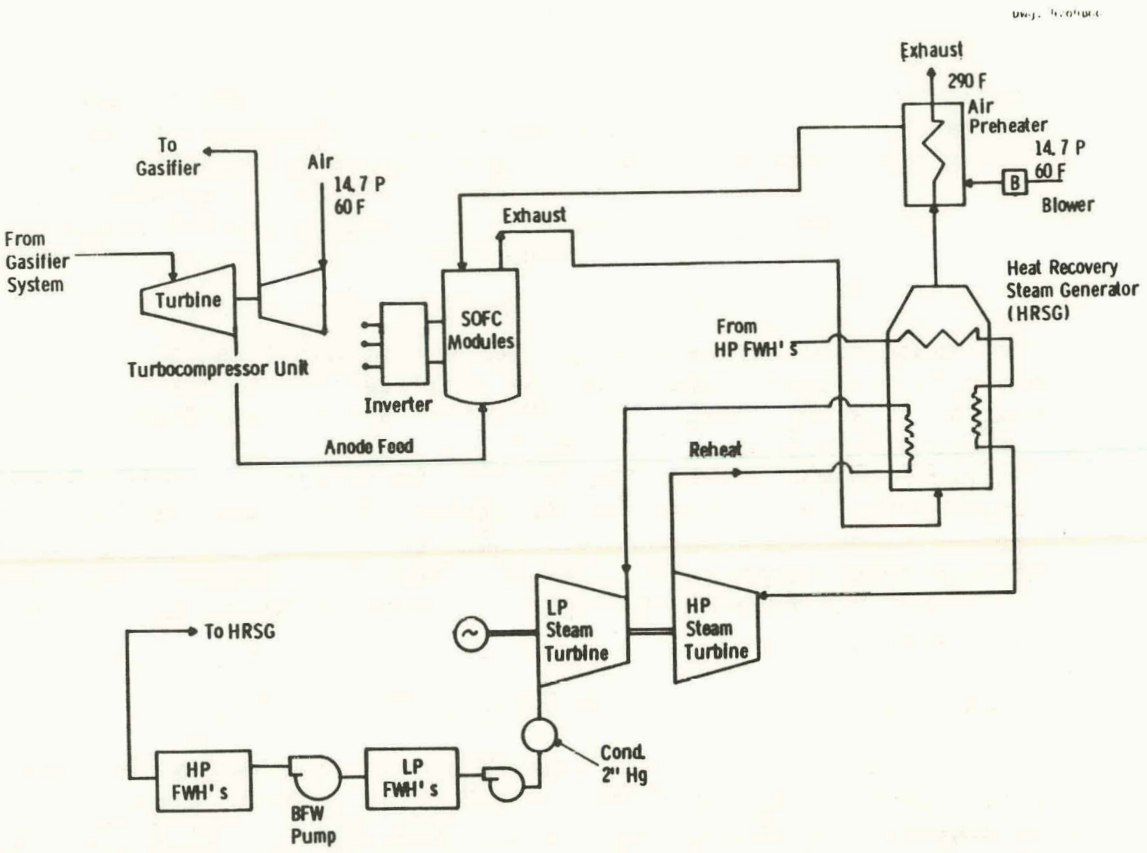

Figure 7. IG/SOFC Steam Turbine Combined Cycle Simplified Flow Diagram

For all three gasifiers, the balance of the power cycle arrangement is similar. Again referring to Figure 7, following expansion of the coal fuel gas to near ambient pressure, fuel and preheated air are ducted directly to the SOFC system. The SOFC generator produces dc power which is then converted through appropriate power conditioning to a net ac electrical output. This power represents about 40 to 60% of the net plant output. The exhaust gas from the combustion of the spent fuel and SOFC air exits the SOFC system at temperatures above 800°C (1470°F). This waste heat is utilized to raise high quality steam through a heat recovery steam generator and, following that, to preheat the incoming SOFC air. Net electrical power is recovered from the steam raised in the HRSG through high performance, reheat steam turbines. The steam plant design includes a deaerating heater and low and high pressure extractive feedwater heating. Net electrical power is generated from the steam turbine system that represents approximately 25 to 40% of the plant net electrical output. Depending on gasifier type as explained earlier, the steam cycle may be directly integrated with gasifier and fuel gas cooling systems. Additionally, for each gasifier system, steam is required for the Zinc Ferrite regeneration step. All or part of this steam may be generated in the gasifier air compressor intercooler (KRW and Lurgi), taken as part of the steam turbine extraction or raised separately in the heat recovery steam generator.

Table 1 shows a comparison of the plant performance of the three different gasifier systems integrated with an SOFC/Steam Turbine power cycle. All three plants assume reheat steam turbine cycles and are based on an 85% SOFC fuel utilization factor and cell operation at 0.6 volts. These results show that the lowest plant heat rate or highest plant efficiency is achieved with the KRW gasifier but that in general each of the gasifiers can be integrated with an SOFC system that operates at near ambient pressure to achieve very attractive plant heat rates. The calculated heat rates for each of the plants all fall below the heat rates projected for the near term and advanced integrated gasification, gas turbine combined cycles.

TABLE 1 - SUMMARY OF PERFORMANCE COMPARING IG/SOFC -STEAM TURBINE COMBINED CYCLES

	KRW-IG/SOFC	Texaco-IG/SOFC	Lurgi-IG/SOFC
Plant Size, MW (nominal)	250	275	300
Gasifier P&T (psia/°F)	330/1850	330/2300	330/1000
SOFC Parameters			
Pressure, psia	17.1	17.1	17.1
Fuel/Air Temp., °F	782/714	646/714	428/714
Performance			
SOFC, MW (at .6V/cell)	130.8	162	202.5
Fuel Expander, MW	36.9	36.3	43.8
Steam Turbine, MW	78.2	115.4	80.0
Auxiliary Power, MW	(9.6)	(38.2)*	(13.0)
Net Power, MW	236.3	275.5	313.3
Plant Heat Rate, Btu/kW hr	7246	7596	7847
Plant Efficiency	47.1	44.9	43.5

* includes O_2 Plant Power as auxiliary requirement

REFERENCE DESIGN

A conceptual design and preliminary plant costs were developed for a nominal 250 MWe KRW IG/SOFC Steam Turbine combined cycle. Figure 8 shows an artist's concept of the plant illustrating arrangement of the gasifier, SOFC power block and HRSG/Air Preheater. The individual SOFC modules which are approximately 3.5 MWe each are stacked into a 3 tier "parking garage" arrangement to form a power block that can produce between 30 to 40 MWe. One gasifier would serve two such power blocks. A 250 MWe central station electric power plant would require two gasifiers and four SOFC power blocks exhausting to a single HRSG and air preheater.

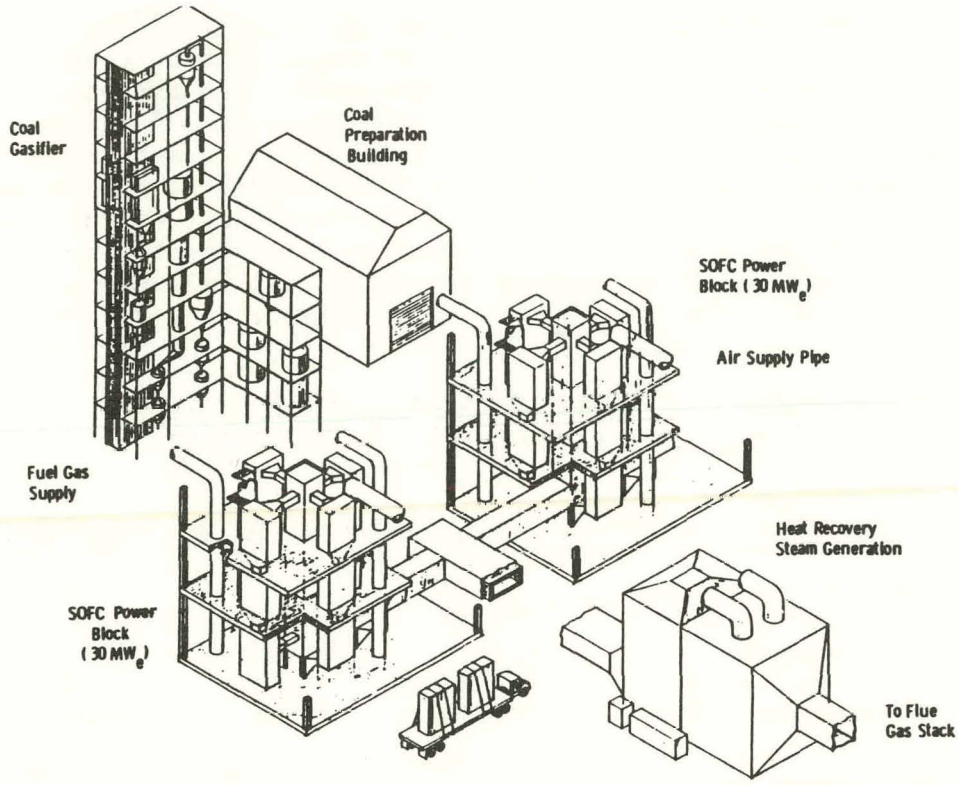

Figure 8. Integrated Gasification, Solid Oxide Fuel Cell Central Station Power Plant

In this fuel cell system, the temperature of the exhaust gas entering the HRSG is fixed by the SOFC fuel utilization factor and excess air that is provided to the SOFC system. In this study, the air flow is taken as four times stoichiometric value while the fuel utilization parameter and cell operating voltage are varied to minimize total cost of electricity (COE).

Figure 9 shows these results for one assumed set of plant economics. The curve shows the relative costs of electricity as a function of cell operating voltage at 85% fuel utilization. The shape of the curve is driven by the cell voltage-current and cell power characteristics that establish the number of cells required to meet the SOFC output. Each point on the curve represent a plant with different heat rate and component costs. Although relatively flat over a voltage range from 0.45 to about 0.60 volts, there is an identifiable minimum that occurs in the COE at about 0.5 volts/cell. For this plant, at the 0.5 volt/cell point, the total capital requirement is estimated (based on EPRI TAG methods (3)) at about 1480 $/kWe with the fuel cell system (including power conditioning) representing about 27% of this total.

POWER CYCLE FOR IG/SOFC GAS TURBINE COMBINED CYCLE

The cycle diagram given in Figure 10 shows the power cycle component arrangement (after gas cleaning) for the IG/SOFC Gas Turbine combined cycle. In this arrangement pressurized fuel gas from the desulfurizers and compresed air are fed to the SOFC system. The exhaust gas from the SOFC are still at high pressure and temperature and suitable for gas turbine operation. The expansion of the gas through the turbine again results in net electrical output. The turbine exhaust gases are still sufficiently hot to raise high quality steam in a heat recovery steam generator. Again, net electrical power is produced from the steam raised in the HRSG using a high performance steam turbine plant.

The performance of this cycle is dependent on a variety of operating and design parameters that are interrelated in a complex manner. These interrelated effects include gasifier type and operating pressure level, fuel gas temperature and control, fuel cell operating voltage and fuel utilization and their effect on gas turbine inlet temperature, the technology limit assumed for the gas turbine (i.e., inlet temperature and operating pressure ratio) and type of gas turbine (with or without steam injection). Presently, systems models are being constructed for different options to investigate the performance potential of this basic power cycle.

6. RESULTS AND ACCOMPLISHMENTS:

An evaluation of IG/SOFC is being conducted to identify potential applications, user requirements, plant design requirements and definition of plant performance and costs.

Nine potential applications for IG/SOFC plants were defined and reviewed by selected utilities. Based on this review, the utilities believed that a 250 MWe coal based central station SOFC power plant is one preferred application for this technology. Other preferred applications include repowering of existing coal, oil and gas units in the 150 to 300 MWe power range and application of small modular 5 to 50 MWe units operating on natural gas. Participation by the utilities in the review process has provided the opportunity to inform potential users of the Solid Oxide Fuel Cell option and to enhance the potential for future coal gasification applications.

Conceptual plant design studies are in progress to define potential IG/SOFC systems for a central station application. Two basic power cycles were identified and then system models developed and parametric studies were conducted for an IG/SOFC-Steam Turbine Combined Cycle Plant. Heat and material balances and plant performance were calculated for this cycle for three basic gasifier types. This study showed that any one of the three gasifier types could be integrated with an SOFC Steam Turbine power

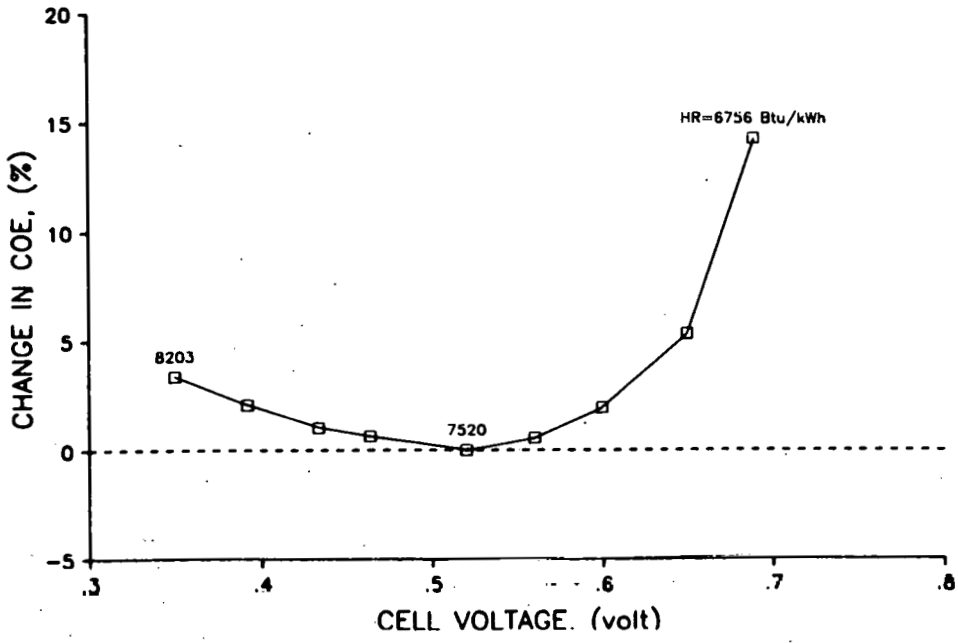

Figure 9. Trend in COE with Cell Operating Voltage for IG/SOFC Steam Turbine Cycle

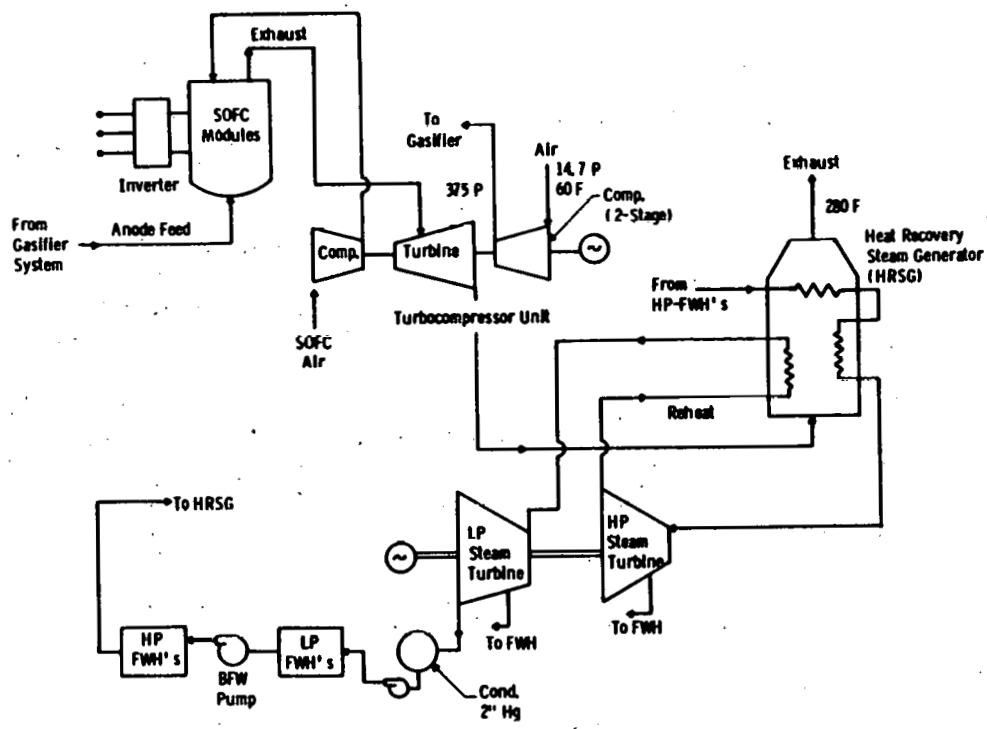

Figure 10. IG/SOFC - Gas Turbine Power Cycle

cycle with resulting plant efficiencies that range from about 43 to 47 percent coal pile to busbar. A reference design study was conducted for the KRW/SOFC - Combined Cycle plant where component costs were estimated and the relative effect of varying fuel cell operating parameters on relative COE was studied.

7. FUTURE WORK:

Parametric studies are continuing to evaluate cell performance and design and costs on system COE. Systems analysis studies are being conducted to define the performance potential of the IG/SOFC - Gas Turbine Combined Cycle Plant. Reference designs for the IG/SOFC Combined Cycle are continuing.

8. REFERENCES:

1. Design, Fabrication and Testing of a Solid Oxide Fuel Cell Stack for a 25 kW to 200 kW Generator - Topical Report User Requirements Test 1.1. Prepared under Contract DE-AC21-80WET17089, April, 1987 (unpublished).

2. An Economic Comparison of Molten Carbonate Fuel Cells and Gas Turbines in Coal Gasification-Based Power Plants, EPRI AP-1543 - Final Report September 1980.

3. Technical Assessment Guide, EPRI P-2410-SR, May 1982.

DYNAMIC SIMULATION MODELS FOR HIGH-TEMPERATURE DESULFURIZATION PROCESSES

1. CONTRACT NUMBER: DE-AC21-86MC23089

CONTRACTOR: Louisiana State University
Department of Chemical Engineering
Baton Rouge, Louisiana 70803

CONTRACTOR PROJECT MANAGER: D. P. Harrison

PRINCIPAL INVESTIGATORS: J. Wang
D. Cockrill
F.R. Groves, Jr.
D.P. Harrison

METC PROJECT MANAGER: S.C. Jain

PERIOD OF PERFORMANCE: September 25, 1986 to
November 24, 1987

2. SCHEDULE/MILESTONES

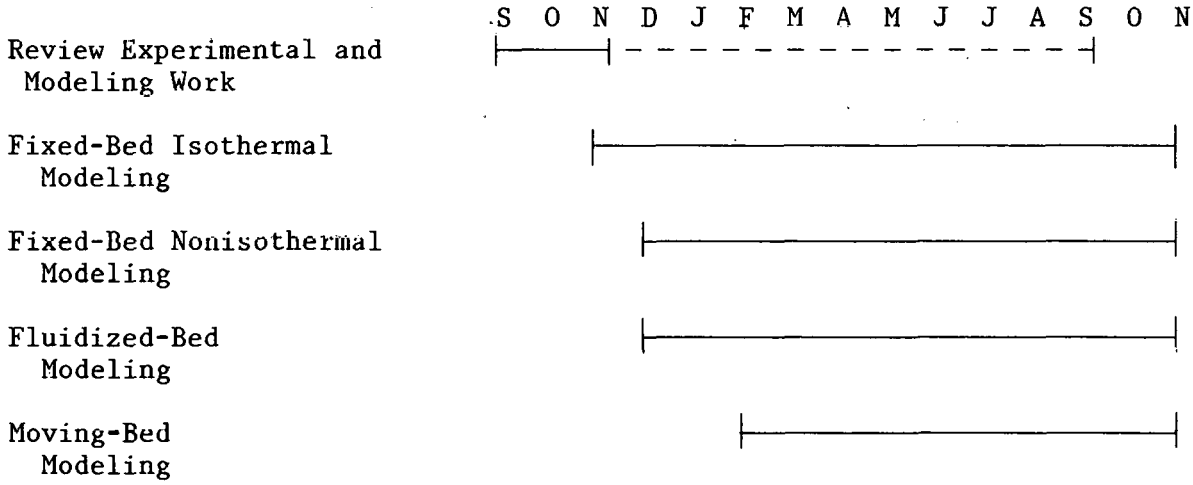

3. OBJECTIVES

The objective of the research is the preparation of dynamic simulation models capable of describing both the sulfidation and regeneration cycles in fixed-, fluidized-, and moving-bed reactors. The models should be capable of matching breakthrough curves, sulfur loadings, and temperature fronts obtained from experimental reactors.

4. BACKGROUND STATEMENT:

The description of high temperature desulfurization/regeneration reactors consists of coupled, nonlinear partial differential equations which can

only be solved by numerical methods. The final equations often represent a compromise in which simplifications are made to satisfy computational constraints. An accurate and detailed model is of little use if the solution cannot be obtained with available computer resources. Likewise, a model which has been so simplified that it no longer mirrors experiment is of little use. Knowledge of numerical mathematics and chemical reaction engineering is required to develop a model which accomplishes both objectives. The reaction engineering analysis must include the heat and mass transfer characteristics, and intrinsic surface chemistry of both the integral reactor and the individual sorbent particles.

The project began with a review of the literature to identify past work on desulfurization reactor modeling and experimental results with which the model predictions could be compared. The studies of Schrodt (1983) and Steinfeld (1980) proved to be of most value in the area of integral reactor modeling, while previous work in this laboratory (Focht, et al., 1986) was used to develop single particle kinetics concepts. Experimental data from fixed-bed reactors in both the sulfidation and regeneration modes has been reported in a series of papers by Grindley and coworkers (1981, 1982, 1983, 1984, 1985a, 1985b, 1986). No relevant experimental results from either fluidized- or moving-bed reactors were identified in the open literature.

5. PROJECT DESCRIPTION:

Material balance equations for all reacting species in both the solid and gaseous phases must be considered. When nonisothermal conditions exist, the material balances must be coupled with energy balances for both phases. The following general simplifications applicable to all reactor configurations have been adopted:

- only one gaseous reactant (H_2S - sulfidation, O_2 - regeneration).
- only one solid reactant (mixed oxides treated as a single specie).
- no reaction in the gas phase.
- no radial or angular gradients in gas concentration or temperature.
- plug flow of gas phase in axial direction.
- negligible accumulation of gaseous reactant and gas phase enthalpy.
- no spatial temperature gradients within the sorbent particles.

Additional simplifications appropriate for individual cases have also been made. For example, energy effects during the sulfidation cycle are known to be small so that an isothermal analysis is reasonable. In contrast, high energy releases during regeneration require that two energy balance equations also be included.

The unreacted core model has been adopted to describe the kinetics of reactions within single particles in both the fixed- and moving-bed

reactors. This model is known to agree quite well with independent single particle kinetic measurements (Focht, et al. (1986)), and its use results in significant mathematical simplification. A homogeneous model has been chosen to describe reaction within the smaller particles used in a fluidized-bed reactor.

For fixed-bed reactors where experimental data is available, the initial numerical effort will be aimed at model validation. That is, parameter values will be chosen so that predicted and experimental results agree within acceptable tolerances. The validated model may then be used for design purposes and to assist in planning additional experimental runs and the analysis of experimental data. For fluidized- and moving-bed reactors, for which no experimental data is available, validation is not feasible. Consequently, certain parameter values must be established by intelligent guesses, and the numerical results can be used for preliminary design studies and for order-of-magnitude comparisons. At the present time, numerical results are available only for the fixed-bed isothermal reactor and further discussion is limited to that case.

6. RESULTS/ACCOMPLISHMENTS

The analysis is applicable to the general chemical reaction

$$A(g) + b\ S(s) \rightarrow \text{prod} \qquad (1)$$

For zinc ferrite reacting with H_2S, b = 0.33. Subject to the simplifications previously described, three material balance equations with boundary conditions are required for the model.

- Gas Phase Component A Material Balance

$$U_o \frac{\partial C_A}{\partial z} = -k_g\, a_v\, (C_A - C_{As}^s) = -r_A^v \qquad (2)$$

with $$C_A = C_{Ao} \text{ at } z = 0 \qquad (3)$$

- Solid Phase Component A Material Balance (for an infinite cylindrical pellet)

$$\frac{\partial(r \frac{\partial C_{As}}{\partial r})}{\partial r} = 0 \qquad \text{for } r_c \leq r \leq R \qquad (4)$$

with $$\frac{\partial C_{As}}{\partial r} = \frac{k_g}{D_e} (C_A - C_{As}^s) \qquad \text{at } r = R \qquad (5)$$

and $$\frac{\partial C_{As}}{\partial r} = \frac{r_A}{D_e} \qquad \text{at } r = r_c \qquad (6)$$

- Solid Phase Component S Material Balance

$$\frac{\partial C_S}{\partial t} = -b\, k_g\, a_p\, (C_A - C_{As}^s) \tag{7}$$

with $$C_S = C_{So} \qquad \text{at } t = 0 \tag{8}$$

The intrinsic reaction rate per unit surface is assumed to be first-order in the concentration of A at the position of the unreacted core and proportional to the molar concentration of S.

$$r_A = k'\, C_{So}\, C_{As}^c \tag{9}$$

The surface rate expression may be converted to a volumetric rate r_A^v by multiplying by the reaction surface area per unit volume.

$$r_A^v = \frac{2\, r_c\, (1 - \varepsilon_v)}{R^2}\; r_A \tag{10}$$

The well-known analytical solution to eqn (4) with boundary conditions (5) and (6) (Szekely, 1976) provides an expression for C_{As} as a function of radial position in the product layer. By setting $r = r_c$, the concentration at the unreacted core may be obtained. This result may be substituted into eqns (9) and (10) to obtain the algebraic expression for the global rate within the pellet.

$$r_A^v = \frac{\dfrac{2(1 - \varepsilon_v)C_A}{R}}{\dfrac{1}{k'C_{So}(1-X)^{\frac{1}{2}}} + \dfrac{R}{D_e} \ln (1-X)^{\frac{1}{2}} + \dfrac{1}{k_g}} \tag{11}$$

where $$X = 1 - \left(\frac{r_c}{R}\right)^2 . \tag{12}$$

By combining equations (2) and (7) through the mass transfer term and substituting equation (11) we obtain the final dimensionless equations for the isothermal fixed bed model

$$\frac{\partial C_A^*}{\partial z^*} = -\frac{\partial X}{\partial t^*} = G(X)\, C_A^* \tag{13}$$

with $$G(X) = \frac{2(1 - \varepsilon_v)L}{U_o\, R} \left[\frac{1}{\dfrac{1}{k'C_{So}\,(1-X)^{\frac{1}{2}}} - \dfrac{R}{D_e} \ln (1-X)^{\frac{1}{2}} + \dfrac{1}{k_g}} \right] \tag{14}$$

The solution to the final equations proceeds in the following manner. All terms in G(X) except X are constant and known. At $t^* = 0$, $X = 0$ for all z^*. Hence, the concentration equation can be integrated for all z^* to obtain $C_A^*(0,z^*)$. Time can then be incremented using the initial values of G(X) and C_A^* to determine $X(t_1^*,z^*)$. This permits G(X) to be reevaluated at t_1^*. The general solution is obtained by alternately solving the concentration and fractional conversion equations until the desired end conditions are reached.

Preliminary numerical results have been obtained using the set of "base-case" parameters listed in Table 1. While these parameter values are reasonable, they are not intended to reproduce actual experimental data. A step-size study was performed using base-case parameters to identify appropriate values of Δt^* and Δz^* and to compare results using a Runge-Kutta (RK) solution method and the LSODE package for solving differential equations. Reduction in Δt^* and Δz^* should improve the accuracy of the solution, but at the expense of added computer time. $\Delta t^* = 0.025$ and $\Delta z^* = 0.02$ proved to be satisfactory for the base-case parameters. The RK and LSODE methods predicted identical concentrations but LSODE required twice the computer time; the RK method is now being used.

Figures 1 through 3 show model results using base-case parameters with $\Delta t^* = 0.025$ and $\Delta z^* = 0.02$ and the RK computational method. Figure 1 presents C_A^* versus z^* profiles at reaction times from 1 to 5 hours, illustrating the movement of the reaction front and the eventual breakthrough. With inlet and breakthrough concentrations approximately 10,000 and 50 ppm (volume) respectively, it is necessary to transform the effluent values of C_A^* to the ppm level with results shown in Figure 2. The definition of breakthrough is arbitrary, but if 50 ppm is selected, the predicted breakthrough time is 3.25 hours. Zero effluent concentration during the initial period of operation results because the desulfurization reaction is assumed irreversible.

Figure 3 shows the sulfur loading within the reactor at breakthrough (3.25 hours). Sulfur concentration is expressed as mass of sulfur per mass of fresh sorbent with complete sulfidation of zinc ferrite sorbent corresponding to 0.398. For these conditions, the first 20% of the bed is completely sulfided, with the reaction occurring over the remaining 80% of the bed length. The overall sorbent utilization at breakthrough is 55%, or 0.22 grams of sulfur captured per gram of initial sorbent.

Table 1. Base Case Parameters for the Fixed-Bed Isothermal Reactor.

ε_v	=	0.74	D_e	=	600 cm^2/hr
L	=	20.3 cm	k_g	=	16,000 cm/hr
U_o	=	47,200 cm/hr	C_{Ao}	=	4.058×10^{-7} mol/cm^3
R	=	0.25 cm	C_{So}	=	8×10^{-3} mol/cm^3
		k' = 1×10^7 $cm^4/mol\ hr$			

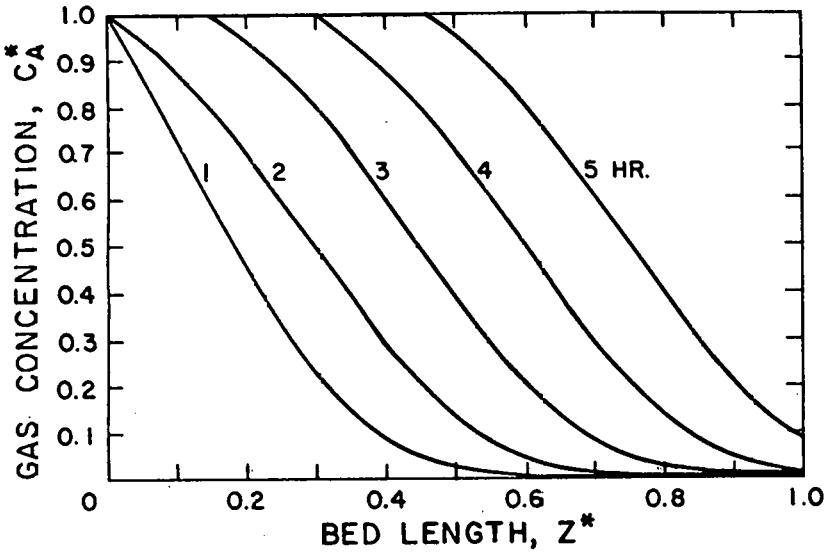

Figure 1. Movement of the Concentration Front Through the Fixed-Bed Reactor: Base-Case Parameters

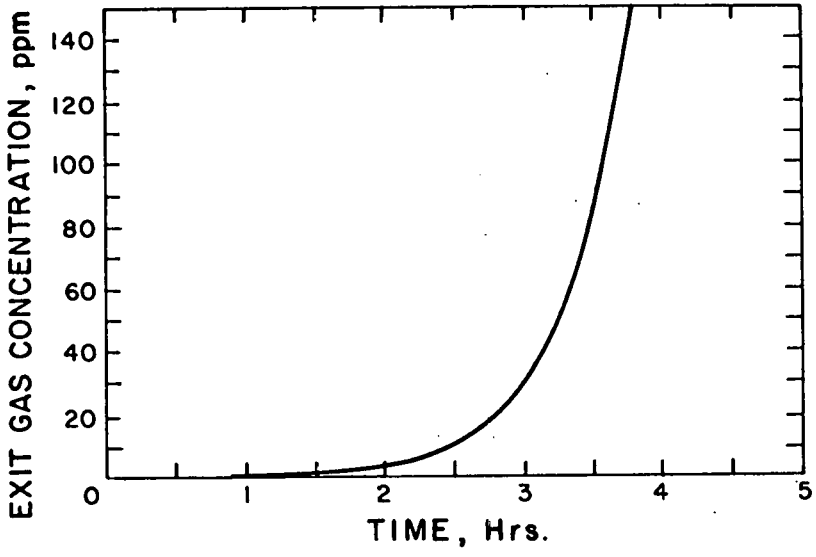

Figure 2. H_2S Breakthrough From the Fixed-Bed Reactor: Base-Case Parameters

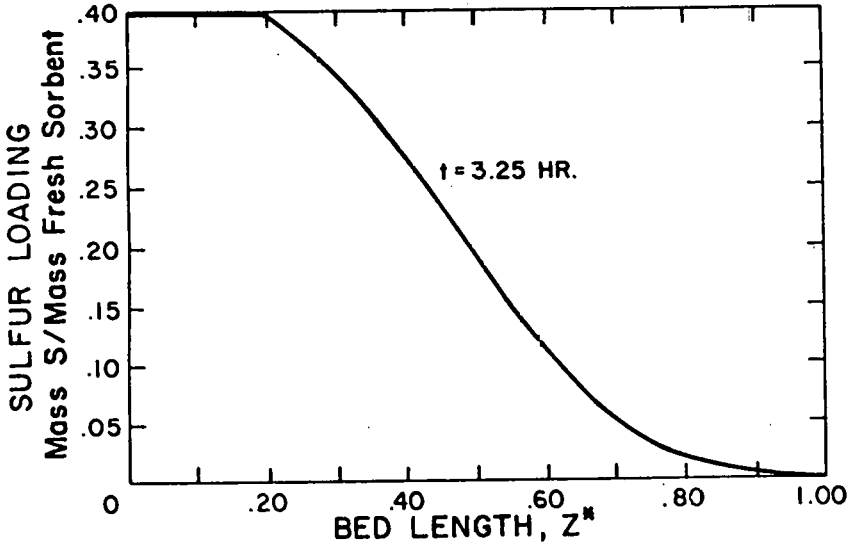

Figure 3. Sorbent Sulfur Loading at Breakthrough: Base-Case Parameters

The concentration fronts in Figure 1 exhibit constant pattern behavior (Ruthven, 1984). Once the concentration front is fully developed at a time corresponding in this case to approximately two hours, it moves through the reactor with a constant velocity of

$$U_f = \frac{U_o \; b \; C_{Ao}}{C_{So} \; (1-\varepsilon_v)} \tag{15}$$

The criterion for the establishment of the constant pattern is

$$\partial C_A^* / \partial z^* = 1 \qquad \text{or} \quad X = 1 \qquad \text{at } z^* = 0 \tag{16}$$

It is necessary to carry out the stepwise integration of the model equations only until the constant pattern develops. Thereafter, the movement of the front can be calculated algebraically in terms of the wave velocity. This simplification results in significant savings in computer time for long reactor beds and sharp reaction fronts. However, if the reaction front extends through the entire bed, breakthrough will occur prior to the establishment of the constant pattern, and no computer savings will be realized.

Variation in individual parameter values may affect the slope of the concentration profiles, the displacement of the profiles, or both. Figure 4a illustrates the effect at t = 4 hours when the inlet gas velocity is changed by ± 25% from the base case value of 47,200 cm/hr. Other parameters are maintained at their base values. Higher velocity (curve 3) reduces the slope and displaces the concentration front to larger values of z^*. The decreased slope results in a longer reaction zone because of the reduced contact time. The displacement occurs because the feed rate of H_2S to the reactor increases proportionally. Decreased velocity (curve 2) has the opposite effect. Breakthrough curves for these cases are shown in Figure 4b. Higher velocity causes the breakthrough to occur earlier (t = 1 hour for 50 ppm effluent concentration), while lower velocity increases the breakthrough time to almost five hours.

In contrast, a change in pellet radius of ± 25% from the base value of 0.25 cm alters only the slope of the concentration profiles as shown in Figure 5a. The smaller pellet (curve 3) exhibits an increased slope, a reduced length of the reaction zone, and the breakthrough time is prolonged as shown in Figure 5b (curve 3). Larger pellets (curve 2) produce the opposite effect. Again, other parameters are maintained at base-case values.

Even though the slope of the concentration profiles may be quite different, this difference is not apparent in the breakthrough curves. At the ppm level, the breakthrough curves are displaced but differences in slope are effectively indistinguishable.

In order to perform a meaningful comparison of experimental results with model predictions, it is necessary that the experimental run be continued past breakthrough to (near) saturation or that the sulfur content of the sorbent be determined as a function of axial position when the run is

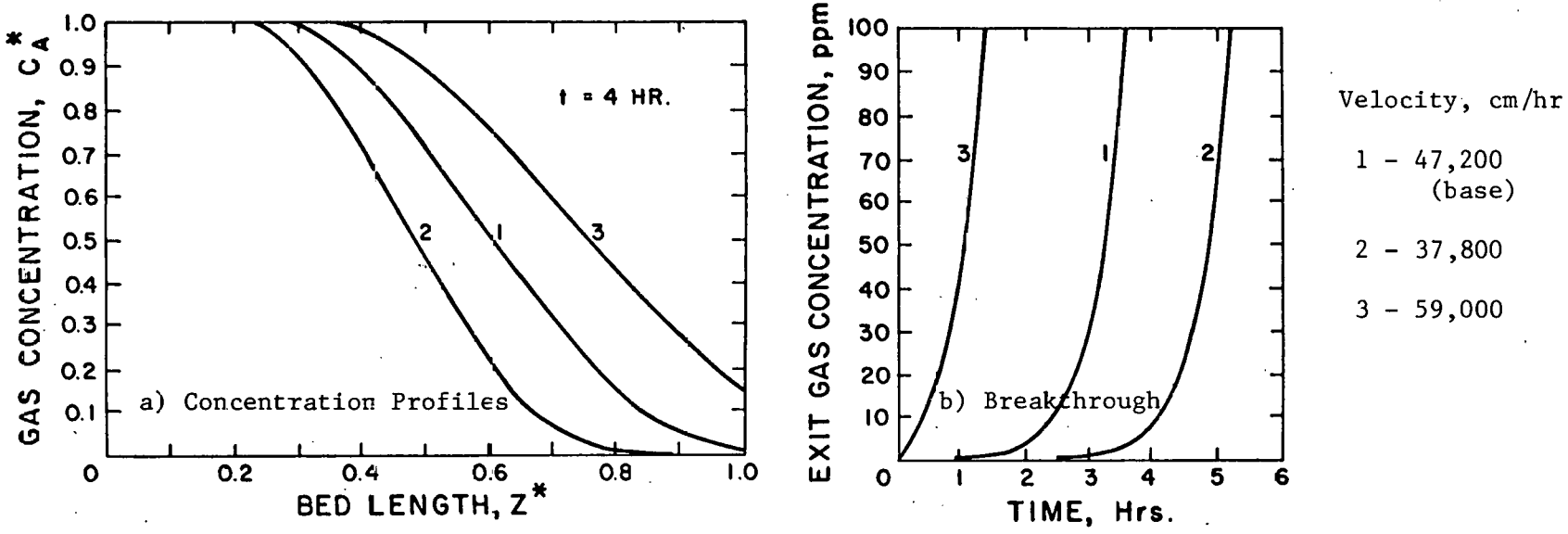

Figure 4. The Effect of Gas Velocity on Reactor Performance

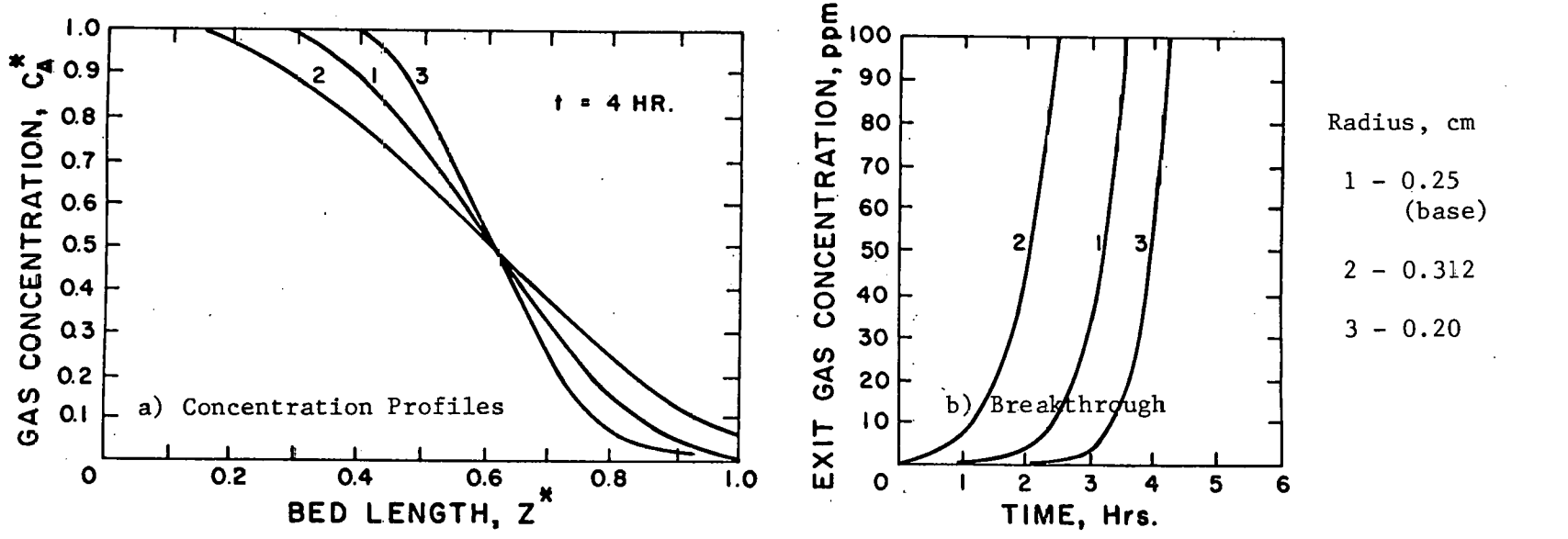

Figure 5. The Effect of Pellet Radius on Reactor Performance

terminated at breakthrough. This severely limits the usefulness of many experimental tests which were terminated at breakthrough. In only a few cases was the sulfur content of the sorbent measured.

7. FUTURE WORK

The isothermal fixed-bed modeling effort has progressed to the stage of identifying relevant experimental results to permit testing and calibration of the model. For the nonisothermal fixed-bed model and the other reactor configurations, the mathematical analysis has been completed, and appropriate numerical techniques have been identified. Preliminary numerical results will be available in the near future.

8. REFERENCES

Focht, G.D., L.N. Sa, P.V. Ranade, D.P. Harrison, 1986, Final Report, DOE Contract DE-AC21-84MC21166.

Grindley, T., et al., DOE/MC/16545-1125; 1982, DOE/METC/82-47, pp. 332-359; 1983, DOE/METC/84-6, pp. 145-171; 1984, DOE/METC/85-3, pp. 314-336; 1985a, DOE/METC/85-6025, pp. 33-62; 1985b, DOE/METC/85-4002; 1986, DOE/METC/86-6042, pp. 190-212.

Ruthven, D.M., 1984, Principles of Adsorption and Adsorption Processes, Wiley-Interscience, New York.

Schrodt, J.T., 1983, DOE/MC/21582-150D.

Steinfeld, G., 1980, DOE/METC/08333-105.

Szekely, J., J.W. Evans, and H.V. Sohn, 1976, Gas-Solid Reactions, Academic Press, New York.

9. NOMENCLATURE

a_p - gas-solid interfacial area per unit volume of particle, ℓ^{-1}

a_v - gas-solid interfacial area per unit volume of bed, ℓ^{-1}

b - stoichiometric coefficient, dimensionless

C_A - molar concentration of A in the gas phase, mol/ℓ^3

C_{Ao} - molar concentration of A at the reactor inlet, mol/ℓ^3

C_{As} - molar concentration of A in the solid phase, mol/ℓ^3

C_{As}^c - molar concentration of A at the unreacted core interface, mol/ℓ^3

C_{As}^s - molar concentration of A at the particle external surface, mol/ℓ^3

C_A^* - dimensionless concentration of A, C_A/C_{Ao}

C_S - molar concentration of S in solid phase, mol/ℓ^3

C_{So} - initial molar concentration of S in solid phase, mol/ℓ^3

D_e - effective diffusivity of A within the pellet, ℓ^2/t

G(X) - function defined by eqn (14)

k' - intrinsic surface rate constant, $\ell^4/mol \cdot t$

k_g - mass transfer coefficient, ℓ/t

L - length of the packed-bed reactor, ℓ

r - radial coordinate within the cylindrical pellet, ℓ

r_A - molar reacton rate of A per unit area, mol A/$t \cdot \ell^2$

r_A^v - molar reaction rate of A per unit volume, mol A/$t \cdot \ell^3$

R - pellet radius, ℓ

t - time, t

t^* - dimensionless time, $t\ U_o\ C_{Ao}/[LC_{So}\ (1 - \varepsilon_v/b)]$

U_f - reaction wave velocity, ℓ/t

U_o - superficial gas velocity, ℓ/t

X - fractional conversion of solid, dimensionless

z - axial position within reactor, ℓ

z^* - dimensionless axial position, $z^* = z/L$

ε_v - bed porosity, dimensionless

DETAILED STUDIES OF NOVEL REGENERABLE SORBENTS FOR HIGH-TEMPERATURE COAL-GAS DESULFURIZATION

1. CONTRACT NUMBER: DE-FC21-85MC22193

CONTRACTOR: Massachusetts Institute of Technology
Department of Chemical Engineering
25 Ames Street
Cambridge, MA 02139
(617)253-3178 (PI)

PROGRAM MANAGER (CONTRACTOR): Maria Flytzani-Stephanopoulos

PRINCIPAL INVESTIGATORS: Maria Flytzani-Stephanopoulos
Kandaswami Jothimurugesan
Susan Lew
George R. Gavalas (Caltech)
Valérie Patrick (Caltech)

METC PROJECT MANAGER: Steven J. Bossart

CONTRACT PERIOD OF PERFORMANCE: October 1, 1985 through July 31, 1987

2. SCHEDULE/MILESTONES:

FY 1987 Program Schedule

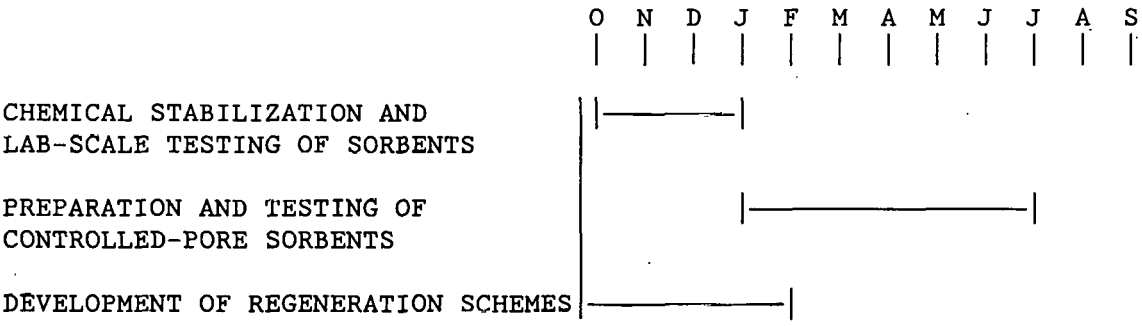

3. OBJECTIVES:

The overall objective of this work is to study in detail the effects of preparation, chemical composition and structural properties on the reactivity, stability, and regenerability of novel mixed oxide H_2S sorbents over the temperature range of 1000°-1500°F. The sorbents selected for this study include both CuO- and ZnO-based materials. The specific objectives of the project are to:

- Investigate the effects of additives such as Al_2O_3 and TiO_2 on the reduction stability and overall performance of CuO- and ZnO-based sorbents.

- Carry out comparative fixed-bed studies of sulfidation-regener-

ation with different compositions of sorbents prepared in granular form, and select most promising sorbent types.

- Conduct parametric studies of regeneration of the selected sorbents and correlate sorbent regenerability and composition of regeneration off-gas to regeneration conditions for each sorbent type.

- Prepare selected sorbents in extruded form (1/8" dia.) with a good balance of porosity and mechanical strength. Test best sorbents in many (10-15) sulfidation-regeneration cycles in a lab-scale, fixed-bed reactor.

4. BACKGROUND STATEMENT:

Detailed experimental studies of the sulfidation/regeneration performance of binary and ternary oxide mixtures of copper and zinc with aluminum, iron, and titanium oxides are being conducted in this project. Results from work carried out since June 1986 are presented here. Accomplishments prior to that date can be found in the 1986 Proceedings of this forum (Flytzani-Stephanopoulos et al., 1986). Earlier reports of work by this research group that led to identification of CuO-based mixed oxides as very promising regenerable sorbents for high-temperature coal gas desulfurization can be found in other publications (Flytzani-Stephanopoulos et al., 1985 a, b; Tamhankar et al., 1986).

A comprehensive approach has been followed in this project to correlate sorbent reactivity, sulfur capacity, and regenerability to the physicochemical properties of the mixed oxide sorbents during reaction. Reduction, sulfidation, and regeneration tests are carried out in lab-scale, fixed-bed reactors and thermobalance apparatus. Structural and composition changes of the solid phases are followed by various analytical techniques. The work aims at optimizing the sorbent composition and physical properties for enhanced desulfurization/regeneration performance over a wide range of operating conditions.

5. PROJECT DESCRIPTION/RESULTS AND ACCOMPLISHMENTS:

The project consists of three major experimental tasks (Tasks 2-4) addressing the contract objectives described above. Tasks 2 and 4 examine the reduction-sulfidation-regeneration characteristics of various compositions of CuO- and ZnO-based mixed oxide sorbents prepared under various conditions in the form of porous granules (-20/+40 mesh). Task 3 involves preparation and testing of selected sorbent compositions in the form of extrusions (1/8" dia.) prepared with a good balance of porosity and mechanical strength.

The effect of additives such as Al_2O_3 and TiO_2, respectively, on the performance of CuO and ZnO sorbents, has been the primary issue in work performed under Tasks 2 and 4. In particular, these additives have been evaluated as stabilizers of CuO and ZnO against reduction (and metallization). In the case of CuO this stabilization results in higher H_2S removal efficiency, while for ZnO loss of volatile Zn metal is sup-

pressed.

Mixed oxide sorbent granules used in Tasks 2 and 4 are prepared in dispersed, porous form by pyrolysis-calcination of homogeneous organic precursors prepared by complexation of aqueous solutions of metal salts with citric acid (Marcilly et al., 1970). Laboratory-scale tests with a fixed bed of sorbent are carried out in quartz microreactors (1-1.5 cm I.D.) heated by a split Lindberg furnace. A description of the microreactor system and associated instrumentation can be found in our previous reports. Also, a Cahn-113X thermogravimetric analyzer (TGA) has been used to study rates of reduction and sulfidation of various Cu-Al-O mixtures and regeneration of ZnS.

Several analytical techniques are used to determine the physicochemical properties of each sorbent. These include X-ray Diffraction (XRD) for crystalline phase identification, Atomic Absorption (AA) spectrometry for elemental composition analysis, Hg-porosimetry for pore volume and pore size distribution determination, BET N_2-desorption for surface area and He-pycnometry for porosity measurements. Also, Scanning Electron Microscopy (SEM) combined with Energy Dispersive X-ray analysis (EDX) is used to examine the porous sorbent morphology, crystallite size, and spatial variation of elemental distribution.

In Task 3 sorbents are prepared in the form of cylindrical extrusions of 1/8" dia. using a Wahlco-Model 20-8 hydraulic piston extruder equipped with a die assembly with 1/8" holes. For extrusion, a paste is prepared by mixing calcined sorbent powders with organic and inorganic binders and the necessary amount of water. After drying and calcining, the extrusions are analyzed by the above techniques, and tested for compressive strength in an Instron-Model 1125 tester machine.

Sulfidation/regeneration testing of sorbents in the quartz microreactor is carried out at P=1 atm, T=550°-800°C, and gas hourly space velocity S.V. $\simeq$ 2000 h^{-1} (STP). A simulated coal gas mixture (air-blown fluidized KRW-gasifier product gas) with a molar composition of 13% H_2, 15% CO, 10% CO_2, 19% H_2O, 1% H_2S, 42% N_2 has been used in several sulfidation tests. Typically, runs are made with a similar sulfidation mixture with carbon oxides made up as nitrogen. Regeneration is conducted with 10 mol% air-90 mol% N_2 as well as various air-steam-N_2 gas mixtures. Each sorbent is evaluated in 2-5 cycles of sulfidation/regeneration at each temperature until stabilized performance is attained.

Cu-Fe-Al-O SORBENTS

A total of fifteen Cu-(Fe, Al)-O mixtures were prepared, characterized and tested in the microreactor under Tasks 2 and 4. The initial results of this study were reported in the 1986 Annual DOE Contractors' Meeting. Over the past year, additional experiments have been performed to correlate the sorbent composition and preparation conditions to the sorbent sulfidation efficiency, sulfur capacity, regenerability and regeneration off-gas composition. The following sections summarize the results from these studies.

Physical Properties. The amorphous citrate technique used in preparation of the Cu-Fe-Al-O sorbents produces materials with well-dispersed oxide phases and high porosity. Effects of calcination temperature and sorbent composition on the physical properties of the resulting mixed oxide materials have been documented in this work. Typically, calcined Cu-Fe-Al-O particles of -20/+40 mesh size have the following properties:

	$T_{calc.}$ = 550°C	$T_{calc.}$ = 650-850°C
Surface Area (m^2/g)	30 - 100	5 - 25
Pore Volume (cm^3/g)	0.4 - 2.0	0.3 - 1.5
Porosity (%)	65 - 90	60 - 85
Bulk Density (g/cm^3)	0.7 - 1.3	1.2 - 1.7

Sorbents with high Al_2O_3-content have higher surface areas and are not well crystallized after calcination at 550°C. XRD analysis indicates the presence of microcrystalline Al_2O_3-rich phases. At higher calcination temperatures sorbents are better crystallized and contain a larger fraction of copper and iron aluminates. The surface area of these sorbents is lower, however their porosity remains high. The latter is due to the fact that more than 60% of the pore volume is in pores larger than 1 μm size, which are not lost at high temperatures. SEM pictures of Cu-Fe-Al-O sorbents typically show a combination of microcrystalline phases and macropores (> 1 μm size). Initial sorbent properties change during sulfidation/regeneration of the material at different temperatures. The main effect is a stabilization of surface area, while pore volume is only slightly affected. The presence of macropores enhances gas diffusion and minimizes pore plugging. A combination of relatively high pore volume (0.4-1.0 cm^3/g) and intermediate surface area (5-15 m^2/g) is adequate for high sorbent conversion.

Chemical Composition Effects. Copper-based sorbents do not suffer from metal volatility problems, hence, they could be used at temperatures up to 800°C or higher. Pure (bulk) copper oxide, however, suffers from thermodynamic as well as kinetic limitations and has not been considered as a practical sorbent.

The association of CuO with Al_2O_3 (or Fe_2O_3) has been employed in this work with the purpose of retarding the rate of CuO reduction to the metal state. The sulfidation equilibria of CuO, Cu_2O, and their compounds with Al_2O_3 (or Fe_2O_3) are vastly superior to Cu. It has been known in the catalysis literature that copper oxide supported on γ-Al_2O_3 is reduced more slowly than the bulk oxide (Voge and Atkins, 1962; Jacono et al., 1982). This reduction retardation was attributed to a monolayer of copper ions on the CuO-Al_2O_3 interface which has been called a "surface" copper aluminate.

During the last year we have studied in the TGA the reduction of a series of CuO-Al_2O_3 mixtures containing varying amounts of CuO, γ-Al_2O_3, and $CuAl_2O_4$ by way of different calcination conditions. These experiments showed that most of the CuO is reduced very fast to Cu, while $CuAl_2O_4$ is reduced slowly first to $CuAlO_2$, and then slowly again to Cu. A small fraction of CuO, possibly at the interface with Al_2O_3, is also

reduced slowly.

The role of iron oxide in both sulfidation and regeneration of the Cu-Fe-Al-O sorbents has been studied in this project. Formation of mixed copper-iron sulfides, e.g. $CuFe_2S_3$, Cu_5FeS_4, etc., from Cu-Fe-O mixtures proceeds with higher H_2S removal efficiency than metallic Cu sulfidation. Also, iron oxide increases the total sulfur capacity of the sorbent, and alters the selectivity of the regeneration reactions towards elemental sulfur formation (see "Regeneration" section below). In the ternary Cu-Fe-Al-O system, complete reduction of iron oxide may also be suppressed by the presence of Al_2O_3.

Sulfidation Performance. Comparative sulfidation experiments with the various Cu-Fe-Al-O formulations were performed in the microreactor at 650°C under conditions essentially free of mass transfer and pore diffusion limitations. As a result, very high breakthrough conversions (70-100% based on the active sorbent oxides) were observed in all tests. Sorbents containing up to 30 wt% Fe_2O_3 showed pre-breakthrough H_2S levels well below the equilibrium values corresponding to metallic copper sulfidation. The main effect of the Al_2O_3 component was to keep the sorbent in dispersed state (high surface area) during sulfidation, and to promote compound (aluminate) formation in regeneration. This in turn stabilized CuO against fast reduction during subsequent sulfidation.

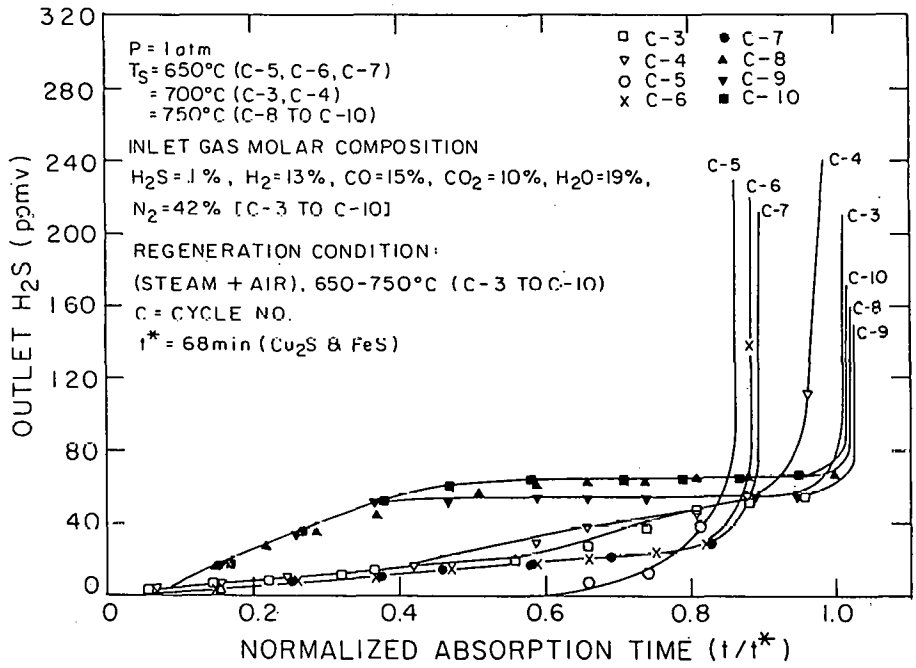

Figure 1. Cyclic Sulfidation of Sorbent C3FA (calcined at 650°C).

From the ternary Cu-Fe-Al-O mixtures, the sorbent C3FA was selected for further parametric sulfidation/regeneration studies. The composition of this sorbent corresponds to an atomic metal ratio of 3Cu:2Fe:2Al (or 47.7 wt% CuO - 31.9 wt% Fe_2O_3 - 20.4 wt% Al_2O_3). Figure 1 shows H_2S breakthrough curves obtained with one batch of this sorbent prepared by calcination in air at 650°C with initial surface area of 21 m^2/g and

high pore volume (~2.0 cm^3/g). The simulated (KRW-gasifier) coal gas mixture was used in these tests at temperatures of 650°, 700° and 750°C. Stable reproducible performance was observed at each temperature, although different regeneration conditions were used between cycles. Breakthrough sorbent conversions of 85-100% were obtained, the conversion improving at higher temperatures. The corresponding sulfur loadings were 18-22 wt%. The pre-breakthrough H_2S levels were below 25 and 60 ppmv, respectively, at 650° and 750°C.

The binary $CuO-Al_2O_3$ sorbents were also selected for further study based on their reduction-sulfidation performance. Sorbents CA_I (calcined at 550°) and CA_{II} (calcined at 850°C), each consisting of 1:1 molar $CuO:Al_2O_3$, were studied in detail. The properties of the fresh, 800°C-sulfided, and 800°C-regenerated CA_I and CA_{II} sorbents as follows:

	CA_I			CA_{II}		
	Fresh	Sulfided	Regenerated	Fresh	Sulfided	Regenerated
Surface Area (m^2/g)	98	13	10	5	8	4
Pore Volume (cm^3/g)	0.39	0.34	0.50	0.36	0.37	0.51
Crystallinity (%)	low	low	75-80	85	low	-
XRD-Phases (wt%)	CuO, $\alpha-Al_2O_3$	Cu_2S(55) $\gamma-Al_2O_3$(45)	$CuAl_2O_4$(69) $CuAlO_2$(31)	$CuAl_2O_4$ (87),CuO (13)	Cu_2S(71) $\gamma-Al_2O_3$ (29)	$CuAl_2O_4$ (59),CuO (41)

CA_I and CA_{II} sorbents were reacted under identical conditions in 12 cycles of sulfidation-regeneration over the temperature range of 550°-800°C. Fresh CA_{II} comprising mainly of $CuAl_2O_4$ of low surface area gave initially a low conversion at 550°C. With cycling, however, the performance of this sorbent improved both in terms of H_2S removal efficiency as well as conversion. At 800°C, both CA_I and CA_{II} sorbents had similar sulfidation performance. Figure 2 shows the data obtained with the CA_I sorbent. Pre-breakthrough H_2S levels well below the equilibrium values for $Cu \rightarrow Cu_2S$ sulfidation can be seen in this figure for all temperatures. In addition, sorbent conversion improves with temperature indicating that gas diffusion is not limiting these systems even at temperatures as high as 800°C.

An interesting feature of $CuO-Al_2O_3$ sorbents is an increase in their surface area (redispersion effect) during sulfidation. As shown in the table above, the 800°C-regenerated CA_{II} sorbent (after 12 cycles) had a surface area of 4 m^2/g compared to 8 m^2/g for the 800°C-sulfided material of the same cycle. Similar data were obtained with the CA_I sorbent as well as several of the Cu-Fe-Al-O mixtures. Thus, it may be concluded that given adequate initial porosity for good conversion, the surface area of $CuO-Al_2O_3$ sorbents will stabilize at a range of intermediate

values with the sulfided and regenerated state alternating between the upper and lower limit, respectively. In regards to Cu-Al-O sorbent stability in H_2-rich sulfidation mixtures, sorbent CA_{II} was superior to CA_I in terms of H_2S removal efficiency at 650°C with a gas containing (in mol%): 20 H_2, 25 H_2O, 1 H_2S, 54 N_2. This may be attributed to the less reducible $CuAl_2O_4$ phase predominant in CA_{II}.

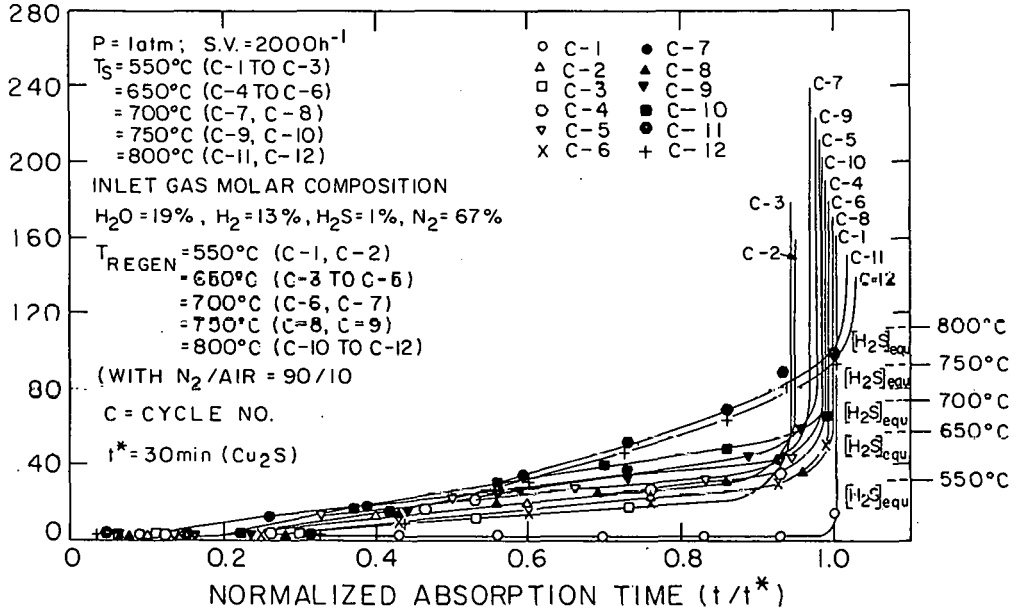

Figure 2. H_2S Breakthrough Curves in Successive Sulfidation Cycles of Sorbent CA_I ($CuO:Al_2O_3$).

Regeneration Performance. Parametric studies of regeneration using different H_2O/air mixtures and temperatures were conducted with the sorbent C3FA, between the sulfidation cycles shown in Figure 1. Isothermal operation was possible by suitable modulation of the furnace heat input to the reactor. The following conditions were employed in these tests:

After sulfidation cycles:
C-2, 3 and 4, T = 700°C, $(H_2O/air)_{mol}$ = 70/30, 80/20, 84/16
C-5, 6 and 7, T = 650°C, $(H_2O/air)_{mol}$ = 70/30, 80/20, 84/16
C-8, 9 and 10, T = 750°C, $(H_2O/air)_{mol}$ = 70/30, 84/16, 80/20

The SO_2 (and H_2S) elution profiles versus regeneration time were obtained by on-line gas chromatography of the exit gas. Elemental sulfur collected in the ice-trap was dissolved in sodium sulfide solution and analyzed by iodometric titration. The SO_2-time profiles have rather broad peaks indicating slow reaction throughout the bed. These peaks shift to longer times at higher H_2O concentrations or higher regeneration temperatures. Correspondingly, the elemental sulfur production is higher under these conditions. In fact, elemental sulfur was always produced in the first few minutes of regeneration and preceded the SO_2 built-up in the product gases. The amount of elemental sulfur produced (in mol% of total sulfur products) is shown below for each of the 9-point parameter

space examined in this work:

ELEMENTAL SULFUR (mol% of total sulfur products)

Temperature (°C)	Regeneration Gas Composition (mol%) 70 Steam 30 Air	80 Steam 20 Air	84 Steam 16 Air
650	3.3	8.7	9.0
700	4.1	9.9	10.7
750	12.1	17.0	20.5

As can be seen from this table the maximum (20.5%) production of elemental sulfur took place at 750°C with a 84% steam - 16% air mixture. The dramatic effect of H_2O on elemental sulfur production from Cu-Fe-Al-O sorbents has been discussed before (e.g., see Flytzani-Stephanopoulos et al., 1986). Actually, dry regeneration with N_2/air mixtures has been repeatedly shown in our work to produce negligible (<1-2%) amounts of sulfur even for sorbents with high iron-content. On the other hand, the presence of iron is crucial for elemental sulfur production in wet regeneration. Thus, the Cu-Al-O sorbents containing no iron show zero selectivity towards elemental sulfur production in regeneration with a 70% steam-30% air mixture.

Sulfate Formation. At the regeneration conditions discussed above, the C3FA sorbent showed evidence of sulfate formation. Thus, after completion of a typical regeneration, the level of SO_2 increased when oxygen was cut and N_2 purge was used in the reactor. This indicates decomposition of residual sulfate. In order to clarify whether sulfate formation would take place even at conditions where its formation would be thermodynamically unstable, additional tests were run with the same batch of C3FA sorbent. Cycles 11 and 12 (not shown in Figure 1) were run at 650° and 750°C sulfidation/regeneration temperatures, respectively. The regeneration mixture used in both cycles had a very low oxygen content (1%), the balance being H_2O (80%) and N_2 (19%). Typically, after 60 minutes, regeneration was more than 99% complete. The SO_2 levels prior to N_2-purge were of the order of 100 ppmv. If no sulfate had formed, SO_2 would decrease to zero levels during N_2 purge. In these tests, steady SO_2 levels of ~50 ppmv were observed during the length of N_2-purge. Thus, it is concluded that a very small amount of sulfate (corresponding to less than 0.5% of the H_2S absorbed in sulfidation) was present at the end of regeneration. It is not clear whether this sulfate came from the Cu (or Fe) components or from the aluminum oxide of the C3FA sorbent.

The sulfation of the low surface area ALCOA T-61 (or T-64) alumina used as inert in the sorbent bed was studied at 750°C with 1% SO_2-99% air mixtures to examine sulfate formation relative to this compound. Based on mass balance calculations, approximately 0.5% of the inlet SO_2 was retained by the alumina in the form of sulfate. Hence, the overall

sulfate contribution of the diluent alumina is negligible during sorbent regeneration.

The dispersed aluminum oxide phase of Cu-Fe-Al-O sorbents, however, may contribute to sulfate formation. In the case of the Cu-Al-O sorbents, CA_I and CA_{II}, regeneration was carried out with a 90% N_2 - 10% air mixture in the temperature range of 550°-800°C. Up to 750°C, sulfate formation was evidenced with the CA_I sorbent, but not the CA_{II} material. Also, the regeneration time (to less than 5 ppmv SO_2) was much shorter for CA_{II} at all temperatures. At 800°C, no sulfate formation took place with either sorbent. These results can be explained in terms of surface sulfate formation in the case of the highly dispersed (high surface area) CA_I sorbent.

Zn-Ti-O SORBENTS

The choice of TiO_2 as an additive to ZnO is a novel approach aiming at stabilizing ZnO against undesired reduction without compromising considerably the good sulfidation equilibria of pure ZnO. The thermodynamic equilibria of direct sulfidation of ZnO-based binary oxides

$$ZnO \cdot M_xO_y + H_2S \longrightarrow ZnS + M_xO_y + H_2O$$

with M_xO_y not forming a bulk sulfide, are less favorable than for ZnO sulfidation. How much inferior the equilibria of the above reaction are is determined by the choice of M_xO_y. For instance, based on available thermodynamic values, compounds of ZnO with Al_2O_3, SiO_2 or TiO_2 are ordered as follows in terms of decreasing sulfidation efficiency:

$$ZnO > Zn_2TiO_4 > Zn_2SiO_4 >> ZnAl_2O_4$$

$ZnAl_2O_4$ is a very poor H_2S sorbent. Zn_2SiO_4 has not been considered in our work; a general problem with silicates is their hydrothermal instability at high temperatures.

During the past year, fourteen Zn-Ti-O binary oxides, three ternary oxides, Zn-Fe-Ti-O, and three batches of pure (bulk) ZnO were synthesized according to the amorphous citrate technique (Marcilly et al., 1970). In addition, two titania-supported ZnO sorbents were prepared by incipient wetness impregnation of TiO_2 granules (anatase, UCI 1090-114). Different conditions used in preparation aimed at synthesizing and studing sorbents of different initial properties. The Zn/Ti atomic ratio was varied in the range of 0.4-2.0/1. Table 1 summarizes the properties of several of the Zn-Ti-O sorbents studied in this work. All sorbents (except ZT-II) were highly crystalline after calcination. Sorbents prepared with excess citric acid (e.g. ZT-IV) or from $TiCl_4$ precursors (e.g. ZT-3, ZT-6) had high pore volume (> 1 cm^3/g). The major phase present in sorbents with Zn/Ti $\leq$ 1 was $ZnTiO_3$. The phase Zn_2TiO_4 was formed at higher than 750°C calcination temperature or for Zn/Ti = 2. The phase $Zn_2Ti_3O_8$ was present only in a few sorbents.

Table 1. Properties of Fresh ZnO-Based Sorbents

SORBENT (Zn:Ti, atomic ratio)	T_{calc} (°C)	TIME (h)	XRD-PHASES[§] (wt%)	SA (m^2/g)	PV (cm^3/g)
ZnO	550	3	--	7	2.7
	650	5	--	3	1.9
	750	5	--	1	0.6
ZT-II (1:1)	550	4	Diffuse Pattern of Z2T3	55	0.9
ZT-I (1:1)	700	12	ZT(70), Z(5), Z2T3(25)	3.5	0.4
ZT-III (0.9:1)	850	4	ZT(69), T(14), Z2T(17)	0.6	0.6
*ZT-IV (1:1)	750	5	ZT(57), Z(11), Z2T3(26), T(6)	20	1.5
#ZT-VIII (0.8:1)	750	5	ZT(50), Z(18), Z2T(26), T(6)	17	0.3
Z2T (2:1)	700	12	Z2T(96), Z(4)	4.4	0.7
+ZT-3 (0.9:1)	700	5	ZT(89), T(11)	6.7	2.3
+ZT-6 (0.5:1)	700	5	ZT(69), T(31)	5	2.0
ZFT-2 (1Zn:2Fe:1Ti)	700	5	T(4), Z(5), M(81), U(5)	7	0.7

§ *Z: ZnO, T: TiO_2 (rutile), ZT: $ZnTiO_3$, Z2T: Zn_2TiO_4, Z2T3: $Zn_2Ti_3O_8$, M: Fe_3O_4+$ZnFe_2O_4$+Zn_2TiO_4, U: Unknown*

* *Prepared with 2:1 molar ratio of citric acid/metals*

\# *Prepared with 0.5:1 molar ratio of citric acid/metals*

\+ *Prepared from $TiCl_4$ + zinc acetate + citric acid*

Sulfidation Performance. Sulfidation tests were carried out at 600° and 650°C with a gas mixture containing (in mol%): 13 H_2, 19 H_2O, 1 H_2S, 67 N_2. Regeneration between cycles was conducted in 10% air-90% N_2 at 700°C. Physical properties such as surface area and pore volume play a crucial role on the Zn-Ti-O sorbent sulfidation performance. In order to attain practical (>20%) sorbent utilization, a minimum pore volume of ~0.4 cm^3/g is required to suppress pore plugging caused by ZnS formation. Sorbents Z2T3 and ZT-VIII, which had low pore volume, almost immediately reached breakthrough during the first cycle of sulfidation. However, succeeding cycles gave sorbent conversion of 45-55% (based on ZnO sulfidation). Limited pore opening and redispersion take place during regeneration, eventually stabilizing the performance of Zn-Ti-O sorbents. Sorbents of high initial surface area (e.g. ZT-II, ZT-IV) gave 100% first-cycle conversion, but gradually stabilized to ~60% conversion in later cycles as their surface area was reduced to 2-4 m^2/g.

Chemical phases also play an important role on sorbent sulfidation performance. Sorbent Z2T containing predominantly Zn_2TiO_4 had better utilization (last cycle, 65% conversion based on ZnO) than sorbents containing mainly $ZnTiO_3$ (e.g. ZT-II, IV) of comparable pore volume and surface area (after final cycle). Furthermore, partially sulfided sorbents contained unreacted $ZnTiO_3$ but not Zn_2TiO_4. Pure (bulk) ZnO with physical properties comparable to those of zinc titanates attained ~100% conversion under similar sulfidation conditions. It appears that the intrinsic kinetics of ZnO sulfidation are faster than those of Zn_2TiO_4 or $ZnTiO_3$.

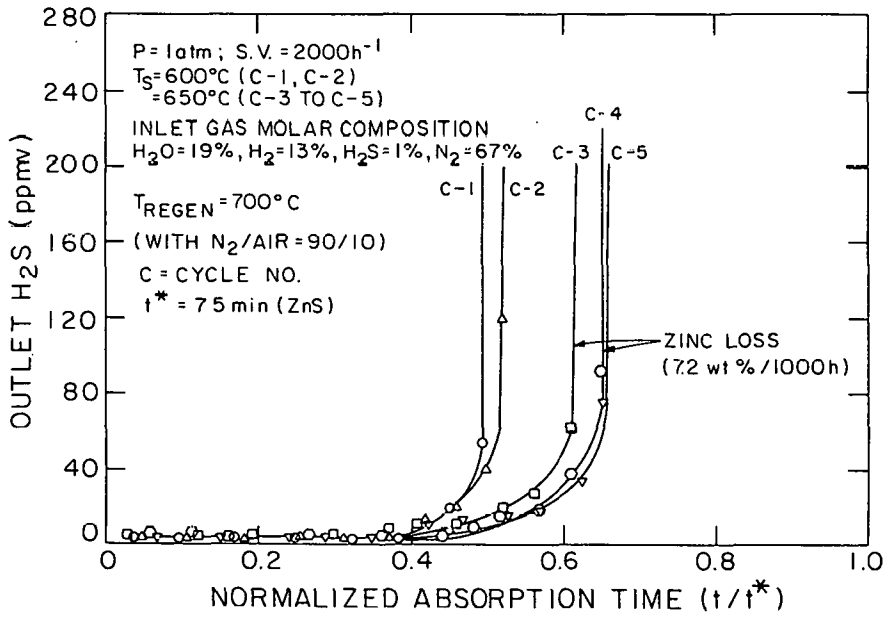

Figure 3. H_2S Breakthrough Curves in Successive Sulfidation Cycles of Sorbent Z2T ($2ZnO:TiO_2$).

Typically, $ZnO-TiO_2$ sorbents prepared in the absence of chloride ion showed a stabilized breakthrough conversion of 50-60%. An example is shown in Figure 3 for sorbent Z2T (100% Zn_2TiO_4). In this case, the pre-breakthrough H_2S levels were below 2-5 ppm, i.e. below the equilibrium for ZnO sulfidation. This is similar to the case of pure ZnO sulfidation. The hypothesis of H_2S chemisorption and surface sulfide formation of different thermodynamic properties than bulk sulfides was used in our previous work to explain this property of ZnO (Flytzani-Stephanopoulos et al., 1985 b). At any rate, the results of Figure 3 indicate that Zn_2TiO_4 breaks down, at least in part, into ZnO and TiO_2. Hence, the ZnO sulfidation properties prevail. At higher conversions, solid state diffusion appears to limit the accessibility to the unreacted titanate. Diffusion through TiO_2 may be the limiting step. Typically, higher conversions of $ZnO-TiO_2$ sorbents were observed at higher temperatures (see Fig. 3). This also indicates kinetic control (either slow intrinsic kinetics or slow diffusion through a solid layer). Rate constants and solid state diffusivities vary exponentially with temperature, while the gas diffusion coefficient is only mildly affected.

Figure 4 shows H_2S breakthrough curves for sorbent ZT-6 prepared in the presence of chloride ion (using $TiCl_4$ in place of the usual Ti-isopropoxide in the precursor solution). This sorbent exceeded 100% conversion (based on ZnO), a result typical with all Zn-Ti-O sorbents prepared in the presence of Cl^- ions. Sub-equilibrium H_2S levels were observed up to ~60% conversion. XRD analysis of the sulfided ZT-6 solid identified α-ZnS (wurtzite, 27 wt%), TiO_2 (rutile, 58 wt%) and unreacted $ZnTiO_3$ (15 wt%). This leaves ~23 wt% sulfur unaccounted for. In sulfur determination performed in a Leco-532 furnace, 10 wt% sulfur was found in the sulfided ZT-6 material.

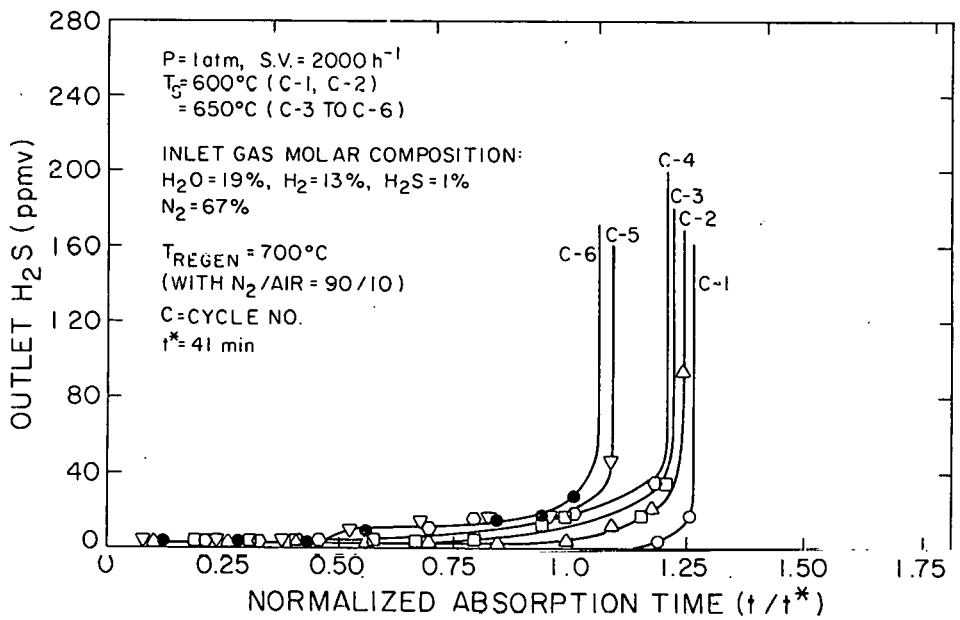

Figure 4. H_2S Breakthrough Curves in Successive Sulfidation Cycles of Sorbent ZT-6 ($0.43ZnO:TiO_2$).

Another explanation for the observed enhanced sulfur capture of this type of Zn-Ti-O sorbents may be offered by the formation of $ZnO-TiO_2$ solid solutions of completely different sulfidation thermodynamics. Interstitial impurities, in this case Cl^-, resulting from sorbent preparation can promote the formation of $ZnO-TiO_2$ solid solutions (Dulin and Rase, 1960). SEM/EDX analysis of the sulfided ZT-6 identified the presence of Cl. However, XRD analysis did not show any oxide solid solutions.

Reduction Stability. During sulfidation at 600° and 650°C, all Zn-Ti-O sorbents stabilized ZnO against reduction. The rate of zinc loss from Zn-Ti-O sorbents was in the range of 3-7 wt%/1000 h at 650°C. This value is much lower than for pure ZnO under similar conditions (~25 wt% Zn/1000 h).

Reduction of ZnO to volatile Zn metal was found to be a surface phenom-

enon. In general, a surface area increase was observed in regenerated ZnO during cycling followed by a higher rate of zinc loss. Zinc loss from zinc titanates, however, was only a weak function of surface area.

The ternary oxide sorbent ZFT-2 (Table 1) containing an atomic ratio of Zn:Fe:Ti = 1:2:1 also showed a low zinc loss (~5.8 wt%/1000 h). Thus, incorporation of TiO_2 into zinc ferrite offers the potential for extending the application of zinc ferrite sorbents to higher temperatures (up to ~650°C).

Regeneration. All Zn-Ti-O mixtures showed excellent phase regenerability in regeneration at 700°C with a dry gas mixture containing 10 mol% air-90 mol% N_2. At these conditions no sulfates were formed. The rate of regeneration was faster than for bulk ZnO regeneration under similar conditions.

TASK 3: PREPARATION AND TESTING OF POROUS SORBENT EXTRUSIONS OF GOOD MECHANICAL STRENGTH

The sorbents C3FA (3Cu:2Fe:2Al), CA (1Cu:2Al) and ZT (1Zn:1Ti) were selected for further study under this task aiming at preparing the sorbents in the form of extrusions of controlled-pore and good mechanical strength. A second goal of this task is to test how well these properties are retained after several cycles of sulfidation/regeneration at 650°C.

Work under this task is in progress. To-date, several batches of sorbent C3FA have been made by extruding powders prepared by the amorphous citrate technique (after 450°C-pyrolysis and 650°C-calcination) with various additives. Extrusion is performed in a Wahlco-Model 20-8 hydraulic-piston extruder through a die with 1/8" holes. Both macropore-formers (organic additives) and inorganic binders are mixed with the powders, and pastes are made by adding the necessary amount of water. After extrusion, the moist cylindrical strands are cut (to several cm lengths), dried in air flow in an oven at ~120°C, cut further to ~1/4" long, and then calcined in air in a muffle furnace for 5 h at 650°C or 850°C. The final products are then characterized for pore surface area and volume by BET-N_2 and Hg-porosimetry, and for compressive crush strength in an Instron-Model 1125 tester machine.

Using bentonite (5 wt%) as binder, the typical properties of the C3FA extrusions are as follows:

T_{calc} (°C)	SA (m^2/g)	PV (cm^3/g)	Porosity (%)	Bulk Density (g/cm^3)	Crush Strength (lb/mm)
650	13	0.47	62	1.3	3.2 - 3.7
850	3.5	0.43	63	1.5	13.7 - 15

When organic binders, such as methocel or mixtures of aluminum formate and formic acid were used along with bentonite, the properties of the 650°C-calcined extrusions were somewhat modified (pore volume: ~0.52

cm^3/g, crush strength: 2.1-3.0 lb/mm).

The two bentonite-extruded C3FA batches (650°- and 850°C-calcined) were tested in sulfidation-regeneration in an 1.5 cm I.D. microreactor. For comparison, (-20/+40 mesh) granules of the C3FA sorbent used in preparation of the paste were tested at the same conditions. The results for both batches of sorbent extrusions were very promising. Figure 5 shows the sulfidation performance of the 650°C-calcined batch. Different flow velocities were used to check for external mass transfer limitations. As shown in Figure 5 this was a problem in our system. Using a higher flow velocity, higher conversion was achieved. More importantly, H_2S pre-breakthrough levels below 5 ppmv were observed up to relatively high sorbent conversions (~30%). Regenerability of performance was excellent. The 850°C-calcined sorbent was tested in three cycles of sulfidation-regeneration at 650°C, S.V.=2000 h^{-1}, and flow velocity of 2.56 cm/sec. The H_2S pre-breakthrough levels were <5 ppmv up to 20% conversion, and below 60 ppmv up to breakthrough (55% conversion).

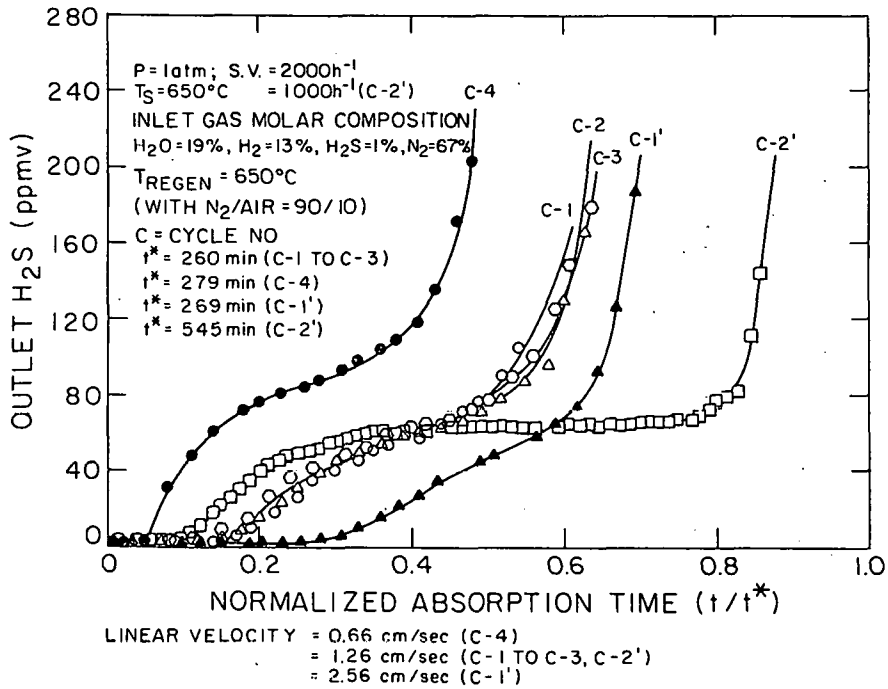

Figure 5. Sulfidation of C3FA - 1/8" dia. Extrusions (calcined at 650°C).

The sulfided and regenerated sorbents had the following properties:

	SA (m^2/g)	PV (cm^3/g)	Bulk Density (g/cm^3)	Crush Strength (lb/mm)
650°C-calc. batch				
sulf'd, 650°C	11	0.37	1.41	1.6
regen'd, 650°C	10	0.54	1.45	1.5
850°C-calc. batch				
sulf'd, 650°C	10	0.37	1.52	2.0
regen'd, 650°C	7	0.39	1.54	5.0

Similar to the sulfidation of powders, surface area increase takes place during pellet sulfidation. Actually, the surface area of the sulfided, 850°C-calcined batch of C3FA, after 3 cycles, is three times as high as in the original material. After regeneration, the crush strength of the extrusions is 5 lb/mm, a value acceptable for practical applications. Additional testing of C3FA will be performed to test the stability of its properties in more cycles (10-15). Also, the CuO-Al_2O_3 and ZnO-TiO_2 sorbents will be prepared and tested in extruded form under similar conditions.

6. CONCLUSIONS:

Results from all phases of this project are very promising and warrant further development of the novel sorbents for coal-gas desulfurization. The complex chemistry involved in sulfidation/regeneration of mixed oxides has come out of these studies. Additional work is needed to obtain kinetic data of reduction-sulfidation and regeneration of the selected Cu-Fe-Al-O and Zn-Ti-O sorbents and develop reaction models that properly account for the complexity of these systems. Also, sorbent preparation with controlled-pore structure and mechanical strength should be given serious attention in bench-scale development of these materials.

7. REFERENCES:

Dulin, F.H., and Rase, D.E. (1960). Phase Equilibria in the System ZnO-TiO_2. J. Am. Ceram. Soc. 43:125-131.

Flytzani-Stephanopoulos, M., Tamhankar, S.S., Gavalas, G.R., Bagajewicz, M.J., and Sharma, P.K. (1985a). High-Temperature Regenerative Removal of H_2S by Porous Mixed Oxide Sorbents. ACS Div. of Fuel Chem. Preprints 30:16-25.

Flytzani-Stephanopoulos, M., Gavalas, G.R., Tamhankar, S.S., and Sharma, P.K. (1985b). Novel Sorbents for High Temperature H_2S Removal. Final Report, DOE/MC/20417-1898.

Flytzani-Stephanopoulos, M., Jothimurugesan, K., Gavalas, G.R., and Sharma, P.K. (1986). Proceedings of the Sixth Annual Contractors' Meeting on Contaminant Control in Coal-Derived Gas Streams, DOE/METC-86/6042.

Jacono, M.L., Cimino, A., and Inversi, M. (1982). J. Catal. 76:320.

Marcilly, C., Courty, P., and Delmon, B. (1970). Preparation of Highly Dispersed Mixed Oxides and Oxide Solid Solutions by Pyrolysis of Amorphous Organic Precursors. J. Am. Ceram. Soc. 53:56-57.

Tamhankar, S.S., Bagajewicz, M., Gavalas, G.R., Sharma, P.K., and Flytzani-Stephanopoulos, M. (1986). Mixed Oxide Sorbents for High-Temperature Removal of Hydrogen Sulfide. Ind. Eng. Chem. Proc. Des. Dev. 25(2): 429-437.

Voge, H.H., and L.T. Atkins (1962). Uniformity of Supported CuO from Rate of Reduction with Hydrogen. J. Catal. 1:171-179.

INTEGRATION AND TESTING OF HOT DESULFURIZATION AND ENTRAINED FLOW GASIFICATION FOR POWER GENERATION SYSTEM

1. COOPERATIVE AGREEMENT NUMBER: DE-FC21-87MC23277

CONTRACTOR: Texaco, Inc.
Montebello Research Laboratory
P.O. Box 400
Montebello, CA 90640
(213) 699-0948

CONTRACT PROJECT MANAGER: Allen M. Robin

PRINCIPAL INVESTIGATORS: Michael W. Becker
Thomas L. Leininger
Allen M. Robin

METC PROJECT MANAGER: Dr. W. S. Liou

CONTRACT PERIOD OF PERFORMANCE: 1987 To 1992

2. SCHEDULE/MILESTONES:

The following schedule has been proposed for the overall five year program.

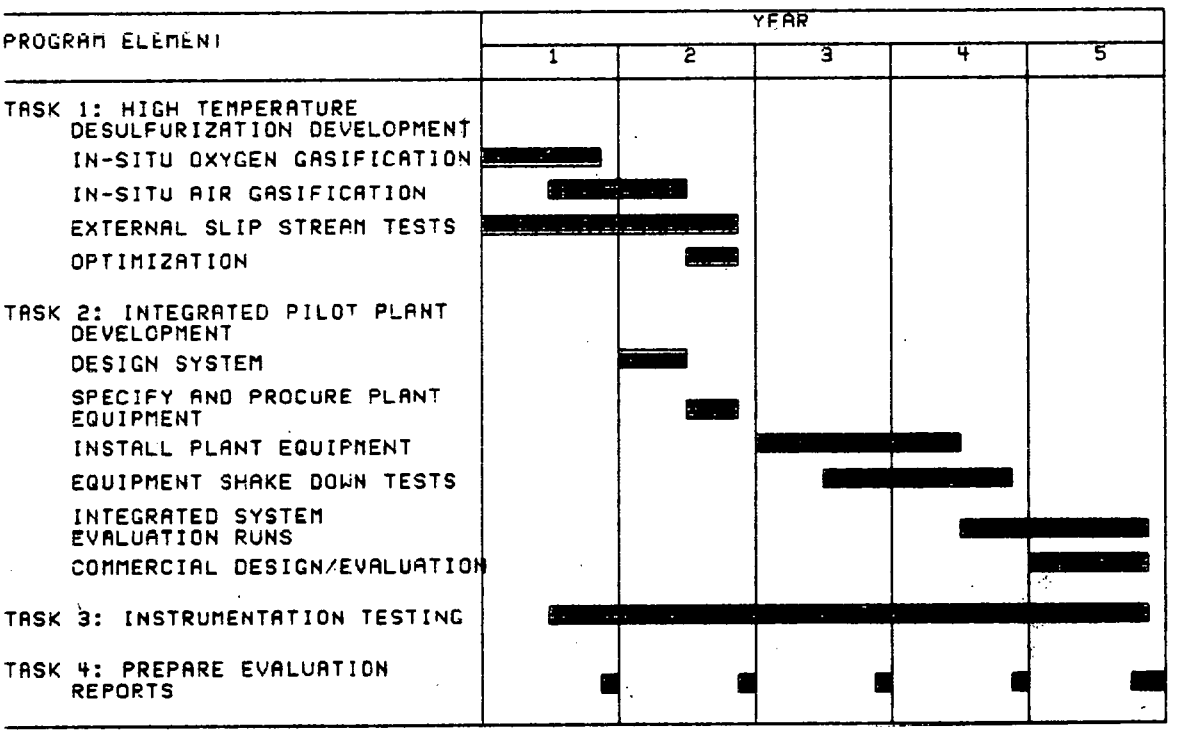

3. OBJECTIVES:

The primary objective of this project is to demonstrate, on a pilot plant scale, an integrated coal gasification combined cycle (IGCC) electric power generation system utilizing hot gas desulfurization and the commercially proven Texaco Coal Gasification Process. Both in-situ and external hot gas desulfurization will be investigated. New specialized instrumentation developed for coal gasification will also be tested during this work.

4. BACKGROUND STATEMENT:

CURRENT STATUS OF THE TCGP

The Texaco Coal Gasification Process (TCGP) utilizes a slagging downflow entrained bed reactor with typical temperatures from 2000°F to 2600°F. Coal is fed to the gasifier as a water slurry. Syngas cooling is accomplished either by waste heat boiler or by direct quench with water depending upon the end use for the gas. Currently, gas contaminant removal is accomplished by conventional methods that require the gas to be cooled to near ambient temperature. Sulfur emissions are reduced to 10% of the New Source Performance Standards (NSPS) at the Cool Water 120 megawatt IGCC electric power plant [1]. In addition, the TCGP is used in three other commercial installations to produce ammonia and petrochemicals. Using the current typical commercial configuration shown in Figure 1, our analysis shows that compared to a conventional pulverized coal plant with stack gas clean-up, a Texaco based IGCC system would be 15% more efficient, and have comparable investment costs.

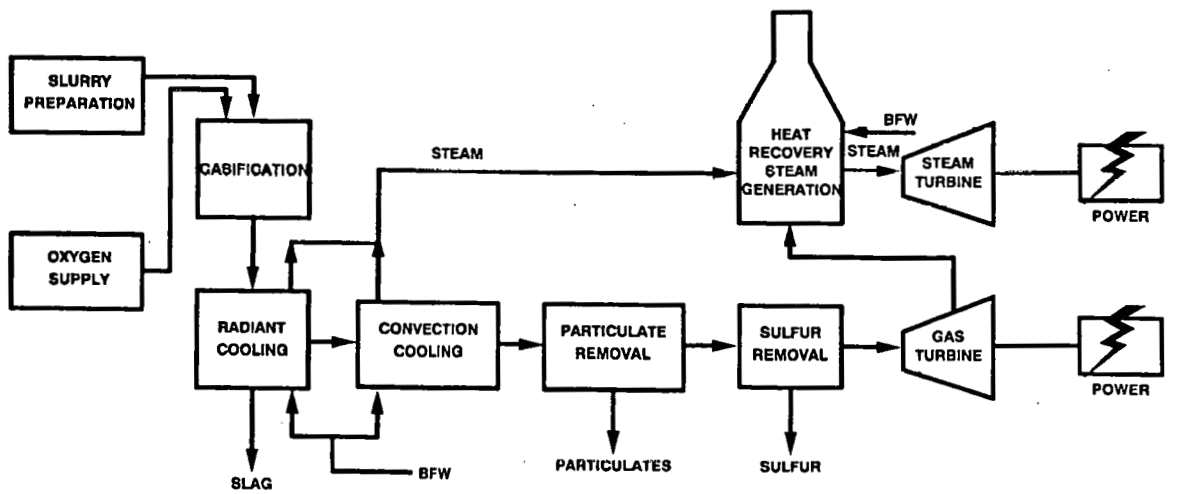

Figure 1. Current Texaco Intergrated Gasification Combined Cycle Power Generation

HIGH TEMPERATURE GAS DESULFURIZATION

An additional increase in process thermal efficiency and a major reduction in capital cost can be realized if the gas does not have to be cooled down to ambient temperature before being fed to a combustion turbine. The high temperature system, however, must still remove the major hot gas contaminants which include sulfur compounds, particulates, volatile metals and nitrogen compounds. Desulfurization can be accomplished either in-situ by feeding a sulfur removal sorbent to the gasification reactor or externally by contacting the sorbent with the gas downstream of the gasifier vessel. In-situ desulfurization could provide the lowest investment cost and simplicity of design. External desulfurization has the potential for very high sulfur removal and the production of a sulfur by-product. A significant amount of work has been done by other investigators in the areas of external desulfurization and in-situ desulfurization using either moving bed or fluidized bed coal gasifiers. However, little work has been done to study high temperature desulfurization in conjunction with an entrained bed gasifier (such as that used in the Texaco process). The initial portion of the research efforts on this project will be devoted to investigating the coupling of hot gas desulfurization to the TCGP.

In 1985, Texaco began to investigate the economics and technical feasibility of utilizing in-situ desulfurization with the TCGP. Based upon preliminary estimates, capturing up to 90% of the sulfur may be feasible for a high sulfur coal [2]. Even higher levels of sulfur removal are projected for external high temperature desulfurization.

Preliminary economic analyses of systems based on both in-situ and external desulfurization show costs and thermal efficiencies better than for the current TCGP IGCC design. Figure 2 shows one potential configuration for an in-situ desulfurization based power generation system. External desulfurization would be similar but would require sulfur removal along with the particulate removal and possibly a sorbent regeneration system. Table 1 compares the various features of the systems shown in Figures 1 and 2.

5. PROJECT DESCRIPTION:

This project will involve a five year test program with costs shared by the U.S. Department of Energy and Texaco. During this period, Texaco will optimize the high efficiency, low cost power system projected by economic studies and demonstrate the system from coal receiving to the gas turbine in an integrated pilot unit. Testing will

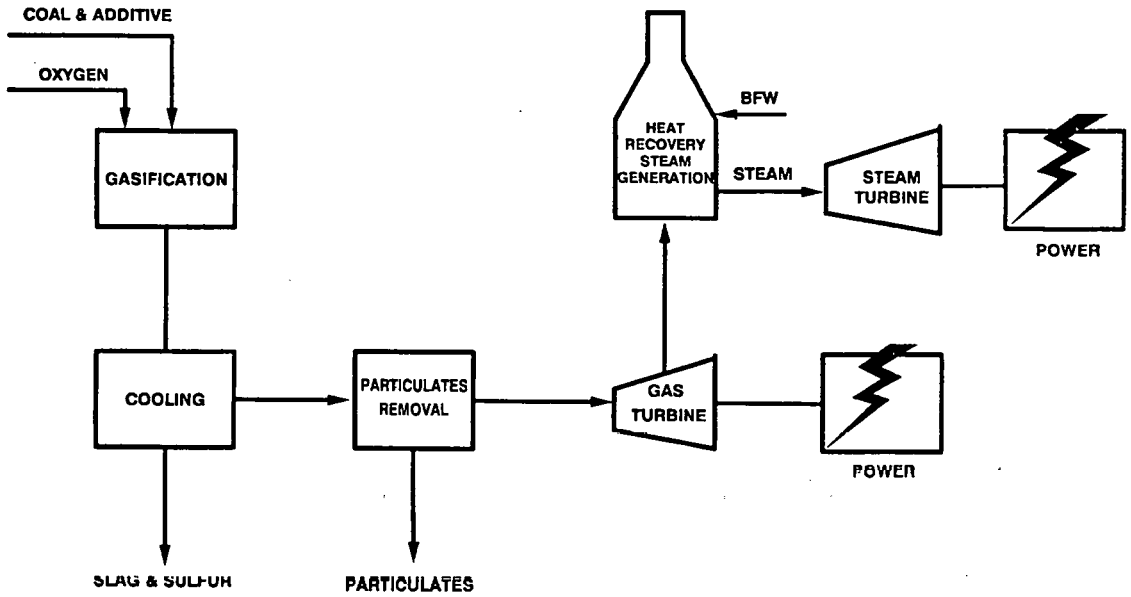

Figure 2. Grass Roots In-Situ Desulfurization

Table 1. Plant Comparisons.

Area	Current Commercial Design	In-situ Desulfurization Design
Gasification	Texaco Gasifier Using O2 or Air	Texaco Gasifier Using O2 or Air
Gas Cooling	To 100°F with Boilers and Exchangers	To 1200°F By Water Injection
Sulfur Removal	Standard Commercial Processing	In-situ Additive
Gas Reheating/ Saturation	Required	None
Particle Removal	Low Temperature	High Temperature
Power System	Advanced Inteqrated Combined Cycle	Advanced Combined Cycle
Heat Rate	8900 BTU/KWH	8500 BTU/KWH
Costs *	1035 $/KW	600 $/KW **

* Supplementary cost: Land, Working Capital, AFUDC, Purchased oxygen assumed.
** Costs below 300 $/KW are anticipated when using existing equipment for power generation to a retrofit application

be done on both a bench and a pilot unit scale. Pilot unit testing will be conducted at the Texaco Montebello Research Laboratory (MRL).

6. RESULTS/ACCOMPLISHMENTS:

Negotiations and review of the contract are currently in progress with signing expected within one month.

7. FUTURE WORK:

HOT GAS DESULFURIZATION SYSTEM DEVELOPMENT

The first two years of the project will be used to determine the most efficient means for removing sulfur from the gas at high temperatures. Both in-situ and external desulfurization will be studied. A high sulfur eastern coal such as Illinois #6 or Pittsburgh #8 will be used for this work. The test program for in-situ desulfurization will include the following work:

- Theoretical Study
- Bench Scale Testing
- Pilot Unit Testing

The theoretical study will identify which sorbents are the most likely candidates for bench scale testing. Sulfur removal efficiencies will be estimated for sorbent/coal ash mixtures using a multi-phase free energy minimization computer program.

Bench scale testing will be conducted to determine the sulfur content of sorbent/coal ash mixtures as a function of the partial pressure of sulfur and oxygen in the gas. The effect of sorbent addition upon slag viscosity will also be addressed.

Pilot unit testing will be conducted in a 350 psig gasifier which is fitted with a syngas cooler. Both air and oxygen (99.5% purity) will be tested as the oxidant. The proposed schedule for pilot unit testing is outlined in Table 2.

The baseline test listed in Table 2 will provide information on gasifier performance and gas composition while using air as the oxidant. Although air gasification work has been well demonstrated in the past, the operating range of interest has not been covered sufficiently for any one coal and the impact of process improvements since those tests is unclear.

Table 2. Proposed Pilot Plant Testing Program For In-Situ Desulfurization.

Type of Test	Oxidant	Sorbent	Schedule
Screening Tests	O_2	*	First Year
Baseline Test	Air	None	Second Year
Screening Tests	Air	*	Second Year
Optimization Tests	Air/O_2	Best	Second Year
Extended Run	Air/O_2	Best	Second Year

* One to three candidate sorbents will be chosen basis the results of the bench scale tests.

The process optimization tests outlined in Table 2 will be used both to determine operating conditions for maximizing sulfur removal and to test corrective action for any operational problems identified during the screening tests. The extended test will be used to demonstrate the best sorbent and operating conditions as determined by the first three phases of the pilot unit testing. Both process economics and operability will be considered while deciding the conditions for the extended test.

During the initial pilot unit testing phase of the project, several other important areas will be investigated in addition to in-situ desulfurization, including the following work:

- Testing of External Desulfurization Sorbents
- Testing of Advanced Instrumentation
- Determination of Contaminant Species
- Characterization of Slag

A variety of external desulfurization sorbents will be evaluated using a slipstream of syngas from the pilot unit. Texaco intends to test sorbents being developed by other investigators in cooperative programs.

Texaco also plans to test and evaluate advanced instrumentation for process control and measurement in entrained bed coal gasification and hot gas cleanup systems. This will provide field testing under commercial type conditions for experimental devices developed by and for METC. Instrumentation of particular interest includes

various devices for gasifier temperature measurement, on-line analysis of coal properties, measurement of various flowrates, and product gas stream particulate and elemental analyses. Testing of instrumentation will continue during subsequent pilot unit tests of the integrated power generation system.

The determination of contaminants in the hot gas is necessary for the design of an integrated power generation system. Contaminants of interest (other than sulfur) include particulates, volatile metals, and nitrogen compounds.

The slag produced via in-situ desulfurization would initially contain sulfide compounds that have to be oxidized either to a sulfate or an oxide prior to disposal. The technical feasibility and economics of treating the slag for disposal or regeneration will be studied.

INTEGRATED SYSTEM DEVELOPMENT AND TESTING

The design, installation and testing of an integrated power generation system is scheduled for the third through the fifth year of the project. Testing of a complete pilot scale integrated power generating system is necessary to verify the operability and controllability of the integrated plant under all operating conditions, including steady state, load following, start-up, shutdown and emergency, as well as to evaluate overall performance. The integrated system will include the following components:

- Slurry Preparation
- Coal Gasification (TCGP)
- Gas Cooling
- Ash Handling
- Gas Contaminant Removal
- Combustion Turbine

A heat recovery steam generator (HRSG) and a steam turbine will not be included in the pilot unit system. No problems are anticipated in designing a commercial size HRSG based upon current knowledge.

The method of desulfurization will be selected after information from the initial pilot unit testing program outlined in Table 2 is available. Modifying the process to include in-situ desulfurization is relatively simple, since

the sorbent can be added during slurry preparation. External desulfurization is slightly more complex, requiring the installation of an additional vessel downstream of the gasifier. Additionally, with many sorbents, the external desulfurization process would include a regeneration step.

Syngas cooling may be accomplished either by a radiant boiler or by partial quenching with water or steam. The final temperature of the syngas will be determined based upon the maximum and/or optimum operating temperature of the various process steps downstream of the syngas cooling step.

Process steps to reduce particulates and volatile metals to acceptable levels will be investigated as required. A number of processes for treating these contaminants are currently under development by other investigators.

8. REFERENCES:

[1] Power Magazine, April 1985, p. 24-25

[2] High temperature phase calculations based on computer simulation, private communication with J. F. Elliot, MIT, 1986

BENCH-SCALE TESTING OF NOVEL DESULFURIZATION SORBENTS

1. CONTRACT NUMBER: DE-AC21-86MC23126

CONTRACTOR: Research Triangle Institute
Research Triangle Park, NC 27709
(919) 541-6255

CONTRACTOR PROJECT MANAGER: Santosh K. Gangwal

PRINCIPAL INVESTIGATORS: Scott M. Harkins
Santosh K. Gangwal

METC PROJECT MANAGER: Steven J. Bossart

CONTRACT PERIOD OF PERFORMANCE: September 29, 1986 to May 31, 1988

2. SCHEDULE/MILESTONES:

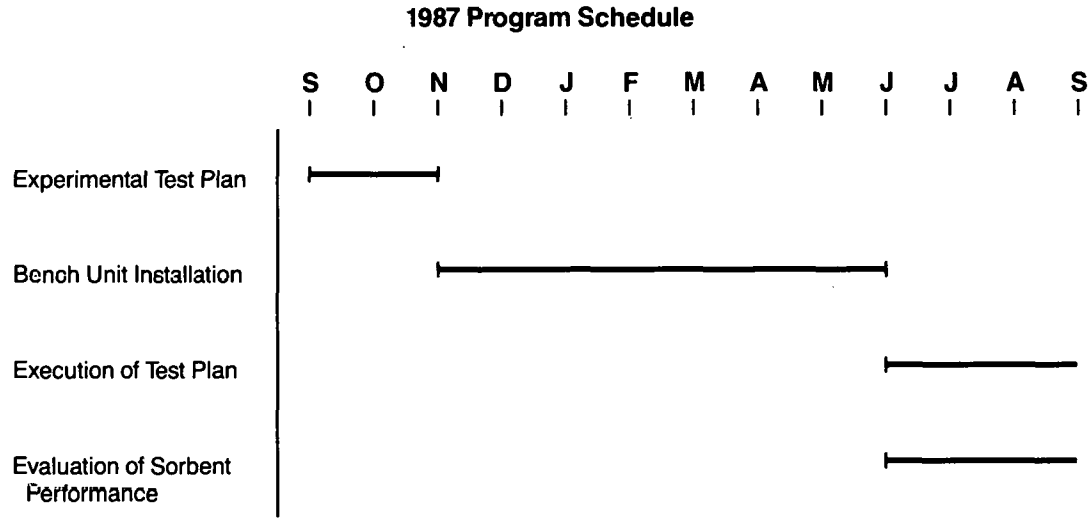

3. OBJECTIVES

The objectives of this contract are to perform bench-scale evaluation and preliminary engineering/economic assessment of novel high temperature desulfurization sorbents which have shown promising results at the laboratory scale. The emphasis is on testing sorbent formulations which have shown potential for high-efficiency hydrogen sulfide removal down to 1 ppmv and/or for stable operation at sulfidation temperatures greater than 650 °C.

4. BACKGROUND STATEMENT

Hot gas desulfurization represents a significant portion of METC's overall hot gas cleanup research program for power generation using coal gasification. The projects comprising the program are aimed at gas streams generated at pressures from 6 to 35 atmospheres and temperatures from 1000 to 1500 °F (538 to 816 °C). These conditions would be typical of integrated gasification combined cycle (IGCC) and gasifier/molten carbonate fuel cell (MCFC) power plants (Office of Technical Management and Office of Basic and Applied Sciences, Morgantown Energy Technology Center, 1986). The focus of the program is to increase power generation efficiency via integrated systems which match gas stream conditions of the gasifier, hot gas desulfurizer and/or other cleanup device, and the power generator.

High-temperature desulfurization research has primarily concentrated on mixed metal oxides which can remove hydrogen sulfide from coal gas to less than 10 ppmv and can be regenerated for multicycle operation. A zinc oxide-iron oxide (zinc ferrite, $ZnFe_2O_4$) sorbent, which can effectively reduce the H_2S level to 5 to 10 ppmv (Grindley and Steinfeld, 1984), is in an advanced stage of development with pilot-scale tests being conducted and demonstration-scale tests being planned. The zinc ferrite sorbent is limited in high temperature use to about 650 °C during the sulfur loading cycle due to possibility of detrimental reduction, zinc vaporization and sintering.

The search for novel sorbents has been motivated by the need for (a) sorbents that can reduce the coal gas sulfur levels to 1 ppmv, the target concentration for MCFC applications, and (b) sorbents that can operate at higher temperatures than zinc ferrite for efficient integration with high temperature fluid-bed gasifiers. Laboratory-scale research on novel sorbents has been extensively carried out by Flytzani-Stephanopoulous et al. (1985). The current focus of this work is on copper oxide-aluminum oxide, zinc oxide-titanium oxide, and copper oxide-iron oxide-aluminum oxide sorbents in different proportions of the individual oxides. These sorbents have shown potential for high H_2S removal efficiency and high temperature stability. Recent research at METC has shown that a copper modified zinc ferrite (zinc ferrite containing approximately 10% copper oxide) may reduce the H_2S in coal gas to below 1 ppmv.

5. PROJECT DESCRIPTION

Based on the laboratory-scale novel sorbent research, DOE/METC selected four sorbent formulations for further bench-scale evaluation under this contract. These formulations and their abbreviated designations are listed below:

- $(ZnO)_{0.86}(CuO)_{0.14}\ Fe_2O_3$ ..... (ZC)F
- $(ZnO)_{0.8}(TiO_2)$ ..... (0.8Z)T
- $(3CuO)(Fe_2O_3)(Al_2O_3)$ ..... (C3)FA
- $(CuO)(Al_2O_3)$ ..... CA

The reasons for the choice of the above sorbents include improved thermodynamics for H_2S removal because of possible copper stabilization as copper oxide, copper aluminate, and/or copper ferrite (rather than as copper metal) and reduced zinc loss at high temperature due to zinc stabilization as zinc titanate.

A detailed experimental test plan has been formulated for bench-scale testing of the novel sorbents. Bench-unit construction is nearing completion and the sorbents are being manufactured by United Catalyst, Inc. (UCI). A simplified schematic of the RTI bench-scale reactor system is shown in Figure 1.

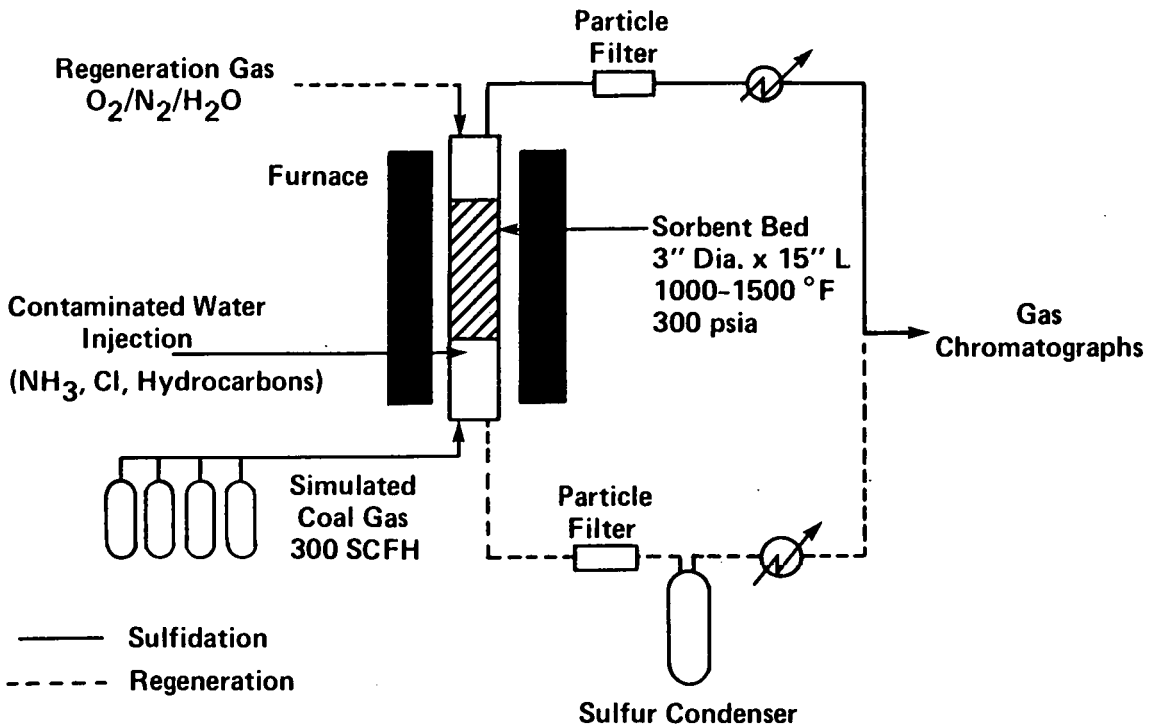

Figure 1. Research Triangle Institute Bench-Scale Desulfurization Reactor.

The bench unit has been designed for a maximum flow of 300 scfh (140 slpm) of simulated coal gas at a maximum pressure of 300 psia and a maximum temperature of 1500 °F (816 °C). The reactor is 3 inches in diameter and the sorbent bed height is 15 inches. The maximum sorbent volume that can be tested is 1.7 liters. The unit has been constructed as a skid mounted system for ease of transportation and the material of construction used is 316 or 304 stainless steel. The wetted parts exposed to coal gas have been Alon processed (a high temperature aluminum vapor treatment) to prevent corrosion of the stainless steel by sulfur gases in presence of steam. The most significant design features of the bench-unit are listed in Table 1.

Table 1. Significant Design Features of Bench-Unit.

- The sorbent cage is easily removable following runs
- Separate lines in opposite direction are provided for regeneration and sulfidation
- Seven high-pressure mass flow controllers allow a high degree of versatility in choosing the simulated coal gas composition
- Automated on-line gas chromatographs with thermal conductivity and flame photometric detectors allow complete gas analysis and sulfur gas speciation down to 1 ppmv
- Sulfur formed during regeneration may be either oxidized to SO_2 or collected in a trap
- A separate line is provided for injecting trace coal gas contaminants directly under the sorbent bed
- Entrained particulates can be captured and measured using removable ceramic filters
- Precise pressure control is provided by two back pressure regulators in series and on-set of reactor plugging may be detected by an electronic differential pressure monitor
- Temperature is monitored at seven positions along the sorbent bed using an Alonized thermowell.

Sorbent manufacture by UCI is progressing parallel to bench-unit construction. Sorbent preparation has been an iterative process in which UCI first prepares several variations of each sorbent. These variations are then evaluated using 1.5 cycle thermogravimetric reactor (TGR) tests, and their physical and chemical properties are measured. The objective is to choose the most promising sorbents for manufacture of large sorbent batches (~1 cubic foot) for bench-unit evaluation. The desired nominal specifications of the sorbent cylindrical extrudates are listed in Table 2.

Table 2. Nominal Sorbent Extrudate Specifications.

Mercury pore volume: ≥ 0.3 cm^3/g	length: 3/8-1/2 inch
BET surface area: ≥ 2 m^2/g	diameter: 3/16 inch
ASTM crush strength: ≥ 1 lb/mm	inorganic binder: $\leq 2\%$

In addition to the specifications in Table 2, porosity, x-ray diffraction crystalline phases (and corresponding crystallite sizes), mercury pore size distribution (and average pore diameter), and attrition

indices of the sorbents are also being measured. The method of sorbent preparation involves high-temperature solid, state reaction of the stoichiometric amounts of the oxides with 2% Bentonite binder. The variations for each sorbent composition involves incorporation of varying levels of organic binder (Methocel) up to 10% during initial preparation. The organic binder burns off during calculation to presumably produce additional porosity within the extrudates. Space limitations do not allow presentation of properties for all variations prepared to date. Typical properties for each sorbent are shown in Table 3.

Table 3. Typical Properties of Novel Sorbents.

	(ZC)F	(Ø.8Z)T	(C3)FA	CA
UCI designation	L-2868	L-2887	L-2889	L-2891
% organic binder	Ø	10	5	5
Bulk density (lb/ft^3)	79.Ø	62.2	78.Ø	52.7
BET Surface Area (m^2/g)	4.Ø	3.25	10.8	48.Ø
Macro-porosity (%)	63.6	59.7	65.8	54.7
Mercury Pore Volume (cm^3/g)	Ø.32	Ø.37	Ø.35	Ø.42
Average pore diameter Angstrom	3125	547Ø	243Ø	175Ø
Crush strength (lb/mm)	3.55	4.7	2.8	1.Ø
Attrition (%)	23	N.M.	N.M.	N.M.
XRD Phases and Crystallite sizes	1. $ZnFe_2O_4$, 166Ø Angstrom 2. CuO (small amount)	1. $Zn_2Ti_3O_8$, >3ØØØ Angstrom 2. α-Zn_2TiO_4, 1ØØØ Angstrom 3. $ZnTiO_3$, (small amount) 4. TiO_2(Anatase) 5. TiO_2(Rutile) 6. ZnO(?)	1. $CuFe_2O_4$, 819 Angstrom 2. $CuAl_2O_4$, 79Ø Angstrom 3. CuO, 5ØØ Angstrom 4. γ-Fe_2O_3	1. $CuAl_2O_4$, 199 Angstrom 2. CuO, 228 Angstrom 3. γ-Al_2O_3

N.M. = not measured.

The (ZC)F sorbent variations were calcined at 1550 °F for 2 hours, whereas the others were calcined at 1600 °F for 2 hours. TGR testing of the variations is being carried out consisting of a 30 minute reduction at 550 °C, followed by 2.5 hour sulfidation at 550 °C, and a 2-hour regeneration at 650 °C. The reduction and sulfidation steps are then repeated for a second cycle. The reducing gas, sulfidation gas and regeneration gas compositions are shown in Table 4.

The coal gas compositions in Table 4 are typical of air-blown fluidized bed gasifier gases.

Table 4. TGR Testing Gas Compositions (%).

	Reducing gas	Sulfidation gas	Regeneration gas
H_2	10.4	10.4	--
CO_2	4.5	4.5	--
CO	16.0	16.0	--
N_2	42.5	39.9	56.0
H_2O	26.6	26.6	41.0
H_2S	--	2.6	--
O_2	--	--	3.0

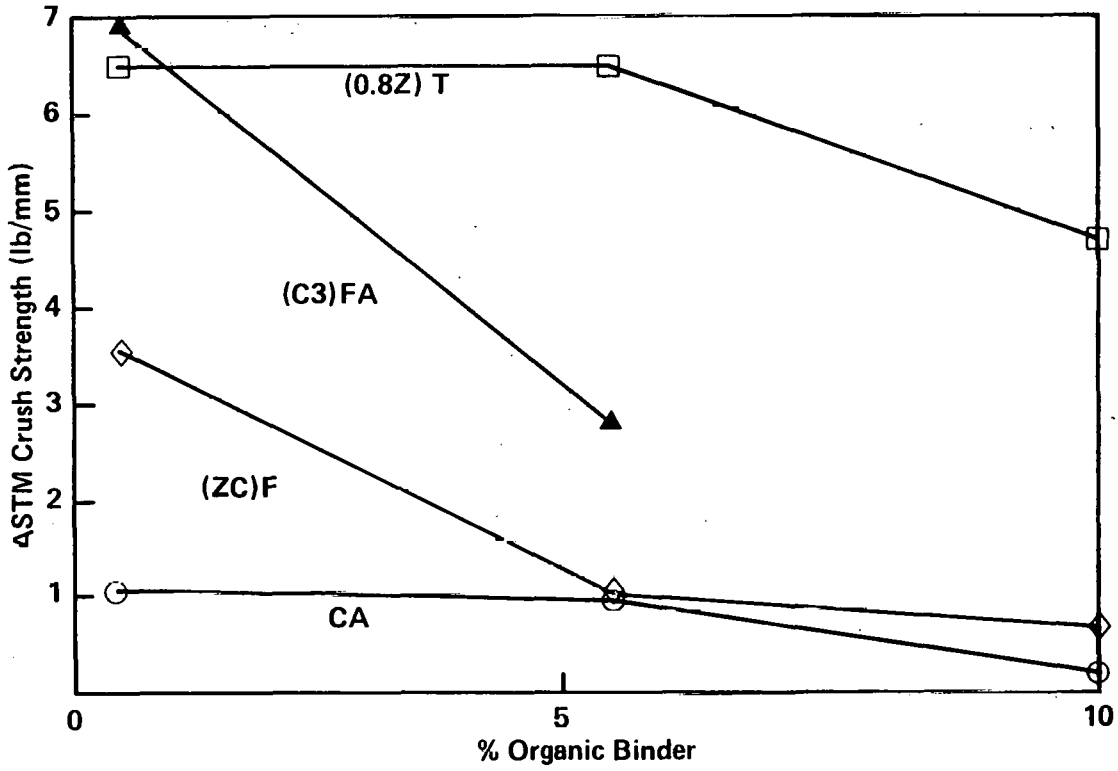

Figure 2. Effect of Organic Binder Content During Preparation on Crush Strength of Calcined Sorbent.

The effect of organic binder concentration during initial preparation on crush strength of the calcined extrudates is shown in Figure 2.

For (ZC)F sorbent, a very detrimental effect of higher organic binder content is seen. The crush strength is acceptable at 0% organic binder level and marginal at 5% organic binder level. The TGR tests did not show any improvement in reactivity for the latter over the former. Clearly, the sorbent of choice for further evaluation on the bench unit is the one prepared with 0% organic binder (UCI designation L-2868). UCI will prepare and supply 1 cubic foot of this sorbent in the near

future. For the (0.8Z)T sorbent, no clearcut choice can be made based on the crush strength results. The TGR tests of the three (0.8Z)T variations are shown in Figure 3.

From Figure 3, the sorbent with 10% organic binder (L-2887) is clearly seen to be superior in reactivity. The mercury pore size distributions of the three (0.8Z)T variations are shown in Figure 4. Most open pore structure is seen to be present in L-2887 (with 10% organic). The fact that the TGR reactivity is highest (Figure 3) for L-2887 and did not change during the second cycle indicates it to be the sorbent of choice for further evaluation on the bench unit. UCI will supply 1 cubic foot of L-2887 in the near future. The TGA results for (C3)FA and CA sorbents are at present preliminary and will be presented in the future.

6. RESULTS/ACCOMPLISHMENTS

- A detailed experimental test plan containing sorbent details, bench-unit design, experimental test matrix, and sorbent evaluation methods was prepared.

- Several novel sorbent variations were prepared and tested using a TGR. Specifications for (ZC)F and (0.8Z)T sorbents were finalized for bench-unit testing. Preliminary TGR tests were completed for all sorbent variations.

- The design and construction of a versatile high-pressure skid mounted bench unit was nearly completed.

7. FUTURE WORK

Formulation and TGR testing of (C3)FA and CA variations will be completed in the near future and specifications of these sorbents will be finalized. Bench-unit construction and commissioning will be completed by late June. Experimental test matrix will then be implemented. Approximately 10, 1.5 cycle bench-unit runs will be carried out for each sorbent with pressure, temperature, H_2S concentration and space velocity as primary variables. Two multicycle runs with and without trace contaminants (Cl, NH_3, tar, CS_2, COS) will also be carried out for each sorbent. Structural properties and XRD phases for the spent sorbent from different levels of the sorbent bench will be measured. The bench unit results will be analyzed and preliminary cost comparison of the sorbents will be carried for applications to 100 MW IGCC and/or gasifier/MCFC power plants.

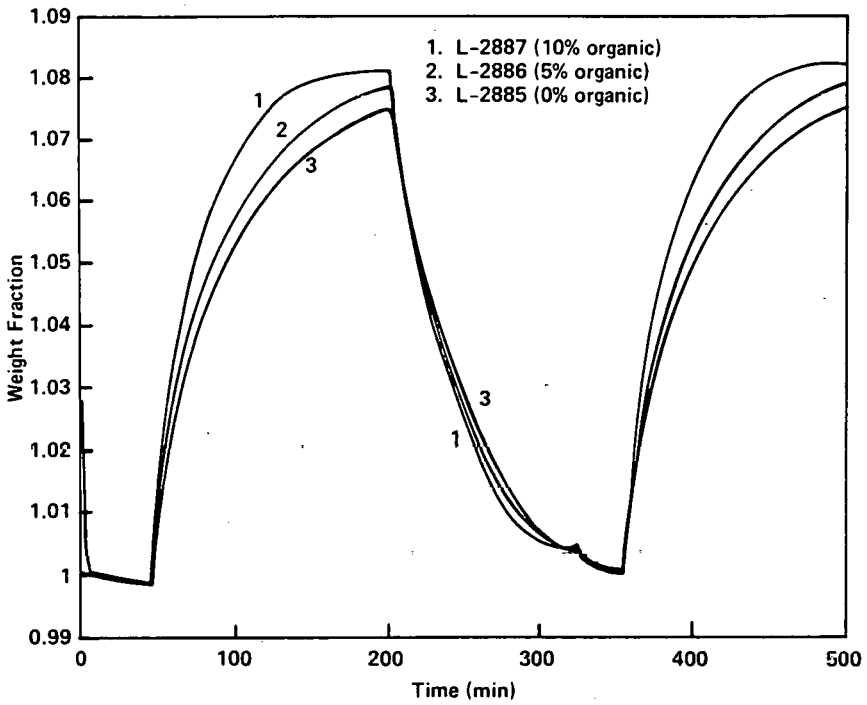

Figure 3. TGR Screening of (0.8Z) T Sorbents.

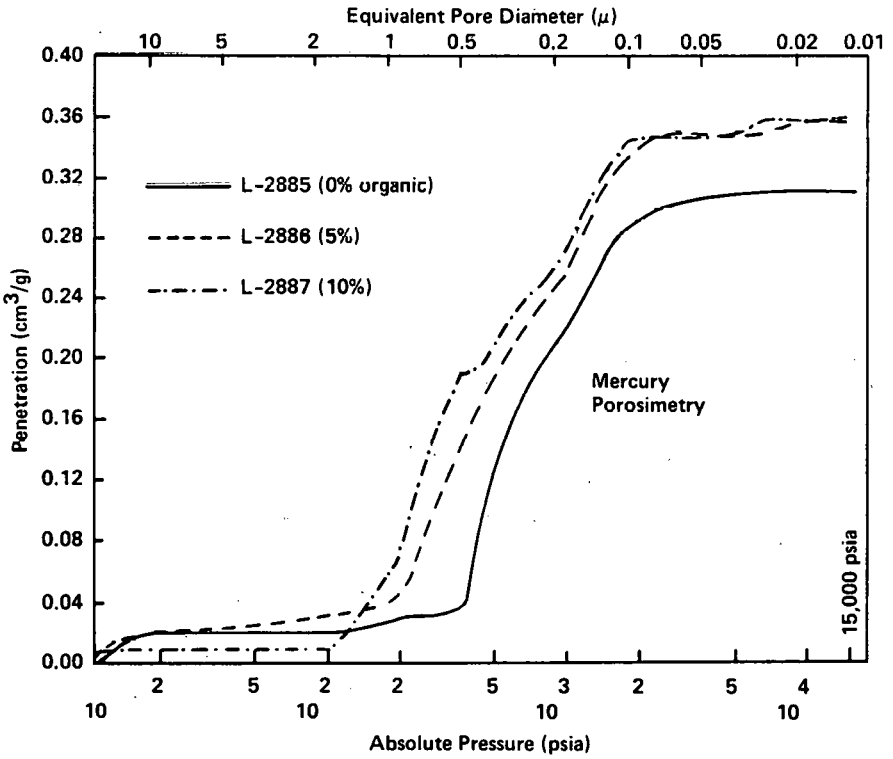

Figure 4. Effect of Organic Binder Content and Subsequent Burnout on Pore Volume Distribution of (0.8Z) T Sorbent.

8. REFERENCES

Office of Technical Management and Office of Basic and Applied Sciences, Morgantown Energy Technology Center, 1986, Hot Gas Cleanup for Electrical Power Generating Systems, DOE/METC-86/6038 (DE86006607).

Grindley, T., and G. Steinfeld, 1984, "Testing of Zinc Ferrite H_2S Absorbent in a Coal Gasifier Side Stream," Proceedings, Fourth Annual Meeting on Contaminant Control in Hot Coal-Derived Gas Streams, DOE/ METC/85-3, pp. 314-336.

Flytzani-Stephanopoulous, M., et al., 1984, "Novel Sorbents for High Temperature Regenerative H_2S Removal, DOE/MC/20417-1898 (DE86004261).

APPENDIX A

TECHNICAL PROGRAM
AGENDA

MONDAY, JUNE 15, 1987

2:00 p.m.	Tour of METC Facilities

TUESDAY, JUNE 16, 1987

7:00 a.m.	Registration, Ballroom Foyer
7:30 a.m.	Speakers Briefing Breakfast, Reflection Dining Room
8:00 a.m.	Morning Coffee and Danish, Ballroom Foyer
8:30 a.m.	Welcome -- Dr. Madhav R. Ghate, Chief, Gasification and Combustion Branch, and Kenneth E. Markel, Jr., Chief, Gas Stream Cleanup Branch, METC
8:35 a.m.	Opening Remarks -- A. A. Pitrolo, Director, METC
8:50 a.m.	Gasification and Gas Stream Cleanup Overview -- Gary E. Voelker, Director of Coal Conversion Systems, Fossil Energy Headquarters
9:00 a.m.	A Summary Status of Coal Gasification Systems and the Prospects for Application in the Electric Power Industry -- Dwain F. Spencer, Vice President, Advanced Power Systems, Electric Power Research Institute

SESSION 1 -- SYSTEM FOR THE PRODUCTION OF CO-PRODUCTS

Co-Chairmen: Suresh C. Jain and Lisa A. Jarr, METC

9:30 a.m.	1.1	Development of a Mild Gasification Process -- Dr. Richard A. Wolfe, UCC Research Corporation
9:55 a.m.	1.2	Steam Conditioning of Coal for Synfuels Production -- Dr. Susan D. Brandes, City College of New York
10:20 a.m.		BREAK
10:50 a.m.	1.3	Investigation of Reaction of Heteroatoms During Coal Gasification -- Dr. Robert F. Zabransky, Institute of Gas Technology
11:15 a.m.	1.4	Measurement and Modeling of Advanced Coal Conversion Processes -- Dr. Peter R. Solomon, Advanced Fuel Research, Inc., and Dr. L. Douglas Smoot, Brigham Young University

Tuesday, June 16, 1987 (Continued)

11:40 a.m. 1.5 Application of Organo-Calcium Chemistry to Control of Contaminant Aromatic Hydrocarbons in Advanced Coal Gasification Processes -- Dr. William A. Peters, Massachusetts Institute of Technology

12:05 p.m. LUNCHEON, University Hall

Master of Ceremonies: John E. Sholes, Deputy Director, Coal Projects Management Division, METC

Dr. William Lueckel, Vice President of Research, International Fuel Cells

"Fuel Cell Applications"

Co-Chairmen: L. Megan Day and Dr. Wen-Shou Liou, METC

1:35 p.m. 1.6 Novel Concept Development of an Internal Recirculation Catalyst for Mild Gasification -- Dr. Suresh P. Babu, Institute of Gas Technology

2:00 p.m. 1.7 Chemical and Physical Development of Char Particles During Devolatilization -- Dr. Peter R. Solomon, Advanced Fuel Research, Inc.

2:25 p.m. 1.8 Study of the Effects of Soot, Particulates, and Other Contaminants on Molten Carbonate Fuel Cells Fueled by Coal Gas -- Dr. Edward A. Pigeaud, Energy Research Corporation

2:50 p.m. BREAK

3:20 p.m. 1.9 Mild Gasification of Coal -- Meyer Steinberg, Brookhaven National Laboratory

3:45 p.m. 1.10 Fundamental Mechanisms of Coal Gasification -- Dr. William A. Peters, Massachusetts Institute of Technology

4:10 p.m. 1.11 Upgrading Condensibles from Coal Devolatilization -- Dr. John E. Mrochek, Oak Ridge National Laboratory

4:35 p.m. 1.12 Assessment of Instrumentation Need for Advanced Coal Conversion Process Applications -- Dr. Eric T. Nelson, Gilbert/Commonwealth, Inc.

POSTER SESSION A

5:30 to 7:00 p.m. Poster Session Displays and Reception

A.1 Particulate Control in a Reduced Entrainment Precipitator -- Dr. Dale A. Furlong, ETS, Inc.

Tuesday, June 16, 1987 (Continued)

A.2 Vaporization of Trace Inorganic Species from Coal Under Combustion Gasification and Conditions -- Dr. Robert D. Brittain, SRI International

A.3 Hot Gas Cleanup Systems Analysis -- Kevin R. Craig and Robert W. Koch, METC

A.4 Experimental Development of a Multi-Solid Fluidized-Bed Reactor Concept -- Robert D. Litt and William G. Steedman, Battelle Columbus Division

A.5 Measurement and Modeling of Advanced Coal Conversion Processes -- Michael A. Serio, Advanced Fuel Research, Inc. and B. Scott Brewster, Brigham Young University

A.6 Mechanisms of Mild Gasification and Low Severity Coal Devolatilization -- Dr. M. Rashid Khan, METC

A.7 Mild Gasification of Coal -- Robert O. Ness, Jr., University of North Dakota Energy Research Center

A.8 Gasification Systems Analysis -- Julianne M. Klara, METC

A.9 Research on Mild Gasification Char Fuel Development -- Dr. Richard A. Wolfe, UCC Research Corporation

A.10 Effects of Halides on the Performance of Coal Gas-Fueled Molten Carbonate Fuel Cell -- H. Russell Kunz, IFC Corporation

A.11 Vessel Cost Reduction -- Samuel C. Leventry, Chicago Bridge and Iron

A.12 Coal Slurry Letdown Device -- Dr. Webb J. Marner, Jet Propulsion Laboratory

A.13 Development of Iron Aluminides for Coal Gasification Systems -- Claudette G. McKamey, Oak Ridge National Laboratory

A.14 Protective Coatings and Claddings: Application/Evaluation -- Nachappa G. Gopalsami, Argonne National Laboratory

WEDNESDAY, JUNE 17, 1987

7:00 a.m. Registration, Ballroom Foyer
7:30 a.m. Speakers Briefing Breakfast, Reflection Dining Room
8:00 a.m. Morning Coffee and Danish, Ballroom Foyer

8:30 a.m. Opening -- Kenneth E. Markel, Jr., Chief, Gas Stream Cleanup Branch, METC

Wednesday, June 17, 1987 (Continued)

SESSION 2 -- SYSTEM FOR THE PRODUCTION OF INDUSTRIAL FUEL GAS

Co-Chairmen: Vijendra P. Kothari and Lisa A. Jarr, METC

8:35 a.m. 2.1 Ash and Slag Characterization -- Sharon K. Falcone-Miller, University of North Dakota Energy Research Center

9:00 a.m. 2.2 Experimental and Theoretical Investigation of Formation and Growth of Ash Agglomerates -- Dr. Ronald H. Carty, Institute of Gas Technology

9:25 a.m. 2.3 Performance Evaluation of a Screenless Counter-Current Granular-Bed Filter on a Subpilot-Scale PFBC -- Keith B. Wilson, Combustion Power Company

9:50 a.m. 2.4 Evaluation of a Sub-pilot Electrostatic Precipitator -- K. Sampath Kumar, Cottrell Environmental Sciences

10:15 a.m. BREAK

10:45 a.m. 2.5 KILnGAS Commercial Module -- Peter G. Garside, Allis-Chalmers Coal Gasification Corporation

SESSION 3 -- ENVIRONMENTAL PROJECTS

11:10 a.m. 3.1 Performance Evaluation of a Ceramic Cross-Flow Filter on a Bench-Scale Gasifier -- Dr. David F. Ciliberti, Westinghouse Electric Corporation

11:35 a.m. 3.2 Environmental Engineering and Analysis -- Dennis P. Raden, Radian Corporation

12:00 p.m. LUNCHEON, University Hall

Master of Ceremonies: Dr. John S. Halow, Director, Coal Projects Management Division, METC

Dr. James Corman, Manager, Thermochemical Processes Branch, General Electric Corporate Research and Development

"Integrated Gasification Combined-Cycle Systems"

Co-Chairmen: Steven J. Bossart and David Dubis, METC

1:30 p.m. 3.3 Advanced Wastewater Treatment -- John R. Gallagher, University of North Dakota Energy Research Center

1:55 p.m. 3.4 Ceramic Cross-Flow Filter Development -- Jeffery M. Gonzales, GTE Products Corporation

Wednesday, June 17, 1987 (Continued)

2:20 p.m.	3.5	A Mechanical Analysis of a Cross Flow Filter -- Dr. David F. Ciliberti, Westinghouse Electric Corporation
2:45 p.m.		BREAK

SESSION 4 -- COMPONENTS AND MATERIALS

3:15 p.m.	4.1	Zirconia Cell Oxygen Source -- Dr. Jerry W. Suitor, Jet Propulsion Laboratory
3:40 p.m.	4.2	Materials Development for JPL Oxygen Plant -- Dr. Timothy E. Easler, Argonne National Laboratory
4:05 p.m.	4.3	Reduction of Erosion in Elbows Due to Flow Field Modifications -- Dr. Kenneth H. Means, West Virginia University
4:30 p.m.	4.4	Ceramic Fiber-Ceramic Matrix Hot-Gas Filters -- David P. Stinton, Oak Ridge National Laboratory

THURSDAY, JUNE 18, 1987

7:00 a.m.	Registration, Ballroom Foyer
7:30 a.m.	Speakers Briefing Breakfast, Reflection Dining Room
8:00 a.m.	Morning Coffee and Danish, Ballroom Foyer
8:30 a.m.	Opening -- Dr. Madhav R. Ghate, Chief, Gasification and Combustion Branch, METC

SESSION 5 -- SYSTEM FOR THE PRODUCTION OF SYNTHESIS GAS

Co-Chairmen: Dr. Norman T. Holcombe and Leland E. Paulson, METC

8:35 a.m.	5.1	Catalytic Gasification Fundamentals -- Dr. Heinz Heinemann, Lawrence Berkeley Laboratory
9:00 a.m.	5.2	Production of Hydrogen from Low-Rank Coals -- Rodney E. Sears, University of North Dakota Energy Research Center
9:25 a.m.	5.3	Biological Degradation of Low-Rank Coal -- Dr. William J. Jones, Georgia Institute of Technology
9:50 a.m.	5.4	Study of Ammonia Removal in Coal Gasification Processes Using an Integrated Systems Approach -- Dr. Ramsay Chang, Acurex Corporation
10:15 a.m.		BREAK

Thursday, June 18, 1987 (Continued)

10:45 a.m. 5.5 Study of Ammonia Removal from Coal Gasification Processes -- Dr. Gopala N. Krishnan, SRI International

11:10 a.m. 5.6 Injection of Densely Loaded Flows into Entrained-Flow Gasifiers -- Dr. Reiner Kollrack, Science Applications International Corporation

11:35 a.m. 5.7 Attrition and Entrainment Studies Related to Fluidized-Bed Gasifiers -- Dr. Ted M. Knowlton, Institute of Gas Technology

12:00 p.m. LUNCHEON, University Hall

Master of Ceremonies: Dr. Paul R. Wieber, Deputy Associate Director, Office for Technical Management, METC

Mr. William Morse, Vice President of Research, Columbia Gas

"The Present and Future of Gas Supplies"

Co-Chairmen: Randall J. Dellefield and Dr. Hsiao-Ya L. Lai, METC

1:30 p.m. 5.8 Mechanisms for Hot Gas Cleanup -- Dr. Jason M. Cook, METC

1:55 p.m. 5.9 Low Temperature, Sulfur Tolerant, Homogenous Catalysts for the Water-Gas Shift Reaction -- Dr. Bernard J. Wood, SRI International

2:20 p.m. 5.10 Removal of H_2S from Gasified Coal -- Dr. Scott Lynn, Lawrence Berkeley Laboratory

2:45 p.m. 5.11 Gas Separation by Pressure Swing Adsorption for Producing Hydrogen from Coal -- Dr. Ralph T. Yang, State University of New York at Buffalo

3:10 p.m. BREAK

3:40 p.m. 5.12 Gas Separation Using Ion Exchange Membranes for Producing Hydrogen from Synthesis Gas -- Dr. Richard D. Noble, National Bureau of Standards

4:05 p.m. 5.13 Separation of Gas Mixtures by Supported Complexes -- Dr. Michael A. Lilga, Pacific Northwest Laboratory

4:30 p.m. 5.14 Measurement of Alkali Vapors in PFBC Process Stream and Their Removal with a Fixed Granular-Bed Sorber -- Dr. Sheldon H. D. Lee, Argonne National Laboratory

4:55 p.m. 5.15 A Study of High Temperature Removal of Alkali in a Pressurized Gasification System -- Dennis M. Bachovchin, Westinghouse Electric Corporation

Thursday, June 18, 1987 (Continued)

POSTER SESSION B

5:30 to 7:00 p.m. Poster Session Displays and Reception

B.1 A Novel Approach to Hydrogen Recovery, Storage, and Transport -- Nicholas L. Krascella, United Technologies Research Center

B.2 Hydrogen Recovery by Novel Solvent Systems -- Dr. Zvi Ludmer, City College of New York

B.3 Low Cost Hydrogen/Novel Membrane Technology for Hydrogen Separation from Synthesis Gas -- Dr. Richard W. Baker, Membrane Technology and Research, Inc.

B.4 Advanced Studies of the Biological Conversion of Synthesis Gas to Methane -- Dr. Edgar C. Clausen, University of Arkansas

B.5 Biological Gasification of Coals -- Dr. Daman S. Walia, Atlantic Research Corporation

B.6 Process Development Unit for Coal Gasification Tied to Regenerative Hot Gas Cleanup -- Albert Calderon, Calderon Energy Company

B.7 Expansion of High-Temperature, High-Pressure Data Set for Coal Gasification -- Dr. Alan W. Scaroni, Pennsylvania State University

B.8 Expansion of High-Temperature, High-Pressure Data Set for Coal Gasification -- Dr. Michael A. Serio, Advanced Fuel Research, Inc.

B.9 Advanced Gasification Entrained Reactor -- Larry A. Bissett, METC

B.10 Sidestream Zinc Ferrite Regeneration Testing -- Dr. Thomas Grindley, METC

B.11 METC Fixed-Bed Gasifier -- Kalman Pater, METC

B.12 Fundamental Studies of In-Situ Sulfur and Alkali Capture -- Dr. George R. Gavalas, California Institute of Technology

B.13 A Mechanistic Study of the Energetic Heterogeneity of Coal Chars -- Dr. Joseph M. Calo, Brown University

B.14 Fundamental Fluidization Research Program -- Dr. Joseph S. Mei, METC

Thursday, June 18, 1987 (Continued)

B.15 Development of a Novel Nested-Fiber Filter Concept for High-Temperature and High-Pressure Physical Cleanup -- Robert D. Litt and H. Nicholas Conkle, Battelle Columbus Division

B.16 Throwaway Processes for Treatment of Regeneration Tail Gases -- Lawrence R. Woodland, Arthur D. Little, Inc.

B.17 Sorbent-Based Recovery of Sulfur from Regeneration Tail Gases -- Scott M. Harkins, Research Triangle Institute

FRIDAY, JUNE 19, 1987

7:00 a.m.		Registration, Ballroom Foyer
7:30 a.m.		Speakers Briefing Breakfast, Reflection Dining Room
8:00 a.m.		Morning Coffee and Danish, Ballroom Foyer
8:30 a.m.		Opening -- Kenneth E. Markel, Jr., Chief, Gas Stream Cleanup Branch, METC

SESSION 6 -- SYSTEM FOR THE PRODUCTION OF POWER

Co-Chairmen: Thomas P. Dorchak and Dr. Justin L. Beeson, METC

8:35 a.m.	6.1	Modeling Hydrodynamic Mixing in Process Design and Development of Fluidized-Bed Gasifiers -- Dr. Thomas R. Blake, University of Massachusetts
9:00 a.m.	6.2	Novel Concepts of System Assessment in Coal Gasification -- Dr. Reuel Shinnar, City College of New York
9:25 a.m.	6.3	Development of a Hot Gas Cleanup System -- Gerald L. Anderson, Institute of Gas Technology
9:50 a.m.	6.4	Sulfur Production from Desulfurization Regenerator Offgas -- Dr. James B. O'Hara, The Ralph M. Parsons Company
10:15 a.m.		BREAK
10:45 a.m.	6.5	KRW Process Development Coal Gasification/Hot Gas Cleanup -- Keven J. Smith, KRW Energy Systems, Inc.
11:10 a.m.	6.6	Design Studies for Hot Gas Cleanup System in a Load Following Mode -- Daniel P. Smith and Dr. Eli Gal, General Electric Corporate Research and Development
11:35 a.m.	6.7	Enhanced Durability and Reactivity for Zinc Ferrite Desulfurization Sorbent -- Dr. Mahesh C. Jha, Amax Research and Development Center

Friday, June 19, 1987 (Continued)

12:00 p.m. LUNCHEON, Reflection Dining Room

Co-Chairmen: Mark C. Williams and Dr. James R. Longanbach, METC

1:00 p.m. 6.8 Integrated Gasification Solid Oxide Fuel Cell System -- Dr. Thomas E. Lippert, Westinghouse Electric Corporation

1:25 p.m. 6.9 Dynamic Simulation Models for High-Temperature Desulfurization Processes -- Dr. Douglas P. Harrison, Louisiana State University

1:50 p.m. 6.10 Detailed Studies of Novel Regenerable Sorbents for High-Temperature Coal-Gas Desulfurization -- Dr. Maria Flytzani-Stephanopoulos, Massachusetts Institute of Technology

2:15 p.m. 6.11 Integration and Testing of Hot Desulfurization and Entrained Flow Gasification for Power Generation -- Michael W. Becker, Texaco, Inc.

2:40 p.m. 6.12 Bench-Scale Testing of Novel Desulfurization Sorbents -- Dr. Santosh K. Gangwal, Research Triangle Institute

3:05 p.m. Closing Remarks -- Kenneth E. Markel, Jr., Chief, Gas Stream Cleanup Branch, and Dr. Madhav R. Ghate, Chief, Gasification and Combustion Branch, METC

APPENDIX B

LIST OF PARTICIPANTS

RAVINDRA K AGRAWAL
DEVELOPMENT ENGR'G & ANALYSIS
KRW ENERGY SYSTEMS, INC.
P.O. BOX 334
MADISON, PA 15663-0334
412-722-6137

SY B ALPERT
TECHNICAL DIRECTOR
ELECTRIC POWER RESEARCH INST.
3412 HILLVIEW AVENUE
PALO ALTO, CA 94304
415-855-2512

GERALD L ANDERSON
ASSISTANT DIRECTOR
INSTITUTE OF GAS TECHNOLOGY
3424 SOUTH STATE STREET
CHICAGO, IL 60616
312-567-5832

KENNY ASHTON
GRADUATE STUDENT
WEST VIRGINIA UNIVERSITY
DEPARTMENT OF GEOLOGY
MORGANTOWN, WV 26506
304-594-2331

SURESH P BABU
ASSOC. DIRECTOR, PROC. DEV.
INSTITUTE OF GAS TECHNOLOGY
3424 S. STATE STREET
CHICAGO, IL 60616
312-567-5758

DENNIS M BACHOVCHIN
SENIOR ENGINEER
WESTINGHOUSE ELECTRIC CORP.
RESEARCH & DEVELOPMENT CENTER
1310 BEULAH ROAD
PITTSBURGH, PA 15235
412-256-2250

RICHARD BAILIE
PROFESSOR
WEST VIRGINIA UNIVERSITY
CHEMICAL ENGINEERING DEPT.
ENGR. SCIENCE BLDG., EVANSDALE
MORGANTOWN, WV 26506
304-293-3351

WILFORD G BAIR
ASSISTANT VICE PRESIDENT
INSTITUTE OF GAS TECHNOLOGY
3424 S. STATE STREET
CHICAGO, IL 60616
312-567-5896

RICHARD A BAJURA
DIRECTOR, ENERGY RESEARCH CTR.
WEST VIRGINIA UNIVERSITY
P.O. BOX 6064
258 STEWART STREET
MORGANTOWN, WV 26506-6064
304-293-2867

RICHARD W BAKER
PRESIDENT
MEMBRANE TECH & RESEARCH, INC.
1030 HAMILTON COURT
MENLO PARK, CA 94025
415-328-2228

FREDERICK J BARAN
MANAGER, COMPLIANCE & CONTROLS
TEXACO, INC.
2000 WESTCHESTER AVENUE
ALTERNATE ENERGY
WHITE PLAINS, NY 10650
914-253-4015

S.P. BARONE
PROJECT MANAGER
GAS RESEARCH INSTITUTE
8600 BRYN MAWR AVENUE
CHICAGO, IL 60631
312-399-8224

DWAYNE G BATESON
EXECUTIVE ASSISTANT
TRANSALTA UTILITIES CORP.
BOX 1900
CALGARY, ALBERTA T2P2M1
CANADA
403-267-7129

SUSHIL K BATRA
SENIOR PROGRAM MANAGER
TECOGEN, INC.
45 FIRST AVENUE
P.O. BOX 9046
WALTHAM, MA 02254-9046
617-890-8700

THOMAS F BECHTEL
ASSOCIATE DIRECTOR, OTM
MORGANTOWN ENERGY TECH CENTER
U.S. DEPARTMENT OF ENERGY
P.O. BOX 880, MS B06
MORGANTOWN, WV 26507-0880
304-291-4147

MICHAEL W BECKER
SENIOR CHEMICAL ENGINEER
TEXACO, INC.
329 NORTH DURFEE ROAD
SOUTH EL MONTE, CA 91733
213-699-0948

JUSTIN L BEESON
PROJECT MANAGER
MORGANTOWN ENERGY TECH CENTER
U.S. DEPARTMENT OF ENERGY
P.O. BOX 880, MS C04
MORGANTOWN, WV 26507-0880
304-291-4671

AUGUST D BENZ
MANAGER, PROCESS PROGRAMS
BECHTEL NATIONAL, INC.
P.O. BOX 3965
SAN FRANCISCO, CA 94119
415-768-5724

MARK H BERGGREN
PROJECT ENGINEER
AMAX EXTRACTIVE R&D, INC.
5950 MCINTYRE STREET
GOLDEN, CO 80403
303-279-7636

LARRY A BISSETT
ACTING CHIEF, CSS
MORGANTOWN ENERGY TECH CENTE
U.S. DEPARTMENT OF ENERGY
P.O. BOX 880, MS N04
MORGANTOWN, WV 26507-0880
304-291-4266

THOMAS R BLAKE
MECHANICAL ENGINEER
UNIVERSITY OF MASSACHUSETTS
DEPT OF MECHANICAL ENGINEERING
AMHURST, MA 01003
413-545-1571

ALAN BLAND
PROGRAM DIRECTOR
KENTUCKY ENERGY CABINET LAB
IRON WORKS PIKE
P.O. BOX 31015
LEXINGTON, KY 40512-3015
606-252-5535

BRADLEY BOCKRATH
CHIEF, COAL CHEMISTRY BRANCH
PITTSBURGH ENERGY TECH CENTER
P.O. BOX 10940
PITTSBURGH, PA 15236
412-675-6082

STEVEN J BOSSART
PROJECT MANAGER
MORGANTOWN ENERGY TECH CENTER
U.S. DEPARTMENT OF ENERGY
P.O. BOX 880, MS C04
MORGANTOWN, WV 26507-0880
304-291-4643

RONNIE A BRADLEY
MANAGER
OAK RIDGE NATIONAL LABORATORY
P.O. BOX X, BUILDING 4508
OAK RIDGE, TN 37831-6098
615-574-6094

SUSAN D BRANDES
RESEARCH ASSISTANT
CITY COLLEGE OF NEW YORK
DEPT. OF CHEMICAL ENGINEERING
140TH AND CONVENT AVENUE
NEW YORK, NY 10031
212-690-8364

SCOTT B BREWSTER
RESEARCH ASSOCIATE
BRIGHAM YOUNG UNIVERSITY
45 CTB
PROVO, UT 84602
801-378-6240

ROBERT D BRITTAIN
SR. PHYSICAL CHEMIST
SRI INTERNATIONAL
MATERIALS RESEARCH LAB
333 RAVENSWOOD AVENUE
MENLO PARK, CA 95014
415-859-2019

CLYDE S BROOKS
CONSULTANT
41 BALDWIN LANE
GLASTONBURY, CT 06033
203-633-7406

JACK T BROWN
DIRECTOR/ELECTROCHEMICAL PROJ.
WESTINGHOUSE ELECTRIC CORP.
1310 BEULAH ROAD
PITTSBURGH, PA 15235
412-256-1950

WENNONA A BROWN
TECHNOLOGY COMMUNICATIONS MGR.
MORGANTOWN ENERGY TECH CENTER
U.S. DEPARTMENT OF ENERGY
P.O. BOX 880, MS C02
MORGANTOWN, WV 26507-0880
304-291-4620

ALBERT CALDERON
PRESIDENT
CALDERON ENERGY COMPANY
P.O. BOX 126
BOWLING GREEN, OH 43402
419-352-4631

JO CALDERON
VICE-PRESIDENT AND TREASURER
CALDERON ENERGY COMPANY
1145 FAIRVIEW AVENUE
P.O. BOX 126
BOWLING GREEN, OH 43402
419-352-4631

JOSEPH M CALO
ASSOCIATE PROFESSOR
BROWN UNIVERSITY
CHEMICAL ENGR'G DEPT, BOX D
PROVIDENCE, RI 02912
401-863-1421

DAVID W CAMP
CHEMICAL ENGINEER
LAWRENCE LIVERMORE NAT'L LAB
P.O. BOX 808, MS L-207
LIVERMORE, CA 94550
415-423-9228

JAMES P CARR
PROGRAM MANAGER
U.S. DEPARTMENT OF ENERGY
FE-22, C-179/GTN
WASHINGTON, DC 20545
202-353-5985

RONALD H CARTY
MANAGER, PROCESS DEVELOPMENT
INSTITUTE OF GAS TECHNOLOGY
3424 SOUTH STATE STREET
CHICAGO, IL 60616
312-567-3751

RAMSAY L CHANG
PROGRAM MANAGER
ACUREX CORPORATION
485 CLYDE AVENUE
MT. VIEW CA 94043
415-961-5700

WALTER L CHEMERYS
MARKETING MGR, SPECIAL PROJ.
UNITED CATALYSTS, INC.
P.O. BOX 32370
LOUISVILLE, KY 40232
502-634-7240

CHARLES I CHU
MANAGER, COAL CONVERSION
UCC RESEARCH CORPORATION
P.O. BOX 128, GLENWAY AVENUE
BRISTOL, VA 24203
703-669-6515

DAVID F CILIBERTI
ADVISORY ENGINEER
WESTINGHOUSE ELECTRIC CORP.
P.O. BOX 355
1310 BEULAH ROAD
PITTSBURGH, PA 15235
412-256-2202

DAVID W CLARK
STAFF ENGINEER
GENERAL MOTORS CORPORATION
ALLISON GAS TURBINE DIVISION
P.O. BOX 420, SPEED CODE O-10
INDIANAPOLIS, IN 46206-0420
317-240-1602
317 687-6067

NIGEL CLARK
ASSOCIATE PROFESSOR
WEST VIRGINIA UNIVERSITY
MECHANICAL & AEROSPACE ENGR.
ENGINEERING SCIENCES BLDG.
MORGANTOWN, WV 26506
304-293-3111

EDGAR C CLAUSEN
PROFESSOR
UNIVERSITY OF ARKANSAS
DEPT. OF CHEMICAL ENGINEERING
3202 BELL ENGINEERING CENTER
FAYETTEVILLE, AR 72701
501-575-4951

NICHOLAS CONKLE
PRINCIPAL RESEARCH ENGINEER
BATTELLE COLUMBUS DIVISION
505 KING AVENUE
COLUMBUS, OH 43201-2693
614-424-5616

JASON M COOK
PHYSICIST
MORGANTOWN ENERGY TECH CENTER
U.S. DEPARTMENT OF ENERGY
P.O. BOX 880, MS AO4
MORGANTOWN, WV 26507-0880
304-291-4718

JAMES CORMAN
MGR, THERMOCHEMICAL PROCESSES
GENERAL ELECTRIC CORPORATE R&D
P.O. BOX 8
SCHENECTADY, NY 12345
518-387-6306

MARGARET S CORNETT
EDITOR, FOSSIL SYNTHETIC FUELS
MCILVAINE COMPANY
2970 MARIA AVENUE
NORTHBROOK, IL 60062
312-272-0010

KEVIN R CRAIG
CHEMICAL ENGINEER
MORGANTOWN ENERGY TECH CENTE
U.S. DEPARTMENT OF ENERGY
P.O. BOX 880, MS EO1
MORGANTOWN, WV 26507-0880
304-291-4560

WILLIAM CRESS
MANAGER, ENGINEER STUDIES
ALLEGHENY POWER SERVICE CORP.
CABIN HILL DRIVE
GREENSBURG, PA 15601
412-838-6720

CECELIA CROPLEY
PROJECT MANAGER
GINER, INC.
14 SPRING STREET
WALTHAM, MA 02254-9147
617-899-7270

L. MEGAN DAY
PROJECT MANAGER
MORGANTOWN ENERGY TECH CENTER
U.S. DEPARTMENT OF ENERGY
P.O. BOX 880, MS CO4
MORGANTOWN, WV 26507-0880
304-291-4074

MARIO DECORSO
MGR, INDUSTRIAL OPERATIONS
SOL-3 RESOURCES
1261 POST HOUSE LA
MEDIA, PA 19063
215-566-7432

RANDALL J DELLEFIELD
PROJECT MANAGER
MORGANTOWN ENERGY TECH CENTER
U.S. DEPARTMENT OF ENERGY
P.O. BOX 880, MS DO4
MORGANTOWN, WV 26507-0880
304-291-4275

DILIP DESHPANDE
SUPERVISORY ENGINEER
ALBERTA POWER LTD.
10035 105TH STREET
EDMONTON, ALBERTA T5J2V6
CANADA
403-420-7177

EDWARD K DIENES
MGR. PROD. DEV./PILOT PLANT
UNITED CATALYSTS, INC.
P.O. BOX 32370
LOUISVILLE, KY 40232
502-634-7402

RAYMOND E DORAZIO
APPLICATION ENGINEER
GTE PRODUCTS CORPORATION
HAWES STREET
TOWANDA, PA 18854
717-265-8983

THOMAS P DORCHAK
PROJECT MANAGER
MORGANTOWN ENERGY TECH CENTER
GRAND FORKS PROJECTS OFFICE
P.O. BOX 7206, UNIV. STATION
GRAND FORKS, ND 58202
FTS-783-0116

DAVID DUBIS
PROJECT MANAGER
MORGANTOWN ENERGY TECH CENTER
U.S. DEPARTMENT OF ENERGY
P.O. BOX 880, MS CO4
MORGANTOWN, WV 26507-0880
304-291-4399

TIMOTHY E EASLER
ARGONNE NATIONAL LABORATORY
9700 SOUTH CASS AVENUE
ARGONNE, IL 60439
FTS-972-4250

B. ZAYNE EGAN
OAK RIDGE NATIONAL LABORATORY
P.O. BOX X
OAK RIDGE, TN 37831-6226
615-574-6868

PAUL EGGERSTEDT
TECHNICAL SPECIALIST
INDUSTRIAL FILTER & PUMP MFG.
5900 OGDEN AVENUE
CICERO, IL 60650
312-656-7800

PHILLIP ENGELER
PROCESS ENGINEER
HELIPUMP CORPORATION
8435 BRECKSVILLE ROAD
CLEVELAND, OH 44141
216-229-3178

SEYED M FATEMI-BADI
GRADUATE ASSISTANT
PENNSYLVANIA STATE UNIVERSITY
410 ACADEMIC ACTIVITIES BLDG.
UNIVERSITY PARK, PA 16802
814-865-4802

HARLAN L FELDKIRCHNER
ASSOCIATE DIRECTOR
INSTITUTE OF GAS TECHNOLOGY
FUNDAMENTAL PROC. RESEARCH
3424 SOUTH STATE STREET
CHICAGO, IL 60616
312-567-5267

PAUL L FELDMAN
MANAGER, CES
RESEARCH COTTRELL, INC.
P.O. BOX 1500
SOMERVILLE, NJ 08876
201-685-4880

JOHN L FERRI
ENGINEER
GTE PRODUCTS CORPORATION
CHEMICAL & METALLURGICAL DIV.
HAWES STREET
TOWANDA, PA 18848
717-265-2121

JOHN T FITZGIBBON
REGIONAL VICE PRESIDENT
FOSTER WHEELER CORP.
FOUR GATEWAY CENTER
SUITE 534
PITTSBURGH, PA 15222
412-281-4887

L. ROBERT FLAIS
SENIOR PLANNING SPECIALIST
BABCOCK & WILCOX COMPANY
1562 BEESON STREET
ALLIANCE, OH 44601
216-821-9110

ROBERT FRUMERMAN
PRESIDENT
FAI
218 SOUTH TRENTON AVENUE
PITTSBURGH, PA 15221
412-371-7800

RICHARD FU
FOSTER WHEELER CORP.
110 SOUTH ORANGE AVENUE
LIVINGSTON, NJ 07039
201-533-4106

DALE A FURLONG
VICE PRESIDENT
ETS, INC.
3140 CHAPARRAL DRIVE, SW
SUITE C-103
ROANOKE, VA 24018-4394

JIM L GADDY
PROFESSOR/DEPT. HEAD
UNIVERSITY OF ARKANSAS
3202 BELL ENGINEERING CENTER
FAYETTEVILLE, AR 72701
501-575-4951

ELI GAL
SENIOR DEVELOPMENT ENGINEER
GENERAL ELECTRIC CORPORATE R&D
200 NORTH 7TH STREET
LABANON, PA 17042
717-274-7049

JOHN R GALLAGHER
RESEARCH SCIENTIST
UNIV OF ND ENERGY RESEARCH CTR
P.O. BOX 8213, UNIV. STATION
GRAND FORKS, ND 58202
701-777-5223

SANTOSH K GANGWAL
SENIOR RESEARCH ENGINEER
RESEARCH TRIANGLE INSTITUTE
P.O. BOX 12194
RESEARCH TRIANGLE PARK NC 2770
919-541-6255

RICHARD E GANNON
DIRECTOR, BUSINESS DEVELOPMENT
AVCO RESEARCH LABORATORY, INC.
ENERGY TECHNOLOGY OFFICE
2385 REVERE BEACH PARKWAY
EVERETT, MA 02149
617-381-4630

CHARLES W GARRETT
PROGRAM MANAGER, TECH COORD.
U.S. DEPARTMENT OF ENERGY
FE-14, B-107/GTN
WASHINGTON, DC 20545
301-353-2819

PETER G GARSIDE
MANAGER, ENGINEERING
ALLIS-CHALMERS COAL GAS CORP.
P.O. BOX 512, 4511-NB
MILWAUKEE, WI 53201-0512
414-475-2643

GEORGE R GAVALAS
PROFESSOR
CALIFORNIA INST OF TECH
1201 E. CALIFORNIA BLVD.
MS 206-41
PASADENA, CA 91125
818-356-4152

MADHAV R GHATE
CHIEF, GASIF & COMBUSTION BR.
MORGANTOWN ENERGY TECH CENTER
U.S. DEPARTMENT OF ENERGY
P.O. BOX 880, MS C04
MORGANTOWN, WV 26507-0880
304-291-4135

BARRY L GILLESPIE
RESEARCH ENGINEER
UCC RESEARCH CORPORATION
P.O. BOX 1280, GLENWAY AVENUE
BRISTOL, VA 24203
703-669-6515

JEFFERY GONZALES
SECTION HEAD
GTE PRODUCTS CORPORATION
CHEMICAL & METALLURGICAL DIV.
HAWES STREET
TOWANDA, PA 18848
717-265-2121

JOHN P GOOCH
ASSOCIATE DIRECTOR
SOUTHERN RESEARCH INSTITUTE
2000 NINTH AVENUE SOUTH
BIRMINGHAM, AL 35255-5305
205-323-6592

NACHAPPA G GOPALSAMI
ELECTRICAL ENGINEER
ARGONNE NATIONAL LABORATORY
9700 SOUTH CASS AVENUE
ARGONNE, IL 60439
FTS-972-5925

ROBERT A GRAFF
PROFESSOR
CITY COLLEGE OF NEW YORK
DEPT OF CHEMICAL ENGINEERING
140TH STREET & CONVENT AVENUE
NEW YORK, NY 10031
212-690-8136

THOMAS GRINDLEY
CHEMICAL ENGINEER
MORGANTOWN ENERGY TECH CENTER
U.S. DEPARTMENT OF ENERGY
P.O. BOX 880, MS N04
MORGANTOWN, WV 26507-0880
304-291-4281

FRANK R GROVES
PROFESSOR
LOUISIANA STATE UNIVERSITY
DEPT. OF CHEMICAL ENGINEERING
BATON ROUGE, LA 70810
504-388-1426

KRISHAN K GUPTA
SR. DEVELOPING TECH SPECIALIST
SARGENT & LUNDY ENGINEERS
MECHANICAL & ANALYTICAL DIV.
55 EAST MONROE STREET
CHICAGO, IL 60603
312-269-6603

GAURANG B HALDIPUR
MANAGER, DEVELOPMENT ENGR'G
KRW ENERGY SYSTEMS, INC.
P.O. BOX 334 WALTZ MILL
MADISON, PA 15663
412-722-6080

JACK S HALOW
DIR., COAL PROJECTS MGMT. DIV.
MORGANTOWN ENERGY TECH CENTER
U.S. DEPARTMENT OF ENERGY
P.O. BOX 880, MS D01
MORGANTOWN, WV 26507-0880
304-291-4109

DAVID O HAM
MGR, ENERGY/ENVIRONMENTAL SCI.
PHYSICAL SCIENCES, INC.
RESEARCH PARK
P.O. BOX 3100
ANDOVER, MA 01810
617-475-9030

SCOTT M HARKINS
CHEMICAL ENGINEER
RESEARCH TRIANGLE INSTITUTE
P.O. BOX 12194
RESEARCH TRIANGLE PARK NC 27603
919-541-5937

DOUGLAS P HARRISON
PROFESSOR
LOUISIANA STATE UNIVERSITY
DEPT. OF CHEMICAL ENGINEERING
BATON ROUGE, LA 70803
504-388-1426

HEINZ HEINEMANN
SENIOR SCIENTIST
UNIVERSITY OF CALIFORNIA
LAWRENCE BERKELEY LABORATORY
1 CYCLOTRON ROAD, BLDG. 62
BERKELEY, CA 94720
415-486-5796

NANDOR H HERTZ
PROJECT MANAGER
ELECTRIC POWER RESEARCH INST.
3412 HILLVIEW AVENUE
P.O. BOX 10412
PALO ALTO, CA 94303
415-855-2338

NORMAN T HOLCOMBE
PROJECT MANAGER
MORGANTOWN ENERGY TECH CENTER
U.S. DEPARTMENT OF ENERGY
P.O. BOX 880, MS E01
MORGANTOWN, WV 26507-0880
304-291-4829

JOHN D HOLMGREN
VICE PRES., TECH. DEVELOPMENT
KRW ENERGY SYSTEMS, INC.
P.O. BOX 334
MADISON, PA 15663-0334
412-722-6030

FRANKLIN I HONEA
CHEMICAL ENGINEER
MORGANTOWN ENERGY TECH CENTER
GRAND FORKS PROJECTS OFFICE
P.O. BOX 7206, UNIV. STATION
GRAND FORKS, ND 58202
FTS-783-0142

PETER S HUGHES
MANAGER, ENERGY PROGRAMS MKTG.
WESTINGHOUSE ELECTRIC CORP.
P.O. BOX 10864
PITTSBURGH, PA 15236
412-382-7091

CARLTON IRWIN
ASSOC. DIR., ENERGY RESEARCH
WEST VIRGINIA UNIVERSITY
258 STEWART STREET
P.O. BOX 6064
MORGANTOWN, WV 26506
304-293-2867

FRED C JAHNKE
SENIOR STAFF ENGINEER
TEXACO, INC.
2000 WESTCHESTER AVENUE
WHITE PLAINS, NY 10650
914-253-7946

SURESH C JAIN
PROJECT MANAGER
MORGANTOWN ENERGY TECH CENTER
U.S. DEPARTMENT OF ENERGY
P.O. BOX 880, MS CO4
MORGANTOWN, WV 26507-0880
304-291-4446

SVEN A JANSSON
MANAGER, SCIENCE & TECHNOLOGY
ASEA PFBC AB
S-612 20
FINSPONG,
SWEDEN
461-228-1110

LISA A JARR
PROJECT MANAGER
MORGANTOWN ENERGY TECH CENTER
U.S. DEPARTMENT OF ENERGY
P.O. BOX 880, MS CO4
MORGANTOWN, WV 26507-0880
304-291-4555

JOHN M JENNINGS
PROGRAM MANAGER
U.S. DEPARTMENT OF ENERGY
OFFICE OF FOSSIL ENERGY
FE-14, B-109/GTN
WASHINGTON, DC 20545
301-353-4251

MAHESH C JHA
MANAGER, MINERAL & ENERGY RE
AMAX EXTRACTIVE R&D, INC.
5950 MCINTYRE STREET
GOLDEN, CO 80403-7499
303-279-7636

DALE A JOHNSON
PROCESS ENGINEER
ANG COAL GASIFICATION
P.O. BOX 1149
BEULAH, ND 58523
701-873-6635

WALTER H JOHNSON
PROGRAM MANAGER
INTERNATIONAL FUEL CELLS CORP.
195 GOVERNORS HIGHWAY
P.O. BOX 739
SOUTH WINDSOR, CT 06040
203-727-2215

WILLIAM J JONES
ASSISTANT PROFESSOR
GEORGIA INST. OF TECHNOLOGY
APPLIED BIOLOGY DEPARTMENT
ATLANTA, GA 30332
404-894-3700

DAVID P KALMANOVITCH
RESEARCH ASSOCIATE
UNIV OF ND ENERGY RESEARCH CTR
P.O. BOX 8213, UNIV. STATION
GRAND FORKS, ND 58202
701-777-5244

FRED S KEMP
PROGRAM MANAGER
INTERNATIONAL FUEL CELLS CORP.
195 GOVERNORS HIGHWAY
P.O. BOX 739
SOUTH WINDSOR, CT 06074
203-727-2212

M. RASHID KHAN
RESEARCH SCIENTIST
MORGANTOWN ENERGY TECH CENTER
U.S. DEPARTMENT OF ENERGY
P.O. BOX 880, MS AO4
MORGANTOWN, WV 26507-0880
304-291-4580

BANG M KIM
CHEMICAL ENGINEER
GENERAL ELECTRIC CORPORATE R&D
P.O. BOX 8
SCHENECTADY, NY 12301
518-387-6596

JIN BAI KIM
PROFESSOR
WEST VIRGINIA UNIVERSITY
MATH DEPARTMENT
MORGANTOWN, WV 26506
304-293-2014

HOBART KING
ADJUNCT PROFESSOR
WEST VIRGINIA UNIVERSITY
DEPARTMENT OF GEOLOGY
MORGANTOWN, WV 26506
304-594-2331

JULIANNE M KLARA
CHEMICAL ENGINEER
MORGANTOWN ENERGY TECH CENTER
U.S. DEPARTMENT OF ENERGY
P.O. BOX 880, MS EO1
MORGANTOWN, WV 26507-0880
304-291-4729

HERMAN KLEIN-TEESELINK
DEVELOPMENT ENGINEER
STORK BOILERS
POSTBUS 20
HENGELO, 7558EG
NETHERLANDS
94 -401-286

TED M KNOWLTON
ASST DIR/FLUIDIZATION RESEARCH
INSTITUTE OF GAS TECHNOLOGY
4201 W 36TH STREET
CHICAGO, IL 60632
312-890-6408

ED KOBETICH
CONSULTANT
BCR NATIONAL LABORATORY
350 HOCHBERG ROAD
MONROEVILLE, PA 15146
412-327-1600

ROBERT W KOCH
CHEMICAL ENGINEER
MORGANTOWN ENERGY TECH CENTER
U.S. DEPARTMENT OF ENERGY
P.O. BOX 880, MS EO1
MORGANTOWN, WV 26507-0880
304-291-4670

REINER KOLLRACK
DEPUTY DIRECTOR
SCIENCE APPLICATIONS INT'L
9760 OWENSMOUTH
CHATSWORTH, CA 91311
818-709-5222

JACK A KOSEK
ASSOCIATE DIRECTOR, ENERGY
GINER, INC.
14 SPRING STREET
WALTHAM, MA 02254-9147
617-899-7270

VIJENDRA P KOTHARI
PROJECT MANAGER
MORGANTOWN ENERGY TECH CENTER
U.S. DEPARTMENT OF ENERGY
P.O. BOX 880, MS CO4
MORGANTOWN, WV 26507-0880
304-291-4579

GARY J KOVACIK
PROJECT OFFICER
ALBERTA RESEARCH COUNCIL
P.O. BOX 429
NISKU, ALBERTA TOC 2GO
CANADA
403-955-7891
037-2147

NICHOLAS L KRASCELLA
RESEARCH ENGINEER
UNITED TECH. RESEARCH CENTER
SILVER LANE
EAST HARTFORD, CT 06108
203-727-7224

GOPALA N KRISHNAN
SENIOR METALLURGIST
SRI INTERNATIONAL
333 RAVENSWOOD AVENUE
MENLO PARK, CA 94025
415-859-2627

K. SAMPATH KUMAR
PROJECT MANAGER
RESEARCH COTTRELL, INC.
COTTRELL ENVIRONMENTAL SCIENCE
P.O. BOX 1500
SOMERVILLE, NJ 08876
201-685-4876

H. RUSSELL KUNZ
PROJECT ENGINEER
INTERNATIONAL FUEL CELLS CORP.
195 GOVERNORS HIGHWAY
P.O. BOX 739
SOUTH WINDSOR, CT 06074
203-727-2284

HSIAO-YA L LAI
PROJECT MANAGER
MORGANTOWN ENERGY TECH CENTER
U.S. DEPARTMENT OF ENERGY
P.O. BOX 880, MS CO4
MORGANTOWN, WV 26507-0880
304-291-4105

EARL LARCHER
PATENT ADVISOR
U.S. DEPARTMENT OF ENERGY
OFFICE OF PATENT COUNSEL
P.O. BOX X
OAK RIDGE, TN 37830
FTS-626-1080

CHUN-WAI LEE
GRADUATE ASSISTANT
PENNSYLVANIA STATE UNIVERSITY
402 ACADEMIC ACTIVITIES BLDG.
UNIVERSITY PARK, PA 16802
814-865-4802

SHELDON H LEE
CHEMICAL ENGINEER
ARGONNE NATIONAL LABORATORY
9700 SOUTH CASS AVENUE
ARGONNE, IL 60439
312-972-4395

YAM Y LEE
RESEARCH SPECIALIST
PYROPOWER CORPORATION
5120 SHOREHAM PLACE
SAN DIEGO, CA 92122
619-458-3012

DENNIS LEPPIN
MANAGER, SURFACE COAL GASIF.
GAS RESEARCH INSTITUTE
8600 W BYRN MAWR AVENUE
CHICAGO, IL 60616
312-399-8286

SAMUEL C LEVENTRY
DESIGN MANAGER
CHICAGO BRIDGE AND IRON
800 JORIE BLVD.
OAK BROOK, IL 60522-7001
312-572-7976

ARTHUR E LEWIS
GEOLOGIST
LAWRENCE LIVERMORE NAT'L LAB
P.O. BOX 808, MS L-207
LIVERMORE, CA 94550
415-422-6453

MICHAEL A LILGA
RESEARCH SCIENTIST
PACIFIC NORTHWEST LABORATORY
P.O. BOX 999
RICHLAND, WA 99352
509-375-2630

YUNG-YI LIN
PROCESS ENGINEER
M. W. KELLOGG
THREE GATEWAY PLAZA
HOUSTON, TX 77046
713-960-2609

WEN-SHOU LIOU
PROJECT MANAGER
MORGANTOWN ENERGY TECH CENTER
U.S. DEPARTMENT OF ENERGY
P.O. BOX 880, MS CO4
MORGANTOWN, WV 26507-0880
304-291-4162

THOMAS E LIPPERT
PRINCIPAL ENGINEER
WESTINGHOUSE ELECTRIC CORP.
1310 BEULAH ROAD, 801-4518
PITTSBURGH, PA 15235
412-256-2440

ROBERT D LITT
ASSOCIATE SECTION MANAGER
BATTELLE COLUMBUS DIVISION
505 KING AVENUE
COLUMBUS, OH 43201-2693
614-424-4818

JAMES LONGANBACH
CHEMIST
MORGANTOWN ENERGY TECH CENTER
U.S. DEPARTMENT OF ENERGY
P.O. BOX 880, MS C04
MORGANTOWN, WV 26507-0880
304-291-4555

ZVI LUDMER
VISITING RESEARCH PROFESSOR
CITY COLLEGE OF NEW YORK
CHEMICAL ENGINEERING DEPT.
140TH ST. AND CONVENT AVENUE
NEW YORK, NY 10031
212-690-4232

WILLIAM LUECKEL
VICE PRESIDENT OF RESEARCH
INTERNATIONAL FUEL CELLS CORP.
195 GOVERNORS HIGHWAY
P.O. BOX 739
SOUTH WINDSOR, CT 06074
203-727-2225

RICHARD H LUNN
BCR NATIONAL LABORATORY
350 HOCHBERG ROAD
MONROEVILLE, PA 15146
412-327-1600

HANS LUTHI
MANAGER, BUSINESS DEVELOPMENT
BROWN, BOVERI, AND COMPANY
DEPARTMENT T-VN
BADEN, CH-5401
SWITZERLAND
56-75 -4303

SCOTT LYNN
PROFESSOR
UNIVERSITY OF CALIFORNIA
LAWRENCE BERKELEY LABORATORY
DEPARTMENT OF CHEMICAL ENGR'G
BERKELEY, CA 94720-9989
415-642-1634

RIPUDAMAN MALHOTRA
SRI INTERNATIONAL
333 RAVENSWOOD AVENUE
MENLO PARK, CA 94025
415-859-4301

MOMTAZ N MANSOUR
PRESIDENT
MGMT & TECH CONSULTANTS, INC.
P.O. BOX 21
COLUMBIA, MD 21045
301-982-1292

KENNETH E MARKEL
CHIEF, GAS STREAM CLEANUP BR.
MORGANTOWN ENERGY TECH CENTER
U.S. DEPARTMENT OF ENERGY
P.O. BOX 880, MS D04
MORGANTOWN, WV 26507-0880
304-291-4505

WEBB J MARNER
MEMBER TECHNICAL STAFF
JET PROPULSION LABORATORY
4800 OAK GROVE DRIVE
PASADENA, CA 91109
818-354-7020

BILL MARSHALL
DEPARTMENT MANAGER
SANDIA NATIONAL LABORATORY
DEPARTMENT 6250
ALBUQUERQUE, NM 87185
505-844-2964

GERALD MAZZELLA
MGR OF TECHNOLOGY OPERATIONS
FOSTER WHEELER CORP.
110 SOUTH ORANGE AVENUE
LIVINGSTON, NJ 07039
201-533-2124

CLAUDETTE G MCKAMEY
DEVELOPMENT ASSOCIATE II
OAK RIDGE NATIONAL LABORATORY
P.O. BOX X
BUILDING 4500-S
OAK RIDGE, TN 37831-6116
615-574-6917

DONALD F MCMILLEN
SRI INTERNATIONAL
333 RAVENSWOOD AVENUE
MENLO PARK, CA 94025
415-859-4301

KENNETH H MEANS
PROFESSOR
WEST VIRGINIA UNIVERSITY
DEPT OF MECHANICAL ENGINEERING
MORGANTOWN, WV 26506
304-293-3111

JOSEPH S MEI
MECHANICAL ENGINEER
MORGANTOWN ENERGY TECH CENTER
U.S. DEPARTMENT OF ENERGY
P.O. BOX 880, MS N04
MORGANTOWN, WV 26507-0880
304-291-4409

SHARON F MILLER
PENNSYLVANIA STATE UNIVERSITY
FUEL SCIENCE DEPARTMENT
324 STIEDLE STREET
UNIVERSITY PARK, PA 16801
- -

BILL MOORE
PROGRAM MANAGER
U.S. DEPARTMENT OF ENERGY
FE-23/GERMANTOWN
GERMANTOWN, MD 20545
301-353-2905

WILLIAM MORSE
VICE PRESIDENT OF RESEARCH
COLUMBIA GAS COMPANY
1600 DUBLIN ROAD
P.O. BOX 2318
COLUMBUS, OH 43216
614-481-1303

JOHN E MROCHEK
CHEMISTRY COORDINATOR
OAK RIDGE NATIONAL LABORATORY
P.O. BOX X
OAK RIDGE, TN 37831-6226
615-574-6840

JOHN C MYCOCK
VICE PRESIDENT
ETS, INC.
3140 CHAPARRAL DRIVE
ROANOKE, VA 24018
703-774-8999

R NAGARAJAN
RESEARCH ASSISTANT PROFESSOR
WEST VIRGINIA UNIVERSITY
MECHANICAL & AEROSPACE ENGR'G
MORGANTOWN, WV 26506
304-293-4111

TOSHIO NAKAYAMA
COAL GASIFICATION SECTION
CRIEPI
261 NAGASAKA YOKOSUKA-SHI
KANAGAWA, 24001
JAPAN
- -
81-468-57-5829

ERIC T NELSON
SENIOR ENGINEER
GILBERT/COMMONWEALTH, INC.
P.O. BOX 1498
READING, PA 19603
215-775-2600

ROBERT O NESS
RESEARCH ENGINEER
UNIV OF ND ENERGY RESEARCH CTR
P.O. BOX 8213, UNIV. STATION
GRAND FORKS, ND 58202
701-777-5209

DUANE G NICHOLS
GROUP LEADER
CONSOL R & D DEPARTMENT
4000 BROWNSVILLE ROAD
LIBRARY, PA 15129
412-854-6614

GRADY B NICHOLS
DIRECTOR OF RESEARCH
SOUTHERN RESEARCH INSTITUTE
2000 NINTH AVENUE SOUTH
BIRMINGHAM, AL 35255-5305
205-323-6592

RICHARD D NOBLE
CHEMICAL ENGINEER
NATIONAL BUREAU OF STANDARDS
CTR FOR CHEM ENG 773.1
BOULDER, CO 80303
303-497-3416

JAMES B O'HARA
DIRECTOR, PROJECTS DEVELOPMENT
RALPH M. PARSONS COMPANY
100 W WALNUT STREET
PASADENA, CA 91124
818-440-2501

GORDON C PAGE
SENIOR PROGRAM MANAGER
RADIAN CORPORATION
8501 MO-PAC BOULEVARD
P.O. BOX 9948
AUSTIN, TX 78766
512-454-4797

KUMAR PARUCHURI
SENIOR RESEARCH ENGINEER
SHELL DEVELOPMENT CORPORATION
3333 HIGHWAY 6 SOUTH
HOUSTON, TX 77082
713-493-7515

KALMAN PATER
MECHANICAL ENGINEER
MORGANTOWN ENERGY TECH CENTER
U.S. DEPARTMENT OF ENERGY
P.O. BOX 880, MS NO4
MORGANTOWN, WV 26507-0880
304-291-4420

LELAND E PAULSON
PROJECT MANAGER
MORGANTOWN ENERGY TECH CENTER
U.S. DEPARTMENT OF ENERGY
P.O. BOX 880, MS D04
MORGANTOWN, WV 26507-0880
304-291-4578

KEITH M PEARSON
MANAGER OF ADMINISTRATION
UCC RESEARCH CORPORATION
P.O. BOX 1280, GLENWAY AVENUE
BRISTOL, VA 24203
703-466-3322

WILLIAM A PETERS
PRINCIPAL RESEARCH ENGINEER
MASSACHUSETTS INST. OF TECH.
77 MASSACHUSETTS AVE, E40-483B
CAMBRIDGE, MA 02139
617-253-3433

MICHAEL PETRIK
PROCESS ENGINEER
HELIPUMP CORPORATION
8435 BRECKSVILLE ROAD
CLEVELAND, OH 44141
216-229-3178

ROBERT L PHEN
MANAGER, FCC TECH. PROGRAMS
JET PROPULSION LABORATORY
4800 OAK GROVE DR., MS 502-307
PASADENA, CA 91109
818-397-7344

EDWARD A PIGEAUD
PROGRAM MANAGER
ENERGY RESEARCH CORPORATION
3 GREAT PASTURE ROAD
DANBURY, CT 06813
203-792-1460

AUGUSTINE A PITROLO
DIRECTOR
MORGANTOWN ENERGY TECH CENTER
U.S. DEPARTMENT OF ENERGY
P.O. BOX 880, MS C02
MORGANTOWN, WV 26507-0880
304-291-4511

MAURICE W PITT
PROGRAM MGR., COAL CONVERSION
U.S. DEPARTMENT OF ENERGY
OFFICE OF FOSSIL ENERGY
WASHINGTON, DC 20545
301-353-3992

DENNIS P RADEN
SENIOR CHEMICAL ENGINEER
RADIAN CORPORATION
8501 MO-PAC BOULEVARD
P.O. BOX 9948
AUSTIN, TX 78766
512-454-4797

LJUBISA RADOVIC
PENNSYLVANIA STATE UNIVERSITY
FUEL SCIENCE PROGRAMS
UNIVERSITY PARK, PA 16802
- -

LAWRENCE K RATH
MGR, PROCESS & PROJECT ENGR.
KRW ENERGY SYSTEMS, INC.
M. W. KELLOGG
P.O. BOX 334
MADISON, PA 15663-0334
412-722-6077

EMERSON R RAY
PROJECT MANAGER
WESTINGHOUSE R&D CENTER
1310 BEULAH ROAD
PITTSBURGH, PA 15243
412-256-2125

LEAH REED
SENIOR SCIENTIST
SHELADIA ASSOCIATES, INC.
15825 SHADY GROVE ROAD
ROCKVILLE, MD 20850
301-258-7474

AMIR REHMAT
MANAGER, UTILITY GAS DIVISION
INSTITUTE OF GAS TECHNOLOGY
3424 SOUTH STATE STREET
CHICAGO, IL 60616
312-567-5899

JOHN REZAIYAN
PROJECT MANAGER
SHELADIA ASSOCIATES, INC.
15825 SHADY GROVE ROAD
ROCKVILLE, MD 20850
301-258-7474

PETER B ROBERTS
MANAGER, ENGR'G TECHNOLOGY
SOLAR TURBINES, INC.
2200 PACIFIC HIGHWAY, MS R-1
SAN DIEGO, CA 92138-5376
619-544-5079

ALLEN M ROBIN
RESEARCH MANAGER
TEXACO, INC.
329 N. DURFEE ROAD
SOUTH EL MONTE, CA 91733
213-699-0948

DAVID ROSS
DEPARTMENT DIRECTOR
SRI INTERNATIONAL
333 RAVENSWOOD AVENUE
MENLO PARK, CA 94025
415-859-2430

MICHAEL D RUTKOWSKI
PROGRAM MANAGER
GILBERT/COMMONWEALTH, INC.
P.O. BOX 1498
READING, PA 19603
215-775-2600

JOSEPH J SANGIOVANNI
SENIOR RESEARCH SCIENTIST
UNITED TECH. RESEARCH CENTER
SILVER LANE, MS 30
EAST HARTFORD, CT 06108
203-727-7328

ALAN W SCARONI
ASSOCIATE PROFESSOR
PENNSYLVANIA STATE UNIVERSITY
404 ACADEMIC ACTIVITIES BLDG.
UNIVERSITY PARK, PA 16802
814-863-3264

JOHN W SCHAEFER
MANAGER, BUSINESS DEVELOPMENT
ACUREX CORPORATION
485 CLYDE AVENUE
P.O. BOX 7044
MT. VIEW, CA 94039
415-961-5700

RICHARD R SCHEHL
DIRECTOR/PROCESS SCIENCES DIV.
PITTSBURGH ENERGY TECH CENTER
U.S. DEPARTMENT OF ENERGY
P.O. BOX 10940
PITTSBURGH, PA 15236
412-892-6012

DALE K SCHMIDT
MANAGER, DEVELOPMENT PROGRAMS
KRW ENERGY SYSTEMS, INC.
P.O. BOX 334
MADISON, PA 15663-0334
412-722-6033

RODNEY E SEARS
RESEARCH SUPERVISOR
UNIV OF ND ENERGY RESEARCH CTR
P.O. BOX 8213, UNIV. STATION
GRAND FORKS, ND 58202
701-777-5163

MOHINDAR SEEHRA
PROFESSOR
WEST VIRGINIA UNIVERSITY
DEPT. OF PHYSICS
MORGANTOWN, WV 26506
304-293-3421

MICHAEL A SERIO
MGR., CHEMICAL ENGR. SCIENCE
ADVANCED FUEL RESEARCH, INC.
87 CHURCH STREET
EAST HARTFORD, CT 06108
203-528-9806

VIJAY SETHI
PROGRAM DIRECTOR
KENTUCKY ENERGY CABINET LAB
IRON WORKS PIKE
P.O. BOX 31015
LEXINGTON, KY 40512-3015
606-252-5535

PRAMOD SHARMA
MEMBER RESEARCH STAFF
JET PROPULSION LABORATORY
4800 OAK GROVE DR., MS 125-112
PASADENA, CA 91109
818-354-3487

REUEL SHINNAR
PROFESSOR
CITY COLLEGE OF NEW YORK
DEPT. OF CHEMICAL ENGINEERING
140TH STREET AT CONVENT AVENUE
NEW YORK, NY 10031
212-690-6679

JOHN E SHOLES
DIRECTOR/GRAND FORKS PROJ OFF.
MORGANTOWN ENERGY TECH CENTER
U.S. DEPARTMENT OF ENERGY
P.O. BOX 880, MS D01
MORGANTOWN, WV 26057-0880
304-291-4305

RICHARD D SKINNER
DIRECTOR, ENVIRONMENTAL ENGR'G
PHILLIPS PETROLEUM COMPANY
PLAZA OFFICE BLDG., RM 1360G
BARTLESVILLE, OK 74004
918-661-5916

STEVEN SMELSER
FLUOR
ADVANCED TECHNOLOGY DIVISION
3333 MICHELSON DRIVE
IRVINE, CA 92730
714-975-5847

CARL SMITH
ADJUNCT PROFESSOR
WEST VIRGINIA UNIVERSITY
DEPARTMENT OF GEOLOGY
MORGANTOWN, WV 26506
304-594-2331

DANIEL P SMITH
MANAGER, PROCESS OPERATION
GENERAL ELECTRIC CORPORATE R&D
P.O. BOX 8, K-1, RM 110
ENGINEERING SYSTEMS BUILDING
SCHENECTADY, NY 12301
518-387-6413

KEVIN J SMITH
PROCESS DEVELOPMENT ENGINEER
KRW ENERGY SYSTEMS, INC.
P.O. BOX 334
MADISON, PA 15663-0334
412-722-6066

MURDO J SMITH
PROGRAM MANAGER
INTERNATIONAL FUEL CELLS CORP.
P.O. BOX 739
SOUTH WINDSOR, CT 06074
203-727-2269

L. DOUGLAS SMOOT
PROFESSOR
BRIGHAM YOUNG UNIVERSITY
COLLEGE OF ENGINEERING SCIENCE
270 CLYDE BUILDING
PROVO, UT 84602
801-378-4327

BRUCE H SOLKA
SENIOR ANALYTICAL CHEMIST
INSTITUTE OF GAS TECHNOLOGY
3424 SOUTH STATE STREET
CHICAGO, IL 60616
312-567-5290

PETER R SOLOMON
PRESIDENT
ADVANCED FUEL RESEARCH, INC.
P.O. BOX 18343
87 CHURCH STREET
EAST HARTFORD, CT 06108
203-528-9806

STRATIS V SOTIRCHOS
PROFESSOR
UNIVERSITY OF ROCHESTER
DEPT. OF CHEMICAL ENGINEERING
ROCHESTER, NY 14627
716-275-4626

VASSILIS STAMOUDIS
PROGRAM MANAGER
ARGONNE NATIONAL LABORATORY
ENVIRONMENTAL RESEARCH BLDG.
9700 SOUTH CASS AVENUE
ARGONNE, IL 60439
312-972-7637

ROGER P STANBRIDGE
VICE PRESIDENT
FOSECO, INC.
20200 SHELDON ROAD
CLEVELAND, OH 44142
216-826-4548

WILLIAM G STEEDMAN
PROJECTS MANAGER
BATTELLE COLUMBUS DIVISION
505 KING AVENUE
COLUMBUS, OH 43201-2693
614-424-4965

MEYER STEINBERG
HEAD, PROCESS SCIENCES DIV.
BROOKHAVEN NATIONAL LABORATORY
ENERGY AND ENVIRONMENT DEPT.
BUILDING 526
UPTON, NY 11973
516-282-3036

GEORGE STEINFELD
PROGRAM MANAGER
ENERGY RESEARCH CORPORATION
3 GREAT PASTURE ROAD
DANBURY, CT 06813
203-792-1460

MARIA F STEPHANOPOULOS
PRINCIPAL RESEARCH ASSOCIATE
MASSACHUSETTS INST. OF TECH.
CHEMICAL ENGINEERING DEPT.
ROOM 66-471
CAMBRIDGE, MA 02139
617-253-3178

DAVE P STINTON
DEVELOPMENT ENGINEER
OAK RIDGE NATIONAL LABORATORY
P.O. BOX X, BLDG. 4515/MS 063
OAK RIDGE, TN 37831
615-574-4556

DAVID STOPEK
PRESIDENT
STOPEK TECHNICAL SERVICES
ROUTE 7, BOX 460
MORGANTOWN, WV 26505
304-594-3294

JERRY W SUITOR
MEMBER TECHNICAL STAFF
JET PROPULSION LABORATORY
4800 OAK GROVE DRIVE
MS 125-177
PASADENA, CA 91109
818-354-4917

FRANK V SUMMERS
R&D SUPERVISOR
KOBE DEVELOPMENT CORPORATION
CHARLOTTE PLAZA
CHARLOTTE, NC 28244
704-373-0329

PAUL R THIBEAULT
CONSULTING ENGINEER
COMBUSTION ENGINEERING, INC.
1000 PROSPECT HILL ROAD
WINDSOR, CT 06095
203-285-4576

DONALD C THOMAS
CHEMICAL ENGINEER
TENNESSEE VALLEY AUTHORITY
2S 91B MISSIONARY BRIDGE PLACE
CHATTANOOGA, TN 37402-2801
615-751-6123

RONALD C TIMPE
RESEARCH ASSOCIATE
UNIV OF ND ENERGY RESEARCH CTR
P.O. BOX 8213, UNIV. STATION
GRAND FORKS, ND 58202
701-777-5219

GORAN B TJELLANDER
MANAGER, FUTURE PFBC TECH.
ASEA PFBC AB
S-612 20
FINGSPONG,
SWEDEN
461-228-1739

ANTHONY J TUCKLEY
MANUFACTURING DIRECTOR
FOSECO, INC.
20200 SHELDON ROAD
CLEVELAND, OH 44142
216-826-4548

RICHARD TURTON
ASSISTANT PROFESSOR
WEST VIRGINIA UNIVERSITY
437 ENGINEERING SCIENCES BLDG.
MORGANTOWN, WV 26506
304-293-3280

DON VAN DER VAART
RESEARCH ENGINEER
RESEARCH TRIANGLE INSTITUTE
P.O. BOX 12194
RESEARCH TRIANGLE PARK NC 2770
919-541-6992

ROBERT VANDERMOLEN
PROJECT MANAGER
COMBUSTION POWER COMPANY, INC.
1020 MARSH ROAD
MENLO PARK, CA 95070
415-324-4744

STEPHEN VERIKIOS
PROGRAM MANAGER
U.S. DEPARTMENT OF ENERGY
FE-22, C-177/GTN
WASHINGTON, DC 20545
202-353-3962

GARY E VOELKER
DIR, COAL CONV. SYSTEMS OFFICE
U.S. DEPARTMENT OF ENERGY
OFFICE OF FOSSIL ENERGY
FE-22, C-152/GTN
WASHINGTON, DC 20545
301-353-2841

DAMAN WALIA
DIRECTOR, COAL MARKETING
ATLANTIC RESEARCH CORP.
5390 CHEROKEE AVENUE
ALEXANDRIA, VA 22312
703-642-4653

LI WENG
STUDENT
CITY COLLEGE OF NEW YORK
477 W. 140 STREET
APARTMENT NO. 51
NEW YORK, NY 10031
212-491-6415

GERALD F WHEELER
PROGRAM MANAGER
U.S. DEPARTMENT OF ENERGY
FE-22, C-179/GTN
WASHINGTON, DC 20545
202-353-3511

GEORGE R WHITE
VICE PRESIDENT FOR RESEARCH
UNIVERSITY OF PITTSBURGH
911 WILLIAM PITT UNION
PITTSBURGH, PA 15260
412-648-7850

PAUL R WIEBER
DEP. ASSOC. DIRECTOR/TECH MGMT
MORGANTOWN ENERGY TECH CENTER
U.S. DEPARTMENT OF ENERGY
P.O. BOX 880, MS BO6
MORGANTOWN, WV 26507-0880
304-291-4364

MARK C WILLIAMS
PROJECT MANAGER
MORGANTOWN ENERGY TECH CENTER
U.S. DEPARTMENT OF ENERGY
P.O. BOX 880, MS EO5
MORGANTOWN, WV 26507-0880
304-291-4134

THOMAS F WILLIAMS
ENGINEER, R&D STUDIES
ALLEGHENY POWER SERVICE CORP.
800 CABIN HILL DRIVE
GREENSBURG, PA 15601
412-838-6733

WARRACK G WILLSON
DIVISION MANAGER
UNIV OF ND ENERGY RESEARCH CTR
P.O. BOX 8213, UNIV. STATION
GRAND FORKS, ND 58202
701-777-5174

KEITH B WILSON
PROJECT MANAGER
COMBUSTION POWER COMPANY, INC.
1020 MARSH ROAD, SUITE 100
MENLO PARK, CA 94025
415-324-4744

WILLIAM G WILSON
PRESIDENT
GAS DESULFURIZATION CORP.
820 HARDEN DRIVE
PITTSBURGH, PA 15229
412-364-1822

RICHARD A WOLFE
EXECUTIVE VICE PRESIDENT
UCC RESEARCH CORPORATION
P.O. BOX 1280, GLENWAY AVENUE
BRISTOL, VA 24203
703-466-3322

WALTER WOLOWODIUK
VICE PRESIDENT
FOSTER WHEELER CORP.
12 PEACHTREE HILL ROAD
LIVINGSTON, NJ 07039
201-533-3639

BERNARD J WOOD
SENIOR CHEMIST
SRI INTERNATIONAL
333 RAVENSWOOD AVENUE
MENLO PARK, CA 94025
415-859-2305

LAWRENCE R WOODLAND
SR. STAFF CHEMICAL ENGR.
ARTHUR D. LITTLE, INC.
20 ACORN PARK
CAMBRIDGE, MA 02140
617-864-5770

ROBERT E WRIGHT
APPLIED RESEARCH TECHNOLOGIST
UCC RESEARCH CORPORATION
P.O. BOX 1280, GLENWAY AVENUE
BRISTOL, VA 24203
703-466-3322

RALPH T YANG
PROFESSOR
STATE UNIVERSITY OF NEW YORK
DEPT OF CHEMICAL ENGINEERING
BUFFALO, NY 14260
716-636-2519

ROBERT F ZABRANSKY
MANAGER
INSTITUTE OF GAS TECHNOLOGY
3424 SOUTH STATE STREET
CHICAGO, IL 60616
312-567-5272

SOLON ZARKANITIS
GRADUATE STUDENT
UNIVERSITY OF ROCHESTER
DEPT. OF CHEMICAL ENGINEERING
ROCHESTER, NY 14627
716-275-4250

ED ZAWADZKI
PRESIDENT
E. A. ZAWADZKI LTD.
100 LANCELOT CIRCLE
MCMURRAY, PA 15317
412-941-9202

JOHN ZONDLO
ASSOCIATE PROFESSOR
WEST VIRGINIA UNIVERSITY
415 ENGINEERING SCIENCE BLDG.
MORGANTOWN, WV 26506
304-293-2619

METC PARTICIPANTS

The participants listed below can all be reached at the following address:

U.S. Department of Energy
Office of Fossil Energy
Morgantown Energy Technology Center
P.O. Box 880
Morgantown, West Virginia 26507-0880

Rita A. Bajura
Fred Bauer
Robert C. Bedick
Louis H. Berkshire
James E. Burchfield
Kent H. Casleton
Floyd Cassidy
James C. Cho
Roger J. Combs
James Copley
Janice Cyzick
Richard A. Dennis
Frederick T. Dyke
John E. France
Gary R. Friggens
Raymond Gansley
Adolf W. Gessner
Leonard E. Graham
Ulrich Grimm
Jack S. Halow
Thomas J. Hand
Richard A. Hargis
Larry C. Headley
Peter A. Hesbach
Doug M. Jewell
Joseph P. Kanosky
Stanley Kasper
Thomas W. Keech
John J. Kovach
Steven C. Lamey
John R. Mallin
Dan Maloney
James McClung
Ted Miin
William R. Miller
Curtis V. Nakaishi
Harvey Ness
Tom O'Brien
Sandy Phares
Massood Ramezan
Nelson Rekos
Lawrence Saroff
Lawrence J. Shadle
Vasant B. Shah
Abolghasen Shamsi
Ken Stone
Larry D. Strickland
Phuoc Xuan Tran
Kaushik K. Vyas
J. Keith Westhusing
Kevin E. Williams
Marvin W. Wilson
Steven D. Woodruff
Paul C. Yue

☆ U. S. GOVERNMENT PRINTING OFFICE: 1987--548-079--60002